

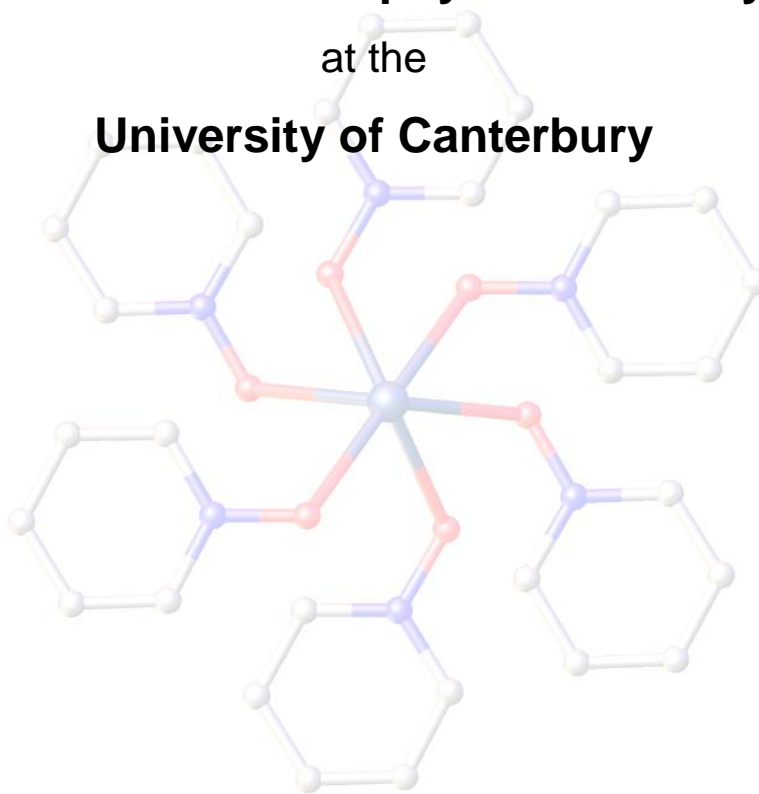
# Pyridine N-oxides as Versatile Ligands for Silver(I)

A thesis submitted in partial fulfilment of the requirements for the degree  
of

**Doctor of Philosophy in Chemistry**

at the

**University of Canterbury**



Submitted by Rakesh Puttreddy

**UC**  
UNIVERSITY OF  
CANTERBURY  
*Te Whare Wānanga o Waitaha*  
CHRISTCHURCH NEW ZEALAND

Department of Chemistry  
University of Canterbury  
Christchurch  
New Zealand  
2013

## Acknowledgements

Firstly I would like to extend my utmost thanks to my supervisor, Professor Peter J. Steel, for his excellent guidance, advice and unwavering support throughout the course of this research work. You were always there when I needed you and have inspired me to keep going through to the end. I owe my deepest gratitude to my supervisor for his patience in the preparation of this thesis and introducing me to the field of X-ray crystallography. Besides my advisor, I would also like to thank my co-supervisor Dr. Chris Fitchett and committee members for their valuable advice and comments. I would also like to thank the Marsden Fund, which has supported me financially throughout my research.

I would like to thank the staff and research students in the Chemistry Department for all your help over the years. I would also like to take this opportunity to thank Dr. Matthew Polson, Dr. Alan Ferguson and Dr. Justine Cottam for their very helpful comments and suggestions during my thesis preparation. Special thanks to Dr. Marie Fitchett for NMR and mass spectrometric analysis, and Drs. Matt Polson and Jan Wikaira for their assistance with X-ray crystallography. I would also like to thank the technical staff Rob, Wayne, Gill, Laurie, Nick and Danny for their background support during my research. And thanks to the Steel group members King, Siji, Solomon, Ryan, Michael and Tom and Team-Fitchett Jayne, Robbie, Paul, Emma, Sam, Will, Anthony and Aimee for being exceptionally friendly.

Last but not least, I would like to thank my parents, Mogilireddy and Prashanthi, brother Rajesh, sister Siji, friends and relatives for their encouragement, love and support through the years.

# Table of contents

Contents	Page No.
Acknowledgements.....	2
Abstract.....	4
<b>Chapter – 1 Introduction</b>	
1.1 Metallosupramolecular chemistry.....	6
1.2 Silver(I) chemistry.....	8
1.3 Pyridine N-oxides.....	11
1.4 Aim of the thesis.....	21
<b>Chapter – 2 Complexes of Pyridine N-oxides</b>	
2.1 Pyridine N-oxides – Introduction.....	25
2.2 Syntheses of pyridine N-oxides.....	26
2.3 Silver(I) complexes of pyridine N-oxides.....	30
2.4 Conclusions.....	97
<b>Chapter – 3 Complexes of Pyridine N,N'-dioxides</b>	
3.1 Pyridine N,N'-dioxides – Introduction.....	102
3.2 Syntheses of pyridine N,N'-dioxides.....	105
3.3 Silver(I) complexes of pyridine N,N'-dioxides.....	109
3.4 Conclusions.....	166
<b>Chapter – 4 Complexes of Pyridine N,N',N''-trioxides</b>	
4.1 Pyridine N,N',N''-trioxides – Introduction.....	171
4.2 Syntheses of pyridine N,N',N''-trioxides.....	172
4.3 Silver(I) complexes of pyridine N,N',N''-trioxides.....	177
4.4 Conclusions.....	195
<b>Chapter – 5 Conclusions</b>	
Conclusions and future prospects.....	197
<b>Chapter – 6 Experimental</b>	
6.1 General information.....	202
6.2 Preparation of pyridine N-oxides.....	203
6.3 Preparation of silver(I) complexes with pyridine N-oxides.....	208
6.4 Preparation of pyridine N,N'-dioxides.....	216
6.5 Preparation of silver(I) complexes with pyridine N,N'-dioxides.....	227
6.6 Preparation of pyridine N,N',N''-trioxides.....	234
6.7 Preparation of silver(I) complexes with pyridine N,N',N''-trioxides.....	236
<b>Appendix</b>	
Crystallographic data.....	239
<b>References.....</b>	<b>255</b>

# Abstract

**Chapter 1** gives a brief introduction to metallocsupramolecular chemistry, silver(I) chemistry and the synthesis and coordination chemistry of pyridine mono-, di- and tri-N-oxides.

**Chapter 2** describes the syntheses of 17 [16 known and 1 new] pyridine N-oxides using either mCPBA or 50% H<sub>2</sub>O<sub>2</sub> as the oxidising agent. It also describes 33 new X-ray crystal structures, of which 23 are silver(I) complexes and the remaining are molecular species, protonated ligands and unreported ligand crystal structures. The N-O group is shown to coordinate with up to three silver atoms with dimensionalities ranging from 0 to 2.

**Chapter 3** describes the syntheses of 21 [16 known and 5 new] bipyridine N,N'-dioxides. This chapter also contains 27 new crystal structures, with 23 being silver(I) complexes, 1 molecular species and three unreported ligand crystal structures. The N,N'-dioxide ligands adopted up to  $\mu_6$ -O,O,O,O',O',O' denticity with polymer dimensionality varying from 0 to 2.

**Chapter 4** involves the syntheses of 4 N,N',N''-trioxides and 7 new silver(I) complexes with 2,6':2',6''-terpyridine N,N',N''-trioxide and 2 ligand crystal structures. This ligand adopted up to  $\mu_6$ -O,O,O',O',O'',O'' with network dimensionality ranging from 0 to 3.

**Chapter 5** summarises the results with final conclusions and future prospects.

**Chapter 6** details the synthetic procedures for the ligands and their silver(I) complexes. All the N-oxide ligands were characterised by melting point, <sup>1</sup>H NMR, <sup>13</sup>C NMR, IR, ESI-MS and elemental analysis, while the silver(I) complexes were characterised by melting point, elemental analysis, IR and ESI-MS.

# **Chapter – 1**

## **Introduction**

## 1.1 Metallosupramolecular chemistry

Metallosupramolecular chemistry<sup>[1]</sup> involves the use of bridging organic ligands and metal atoms to assemble discrete or 1-, 2- or 3-D polymeric species.<sup>[2]</sup> Self-assembly of metallosupramolecular structures by the directional bonding approach is a subject of current interest; the major requirement for this directional self-assembly approach is the use of rigid precursors of appropriate size and shape. The structure, conformation and topology of these supramolecules depend on the nature of the organic bridging ligand and also on the nature of the metal-ligand interactions.

The goals for the construction of metallosupramolecular networks are to obtain materials that show specific multifunctional properties. Among various supramolecular assemblies, porous networks that contain empty spaces where guest molecules are occupied are of particular interest, because they have many potential applications. For this purpose, heterocycles are widely employed as useful building blocks in the construction of molecular recognition and supramolecular assembly systems with various species both in solution and solid states. N-Heterocycles, especially pyridines and their derivatives [bipyridines, terpyridines etc.,] are often used as building blocks for the construction of sophisticated molecular architectures, which may also incorporate hydrogen bonding, electrostatics, metal coordination bonds,  $\pi$ - $\pi$  interactions, and other attractive weak forces.

The number and spatial arrangement of the metal-binding domains allows the assembly of a wide range of discrete molecular or nanostructured materials. For example, the Steel group<sup>[3]</sup> designed and synthesized a set of heterocycles, which can act as convergent 1.1a, ambivergent 1.1b and divergent 1.1c organic connectors for the construction of supramolecular assemblies, as shown in figure 1.1. The ligands were designed and synthesized based on their applicability and desired network construction; the 'convergent' approach targets molecular recognition, whereas the 'divergent' ligands lead to supramolecular assembly.

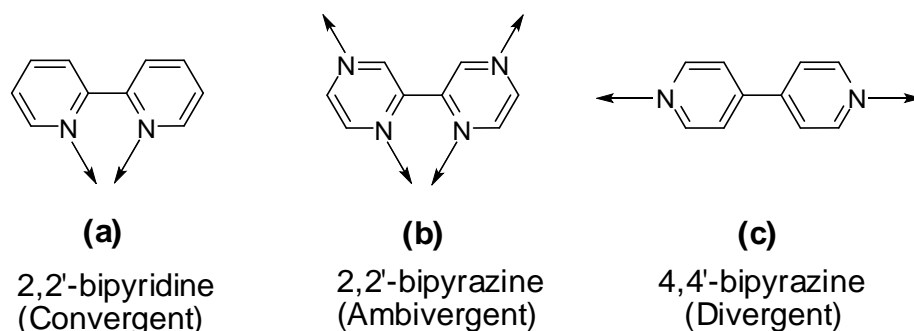


Figure 1.1 – Coordination characteristics of three symmetrical heterocycles.

Sauvage *et al.* successfully employed 1,10-phenanthroline derivatives in the metal-templated synthesis of catenanes [figure 1.2a], where the two phenanthroline units cooperatively coordinate to the same copper(I) center.<sup>[4]</sup>

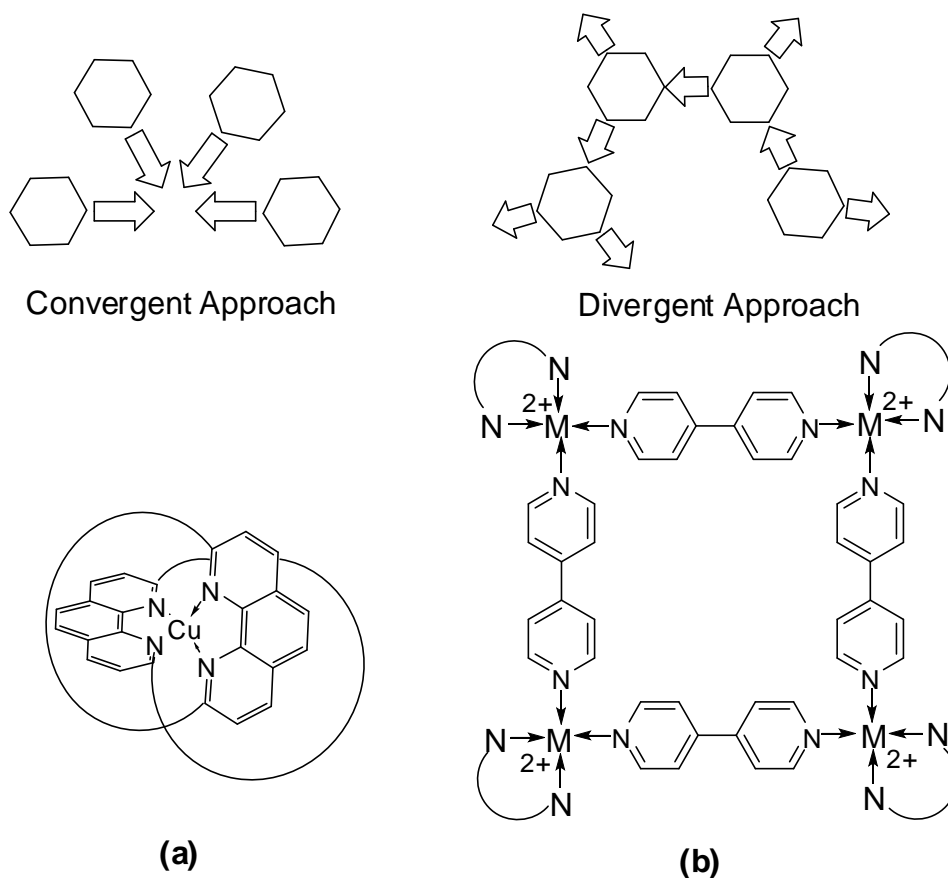


Figure 1.2 – Convergent and divergent approaches based on metallosupramolecular assemblies.

Fujita *et al.* used 4,4'-bipyridine derivatives<sup>[5]</sup> in the synthesis of the molecular squares [figure 1.2b], wherein each 4,4'-bipyridine unit moiety acted independently. When *cis*-protected Pd<sup>2+</sup> species were complexed, a large metallocycle was derived from 4,4'-bipyridine units and four Pd<sup>2+</sup> centers.<sup>[6]</sup>

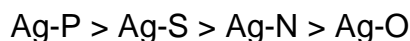
N-Donor containing ligands have been widely used in the self-assembly of coordination polymers because of the facile formation of metal-N-bonds. Commonly used organic ligands containing pyridyl,<sup>[7]</sup> imidazolyl,<sup>[8]</sup> pyrazolyl,<sup>[9]</sup> pyrimidyl,<sup>[10]</sup> triazolyl,<sup>[11]</sup> pyrazine,<sup>[12]</sup> or nitrile<sup>[13]</sup> terminal groups are good examples. The N-atom in these terminal groups have only one lone electron pair, and thus each N donor usually coordinates to a single metal ion. Compared with pyridine containing ligands, pyridine N-oxide ligands differ in several aspects.

- 1) Oxygen is a harder donor than nitrogen.
- 2) The coordination preference between a pyridine N-oxide and a pyridine is quite different; each oxygen site in a pyridine N-oxide may bridge two or more metal centers, while the pyridine nitrogen is coordinated to only one metal center.
- 3) The pyridine N-oxide is a longer spacer which allows for the formation of more porous frameworks.

With all the points mentioned in the literature<sup>[14]</sup> about pyridine N-oxides, we were interested to study pyridine N-oxides coordination ability with the  $d^{10}$  silver(I) metal ion.

## 1.2 Silver chemistry

In metallosupramolecular chemistry the silver ion has been widely used due to the soft acceptor characteristics of this cation,<sup>[15]</sup> as well as its flexible coordination sphere. The silver(I) ion, with its  $d^{10}$  electronic configuration, has zero ligand field stabilization energy [LFSE] and forms labile complexes in which there is rapid exchange of the original ligand set for new ligands available from the surroundings. Studies on ligand-exchange reactions have suggested the relative stability of silver bonds to be:



The flexibility of the silver(I) ion affords an opportunity to investigate the self-assembly process influenced by modifications of the ligand denticity, ligand to metal ratio,<sup>[16]</sup> counterions,<sup>[17]</sup> and non-covalent interactions.<sup>[18]</sup>

Insight into the self assembly process can be obtained by carrying out systematic studies using a series of similar complexes obtained by assembling from a specific ligand and the same metallic center, while imposing the subtle alterations in the environment such as changing the anions<sup>[19]</sup> and the crystallisation solvent.<sup>[16-18]</sup> Extensive work has been done in the construction of silver(I) coordination polymers using rigid ligands,<sup>[20]</sup> because they allow a better prediction of the overall shape.

### 1.2.1 Supramolecular silver(I) interactions in coordination polymers

The strategy for supramolecular design proposed by Desiraju<sup>[20-21]</sup> in 1995 is based on the interpretation of crystal structures in terms of “supramolecular interactions” and “supramolecular synthons”, allowing the consideration of structure of the “supermolecule” governed by discrete non-covalent intermolecular contacts.



These contacts include  $\text{Ag}\cdots\text{Ag}$ ,  $\text{Ag}\cdots\text{aromatic}$ , and  $\text{Ag}\cdots\text{anion}$  interactions and electrostatic repulsions. Most of the information about these types of interactions has been obtained from the discrete molecular models designed to investigate the nature of specific supramolecular interactions. However, in a supramolecular array these intermolecular contacts combine so that the overall structure is a compromise between various interactions of different energies.<sup>[21]</sup>

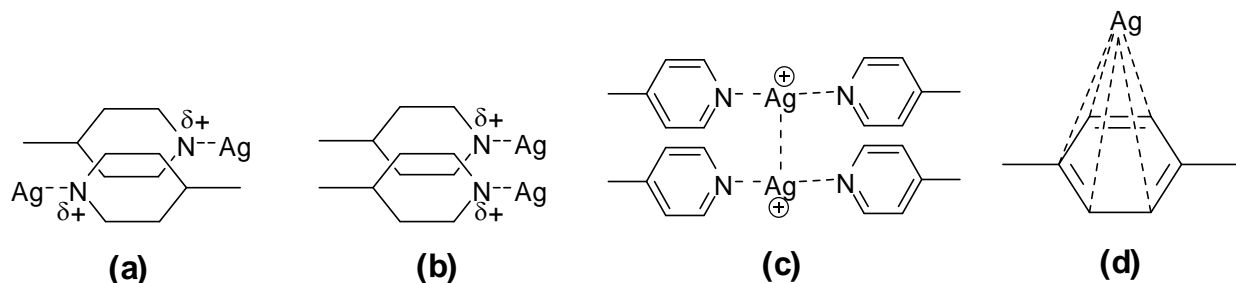
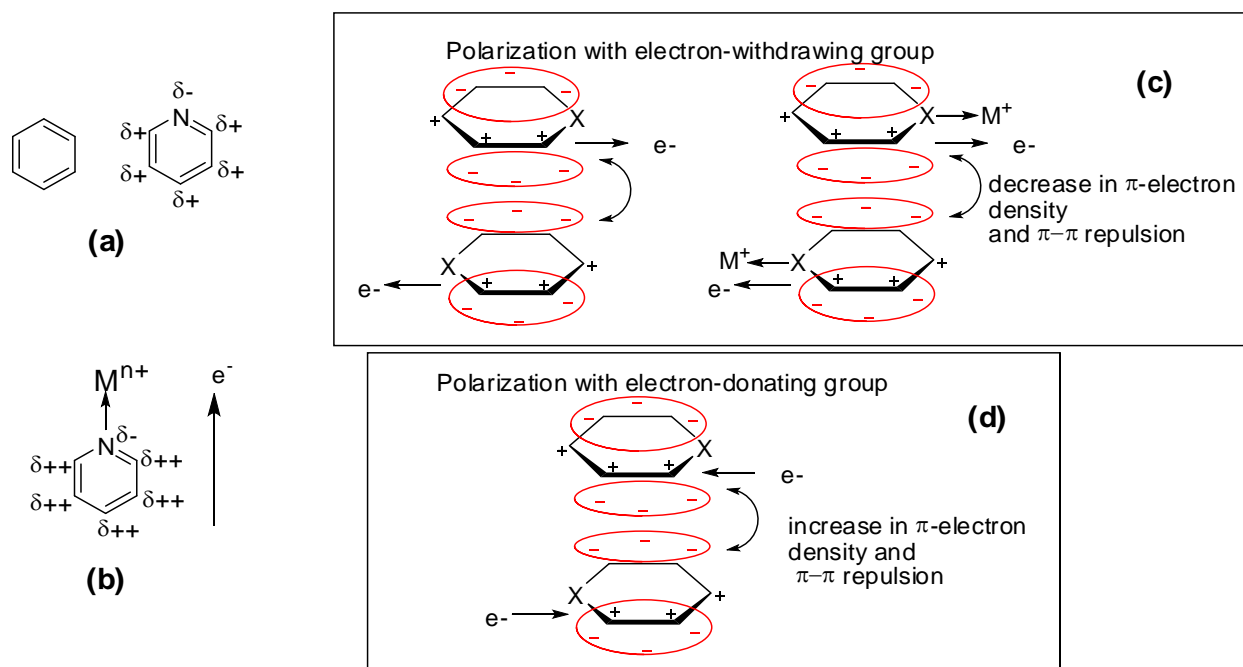


Figure 1.3 – Weak interactions observed in silver(I) coordination polymers (a) favourable head-to-tail  $\pi$ -aromatic interactions, (b) less-favoured head to head aromatic  $\pi$ - $\pi$  interactions, (c)  $\text{Ag}\cdots\text{Ag}$  interactions, (d)  $\text{Ag}\cdots\text{aromatic}$  interactions.

For example, a metal which is coordinated to a nitrogen heteroatom will further enhance the electron-withdrawing effect through its positive charge, as shown in figure 1.4b. Hence, aromatic nitrogen heterocycles should in principle be well suited for  $\pi$ - $\pi$  interactions because of their lower  $\pi$ -electron density than neutral ring systems [figure 1.4c].



X = substituent or heteroatom  
 $\text{X-M}^+$  = heteroatom with co-ordinated metal

Figure 1.4 – (a & b) Outlines the localization of electron density on heteroatom and delocalization of charge over the aromatic ring after heteroatom-metal coordination, (c & d) role of electron withdrawing and electron donating groups in  $\pi$ - $\pi$ -aromatic interactions. For simplicity the arene moieties are drawn in perfect face-to-face alignment and with a uniform decrease or increase in  $\pi$ -electron density. Not shown is the still present  $\pi$ - $\sigma$  attraction which competes with  $\pi$ - $\pi$  repulsion.

### 1.2.2 Metal – Pi interactions

Many transition metal cations can accept electrons from unsaturated organic molecules and, thus, form very stable organometallic species. The silver(I) cation is known to form comparatively weak interactions with aromatic molecules. Hence, measurements of association constants of silver(I) with simple aromatic hydrocarbons led to a conclusion that the broader a conjugated electronic system the stronger would be the silver(I) interaction.<sup>[22]</sup> It would be expected that smaller or more electron deficient aromatic molecules would less readily interact with silver(I) and thus form weaker contacts. It is also logical that interactions between weakly coordinating anions and silver(I) will affect the strength of any Ag–aromatic interaction. The observation that strongly coordinating anions [ $\text{SO}_4^{2-}$ ,  $\text{PhCO}_2^-$ ,  $\text{MeCO}_2^-$ ] completely diminish the metal–aromatic interaction<sup>[23]</sup> means that the anion effect should be taken into consideration when silver(I)–aromatic interactions are used during polymer construction.

### 1.2.3 Metal – metal interactions

Argentophilicity is the tendency of silver(I) ions to aggregate at distances below the van der Waals diameter of 3.44 Å. As a  $d^{10}$  metal cation, Ag ions can form ligand-supported or ligand-unsupported  $\text{Ag}\cdots\text{Ag}$  interactions.<sup>[24]</sup> Although  $\text{Ag}\cdots\text{Ag}$  interactions are comparatively weak, they play an important role in the assembly of functional silver(I) coordination polymers, and the existence of  $d^{10}$ - $d^{10}$  interactions between two closed shells of silver(I) atoms can not only contribute to the structural diversities of the final structures by increasing the structural dimensionalities, but also endow the silver(I) coordination polymers with various properties [e.g. semiconductivity, luminescence]. Since the publication of two early papers on  $\text{Ag}\cdots\text{Ag}$  interactions by Robinson and Zaworotko in 1995<sup>[25]</sup> and by Yaghi and Li in 1996,<sup>[26]</sup> argentophilic interactions in either a ligand-supported<sup>[27]</sup> or ligand unsupported<sup>[28]</sup> way have received wide attention. Raman spectra and semiconductivity have been used to provide evidence of the existence of  $\text{Ag}\cdots\text{Ag}$  interactions.

### 1.2.4 Anion bridging

Many coordination networks and polymers are based on silver(I) ions. Usually, these extended structures are prepared by mixing the metal salt with the mono or multipodal ligand in the appropriate stoichiometry. Since there are several potential ways in which the components can assemble together due to flexible coordination geometry around these metal centers, the choice of the final assembly is also strongly influenced by the experimental conditions and the nature of the metal's counteranions.<sup>[29]</sup> The energy of anion coordination in supramolecular structures can vary

over a wide range and its influence is difficult to predict. Even a weak bridging interaction can distort a polymeric structure significantly when compared with an analogous structure formed in the presence of a non-coordinated anion. Champness<sup>[30]</sup> and others<sup>[31]</sup> have carried out a detailed investigations on the impact of anions in the formation of metal organic networks with silver(I) ions.

## 1.3 Pyridine N-oxides

### 1.3.1 Introduction

The introduction of substituents into a pyridine ring has long been a difficult problem. The principal reason is that pyridine, because of the polar effect of the nitrogen atom, is very resistant to electrophilic substitution. Pyridine N-oxide was first made by Meisenheimer<sup>[32]</sup> in 1926, and become commercially available<sup>[33]</sup> in 1954. Thus the synthesis of N-oxides was a boon to pyridine chemistry, as it proved to be an important intermediate for pyridine chemists to synthesize a number of substituted pyridines with good yields under less harsh conditions. Pyridine N-oxide chemistry has been much reviewed by Katritzky,<sup>[34]</sup> Shaw,<sup>[35]</sup> Abramovitch and Saha,<sup>[36]</sup> and Ochiai.<sup>[37]</sup>

### 1.3.2 Structure and reactivity

It is of interest, both from the electronic structure as well as the chemical reactivity, to compare the dipole moment of the N-oxides with their corresponding bases [i.e., deoxygenated species]. In fact, the observation made by Linton<sup>[38]</sup> that the difference in dipole moment between pyridine [2.22D] and pyridine N-oxide [4.24D] is considerably smaller than that between trimethylamine [0.65D] and trimethylamine N-oxide [5.02D], which led Ochiai to conclude that the pyridine ring is activated on N-oxidation. This conclusion was substantiated by the facile nitration of pyridine N-oxide, as against the resistance towards pyridine of the same reaction, to yield 4-nitropyridine N-oxide in good yields with small amounts of 2-nitropyridine N-oxide. This was equally confirmed and supported by using quinoline N-oxide.<sup>[39]</sup>

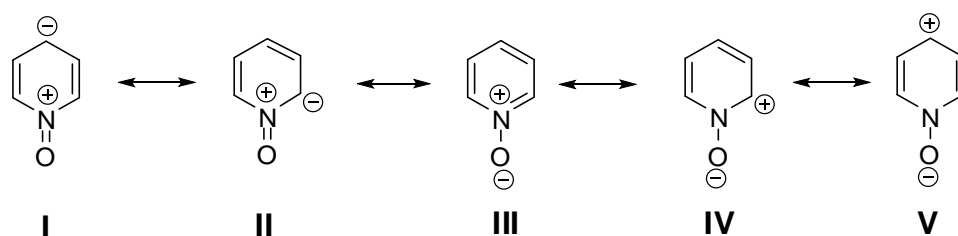


Figure 1.5 – Possible resonance structures of pyridine N-oxide.

In pyridine, the nitrogen lone pair of electrons is in a  $sp^2$  orbital. Thus, in the pyridine N-oxides the N-O bond is in the same plane as the aromatic ring and the oxygen  $2p\pi$  electrons interact directly with the  $\pi$ -system of the ring. The contribution of resonance structures I to V [figure 1.5] depends on the nature of the substituents at the 4-position.<sup>[40]</sup> The dipole moments of 4-substituted pyridine N-oxides show that the pyridine N-oxide ring can either have a deficiency or an excess of electrons at the 4-position depending upon the substituents. When the substituents are electron donating the mesomeric moment shifts are positive, and if it is electron withdrawing the mesomeric shifts to negative values; thereby permitting both the nucleophilic and electrophilic attack by  $\sigma$ -electron withdrawing and  $\pi$ -back bond donating character of the N-oxide moiety.

### 1.3.3 Methods of preparation

Heterocyclic N-oxides can be prepared either by catalytic<sup>[41]</sup> or non-catalytic oxidation<sup>[32, 42]</sup> systems. Among the oxidants, the hydroperoxides have a prominent position. Among them, hydrogen peroxide [ $H_2O_2$ ] and *t*-butyl hydroperoxide [TBHP] are commonly used as laboratory oxidants. Both of them are relatively stable, easy to store, commercially available, relatively cheap reagents of low molecular weight which can be used for laboratory and industrial purposes. They contain relatively high amounts of active oxygen [ $H_2O_2$  – 47% and TBHP – 17.8% by weight], and are environmentally friendly since water and *t*-butanol are easy to recover from the reaction mixture [products of their reduction]. Hydrogen peroxide is supplied mainly as a 30% aqueous solution [also commercial grades are available from 50% to 100%] and TBHP as a 70% aqueous solution or 5.0 – 6.0 M solution in decane or nonane.

### 1.3.4 Coordination compounds of metals with pyridine N-oxides

In the field of supramolecular coordination chemistry, pyridine N-oxides are of interest for investigating the denticity of oxygen of the N-oxide. Since the oxygen of the N-oxide is in conjugation with the aromatic pyridine ring system, the nature of substituents in the pyridine ring influences the basicity of the N-oxide and their coordination behaviour with metals. The dependence of pKa values of pyridine N-oxides based on the nature of the substituents has been described in detail using Hammett constants. The stability of the complexes of pyridine N-oxides decrease as the electron attracting power of the ring substituent increases. The basicity and bonding in aromatic N-oxides with metals can be systematically varied by appropriate substitution<sup>[43]</sup> on the aromatic ring with a concomitant minimal charge in steric interaction at the reaction site. The desired directionality of polymers can be constructed by suitable ligand design and metal choice.

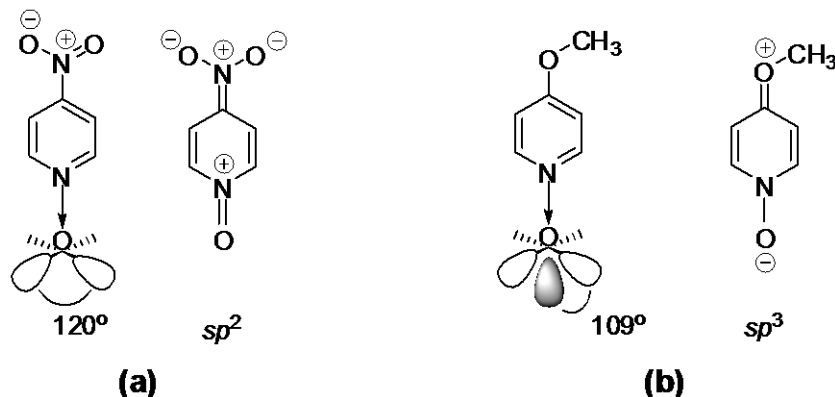


Figure 1.6 – The interaction of O-atom of N-oxide with metals upon change in the O-atom hybridization in compound with (a) an electron-acceptor and (b) an electron donor functional groups.

The oxygen in an N-oxide is available in  $sp^2$  and  $sp^3$  hybridization states and interacts with metals based on the substituents in the pyridine ring. For example, 4-nitropyridine N-oxide [–M effect] in the crystalline state is found in the quinonoid<sup>[44]</sup> form, whereas in 4-methoxypyridine N-oxide [+M effect], the oxygen retains three pairs of electrons available for coordination, as shown in figure 1.6.

The coordination sites of these ligand systems are accessible for metals sometimes if one or both the  $\alpha$ -positions are occupied by bulkier substituents. With these ligands, usually the complexes have octahedral geometry with some distortion, however, complexes with metal coordination numbers from 2 to 9 are also known.

### 1.3.5 Coordination chemistry of pyridine and substituted pyridine N-oxides

Monodentate pyridine N-oxides have the ability to form complexes yielding maximum coordination numbers for most metal ions.<sup>[45]</sup> The most common coordination numbers for metals obtained with pyridine N-oxide is in complexes of the type  $[ML_6]^{n+}$  [where  $M = Mn^{+2}, Fe^{+2}, Co^{+2}, Cu^{+2}, Zn^{+2}$  and  $n = 2$  or  $3$ ],<sup>[46]</sup> which have been reported in great number. The N-oxides, such as pyridine N-oxide, quinoline N-oxide and isoquinoline N-oxide, do not introduce severe steric hindrance during the formation of cationic metal complexes and are formed during the interactions of these ligands with most  $3d$  metal perchlorates, tetrafluoroborates and, in certain cases in the presence of excess ligand. Interestingly, the presence of 3- and 4- substituents<sup>[46a]</sup> in the pyridine N-oxide ring and 4- and 6- substituents in that of quinoline N-oxide ring also does not introduce steric interference in the complexes of the type  $[ML_6]^{n+}$ .

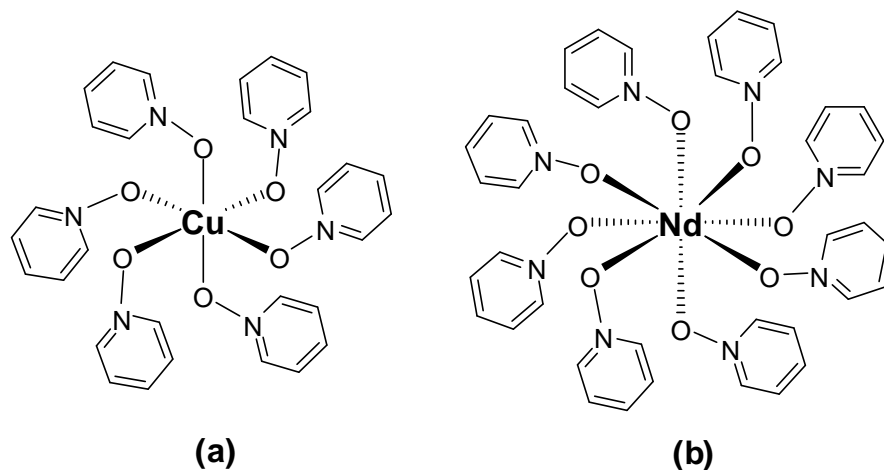


Figure 1.7 – Pyridine N-oxide complexes with metals (a)  $\text{Cu}^{+2}$  and (b)  $\text{Nd}^{+3}$  of the type  $[\text{ML}_6]^{n+}$  and  $[\text{ML}_8]^{n+}$ .<sup>[47]</sup>

Substituents with certain functional groups on pyridine N-oxides, as shown in figure 1.8, can also serve as donor sites leading to the formation of chelate complexes. For example, 2-substituted pyridine N-oxides are capable of bidentate coordination with metals, similar to 2,2'-bipyridine N,N'-dioxide.

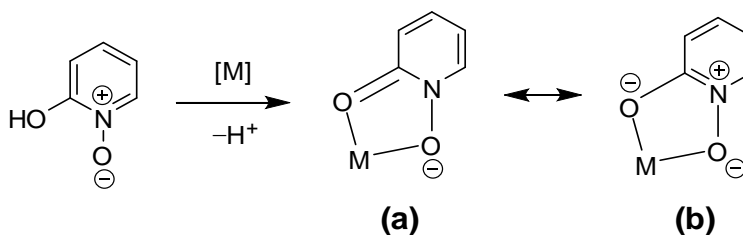


Figure 1.8 – Coordination modes of 2-substituted pyridine N-oxides.

Based on a CSD search, 2-mercaptopyridine N-oxide<sup>[48]</sup> and 2-hydroxypyridine N-oxide<sup>[49]</sup> are the most studied ligands in the 2-substituted pyridine N-oxide family after pyridine carboxylic acid N-oxides. Each ligand chelates to the metal with two, three and four ligands per metal with the general formula  $\text{ML}_2$ ,  $\text{ML}_3$  and  $\text{ML}_4$ , as shown in figure 1.9. These two ligands have been extensively investigated as new sequestering agents for actinide(IV) ions and selective metal extractions based on the similarities in the chelating groups of microbial Fe(III) sequestering agents, siderophores by Raymond and his group.<sup>[50]</sup>

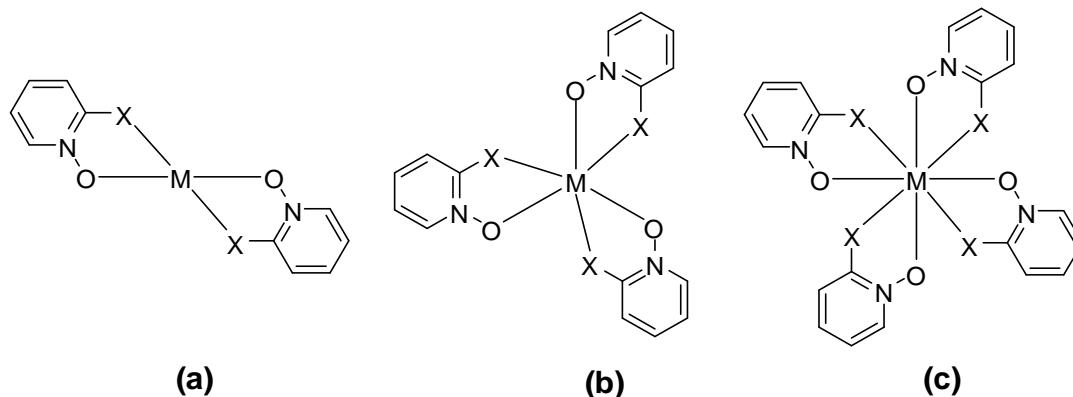


Figure 1.9 – Possible arrangement of 2-substituted pyridine N-oxides around the metal center.

Due to tautomeric reasons, except for 2-aminopyridine N-oxide,<sup>[51]</sup> other 2-aminosubstituted pyridine N-oxides were found to form complexes of the type shown in figure 1.10. However, the  $\text{-NH}_2$  group appears to be non-coordinating with metals, forming complexes of the type  $[\text{ML}_6]^{n+}$  through the oxygen of the N-oxide, as shown in figure 1.7a. The deprotonated 2-aminoalkyl pyridine N-oxides form complexes of the type  $[\text{ML}_2]$  which have square planar geometry and O,N-chelation in a *trans* arrangement, as shown in figure 1.10.

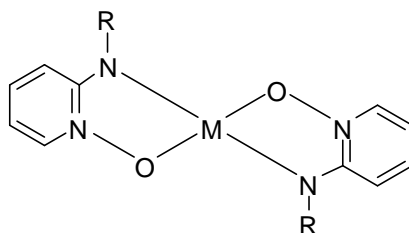


Figure 1.10 – *Trans* arrangement of 2-alkylamino pyridine N-oxides in square planar geometry with O,N-chelation.

Since 1961, considerable interest has been shown in metal complexes of the mono-carboxylic acid pyridine N-oxides. Several complexes have been synthesized and reported by Knuuttila<sup>[52]</sup> and other groups<sup>[53]</sup>. According to Knuuttila, the positions of the substituents of the pyridine mono-carboxylic acid N-oxide appear to play a significant role in the coordination chemistry with specific metals. For example, in picolinic acid N-oxide, the N-oxide is *ortho* to the  $\text{-COOH}$  functional group, thus resulting in a stable six-membered ring generated through the N-oxide and carboxylate groups, as shown in figure 1.11a.

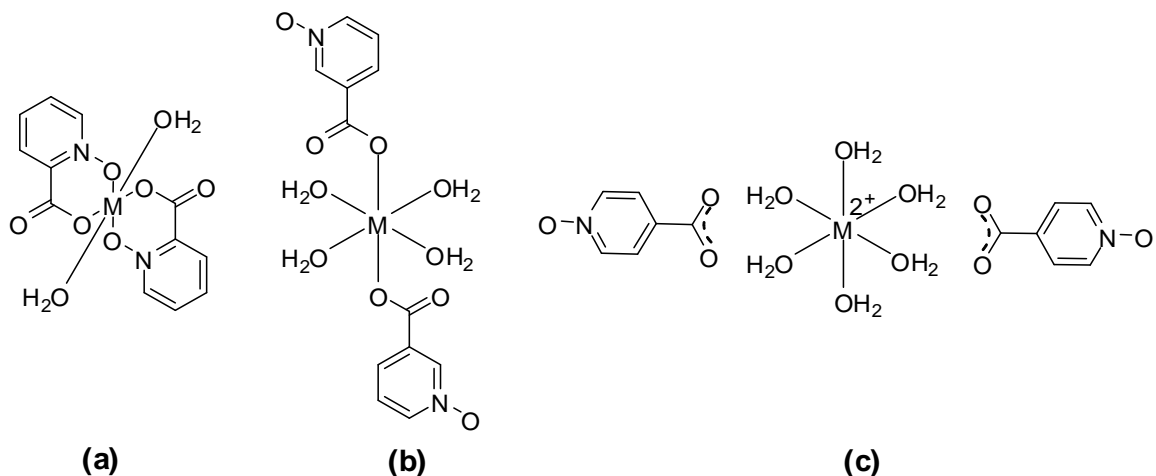


Figure 1.11 – Possible coordination modes of 2-, 3- and 4-pyridine carboxylic acid N-oxide.

In nicotinic acid N-oxide, the N-oxide group is *meta* to the  $-\text{COOH}$  group and does not coordinate to the metal. Coordination occurs only through one carboxylato atom, as shown in figure 1.11b. In isonicotinic acid N-oxide, where the N-oxide and  $-\text{COOH}$  groups are *para*, neither group is coordinated to the metals Co(II), Ni(II), Fe(II), Mg(II) or Zn(II), and the compounds formed are ionic with hexaaquametal(II) cations and isonicotinate N-oxide anions, as shown in figure 1.11c. Thus, in this case, the coordination ability of the N-oxide group of pyridine mono-carboxylic acid N-oxides clearly decreases in the order picolinic N-oxide > nicotinic acid N-oxide > isonicotinic acid N-oxide in aqueous solution.

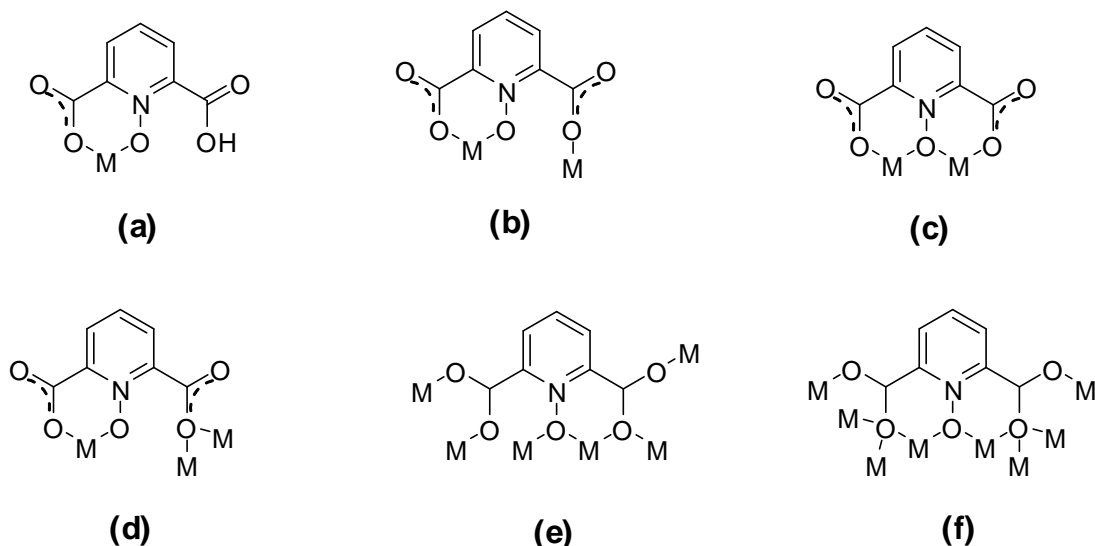


Figure 1.12 – Coordination modes of pyridine 2,6-dicarboxylic acid N-oxide.

Pyridine 2,6-dicarboxylic acid N-oxide is a typical example of a semi-rigid dicarboxylate ligand, which has limited steric hindrance, weak stacking interactions and can offer possibilities to form



complicated coordination polymers through its versatile coordination modes, as shown in figure 1.12.<sup>[54]</sup>

### 1.3.6 Coordination chemistry of N,N'-dioxides

When two ligands approach a metal ion they repel each other, with an unfavourable enthalpy change upon complex formation, but in the case of a chelating ligand this repulsion has been already been built into the ligand. 2,2'-Bipyridine N,N'-dioxides act as chelating ligands with some distortion of the ideal bond angles upon complex formation [figure 1.13]. This can be unfavorable as compared with monodentate complex formation if the distance of the donor atoms are not ideally suited to the metal.

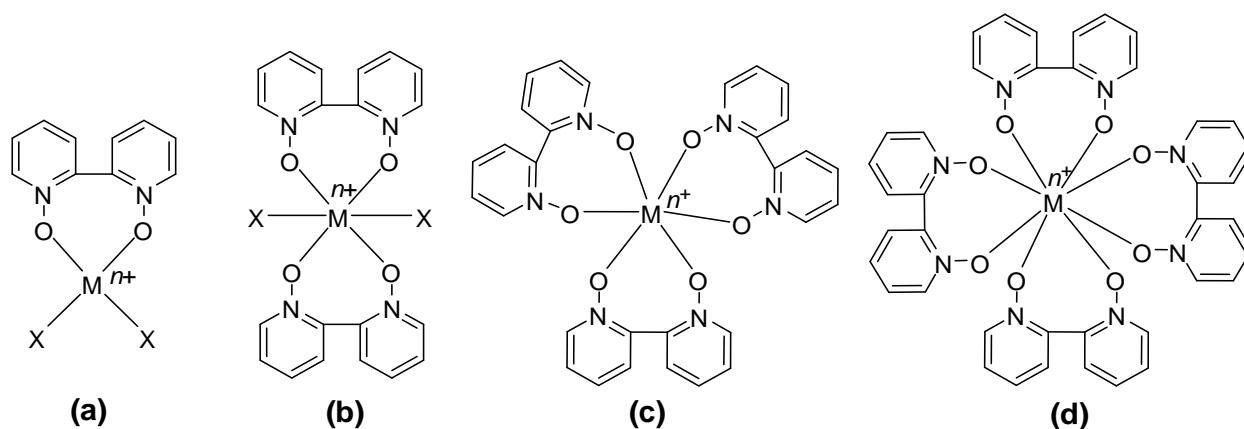


Figure 1.13 – General representation of 2,2'-bipyridine-N,N'-dioxide metal complexes of the type  $[ML]^{n+}$  (a),  $[ML_2]^{n+}$  (b),  $[ML_3]^{n+}$  (c) and  $[ML_4]^{n+}$  (d).

The skewed seven-membered chelate ring produces a pair of optical isomers  $\delta$  and  $\lambda$ , as shown in figure 1.14, that can change its conformation [ $\delta \leftrightarrow \lambda$ ] easily. The stereochemical conclusions were mainly obtained by NMR, absorption and circular dichroism [CD] spectral studies, but no crystal structures were reported.<sup>[55]</sup> A large number of metal complexes with skew conformations, including the resolution of diastereoisomers in mixed-ligand systems have been published by Kanno and Fujita<sup>[56]</sup>, and by other groups. The rate of racemization can be reduced with an increase in the electron donating ability of the 4,4'-substituents.

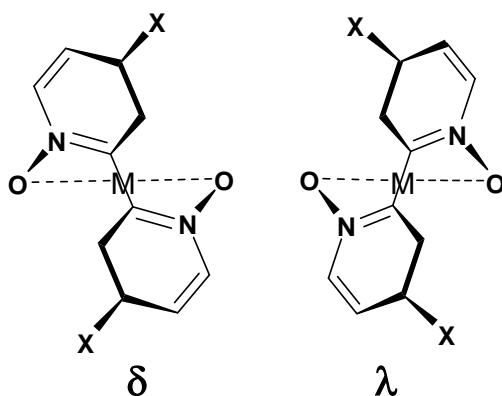


Figure 1.14 – Chiral skew conformations of 4,4'-disubstituted-2,2'-bipyridine N,N'-dioxides.

Valigura *et al.*<sup>[57]</sup> reported two isomeric complexes of composition  $\text{Cu}(\text{bipyo})\text{Cl}_2$ , green and yellow-orange crystals obtained by changing the reaction [temperature] conditions, as shown in figure 1.15. The author described this as “bridge-bond isomerism”, as the color and magnetic properties of these isomers differ by the bonding mode of the oxygen of the N-oxide and the chlorine of the copper(II) salt.

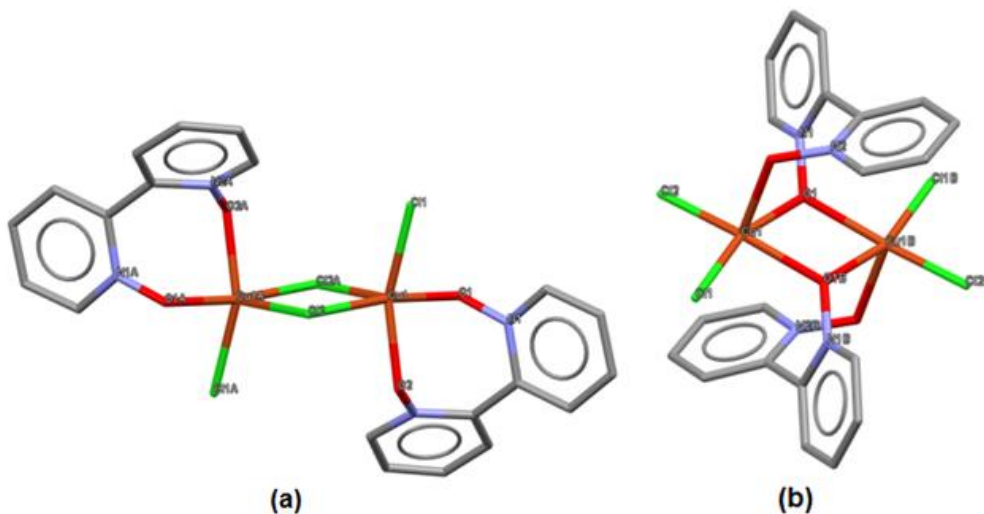


Figure 1.15 – Molecular structures of green (a) and yellow-orange (b) isomers of  $\text{Cu}(\text{bipyo})\text{Cl}_2$  complexes.<sup>[57]</sup>

Exo-bidentate ligands such as pyrazine or 4,4'-bipyridine N,N'-dioxides<sup>[58]</sup> have been widely used and exploited as building blocks in multidimensional polymers. They are linear spacer molecules, but the coordination behavior of the metal and metal to ligand ratio is crucial. The O-donor ligand, 4,4'-bipyridine N,N'-dioxide has been used widely for the construction of multidimensional arrays, especially with lanthanides.<sup>[59]</sup>

3-Dimensional networks can be obtained based on the high coordination numbers [ $\geq 7$ ] of the metals employed. With first row transition metals, 1D coordination polymers have been reported.

Only a few examples exist of homoleptic higher dimensional polymers. The relatively low steric demand of the pyridyl N-oxide donor group, combined with the orientation of the lone pairs on the pyridyl N-oxide oxygen atom, results in relatively high flexibility regarding its coordination behavior. Champness *et al.*<sup>[59]</sup> showed the possible binding modes of 4,4'-bipyridine N,N'-dioxides by complexing them with lanthanide metal ions, as shown in figure 1.16.

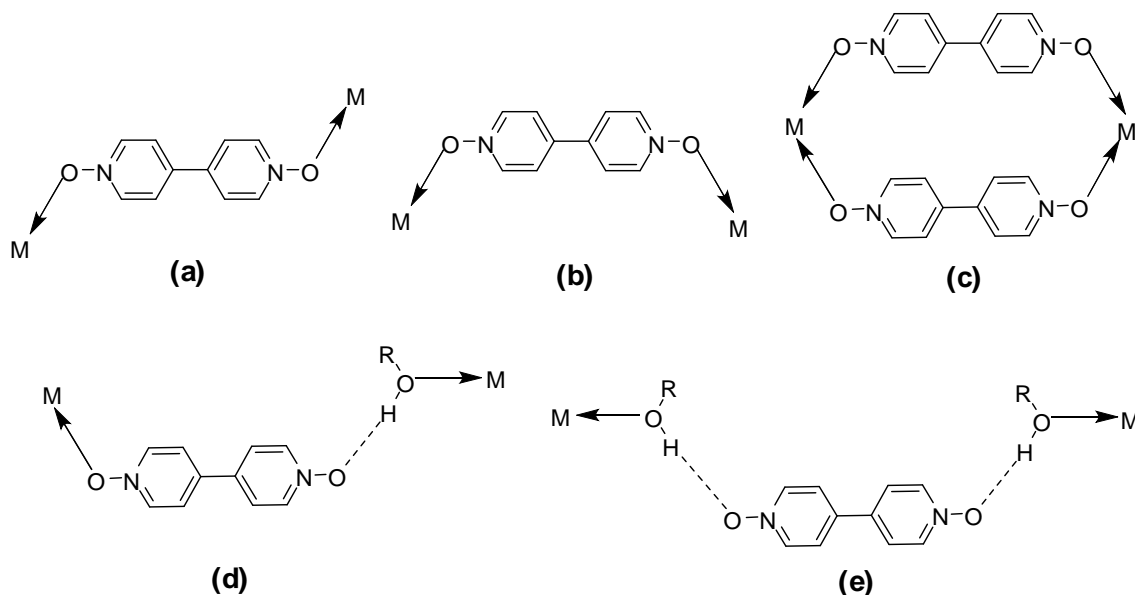


Figure 1.16 – (a) *Anti*<sup>[60]</sup> and, (b) *syn*<sup>[45b, 61]</sup> and (c) double bridge formation<sup>[45a]</sup> of 4,4'-bipyridine N,N'-dioxide coordination modes with metal centers. Potential hydrogen bonding interactions<sup>[62]</sup> involving coordinated solvent molecules (d) [water (R = H) or (e) methanol (R = CH<sub>3</sub>)].

Besides being a strongly coordinating ligand, 4,4'-bipyridine N,N'-dioxide is a good H-bond acceptor [figure 1.16d and 1.16e], which can be used to construct multidimensional H-bonded polymers<sup>[58b, 63]</sup>. The neighboring C-H function in the aromatic ring can lead to the formation of H-bonds between the coordinated 4,4'-bipyridine N,N'-dioxide molecules, resulting in the stabilization of metal coordination polyhedron, as shown in figure 1.17.

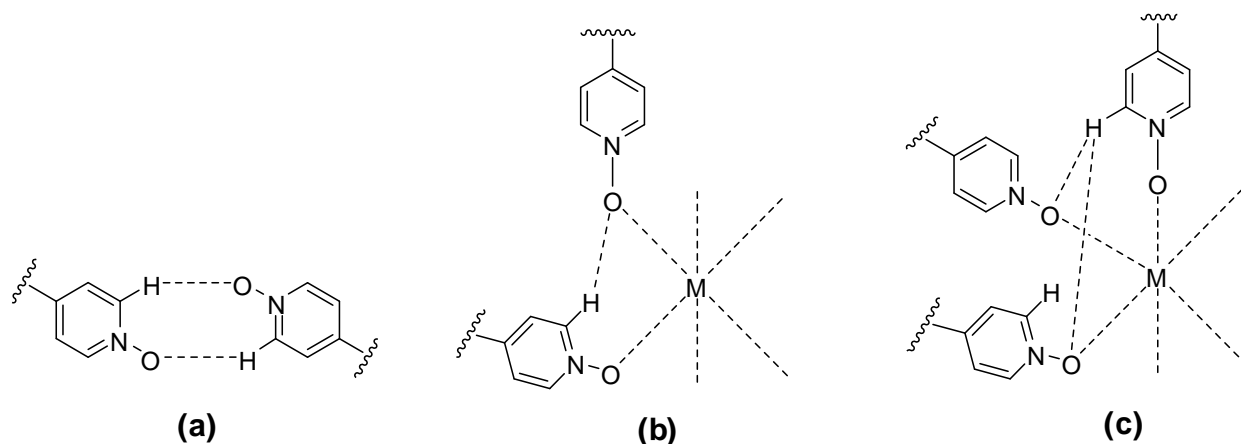


Figure 1.17 – (a) H-Bonding in 4,4'-bipyridine N,N'-dioxide and (b & c) its metal complexes.

Mak *et al.*<sup>[14, 64]</sup> proposed and reported the conformations of 1,2-bis(4-pyridyl)ethane N,N'-dioxide in porous coordination networks generated from lanthanide metal salts using 1,2-bis(4-pyridyl)ethane N,N'-dioxide [**L1**] and isonicotinic acid [**L2**] as mixed ligand donors.

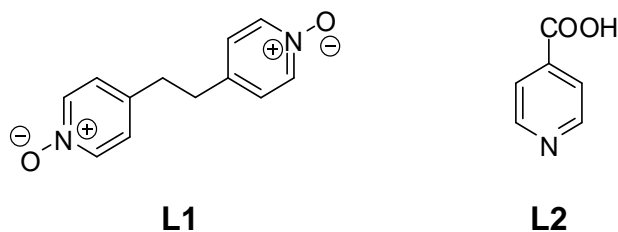


Figure 1.18 – 1,2-Bis(4-pyridyl)ethane N,N'-dioxide [**L1**] and isonicotinic acid [**L2**] as mixed ligand donors. By altering the molar ratio of **La:L1:L2** from 1:1:1.5 to 1:2:1, the coordination modes of **L1** changed between the modes shown in figure 1.19.

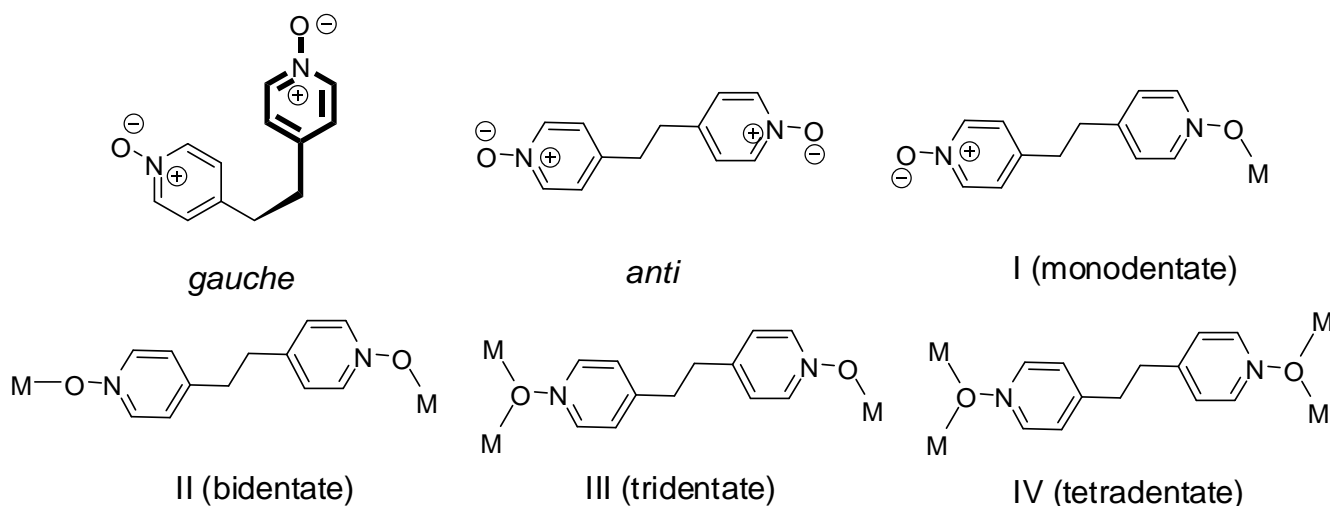


Figure 1.19 – Coordination modes of 1,2-bis(4-pyridyl)ethane N,N'-dioxide [**L1**].

### 1.3.7 Coordination chemistry of higher pyridine N-oxides

Metal complexes of higher pyridine N-oxides have been less studied, the only known higher pyridine N-oxides are shown in figure 1.20. A few reports have been published on the metal complexes of 2,2':2,6''-terpyridine N,N',N''-trioxide including crystal structures, and two metal complexes<sup>[65]</sup> with 4,4-diphenyl-2,2':6',2'':6'',2''':6''',2''''-quaterpyridine N,N',N'',N'''-tetraoxide. The coordination chemistry of both ligands shown in figure 1.20 has been studied, including their stereochemistry, by Amoroso<sup>[66]</sup> and a few other groups.<sup>[67]</sup>

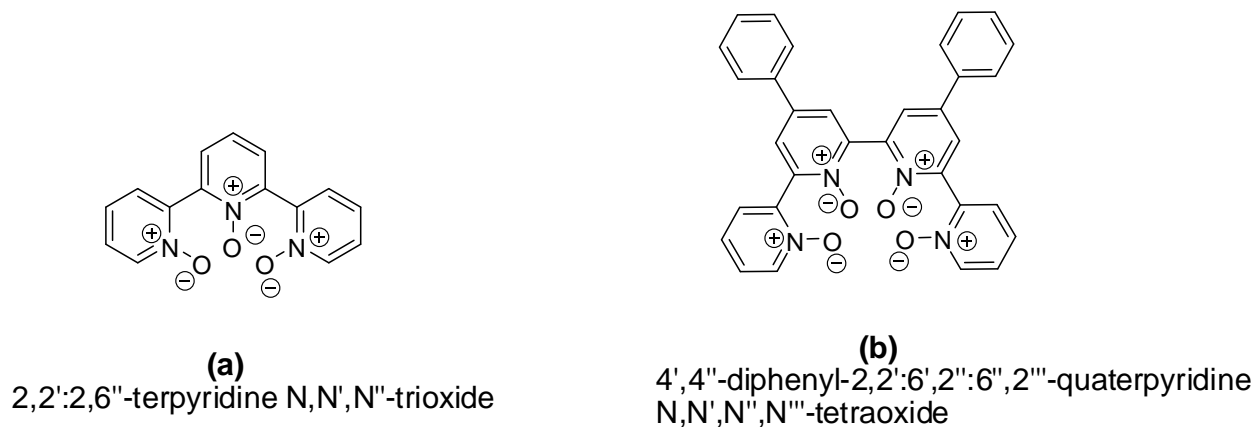


Figure 1.20 – Reported higher pyridine N-oxides.

A notable point of interest in terpyridine N,N',N''-trioxide transition metal complexes is that the seven-membered chelate rings produce an unstrained structure that contains the ligand in a facial coordination mode, rather than the meridional arrangement typical for the parent pyridyl ligand.<sup>[68]</sup> Two possible facial arrangements of these ligands exist, although only one is generally observed in the crystal structures, as shown in figure 1.21.

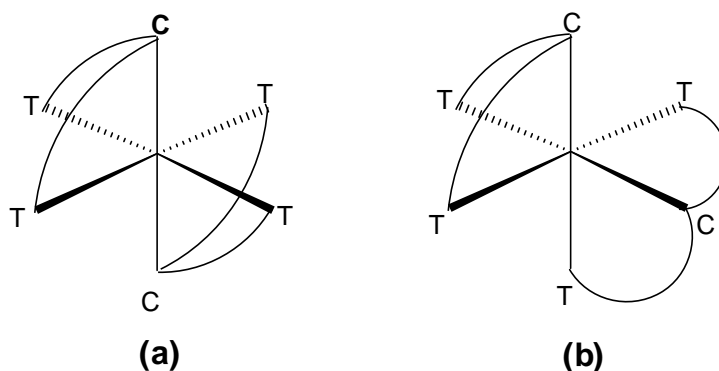


Figure 1.21 – Possible facial arrangements of terpyridine N,N',N''-trioxide about an octahedral center.

#### 1.4 Aims of the thesis

Since the availability of electrons on the oxygen of pyridine N-oxide can be altered by changing the substituents on the pyridine ring, the present study was directed towards examining the different coordination modes of N-oxides with the  $d^{10}$  silver(I) metal, as shown in figure 1.22.

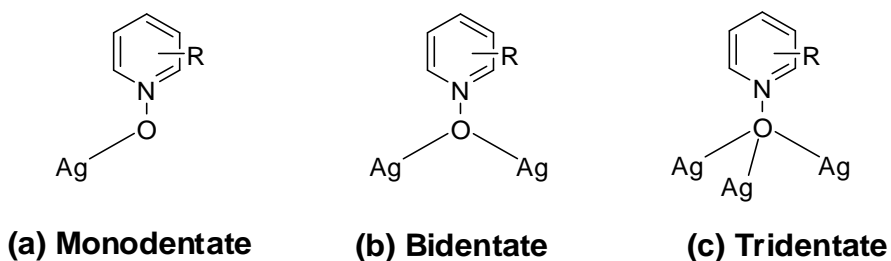


Figure 1.22 – N-Oxide of pyridine showing the coordination of the oxygen atom to one, two and three different silvers.

Research in the Steel group has been extensively directed towards the study of bridging heterocyclic ligands that are unidirectional and are able to coordinate to metals in a monodentate fashion. However, from our very first X-ray crystal structure, we found that the oxygen of pyridine N-oxide can coordinate up to three independent silver(I) metal ions, as shown in figure 1.23.

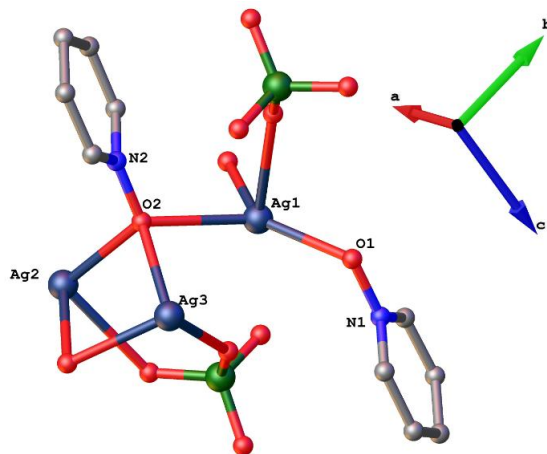


Figure 1.23 – The oxygen of pyridine N-oxide showing coordination to three different silver ions. [The detailed coordination chemistry of this N-oxide will be discussed in the next chapter].

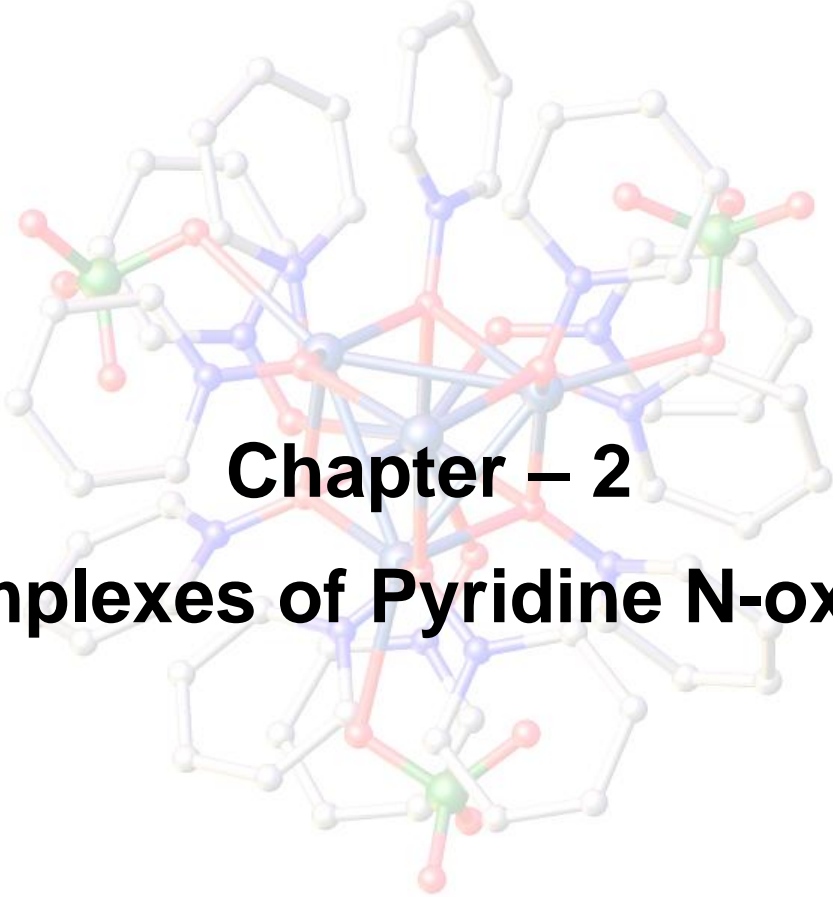
The emphasis of the current study is on the coordination pattern of silver(I) salts, with different pyridine N-oxides. The ligands were designed and synthesized to complex with silver(I) salts to study:

- 1) The electronic and substituent effect of the oxygen of the pyridine N-oxide when coordinated with a silver(I) ion.
- 2) The effect of flexible and rigid spacers within the N,N'-dioxides.
- 3) The effect of counterions, solvent, temperature and the stoichiometric ratio of ligand to silver(I) salt.

To the best of our knowledge, using Scifinder and a CCSD search, surprisingly few silver(I) complex crystal structures have been reported to date, as shown in table 1.

Table – 1 Reported literature on silver(I)-pyridine N-oxide complexes to date.

Entry	Pyridine N-oxide	Characterization	Reference
1	2-, 3- and 4-cyanopyridine N-oxide	EA , IR	[69]
2	2,2'-bipyridine N,N'-dioxide	EA, IR	[70]
3	2-Methyl-, 3-methyl-, 4-methyl-, 2- <i>n</i> -propyl-, 2-isopentyl- and 2,6- dimethylpyridine N-oxides	EA, IR	[71]
4	Pyrazine N-oxide 3-Methyl-, 2,5-dimethyl-, 3,5- dimethylpyrazine N-oxide 2,6-Dimethylpyrazine N,N'-dioxide 2-Chloro-3-methylpyrazine 1-, and 4- oxide	EA, IR	[72]
5	2-Mercaptopyridine N-oxide	EA, IR and X-ray	[73]
6	4-Nitropyridine N-oxide	X-ray	[74]
7	Pyridine 4-carboxylic acid N-oxide	EA, IR and X-ray	[75]
8	Pyridine 2,6-dicarboxylic acid N-oxide	EA and IR	[54]
9	1,3-Bis(4-pyridyl)propane N,N'-dioxide	EA, IR and X-ray	[14]



**Chapter – 2**  
**Complexes of Pyridine N-oxides**



## 2.1 Introduction

The importance of different pyridine N-oxides, their possible coordination modes and the effect of substituent groups on supramolecular networks has been previously outlined in Chapter 1. The molecular complexes described in the literature consider several potential donor sites for the aromatic N-oxides, such as the  $\pi$ -system of the heterocyclic group, the oxygen atom of the N-oxide group, or ring substituents, which interact with different acceptors. In order to study the electronic and substituent effect of the N-oxides in silver(I) complexes, a series of substituted pyridine N-oxide ligands were synthesised, as shown in figure 2.1. Since the N-oxide can back donate electrons to the pyridine ring system based on the substituents, we chose mono pyridine N-oxides in which the substituents can affect the geometry of the complexes depending on the size and basic strength of the N-oxides.

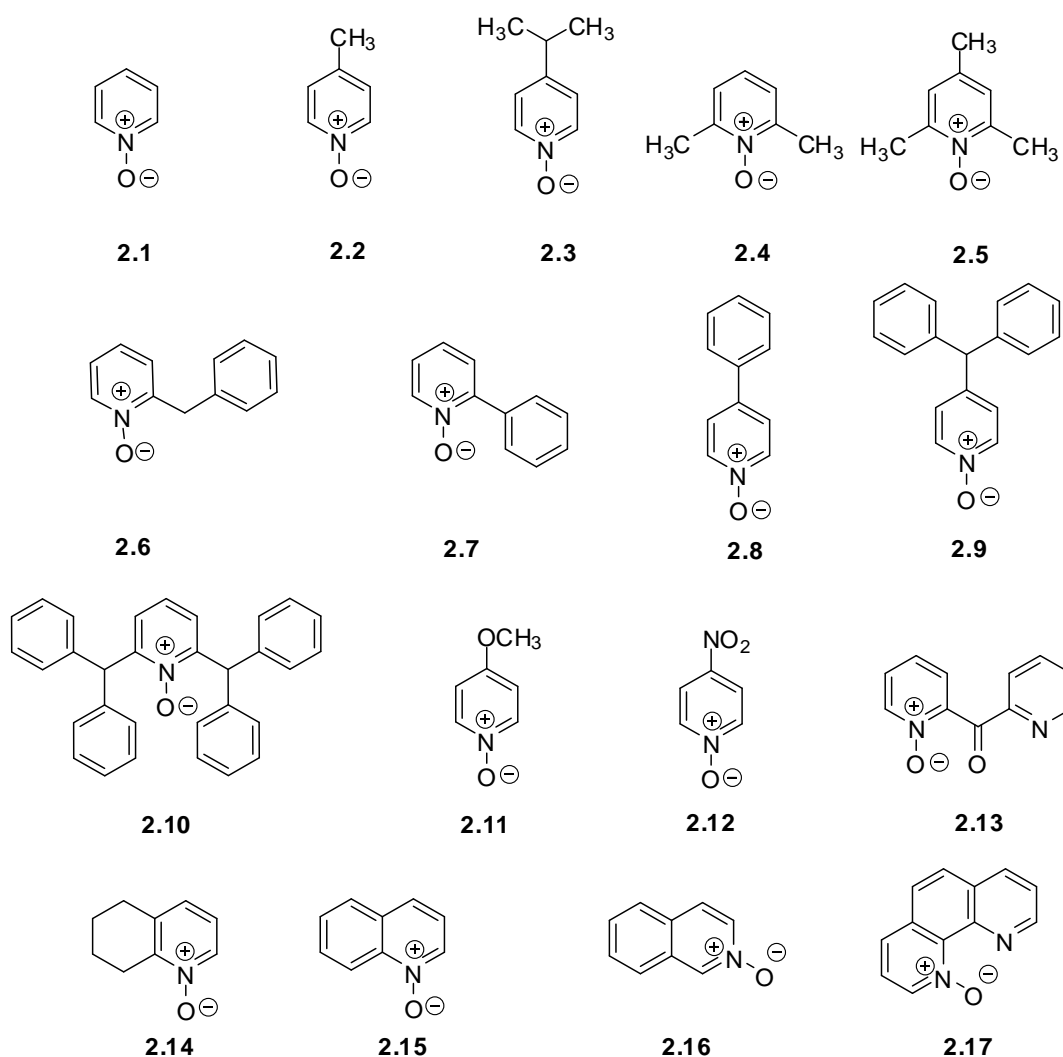
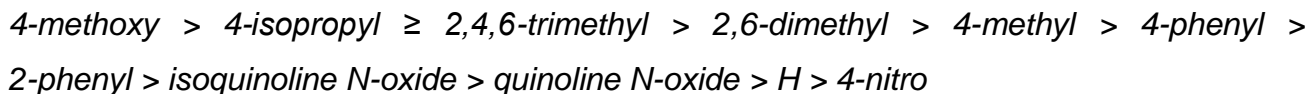


Figure 2.1 – List of mono-N-oxides.

As the basic strength of the N-oxide increases, the coordination ability of the ligand increases; thus increasing the stability constant of the complexes. Based on the pKa values reported by Katritzky<sup>[76]</sup> and others,<sup>[77]</sup> the order of the base strength of the N-oxides shown in figure 2.1 can be arranged as follows:

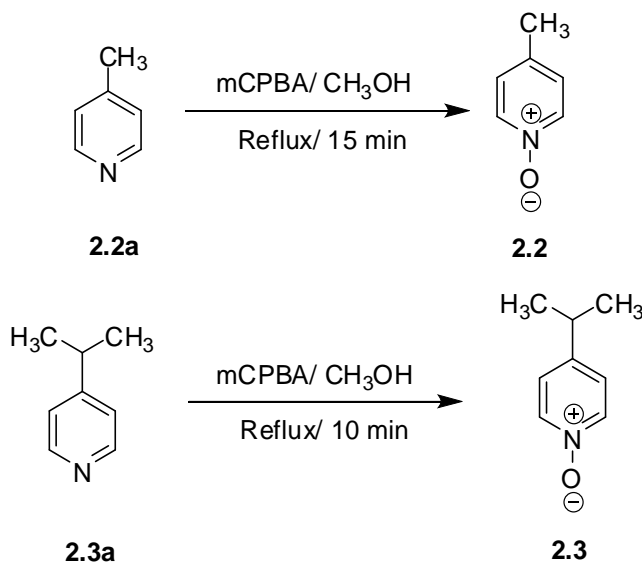


Introduction of alkyl groups [+I effect] increases the basicity of the N-oxides, with the 4-substituted being more basic than 2-substituted N-oxides, due to the lower stability of the *ortho*-quinonoid structure in comparison to the *para*-quinonoid structure. The phenyl substituted pyridine N-oxides are less basic than methyl substituted ones.

## 2.2 Syntheses of ligands

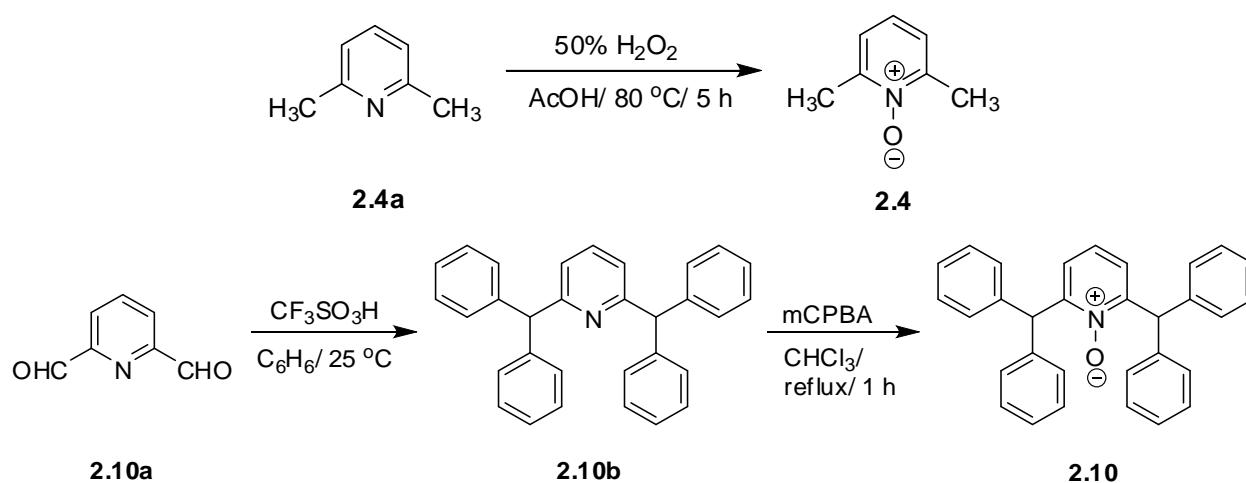
The syntheses of all the ligands shown in figure 2.1 utilize known procedures, except for ligands 2.1, 2.8, 2.11 and 2.12, which are commercially available.

Ligands 2.2 and 2.3 are known compounds and were prepared according to literature methods using 3-chloroperbenzoic acid [mCPBA] in reasonable yields. MCPBA was found to be a very effective oxidizing agent for the synthesis of various pyridine N-oxides. Unfortunately, trace amounts of the oxidant were found to crystallise with the silver(I) salts, therefore the acid was used to synthesise only a few pyridine N-oxides in the early stages of the project.



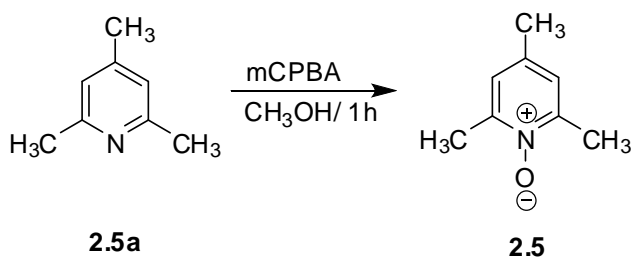
Scheme 2.1 – Synthesis of ligands 2.2 and 2.3.

After synthesising ligands with substituents at the position '4' of the pyridine ring, the focus turned to generating ligands which are more sterically crowded on either side of the N-oxide group; i.e. at positions '2' and '6' of the heterocyclic ring. Thus, ligands **2.4** and **2.10** were synthesised. These two ligands were chosen to illustrate the steric hindrance of both methyl and aromatic substituents on a central heterocyclic ring. Ligand **2.4** was obtained in one step by oxidising 2,6-lutidine **2.4a** with 50% hydrogen peroxide in acetic acid, whereas **2.10** was made in a two-step process, as shown in scheme 2.2. The synthesis of ligand **2.10** involves the condensation reaction of 2,6-pyridinedicarboxaldehyde **2.10a** with benzene in the presence of the Bronsted superacid  $\text{CF}_3\text{SO}_3\text{H}$  to give precursor **2.10b**<sup>[78]</sup> in 61% yield. The precursor **2.10b** was then oxidised with mCPBA in chloroform to give ligand **2.10**, which is a new compound.



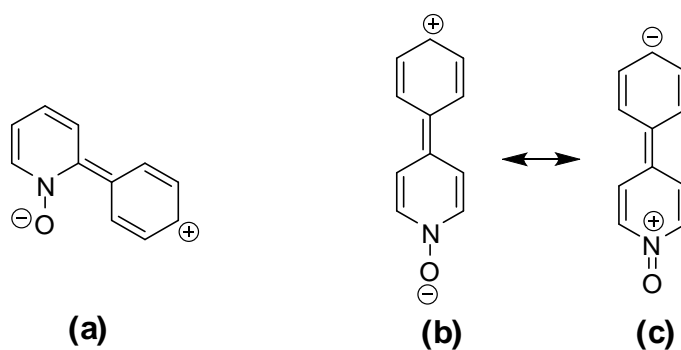
Scheme 2.2 – Synthetic methods for the preparation of ligands **2.4** and **2.10**.

Ligand **2.5**<sup>[79]</sup> is a known compound and was synthesised by oxidising 2,4,6-collidine [**2.5a**] with mCPBA. Ligand **2.5** is capable of showing both a +I effect and also has steric hindrance due to extra alkyl groups around the ring, as shown in scheme 2.3. It is evident from some experimental studies carried out by Andreev and co-workers,<sup>[43]</sup> that the introduction of alkyl groups at positions 2 and 6 increases the stability of the complexes, due to the +I effect. However, at the same time, due to the associated steric hindrance of these extra alkyl groups complex decomposition accelerates much faster than for other alkyl substituted pyridine N-oxides. Important applications of sterically hindered 2,6-di-<sup>[80]</sup> and 2,4,6-tri-substituted<sup>[81]</sup> pyridine N-oxide derivatives are as oxidants or potent ligands in the epoxidation of olefins in the presence of catalytic amounts of ruthenium(IV) porphyrin with high efficiency and selectivity under mild conditions.



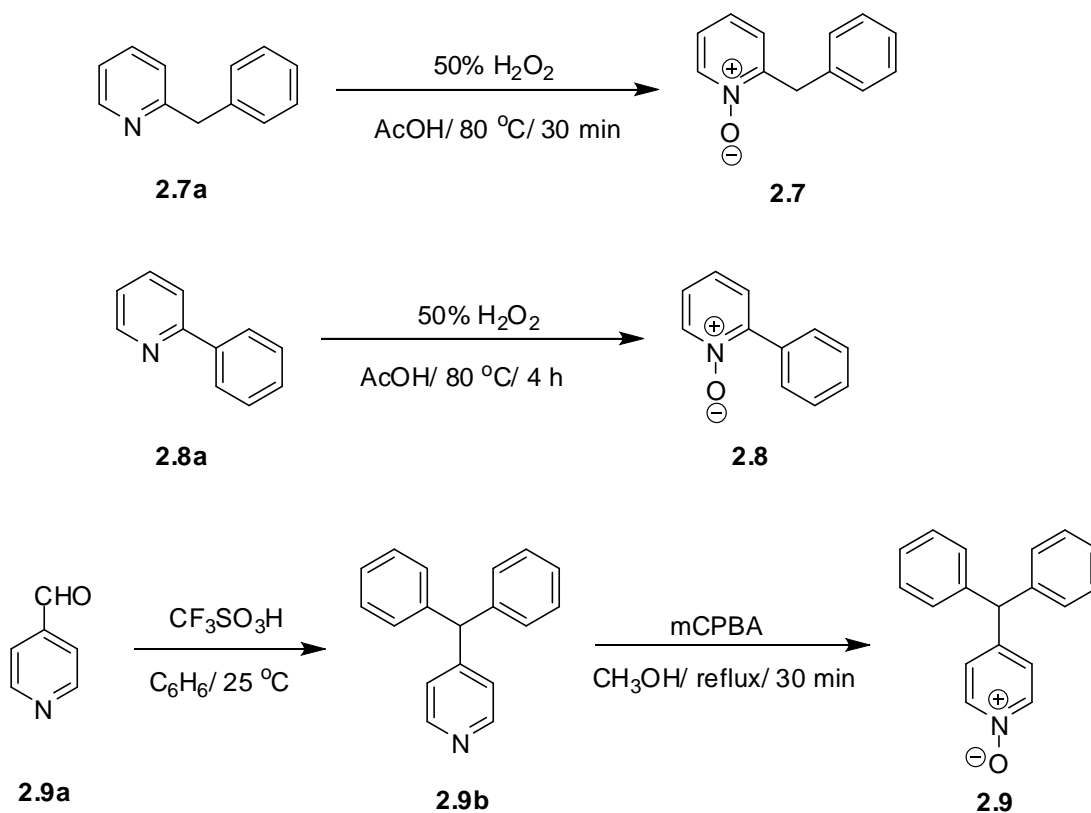
Scheme 2.3 – Synthetic scheme for the preparation of ligand **2.5**.

In order to study the effect of phenyl rings on pyridine N-oxides, four phenyl substituted pyridine N-oxides ligands **2.6**, **2.7**, **2.8** and **2.9** were synthesised. In ligands **2.7** and **2.8** the phenyl rings are in resonance with the pyridine ring system, which stabilise their *ortho*- and *para*-quinonoid structures,<sup>[82]</sup> as shown in scheme 2.4. In contrast, in ligands **2.7** and **2.9** the phenyl rings are separated by an alkyl group so that the  $\pi$ -delocalisation no longer exists. 4-Substituted pyridine N-oxides, which are capable of showing *para*-quinonoid structures, have been used for the synthesis of non-linear optical crystals to produce second harmonic generators [SHG].<sup>[83]</sup> These second order effects in organic or inorganic materials result from the enhancement of polarization in one direction and inhibition in another direction; for example ligands **2.2**, **2.8** and **2.12** are extensively used for SHG studies.

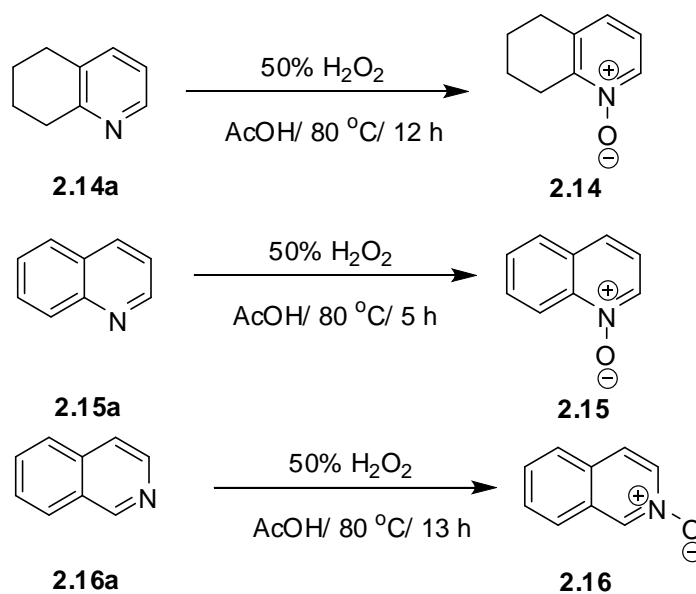


Scheme 2.4 – *Ortho*- and *para*-quinonoid resonating structures for 2- and 4-phenylpyridine N-oxides.

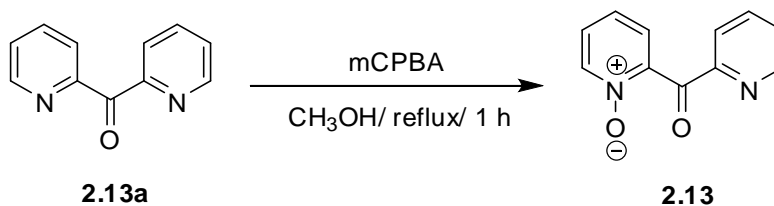
Ligands **2.7**<sup>[84]</sup> and **2.8**<sup>[85]</sup> are known compounds and were synthesized in one step from the precursors **2.7a** and **2.8a** using 50% hydrogen peroxide in acetic acid. Ligand **2.9**<sup>[86]</sup> is also a known compound and was synthesised by condensation of pyridine 4-carboxaldehyde **2.9a** with benzene in Bronsted superacid  $\text{CF}_3\text{SO}_3\text{H}$  to yield **2.9b**,<sup>[78]</sup> which was then oxidized to **2.9** with mCPBA in methanol, as shown in scheme 2.5.

Scheme 2.5 – Syntheses of ligands **2.7**, **2.8** and **2.9**.

The structure of the heterocycles can also influence the basicity of the N-oxides. For example, the basicity<sup>[43]</sup> of N-oxides increases from: *Pyridine* < *quinoline* < *isoquinoline* < *acridine*. Ligands **2.14**,<sup>[87]</sup> **2.15**<sup>[88]</sup> and **2.16**<sup>[89]</sup> are all known compounds and were synthesised to study the effect of a fused ring system in their silver(I) complexes.

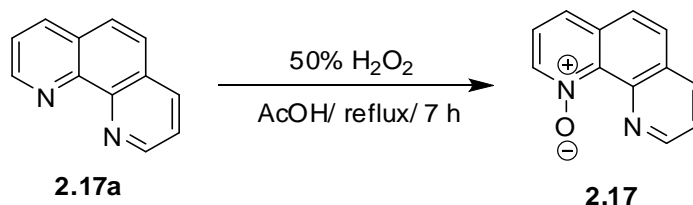
Scheme 2.6 – Syntheses of ligands **2.14**, **2.15** and **2.16**.

Ligand **2.13** was obtained as a by-product when attempting to prepare the N,N'-dioxide of **2.13a**. The synthesis involves oxidation of the precursor 2,2'-dipyridyl ketone **2.13a** using mCPBA yielding 66% of **2.13**. A subsequent Scifinder search revealed only two reports for the synthesis of **2.13**. Both the literature<sup>[90]</sup> methods employed perfluoro-*cis*-2-*n*-butyl-3-*n*-propyloxaziridine as the oxidant to yield ligand **2.13** in 50% yield.



Scheme 2.7 – Synthesis of ligand **2.13**.

Ligand **2.17**<sup>[91]</sup> is also a known compound and was obtained as the main product while trying to prepare the N,N'-dioxide of **2.17a**. The synthesis involved a well-established procedure of oxidizing the precursor 1,10-phenanthroline **2.17a** using 50% hydrogen peroxide in acetic acid to yield 74% of **2.17**.



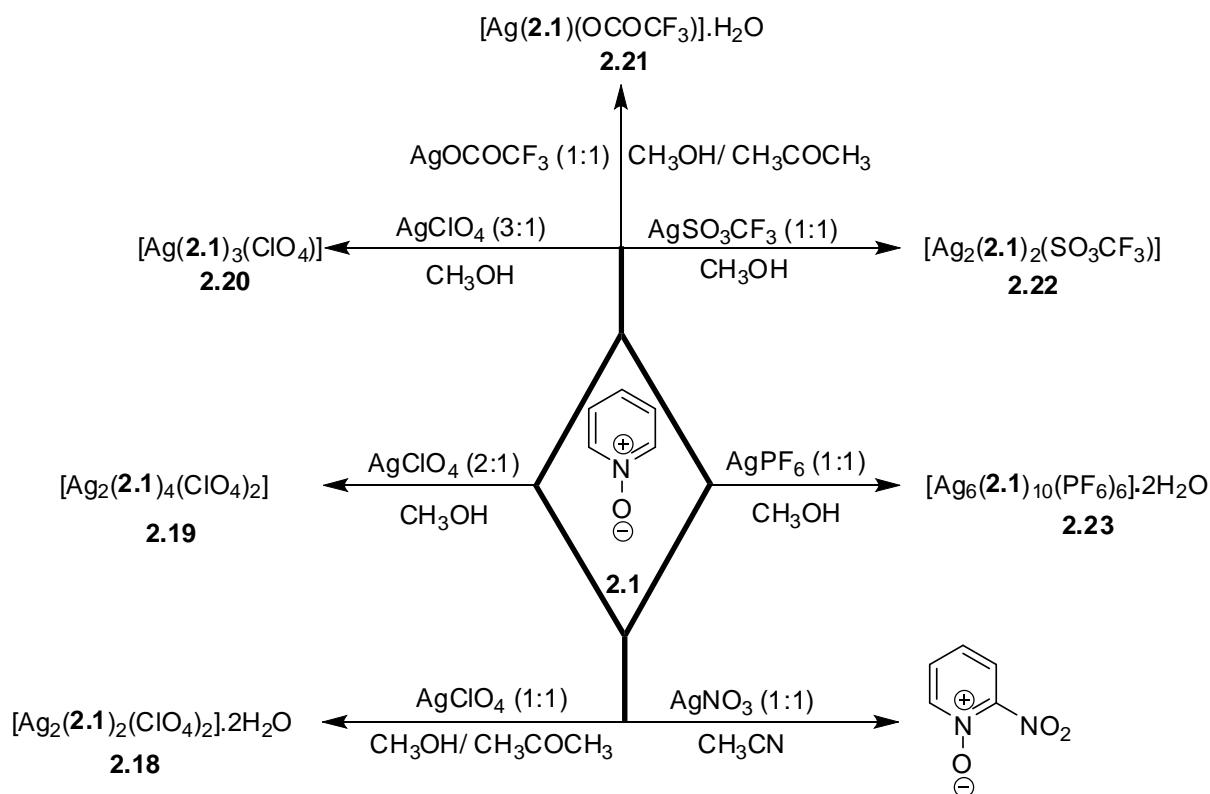
Scheme 2.8 – Synthesis of ligand **2.17**.

## 2.3 Silver(I) complexes of pyridine N-oxides

### 2.3.1 Complexes with pyridine N-oxide **2.1**

Three different one-dimensional polymeric complexes **2.18**, **2.19** and **2.20** were obtained when ligand **2.1** was reacted with silver(I) perchlorate in 1:1, 2:1 and 3:1 stoichiometric ratios, with their asymmetric unit compositions shown in scheme 2.9. Increasing the ratio of ligand **2.1** resulted in a decrease of ligand denticity from  $\mu_3$ -O,O,O to  $\mu_2$ -O,O with an increase in the coordination number of the silver(I) ion from 6 to 8. Increased ratios of ligand **2.1** also led the perchlorate anions to change its nature from coordinating to non-coordinating, due to the increased probability of ligand [**2.1**] binding to silver(I) ions. Although complexes **2.18** and **2.21** were synthesised under similar conditions, the structure of the final silver(I) complex was influenced by the anions employed. Self assembly of ligand **2.1** with  $\text{AgClO}_4$  and  $\text{AgOCOCF}_3$  produced 1D polymer chains with the water molecules playing an important structural role.

Ligand **2.1** adopted a  $\mu_3$ -O,O,O coordination mode in complexes **2.18**, **2.22** and **2.23**, though the anions employed were different in each case. Mixing acetonitrile solutions of ligand **2.1** and AgNO<sub>3</sub> in a 1:1 stoichiometric ratio followed by slow evaporation at room temperature, resulted in colourless crystals of 2-nitropyridine N-oxide confirmed by X-ray crystallography. Though the crystal structure of 2-nitropyridine N-oxide was reported by Gatilov *et al.*,<sup>[92]</sup> the structure has not been deposited in the *Cambridge Crystallographic Database* to date.



Scheme 2.9 – Syntheses of complexes **2.18** – **2.23**.

### With silver(I) perchlorate (1:1) **2.18**

Complex **2.18** crystallised and solved in the triclinic *P*-1 space group and the asymmetric unit is shown in figure 2.2 with selected labels and bonding parameters. Three independent silver(I) ions, two of which lie on crystallographic inversion centers, two ligands, two perchlorate anions and two water molecules are present in the asymmetric unit of **2.18**. This shows that the complex has a 1:1 ligand **2.1** to silver(I) ratio. The ligand oxygen O1 coordinates to Ag1 in a monodentate fashion, while O2 adopts a  $\mu_3$ -O,O,O tridentate coordination mode with Ag1, Ag2 and Ag3, with an average Ag-O<sub>ligand</sub> distance of 2.428(1) Å and N-O<sub>ligand</sub>-Ag angles ranging from 112.91(9)° to 122.97(2)°. The Ag-O<sub>ligand</sub> bond distances are close to previously reported values<sup>[14]</sup> for N-oxide complexes

showing mono- and tridentate coordination with silver(I) ions. The angles made by the tridentate ligand oxygen O2 with Ag1, Ag2 and Ag3 range from  $92.81(4)^\circ$  to  $113.37(5)^\circ$ .

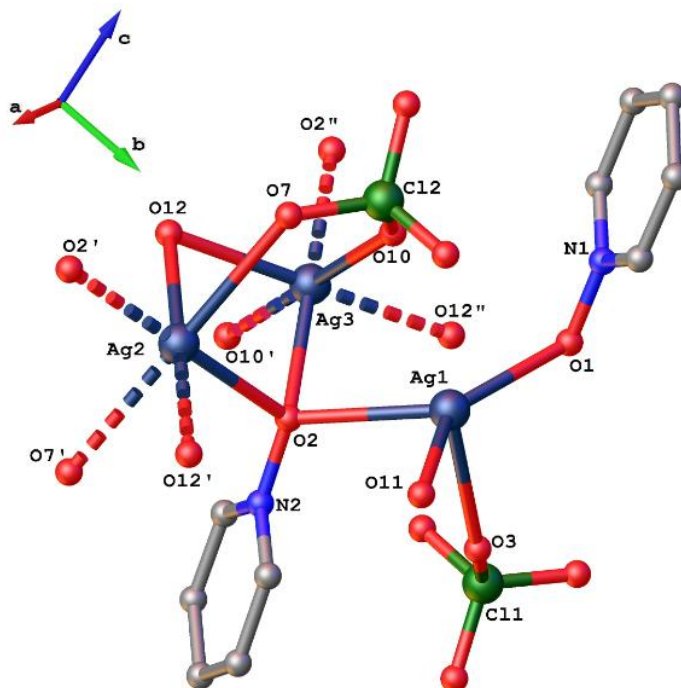


Figure 2.2 – Asymmetric unit of complex **2.18**. Hydrogen atoms are excluded for clarity. Selected bond lengths (Å) and bond angles ( $^\circ$ ): N1-O1 = 1.347(2), N2-O2 = 1.348(2), Ag1-O1 = 2.335(1), Ag1-O2 = 2.457(1), Ag2-O2 = 2.412(1), Ag3-O2 = 2.510(1), N1-O1-Ag1 = 115.65(2), N2-O2-Ag2 = 112.91(9), N2-O2-Ag1 = 115.11(9), N2-O2-Ag3 = 122.97(2), Ag2-O2-Ag1 = 113.37(5), Ag2-O2-Ag3 = 97.31(4), Ag1-O2-Ag3 = 92.81(4).

Two silvers, Ag2 and Ag3, lie on inversion centers. Ag3 has distorted octahedral geometry with an  $O_6$  environment while Ag1 [ $\tau_4 = 0.67$ ] is four-coordinate with an  $O_4$  environment. The N- $O_{\text{ligand}}$  bond distances, 1.347(2) Å [N1-O1] and 1.348(2) Å [N2-O2], show that the oxygen atoms are  $sp^3$  hybridized, which is also supported by its tridentate behaviour. The perchlorate oxygen O3 is monodentate with Ag1, while the Cl2 oxygens O7 and O10 are bridging Ag2 and Ag3, as shown in figure 2.2.

Consideration of the N2-O2-Ag and Ag-O-Ag angles reveal a distorted tetrahedral geometry, as shown in figure 2.3a. The distorted octahedral silver(I) ions are arranged in a vertex-sharing mode and further extend to a 1D polymeric chain along the *a*-axis.



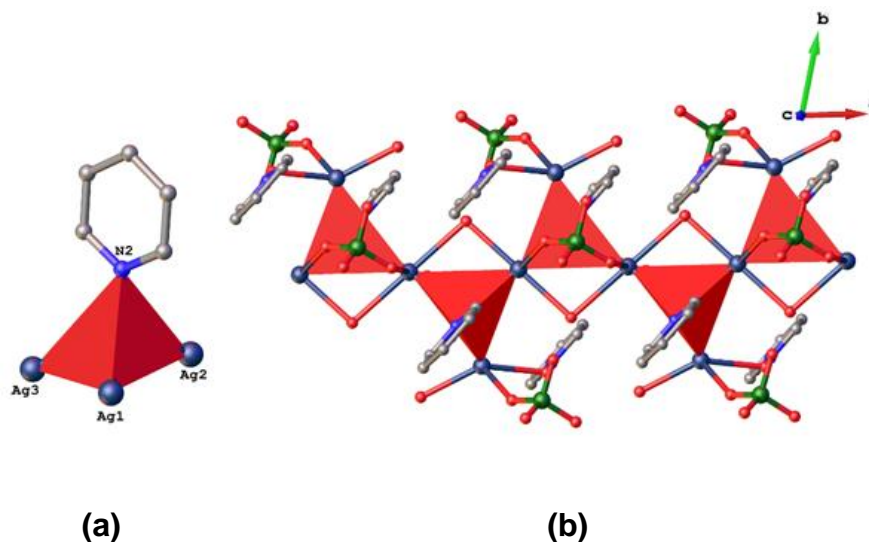


Figure 2.3 – (a) The tridentate pyridine N-oxide coordination mode with three different silvers Ag1, Ag2 and Ag3 (b) vertex-sharing representation of the 1D polymeric structure of complex **2.18** viewed down the *c*-axis. Hydrogen atoms are excluded for clarity.

Interestingly in this 1D polymeric structure, the perchlorate anion is found between two pyridine N-oxide rings preventing any  $\pi$ - $\pi$  interactions, as shown in the figure 2.4.

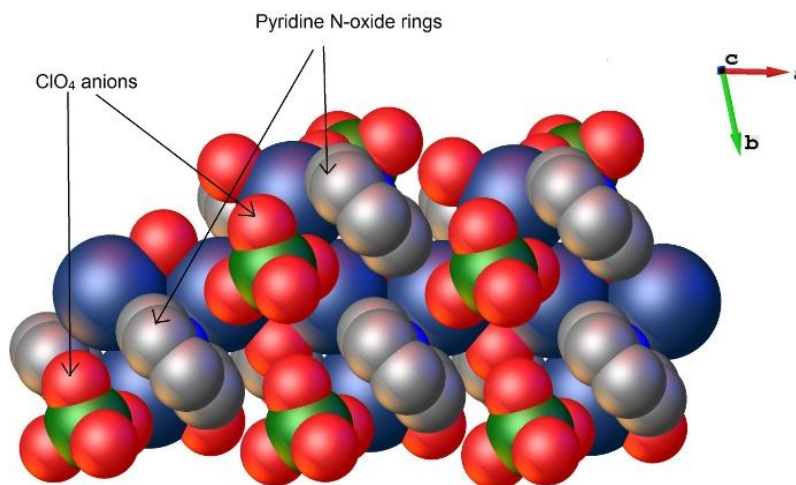


Figure 2.4 – 1D polymeric space filling model of complex **2.18** showing the absence of  $\pi$ - $\pi$  interactions, due to the perchlorate anions. Hydrogen atoms are excluded for clarity.

In the crystal lattice, each of the 1D polymers propagates in two-dimensions with hydrogen bond interactions along the *b*-axis but no interactions along the *c*-axis, as seen in figure 2.5.

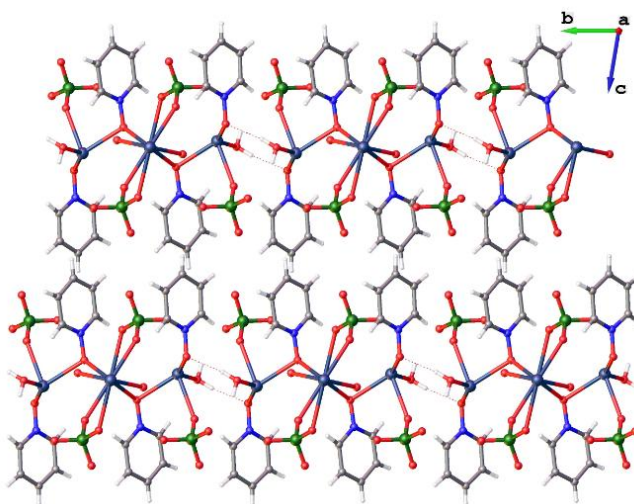


Figure 2.5 – Hydrogen bond assisted 2D crystal packing of complex **2.18** viewed down the *a*-axis.

### With silver(I) perchlorate (2:1) **2.19**

Colourless crystals of complex **2.19** were obtained when ligand **2.1** was reacted with silver(I) perchlorate in a 2:1 stoichiometric ratio, and these crystallised in the trigonal *R*3 space group. Single crystal X-ray analysis revealed the asymmetric unit of complex **2.19** contains four ligand **2.1** molecules, and four silver(I) ions with one coordinated [C11] and one non-coordinated [C12] perchlorate anion, as shown in the figure 2.6. The bond distance between the monodentate perchlorate oxygen O5 and Ag2 is 2.521(3) Å. Complex **2.19** has a 2:1 ligand to silver(I) ratio, with Ag1, Ag3 and Ag4 lying on 3-fold rotation axes, while Ag2 has full occupancy.

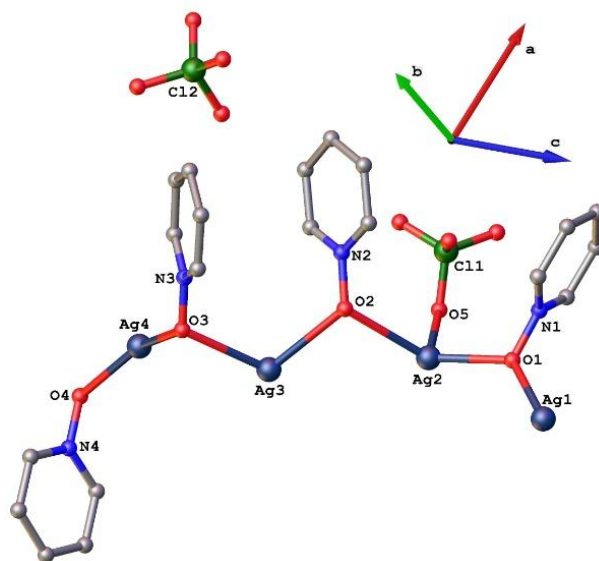


Figure 2.6 – Asymmetric unit of complex **2.19**. Hydrogen atoms are excluded for clarity. Selected bond lengths (Å): Ag1-O1 = 2.471(2), Ag2-O1 = 2.192(2), Ag2-O2 = 2.275(2), Ag2-O5 = 2.521(3), Ag3-O2 = 2.515(2), Ag3-O3 = 2.475(2), Ag4-O3 = 2.490(2), Ag4-O4 = 2.464(2).

Complex **2.19** is a 1D polymer with all four silver(I) ions adopting a six-coordinate geometry and ligands **2.1** opting for both  $\mu_2$ -O,O bidentate and  $\mu_3$ -O,O,O tridentate coordination modes, as shown in figure 2.7b. The 1D polymer of complex **2.19** is divided into two parts, units – A and B, which are repeated to extend one-dimensionally along the *c*-axis, as shown in figure 2.7a. The aromatic rings of the ligand are twisted and take a spiral form around the distorted octahedral silver(I) centers to allow  $\pi$ - $\pi$  interactions, with centroid-centroid distances of 3.569 Å, 3.603 Å and 3.756 Å, as shown in figure 2.7b. These  $\pi$ - $\pi$  interactions between unit – A and unit – B pyridine rings are separated by triangular Ag<sub>3</sub> units formed from the Ag<sub>2</sub> centers, each of which has a monodentate perchlorate anion, as shown in figure 2.8b.

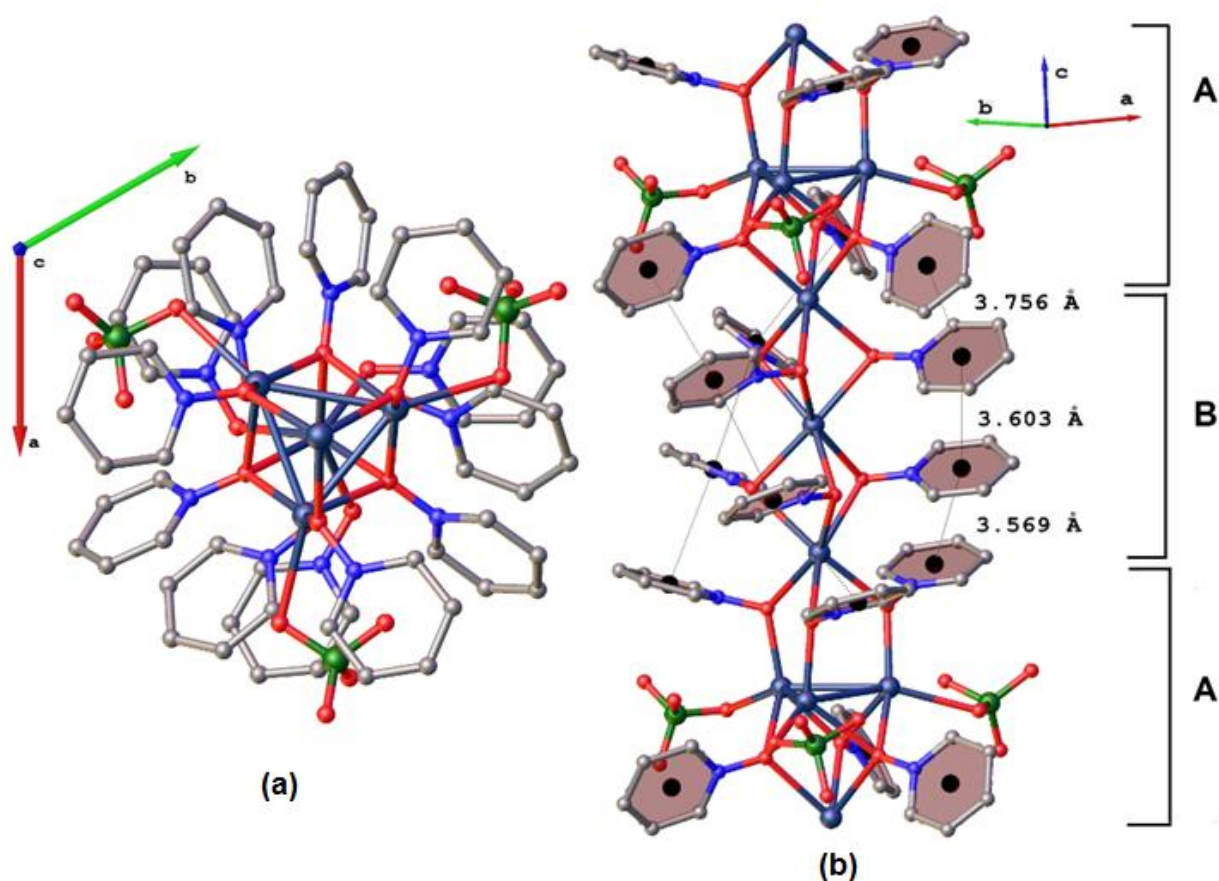


Figure 2.7 – (a) 1D Polymeric structure of complex **2.19** viewed down the *c*-axis, and (b) spiral like arrangement of aromatic  $\pi$ -stacking of the 1D polymer. Hydrogen atoms are excluded for clarity.

Unit – A contains five silver(I) ions, three bidentate ligands and three tridentate ligands, as shown in figure 2.8a. The bidentate N-O [1.354(3) Å] bond distances are longer than in the tridentate N-O [1.346(3) Å] groups, which is contrary to those obtained in complex **2.18**. The Ag-O<sub>ligand</sub> bond distances of the  $\mu_2$ -O,O bidentate O1 [2.331 Å] are shorter than the tridentate O2 [2.441 Å] ligand **2.1** molecules. The coordination angles range between 113.08(2)° and 123.04(2)°. Three highly

distorted octahedral Ag<sub>2</sub> silver(I) centers form a triangle, with Ag<sup>⋯</sup>Ag distances of 3.019(4) Å and monodentate perchlorate anions coordinated to each Ag<sub>2</sub> center, as shown in figure 2.8b. The Ag<sub>2</sub>-Ag<sub>2</sub>'-Ag<sub>2</sub>'' interactions form an equilateral triangle bridged by three μ<sub>2</sub>-O,O ligand **2.1** oxygens, O1, at angles of 126.57(1)°, whilst the Ag<sub>3</sub> is connected to the triangle through three μ<sub>3</sub>-O,O,O ligand **2.1** oxygens [O2]. The non-bonding distances between oxygens from μ<sub>3</sub>-O,O,O [O2-O2'' = 3.080 Å] ligands are shorter than the μ<sub>2</sub>-O,O [O1-O1' = 3.240 Å] oxygens. The non-bonded distance between Ag1-Ag3 is 7.199 Å.

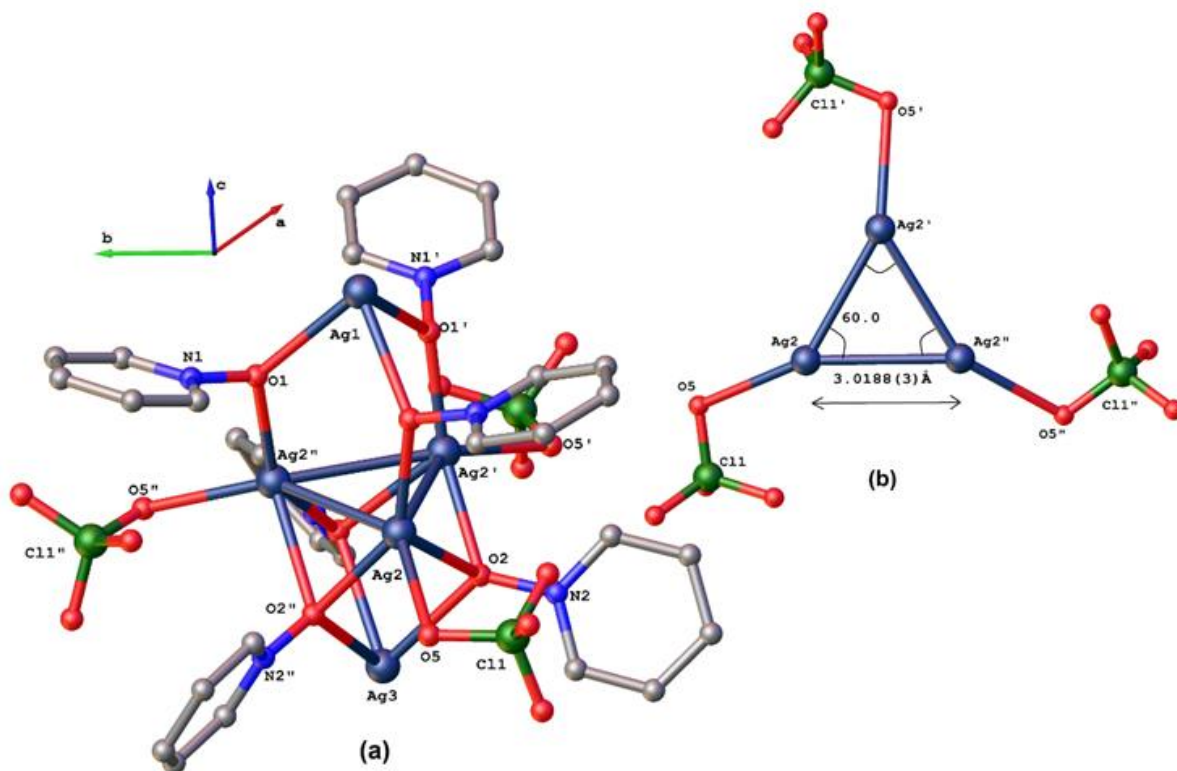


Figure 2.8 – (a) Unit – A in the 1D polymeric structure of complex **2.19**. Hydrogen atoms are omitted for clarity. (b) Equilateral triangle arrangement of Ag<sub>2</sub> centers. Selected bond lengths (Å) and bond angles (°): N1-O1 = 1.354(3), N2-O2 = 1.346(3), Ag1-O1 = 2.471(2), Ag2''-O1 = 2.192(2), Ag2''-O2'' = 2.275(2), Ag2-O2'' = 2.533(2), Ag3-O2'' = 2.515(2), O1-O1' = 3.240, O2-O2'' = 3.080, Ag2-Ag2' = 3.019(4), Ag1-Ag3 = 7.199, N1-O1-Ag1 = 113.40(2), N1-O1-Ag2'' = 113.06(2), N2-O2-Ag2 = 120.0(2), N2-O2-Ag3 = 123.04(2), N2-O2-Ag2'' = 121.07(2), Ag2-Ag2'-Ag2'' = 60.0(2), Ag2''-O1-Ag1 = 126.57(1).

The unit – B of complex **2.19** comprises six μ<sub>2</sub>-O,O bidentate ligand **2.1** molecules and one six-coordinate Ag<sub>4</sub> center. These six ligand **2.1** molecules bridge Ag<sub>4</sub> and Ag<sub>1</sub>, Ag<sub>3</sub> centers from unit – A in two trigonal bipyramidal arrangements, as shown in figure 2.9. The distorted octahedral Ag<sub>4</sub> and Ag<sub>1</sub> ions are bridged by O4 oxygens at near right angles [88.68(7)°], while Ag<sub>4</sub> and Ag<sub>3</sub> are bridged by O3 oxygens at 86.50(7)°. The N-O bond distances 1.336(3) Å [N3-O3] and 1.335(3) Å [N4-O4], their average coordination distances 2.482 Å [Ag-O3] and 2.484 Å [Ag-O4] and

coordination angles  $117.58^\circ$  [N-O3-Ag] and  $114.98^\circ$  [N-O4-Ag] are similar. The non-bonded distances between Ag1-Ag4 [3.473 Å] are slightly longer than Ag3-Ag4 [3.402 Å].

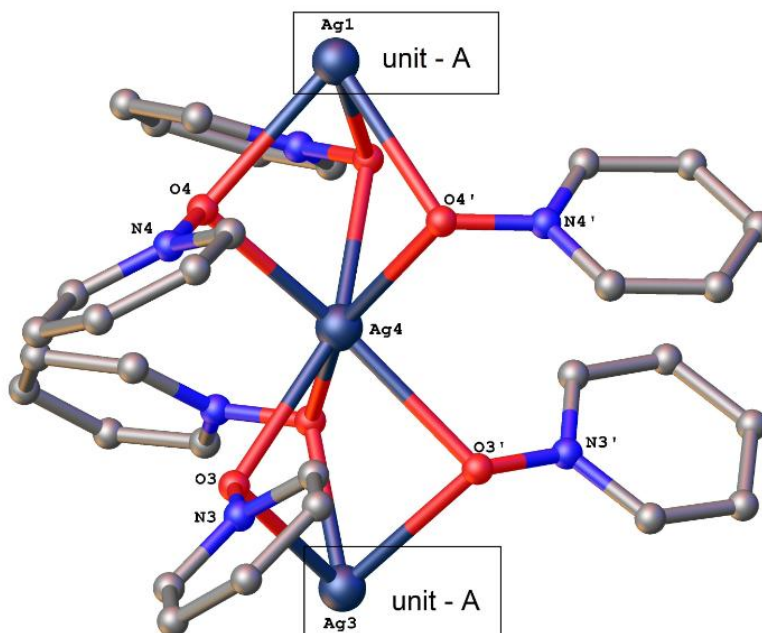


Figure 2.9 – Unit – B in the 1D polymeric structure of complex **2.19**. Hydrogen atoms are omitted for clarity. Selected bond lengths (Å) and bond angles ( $^\circ$ ): N3-O3 = 1.336(3), N4-O4 = 1.335(3), Ag3-O3 = 2.475(2), Ag4-O3 = 2.490(2), Ag1-O4 = 2.504(2), Ag4-O4 = 2.464(2), N3-O3-Ag3 =  $117.18(2)$ , N3-O3-Ag4 =  $117.99(2)$ , N4-O4-Ag1 =  $118.53(2)$ , N4-O4-Ag4 =  $111.44(2)$ , Ag4-O4-Ag1 =  $88.68(7)$ , Ag3-O3-Ag4 =  $86.50(7)$ .

### With silver(I) perchlorate (3:1) **2.20**

Large yellow crystals of complex **2.20** were obtained by slow evaporation of a methanol solution containing a 3:1 ratio of ligand **2.1** and the  $\text{AgClO}_4$ . The complex **2.20** crystallised in the hexagonal  $P6_3/m$  space group with the asymmetric unit comprising one ligand **2.1** molecule coordinated to an Ag1 center in a monodentate fashion and a non-coordinated perchlorate [Cl1] anion, as shown in figure 2.10. The perchlorate anion is disordered with a three-fold rotation axis passing through the O3 oxygen, with the O3 oxygen occupancies being 16.6% each and O2 being 50%. The Ag1 and Cl1 atoms each have 16.6% occupancy. The ligand **2.1** is present in a  $\mu_2$ -O,O bidentate coordination mode, bridging Ag1 ions at angles of  $74.23(1)^\circ$  with an N-O bond distance of 1.326(6) Å. The silver(I) ions display an eight-coordinate geometry with an  $\text{Ag}_2\text{O}_6$  environment, as shown in figure 2.10. Each Ag1 is linearly coordinated with adjacent Ag1 ions at distances of 2.996(1) Å, with the coordination sphere being completed by six oxygens supplied by ligand **2.1** molecules at distances of 2.483(3) Å, with coordination angles of  $117.4(3)^\circ$ .

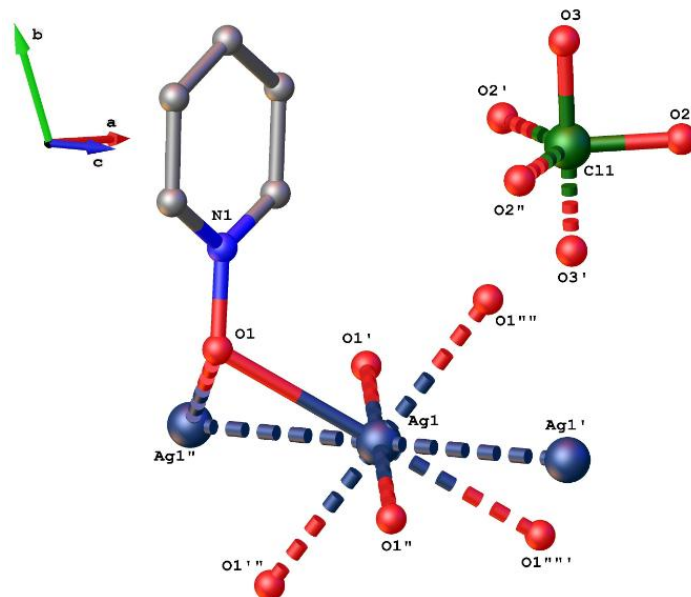
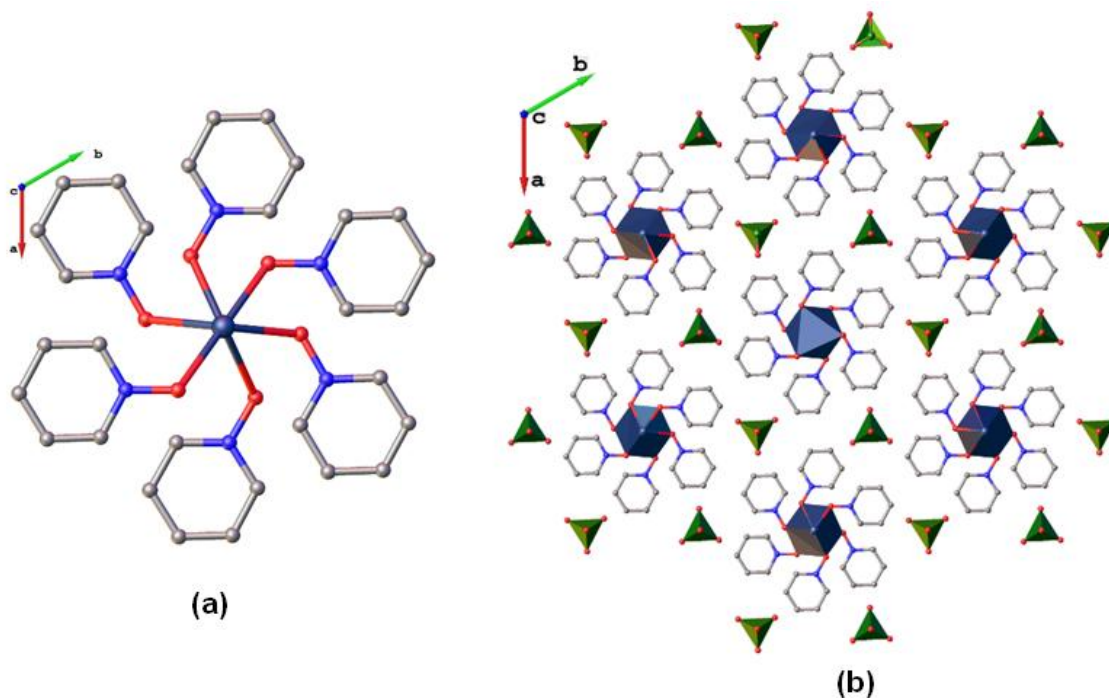


Figure 2.10 – Asymmetric unit of complex **2.20**. Hydrogen atoms are omitted for clarity. Selected bond lengths (Å) and bond angles (°): N1-O1 = 1.326(6), Ag1-O1 = 2.483(3), Ag1-Ag1' = 2.996(1), N1-O1-Ag1 = 117.4(3), Ag1-O1-Ag1 = 74.23(1), Ag1''-Ag1-Ag1' = 180.0.

The complex **2.20** extends into a 1D polymer along the *c*-axis with three  $\mu_2$ -O,O bidentate ligands **2.1** bridged each Ag $\cdots$ Ag interaction, as shown in figure 2.11c. The centroid-centroid distances between the aromatic rings along the *c*-axis are 5.992 Å. The crystal packing [figure 2.11b] illustrates how each 1D polymer [figure 2.11a] is surrounded by six perchlorate anions.



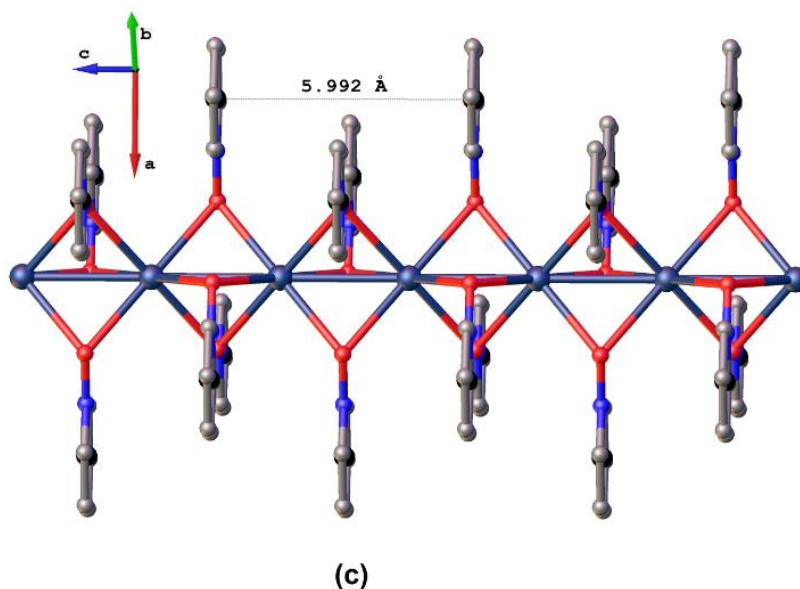


Figure 2.11 – (a & c) 1D Polymeric structure of complex **2.20** as viewed down the *c*- and *b*-axis, respectively (b) crystal packing of complex **2.20**. Hydrogen atoms are omitted for clarity.

#### With silver(I) trifluoroacetate (1:1) **2.21**

Complex **2.21**, formed by the reaction of silver(I) trifluoroacetate with ligand **2.1**, was solved in the monoclinic  $P2_1/c$  space group. The asymmetric unit [figure 2.12a] contains one ligand molecule and  $\text{AgOCOCF}_3$  in a 1:1 ligand to silver(I) ratio with a coordinating water molecule. A discrete structure [figure 2.12b] formed in which each silver(I) center is four-coordinate [ $\tau_4 = 0.37$ ] with an  $\text{Ag}_1\text{O}_3$  environment. The coordinating oxygen atoms are supplied by two water molecules and two trifluoroacetate anions, as shown in figure 2.12b. The bidentate trifluoroacetate anions bridge silver(I) ions [ $\text{Ag1} \cdots \text{Ag1}'$  bond] at a distance of 2.936(3) Å with two waters in a *trans*-like arrangement at angles 145.96(4)° [ $\text{O4-Ag1-Ag1}'$ ]. The  $\text{N-O}_{\text{ligand}}$  bond distances, 1.335(2) Å [ $\text{N1-O1}$ ], are smaller than the  $\text{N-O}_{\text{ligand}}$  distances observed in complex **2.18** [1.348(2) Å]; this implies that the oxygen orbitals are  $\text{sp}^2$  hybridized with slight double bond character. Alternatively, since there is no coordination between silver(I) ions and ligands **2.1**, the  $\pi$ -electrons on oxygen atoms are donated to the aromatic ring, a commonly observed property in pyridine N-oxides. Based on the results from this work on silver(I) trifluoroacetate complexes with various pyridine N-oxides, this silver(I) salt prefers to form  $\text{Ag} \cdots \text{Ag}$  bonds and bind water molecules rather than N-oxide ligands. This results in supramolecular frameworks in which the N-oxides form hydrogen bonds with the water molecules, as seen in figure 2.13.

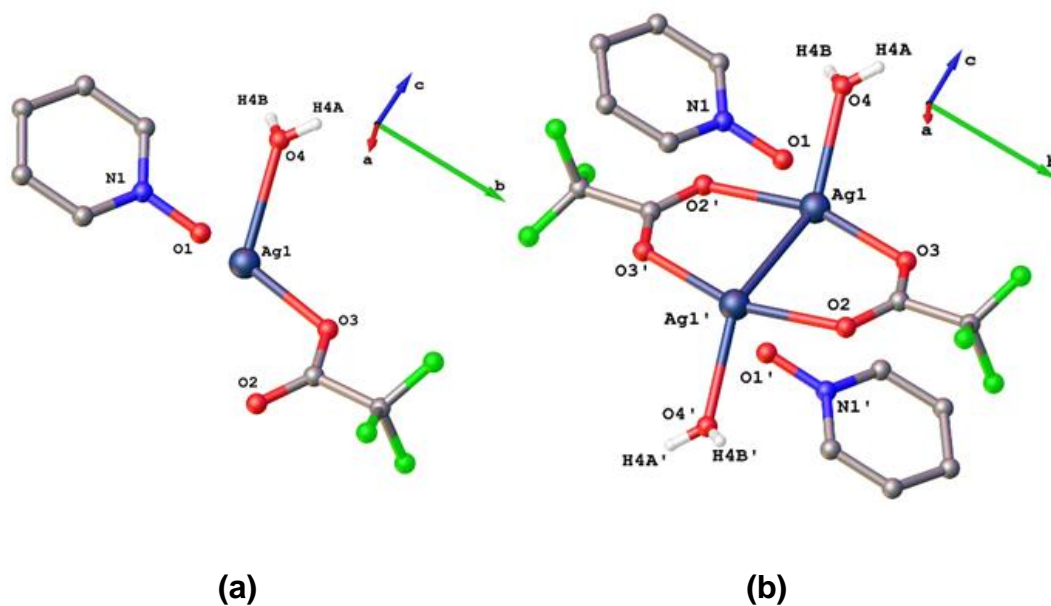


Figure 2.12 – (a) Asymmetric unit of complex **2.21**; (b) Discrete structure of complex **2.21**. Selected hydrogen atoms are excluded for clarity. Selected bond lengths (Å) and bond angles (°): N1-O1 = 1.335(2), Ag1-O2' = 2.309(1), Ag1-O3 = 2.258(1), Ag1-O4 = 2.409(2), Ag1-Ag1' = 2.936(3), O4-Ag1-Ag1' = 145.96(4).

Complex **2.21** extends into a 1D staircase-like polymer with alternating Ag $\cdots$ Ag and hydrogen bonding interactions, as shown in figure 2.13. The oxygens O1 and O1' of the N-oxide interact with hydrogens H4A', H4B and H4B', H4A of water molecules, which are positioned *trans*- over Ag1-Ag1' bonds to generate four-membered rings. These rings are planar, i.e. the oxygens [O1, O4', O1' and O4] lie in the same plane, as shown in figure 2.14, and the D-H $\cdots$ A angles are close to 180°, as shown in table 2.1.

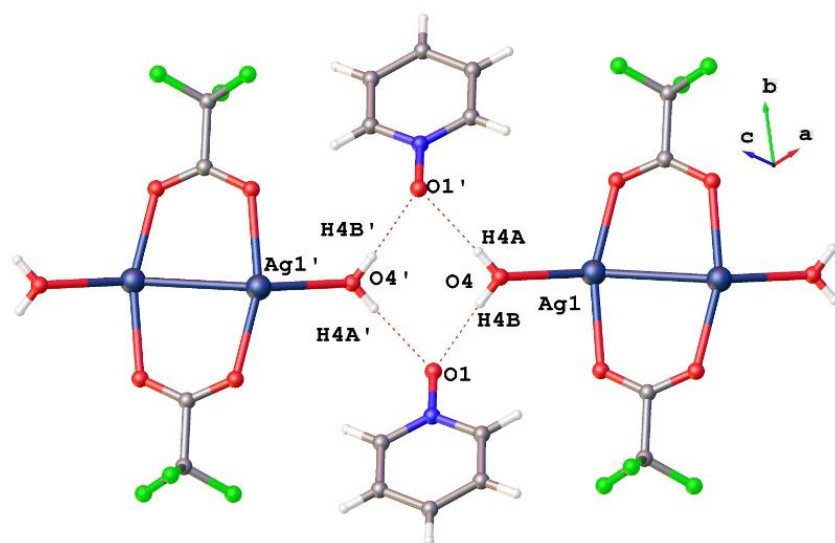


Figure 2.13 – Depiction of the hydrogen bonded ligand dimeric interaction with the water molecules.



Table – 2.1 Hydrogen bond parameters in complex **2.21**.

D-H...A	$d_{D-H}$ (Å)	$d_{H...A}$ (Å)	$d_{D...A}$ (Å)	$\angle D-H...A$ (°)
O4-H4A...O1'	0.773	2.028	2.800	176.99
O4-H4B...O1	0.779	2.020	2.796	175.03

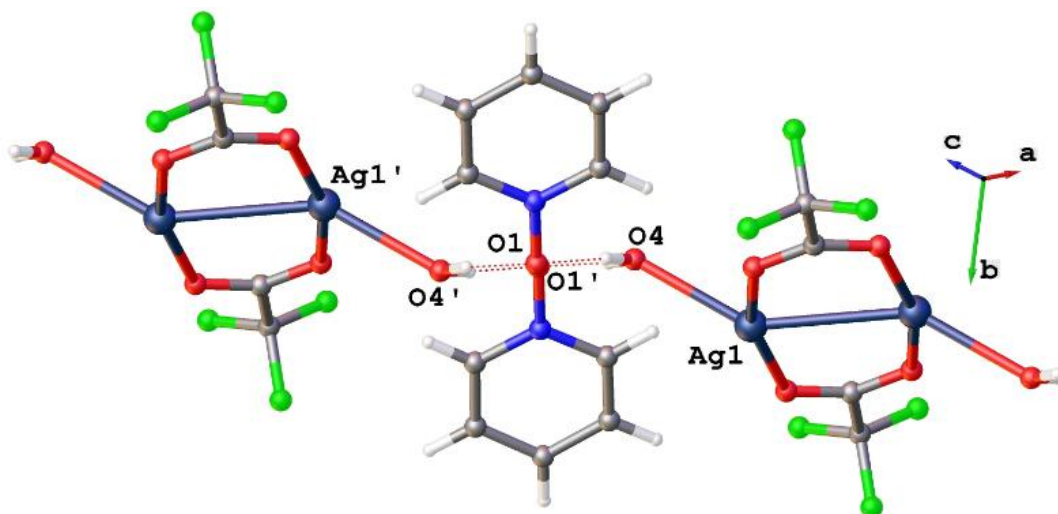


Figure 2.14 – View illustrating how the hydrogen bonding interactions are planar.

### With silver(I) triflate (1:1) **2.22**

Complex **2.22** solved in the triclinic  $P-1$  space group and the asymmetric unit contains two ligands and two silver(I) triflate units, as shown in figure 2.15. Complex **2.22** has a 1:1 ligand [**2.1**] to silver(I) ratio. The ligands [**2.1**] and triflate anions are both in  $\mu_2$ -O,O bidentate and  $\mu_3$ -O,O,O tridentate coordination modes, as shown in figure 2.15. The tridentate N1-O1 [1.349(2) Å] bond distances are longer than the bidentate N2-O2 [1.336(2) Å] bonds, which is similar to complex **2.18** but different to complexes **2.19** and **2.20**. Although the observed long N1-O1 and short N2-O2 bond distances are consistent with their tridentate and bidentate coordination modes with silver(I) ions, the coordination abilities of N1-O1 [Ag-O1 = 2.411(2) Å] and N2-O2 [Ag-O2 = 2.395(2) Å] are similar. The long Ag1''-Ag2 [4.203(4) Å] and Ag1'-Ag2 [4.109(4) Å] distances result from bridging angles of 124.44(7)° [Ag1''-O2-Ag2] and 117.44(6)° [Ag1'-O1-Ag2] for bidentate and tridentate **2.1** ligand molecules. The non-bonding distances between Ag1 and Ag2 is 3.381(4) Å.

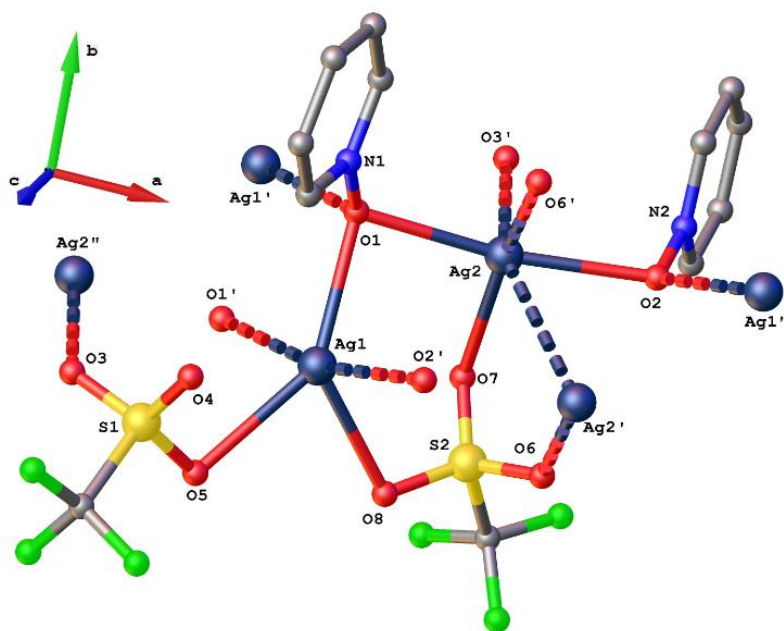


Figure 2.15 – Asymmetric unit of complex **2.22**. Hydrogens atoms are omitted for clarity. Selected bond lengths (Å): N1-O1 = 1.349(2), N2-O2 = 1.336(2), Ag1-O1 = 2.417(2), Ag1'-O1 = 2.399(2), Ag2-O1 = 2.418(2), Ag1''-O2 = 2.371(2), Ag2-O2 = 2.380(2), Ag1-O5 = 2.528(2), Ag2'-O6 = 2.456(2), Ag2-O7 = 2.479(2), Ag1-O8 = 2.464(2), N1-O1-Ag1' = 112.19(1), N1-O1-Ag1 = 118.95(1), N1-O1-Ag2 = 116.41(1), N2-O2-Ag1'' = 113.14(1), N2-O2-Ag2 = 110.07(1), Ag1''-O2-Ag2 = 124.44(7), Ag1'-O1-Ag2 = 117.44(6), Ag1''-Ag2 = 4.203(4), Ag1'-Ag2 = 4.109(4), Ag1-Ag2 = 3.381(4).

Complex **2.22** is a 1D polymer and propagates along the *a*-axis with six- [Ag2] and five- [Ag1( $\tau_5 = 0.38$ )] coordinate silver(I) ions, as shown in figure 2.16. Interestingly, the oxygens O6/O6' and O7/O7' of the tridentate triflate anions S2/S2' are bridging across Ag2 $\cdots$ Ag2' with interactions similar to trifluoroacetate anion in the dimeric arrangement observed in complex **2.21**. These triflate bridged Ag2 interactions are weak with distances of 3.247(3) Å, which was surprising since trifluoroacetate anion bridged Ag $\cdots$ Ag interactions are usually quite strong. Also, the bidentate and tridentate ligands [**2.1**] are separated by bidentate and tridentate triflate anions as shown in figure 2.16. The centroid-centroid distances between the bidentate and tridentate aromatic rings are 8.267 Å, the length of the *a*-axis.

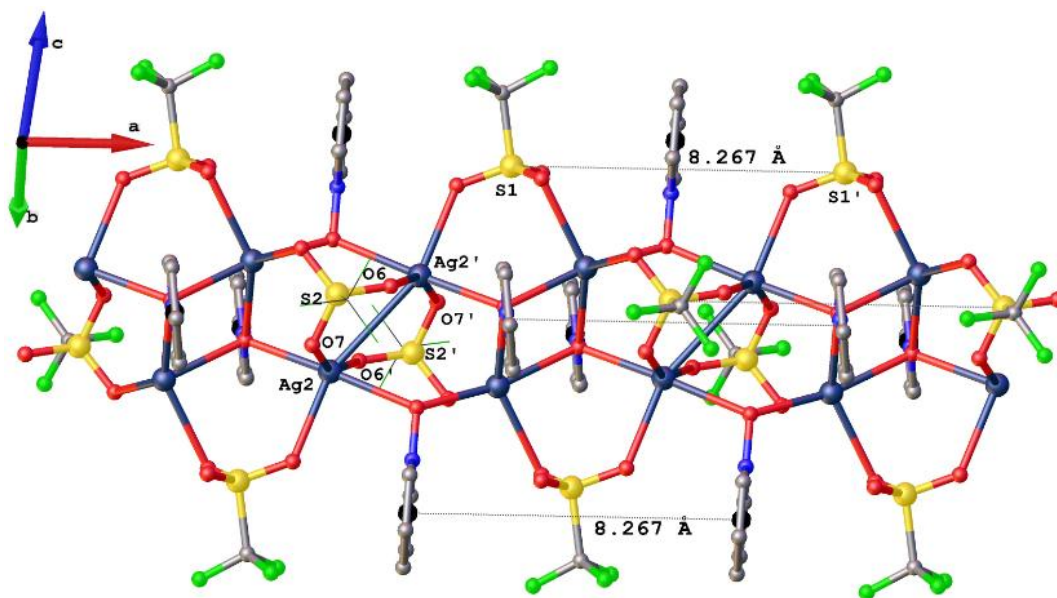


Figure 2.16 – 1D Polymeric structure of complex **2.22**. Hydrogens atoms are omitted for clarity. Selected bond lengths (Å): Ag2-Ag2' = 3.247(3), Ag2-O6 = 2.456(2), Ag2-O7 = 2.479(2), S1-S1' = 8.267.

### With silver(I) hexafluorophosphate (1:1) **2.23**

X-ray analysis of complex **2.23** showed the asymmetric unit to contain ten ligand molecules [**2.1**], six silver(I) ions, six hexafluorophosphate anions and two water molecules [O11 and O12], as shown in figure 2.17. The complex solved in the monoclinic  $P2_1/c$  space group and has a 5:3 ligand to silver(I) ratio. The asymmetric unit of complex **2.23** contains two independent units – A and B, each with five ligand molecules **2.1** and three silver(I) ions, as shown in figure 2.17. Unit – A has a monodentate water molecule [O12] coordinated to Ag4 at a distance of 2.422(6) Å. In unit – B, the water molecule [O11] bridges silver(I) ions (Ag1 and Ag3) at distances of 2.499(6) Å and 2.515(6) Å, respectively. The O12 atom also has a long contact to Ag6 at a distance of 2.607(6) Å. These two units extend along the *b*-axis with  $\mu_2$ -O,O and  $\mu_3$ -O,O,O ligand molecules **2.1**, as will be discussed in the following sections.

The one-dimensional unit – A contains one three- [Ag6] and two five-coordinate [Ag5 ( $\tau_5 = 0.05$ ) and Ag4 ( $\tau_5 = 0.41$ )] silver(I) ions with three bidentate [O6, O7 and O8] and two tridentate [O9 and O10] ligand **2.1** molecules, as shown in figure 2.18. The average Ag-O<sub>ligand</sub> bond lengths for bidentate [2.390 Å] ligand **2.1** oxygens [O6, O7, and O8] are shorter than the tridentate oxygens O9 and O10 [2.458 Å]. The bidentate oxygen O6 bridges Ag6 and Ag5 with larger angles of 107.2(2)° in comparison to the other two bidentate oxygens O7 [99.0(2)°] and O8 [104.9(2)°].

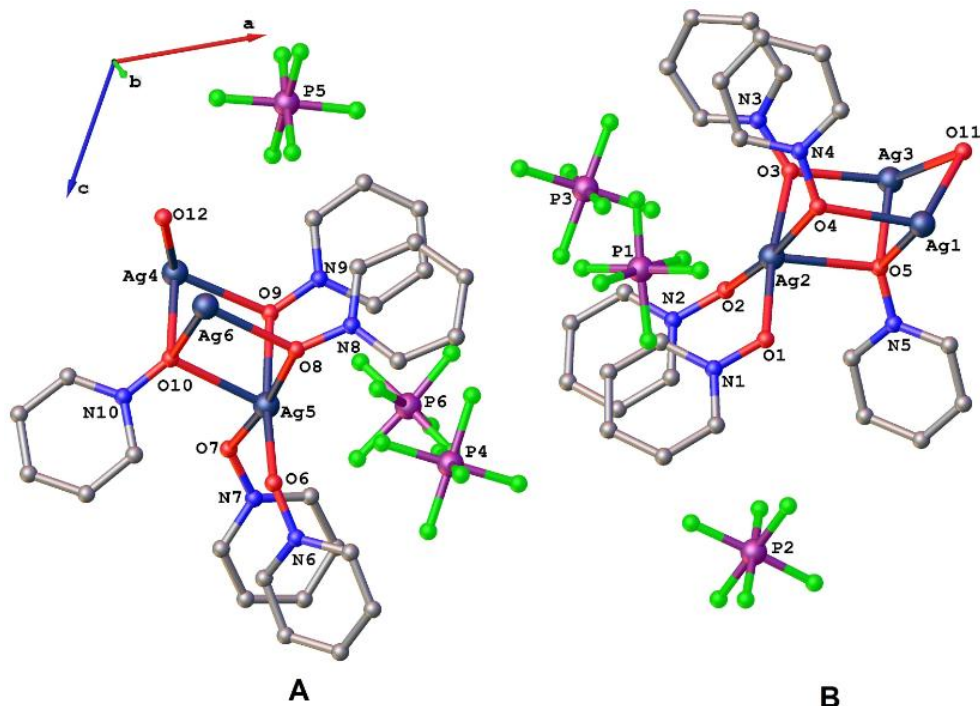


Figure 2.17 – Asymmetric unit of complex **2.23**. Hydrogens atoms are omitted for clarity. Selected bond lengths (Å): Ag1-O11 = 2.499(6), Ag3-O11 = 2.515(6), Ag4-O12 = 2.422(6).

Another structural feature in complex **2.23** is the presence of seven  $\text{Ag}_2\text{O}_2$  fused rings that are formed by two bidentate [O7 and O8] and two tridentate [O9 and O10] ligand **2.1** oxygens between Ag4, Ag5 and Ag6 ions, as shown in figure 2.18. The groups of seven  $\text{Ag}_2\text{O}_2$  rings are bridged by two N6-O6 groups at Ag5 and Ag6 to extend one-dimensionally along the *b*-axis. Two monodentate water oxygens [O12 and O12'] are coordinated in a *trans*- arrangement across the four-membered ring formed by O9, O9', Ag4 and Ag4'. The coordination angles for the ligands [**2.1**] vary from 115.0(4)° to 128.0(4)°, as shown in figure 2.18.

The 1D polymeric unit – B has three five-coordinate [Ag1 ( $\tau_5 = 0.28$ ), Ag2 ( $\tau_5 = 0.04$ ) and Ag1 ( $\tau_5 = 0.14$ )] silver(I) centers with two bidentate [O1 and O2] and three tridentate [O3, O4 and O5] ligand **2.1** molecules, as shown in figure 2.19. The bidentate N-O group [N1-O1 = 1.350(8) Å and N2-O2 = 1.352(8) Å] bond distances are similar to the tridentate N-O groups [N3-O3 = 1.352(8) Å, N4-O4 = 1.347(8) Å and N5-O5 = 1.341(8) Å]. The Ag3...Ag3' [3.329(1) Å] interaction is the shortest of the Ag-Ag distances in unit – B. The N-O bond distances are contrary to those expected, with the average Ag-O<sub>ligand</sub> bond distances of bidentate [Ag-O = 2.373(5) Å] being shorter than tridentate [Ag-O = 2.472(5) Å] ligand **2.1** molecules.

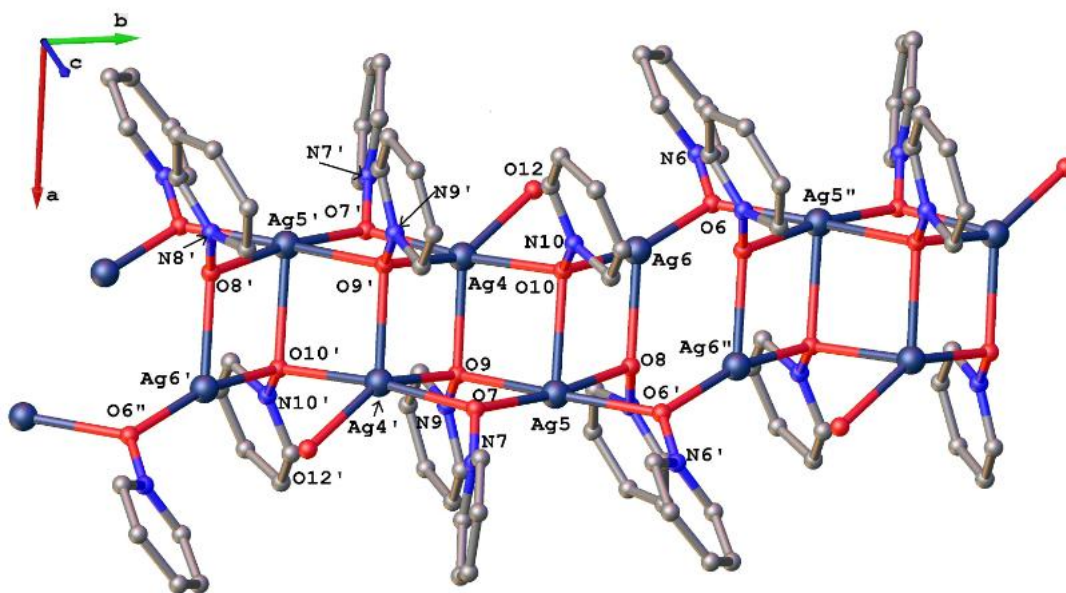


Figure 2.18 – 1D Polymeric structure of unit – A in complex **2.23**. Hydrogen atoms are omitted for clarity. Selected atoms and bonds in the aromatic rings are shown in wireframe for clarity. Selected bond lengths (Å) and bond angles (°): N6-O6 = 1.339(8), N7-O7 = 1.346(8), N8-O8 = 1.345(8), N9-O9 = 1.345(8), N10-O10 = 1.356(8), Ag5'-O6 = 2.427(6), Ag6-O6 = 2.274(6), Ag4'-O7 = 2.434(6), Ag5-O7 = 2.369(6), Ag5-O8 = 2.449(6), Ag6-O8 = 2.387(5), Ag4'-O9' = 2.422(6), Ag4-O9' = 2.430(5), Ag5-O9' = 2.507(6), Ag4-O10 = 2.455(6), Ag5-O10 = 2.540(5), Ag6-O10 = 2.393(6), N6-O6-Ag6 = 122.0(5), N6-O6-Ag5' = 125.3(5), N7-O7-Ag5 = 121.4(4), N7-O7-Ag4' = 117.6(4), N8-O8-Ag6 = 128.0(4), N8-O8-Ag5 = 116.3(4), N9'-O9'-Ag4' = 120.4(4), N9'-O9'-Ag4 = 122.2(4), N9'-O9'-Ag5 = 123.2(4), N10-O10-Ag6 = 119.5(4), N10-O10-Ag4 = 124.8(4), N10-O10-Ag5 = 115.0(4), Ag6-O6-Ag5'' = 107.2(2), Ag5-O7-Ag4' = 99.0(2), Ag6-O8-Ag5 = 104.9(2).

The angles made by the bidentate bridging water molecule [O11] with Ag1 and Ag3 [94.2(2)°] are close to those of the bidentate bridging of O1 [99.06(2)°] and O2 [105.8(2)°] ligand **2.1** oxygens.

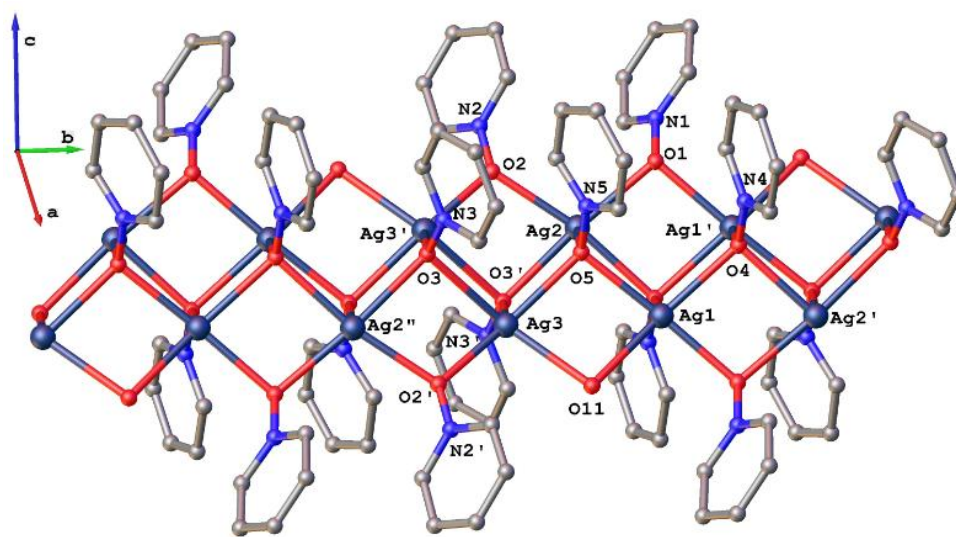


Figure 2.19 – 1D Polymeric structure of unit – B in complex **2.23**. Hydrogens atoms are omitted for clarity and selected aromatic rings are shown in wireframe for clarity. Selected bond lengths (Å) and bond angles

(°): N1-O1 = 1.350(8), N2-O2 = 1.352(8), N3-O3 = 1.352(8), N4-O4 = 1.347(8), N5-O5 = 1.341(8), Ag3-Ag3' = 3.329(1), Ag1'-O1 = 2.375(5), Ag2-O1 = 2.406(5), Ag2-O2 = 2.400(5), Ag3'-O2 = 2.312(5), Ag2''-O3 = 2.486(5), Ag3'-O3 = 2.371(5), Ag3-O3 = 2.582(6), Ag1-O4 = 2.453(5), Ag1'-O4 = 2.483(5), Ag2'-O4 = 2.460(5), Ag1-O5 = 2.400(5), Ag2-O5 = 2.553(5), Ag3-O5 = 2.460(5), N1-O1-Ag1' = 117.4(4), N1-O1-Ag2 = 122.4(4), N2-O2-Ag3' = 124.2(4), N2-O2-Ag2 = 125.0(4), N3-O3-Ag3' = 127.3(4), N3-O3-Ag2'' = 119.1(4), N3-O3-Ag3 = 112.8(4), N4-O4-Ag1 = 125.5(4), N4-O4-Ag2' = 118.9(4), N4-O4-Ag1' = 120.5(4), N5-O5-Ag1 = 119.2(4), N5-O5-Ag3 = 124.6(4), N5-O5-Ag2 = 113.2(4), Ag1'-O1-Ag2 = 99.06(2), Ag3'-O2-Ag2 = 105.8(2), Ag1-O11-Ag3 = 94.2(2).

Complex **2.23** also exhibits  $\pi$ - $\pi$  aromatic interactions with centroid-centroid distances ranging from 3.473(7) Å to 3.979(8) Å. The motifs for units – A and B in complex **2.23** are shown in figure 2.20.

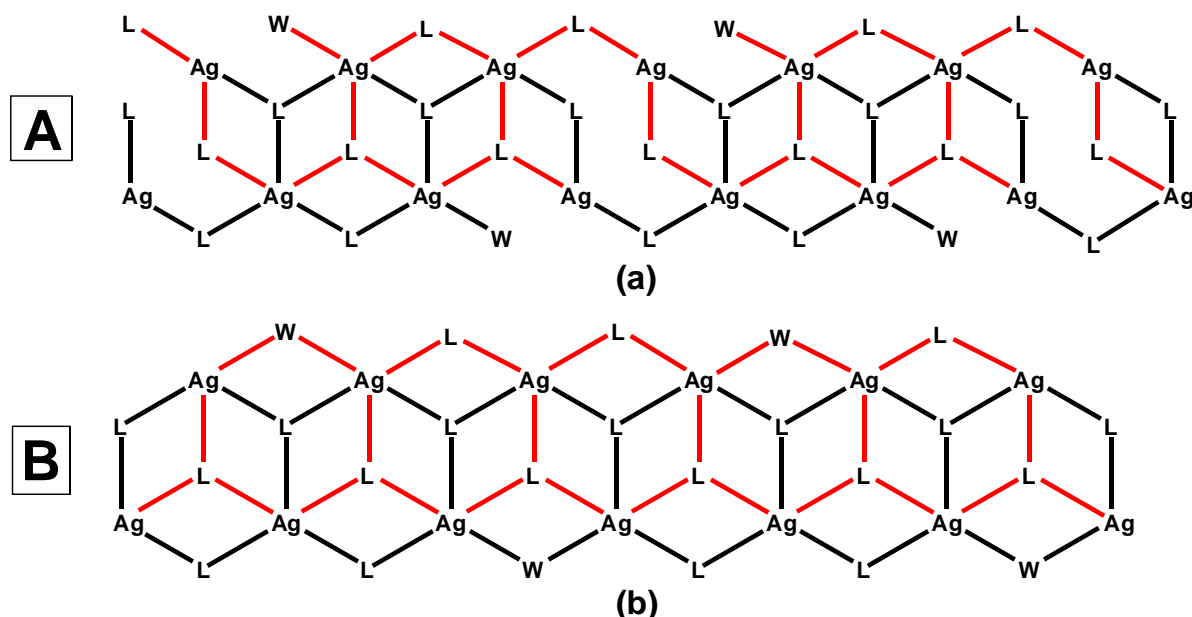


Figure 2.20 – One-dimensional pattern for units – A and B in complex **2.23** [L represents ligand molecules **2.1** and W represents water molecules].

A number of attempts to grow crystals of complexes with ligands **2.2** and **2.3** were unsuccessful. Several different crystal growing techniques were attempted but failed to produce crystals suitable for X-ray analysis. We therefore proceeded to study the sterically hindered ligand **2.4** in the series mentioned in figure 2.1.

### 2.3.2 Complexes with 2,6-dimethylpyridine N-oxide **2.4**

Watson *et al.*<sup>[93]</sup> and Wootton *et al.*<sup>[94]</sup> have produced the most interesting investigations of the interactions between heteroaromatic N-oxides and copper(II) salts. They studied a large number of CuCl<sub>2</sub> and CuBr<sub>2</sub> complexes with various 2,6-disubstituted pyridine N-oxides, and confirmed the formation of these complexes with X-ray crystal structures. Depending on the basicity of the ligands, dimers or even polymers formed linked by oxygen bridges as shown in figure 2.21. These

bridges with metals are likely for 2,6-disubstituted pyridine N-oxides, due to the steric hindrance produced by the bulky substituents.

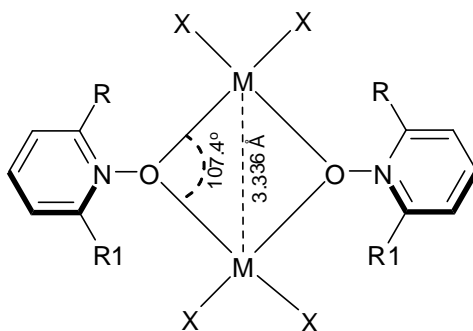
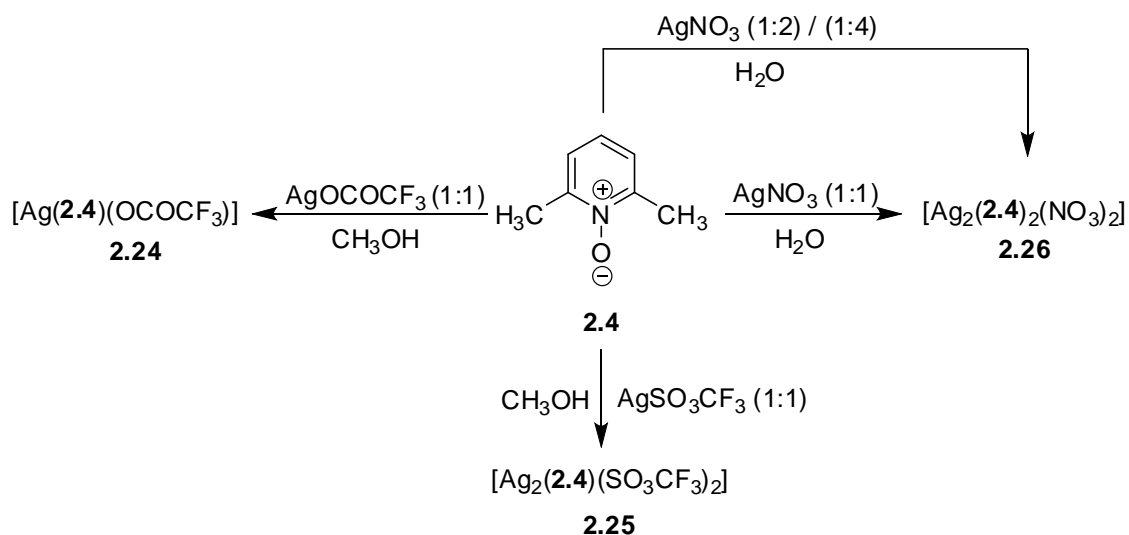


Figure 2.21 – Oxygen-type bridge formations for 2,6-disubstituted pyridine N-oxides.

In order to further investigate the formation of such bridging motifs in 2,6-disubstituted pyridine N-oxides with silver(I) salts, three complexes using ligand **2.4** were synthesised and then characterised by X-ray crystallography, as shown in scheme 2.10. In all three synthesised silver(I) complexes, the ligand [**2.4**] exhibits a  $\mu_2$ -O,O bidentate coordination mode. The asymmetric unit compositions of the synthesised complexes are shown in scheme 2.10.

Attempts to synthesise complexes with varying ratios of ligand to silver(I) triflate and silver(I) trifluoroacetate were unsuccessful, but with silver(I) nitrate the 1:2 and 1:4 ligand to silver(I) ratios produced structures similar to complex **2.26**, which was prepared from a 1:1 ligand to silver(I) nitrate ratio. In order to confirm the obtained 1:2 and 1:4 ratio complexes were truly the 1:1 ligand to silver(I) ratios, X-ray powder diffraction (XRPD) experiments were carried out, as shown in figure 2.22.



Scheme 2.10 – Syntheses of complexes **2.24** – **2.26**.

Although the 1:1 ligand to silver(I) pattern is slightly broadened in comparison to the 1:2 and 1:4 ratios, it is clear that all of the synthesised samples are identical from the values marked over the peaks.

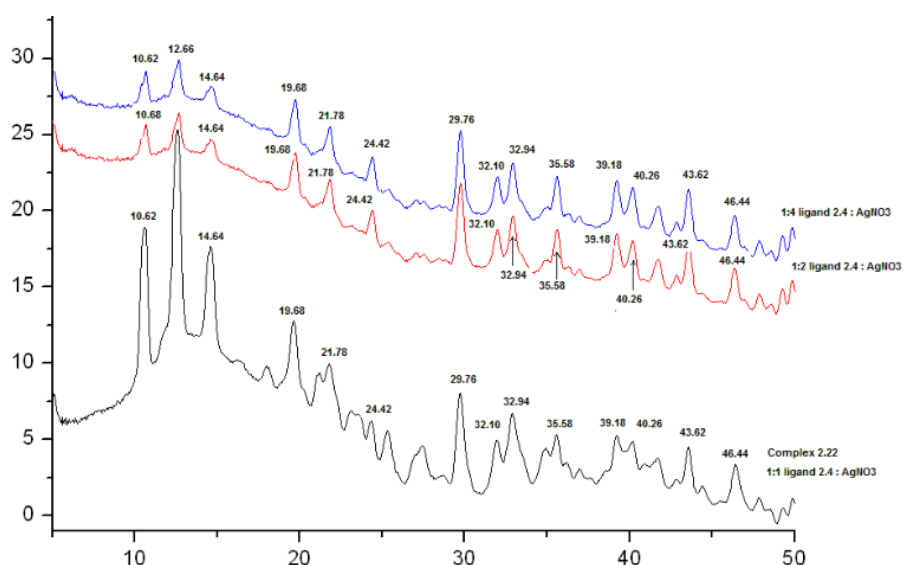


Figure 2.22 – XRPD pattern of complex **2.26** in 1:1 [black], 1:2 [red] and 1:4 [blue] ligand **2.4** to  $\text{AgNO}_3$  ratios.

#### With silver(I) trifluoroacetate (1:1) **2.24**

The silver(I) trifluoroacetate complex **2.24** with ligand **2.4** was solved in the monoclinic  $P2_1/c$  space group and is shown in figure 2.23. The asymmetric unit contains one ligand and a silver salt, with a disordered  $-\text{CF}_3$  group in a 77:23 occupancy ratio. The complex has a 1:1 ligand **2.4** to silver(I) ratio. The ligand [**2.4**] is in  $\mu_2$ -O,O bidentate bridging coordination mode with  $\text{Ag1}$  and  $\text{Ag1}'$  at distances of 2.432(2) Å [ $\text{Ag1-O1}$ ] and 2.375(2) Å [ $\text{Ag1}'\text{-O1}$ ] and bridging angles of 106.90(6)° [ $\text{Ag1-O1- Ag1}'$ ]. These values are close to the values reported in the pyridine N-oxide copper complex.<sup>[95]</sup> The non-bonded  $\text{Ag1-Ag1}'$  distance is 3.862(3) Å. The N-O<sub>ligand</sub> bond distances of 1.329(2) Å [ $\text{N1-O1}$ ] and coordination angles of 120.58(2)° [ $\text{N1-O1-Ag1}$ ] emphasize that the oxygen orbitals are  $\text{sp}^2$  hybridized with partial N-O double bond character.

The five-coordinate  $\text{Ag1}$  [ $\tau_5 = 0.38$ ] has an  $\text{Ag}_1\text{O}_4$  environment with the oxygens supplied by two trifluoroacetate anions [ $\text{O2}$  and  $\text{O3}''$ ] and two ligand molecules **2.4** [ $\text{O1}$  and  $\text{O1}'$ ], and interacts strongly with  $\text{Ag1}''$  at a distance of 2.982(3) Å, as shown in figure 2.23.



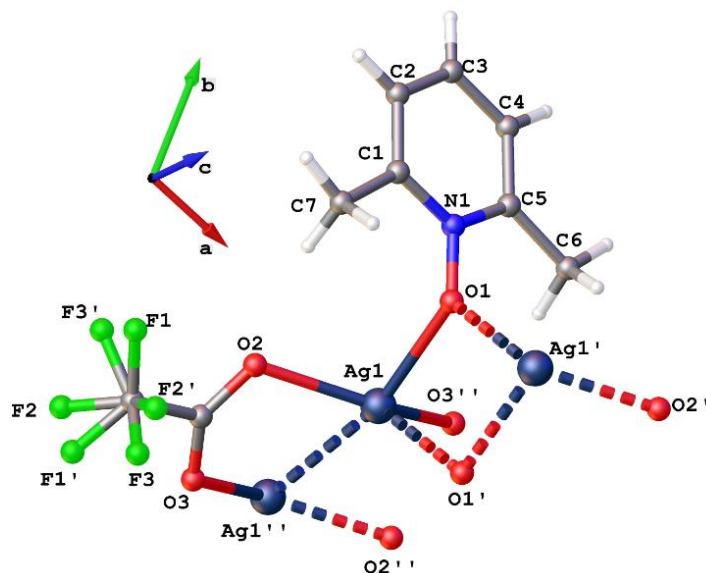


Figure 2.23 – Asymmetric unit of complex **2.24**. Selected bond lengths (Å) and bond angles (°): N1-O1 = 1.329(2), Ag1-O1 = 2.432(2), Ag1'-O1 = 2.375(2), N1-O1-Ag1 = 120.58(2), Ag1-O1- Ag1 = 106.90(6), Ag1-Ag1' = 2.982(3).

Complex **2.24** is a 1D linear polymer extending along the *c*-axis with dimeric silver(I) units bridged by trifluoroacetate anions and connected by two ligand molecules along the *b*-axis, as shown in figure 2.24. Each of the 1D polymers has  $\pi$ - $\pi$  interactions along the *c*-axis to adjacent chains with a centroid-centroid distance of 3.559(6) Å, extending two-dimensionally as shown in figure 2.24.

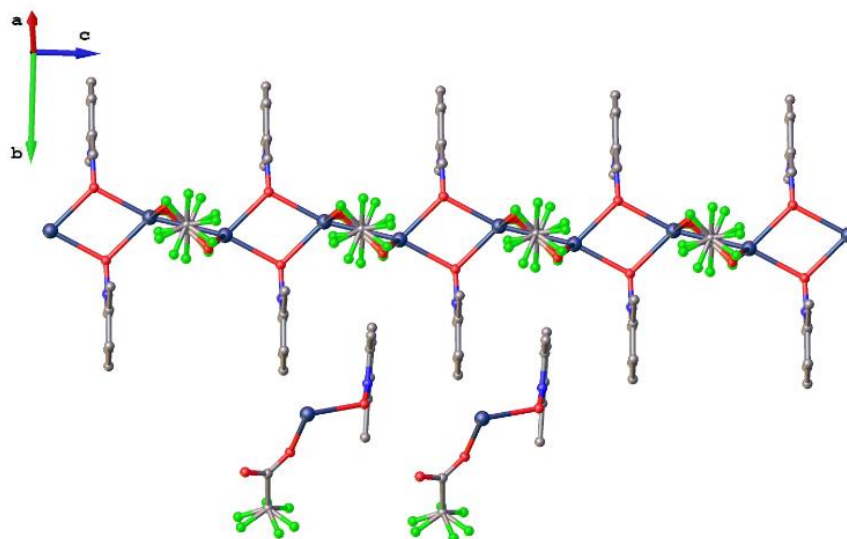


Figure 2.24 – 1D polymeric view of complex **2.24** showing  $\pi$ -stacking. Hydrogen atoms are omitted for clarity.

### With silver(I) triflate (1:1) 2.25

The silver(I) triflate complex **2.25** solved in the triclinic  $P-1$  space group and is shown in figure 2.25. The asymmetric unit has a 1:2 ligand to silver(I) ratio, with ligand **2.4** adopting a  $\mu_2$ -O,O bidentate bridging coordination mode with Ag1 and Ag2. The N-O<sub>ligand</sub> bond distance is 1.344(4) Å, with coordination angles of 116.36(2)° [N1-O1-Ag2] and 110.57(2)° [N1-O1-Ag1]. The angle made by the  $\mu_2$ -O,O bridging oxygen [O1] with Ag1 and Ag2 is 133.03(2)°, with distances of 2.313(2) Å [Ag1-O1], 2.400(3) Å [Ag2-O1]. This bridging angle is greater than that seen in complex **2.24**, and also in other pyridine N-oxide complexes reported to date.<sup>[96]</sup> The four-coordinate Ag1 [ $\tau_4 = 0.38$ ] and Ag2 [ $\tau_4 = 0.55$ ] have O<sub>4</sub> environments, as seen in figure 2.25.

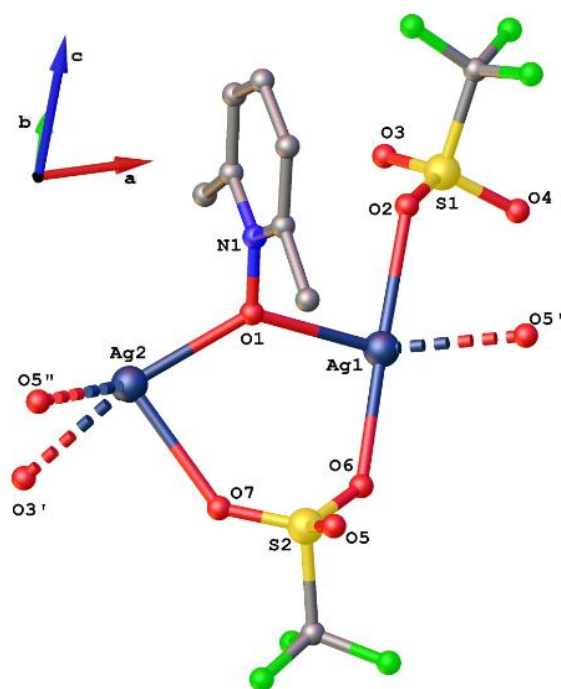


Figure 2.25 – Asymmetric unit of complex **2.25**. Hydrogen atoms are excluded for clarity. Selected bond lengths (Å) and bond angles (°): N1-O1 = 1.344(4), Ag1-O1 = 2.313(2), Ag2-O1 = 2.400(3), N1-O1-Ag2 = 116.36(2), N1-O1-Ag1 = 110.57(2), Ag1-O1-Ag2 = 133.03(2).

The asymmetric unit extends into a 2D polymeric network in the  $ab$ -plane as seen in figure 2.26a, with triflate anions being bidentate or tetradentate. The polymer has bidentate triflate,  $\mu_2$ -O,O bidentate bridging ligands **2.4** and tetradentate triflate 'above and below' [ $+c$  and  $-c$ -directions] the silver(I) lattice, as shown in figure 2.26b.

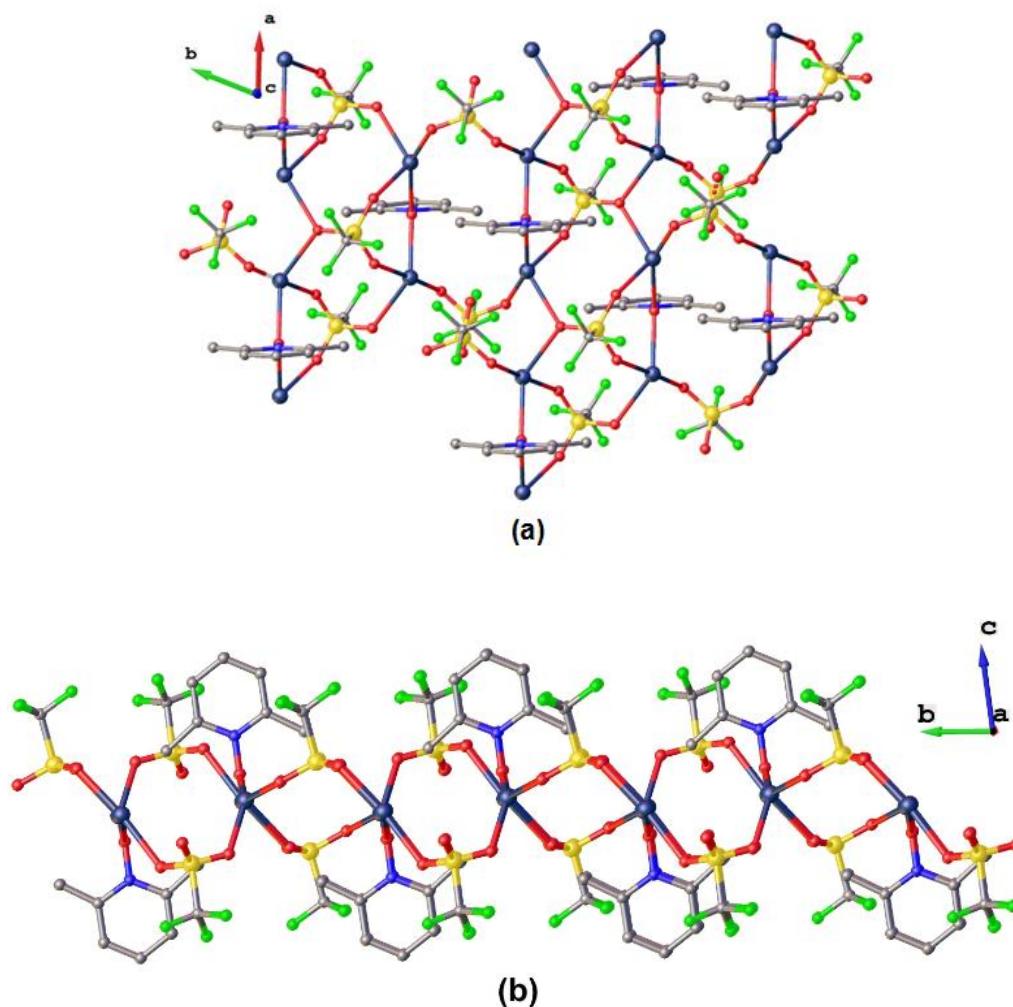


Figure 2.26 – 2D Polymer of complex **2.25** viewed along (a) *c*-axis, and (b) *a*-axis. Hydrogen atoms are omitted for clarity.

#### With silver(I) nitrate (1:1) **2.26**

The silver(I) nitrate complex **2.26** solved in the monoclinic  $P2_1/n$  space group and is shown in figure 2.27 with selected atom labels and bonding parameters. The asymmetric unit contains two ligands **2.4** and two silver(I) ions in a 1:1 ligand to silver(I) ratio. The oxygens, O1 and O2, of the ligand molecules are in a  $\mu_2$ -O,O bidentate bridging coordination mode with Ag1 and Ag2 at distances ranging from 2.320(2) Å to 2.401(2) Å. The N-O bond lengths 1.329(2) Å [N1-O1] and 1.324(3) Å [N2-O2] are close to double bond character with  $sp^2$  hybridized oxygen orbitals evidenced by the  $\mu_2$ -O,O bridging mode with coordination angles ranging from 124.43(1)° to 133.77(2)°. The ligand oxygens [O1 and O2] bridge silver ions [Ag1 and Ag2] at average angles of 101.45° [Ag-O<sub>ligand</sub>-Ag] to form a non-planar rectangle, with ligands [**2.4**] being orthogonal to this plane; 88.44(2)° [Ag2-O1-N1-C6].

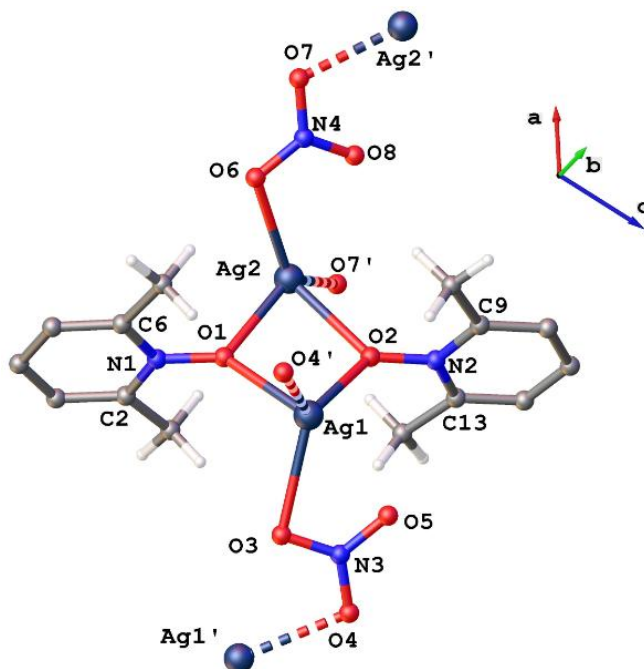


Figure 2.27 – Asymmetric unit of complex **2.26**. Selected hydrogen atoms are excluded for clarity. Selected bond lengths (Å) and bond angles (°): N1-O1 = 1.329(2), N2-O2 = 1.324(3), Ag1-O2 = 2.341(2), Ag1-O1 = 2.401(2), Ag2-O1 = 2.320(2), Ag2-O2 = 2.375(2), N1-O1-Ag2 = 124.43(1), N1-O1-Ag1 = 133.77(1), N2-O2-Ag1 = 129.66(2), N2-O2-Ag2 = 128.37(1), Ag2-O1-Ag1 = 101.38(6), Ag1-O2-Ag2 = 101.53(7).

The four-coordinate silver(I) ions [Ag1 ( $\tau_4 = 0.73$ ) and Ag2 ( $\tau_4 = 0.37$ )] have four oxygen donors supplied from the ligands and nitrate anions, as shown in figure 2.27. The asymmetric unit grows into a 2D polymeric network, as shown in figure 2.28, with Ag1 centers linked by unsymmetrical bidentate nitrate anions, while the Ag2 centers are linked by symmetrical bidentate nitrate anions.

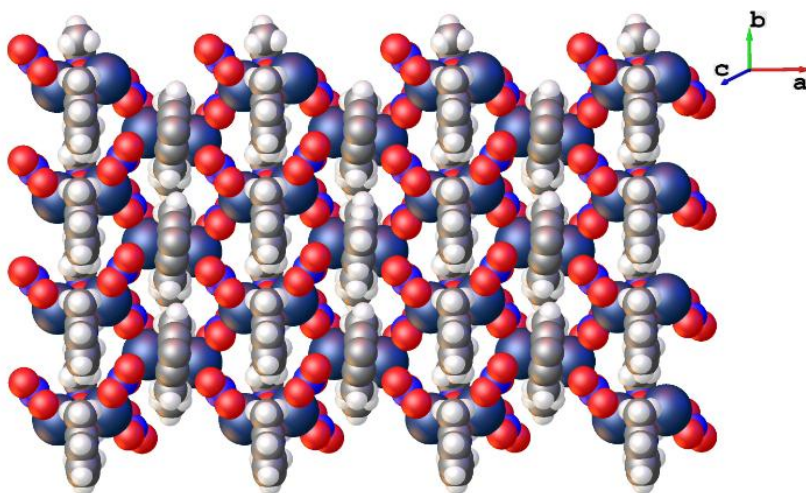


Figure 2.28 – 2D Polymeric view of complex **2.26** using a space filling model.

The section of the 2D polymer shown in figure 2.29a will be used to discuss the bridging modes of the nitrate anions and Ag<sup>+</sup>–Ag relationships. The polymer uses four bridging ligands, six silver ions and four bridging nitrate anions to form a 20-membered ring system [figure 2.29a]. Within the ring system, Ag1–Ag1' and Ag1'–Ag1'', are joined by unsymmetrical bidentate nitrate anions [figure 2.29b], whereas the silver ions Ag2''–Ag2''' and Ag2'''–Ag2 are linked by symmetrical bidentate nitrate anions [figure 2.29c]. The silver(I) ions, Ag1–Ag2 and Ag1''–Ag2'', are separated by a distance of 3.654 Å and are held together by two ligands bridging on either side. The Ag1–Ag1' and Ag1'–Ag1'' distances [5.245 Å] are shorter than the Ag2''–Ag2''' and Ag2'''–Ag2 distances [5.542 Å]; the difference is due to the fact that the distance required for symmetrical nitrate bridging is larger than for unsymmetrical bridging.

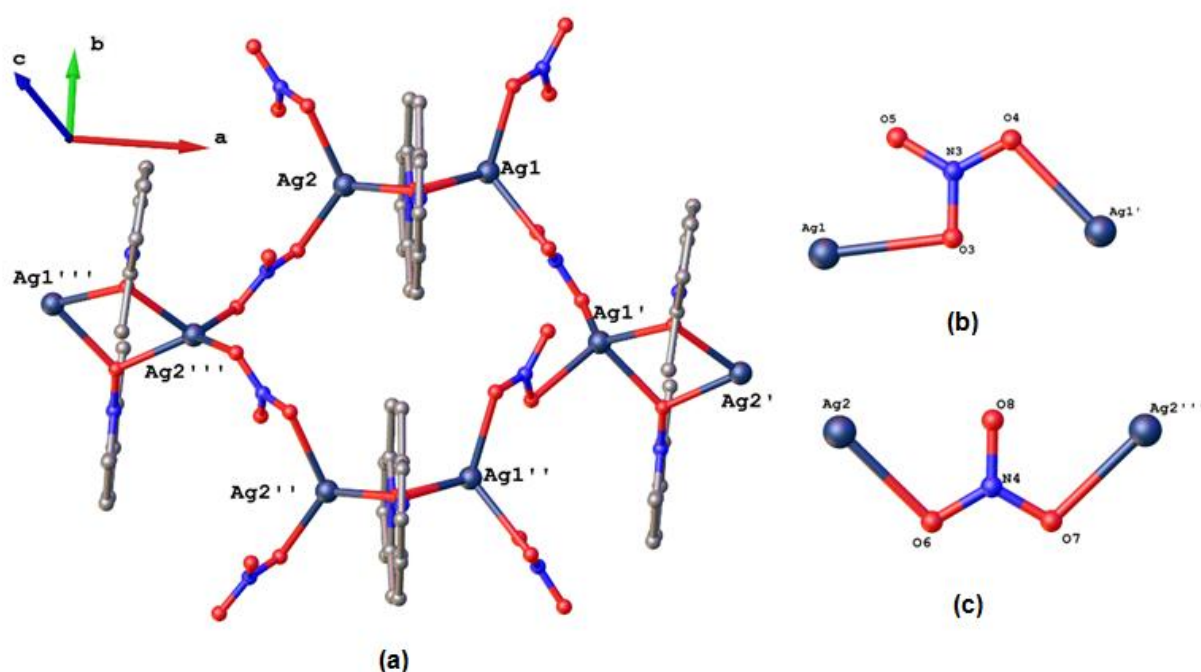


Figure 2.29 – (a) Section of the cyclic 20-membered repeating unit of complex **2.26**, (b) unsymmetrical bridging mode of the bidentate anion, and (c) symmetrical bridging mode of the bidentate nitrate anion. Hydrogen atoms are omitted for clarity.

The polymer grows two-dimensionally in the *ab*-plane to form 2D sheets, with adjacent sheets having  $\pi$ - $\pi$  interactions along the *a*-axis with centroid-centroid distances of 3.856 Å, as shown in figure 2.30.

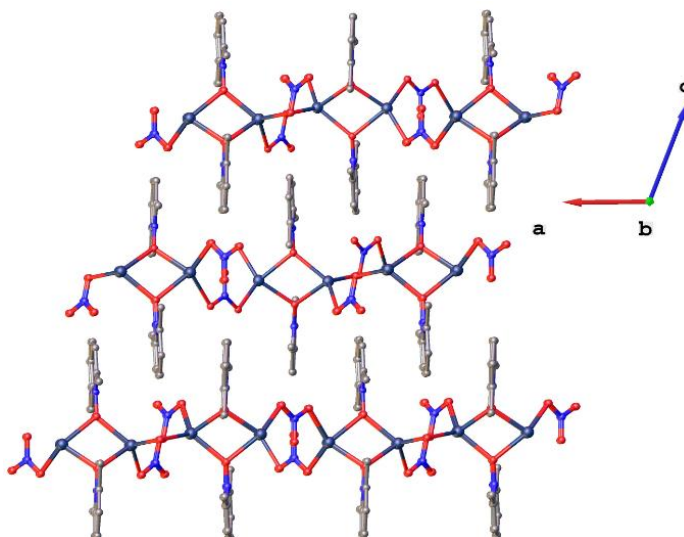
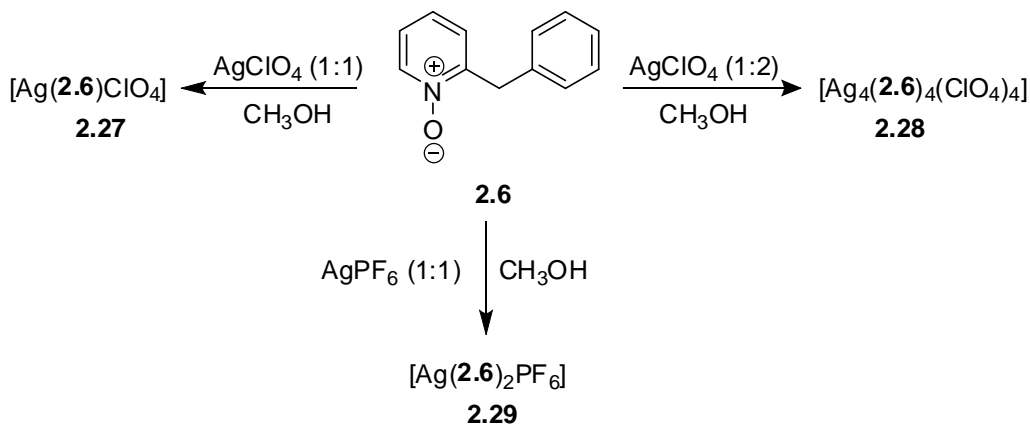


Figure 2.30 – Three-dimensional  $\pi$ -stacking view of the 2D polymeric structure of complex **2.26** viewed down the  $b$ -axis. Hydrogen atoms are omitted for clarity.

A number of attempts to grow crystals of complexes with ligand **2.5** were unsuccessful using different crystal growth techniques and solvent conditions. So we moved to synthesise complexes with ligand **2.6** in the listed pyridine N-oxides shown in figure 2.1.

### 2.3.3 Complexes with 2-benzylpyridine N-oxide **2.6**

The N-O group of ligand **2.6** not only provides an oxygen donor similar to the complexes discussed with ligand **2.4**, but also ligand **2.6** offers an additional site to interact with silver(I) ions in the form of the phenyl ring. Also, ligand **2.6** is the basis for comparison of ligands **2.9** and **2.10** with the  $-\text{CH}-$  functionalities to check for the formation of  $\text{Ag}\cdots\text{C}$  contacts in silver(I) complexes. Three complexes were successfully synthesised but attempts to grow crystals with other silver(I) salts were unsuccessful.



Scheme 2.11 – Syntheses of complexes **2.27** – **2.29**.

### With silver(I) perchlorate (1:1) 2.27

X-Ray analysis demonstrated that complex **2.27** has a 1:1 ligand **2.6** to AgClO<sub>4</sub> ratio. The asymmetric unit of complex **2.27** in the monoclinic  $P2_1/c$  space group comprises one ligand [**2.6**] and a silver(I) perchlorate, as shown in figure 2.31. The oxygen of the N-oxide group adopts a  $\mu_2$ -O,O bidentate bridging coordination mode with Ag1 and Ag1' at distances of 2.479(2) Å [Ag1-O1] and 2.275(2) Å [Ag1'-O1]. The coordination angles 127.45(9)° [N1-O1-Ag1] are close to  $sp^2$  hybridization angles, with bond distances of 1.339(2) Å [N1-O1]. The silver(I) ion is four-coordinate [ $\tau_4 = 0.48$ ] bound to oxygens from two ligands [O1 and O1'], a perchlorate anion [O2] and a Ag- $\pi$  aromatic interaction [C10 and C11], as shown in figure 2.31. The Ag-C [Ag1''-(C10,11)] contact has a distance of 2.378(2) Å.

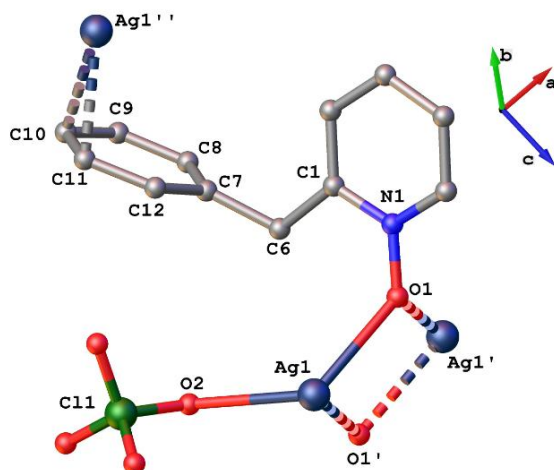


Figure 2.31 – Asymmetric unit of complex **2.27**. Hydrogen atoms are excluded for clarity. Selected bond lengths (Å) and bond angles (°): N1-O1 = 1.338(2), Ag1-O1 = 2.479(2), Ag1'-O1 = 2.275(2), Ag1''-(C10,11) = 2.378(2), N1-O1-Ag1 = 127.45(9), Ag1-O1-Ag1' = 106.80(5).

The oxygens [O1 and O1'] of two ligand molecules bridge the silver(I) ions about a center of inversion, as shown in figure 2.32. As a consequence the Ag<sub>2</sub>O<sub>2</sub> ring is planar, with a non-bonded Ag...Ag distance of 3.819 Å. The two bridging ligand molecules are orthogonal to the four-membered Ag<sub>2</sub>O<sub>2</sub> parallelograms. The internal angles subtended in the parallelogram are 106.80(5)° [Ag1'-O1-Ag1] and 73.21(5)° [O1-Ag1'-O1']. Additionally, two perchlorate anions [O2 and O2'] are coordinated to Ag1 and Ag1' in a *trans*-fashion with respect to the Ag<sub>2</sub>O<sub>2</sub> plane. The bond distances and angles made by the perchlorate oxygens with silver(I) ions are 2.598(1) Å [Ag1-O2] and 120.30(8)° [Cl1-O2-Ag1]. The complex **2.27** is a 2D polymer that propagates in the *bc*-plane, as shown in figure 2.33.

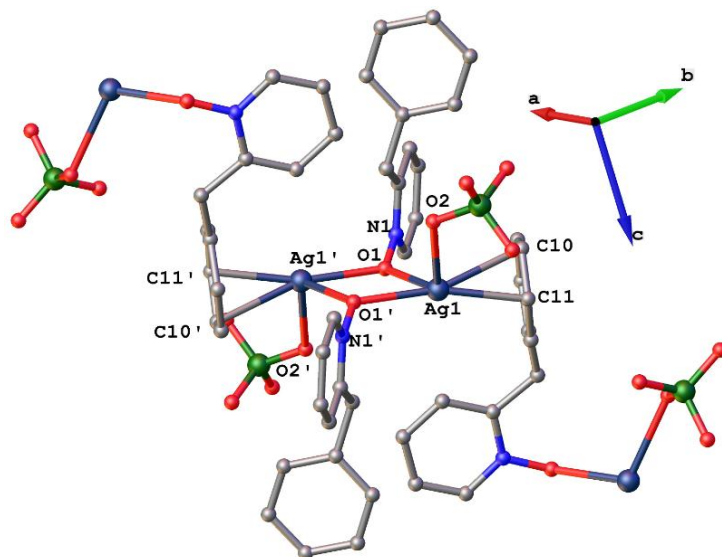


Figure 2.32 – A Section of the 2D polymeric unit of complex **2.27**. Hydrogen atoms are omitted for clarity. Selected bond lengths (Å) and bond angles (°); Ag1-O1 = 2.480(1), Ag1-O2 = 2.599(5), Ag1'-O1-Ag1 = 106.80(5), O1-Ag1'-O1' = 73.21(5), C11-O2-Ag1 = 120.30(8), Ag1-(C10,11) = 2.378(2).

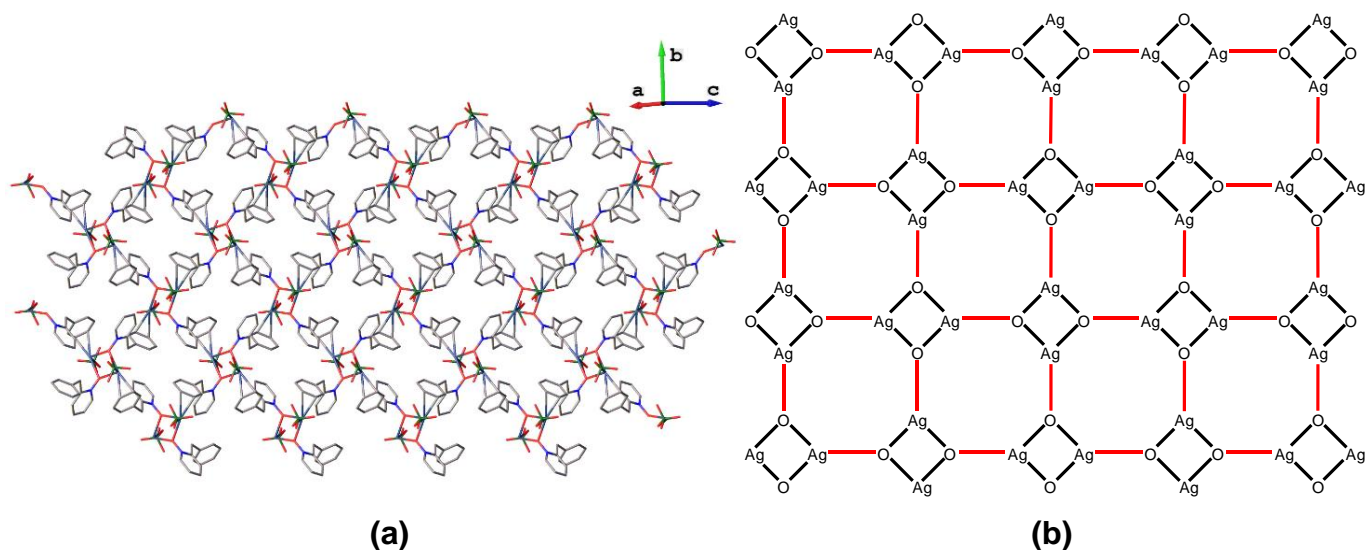


Figure 2.33 – (a) 2D polymeric view of complex **2.27**, (b) Topological view of complex **2.27** [the red coloured lines indicate phenyl rings coordinated to silver(I) ions].

### With silver(I) perchlorate (1:2) **2.28**

The complex **2.28** was prepared by reacting 1:2 stoichiometric ratios of ligand **2.6** to silver(I) perchlorate. The asymmetric unit of complex **2.28** in the monoclinic  $P2_1/c$  space group contains four ligand [**2.6**] molecules and four silver(I) ions in a 1:1 ligand to silver(I) ratio. The asymmetric unit also has three monodentate and one non-coordinated perchlorate anions. The ligands [**2.6**] exhibit  $\mu_2$ -O,O,  $\mu_3$ -O,O,C<sub>44</sub>,  $\mu_3$ -O,O,C<sub>9,10</sub>, and  $\mu_4$ -O,O,C<sub>33,34</sub>,C'<sub>36</sub> coordination modes, as shown in figure 2.34. Though the coordination modes of the phenyl ring vary for different ligands **2.6** in the



asymmetric unit, the denticity observed for all N-O groups is two. The three monodentate perchlorate anions are coordinated to silver(I) ions at distances of 2.411(3) Å [Ag2-O5], 2.582(3) Å [Ag3-O9], 2.397(3) Å [Ag4-O13].

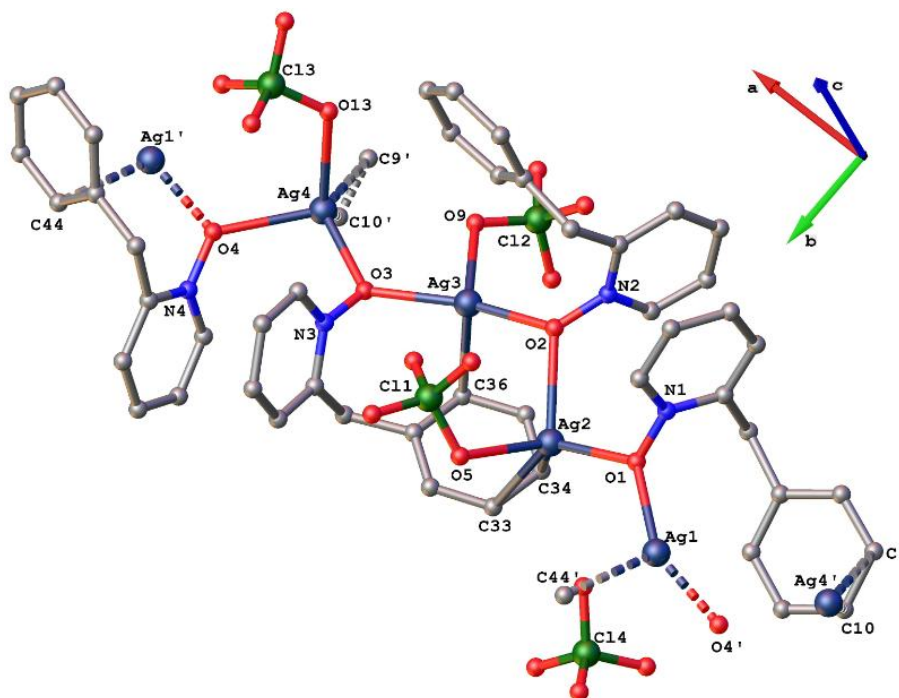


Figure 2.34 – Asymmetric unit of complex **2.28**. Hydrogen atoms are excluded for clarity. Selected bond lengths (Å) and bond angles (°): N1-O1 = 1.342(4), N2-O2 = 1.339(5), N3-O3 = 1.351(4), N4-O4 = 1.332(5), Ag1-O1 = 2.309(3), Ag2-O1 = 2.305(3), Ag2-O2 = 2.403(3), Ag3-O2 = 2.279(3), Ag3-O3 = 2.318(3), Ag4-O3 = 2.310(3), Ag4-O4 = 2.379(3), Ag1'-O4 = 2.311(3), Ag2-O5 = 2.411(3), Ag3-O9 = 2.582(3), Ag4-O13 = 2.397(3), N1-O1-Ag2 = 117.2(2), N1-O1-Ag1 = 111.9(2), N2-O2-Ag3 = 120.2(2), N2-O2-Ag2 = 124.2(2), N3-O3-Ag4 = 117.7(2), N3-O3-Ag3 = 109.1(2), N4-O4-Ag1' = 115.5(2), N4-O4-Ag4 = 125.1(2), Ag2-O1-Ag1 = 127.04(1), Ag3-O2-Ag2 = 102.15(1), Ag4-O3-Ag3 = 129.10(1), Ag1'-O4-Ag4 = 110.51(1), Ag1'-C44 = 2.645(5), Ag4'-C9 = 2.542(4), Ag4'-C10 = 2.427(4), Ag2-C34 = 2.458(4), Ag2-C33 = 2.542(4), Ag3-C36 = 2.692(4), Ag4'-(C9,10) = 2.384(4), Ag2-(C33,34) = 2.400(4).

The N-O bond distances vary from 1.332(5) Å to 1.351(4) Å, with an average value of 1.341 Å, which is close to the values obtained for the  $\mu_2$ -O,O ligands **2.6** observed in complex **2.27**. There are one three- [Ag1] and three four- [Ag2 ( $\tau_4 = 0.80$ ), Ag3 ( $\tau_4 = 0.53$ ) and Ag4 ( $\tau_4 = 0.84$ )] coordinate geometry silver(I) ions, as shown in figure 2.34. The average Ag-O<sub>ligand</sub> bond lengths of ligands **2.6** in complex **2.28** [2.326(3) Å] are close to the values observed in complex **2.27** [2.377(2) Å]. The ligand oxygens bridging and coordination angles range from 102.15(1)° to 129.10(1)° and 109.1(2)° to 125.1(2)° respectively. The Ag-C contacts are at distances of 2.645(5) Å [Ag1'-C44], 2.692(4) Å [Ag3-C36], 2.384 (4) Å [Ag4'-(C9,10)] and 2.400(4) Å [Ag2-(C33,34)], and all fall in the range of reported Ag(I)- $\pi$  distances.<sup>[97]</sup>

The complex is a 1D polymer with three-coordinate [Ag1] and four-coordinate [Ag2, Ag3 and Ag4] silver(I) ions with multiple  $\pi$ - $\pi$  interactions in the crystal packing. Every aromatic ring of the ligand **2.6** molecules exhibits  $\pi$ - $\pi$  interactions, as shown in figure 2.35. The shortest  $\pi$ - $\pi$  interaction is observed between the pyridine rings of ligand **2.6** molecules at a centroid-centroid distance of 3.511 Å. The next shortest distance of 3.660 Å is observed between  $\mu_3$ -O,O,C<sub>44</sub> and  $\mu_2$ -O,O coordination mode ligand **2.6** molecules of two different 1D polymers in the crystal packing. Similar  $\pi$ - $\pi$  interactions are also observed between the  $\mu_3$ -O,O,C<sub>9,10</sub> and  $\mu_2$ -O,O ligands at a distance of 3.696 Å, and between two  $\mu_2$ -O,O ligands at a distance of 3.904 Å, as shown in figure 2.35.

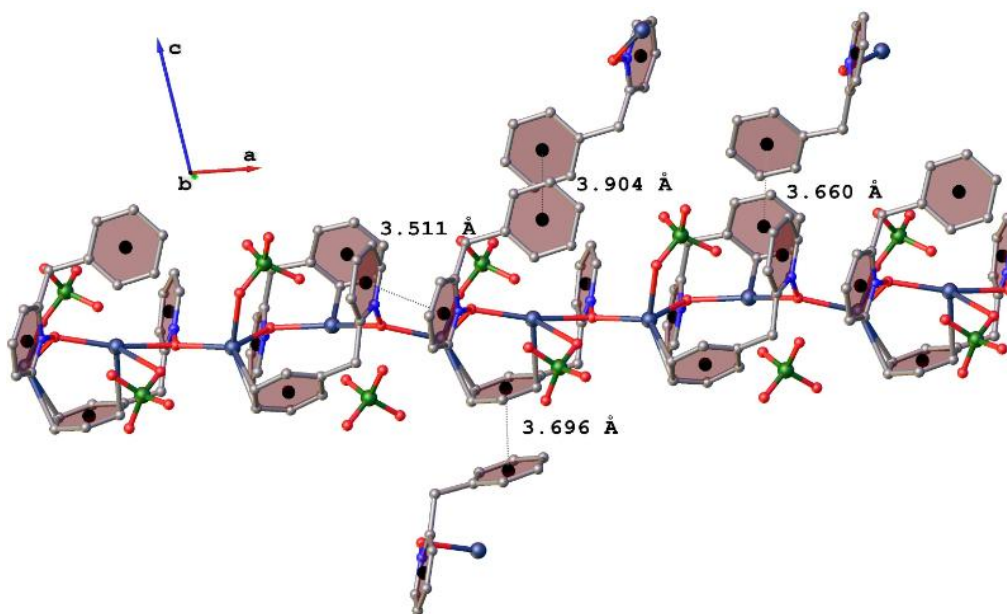


Figure 2.35 – Crystal packing diagram of complex **2.28** showing the  $\pi$ - $\pi$  interactions. Hydrogen atoms are omitted for clarity.

#### With silver(I) hexafluorophosphate (1:1) **2.29**

The discrete structure of complex **2.29** solved in the triclinic *P*-1 space group and has ligand **2.6** molecules in  $\mu_3$ -O,O,C<sub>20,21</sub> and  $\mu_3$ -O,O,C<sub>7,12</sub> coordination modes, as shown in figure 2.36. The asymmetric unit of complex **2.29** comprises two ligands and one silver(I) cation with a non-coordinated PF<sub>6</sub> anion. The complex **2.29** has a 2:1 ligand to silver(I) ratio. The phenyl rings, and their respective monodentate N1-O1 and bidentate N2-O2, form six- and seven-membered ring systems at the five-coordinate Ag1 [ $\tau_5 = 0.18$ ] centers, as shown in figure 2.36. The monodentate N1-O1 [1.317(2) Å] bond is shorter than the bidentate N2-O2 [1.330(2) Å] bond. Though ligand **2.6** exhibits different N-O bond distances, the average coordination abilities of N1-O1 [Ag1-O1 =

2.387(1) Å] and N2-O2 [Ag1-O2 = 2.388(1) Å] are similar. The coordination angles of the monodentate N1-O1 groups [134.24(1)°] are greater than the bidentate N2-O2 [124.56(9)°] groups.

The two  $\mu_2$ -O,O oxygens [O2 and O2'] and two silver ions [Ag1 and Ag1'] form a four-membered ring with unequal sides of 2.374(1) Å [Ag1'-O2] and 2.388(1) Å [Ag1-O2], as shown in figure 2.36. As a result of symmetry, the Ag<sub>2</sub>O<sub>2</sub> ring is planar in the form of a parallelogram with internal angles of 110.33(4)° [Ag1-O2-Ag1'] and 69.67(4)° [O2-Ag1-O2']. The two pyridine rings of the bidentate oxygens [O2] are orthogonal to the Ag<sub>2</sub>O<sub>2</sub> ring with torsional angles of 98.64(2)° [C17-N2-O2-Ag1]. However, the monodentate N1-O1 is coordinated to the Ag<sub>2</sub>O<sub>2</sub> ring at an angle of 143.77(2)° [N1-O1-Ag1-O2]. The distance between the two non-bonded silver(I) ions is 3.908 Å, which were longer than the values observed for complex **2.28**. The phenyl rings are coordinated to Ag1 ions at distances of 2.482(2) Å and 2.682(2) Å. The aromatic carbons C20,21/C20',21' are coordinated at Ag1 centers in a *trans*- arrangement to the Ag<sub>2</sub>O<sub>2</sub> ring at an angle of 83.47(2)° [C20,21-Ag1-O2], as shown in figure 2.36. The Ag-C contact distances of 2.482(2) Å are also similar to the values observed in complex **2.28**.

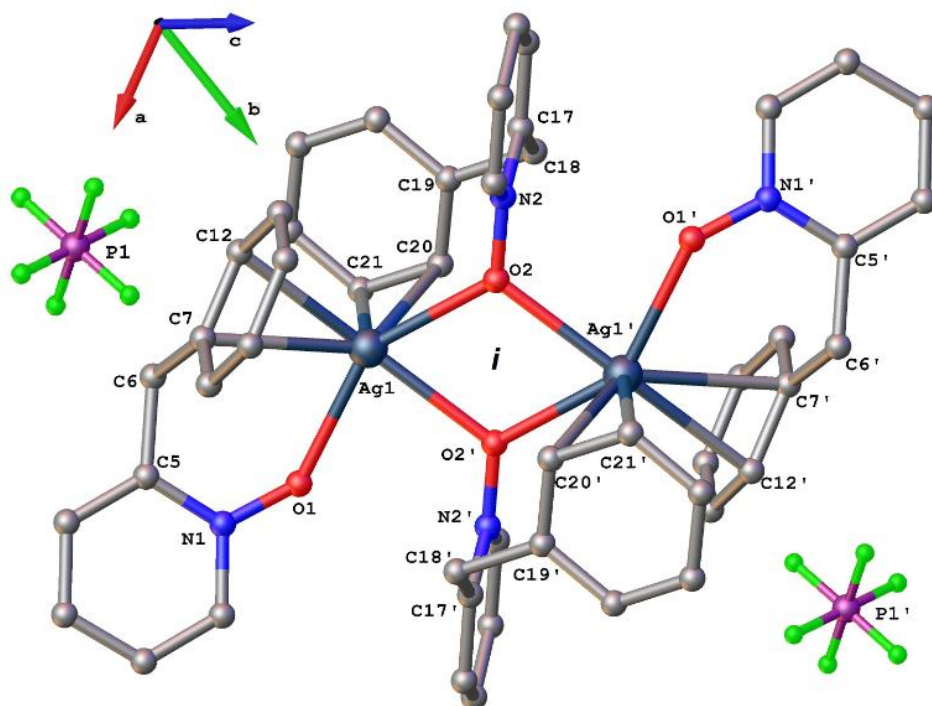


Figure 2.36 – Discrete structure of complex **2.29**. Hydrogen atoms are excluded for clarity. Selected bond lengths (Å) and bond angles (°): N1-O1 = 1.317(2), N2-O2 = 1.330(2), Ag1-O1 = 2.387(1), Ag1'-O2 = 2.374(1), Ag1-O2 = 2.388(1), Ag1-Ag1' = 3.908, Ag1-(C20,21) = 2.682(2), Ag1-(C7,12) = 2.482, Ag1-O2-Ag1' = 110.33(4), O2-Ag1-O2' = 69.67(4), N1-O1-Ag1 = 134.24(1), N2-O2-Ag1 = 121.98(9), N2-O2-Ag1' = 127.15(9), C17-N2-O2-Ag1 = 98.64(2), N1-O1-Ag1-O2 = 143.77(2), C20,21-Ag1-O2 = 83.47(2).

In the crystal packing of complex **2.29** the pyridine rings of the monodentate N1-O1 groups exhibit  $\pi$ - $\pi$  interactions at distances of 3.527 Å, as shown in figure 2.37.

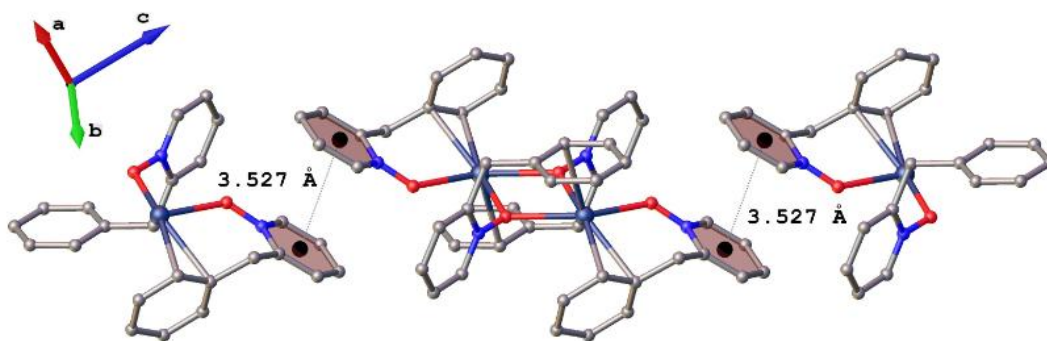
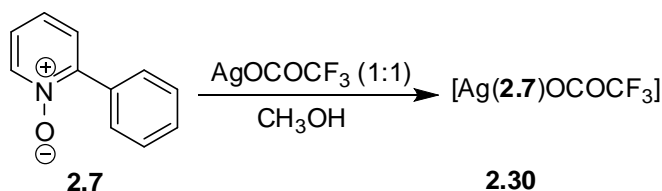


Figure 2.37 – Crystal packing diagram of complex **2.29** illustrating  $\pi$ - $\pi$  interactions. Hydrogen atoms are omitted for clarity.

### 2.3.4 Complexes with 2-phenylpyridine N-oxide **2.7**

To date, crystal structures have been reported where 2-phenylpyridine has been employed as a cyclometallating ligand in palladium,<sup>[98]</sup> platinum,<sup>[99]</sup> iridium<sup>[100]</sup> and ruthenium<sup>[101]</sup> complexes. To the best of our knowledge, no X-ray crystal structures of metal complexes of ligand **2.7** have been reported. Several attempts were made to grow crystals with various silver(I) salts with ligand **2.7** using different crystal growth methods; however all of these were unsuccessful except with AgOCOCF<sub>3</sub>. The obtained silver(I) complex is discrete, with the asymmetric unit composition shown in scheme 2.12. Attempts were made to crystallise more complexes with varied AgOCOCF<sub>3</sub> to ligand **2.7** ratios in order to construct a polymeric network but these were unsuccessful.



Scheme 2.12 – Synthesis of complex **2.30**.

#### With silver(I) trifluoroacetate (1:1) **2.30**

The crystal structure of complex **2.30** solved in the triclinic *P*-1 space group and contains one ligand molecule [**2.7**] and one silver(I) trifluoroacetate in a 1:1 ligand to silver(I) ratio, as shown in figure 2.38a. The N-oxide groups of the ligand [**2.7**] are monodentate and the silver(I) ions are four-coordinate [ $\tau_4 = 0.40$ ] with an Ag<sub>1</sub>O<sub>3</sub> environment, as shown in figure 2.38b. The coordination angle of 110.71(8)° [N1-O1-Ag1] and short bond distance of 1.317(2) Å [N1-O1] implies that the oxygen orbitals are sp<sup>2</sup> hybridized. Complex **2.30** is a discrete structure with trifluoroacetate anions bridging on either side of strongly interacting silver-silver bonds with distances of 2.988(2)

Å [Ag1 $\cdots$ Ag1']. The two phenyl substituents in the discrete structure are twisted at angles of 132.1(2)° [N1-C5-C6-C7] in parallel fashion to the Ag $\cdots$ Ag interactions at a distance of 3.173 Å [closest distance Ag1'-C8].

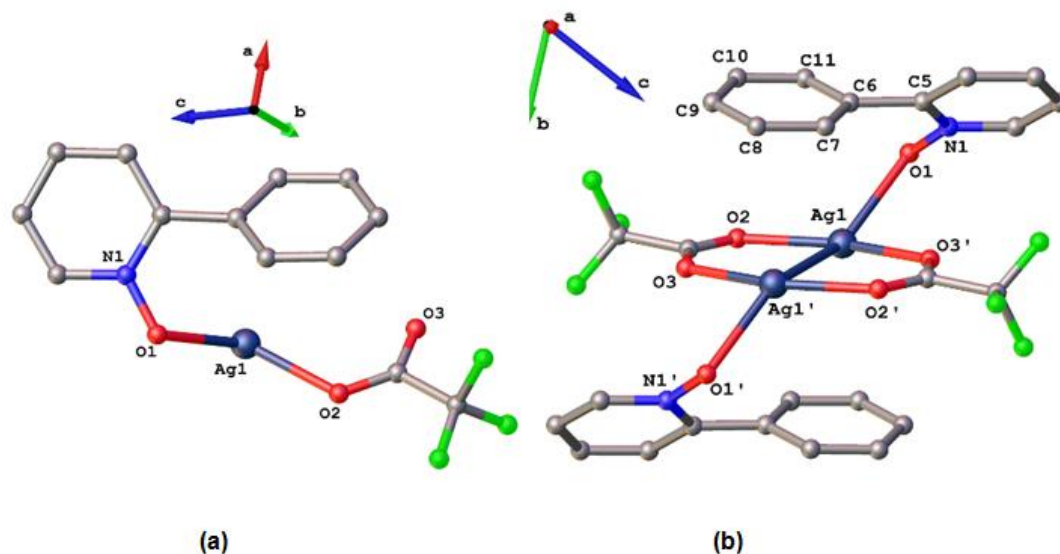
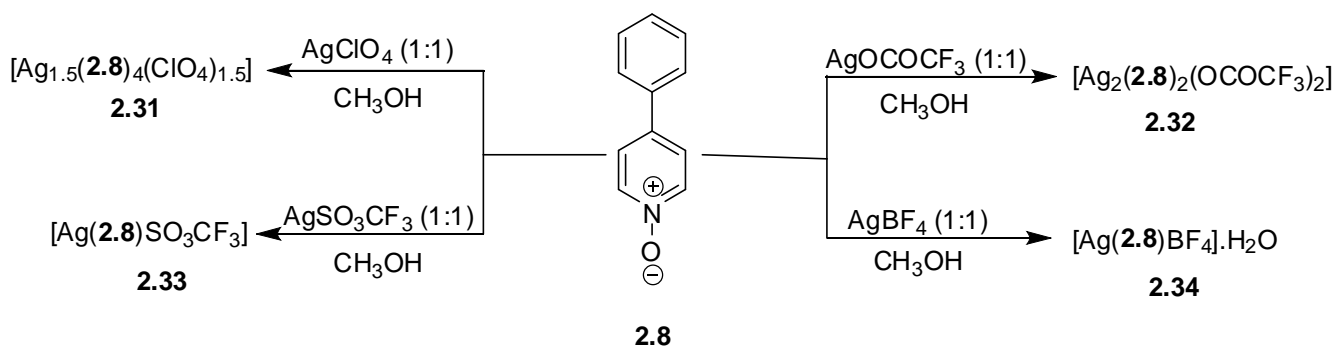


Figure 2.38 – (a) Asymmetric unit of complex **2.30**, (b) discrete dimeric assembly of complex **2.30**. Hydrogen atoms are excluded for clarity. Selected bond lengths (Å) and bond angles (°): N1-O1 = 1.317(2), Ag1-O1 = 2.443(2), Ag1-O2 = 2.243(2), Ag1'-O3 = 2.261(2), Ag1-Ag1' = 2.988(2), N1-O1-Ag1 = 110.71(8), N1-C5-C6-C7 = 132.1(2).

### 2.3.5 Complexes with 4-phenylpyridine N-oxide **2.8**

Four complexes were synthesised under similar solvent conditions with a 1:1 ligand **2.8** to silver(I) salt ratios, as shown in scheme 2.13. All four complexes have different dimensionalities based on the role played by the anion employed. In complex **2.31**, the perchlorate anion is non-coordinated with multiple Ag $\cdots$ Ag interactions. Complex **2.32** has a 1D chain with the expected dimeric trifluoroacetate Ag $\cdots$ Ag contacts similar to complex **2.24**, and complex **2.33** is two-dimensional similar to complex **2.21**. Complex **2.34** is a 1D linear staircase polymer with extended Ag-C contacts from the phenyl rings of ligand **2.8**.



Scheme 2.13 – Syntheses of complexes **2.31** – **2.34**.

The phenyl ring of ligand **2.8** afforded some  $\pi$ - $\pi$  interactions to extend complexes **2.31** and **2.32** three-dimensionally and **2.34** in two-dimensions. The results revealed that the nature of the counterion and ligand has a great impact on the structure of the complexes. In addition, the phenyl substituent plays an important role, linking low dimensional entities into higher dimensional frameworks.

#### With silver(I) perchlorate (1:1) **2.31**

Complex **2.31** solved in the triclinic *P*-1 space group with four ligands **2.8** and one and a half silver(I) perchlorates in a 4:1.5 ligand to silver(I) ratio, as shown in figure 2.39. The two perchlorate anions are non-coordinated in this structure. The complex **2.31** consists of one monodentate and three  $\mu_2$ -O,O bidentate ligand **2.8** molecules, as shown in figure 2.39b. The  $\mu_2$ -O,O bidentate ligands **2.8** are bridging over Ag1, Ag2 and Ag1', which are interacting linearly at a distance of 3.258(4) Å [Ag1-Ag2]. The N2-O2 and N3-O3 bond distances are 1.326(4) Å and 1.337(5) Å with bridging angles 81.57(9)° [Ag2-O2-Ag1'] and 83.40(9)° [Ag1-O3-Ag2], respectively. The Ag-O<sub>ligand</sub> bond lengths of N2-O2 and N3-O3 bridging across Ag1-Ag2-Ag1' range from 2.403(3) Å to 2.581(3) Å.

The silvers Ag1 and Ag2 are both six-coordinate with Ag<sub>1</sub>O<sub>5</sub> and Ag<sub>2</sub>O<sub>4</sub> environments, respectively, as shown in figure 2.39b. Two bidentate N1-O1 and N1'-O1' groups bridge Ag1 and Ag1'' forming a four-membered Ag<sub>2</sub>O<sub>2</sub> ring, as shown in figure 2.39b. The N1-O1 bond distance [1.347(4) Å] is longer than the other bidentate N-O groups observed in the complex. The internal angles in the Ag<sub>2</sub>O<sub>2</sub> ring are 89.81(1)° [Ag1-O1-Ag1'] and 90.39(1)° [O1-Ag1-O1'] with two unequal coordination distances of 2.287(3) Å [Ag1-O1] and 2.553(3) Å [Ag1''-O1], and two coordination angles of 127.7(3)° [N1-O1-Ag1] and 121.8(2)° [N1-O1-Ag1'']. The non-bonded distance between Ag1 and Ag1'' [3.419 Å] is longer than Ag $\cdots$ Ag distances observed in complex **2.31**.

Two monodentate oxygens O4 and O4' of ligand **2.8**, as shown in figure 2.39b, are coordinated to Ag1 ions in a *trans*- fashion across the four-membered Ag<sub>2</sub>O<sub>2</sub> ring at a distance of 2.216(4) Å [Ag1/Ag1''-O4], with coordination angles of 115.3(3)° [N4-O4-Ag1]. The monodentate N4-O4 [1.328(5) Å] groups have shorter Ag-O<sub>ligand</sub> bond lengths than the bidentate groups. The two aromatic rings are twisted with respect to each other about the C-C bond, and their torsional angles range from 25.6(6)° to 31.6(6)°.

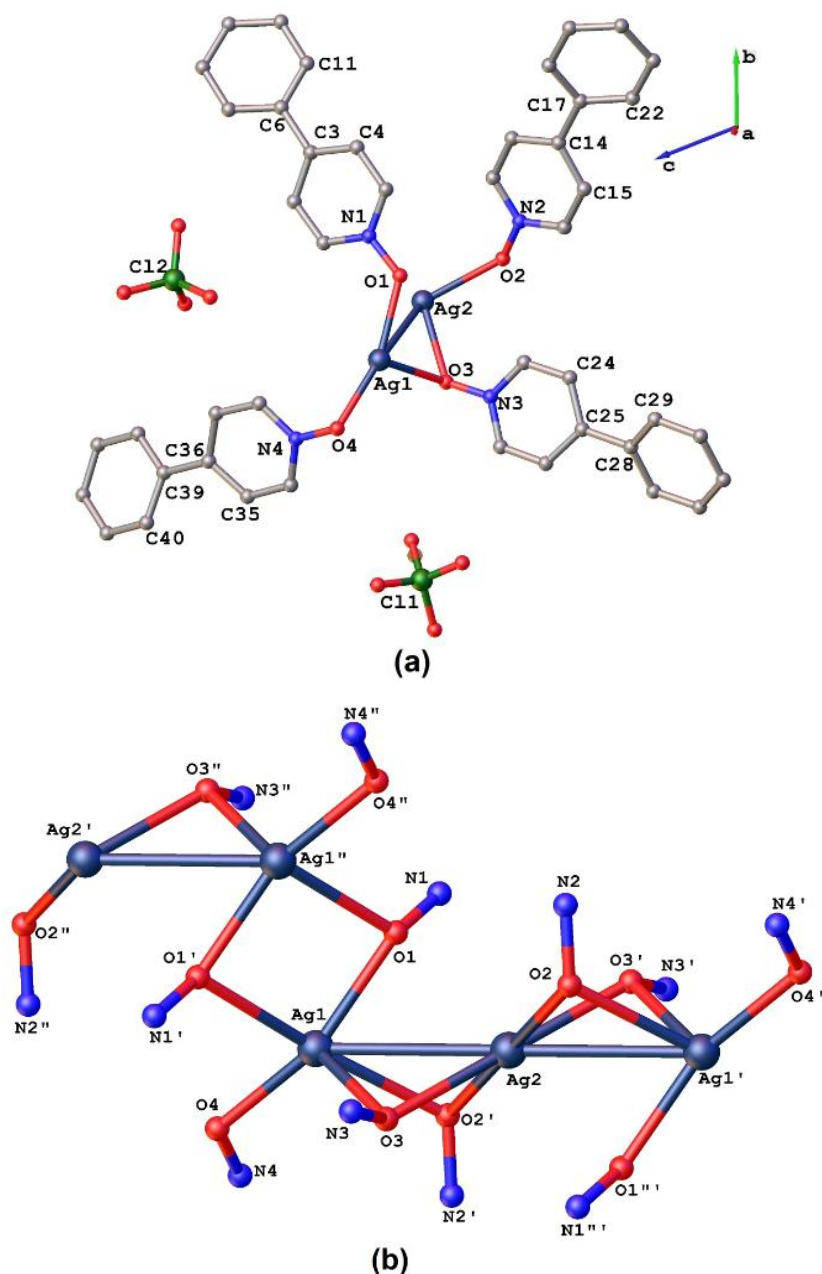


Figure 2.39 – (a) Asymmetric unit of complex **2.31**, hydrogen atoms are excluded for clarity. (b) Central coordination view of complex **2.31** constructed using Ag, O and N atoms. Selected bond lengths (Å) and bond angles (°): N1-O1 = 1.347(4), N2-O2 = 1.326(4), N3-O3 = 1.337(5), N4-O4 = 1.328(5), Ag1-O4 = 2.216(4), Ag1-O1 = 2.287(3), Ag1-O3 = 2.457(3), Ag1-O1' = 2.553(3), Ag1-O2' = 2.581(3), Ag2-O2 = Ag2-O2' = 2.403(3), Ag2-O3 = Ag2-O3' = 2.441(3), Ag1-O3 = 2.457(3), N2-O2-Ag2 = 125.5(2), N2-O2-Ag1' = 122.2(2), N3-O3-Ag2 = 129.7(2), N3-O3-Ag1 = 116.0(2), Ag1-O3-Ag2 = 83.40(9), Ag2-O2-Ag1' = 81.57(9), Ag1-Ag2 = 3.258(4), C4-C3-C6-C11 = 30.3(6), C15-C14-C17-C22 = 25.6(6), C24-C25-C28-C29 = 31.6(6), C35-C36-C39-C40 = 27.8(6).

Complex **2.31** is a 1D polymer extending along the *a*-axis, with silver(I) ions in six-coordinate geometry, as shown in figure 2.40.

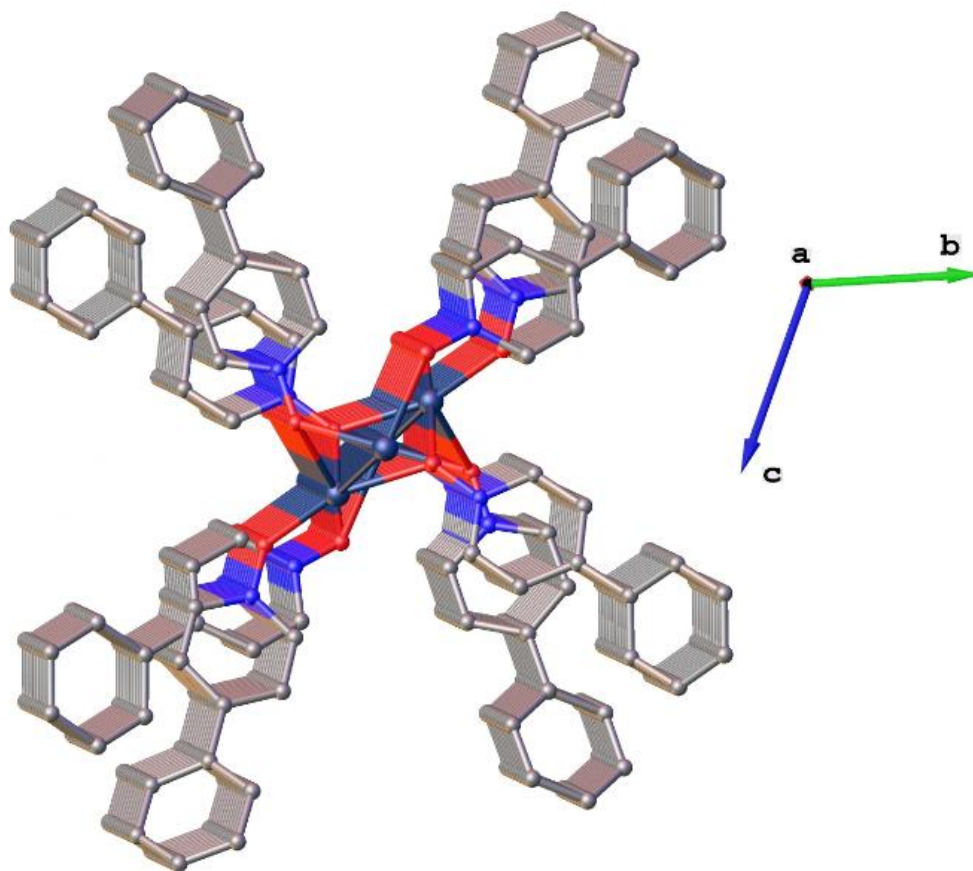


Figure 2.40 – 1D polymeric view of the complex **2.31** along the  $a$ -axis. The anions and hydrogen atoms are excluded for clarity.

Complex **2.31** has  $\pi$ - $\pi$  interactions between monodentate ligands from different 1D polymers at centroid-centroid distances of 3.675 Å to give an extended 3D network; as shown in figure 2.41. There also exist intramolecular  $\pi$ - $\pi$  interactions between monodentate and bidentate ligands at distances of 3.486 Å, as shown in figure 2.41.



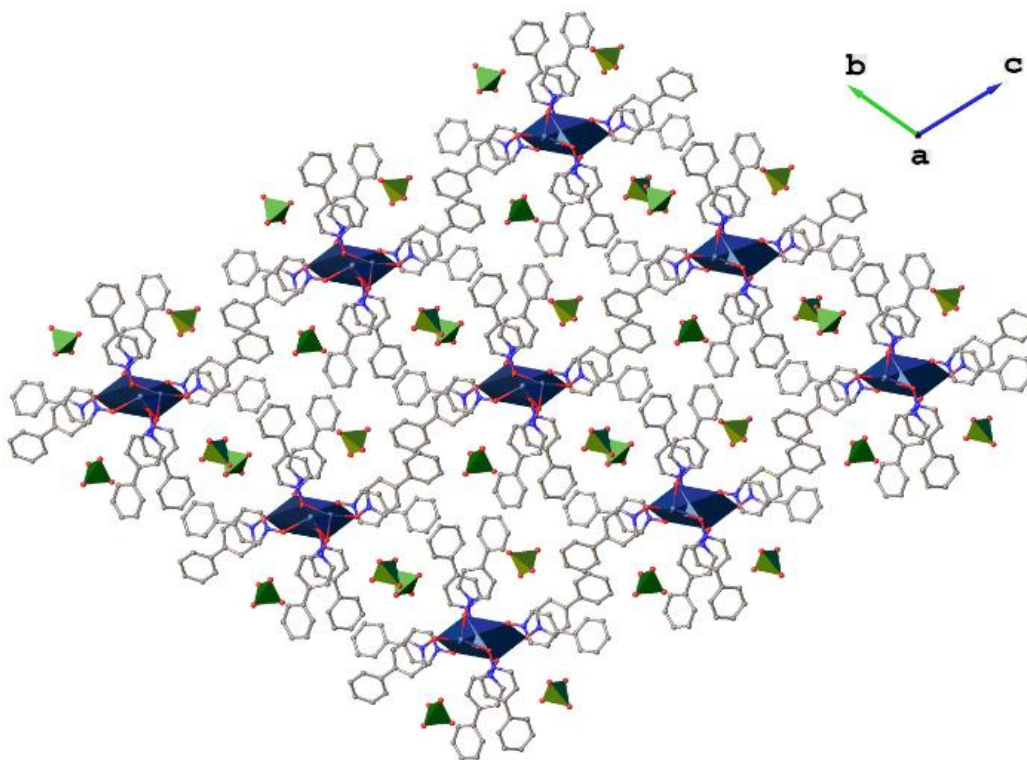


Figure 2.41 – Crystal packing diagram of complex **2.31**, viewed down the *a*-axis. Hydrogen atoms are omitted for clarity.

#### With silver(I) trifluoroacetate (1:1) **2.32**

The asymmetric unit of complex **2.32**, shown in figure 2.42, was solved in the tetragonal  $P4_12_12$  space group and comprises two ligands [**2.8**] and two silver(I) trifluoroacetates in a 1:1 ligand to silver(I) ratio. The ligands in the complex exhibit  $\mu_2$ -O,O bidentate bridging coordination modes with average N-O<sub>ligand</sub> bond distances of 1.331(5) Å. The ligand oxygens, O1 and O2, bridge Ag1, Ag2' and Ag1' forming irregular Ag<sub>2</sub>O<sub>2</sub> rings with unequal sides with lengths of 2.468(3) Å [Ag1-O1], 2.426(3) Å [Ag2'-O1], 2.475(3) Å [Ag2-O2] and 2.502(3) Å [Ag1'-O2]. The internal angles in the Ag<sub>2</sub>O<sub>2</sub> rings, formed by O1 and O2 oxygens, are 90.33(2)° [Ag2-O1-Ag1'], 88.45(2)° [Ag2-O2-Ag1'], 84.70(12)° [O1-Ag2-O2] and 83.24(2)° [O1-Ag1-O2].

The N-O<sub>ligand</sub>-Ag bond angles range from 113.9(2)° to 133.4(3)°, and these coordination angles are similar to those observed in reported complexes of ligand **2.8**.<sup>[102]</sup> The phenyl rings are twisted about the C-C bond at torsional angles of 37.8(8)° [C4-C3-C6-C11] and 41.7(7)° [C13-C14-C17-C18].

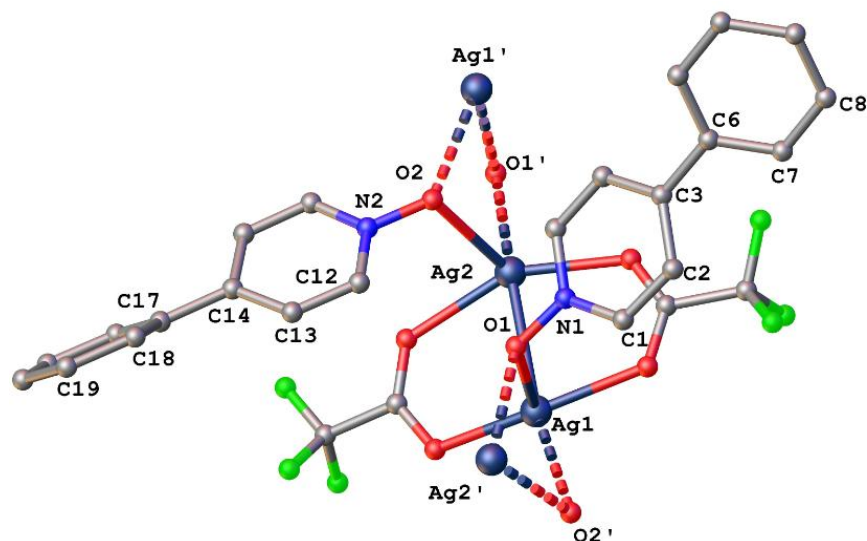
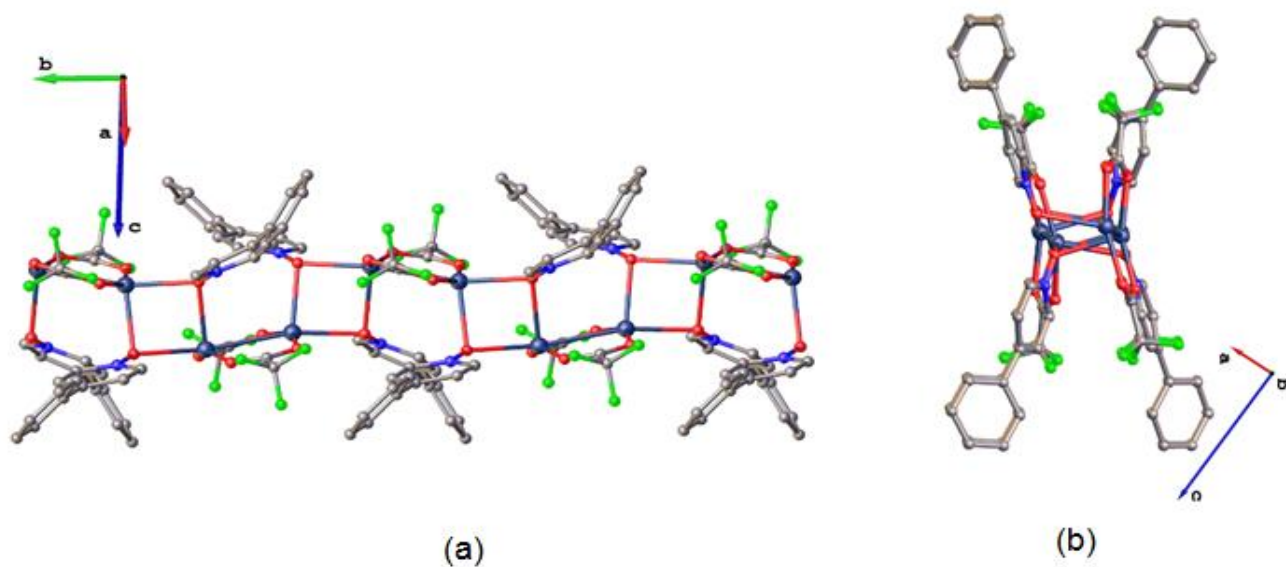


Figure 2.42 – Asymmetric unit of complex **2.32** with ligand **2.8**. Hydrogen atoms are removed for clarity. Selected bond lengths (Å) and bond angles (°): N1-O1 = 1.330(4), N2-O2 = 1.333(4), Ag1-O1 = 2.468(3), Ag2'-O1 = 2.426(3), Ag2-O2 = 2.475(3), Ag1'-O2 = 2.502(3), N1-O1-Ag2' = 125.2(3), N1-O1-Ag1 = 117.8(3), N2-O2-Ag2 = 113.9(2), N2-O2-Ag1' = 133.4(3), Ag2-O1-Ag1' = 90.33(2), Ag2-O2-Ag1' = 88.45(2), Ag1-Ag2 = 2.949(1), O1-Ag2-O2' = 84.70(2), O1-Ag1-O2' = 83.24(2), C2-C3-C6-C7 = 37.4(7), C13-C14-C17-C18 = 42.4(6).

The silver(I) [Ag1 ( $\tau_5 = 0.20$ ) and Ag2 ( $\tau_5 = 0.22$ )] ions adopt a five-coordinate distorted square-pyramidal geometry with an  $\text{Ag}_1\text{O}_4$  environment. Ag1...Ag2 ions exhibit a strong interaction at a distance of 2.944(4) Å, with trifluoroacetate anions bridged on either side. These dimeric  $(\text{CF}_3\text{OCO})\text{Ag1-Ag2}(\text{OCOCF}_3)$  arrangements are identical to those previously reported,<sup>[103]</sup> and are further bridged by  $\mu_2\text{-O,O}$  ligands to give a one-dimensional polymeric structure extending along the *b*-axis, as shown in figure 2.43.



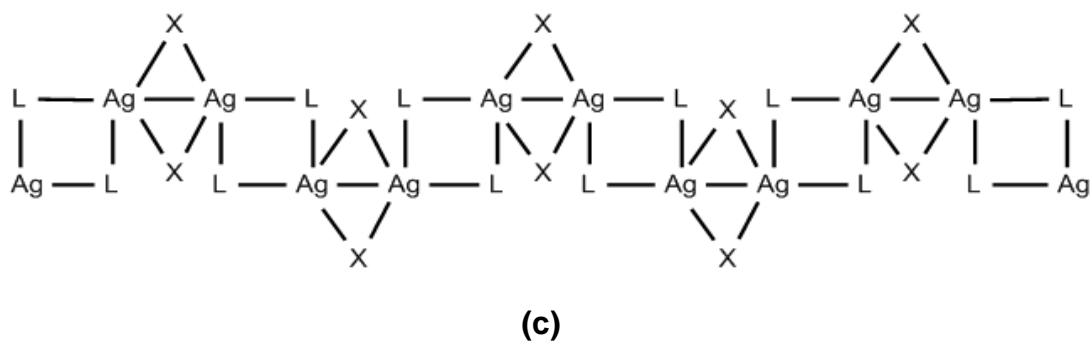


Figure 2.43 – (a) 1D polymeric structure of complex **2.32**. Hydrogen atoms are excluded for clarity. (b) ‘H-shaped’ 1D polymer of complex **2.32**, viewed along *b*-axis (c) Topological structure related to complex **2.32** [X = CF<sub>3</sub>COO<sup>-</sup> and L = ligand **2.8**].

The 1D polymer, when viewed down the *b*-axis, is ‘H-shaped’, as shown in figure 2.43b. Each ‘H-shaped’ polymer exhibits a  $\pi$ - $\pi$  interaction [figure – 2.44b] with a centroid-centroid distances of 3.801 Å, to give a 3 dimensional network, as shown in figure 2.44a.

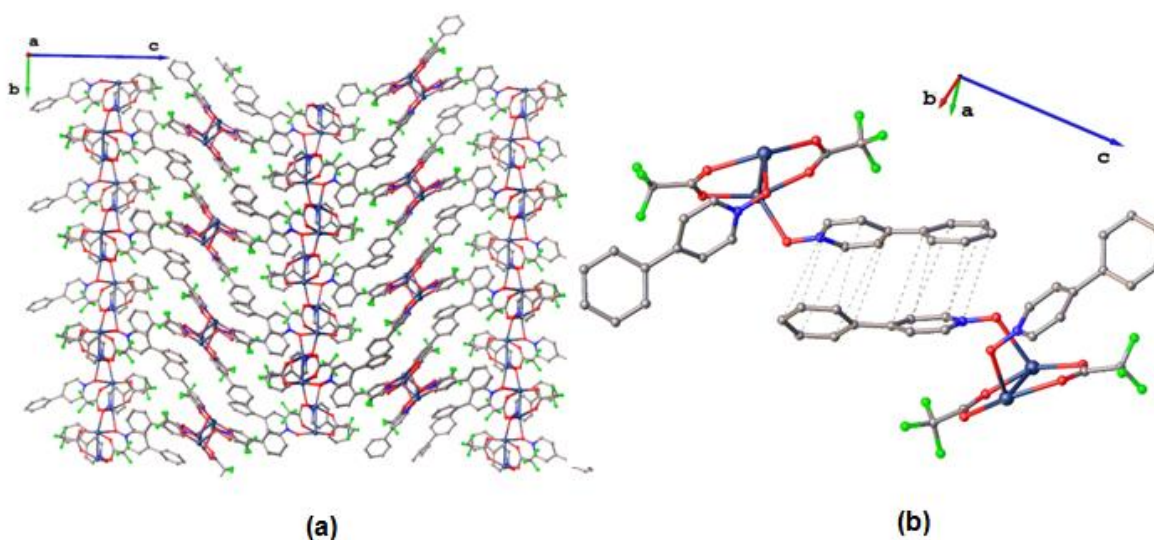


Figure 2.44 – (a) 3D Polymer of complex **2.32** generated with  $\pi$ - $\pi$  interactions when viewed down the *a*-axis. (b) Section of 3D polymer showing  $\pi$ - $\pi$  interactions between the ligands.

### With silver(I) triflate (1:1) **2.33**

The structure of complex **2.33**, depicted in figure 2.45a, was solved in the orthorhombic *Pbca* space group, with a ligand **2.8** molecule coordinated to one AgSO<sub>3</sub>CF<sub>3</sub>. This shows the complex **2.27** has a 1:1 ligand to silver(I) ratio. The ligand oxygen, O1, bridges Ag1 and Ag1'' at an angle of 128.64(2)° [Ag1-O1-Ag1''], with bond distances of 2.287(3) Å [Ag1-O1] and 2.377(3) Å [Ag1''-O1]. The bond distance of 1.341(4)° [N1-O1] and the coordination angle 112.2(2)° [N1-O1-Ag1] are similar to those found in previously reported ligand **2.8** complexes.<sup>[102]</sup> The silver(I) ions are five-

coordinate [ $\tau_5 = 0.37$ ] with an  $O_5$  coordination sphere with two oxygens supplied by the N-oxide ligands and three oxygens from triflate anions, as seen in figure 2.45b.

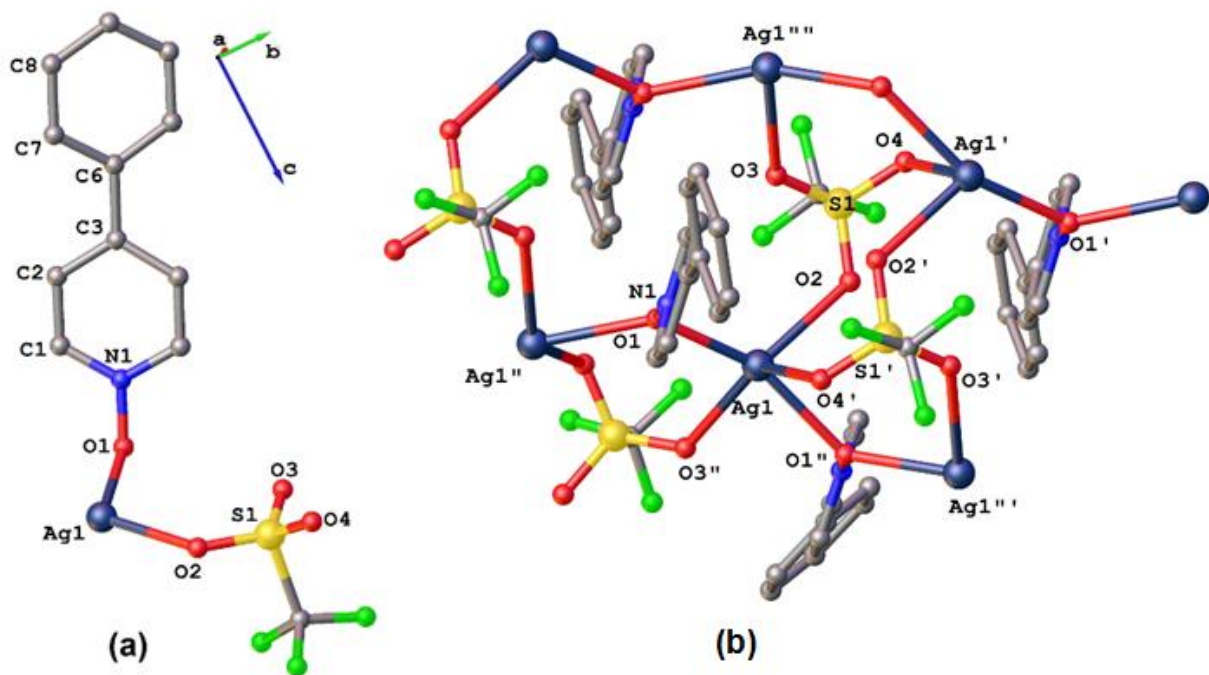


Figure 2.45 – (a) Asymmetric unit of complex **2.33**, (b) section of the 2D polymeric structure of complex **2.33**. Hydrogen atoms are omitted for clarity. Selected bond lengths (Å) and bond angles (°): N1-O1 = 1.341(4), Ag1-O1 = 2.287(3), Ag1''-O1 = 2.377(3), N1-O1-Ag1 = 112.2(2), Ag1-O1-Ag1'' = 128.64(2).

The tridentate triflate anions and bidentate bridging ligands **2.8** with five-coordinate silver(I) ions grow two-dimensionally in the *ab*-plane, as shown in figure 2.46a. The ligand **2.8** molecules and tridentate triflate anions are placed along the *c*-axis in a 1:1 ratio, with every two ligands isolated by a tridentate triflate anion that propagates two-dimensionally along the *ab*-plane. There is no possibility for the 2D sheets to interact with each other through  $\pi$ - $\pi$  interactions, as those spaces are filled with tridentate triflate anions on both sides of the polymeric sheet, as shown in figure 2.46b.

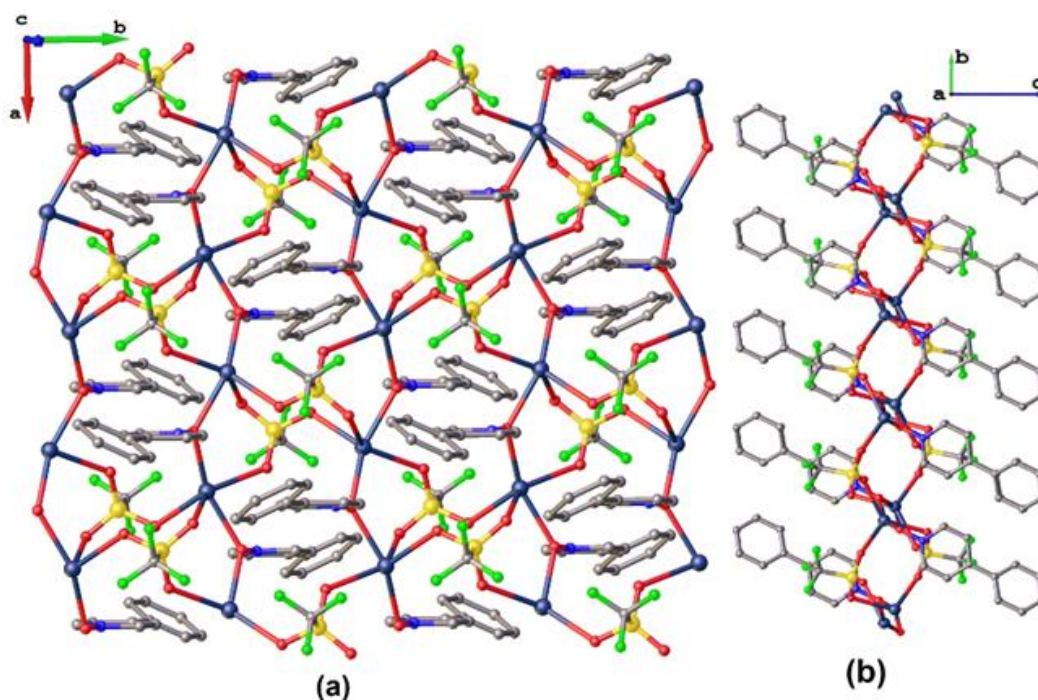


Figure 2.46 – 2D polymeric network of complex **2.33** viewed down the (a) *c*-axis and (b) *a*-axis. Hydrogen atoms are excluded for clarity.

#### With silver(I) tetrafluoroborate (1:1) **2.34**

Complex **2.34** crystallised in the triclinic *P*-1 space group with its asymmetric unit composed of one ligand **2.8** and a water molecule coordinated to silver, with a non-coordinating BF<sub>4</sub> anion. This shows the complex has a 1:1 ligand to silver(I) ratio, as shown in figure 2.47a. The extended structure is shown in figure 2.47b. Again the ligand **2.8** adopts a  $\mu_2$ -O,O bidentate coordination mode, bridging Ag1 and Ag1' at an angle of 105.67(6)° [Ag1-O1-Ag1]. The silver(I) ions are four-coordinate with a CO<sub>3</sub> coordination sphere. The bond distances 1.333(2) Å [N1-O1] and coordination angles 105.67(6)° [N1-O1-Ag1] are close to those previously reported.<sup>[102]</sup> Also, the observed Ag(I)- $\pi$  distances of 2.480 Å are similar to that seen in complex **2.29**.

Two bidentate ligands **2.8** bridge two silver(I) ions at distances of 2.402(2) Å [Ag1-O1 ] and 2.337(2) Å [Ag1'-O1], forming a four-membered Ag<sub>2</sub>O<sub>2</sub> ring, as shown in figure 2.47b. The ligands coordinated across the Ag<sub>2</sub>O<sub>2</sub> ring are twisted at angles of 48.8(3)° [Ag1-O1-N1-C5], which is smaller than the values observed in complex **2.29**. The non-bonding Ag $\cdots$ Ag distance [3.778 Å] is shorter than the values observed in complex **2.29**. Two water molecules [O2, O2'] and the phenyl rings are *trans*-coordinated to the silvers [Ag1 and Ag1'] with respect to the four-membered ring.

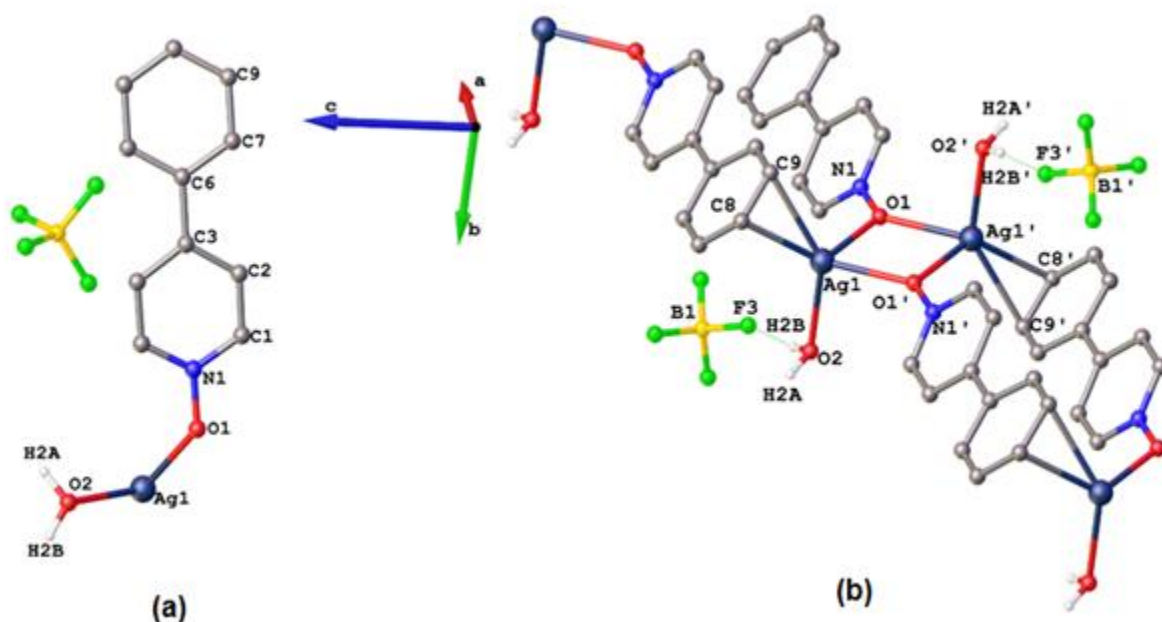


Figure 2.47 – (a) Asymmetric unit of complex **2.34**, (b) a section of the 1D polymeric structure of complex **2.34**. Selected hydrogen atoms are excluded for clarity. Selected bond lengths (Å) and bond angles (°): N1-O1 = 1.333(2), Ag1-O1 = 2.402(2), Ag1-O1 = 2.337(2), Ag1-(C8,9) = 2.480(2), N1-O1-Ag1 = 105.67(6), Ag1-O1-Ag1 = 105.67(6), Ag1-O1-N1-C5 = 48.8(3), C2-C3-C6-C7 = 5.7(3).

Complex **2.34** is a linear 1D polymer with  $\text{BF}_4$  anions interacting with the hydrogens [H2B and H2B'] from the water molecules [ $d(\text{O2}\cdots\text{F3}) = 2.704 \text{ \AA}$ ] coordinated along the  $b$ -axis, as seen in the figure 2.48 in the crystal packing. There is a  $\pi$ - $\pi$  interaction between the electron rich phenyl rings and electron deficient pyridine N-oxide rings with centroid-centroid distances of  $3.678 \text{ \AA}$ .

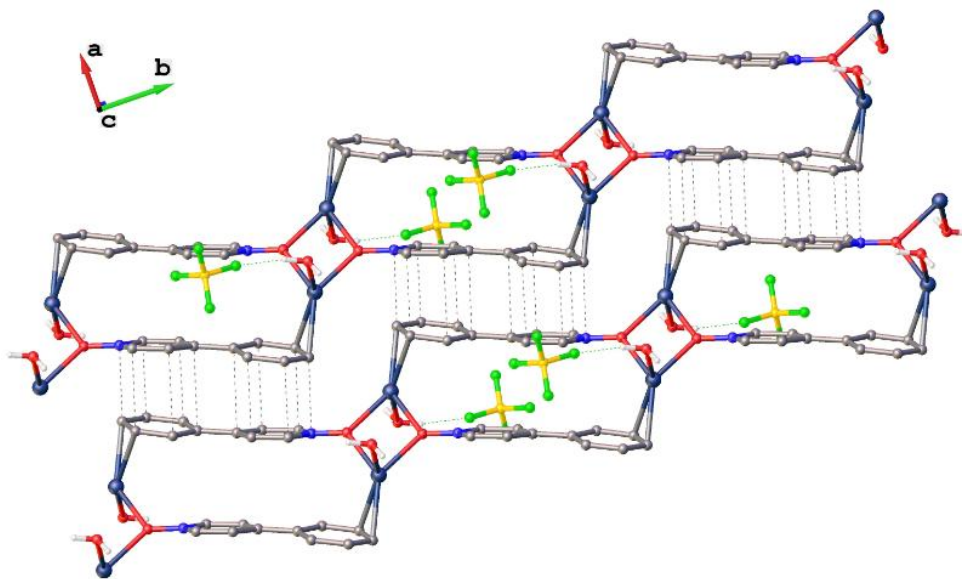
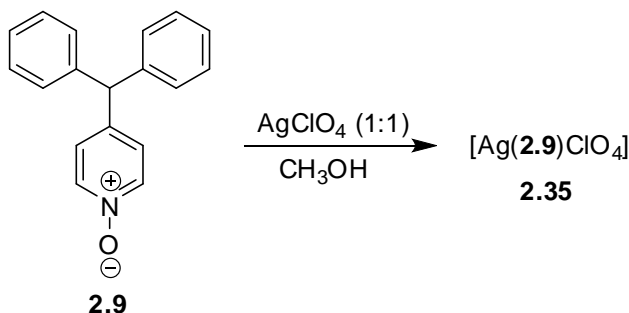


Figure 2.48 – Crystal packing of complex **2.34** illustrating  $\pi$ - $\pi$  interactions as viewed down the  $c$ -axis. Hydrogen atoms are excluded for clarity.

### 2.3.6 Complexes with 4-diphenylmethyl pyridine N-oxide 2.9

The interesting coordination chemistry seen with ligand **2.6** encouraged us to change the ligand substituents to the two phenyl substituents with –CH– spacers at position 4. We expected this would result in 3D networks when reacted with silver(I) salts, through Ag-C contacts. However, despite numerous attempts to crystallise complexes with other silver(I) salts, all endeavours were unsuccessful. We were however successful with silver(I) perchlorate, which produced a 2D network similar to complex **2.29** [scheme 2.14].



Scheme 2.14 – Synthesis of complex **2.35**.

#### With silver(I) perchlorate (1:1) 2.35

X-ray analysis of complex **2.35** solved in the monoclinic  $P2_1/n$  space group. The asymmetric unit contains one ligand **2.9**, one perchlorate and a four-coordinate silver(I) ion, as shown in figure 2.49. The ligand oxygen displays a  $\mu_2$ -O,O bidentate bridging coordination mode, similar to ligand **2.6**, with Ag1 and Ag1' at bond distances of 2.344(4) Å [Ag1-O1] and 2.278(4) Å [Ag1'-O1]. The N1-O1 bond distance in the complex is 1.335(6) Å, with a bridging angle of 103.8(1)° [Ag1-O1-Ag1']. The coordination angles with Ag1 and Ag1' are 121.9(3)° [N1-O1-Ag1] and 127.3(3)° [N1-O1-Ag1'], which are similar to the angles reported in other pyridine N-oxide complexes.<sup>[75]</sup> The N-O bond distances and coordination angles indicate that the oxygen orbitals are  $sp^2$  hybridized.

The silver(I) ion [Ag1( $\tau_4 = 0.61$ )] exhibits a seesaw geometry with a  $CO_3$  coordination sphere, with oxygens supplied from two ligand **2.9** molecules, a perchlorate anion and the carbons of the phenyl ring [C16 and C17], as shown in figure 2.49.

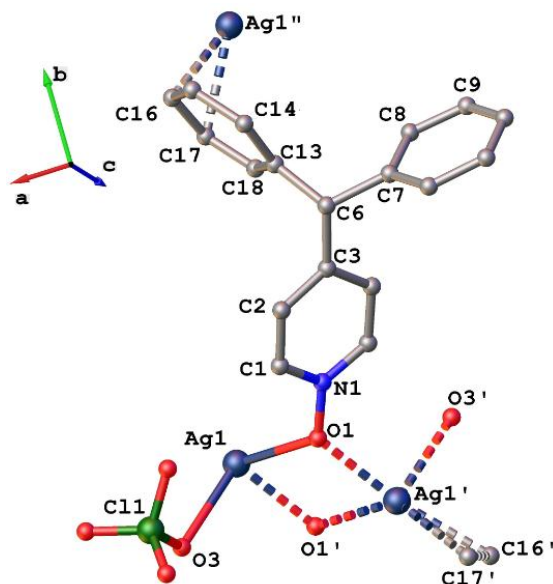


Figure 2.49 – Asymmetric unit of complex **2.35**. Hydrogen atoms are excluded for clarity. Selected bond lengths (Å) and bond angles (°): N1-O1 = 1.335(6), Ag1-O1 = 2.344(4), Ag1'-O1 = 2.278(4), Ag1''-(C16,17) = 2.312(6), N1-O1-Ag1 = 121.9(3), N1-O1-Ag1' = 127.3(3), Ag1-O1-N1-C1 = 68.0(6).

Once again the ligands bridge silver(I) ions to form a four-membered  $\text{Ag}_2\text{O}_2$  ring, similar to complexes **2.29** and **2.34**, as shown in figure 2.50. The torsional angles [ $\text{Ag1-O1-N1-C1} = 68.0(6)^\circ$ ] of the ligands coordinated across the  $\text{Ag}_2\text{O}_2$  ring are smaller than the values observed in **2.29** but greater than those observed in complex **2.34**. The non-bonded  $\text{Ag}\cdots\text{Ag}$  distance in the  $\text{Ag}_2\text{O}_2$  ring is 3.637 Å, close to the values seen in complex **2.34**. The perchlorate oxygens O3 and O3' are *trans*- to each other, coordinating Ag1 and Ag1' at a distance of 2.524(5) Å, with vertex angles of  $103.79(2)^\circ$  [ $\text{Ag1'-O1-Ag1}$ ] and  $76.21(2)^\circ$  [ $\text{O1-Ag1-O1'}$ ].

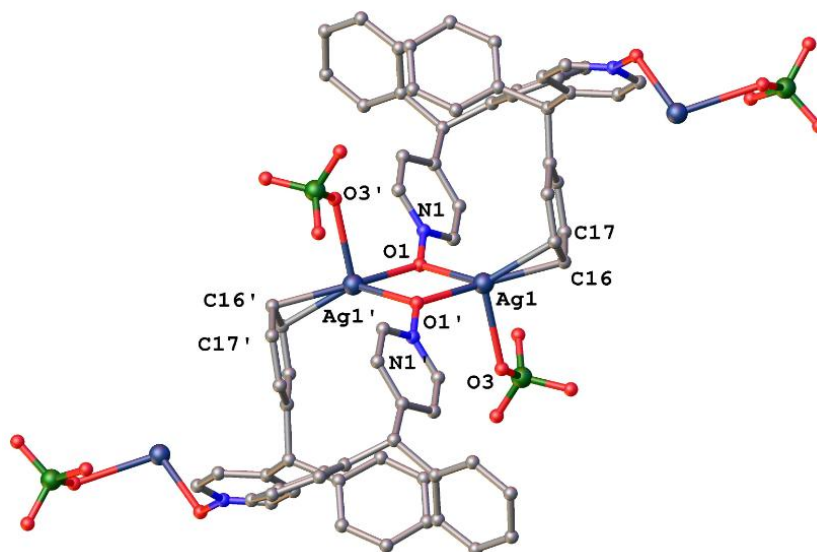


Figure 2.50 – A section of the 2D polymeric structure of complex **2.35**. Hydrogen atoms are excluded for clarity. Selected bond lengths (Å) and bond angles (°):  $\text{Ag1'-O1-Ag1} = 103.79(2)$ ,  $\text{O1-Ag1-O1'} = 76.21(2)$ .



The whole structure can be described as a 2D polymer with repeating units [figure 2.50] forming 'Z-shaped' [4+4] metallocycles, as shown in figure 2.51. Each of these 'Z-shaped' units contains four ligands and four silver(I) ions, with the perchlorates oriented above and below the polymer along the *c*-direction, as shown in figure 2.51.

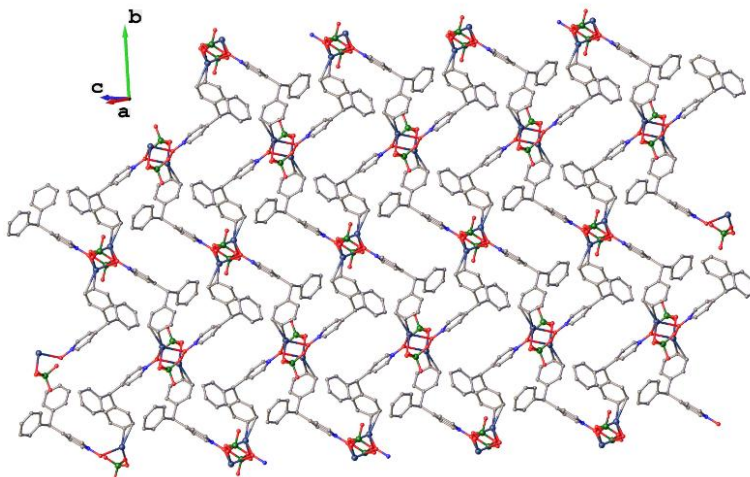


Figure 2.51 – Depiction of the 2D polymeric network of complex **2.35** with hydrogen atoms omitted for clarity.

### 2.3.7 Complexes with 2,6-bis(diphenylmethyl)pyridine N-oxide **2.10**

Several attempts were made to synthesise silver(I) complexes with ligand **2.10**, however, the ligand exclusively crystallises out, thus preventing the formation of complexes. This inability to form complexes with ligand **2.10** is possibly due to the sterically crowded phenyl rings at positions 2 and 6. Ligand **2.10** itself solved in the orthorhombic *Pbca* space group with a planar pyridine ring A, and twisted phenyl rings B, C, D, and E, as depicted in figure 2.52. The ligand has the shortest bond distance [N1-O1 = 1.306(2) Å] of all the pyridine N-oxides discussed so far. A list of angles and torsional angles between the ring systems A, B, C and D are shown in table 2.2.

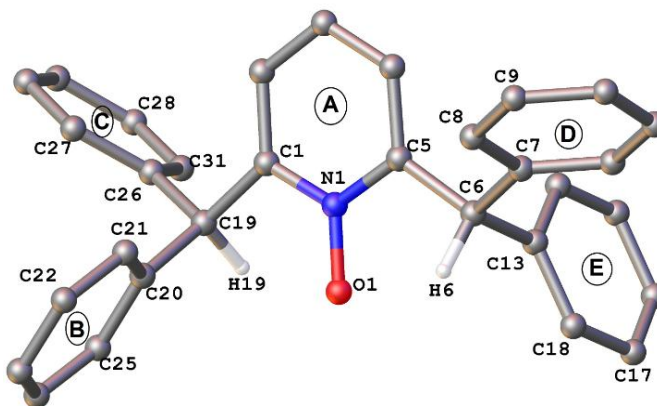


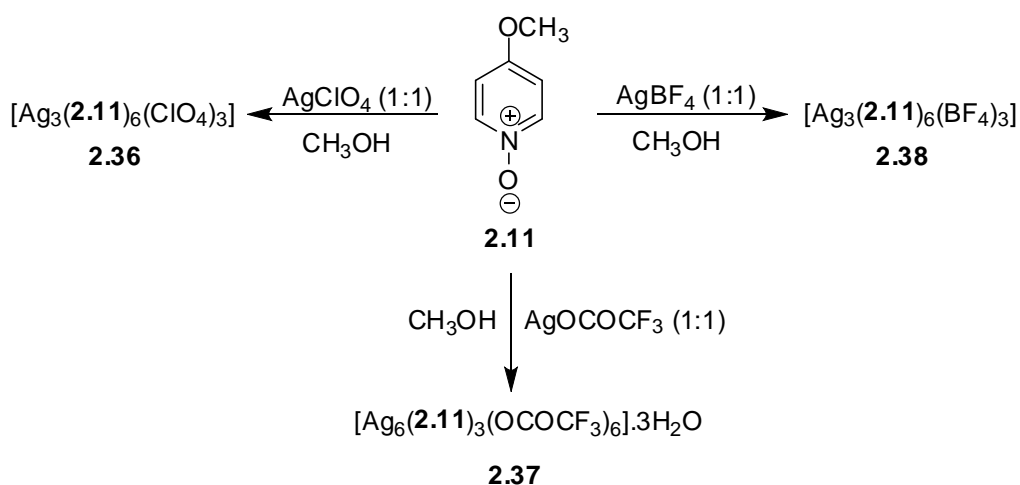
Figure 2.52 – Asymmetric unit of ligand **2.10**. Aryl hydrogen atoms are excluded for clarity. Selected bond lengths (Å): N1-O1 = 1.306(2), C5-C6 = 1.505(2), C1-C19 = 1.507(2).

Table – 2.2 Bond and torsional angles in ligand **2.10**.

Angles (°)			Torsional angles (°)
113.09(2)	C5-C6-C7	N1-C5-C6-C7	23.03(1)
110.19(2)	C5-C6-C13	N1-C5-C6-C13	75.07(1)
113.65(2)	C1-C19-C20	N1-C1-C19-C20	73.16(2)
111.85(2)	C1-C19-C26	N1-C1-C19-C26	19.53(1)

### 2.3.8 Complexes with 4-methoxypyridine N-oxide **2.11**

Three complexes were successfully synthesised from ligand **2.11**, with their asymmetric unit compositions shown in scheme 2.15. The complexes **2.36** and **2.38** crystallised in a 2:1 ligand to silver(I) ratio and were solved in the monoclinic  $P2_1/n$  and triclinic  $P-1$  space groups respectively, with anions non-coordinated. These complexes are 1D polymers with the ligand **2.11** molecules showing monodentate, bidentate and tridentate coordination modes in **2.36**, while in complex **2.38** the ligand **2.11** denticity is two. As expected, complex **2.37** is similar to complex **2.21** with the trifluoroacetate anions forming dimeric bridges across  $Ag \cdots Ag$  interactions with the exclusion of ligand **2.11** molecules. Their oxygens show H-bonding interactions with water molecules. Attempts to crystallise  $AgOCOCF_3$  complexes of ligand **2.11** using different solvent conditions and silver(I) salt ratios were unsuccessful.

Scheme 2.15 – Syntheses of complexes **2.36** – **2.38**.

### With silver(I) perchlorate (1:1) **2.36**

Complex **2.36** crystallised and solved in the monoclinic  $P2_1/n$  space group, as shown in figure 2.53. The asymmetric unit contains six ligand **2.11** molecules and three silver(I) ions in a 2:1 ligand **2.11** to silver(I) ratio. Although the silver(I) ions are six- [Ag1 and Ag2] and five- [Ag3 ( $\tau_5 = 0.37$ )] coordinate similar to complex **2.38**, it is interesting to see the ligand **2.11** oxygens are present in monodentate,  $\mu_2$ -O,O bidentate bridging and  $\mu_3$ -O,O,O tridentate coordination modes within the polymeric structure. The  $\mu_2$ -O,O ligand **2.11** oxygens, O3 and O9, bridge Ag1...Ag1' and Ag1...Ag2, which are interacting weakly at distances of 3.061(6) Å and 3.340(4) Å, while there were no **2.11** bridging ligands across silver(I) ions Ag2 and Ag3 which are interacting strongly at a distance of 2.983(5) Å. The N-O<sub>ligand</sub> bond distances range from 1.348(4) Å to 1.364(4) Å, which clearly indicates the N-O<sub>ligand</sub> bond lengths have single bond character, due to the electron donating -OCH<sub>3</sub> group.

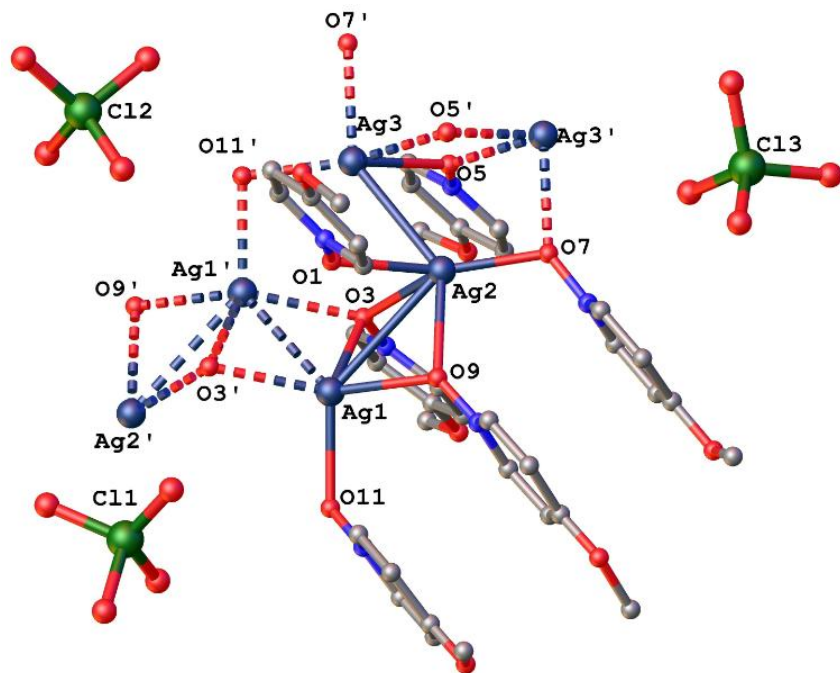


Figure 2.53 – Asymmetric unit of complex **2.36**. Hydrogen atoms are excluded for clarity. Selected bond lengths (Å) and bond angles ( $^\circ$ ): N1-O1 = 1.354(4), N2-O3 = 1.353(4), N3-O5 = 1.348(4), N4-O7 = 1.351(5), N5-O9 = 1.350(4), N6-O11 = 1.364(4), Ag1-O3 = 2.534(3), Ag1-O9 = 2.417(3), Ag1-O11 = 2.372(3), Ag2-O7 = 2.192(3), Ag2-O1 = 2.368(3), Ag2-O3 = 2.412(3), Ag2-O9 = 2.564(3), Ag3-O11' = 2.257(3), Ag3-O5 = 2.348(3), Ag3-O5' = 2.392(3), Ag3'-O7 = 2.532(3), N1-O1-Ag2 = 116.4(2), N2-O3-Ag2 = 119.61(2), N2-O3-Ag1 = 117.88(2), N2-O3-Ag1' = 123.1(2), N3-O5-Ag3 = 124.8(2), N3-O5-Ag3' = 124.5(2), N4-O7-Ag2 = 117.4(2), N4-O7-Ag3' = 145.9(2), N5-O9-Ag1 = 130.5(2), N5-O9-Ag2 = 140.7(2), N6-O11-Ag3' = 112.09(2), N6-O11-Ag1 = 118.77(2), Ag1-O3-Ag1' = 74.60(7), Ag2-O3-Ag1 = 85.30(9), Ag2-O3-Ag1' = 116.51(2), Ag3-O5-Ag3' = 110.31(2), Ag2-O7-Ag3' = 96.62(2), Ag1-O9-Ag2 = 84.18(8), Ag3-O11-Ag1' = 97.10(2), Ag1-Ag1' = 3.061(6), Ag1-Ag2 = 3.340(4), Ag2-Ag3 = 2.983(5), Ag1'-Ag1-Ag2 = 82.047(2), Ag3-Ag2-Ag1 = 99.65(2).

The six-coordinate Ag2 ion is bound by four **2.11** ligands molecules, which are monodentate [O1],  $\mu_2$ -O,O, bidentate bridging [O9] between Ag2-Ag1 and [O7] between Ag2 and Ag3' and  $\mu_3$ -O,O,O tridentate, [O3] over Ag2-Ag1-Ag1', as shown in figure 2.53. Interestingly, the oxygens, O7 and O11', which bridge Ag2, Ag3' and Ag1', Ag3 at angles  $96.62(2)^\circ$  and  $97.10(2)^\circ$  with no Ag $\cdots$ Ag interactions have similar average Ag-O<sub>ligand</sub> bond distances of 2.362(3) Å and 2.314(3) Å. On the other hand, oxygens, O3 and O9 bridging Ag1 and Ag2 centers at angles ranging from  $74.60(7)^\circ$  to  $116.51(2)^\circ$  have similar average Ag-O<sub>ligand</sub> bond distances of 2.447(3) Å and 2.490(3) Å.

It is worth discussing the Ag $\cdots$ Ag interactions, which allow the polymer to grow one-dimensionally along the *b*-axis. Four six-coordinate silver(I) centers [Ag2', Ag1, Ag1' and Ag2] and two five-coordinate silver ions [Ag3 and Ag3'] generate an 'S' shaped chain, as shown in figure 2.54. The angles between Ag3-Ag2-Ag1' and Ag1'-Ag1-Ag2 are  $99.65(2)^\circ$  and  $82.047(2)^\circ$ , respectively. Each of these 'S' shaped silver chains has two monodentate and two  $\mu_3$ -**2.11** ligands [figure 2.54], which in turn are connected by four  $\mu_2$ -**2.11** ligands to extend one-dimensionally, as shown in figure 2.54. The 'S' shape chain comprises two strong Ag $\cdots$ Ag interactions [Ag3'-Ag2'/Ag2-Ag3 = 2.983(5) Å] and three weak ones [Ag1-Ag1' = 3.061(6) Å and Ag2'-Ag1/Ag1'-Ag2 = 3.340(4) Å].

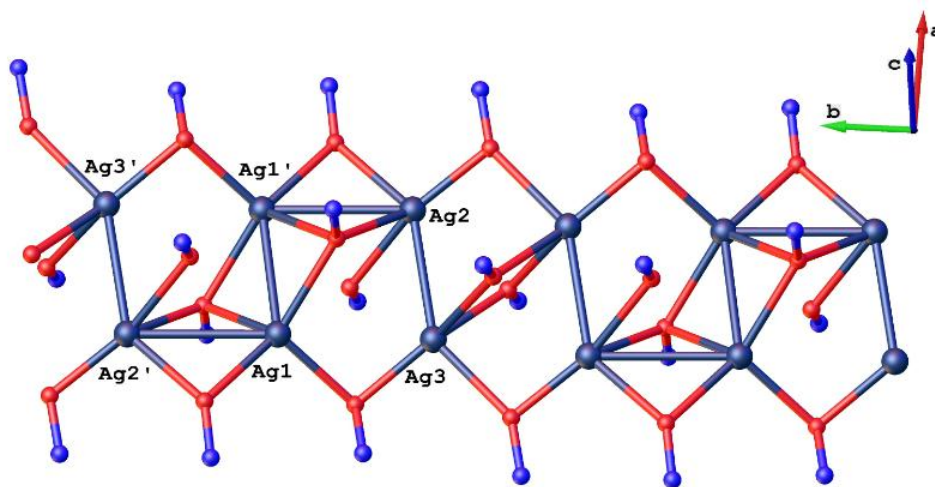


Figure 2.54 – The central coordination skeletal structure of complex **2.36** constructed using Ag [deep blue], O [red] and N [blue] atoms to show the bridging modes of the 1D polymer. Carbon atoms and  $-\text{OCH}_3$  groups of ligands **2.11** are omitted for clarity.

#### With silver(I) trifluoroacetate (1:1) **2.37**

The overall structure of complex **2.37** is a discrete assembly, as shown in figure 2.55 with the solid bonds representing the asymmetric unit, which has a 1:2 ligand to silver(I) ion ratio. The complex **2.37** was solved in the monoclinic  $P2_1/n$  space group and contains six silver(I) trifluoroacetates and three water molecules with their hydrogens interacting with three ligand **2.11** molecules, as

shown in figure 2.55. The N-O<sub>ligand</sub> bond distances range from 1.349(4) Å to 1.353(3) Å. Their average [1.351 Å] is higher than the N-O distances seen in complex **2.21** [1.335(3) Å] of ligand **2.1** showing similar hydrogen bonding interactions. Out of the six trifluoroacetate groups, three of them are disordered over six fluorine atom sites at C24 and C22 with 50:50 and 20:80 occupancy ratios, respectively, and over one fluorine atom at C20 with 26:74 occupancy ratio. In a similar result to complex **2.21**, the trifluoroacetate anions coordinate strongly to the silver(I) ions to form dimeric units linked into tetranuclear complexes via the bridging water molecules.

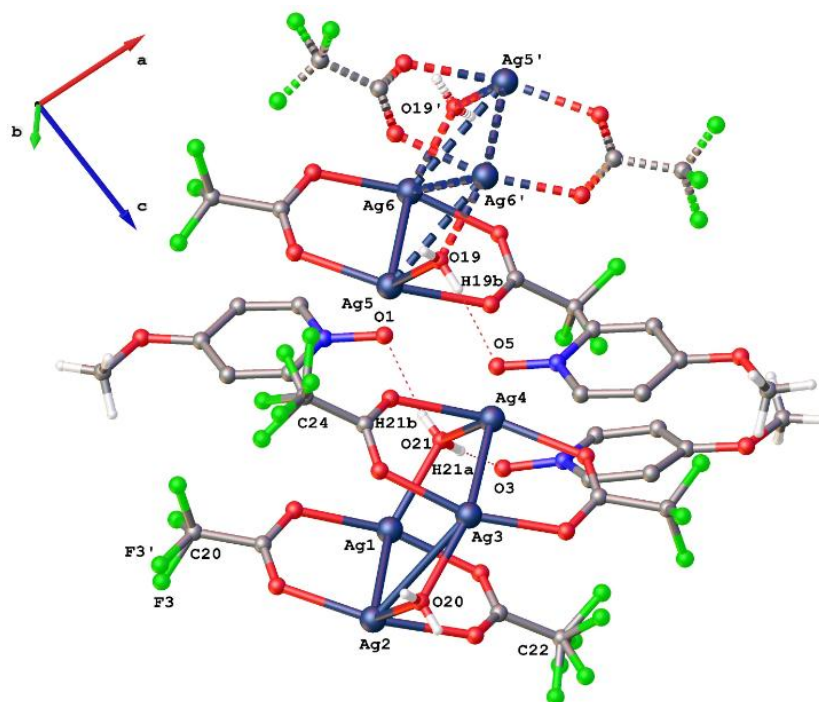


Figure 2.55 – Asymmetric unit of complex **2.37**. Selected hydrogen atoms are excluded for clarity. Selected bond lengths (Å) and bond angles (°): N1-O1 = 1.349(4), N2-O3 = 1.353(3), N3-O5 = 1.351(3), Ag1-Ag2 = 2.896(4), Ag2-Ag3 = 3.323(4), Ag3-Ag4 = 2.886(4), Ag5-Ag6 = 2.874(4), Ag5-Ag6' = 3.354(4), Ag6-Ag6' = 3.350(6).

Complex **2.37** contains two four- [Ag1 and Ag4], three five- [Ag2, Ag3 and Ag5] and one six-coordinate [Ag6] silver(I) ion as shown in figure 2.55. The four-coordinate Ag1 and Ag4 centers have seesaw coordination geometry with  $\tau_4$  indexes of 0.32 and 0.60. The  $\tau_5$  parameters of Ag2 and Ag5 centers are both 0.66, while the Ag3 value is 0.05, being close to square pyramidal coordination geometry. As seen previously there are strong Ag1 $\cdots$ Ag2 and Ag3 $\cdots$ Ag4 interactions at distances of 2.896(4) Å and 2.886(4) Å, respectively, with trifluoroacetate anions bridging on either side. These two strongly bonded silver(I) ions are capped by two water molecules, O20 and O21 at Ag1, Ag4 and Ag2, Ag3 to form six-membered rings, with a weak interaction between Ag2 $\cdots$ Ag3 at a distance of 3.323(4) Å. In the neighboring complex, Ag5 $\cdots$ Ag6 and the symmetry generated Ag5' $\cdots$ Ag6' show strong interactions at a distance of 2.874(4) Å. There also exists weak

interactions between Ag5 $\cdots$ Ag6' and Ag6 $\cdots$ Ag6' at distances of 3.354(4) Å and 3.350(6) Å respectively. The weakly interacting silver(I) ions [Ag5, Ag5', Ag6 and Ag6'] are capped with two water molecules [O19 and O19'] to form six-membered rings, as shown in figure 2.55. The ligand oxygens O1, O3 and O5 are hydrogen bonded to H21b, H21a and H19b, as shown in the asymmetric unit, with symmetry generated Ag5' and Ag6' indicated by the broken bonds. The hydrogen bond parameters are shown in table 2.3.

Table – 2.3 Selected hydrogen bond parameters for complex **2.37**.

D-H $\cdots$ A	dD-H(Å)	dH $\cdots$ A(Å)	dD $\cdots$ A(Å)	<D-H $\cdots$ A(°)
O21-H21a $\cdots$ O3	0.773	1.937	2.707	172.97
O21-H21b $\cdots$ O1	0.718	2.467	2.005	168.68
O19-H19b $\cdots$ O5	0.779	1.944	3.617	169.68

#### With silver(I) tetrafluoroborate (1:1) **2.38**

Single crystal X-ray analysis reveals that the asymmetric unit of complex **2.32** comprises two six-coordinate silver(I) ions [Ag1 and Ag3] and a five-coordinate silver [Ag2 ( $\tau_5 = 0.01$ )], as shown in figure 2.56. The complex **2.38** was solved in the triclinic *P*-1 space group. The asymmetric unit has six ligand **2.11** molecules and three silver(I) ions in a 2:1 ligand to silver(I) ratio. Two of the tetrafluoroborates [B1 and B3] are disordered with an occupancy ratio of 40:60 on B1 and 35:65 on B3. Interestingly, all six ligands are showing  $\mu_2$ -O,O bidentate bridging modes. The  $\mu_2$ -O,O oxygens [O5, O9 and O11] are bridging Ag1 and Ag3 ions in a pyramidal arrangement, with weak Ag $\cdots$ Ag interactions at a distances of 3.272(3) Å, while O7 and O3 are bridging Ag2-Ag3' and Ag2-Ag2', respectively with no Ag $\cdots$ Ag interactions. The ligand oxygen, O1, bridges Ag1 and Ag2', as shown in figure 2.56.

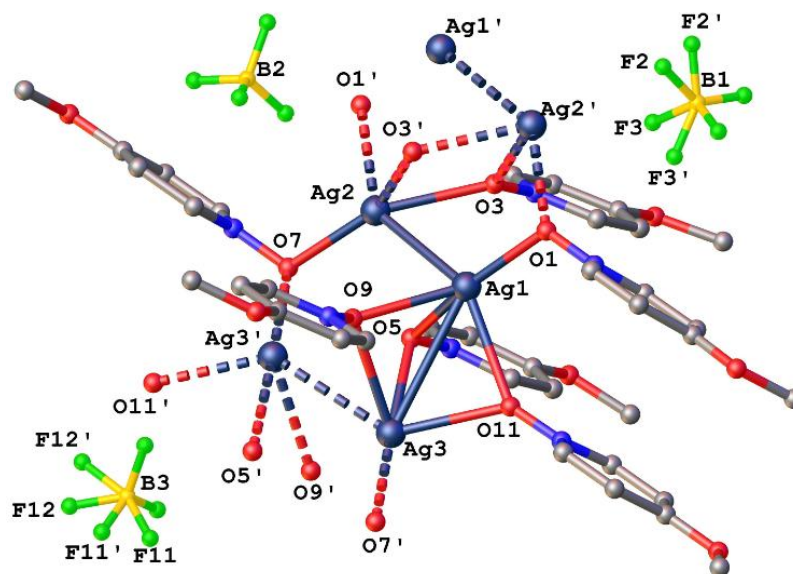


Figure 2.56 – Asymmetric unit of complex **2.38**. Hydrogen atoms are excluded for clarity. Selected bond lengths (Å) and bond angles (°): N1-O1 = 1.356(4), N2-O3 = 1.355(3), N3-O5 = 1.359(3), N4-O7 = 1.362(3), N5-O9 = 1.348(3), N6-O11 = 1.343(3), Ag1-O1 = 2.179(3), Ag1-O9 = 2.399(2), Ag1-O5 = 2.405(2), Ag1-O11 = 2.543(2), Ag2-O7 = 2.280(2), Ag2-O3 = 2.342(2), Ag2-O3' = 2.434(2), Ag2-O1' = 2.474(3), Ag3-O7' = 2.312(2), Ag3-O5 = 2.474(2), Ag3-O11 = 2.501(2), Ag3-O9 = 2.530(2), Ag2'-O3 = 2.342(2), Ag3'-O7 = 2.312(2), Ag2'-O1 = 2.474(3), N1-O1-Ag1 = 119.2(2), N1-O1-Ag2 = 140.6(3), N2-O3-Ag2 = 121.25(2), N2-O3-Ag2' = 129.85(2), N3-O5-Ag1 = 115.05(2), N3-O5-Ag3 = 119.24(2), N4-O7-Ag2 = 114.16(2), N4-O7-Ag3 = 116.82(2), N5-O9-Ag1 = 122.09(2), N5-O9-Ag3 = 116.49(2), Ag1-O5-Ag3 = 84.22(6), Ag2-O3-Ag2' = 108.57(8), Ag3-O11-Ag1 = 80.90(6), Ag1-O9-Ag3 = 83.14(6), Ag2'-O7-Ag3 = 101.97(8), Ag1-O1-Ag2' = 95.88(2), Ag1-Ag2 = 3.016(3), Ag1-Ag3 = 3.272(3), Ag2-Ag1-Ag3 = 96.13(9), Ag3-Ag3-Ag1 = 86.88(2).

The Ag1 $\cdots$ Ag2 interaction at a distance of 3.016(3) Å with no  $\mu_2$ -**2.11** bridging ligand is stronger than the Ag1 $\cdots$ Ag3 [3.272(3) Å] interaction, which has three  $\mu_2$ -**2.11** ligands. The Ag $\cdots$ Ag interactions are almost at right angles [Ag2-Ag1-Ag3 = 96.13(9)° and Ag3'-Ag3-Ag1 = 86.88(2)°]. The N-O<sub>ligand</sub> bond distances range from 1.343(3) Å to 1.359(3) Å, which implies that the oxygen orbitals are sp<sup>3</sup> hybridised due to the electron donating -OCH<sub>3</sub> group. The complex **2.38** propagates along the *a*-axis to give a 1D polymer, as shown in the figure 2.57.

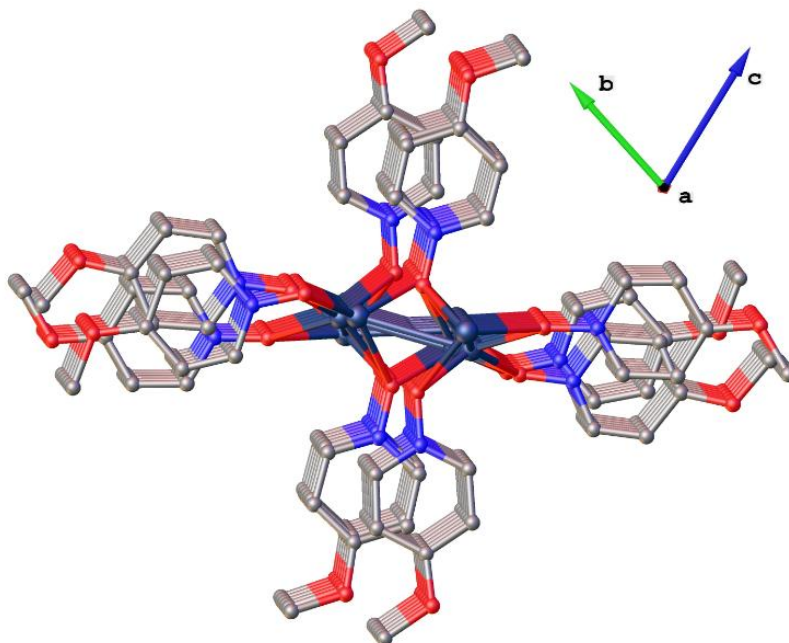


Figure 2.57 – 1D Polymer of complex **2.38** viewed down the *a*-axis. Hydrogen atoms and anions are excluded for clarity.

Though the N-O<sub>ligand</sub> bond distances and their corresponding coordination angles suggest they are in a sp<sup>3</sup> hybridization state, their coordination ability [Ag-O<sub>ligand</sub>] vary greatly in the polymer, as seen in figure 2.56. The average Ag-O<sub>ligand</sub> bond distances of  $\mu_2$ -**2.11** oxygen O7, bridging Ag2-Ag3' at distance of 2.296(2) Å is shorter compared to oxygens O5, O9 and O11, bridging Ag1-Ag3 at an average distance of 2.475(2) Å. Also, these oxygens O5, O9 and O11 which bridge Ag1 and Ag3 have small Ag-O<sub>ligand</sub>-Ag angles [Ag1-O5-Ag3 = 84.22(6), Ag3-O11-Ag1 = 80.90(6), Ag1-O9-Ag3 = 83.14(6)] compared to O3, O7 and O1 bridging silver(I) ions with no Ag...Ag interactions [Ag2-O3-Ag2' = 108.57(8), Ag2'-O7-Ag3 = 101.97(8), Ag1-O1-Ag2' = 95.88(2)], as shown in figure 2.58.

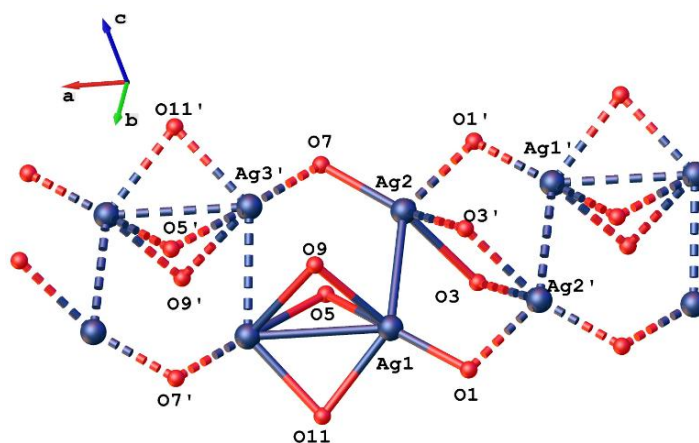


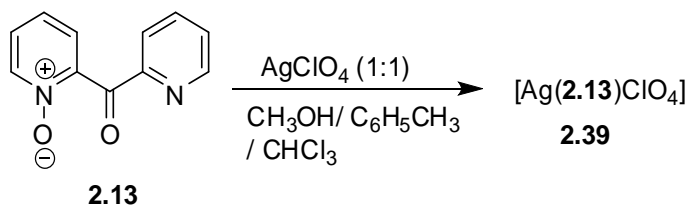
Figure 2.58 – The central coordination skeletal structure of complex **2.38** constructed using Ag [blue] and O [red] atoms showing the bridging modes of ligands **2.11** in the 1D polymer.



Attempts to grow crystals of complexes with ligand **2.12** with various silver(I) salts, using various crystal growth techniques and solvent conditions were unsuccessful and resulted in crystallisation of ligand **2.12**. A possible reason for this might be the strong electron withdrawing nature of the nitro group, which makes the oxygen electrons un-available for complex formation with silver(I) ions. An increase in reaction ratio from 1:1 to 1:20 for  $\text{AgBF}_4$  with ligand **2.12** to check for possible complex formation was unsuccessful, and only provided crystals of ligand **2.12**. Therefore, we began synthesis of complexes with ligand **2.13**.

### 2.3.9 Complexes with di-(2-pyridyl)ketone N-oxide **2.13**

Several attempts to synthesise silver(I) complexes with ligand **2.13** using different solvent conditions and crystal growth techniques were unsuccessful. Finally, we succeeded to isolate green block like crystals of complex **2.39**, when two equivalents of  $\text{AgClO}_4$  dissolved in methanol were added to one equivalent of ligand **2.13** dissolved in a 1:1 ratio of toluene and chloroform using the slow evaporation technique. The asymmetric unit composition of the crystal structure is shown in scheme 2.15.



Scheme 2.15 – Synthesis of complex **2.39**.

Although ligand **2.13** was obtained as a second product during the synthesis of ligand **3.8**, it offered interesting silver(I) coordination chemistry. The possible coordination modes of ligand **2.13** with silver(I) ions are shown in figure 2.59.

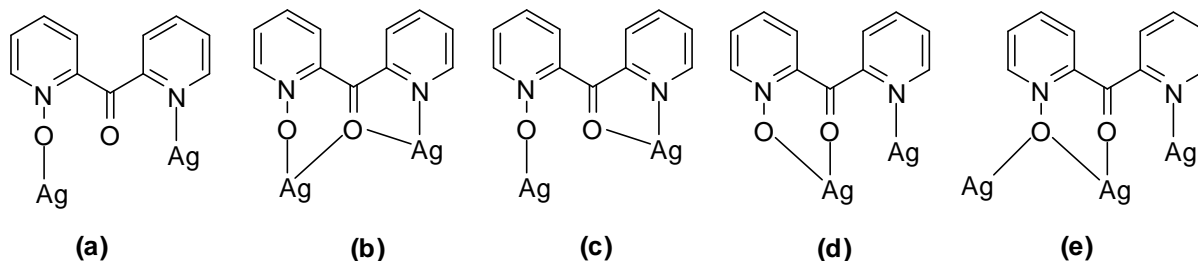


Figure 2.59 – Overview of the possible coordination modes of ligand **2.13** with silver(I) ions.

### With silver(I) perchlorate (1:1) **2.39**

The crystal structure of complex **2.39** solved in the triclinic *P*-1 space group and contains a ligand **2.13** coordinated to one silver(I) [Ag1] through the nitrogen atom and a non-coordinated perchlorate anion, which is disordered over three oxygens with an occupancy ratio of 44:56, as shown in figure 2.60. The N1-O1 groups are monodentate with bond distances of 1.329(3) Å and coordination angles of 116.81(1)° [N1-O1-Ag1]. Each Ag1 ion is linked via nitrogen [N2] and oxygen [O1'] in a near linear coordination angle of 174.59(7)° [O1'-Ag1-N2] to form [2+2] macrocycles. Each of the macrocycles is linked together by the silver [Ag1] centers which adopt a distorted T-shaped geometry with angles 82.36(5)° [N2-Ag1-Ag1''].

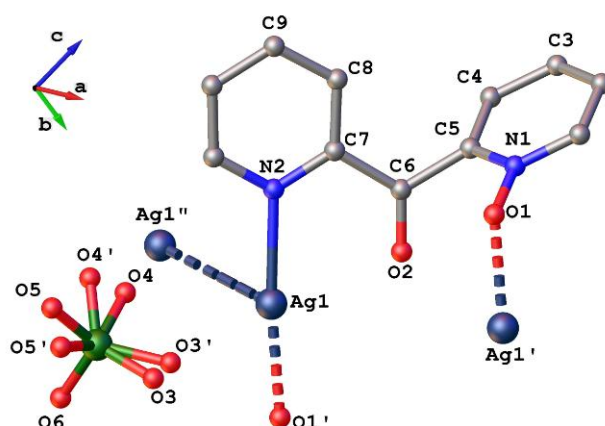


Figure 2.60 – Asymmetric unit of complex **2.39**. Hydrogen atoms are excluded for clarity. Selected bond lengths (Å) and bond angles (°): N1-O1 = 1.329(3), N2-Ag1 = 2.222(2), Ag1''-O1 = 2.215(2), N1-O1-Ag1 = 116.81(1), O1'-Ag1-Ag1' = 100.56(5), O1-Ag1-N2 = 174.59(7), N2-Ag1-Ag1'' = 82.36(5), C7-C6-C5-N1 = 107.5(2).

Complex **2.39** is a 1D linear polymer that extends along the *a*-axis, as shown in figure 2.61a, with [2+2] macrocycles joined by weak Ag $\cdots$ Ag interactions at distances of 3.246(4) Å, as shown in figure 2.61b. The non-bonded distance between the carbonyl oxygen [O2] and Ag1 is 2.633(2) Å, which is slightly longer than other reported Ag-O<sub>keto</sub> distances [2.592(5) Å] in 2,2'-dipyridylketone silver(I) complexes.<sup>[104]</sup> Interestingly, the pyridine N-oxide ring is twisted at a torsional angle of 107.5(2)° [C7-C6-C5-N1] parallel to the nitrogen atom [N2] to coordinate Ag1 centers at distances 2.215(2) Å [O1-Ag1''] and 2.222(2) Å [N2-Ag1], as shown in figure 2.61a.

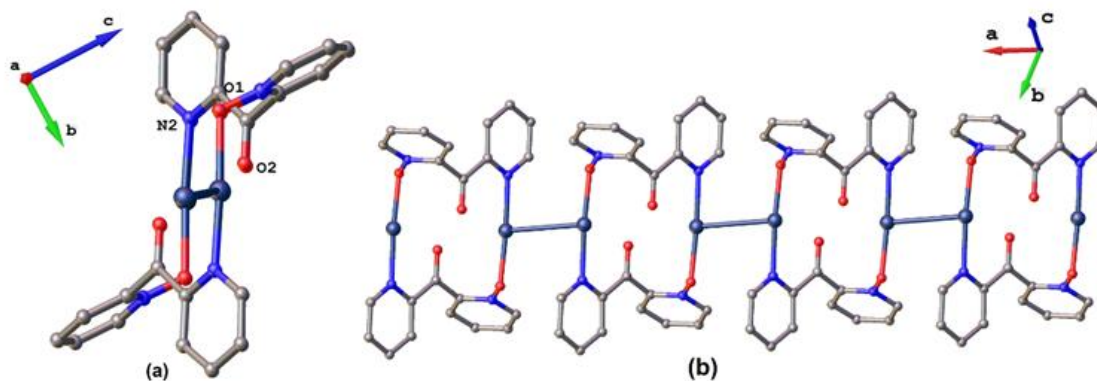


Figure 2.61 – (a) A section of the one-dimensional polymer of complex **2.39** as viewed down the *a*-axis, showing that the O-Ag and N-Ag bond lengths are similar and, (b) 1D polymeric structure showing each [2+2] metallocycle joined by Ag...Ag interactions.

Crystal packing revealed  $\pi$ - $\pi$  interactions between two coplanar pyridine ring systems of adjacent 1D polymeric chains at centroid-centroid distances of 3.515 Å, as shown in figure 2.62.

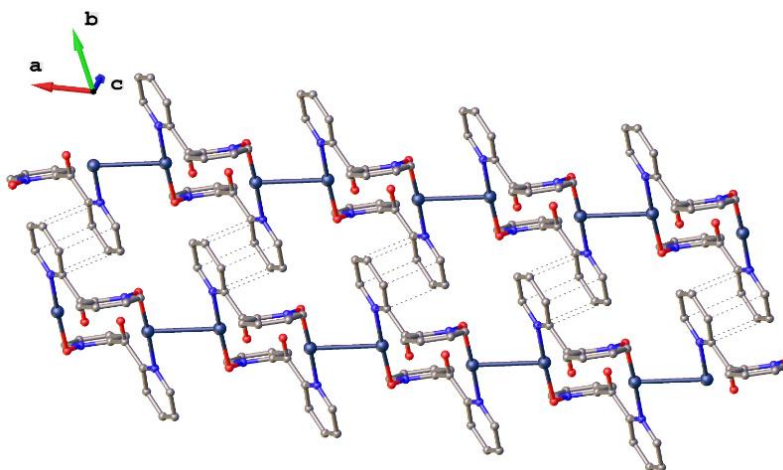
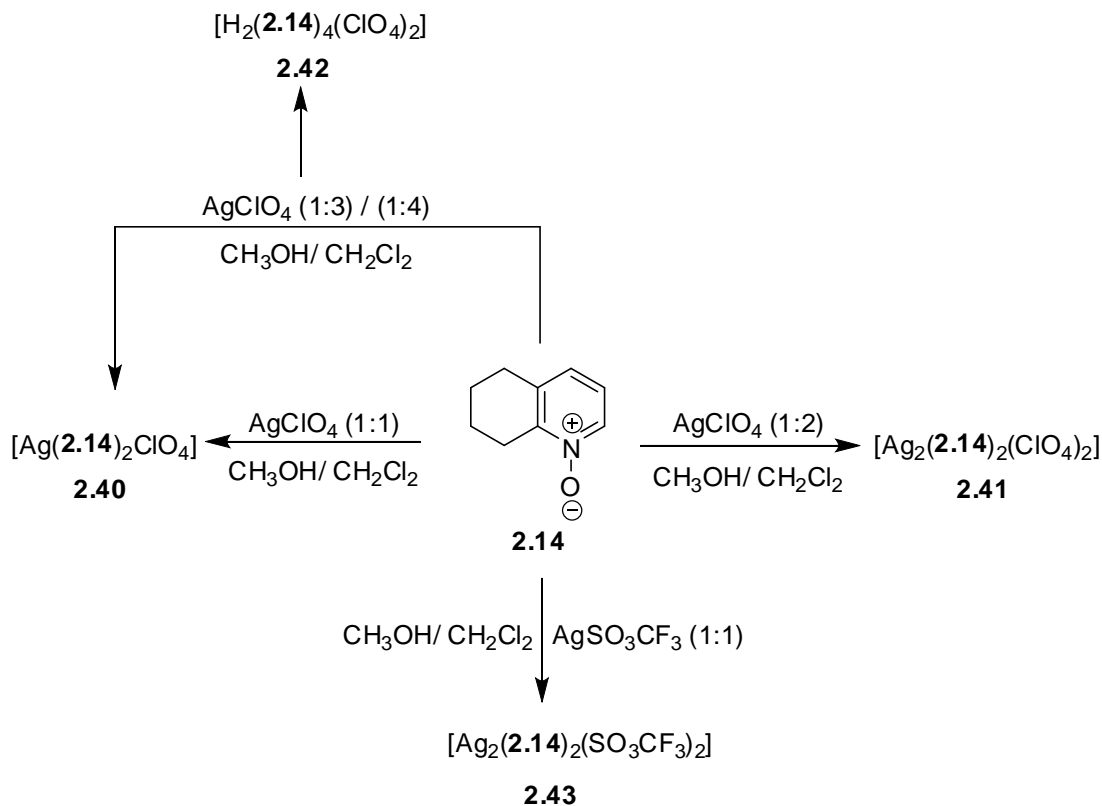


Figure 2.62 – A section of the crystal packing structure showing  $\pi$ - $\pi$  interactions between 1D polymeric units. Hydrogen atoms are omitted for clarity.

### 2.3.10 Complexes with 5,6,7,8-tetrahydroquinoline N-oxide **2.14**

Two complexes, **2.40** and **2.43**, were synthesised with  $\text{AgClO}_4$  and  $\text{AgSO}_3\text{CF}_3$ , using ligand **2.14**, as shown in scheme 2.16. Though the complex **2.41** produced good quality crystals and refined well [ $R_1 = 2.65\%$ ], the elemental analysis did not provide satisfactory results for the expected 1:1 ligand **2.14** to silver(I) ratio. Though cell checks for randomly picked crystals from 1:3 ratio and 1:4 ratio batch samples matched complexes **2.40** and **2.41**, the 1:3 reaction ratio samples also contained a protonated ligand **2.14** with two non-coordinated perchlorates (**2.42**), which will be discussed in detail later.

Scheme 2.16 – Syntheses of complexes **2.40** – **2.43**.With silver(I) perchlorate (1:1) **2.40**

Complex **2.40** was prepared through evaporation of a solution of the ligand **2.14** and  $\text{AgClO}_4$  in a 1:1 mixture of methanol and dichloromethane. The slow evaporation of solvent left colourless needle-like crystals covered in large amounts of unknown black material. These crystals solved in the monoclinic  $P2_1/n$  space group. The asymmetric unit contains two ligand **2.14** molecules, one silver(I) ion and a monodentate  $\text{ClO}_4$  anion with 2:1 ligand to silver(I) ratio, as shown in figure 2.63. The silver(I) ions are five-coordinate [ $\text{Ag1}$  ( $\tau_5 = 0.52$ )] with an  $\text{O}_5$  environment with oxygen donor atoms supplied from four ligands and a perchlorate anion. The N1-O1 and N2-O2 bond distances are 1.339(8) Å and 1.336(4) Å, respectively, which are longer than any other reported bond lengths for ligand **2.14** [1.310(2) Å].<sup>[105]</sup> The ligand **2.14** oxygens, O1 and O2, adopt a  $\mu_2$ -O,O bidentate bridging mode with Ag1, Ag1'' and Ag1, Ag' ions with Ag-O<sub>ligand</sub> distances ranging from 2.347(1) Å to 2.450(1) Å. The coordination angles of N1-O1-Ag1 and N2-O2-Ag1 are 126.53(1)° and 129.02(1)°, and their average bridging angles [Ag-O<sub>ligand</sub>-Ag] are larger than those reported for copper(II) complexes with ligand **2.15**.<sup>[106]</sup>

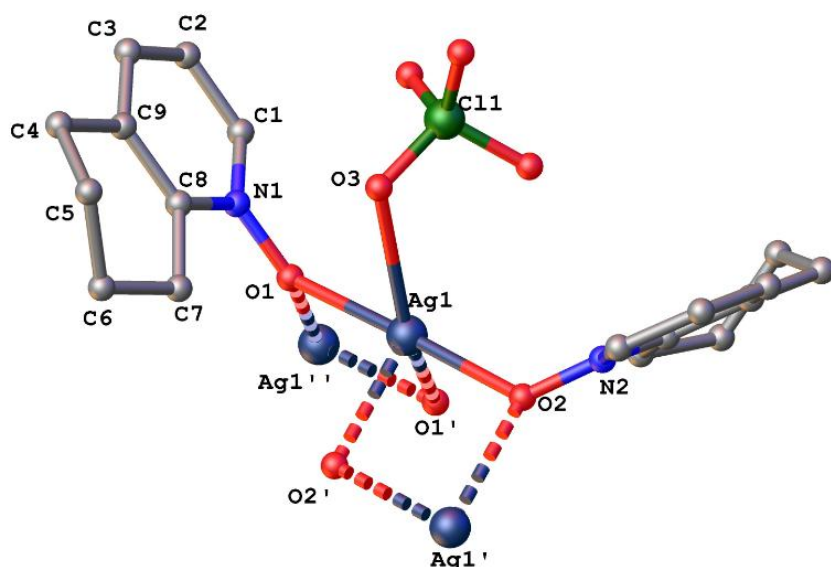
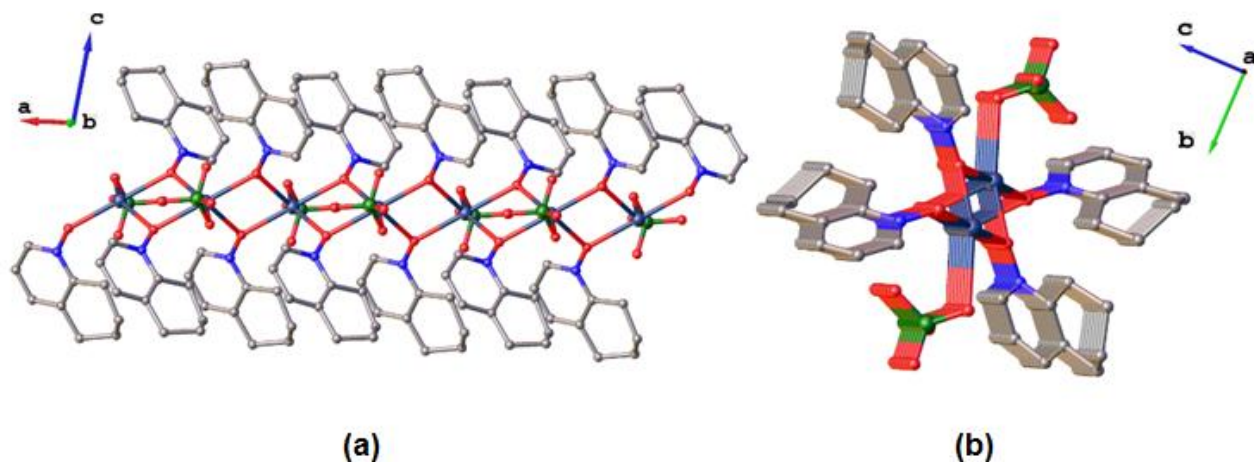


Figure 2.63 – Asymmetric unit of complex **2.40**. Hydrogen atoms are excluded for clarity. Selected bond lengths (Å) and bond angles (°): N1-O1 = 1.339(8), N2-O2 = 1.336(4), Ag1-O1 = 2.361(1), Ag1-O2 = 2.347(1), Ag1'-O1 = 2.426(1), Ag1'-O2 = 2.450(1), N1-O1-Ag1 = 126.53(1), N2-O2-Ag1 = 129.02(1), Ag1-O1-Ag1' = 106.28(5), Ag1-O2-Ag1' = 105.53(5).

The pyridine N-oxide ring in the fused ring structure is planar, while the cyclohexyl- fragment has twisted to adopt a half-chair arrangement, as shown in figure 2.63. The dihedral angles of  $39.5(2)^\circ$  [C5-C6-C7-C8] and  $53.1(2)^\circ$  [C9-C4-C5-C6] are very slightly larger than the reported values for ligand **2.14** [ $38.1^\circ$  and  $51.2^\circ$ ].<sup>[105]</sup> The asymmetric unit grows into a 1D polymer along the *a*-axis [figure 2.64a], with four-membered rings formed by two ligands bridging two silvers [Ag1-O1-Ag1''-O1' and Ag1-O2-Ag1'-O2']. Their respective perchlorates are directed along the *b*-axis, as shown in figure 2.64c.



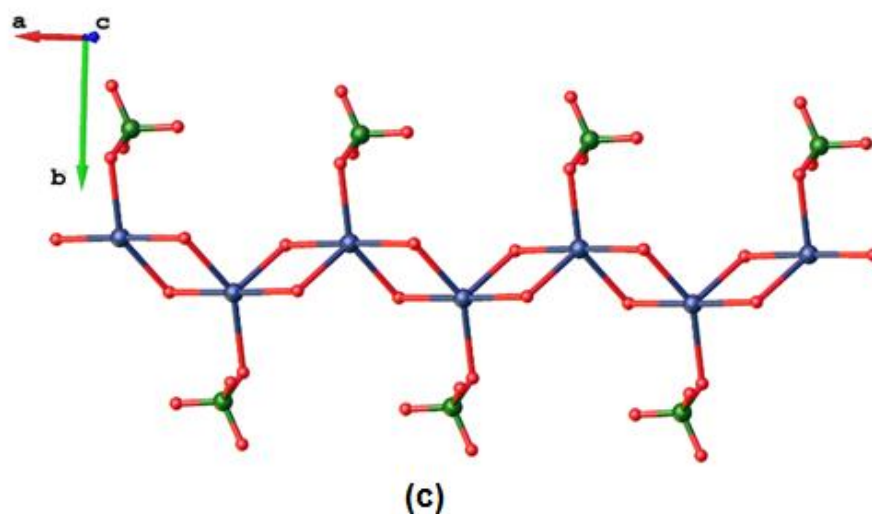


Figure 2.64 – One-dimensional polymer of complex **2.40** as viewed down the (a) *b*-axis, (b) *a*-axis (c) skeletal view of the  $\text{Ag}_2\text{O}_2$  rings formed in the 1D polymeric chain of complex **2.40** as viewed down the *c*-axis [constructed using Ag, O and Cl atoms]. Ligands **2.14** are excluded for clarity. In structures (a) and (b) the hydrogen atoms are omitted for clarity.

#### With silver(I) perchlorate (1:2) **2.41**

A single crystal of the silver(I) complex **2.41** suitable for X-ray crystallographic analysis was isolated from a mixture containing a 1:2 ligand to  $\text{AgClO}_4$  stoichiometric ratio. Again the rectangular crystal plates were grown and picked from an unknown black material. The complex **2.41** crystallised and solved in the triclinic *P*-1 space group. The asymmetric unit contains two ligands **2.14** and two coordinated monodentate perchlorate anions at Ag1 and Ag2, with one perchlorate [Cl2] being disordered over two oxygens atoms, O8 and O9, in 77:23 occupancy ratio, as shown in figure 2.65. The complex **2.41** has a 1:1 ligand to silver(I) ratio. The bond distances of N1-O1 and N2-O2 are 1.362(3) Å and 1.360(3) Å, respectively, which are longer than the values seen in complex **2.40**. The Ag-O<sub>ligand</sub> bond distances vary from 2.275(2) Å to 2.357(2) Å, with their average 2.313(2) Å, shorter than the values observed in complex **2.40**. The coordination angles are 118.21(1)° [N1-O1-Ag2], 114.36(1)° [N1-O1-Ag1], 112.34(4)° [N2-O2-Ag1] and 111.81(1)° [N2-O2-Ag2]; these values are found to be smaller than in complex **2.40**.

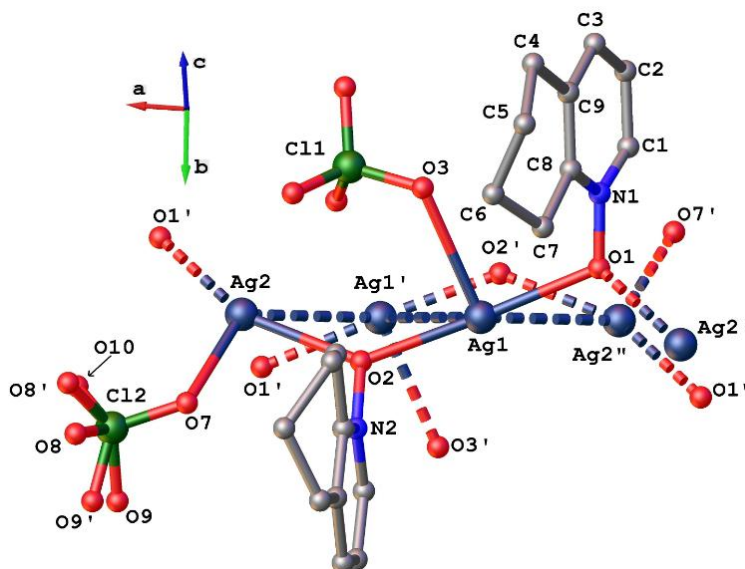


Figure 2.65 – Asymmetric unit of complex **2.41**. Hydrogen atoms are excluded for clarity. Selected bond lengths (Å) and bond angles (°): N1-O1 = 1.362(3), N2-O2 = 1.360(3), Ag2'-O1 = 2.306(2), Ag1-O1 = 2.315(2), Ag1-O2 = 2.275(2), Ag2-O2 = 2.357(2), N1-O1-Ag2' = 118.21(1), N1-O1-Ag1 = 114.36(14). N2-O2-Ag1 = 112.34(1), N2-O2-Ag2 = 111.81(1), Ag1-O1-Ag2' = 115.43(8), Ag1-O2-Ag2 = 135.53(8).

As usual, the pyridine rings are planar, while the cyclohexane ring systems are twisted to adopt a half-chair conformation, similar to complex **2.40**, with torsional angles 43.9(5)° [C5-C6-C7-C8] and 45.0(7)° [C9-C4-C5-C6]. Their average torsional angles [44.5(5)°] are similar to the values observed in complex **2.40** [46.3(2)°]. Complex **2.41** is a 1D linear polymer propagating along the *a*-axis, as shown in figure 2.66.

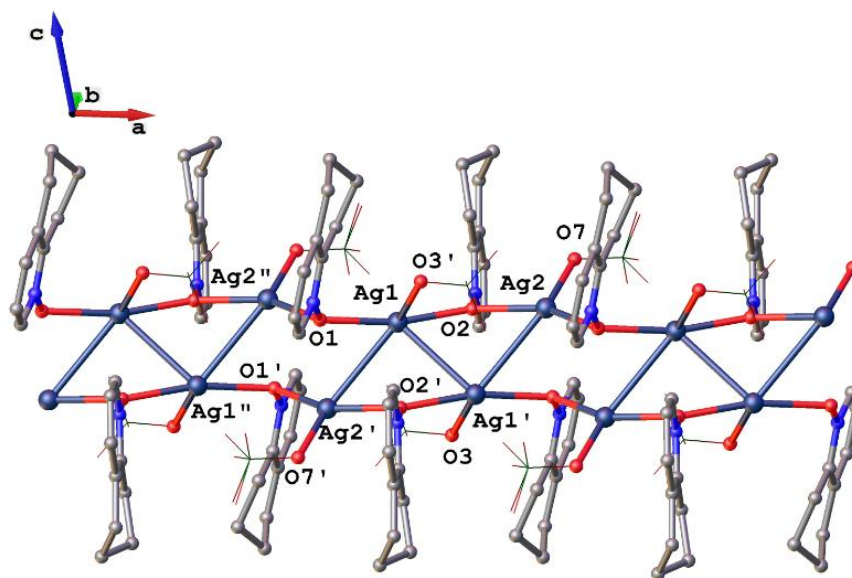


Figure 2.66 – 1D Polymeric structure of complex **2.41**. Selected atoms are labeled for description and hydrogen atoms are omitted for clarity.

As seen in figure 2.66, the silvers Ag1 [ $\tau_5 = 0.51$ ] and Ag2 [ $\tau_4 = 0.50$ ] are five- and four-coordinate, and interact in a 'Z' shape at an average distance of 3.143 Å, with an angle of 85.93(1)° [Ag1-Ag1'-Ag2]. Each of these 'Z'-shaped Ag $\cdots$ Ag units are bridged by a ligand oxygen O2 at an angle of 135.53(8)° [Ag1-O2-Ag2], and each 'Z'-shaped Ag $\cdots$ Ag unit is linked by ligand **2.14** oxygen [O1] at an angle of 115.43(8)° [Ag1-O1-Ag2'].

#### With silver(I) perchlorate (1:3) **2.42**

The crystal structure of salt **2.42** was solved in the monoclinic  $P2_1/c$  space group. The crystal for X-ray crystal analysis was taken from a 1:3 ligand to AgClO<sub>4</sub> reaction mixture. The asymmetric unit of **2.42** is comprised of four ligand molecules, two of which are protonated, and two non-coordinated perchlorate anions, as shown in figure 2.67. The positive charge on the two protonated ligand molecules is balanced by two perchlorate anions. The average N-O<sub>ligand</sub> bond length, 1.361(9) Å, is greater than that of the average bond distance seen in complex **2.40** [1.339(4) Å], and it is equal to complex **2.41** [1.361(3) Å]. The angles between the protons [H3 and H4] and ligand oxygens are 165.02° [O1'-H3-O3] and 138.42° [O2-H4-O4]. The pyridine rings are planar with twisted cyclohexane ring systems adopting half-chair conformations with torsional angles ranging from 42.5(1)° to 50.1(1)°, their average, 46.23(1)°, is close to that observed in the previously reported hydrogen bonded networks of ligand **2.14** [44.65°].<sup>[105]</sup>

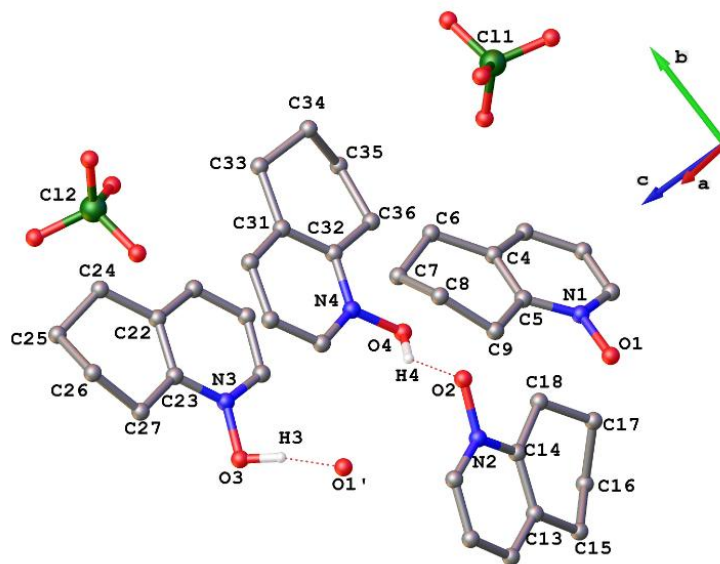


Figure 2.67 – Asymmetric unit of compound **2.42**. Selected hydrogen atoms are excluded for clarity. Selected bond lengths (Å) and bond angles (°): N1-O1 = 1.374(1), N2-O2 = 1.355(9), N3-O3 = 1.353(9), N4-O4 = 1.362(9), O3-H3 = 0.92(6), O4-H4 = 0.97(6), O1'-H3-O3 = 165.02, O2-H4-O4 = 138.42, C4-C6-C7-C8 = 47.0(1), C5-C9-C8-C7 = 46.1(1), C13-C15-C16-C17 = 48.4(1), C14-C18-C17-C16 = 42.5(1), C23-C27-C26-C25 = 43.8(1), C22-C24-C25-C26 = 50.1(1), C32-C36-C35-C34 = 42.7(1), C31-C33-C34-C35 = 49.3(1).



### With silver(I) triflate (1:1) **2.43**

The crystal structure of ligand **2.14** with  $\text{AgSO}_3\text{CF}_3$  was crystallised and solved in the triclinic  $P-1$  space group. The asymmetric unit contains two ligand **2.14** molecules and two silver(I) ions in a 1:1 ligand to silver(I) ratio, as shown in figure 2.68. The complex **2.43** has two coordination modes, with  $\mu_3$ -O,O,O tridentate ligands at N1-O1 groups and a  $\mu_2$ -O,O bidentate bridging at N2-O2, with distances of 1.355(3) Å and 1.349(3) Å, respectively. The average N-O<sub>ligand</sub> bond distance of 1.352(3) Å is greater than that observed in the silver(I) perchlorate complex **2.40** [1.339(4) Å] and less than **2.41** [1.361(3) Å]. The average Ag-O<sub>ligand</sub> bond distance of 2.436(2) Å shows that the coordination ability of ligand **2.14** in complex **2.43** is weaker than that seen in complexes **2.40** [2.396(1) Å] and **2.41** [2.313(2) Å]. As usual, the pyridine rings are planar, while the fused cyclohexane ring is twisted to adopt half-chair formations with torsional angles [C5-C6-C7-C8 = 37.2(4)° and C9-C4-C5-C6 = 53.9(4)°] similar to complex **2.40**.

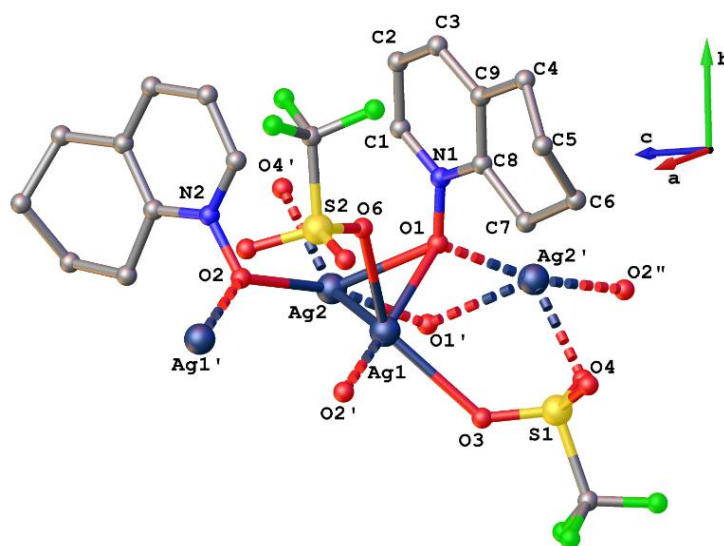


Figure 2.68 – Asymmetric unit of complex **2.43**. Hydrogen atoms are excluded for clarity. Selected bond lengths (Å) and bond angles (°): N1-O1 = 1.355(3), N2-O2 = 1.349(3), Ag1-O1 = 2.384(2), Ag2-O1 = 2.580(2), Ag2-O2 = 2.346(2), N1-O1-Ag2 = 116.06(2), N1-O1-Ag1 = 117.13(1), N1-O1-Ag2 = 122.15(2), N2-O2-Ag1' = 112.22(2), N2-O2-Ag2 = 109.59(2), Ag2-O1-Ag2' = 104.11(7), Ag1-O1-Ag2 = 74.36(5), Ag1-O1-Ag2' = 116.07(8), Ag1'-O2-Ag2 = 137.77(9), Ag1-Ag2 = 3.004(3).

The coordination angles of the bidentate and tridentate ligands with the silver(I) ions range from 109.59(2)° to 122.15(2)°. The two five coordinate Ag1 [ $\tau_5 = 0.41$ ] and Ag2 [ $\tau_5 = 0.42$ ] centers are interacting at a distance of 3.004(3) Å; with the O2 oxygen of ligand **2.14** bridging Ag1 and Ag2 at an angle of 74.36(5)°. Complex **2.43** is a 1D linear polymer which grows along the *a*-axis, as shown in figure 2.69a. The triflate anions of complex **2.43** are monodentate and bidentate, as

seen in figure 2.69b. The monodentate and bidentate triflate anions are pointing up and down along the *b*-axis in opposite directions to the bidentate and tridentate ligands.

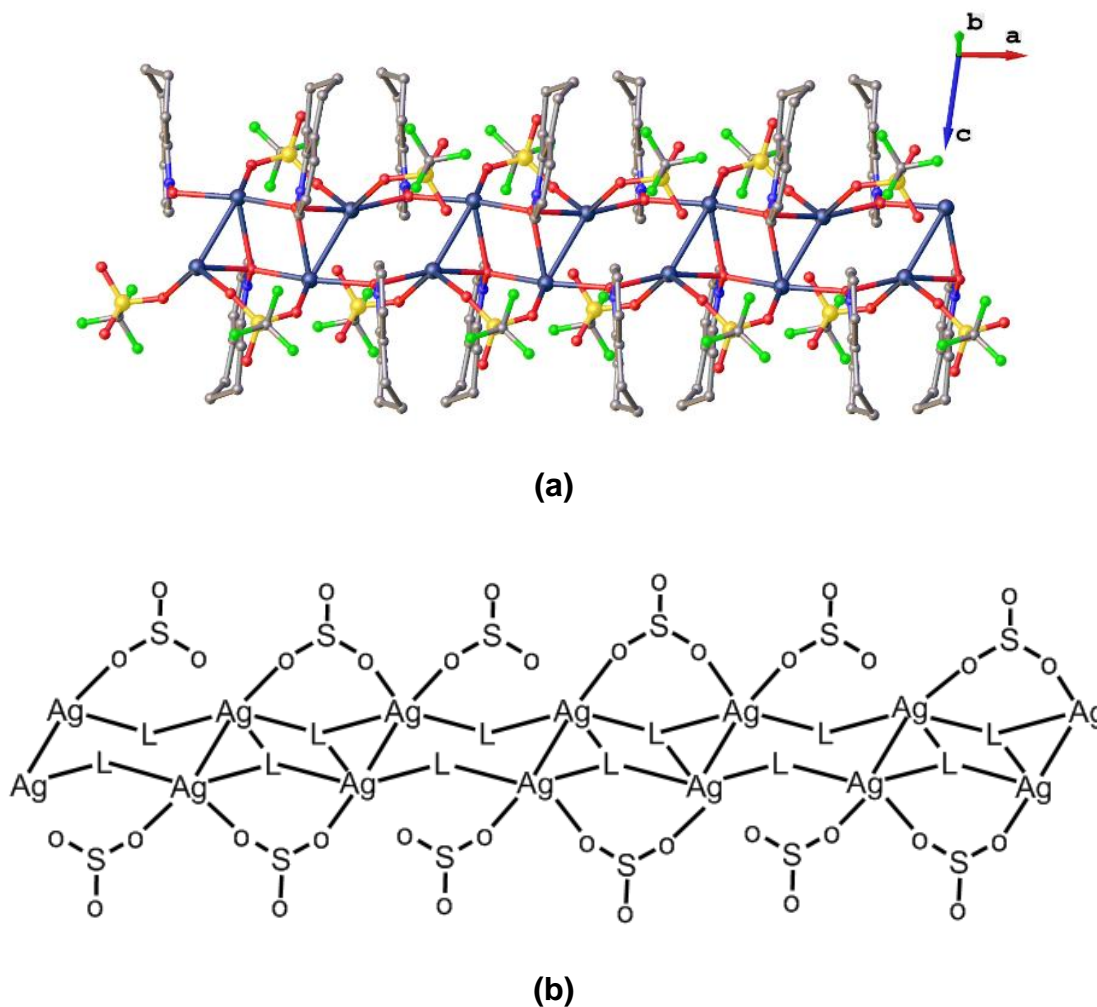
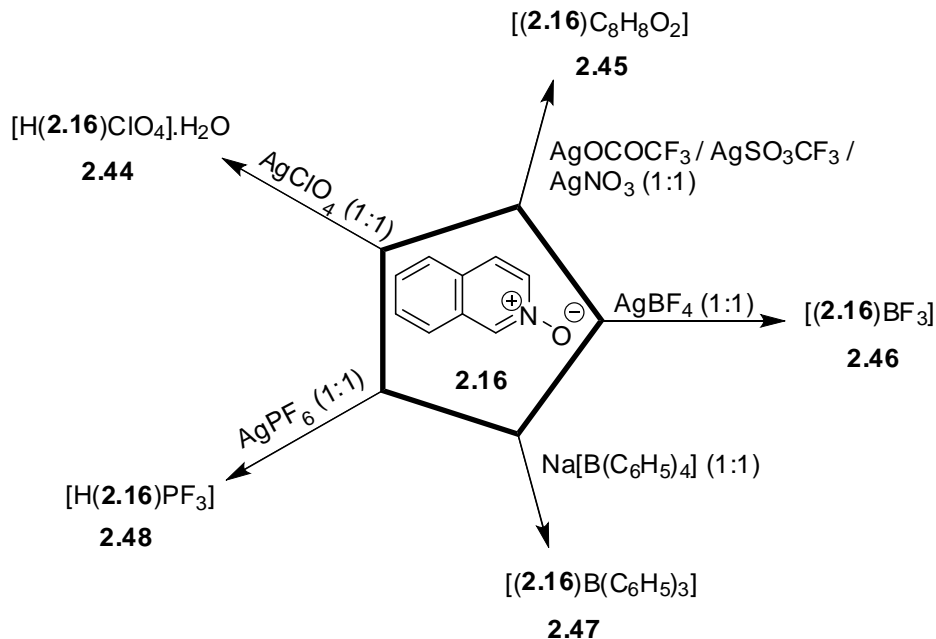


Figure 2.69 – (a) 1D Polymer of complex **2.43** with the hydrogen atoms excluded for clarity. (b) Topological view for the above 1D polymer.

### 2.3.11 Reactions with isoquinoline N-oxide **2.16**

All the compounds shown in scheme 2.17 were prepared in 1:1 methanol to acetonitrile solvent ratios and crystals were obtained by slow evaporation of the solution. When ligand **2.16** was reacted with  $\text{AgClO}_4$ ,  $\text{AgBF}_4$  and  $\text{AgPF}_6$  it gave three different compounds [**2.44**, **2.46** and **2.47**] under similar solvent and reaction conditions, whereas when ligand **2.16** was reacted with  $\text{AgOCOCF}_3$ ,  $\text{AgSO}_3\text{CF}_3$  and  $\text{AgNO}_3$  they all formed co-crystal **2.45**.

It is known from previous literature that some pyridine N-oxides are capable of forming adducts with boron compounds,<sup>[44, 107]</sup> such as **2.46**. We also successfully crystallised adduct **2.47**, similar to **2.46**, when ligand **2.16** was treated with  $\text{Na}[\text{B}(\text{C}_6\text{H}_5)_4]$  under similar reaction conditions to prepare complex **2.46**. Compound **2.48** is closely related to compound **2.42**.



Scheme 2.17 – Syntheses of compounds **2.44** – **2.48**.

#### With silver(I) perchlorate (1:1) **2.44**

Due to the high reactivity of oxygen in the N-oxide molecules, they are more reactive towards proton donor molecules, forming two possible structures, (a) and (b), which are depicted in figure 2.70.<sup>[108]</sup> A structure 2.70a has formed in most cases e.g., in tris[hydrogenbis(pyridine N-oxide)] and in the complex of 2,6-dimethylpyridine N-oxide with pentachlorophenol,<sup>[109]</sup> while the structure type 2.70b is inherent in a few commercially available N-oxides e.g., 4-dimethylaminopyridine N-oxide,<sup>[110]</sup> 4-methoxy pyridine N-oxide and HX (X = ClO<sub>4</sub>, CH<sub>3</sub>CO<sub>2</sub>) salts<sup>[111]</sup> where protonated cationic complexes of pyridine N-oxides are stabilized by their respective anions.

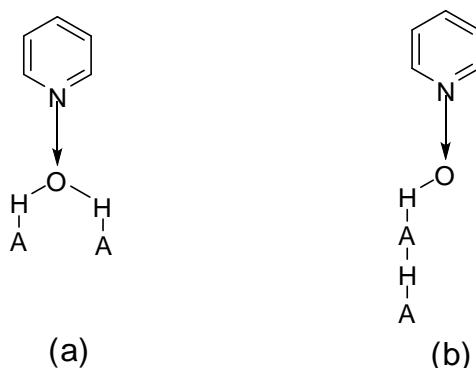


Figure 2.70 – Possible products from reactions of pyridine N-oxides with protic solvents.

The crystal structure of ligand **2.16** with AgClO<sub>4</sub> was solved in the triclinic *P*-1 space group, as shown in figure 2.71. The asymmetric unit contains a water molecule that interacts with a protonated ligand **2.16**, [H(C<sub>9</sub>H<sub>7</sub>NO)]<sup>+</sup> stabilized by a perchlorate anion. The N1-O1 [1.374(3) Å]

bond distance is longer than the usual N-O single bond distances previously reported for hydrogen bonded pyridine N-oxides.<sup>[112]</sup> The bond angle, 109.5° [N1-O1-H1], shows that the oxygen orbitals are sp<sup>3</sup> hybridised with a hydrogen bonded N-oxide group [ $d(\text{O1}\cdots\text{O2}) = 2.513 \text{ \AA}$ ], similar to other reported protonated pyridine N-oxide ring systems.<sup>[112]</sup>

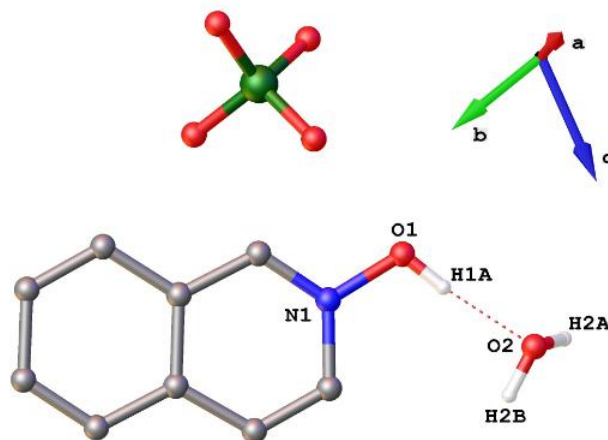


Figure 2.71 – Asymmetric unit of salt **2.44**. Selected hydrogen atoms are excluded for clarity. Selected bond lengths (Å) and bond angles (°): N1-O1 = 1.374(3), O1-H1A = 0.8200, N1-O1-H1A = 109.5, H2A-O2-H2B = 109.5.

#### With silver(I) trifluoroacetate/ triflate/ nitrate (1:1) **2.45**

Compound **2.45** solved in the triclinic *P*-1 space group, and contains a ligand molecule interacting with a protonated 1,2-benzenedicarboxylic acid, as shown in figure 2.72. The formation of phthalic acid could be either from oxidation of ligand **2.16** by silver(I) salts or contamination from hydrolysed dibutyl phthalate in plastic vial caps used during crystal growth. The N1-O1 [1.346(5) Å] bond distance is shorter than that seen in complex **2.44**. In compound **2.45**, the O-H group of the carboxylic acid and the N-O group are interacting through a hydrogen bond. The O1-H5A, O5 $\cdots$ O1, O3-H3A and O3-O1' distances are 0.920(2) Å, 2.618(2) Å, 0.938(7) Å and 2.618(2) Å respectively, with bond angles 168.31(1)° [O5-H5A $\cdots$ O1] and 165.72(2)° [O3-H3A $\cdots$ O1'] which are close to the reported crystal structures of isoquinoline N-oxide with 2-nitrobenzoic acid.<sup>[113]</sup>

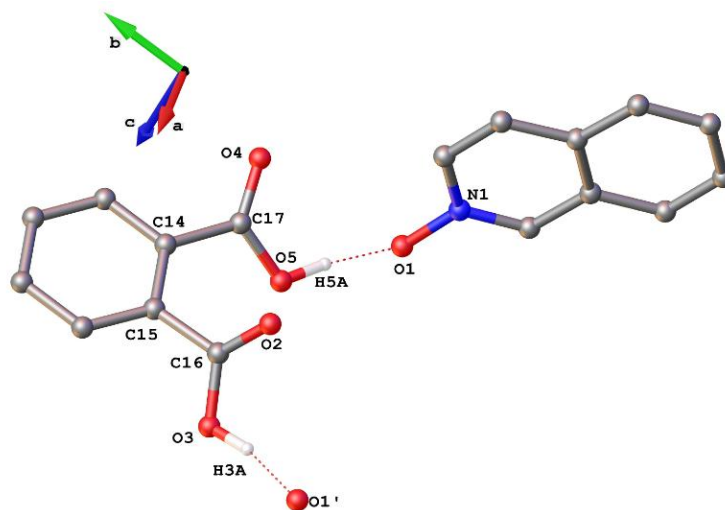


Figure 2.72 – Asymmetric unit of **2.45**. Selected hydrogen atoms are excluded for clarity. Selected bond lengths (Å) and bond angles (°): N1-O1 = 1.346(5), C16-O2 = 1.211(2), C16-O3 = 1.319(2), C17-O4 = 1.214(2), C17-O5 = 1.319(2), O2-C16-O3 = 124.18(1), O4-C17-O5 = 124.06(1).

#### With silver(I) tetrafluoroborate (1:1) **2.46**

The asymmetric unit of compound **2.46** solved in the orthorhombic *Pbca* space group, with one ligand **2.16** and a BF<sub>3</sub> adduct in a 1:1 ratio, as shown in the figure 2.73. The oxygen [O1] and BF<sub>3</sub> anion have a tetrahedral arrangement with angles 109.62(3)° [F1-B1-O1], 109.03(2)° [F2-B1-O1] and 104.55(2)° [F3-B1-O1]. The N1-O1 bond distance [1.374(1) Å] and angle 111.45(1)° [N1-O1-B1] clearly shows that the oxygen orbitals are once again sp<sup>3</sup> hybridised. The bond distances 1.374(1) Å [N1-O1] and 1.511(1) Å [B1-O1] are close to the reported single bond distances in complexes of a similar type.<sup>[114]</sup>

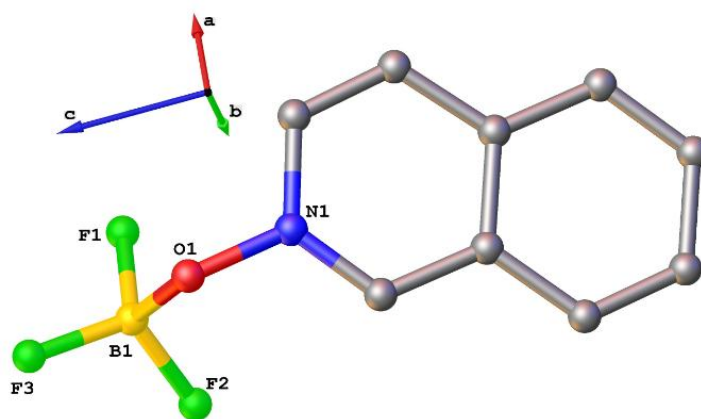


Figure 2.73 – Asymmetric unit of complex **2.46**. Hydrogen atoms are excluded for clarity. Selected bond lengths (Å) and bond angles (°): N1-O1 = 1.374(1), N1-O1-B1 = 111.35(1), B1-F1 = 1.385(2), B1-F2 = 1.381(2), B1-F3 = 1.367(2), B1-O1 = 1.510(2), F1-B1-O1 = 109.52(1), F2-B1-F1 = 108.83(1), F2-B1-O1 = 109.92(1), F3-B1-F1 = 112.03(1), F3-B1-F2 = 112.01(1), F1-B1-O1 = 109.62(3), F2-B1-O1 = 109.03(2), F3-B1-O1 = 104.45(1).

### With sodium(I) tetraphenylborate (1:1) **2.47**

Compound **2.47** was prepared in a 1:1 ligand **2.16** to  $\text{Na}[\text{B}(\text{C}_6\text{H}_5)_4]$  stoichiometric ratio to give pale orange blocks which are highly hygroscopic in nature. The structure was solved in the monoclinic  $P2_1/c$  space group. The actual asymmetric unit composition contains five 1:1 ligand **2.14** to  $\text{B}(\text{C}_6\text{H}_5)_3$  adducts, as shown in figure 2.74. Due to disorder problems over isoquinoline aromatic rings, the asymmetric unit is not shown in full. The chemistry between ligand **2.16** and  $\text{Na}[\text{B}(\text{C}_6\text{H}_5)_4]$  is similar to that with  $\text{AgBF}_4$  [compound **2.46**], replacing a phenyl ring to form a B-O bond. Compound **2.47** has short N1-O1 [1.356(5) Å] and long B1-O1 [1.581(7) Å] bond distances when compared to **2.46**.

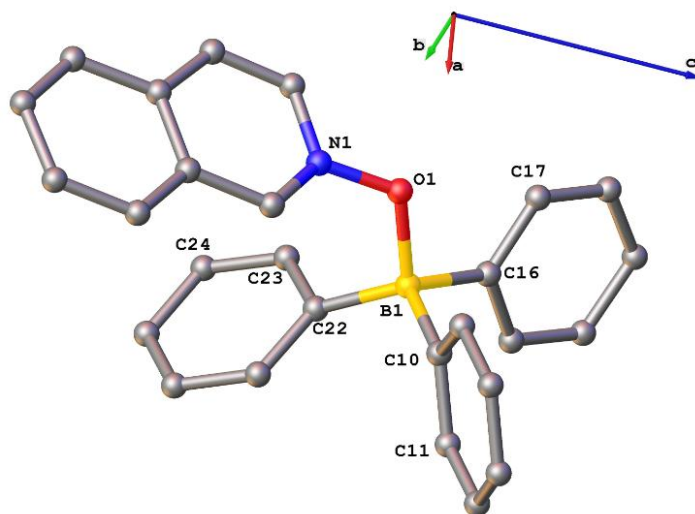


Figure 2.74 – Asymmetric unit of **2.47**. Hydrogen atoms are excluded for clarity. Selected bond lengths (Å) and bond angles (°): N1-O1 = 1.356(5), B1-O1 = 1.581(7), N1-O1-B1 = 118.2(4), O1-B1-C22-C23 = 63.6(7), O1-B1-C16-C17 = 6.0(7), O1-B1-C10-C11 = 176.4(5).

### With silver(I) hexafluorophosphate (1:1) **2.48**

Pyridine N-oxides primarily form two types of compounds: (i) complexes with the N-oxides acting as bridging or monodentate ligands that are coordinated to the metal or (ii) di-adducts of the N-oxide,<sup>[115]</sup> which form protonated  $[\text{H}(\text{N-oxide})_2]^+$  ions, stabilized by anions, as shown in figure 2.75.

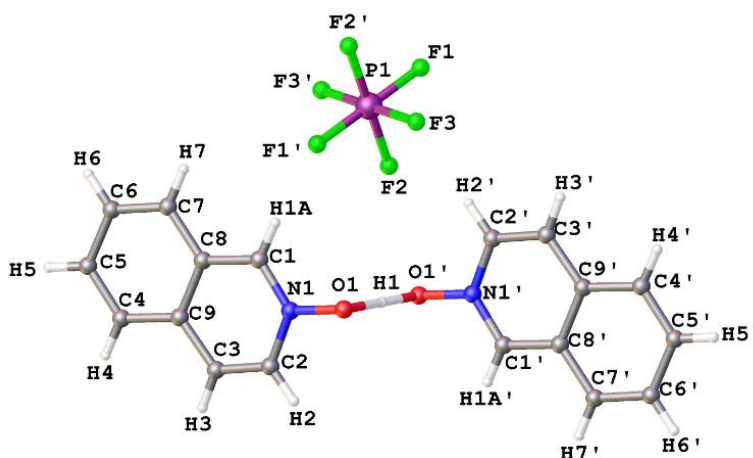


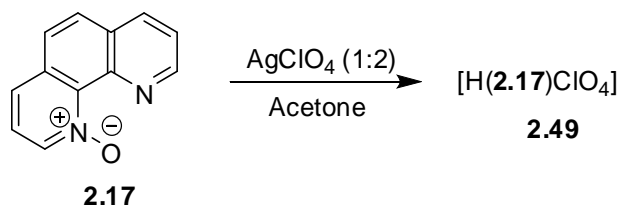
Figure 2.75 – Asymmetric unit of **2.48**. Selected bond lengths (Å) and bond angles (°): N1-O1 = 1.357(2), O1-H1 = 1.201(1), O1-H1-O1' = 180.0(1).

The asymmetric unit of **2.48**, solved in the monoclinic  $C2/c$  space group, contains one ligand **2.16** and half a  $PF_6$  anion with a hydrogen shared between two ligand molecules, as shown in figure 2.75. The N1-O1 bond length of 1.357(2) Å agrees well with other reported distances 1.358(2) Å of hydrogen bonded di-adducts with mono-N-oxides. The symmetry related O-H bond in the dimeric cation  $[H(C_9H_8NO)_2]^+$  has a length of 1.201(1) Å [O1-H1] with an extremely short O1...O1' separation of 2.402 Å, close to the shortest O...O distance of 2.290 Å reported to date for  $[H_3O]^+$ , which also has an inversion center.<sup>[116]</sup>

### 2.3.12 Reactions of 1,10-phenanthroline N-oxide **2.17**

#### With silver(I) perchlorate (1:2) **2.49**

Predictable results were obtained with the reaction of ligand **2.17** and silver(I) perchlorate in a methanol and acetonitrile mixture. Attempts to grow complexes in aprotic solvents were unsuccessful. The crystal structure with silver(I) perchlorate was solved in the triclinic  $P-1$  space group, and contains a perchlorate anion and a ligand protonated at nitrogen [N15], which in turn is interacting with the adjacent oxygen [O1], as seen in figure 2.76. The bond distance [N2-O1 = 1.315(2) Å] distinctly reveals that N-O is of double bond character.



Scheme 2.18 – Synthesis of **2.49**.

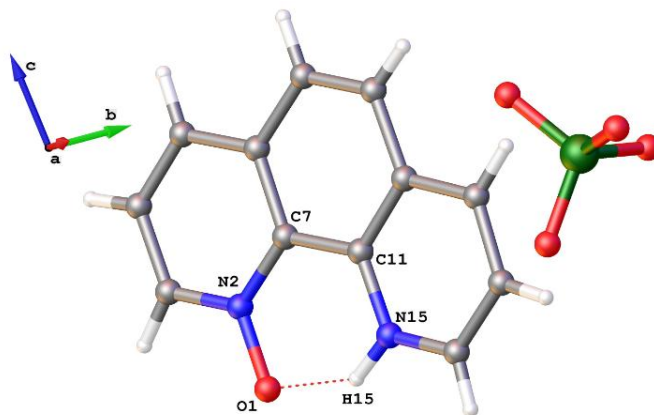


Figure 2.76 – Asymmetric unit of **2.49**. Selected bond lengths (Å): N2-O1 = 1.315(2), N15-H15 = 0.920(2).

The asymmetric unit assembles into a three-dimensional polymeric network using weak interactions, which are provided by the electron rich and deficient aromatic ring systems, as shown in figure 2.77. The interaction between O1 and H15 forms a six-membered ring. The  $sp^2$  hybridised oxygen atoms, O1 and O1' are interacting with hydrogens H3 and H3' to form an eight-membered ring, while the electron rich pyridine N-oxide ring system has  $\pi$ -stacking with an electron deficient pyridine ring at centroid-centroid distances 3.593 Å, as seen in figure 2.77. The hydrogen bonding parameters are shown in table 2.4.

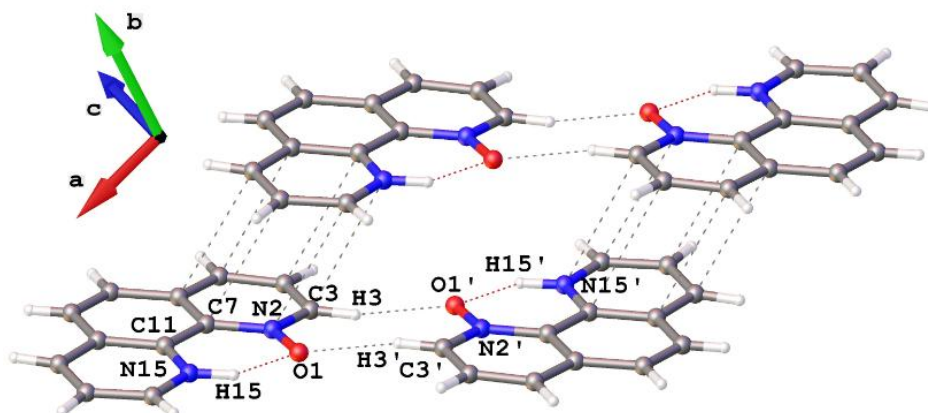


Figure 2.77 – Hydrogen bonded network and  $\pi$ -stacking for **2.49**.

Table – 2.4 Hydrogen bond parameters in **2.49**.

D-H...A	$d_{D-H}$ (Å)	$d_{H...A}$ (Å)	$d_{D...A}$ (Å)	$\angle D-H...A$ (°)
N15-H15...O1	0.919	1.752	2.527	140.11
C3'-H3'...O1	0.956	2.314	3.238	162.64



## 2.4 Conclusions

In this chapter, we described the syntheses of various pyridine N-oxides that have been prepared by oxidizing their respective nitrogen heterocycles using either mCPBA or 50% hydrogen peroxide. Most of the work investigates the complexation of a family of pyridine N-oxides with silver(I) salts. Single crystal analyses of these silver(I) complexes provided information about the interactions and other factors that may direct one to the formation of particular arrays.

In all the pyridine N-oxide silver(I) perchlorate complexes discussed in this chapter, the polymers obtained are one-dimensional [excluding weak interactions], whether the perchlorate anion is coordinated or non-coordinated. Three types of perchlorate anions are commonly observed, non-coordinated, monodentate and bridging bidentate; of which the first two are the most commonly observed, while the bidentate bridging is only seen in complex **2.18**. Interestingly, in all the silver(I) perchlorate complexes, ligands adopted a maximum denticity of either two or three, for the electron rich pyridine N-oxide ligands, such as **2.1**, **2.11** and **2.12**. Also, in silver(I) complexes of non-coordinated and bidentate perchlorates, silver(I) ions adopted a six-coordinate geometry, as observed in complexes **2.18** and **2.36**.

In the silver(I) trifluoroacetate complexes, a secondary binding unit [SBU],<sup>[103a, 103b]</sup> linearly links  $\mu_2$ -O,O bidentate bridging ligands to yield one-dimensional polymers, as shown in figure 2.78. Most of these complexes adopted one-dimensional networks with strong Ag $\cdots$ Ag interactions with bidentate trifluoroacetate anions on both sides. A maximum denticity of two was attained by these pyridine N-oxides with six-coordinate silver(I) ions. In some complexes, such as **2.21** and **2.37**, these trifluoroacetate anions prefer to coordinate water molecules than pyridine N-oxide ligands giving rise to hydrogen bonded networks.

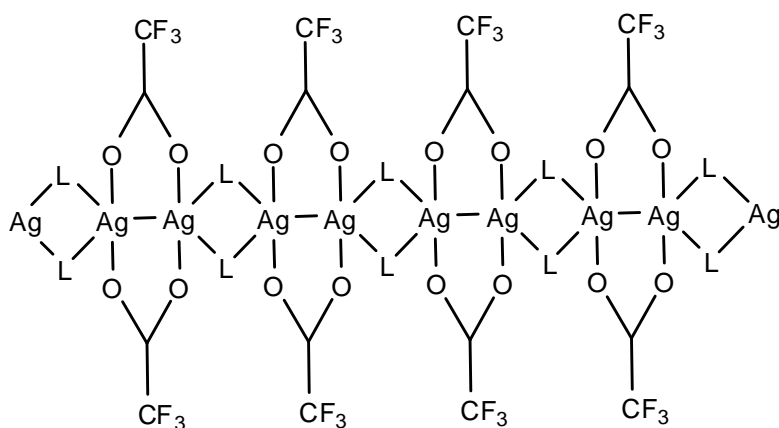


Figure 2.78 – 1D Topological type polymer showing secondary binding units [SBU] joined by  $\mu_2$ -O,O bidentate bridging ligands.

It is apparent from some of the silver(I) trifluoroacetate complexes that these trifluoroacetate bridged  $\text{Ag}\cdots\text{Ag}$  interactions resulted in consistent structural motifs with different pyridine N-oxides, as shown in figure 2.79. Hence, these complexes offer the prospect for control of the overall structure arrangement, while maintaining some flexibility.

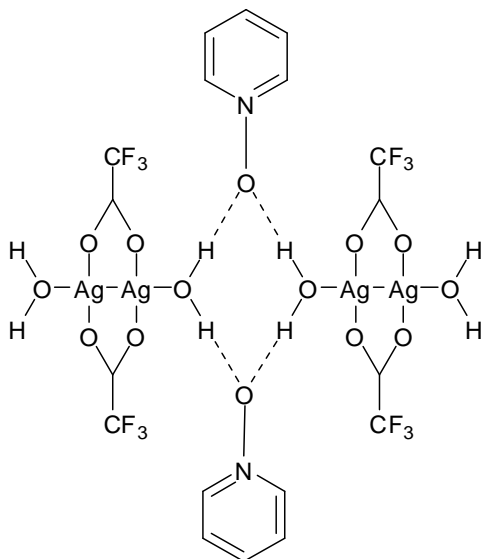


Figure 2.79 – General representation of the hydrogen bonded networks seen in the pyridine N-oxide silver(I) trifluoroacetate complexes.

In silver(I) triflate complexes, the motifs obtained depend on the type of coordination mode adopted by the triflate anion or the ligand type used. Out of the four silver(I) triflate complexes synthesised [**2.22**, **2.25**, **2.33** and **2.43**], **2.25** and **2.33** were two-dimensional with the triflates in tridentate and tetradentate coordination modes, while complexes **2.22** [ $\mu_2$ - and  $\mu_3$ -triflates] and **2.37** [ $\mu$ - and  $\mu_2$ -triflates] are 1D polymers. In complexes **2.25** and **2.33**, the triflate anions are tri- and tetradentate, giving ligands **2.4** and **2.8** a  $\mu_2$ -bidenticity, whereas in complex **2.43** the triflates are mono and bidentate with more ligands [**2.14**] and silver(I) ion interactions, resulting in maximum denticity for the pyridine N-oxides and coordination geometries for silver(I) ions from 3 to 6, as shown in figure 2.80.

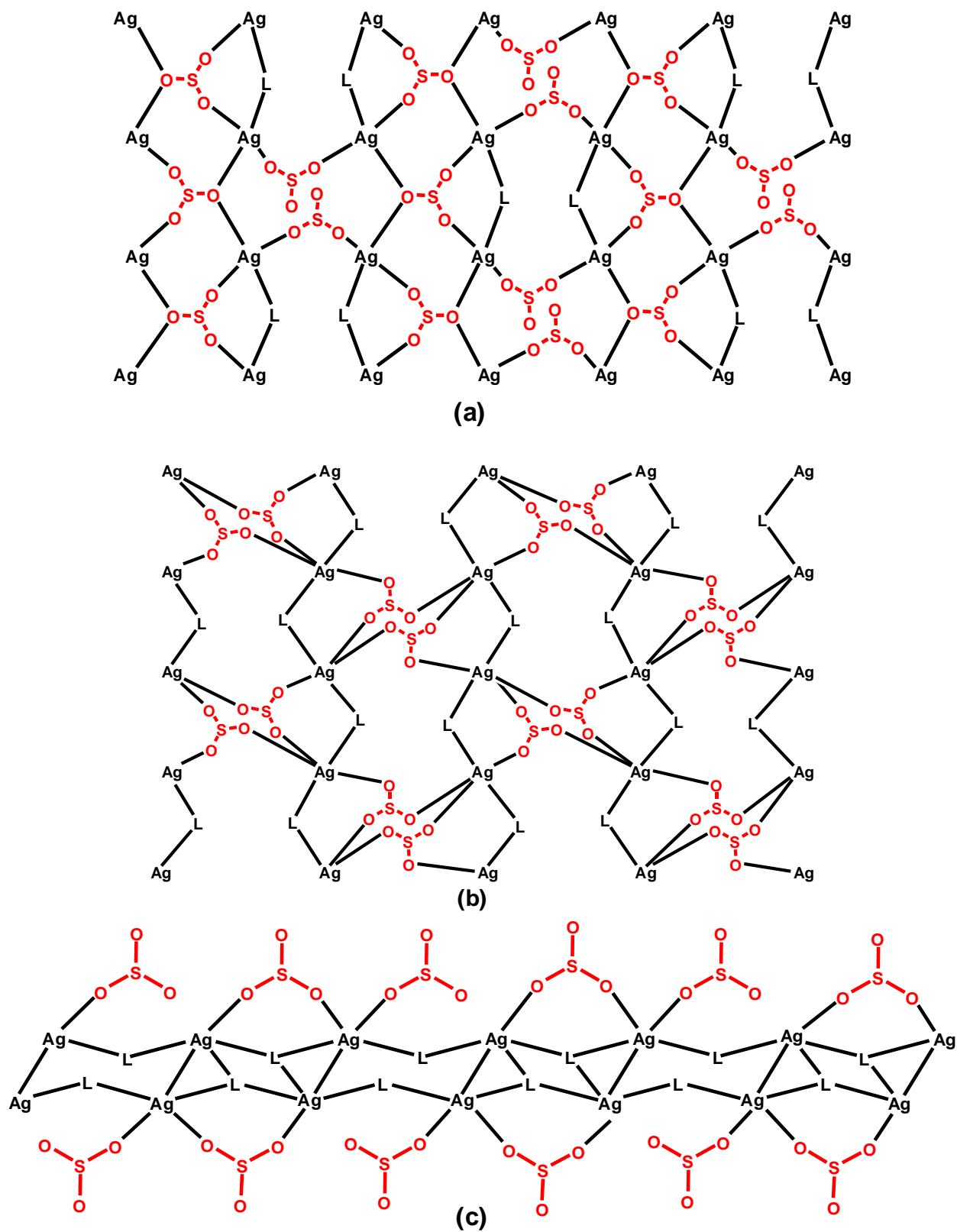


Figure 2.80 – Types of 1D and 2D polymers obtained from silver(I) triflate with (a) ligand **2.4** (b) ligand **2.8** and (c) ligand **2.14**.

The advantages of a substituted rigid phenyl ring in ligand **2.8** offered some interesting crystal packing features compared to ligands **2.1**, **2.4** and **2.11**. In general, the complexes of the type shown in figure 2.81a interact with anions and solvent molecules in the crystal lattice. The ligand **2.8** offers two types of  $\pi$ - $\pi$  interactions in complexes **2.31** and **2.32**, as shown in figures 2.81b and 2.81c.

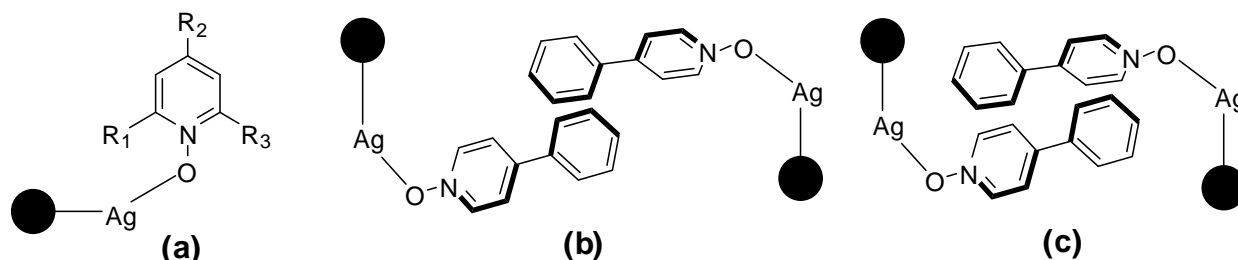


Figure 2.81 – (a) General representation of ligands **2.1**, **2.4** and **2.11** interacting with silver(I) ions with no observed  $\pi$ - $\pi$  interactions (b & c)  $\pi$ - $\pi$  interactions observed in complexes **2.31** and **2.32** of ligand **2.8**.

The interaction between the silver(I) cations and aromatic rings of the ligand can also be a driving force to different supramolecular networks, as seen in the silver(I) complexes **2.27**, **2.28**, **2.29**, and **2.35**. In ligands **2.6** and **2.9**, the coordination site of the pyridine N-oxides and phenyl rings are isolated by  $-\text{CH}_2-$  and  $-\text{CH}-$  functionalities. These two complexes extend two-dimensionally with the help of Ag-aromatic interactions, as seen in figure 2.82.

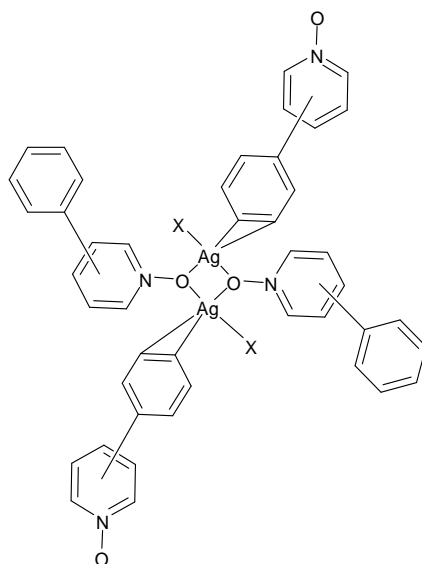
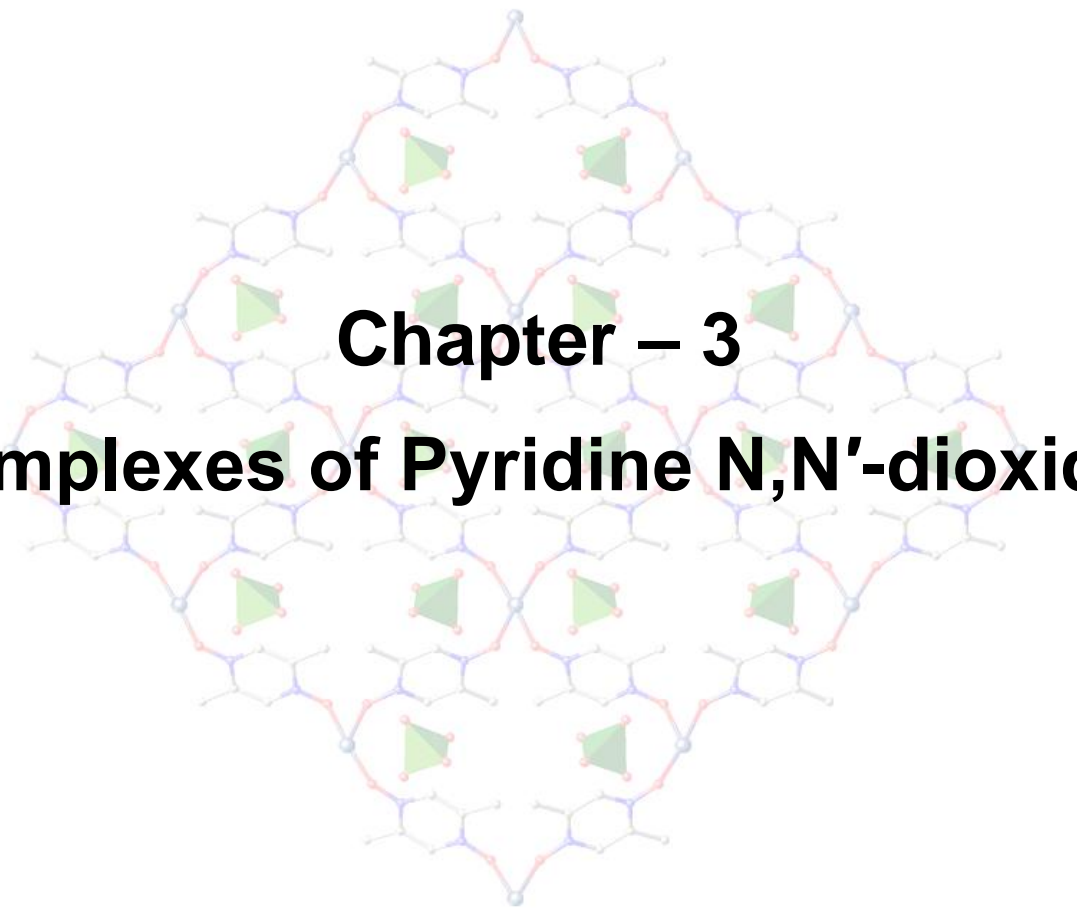


Figure 2.82 – General representation of 'oxygen-bridge' type complex formation.

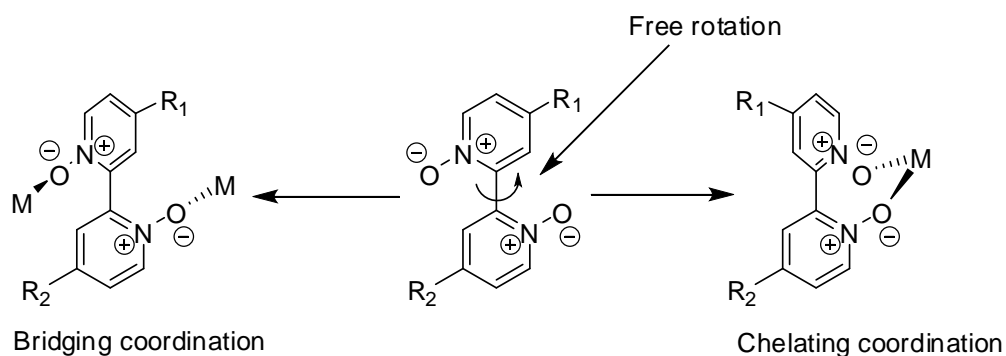


**Chapter – 3**  
**Complexes of Pyridine N,N'-dioxides**

### 3.1 Introduction

N,N'-Dioxides are of interest as ligands in coordination chemistry and also serve as important precursors for the syntheses of substituted 2,2'-bipyridines. Interest in N,N'-dioxides has increased because of their biological activities due to their strong affinities and chelating properties;<sup>[117]</sup> Researchers have also reported several N,N'-dioxide derivatives capable of forming biologically active metal complexes.<sup>[118]</sup> Apart from these, coordination complexes of N,N'-dioxides are also known to have extensive applications as magnetic materials,<sup>[119]</sup> in catalysis<sup>[120]</sup> as well as in supramolecular systems.<sup>[121]</sup>

2,2'-Bipyridine N,N'-dioxides can act as either chelating or bridging ligands, facilitated by rotation around the C-C bond that connects the two pyridine N-oxide rings, as shown in scheme 3.1. The N,N'-dioxide derivative can bridge the metal centers with a range of distances between the coordinating metals.<sup>[122]</sup>



Scheme 3.1 – Bridging and chelating coordination modes of 2,2'-bipyridine N,N'-dioxides.

This chapter discusses the coordination modes of 2,2'-bipyridine N,N'-dioxides and their analogues as listed in figure 3.1. The chelating ability of these ligands is not their only unique property and the  $\pi$ -delocalized systems of the pyridine rings can also impart secondary effects on coordination with metals by suitable substitutions. The spacer unit in the N,N'-dioxide is another aspect of interest, which has proven to be a useful tool in supramolecular chemistry<sup>[123]</sup> and crystal engineering for the construction of high dimensionality networks.<sup>[124]</sup> The most popular bridging ligand is **3.11**, which is useful for designing metal coordination networks, since it can act as both a bridging and terminal ligand. Ligand **3.11** has also been found occasionally as a non-coordinated guest molecule. All of these terminal spacer ligand systems may also be further involved in hydrogen bonding<sup>[125]</sup> or  $\pi$ -stacking interactions,<sup>[125b, 126]</sup> which are dependent on the reaction conditions adopted, such as ratios of reactants, type of metal employed, and the anions used.

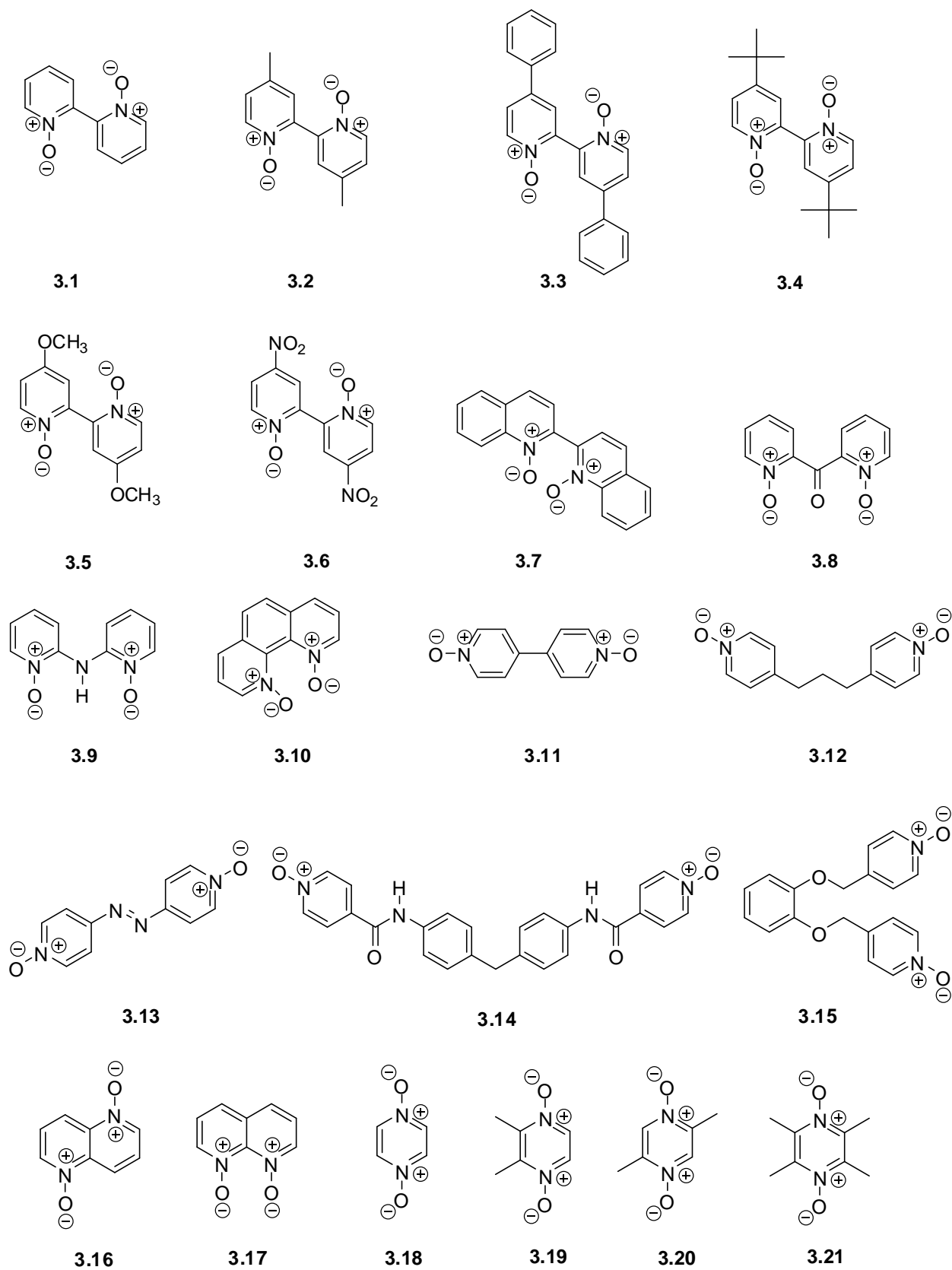


Figure 3.1 – List of N,N'-dioxides.

In order to study the coordination chemistry of such bridging ligands, several conformationally rigid [3.11 and 3.13] and non-rigid [3.12 and 3.14] ligands were synthesised, as depicted in figure 3.2. Ligand 3.11 has a relatively low space demand [9.7 Å] of the pyridine N-oxide donor groups, combined with the orientation of the lone pairs on the pyridyl-N-oxide atoms. This results in a highly labile coordination behaviour, which causes structural diversity. Besides being a strongly coordinating ligand, 3.11 is a good hydrogen bond acceptor<sup>[127]</sup> and its related hydrogen bonding networks were described previously in chapter 1. Ligands 3.11 and 3.13 can adopt both *cis*- and *trans*- coordination modes<sup>[128]</sup> with metals due to their characteristic rigidity, whereas ligands 3.12 and 3.14 are more flexible<sup>[129]</sup> due to the –CH<sub>2</sub>– moieties. Thus, 3.12 can exhibit *anti-anti*, *gauche-anti* and two different *gauche-gauche* [*cis-trans*] conformations while ligand 3.14 can only adopt various conformations when coordinating to metals.<sup>[130]</sup>

Ligands like 3.13 are currently of interest in supramolecular assemblies, since these systems are photoactive and electrochemically active,<sup>[131]</sup> due to the presence of the –N=N– bond between two aromatic rings. Ligand 3.13 crystallises and exists in the stable *trans*- form<sup>[132]</sup> and can be used to construct either *cis*-, *trans*-<sup>[133]</sup> or a combination<sup>[134]</sup> of both in hydrogen bond networks.

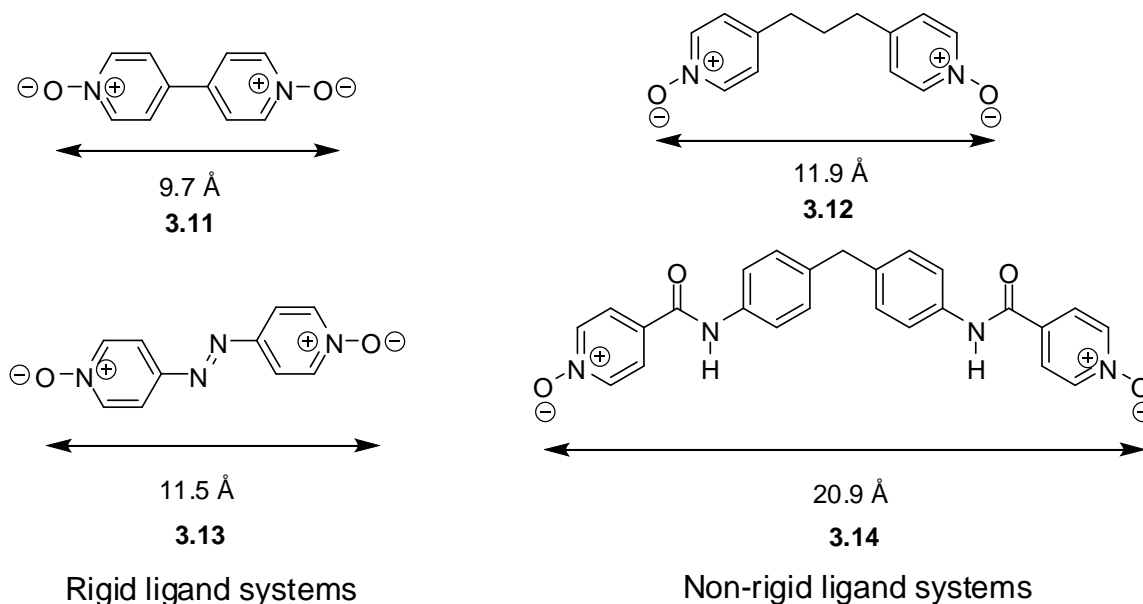


Figure 3.2 – Observed distances within the spacer ligands.

Ligand 3.15 [figure 3.1] is another spacer ligand, which is flexible and has better electron donating properties. The distance between non-bonding oxygens of ligand 3.15 is 9.1 Å, which is similar to 3.11 but with better coordination abilities. Ligands 3.10 and 3.17 [figure 3.1] are potentially important ligands in coordination chemistry; unfortunately these ligands have eluded chemists to date, as they prove to be extremely difficult to synthesise and isolate.



The coordination chemistry of pyrazine N,N'-dioxides has generated interest in recent years because the magnetic properties<sup>[135]</sup> can be adjusted and tuned depending on the type of pyrazine N,N'-dioxide [3.18 – 3.21] employed. Several literature reports have shown that the electron densities of the oxygen atoms in the pyrazine N,N'-dioxides and their derivatives are larger than other N-oxides with longer aromatic spacer groups. The distances between the oxygen atoms of ligands 3.18 – 3.21 is about 5.3 Å [figure 3.3], which is about half the distance observed in ligand 3.11. The denticity and their coordination modes in pyrazine N,N'-dioxides can be switched<sup>[136]</sup> by simply increasing or decreasing the number of methyl substituents, in order to obtain diverse polymeric topologies.<sup>[137]</sup>

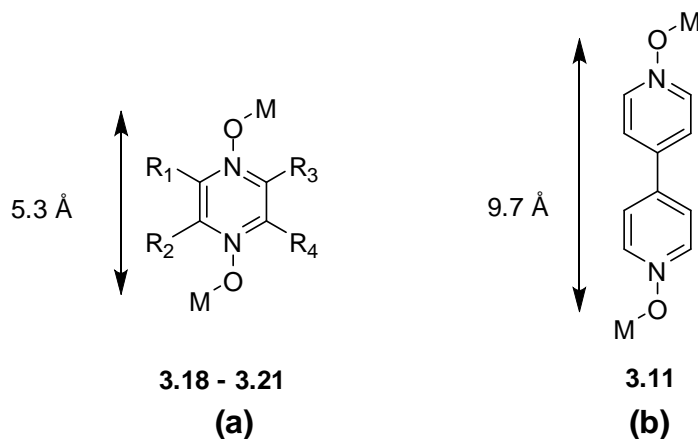
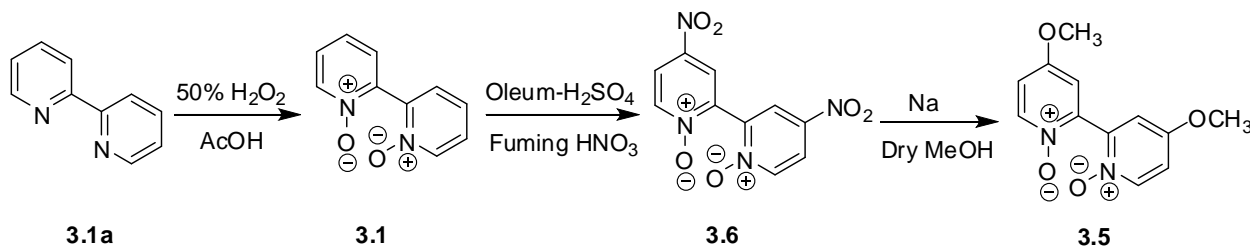


Figure 3.3 – Comparison of O...O distances between ligands (a) and (b).

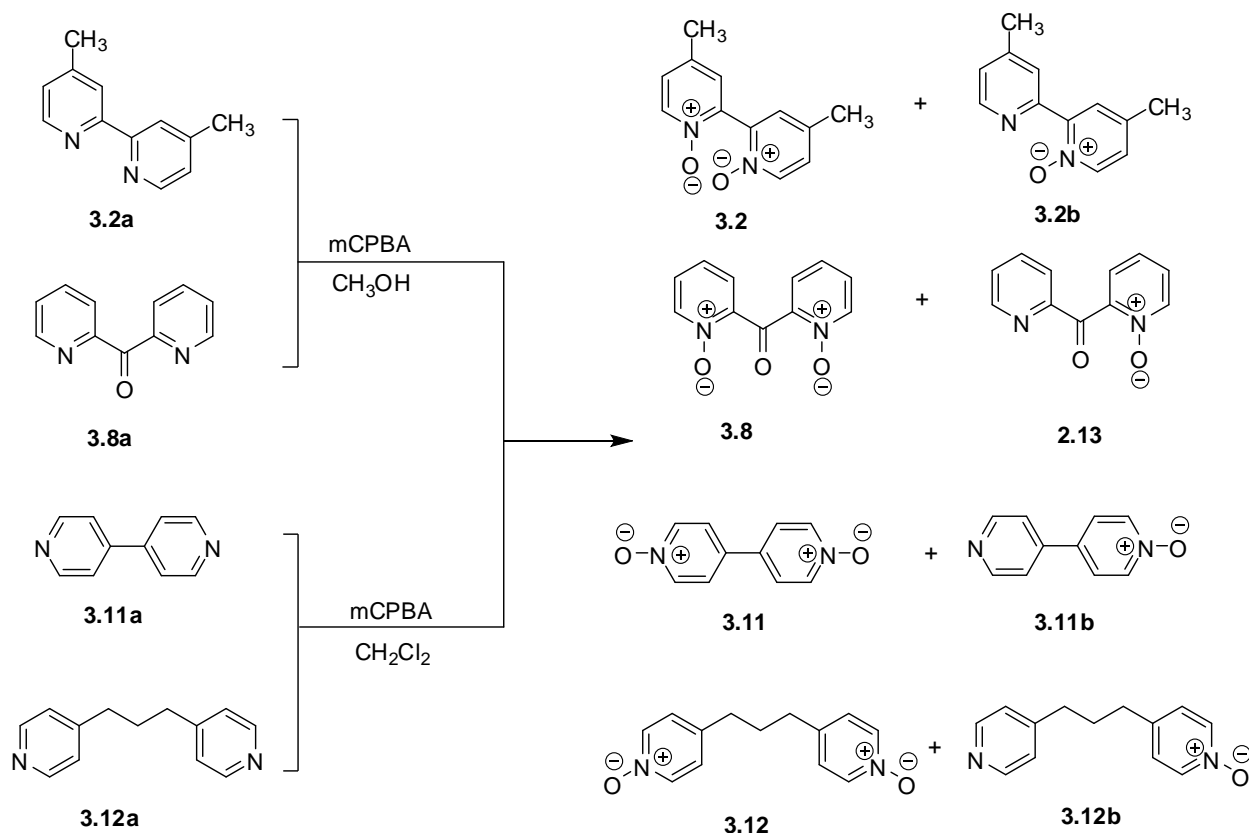
### 3.2 Syntheses of ligands

The three ligands 3.1, 3.5 and 3.6 were synthesised<sup>[138]</sup> from precursor 3.1a using a linear synthetic strategy, as shown in scheme 3.2. Ligand 3.1 was obtained in 76% yield after treatment of 3.1a with 50% H<sub>2</sub>O<sub>2</sub> in glacial acetic acid at 70 – 80°C. The crystalline white powder of ligand 3.1 was then converted to 3.6 [17%] yielding a yellow powder, which precipitates out when poured over crushed ice, after heating 12 hours at 80°C. The nitro groups of ligand 3.6 were replaced with –OCH<sub>3</sub> groups in 35% yield using sodium methoxide in dry methanol.<sup>[139]</sup>



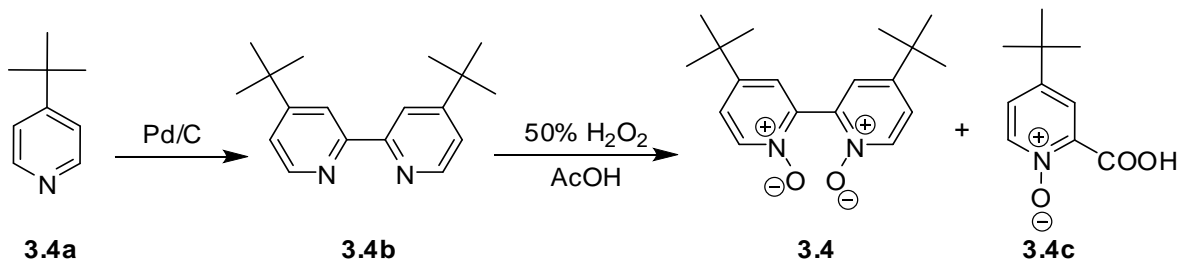
Scheme 3.2 – Syntheses of ligands 3.1, 3.5 and 3.6.

All of the ligands shown in scheme 3.3, except **3.8** and **3.12b** are well-known and were able to be synthesised using well established procedures. The ligands **3.2**,<sup>[140]</sup> **3.8**, **3.11**<sup>[59]</sup> and **3.12**<sup>[141]</sup> were synthesised by the reaction conditions shown in scheme 3.3. Oxidation of the corresponding N-heterocycles with mCPBA gave mono- and dioxides, which were separated by flash chromatography (**3.2b**,<sup>[142]</sup> **3.11b**<sup>[143]</sup> and **3.12b** are not further discussed in this thesis).

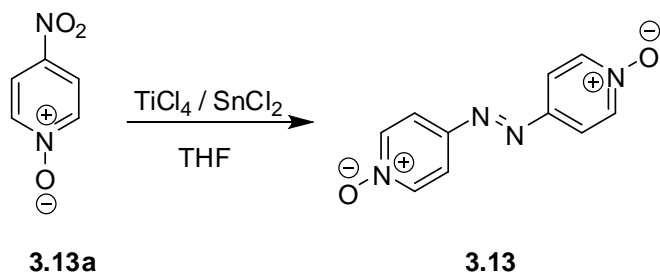


Scheme 3.3 – Syntheses of ligands **3.2**, **3.8**, **3.11** and **3.12**.

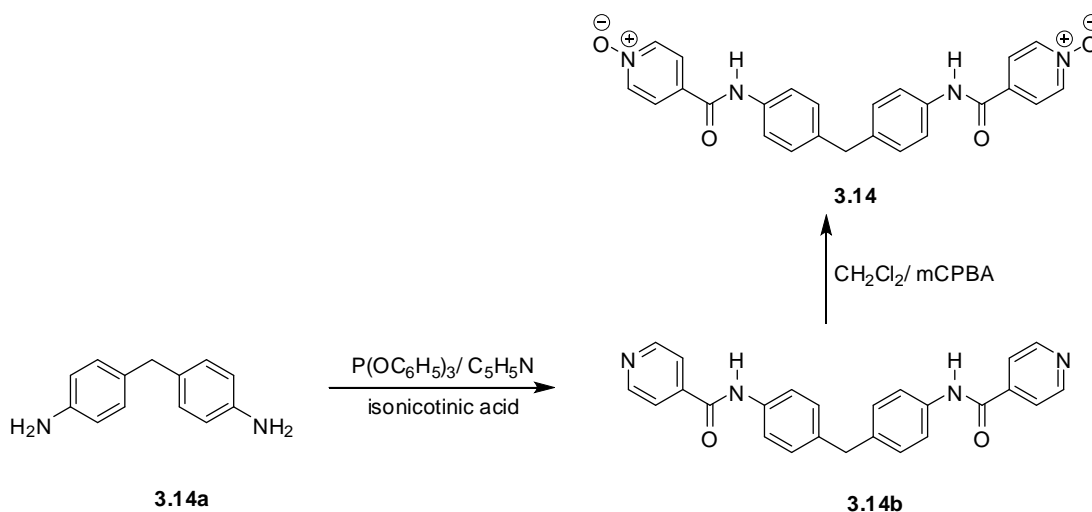
Ligand **3.4** can be prepared in several ways and for this work a traditional method of making **3.4b** by C-C coupling of **3.4a** using Pd/C as a catalyst was used, as shown in scheme 3.4. A TLC plate of the reaction mixture showed a number of spots in addition to **3.4b**, which were possibly due to the formation of higher oligopyridines [e.g. terpyridines]. Extraction of the reaction mixture with chloroform, followed by filtration through Celite to remove the catalyst and subsequent distillation of unreacted **3.4a**, gave a mixture of **3.4b** with other unknown products. Pure **3.4b** was obtained by repeated crystallisations of the crude material from pentane to give a white powder in 6% yield. The obtained ligand **3.4b** was then oxidized to **3.4** [50% yield] and a by-product **3.4c** using 50% H<sub>2</sub>O<sub>2</sub> in acetic acid. These were separated using silica gel chromatography. Interestingly, ligand **3.4c** was initially isolated thinking that it was the mono-N-oxide; however, X-ray analysis confirmed the actual structure as **3.4c**.

Scheme 3.4 – Synthesis of ligand **3.4**.

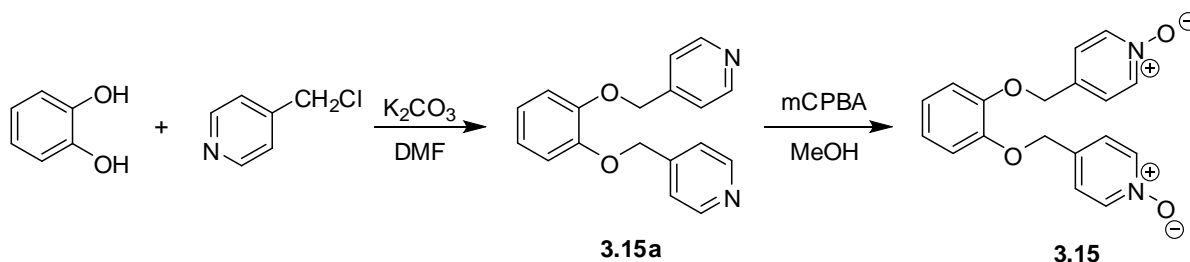
To date, only two synthetic procedures<sup>[144]</sup> for making ligand **3.13** are known. The procedure adopted, as reported by Malinowski *et al.*,<sup>[145]</sup> uses  $\text{TiCl}_4/\text{SnCl}_2$  as catalyst, which gave **3.13** in 34% yield, as shown in scheme 3.5. Attention needs to be paid to the ratio of catalyst used in this reaction, since a change in ratio can lead to different azo bipyridine products as reported in the literature.<sup>[145-146]</sup>

Scheme 3.5 – Synthesis of ligand **3.13**.

The amide spacer ligand **3.14b** was made using well-known literature procedures,<sup>[147]</sup> and then oxidized with mCPBA to give ligand **3.14** in 20% yield, as shown in scheme 3.6.

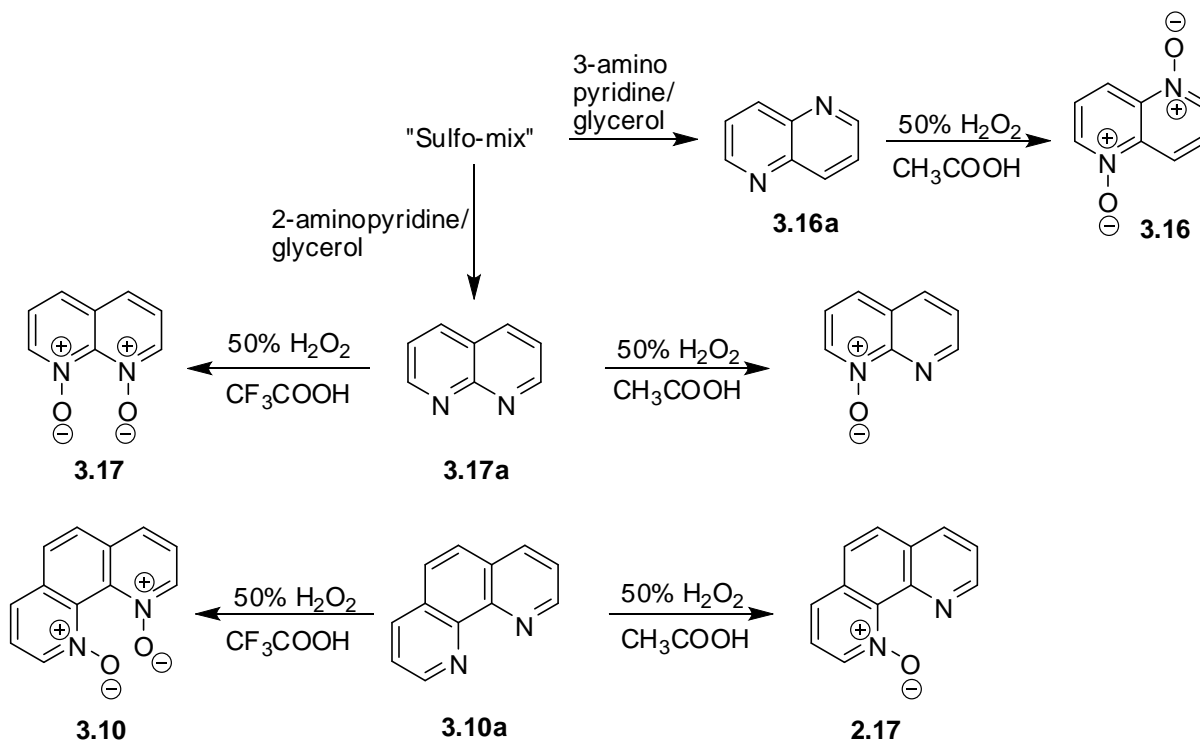
Scheme 3.6 – Synthesis of ligand **3.14**.

Ligand **3.15a** was oxidized with mCPBA to give ligand **3.15** in only 7% yield.



Scheme 3.7 – Synthesis of ligand **3.15**.

The syntheses of ligands **3.16a** and **3.17a** were achieved using a classical Skraup reaction,<sup>[148]</sup> which involves reacting amino pyridines with glycerol in “sulfo-mix” (a mixture of sulphuric acid and a nitrobenzene oxidizing agent) at 140°C for 48 hours, as shown in scheme 3.8. The product **3.16a** was then oxidized to ligand **3.16**<sup>[149]</sup> with 50% hydrogen peroxide in acetic acid. Syntheses of ligands **3.10** and **3.17** were difficult, as oxidation results in steric repulsions between oxygens. Also, due to high solubility of the resultant product, isolation was challenging.

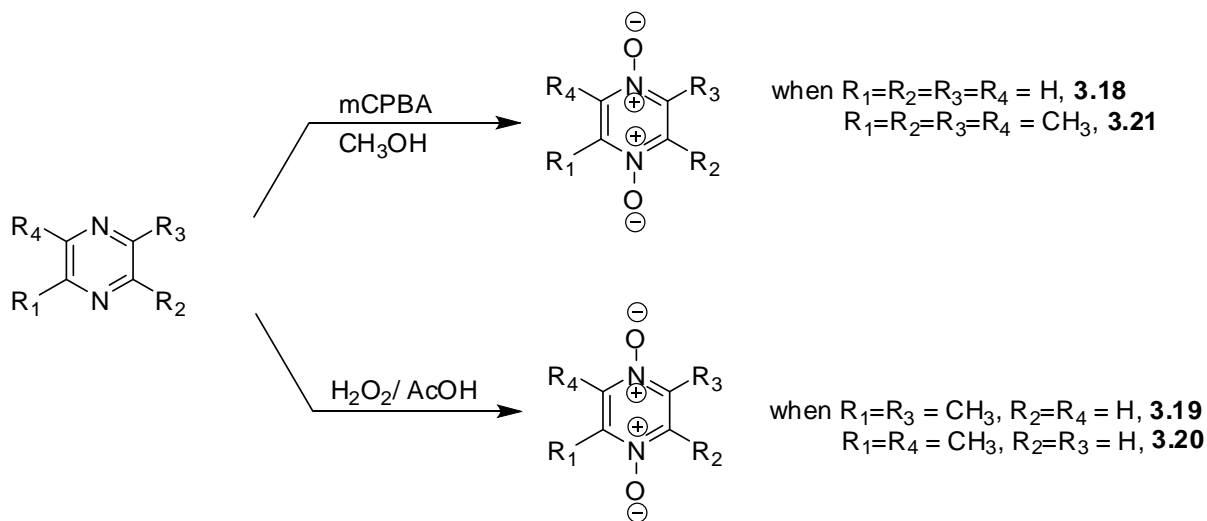


Scheme 3.8 – Syntheses of ligand **3.10**, **3.16** and **3.17**.

To date, only one literature source has reported<sup>[150]</sup> the synthesis of ligand **3.10**, as depicted in scheme 3.8. Rozen<sup>[150]</sup> mentioned that the initial trials to synthesise ligand **3.10** with different peroxides were unsuccessful. Initially, the mono-N-oxides<sup>[151]</sup> of **3.10a** and **3.17a** were synthesized with 50% H<sub>2</sub>O<sub>2</sub> in acetic acid. Then with these mono-N-oxides as a TLC reference,

ligands **3.10** and **3.17** were synthesised in 50% H<sub>2</sub>O<sub>2</sub> in trifluoroacetic acid, as shown in scheme 3.8. Ligand **3.17** was stirred in a oil bath at 140°C for 8 days to drive the reaction to completion and the obtained product was subsequently purified over silica gel. It was then characterized by NMR and mass spectroscopy.

Four pyrazine 1,4-dioxide<sup>[41a, 152]</sup> ligands were prepared by simply heating the reactants for longer periods to attain better yields. About 2.5 to 3 equivalents of the respective oxidants shown in scheme 3.9 were employed. One half of the equivalents of oxidants were added initially and the remainder midway through the heating period, in order to oxidize any mono-N-oxides formed. Addition of the oxidants all at once gives a mixture of mono- and dioxides.



Scheme 3.9 – Syntheses of ligand **3.18** – **3.21**.

### 3.3 Syntheses of silver(I) complexes with N,N'-dioxides

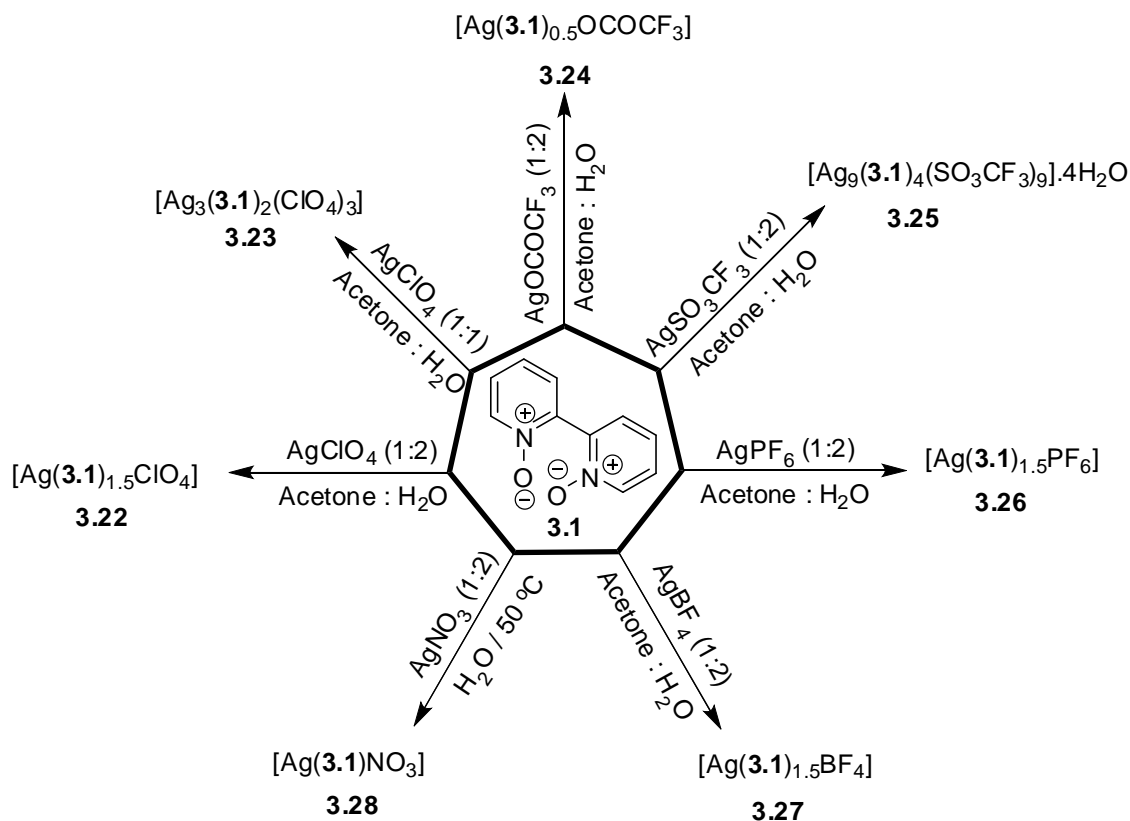
#### 3.3.1 Complexes with 2,2'-bipyridine N,N'-dioxide **3.1**

2,2'-Bipyridine N,N'-dioxide proved to be the most successful ligand for making silver(I) complexes compared to any other N,N'-dioxide listed in figure 3.1. All the complexes, shown in Scheme 3.10, synthesised with ligand **3.1**, were obtained by slow evaporation of the solutions, unless otherwise mentioned. Complexes **3.22**, **3.26** and **3.27** were synthesised in a 1:2 ligand to AgX [X = ClO<sub>4</sub>, PF<sub>6</sub> and BF<sub>4</sub>] ratio, which resulted in similar 1D polymers [excluding anions].

A change in ligand to AgClO<sub>4</sub> ratio from 1:2 to 1:1 resulted in the formation of complex **3.23**, which had a different polymeric network due to coordination of the perchlorate anion with silver(I) ions. Complex **3.24** had trifluoroacetate anions bridging to either side of strong Ag<sup>+</sup>⋯Ag interactions and ligands **3.1** adopted an *anti*-coordination mode with two unique silver(I) ions. Ligands **3.1** achieved maximum denticity in complex **3.25**. After a number of unsuccessful attempts to get silver(I)

complexes of ligand **3.1** with  $\text{AgNO}_3$ , a discrete complex **3.28** was finally obtained by adding a solution of  $\text{AgNO}_3$  in water at  $50^\circ\text{C}$  to a solution of the ligand, also in water, at  $50^\circ\text{C}$ .

Since the ligands and silver(I) ions discussed have similar coordination chemistries in complexes **3.22**, **3.26** and **3.27** with only slight changes in bond parameters, the crystal structure descriptions will be discussed in detail for complex **3.22** only. The other two complexes [**3.26** and **3.27**] will subsequently be compared, while keeping the atom labels the same, as discussed later.



Scheme 3.10 – Syntheses of complexes **3.22** – **3.28**.

### With silver(I) perchlorate (1:2) **3.22**

Colourless block crystals were obtained when ligand **3.1** was reacted with silver(I) perchlorate in 1:2 stoichiometric ratio. The asymmetric unit of complex **3.22**, solved in the monoclinic  $C2/c$  space group, comprises two half occupancy silver(I) ions, Ag1 and Ag2, and a perchlorate anion disordered over three oxygens [O4, O5 and O6], as seen in figure 3.4. The complex **3.22** has a 3:2 ligand to silver(I) ratio. The **3.1** ligand molecules have  $\mu_3\text{-O}, \text{O}', \text{O}'$  and  $\mu_2\text{-O}, \text{O}'$  coordination modes with an average N-O bond distance of  $1.319(3)$  Å. The N2-O2 has  $\mu_2\text{-O}, \text{O}$  bidentate bridging coordination mode with Ag1 and Ag2, while N1-O1 and N3-O3 are monodentate with Ag1 and Ag2 respectively. The bond lengths of a bidentate N2-O2 [average  $\text{Ag-O}_{\text{ligand}} = 2.394(2)$  Å] are

found to be longer than the monodentate N1-O1 and N3-O3 [average  $\text{Ag-O}_{\text{ligand}} = 2.312 \text{ \AA}$ ] with coordination angles  $[\text{N-O}_{\text{ligand}}-\text{Ag}]$  ranging from  $115.24(5)^\circ$  to  $124.18(3)^\circ$ .

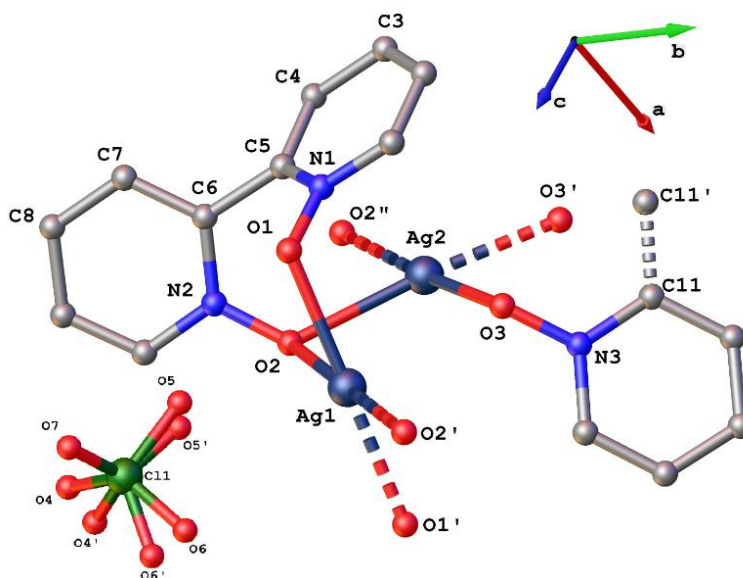


Figure 3.4 – Asymmetric unit of complex **3.22**. Hydrogen atoms are excluded for clarity. Selected bond lengths ( $\text{\AA}$ ) and bond angles ( $^\circ$ ): N1-O1 = 1.321(3), N2-O2 = 1.315(3), N3-O3 = 1.323(3), Ag1-O1 = 2.311(2), Ag1-O2 = 2.428(5), Ag2-O2 = 2.361(3), Ag2-O3 = 2.314(2), N1-O1-Ag1 =  $115.24(5)^\circ$ , N2-O2-Ag2 =  $124.18(3)^\circ$ , N2-O2-Ag1 =  $119.91(4)^\circ$ , N3-O3-Ag2 =  $118.14(4)^\circ$ .

Complex **3.22** is a 1D linear polymer propagating along the *c*-axis with distorted square planar silver(I) ions Ag1 [ $\tau_4 = 0$ ] and Ag2 [ $\tau_4 = 0$ ], which are in an  $\text{O}_4$  environment, as seen in figure 3.5a. In the 1D polymeric structure, ligand **3.1** exhibits two types of coordination modes, Bipy – 1 and Bipy – 2, as shown in figure 3.5b. The dihedral angles between the pyridine rings in Bipy – 1 and Bipy – 2 ligands are  $64.76^\circ$  and  $66.38^\circ$ , respectively, with distances between the metal bound oxygens of  $2.960 \text{ \AA}$  [O3-O3'] and  $2.927 \text{ \AA}$  [O2-O1], respectively. Hydrogens H15 and H15' of Bipy – 1 are interacting with the oxygens O1 and O1' of the monodentate N-O groups of Bipy – 2 at distances  $\text{O}\cdots\text{H} = 2.175 \text{ \AA}$ , as shown in figure 3.5a. The hydrogen bond parameters related to the C15-H15 $\cdots$ O1 interaction are shown in table 3.1.

Table – 3.1 Hydrogen bond parameters of complex **3.22**.

D-H $\cdots$ A	$d_{\text{D-H}}(\text{\AA})$	$d_{\text{H}\cdots\text{A}}(\text{\AA})$	$d_{\text{D}\cdots\text{A}}(\text{\AA})$	$\angle\text{D-H}\cdots\text{A}(^\circ)$
C15-H15 $\cdots$ O1	0.950	2.175	3.114	169.7

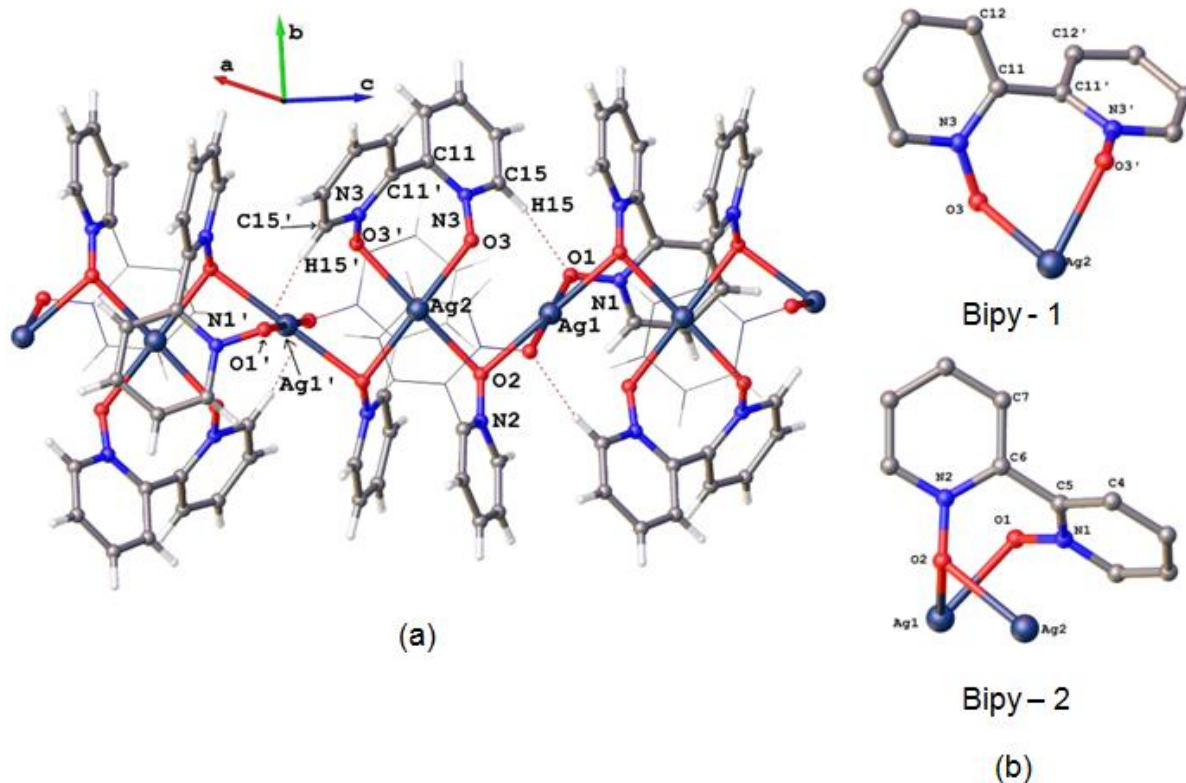


Figure 3.5 – (a) 1D Polymeric structure of complex **3.22** showing hydrogen bond interactions, and (b) coordination modes of ligand **3.1** in complex **3.22**. Hydrogen atoms in figure 3.5b are excluded for clarity.

In the crystal structure, the Ag1 and Ag2 atoms are on a center of inversion and a two-fold rotation axis, respectively, which provides two unique Ag-O bond lengths around each of the silver(I) ions. The planar Ag1 and Ag2 ions are bridged by O2 oxygen atoms to give a one-dimensional polymer. As seen in figure 3.6, Ag1 is surrounded by the oxygens [O1, O1', O2 and O2'] supplied by only Bipy –2 ligands, whereas for Ag2, the oxygens [O2, O2'', O3 and O3'] are supplied from Bipy –1 and Bipy –2 ligand molecules. The bond distances around the Ag(I) ion centers are 2.311(2) Å [Ag1-O1/O1'], 2.428(5) Å [Ag1-O2/O2''], 2.314(2) Å [Ag2-O3/O3'] and 2.361(3) Å [Ag2-O2/O2''], their average  $\text{Ag-O}_{\text{ligand}} = 2.353$  Å falls into the acceptable range of O-donor silver(I) square planar complexes reported by Hanton *et al.*<sup>[153]</sup> and other groups.<sup>[154]</sup> The angles between the *trans*-oxygens around Ag1 and Ag2 are 180° and 175.34°, respectively and the sum of the internal angles around each Ag(I) center is 360°. These values are in good agreement with the other reported square planar complexes.<sup>[153]</sup>



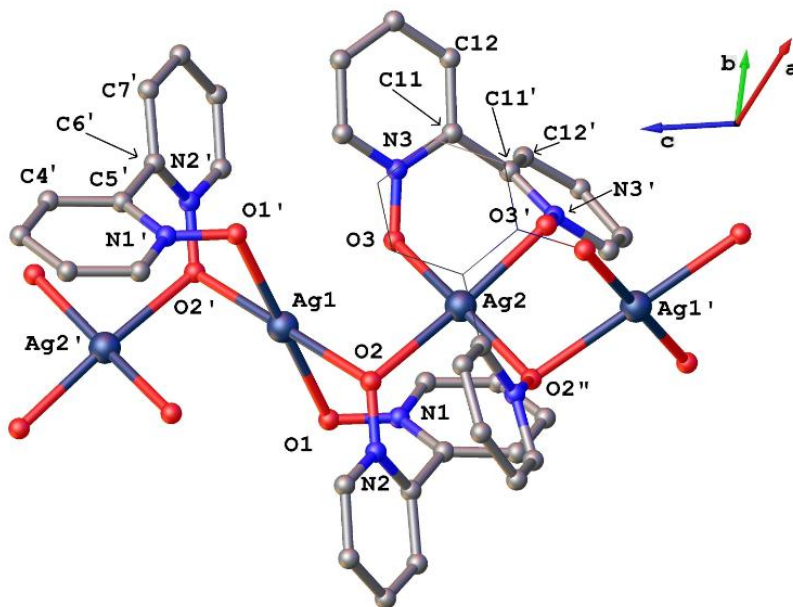
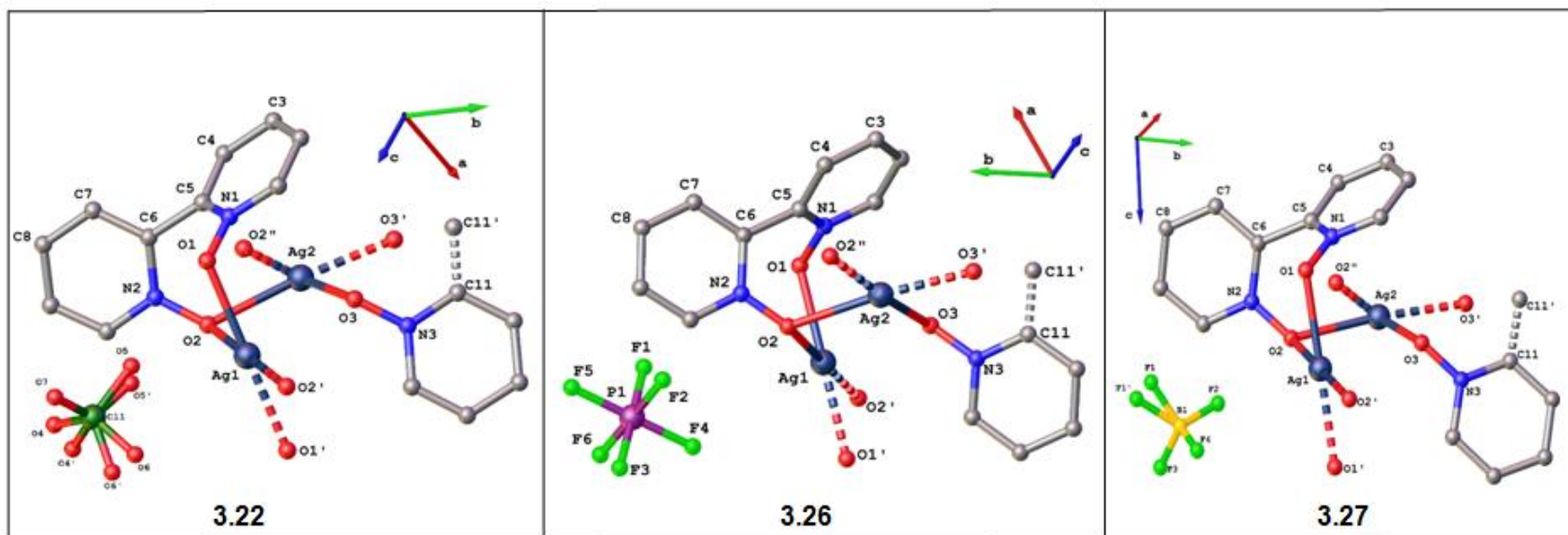


Figure 3.6 – Perspective view of the 1D polymeric structure showing the silver(I) geometry. Hydrogen atoms are excluded for clarity, and selected aromatic rings are shown in wireframe for clarity. Selected bond lengths (Å) and bond angles (°): Ag1-O1/O1' = 2.311(2), Ag1-O2/O2'' = 2.428(5), Ag2-O3/O3' = 2.314(2), Ag2-O2/O2'' = 2.361(3), O1-Ag1-O1' = 180.0, O2-Ag1-O2' = 180.0, O1-Ag1-O2' = 103.74(6), O1-Ag1-O2 = 76.26(6), O3-Ag2-O2'' = 175.34(7), O3'-Ag2-O2 = 175.34(7), O3-Ag2-O2 = 100.30(7), O2-Ag2-O2'' = 80.25(9), O3-Ag2-O3' = 79.53(9).

The crystals structures of three isomorphous complexes **3.22**, **3.26** and **3.27** and their crystal data are shown in figure 3.7 and table 3.2, respectively. Also, table 3.3 shows the comparison of hydrogen bond parameters in complexes **3.22**, **3.26** and **3.27**.



	Complex <b>3.22</b>	Complex <b>3.26</b>	Complex <b>3.27</b>
Formula	$C_{15}H_{12}N_3O_7ClAg$	$C_{15}H_{12}N_3O_3PF_6Ag$	$C_{15}H_{12}N_3O_3BF_4Ag$
Formula weight	489.60	535.12	476.96
Crystal system	monoclinic	monoclinic	monoclinic
Space group	$C2/c$	$C2/c$	$C2/c$
$a/\text{\AA}$	22.5763(9)	23.4319(6)	22.655(5)
$b/\text{\AA}$	13.0278(5)	13.14761(16)	12.852(3)
$c/\text{\AA}$	13.5406(5)	13.5859(4)	13.556(3)
$\alpha/\text{deg}$	90.00	90.00	90.00
$\beta/\text{deg}$	123.260(2)	123.536(4)	124.17(3)
$\gamma/\text{deg}$	90.00	90.00	90.00
$V/\text{\AA}^3$	3330.2(2)	3488.71(14)	3265.5(11)
Z	8	8	8
T/K	110.0	120.0	120.0

Figure 3.7 – Comparison of the asymmetric units in isomorphous complexes **3.22**, **3.26** and **3.27**.

Table – 3.2 Comparison of the bond parameters in complexes **3.22**, **3.26** and **3.27**.

Bond parameter	Complex <b>3.22</b>	Average	Complex <b>3.26</b>	Average	Complex <b>3.27</b>	Average
N1-O1 (Å)	1.321(3)	1.319	1.312(2)	1.318	1.315(2)	1.318
N2-O2 (Å)	1.315(3)		1.318(2)		1.318(2)	
N3-O3 (Å)	1.323(3)		1.324(2)		1.321(2)	
Ag1-O1 (Å)	2.311(2)	2.354	2.325(2)	2.345	2.302(2)	2.348
Ag1-O2 (Å)	2.428(5)		2.399(2)		2.424(2)	
Ag2-O2 (Å)	2.361(3)		2.344(2)		2.350(2)	
Ag2-O3 (Å)	2.314(2)		2.311(2)		2.315(2)	
N1-O1-Ag1 (°)	115.24(5)	119.36	117.08(1)	119.44	115.35(1)	119.19
N2-O2-Ag2 (°)	124.18(3)		124.18(1)		124.40(1)	
N2-O2-Ag1 (°)	119.91(4)		120.11(1)		119.13(1)	
N3-O3-Ag2 (°)	118.14(4)		116.39(1)		117.91(1)	
N1-C5-C6-N2 (°)	66.38		66.41		68.41	
N3-C11-C11'-N3'(°)	64.76		63.90		64.31	

Table – 3.3 Comparison of hydrogen bond parameters in complexes **3.22**, **3.26** and **3.27**.

Complex, X	D-H...A	<i>d</i> D-H(Å)	<i>d</i> H...A(Å)	<i>d</i> D...A(Å)	<D-H...A(°)
<b>3.22</b>	C15-H15...O1	0.950	2.175	3.114	169.73
<b>3.26</b>	C15-H15...O1	0.930	2.183	3.104	170.48
<b>3.27</b>	C15-H15...O1	0.930	2.169	3.089	169.54

### With silver(I) perchlorate (1:1) **3.23**

The reaction of ligand **3.1** with AgClO<sub>4</sub> in a 1:1 ratio resulted in a 2:3 ligand to silver(I) ratio in the asymmetric unit. The asymmetric unit contains two ligand molecules, three silver(I) perchlorates and a water molecule [O17], as shown in figure 3.9. Although the complex **3.23** solved in the monoclinic *P*2<sub>1</sub>/*n* space group with reasonable refinement [*R*<sub>1</sub>= 5.43%], it had some serious disorder problems involving the two silver(I) ions, Ag2 and Ag3, and a perchlorate anion Cl1. The perchlorates Cl2 and Cl3 are monodentate, while Cl1 is bidentate. The oxygen O6 of the monodentate perchlorate anion is bridging Ag2' and Ag3', with further bridging by water [O17] to form a four-membered ring [O17-Ag2'-O6-Ag3']. The ligands **3.1** show μ<sub>4</sub>-O,O,O',O' coordination modes with the Ag1 ions having distorted square planar geometry, which is similar to the complexes **3.22**, **3.26** and **3.27**.

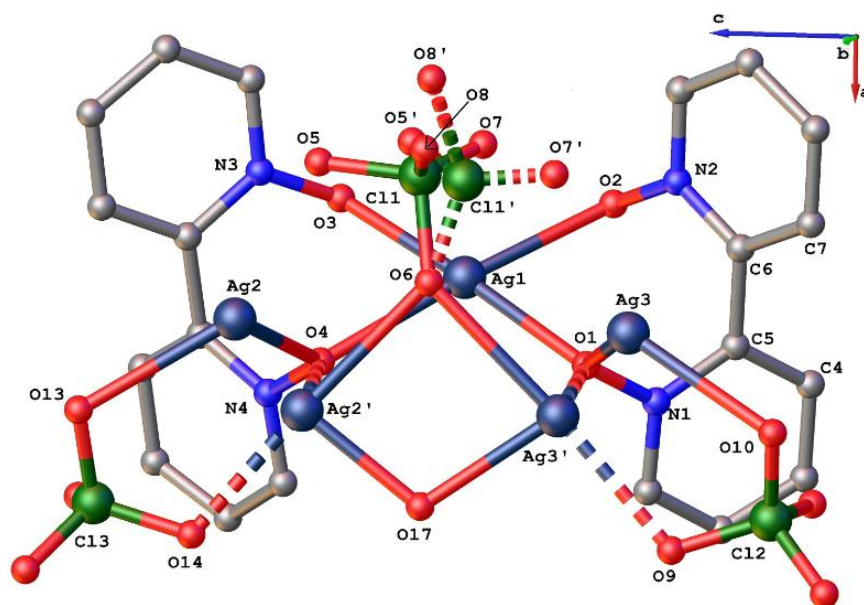


Figure 3.9 – Asymmetric unit of complex **3.23**. Selected hydrogen atoms and acetonitrile molecule are omitted for clarity. The broken lines represent the disordered component. Selected bond lengths (Å): N1-O1 = 1.341(6), N2-O2 = 1.341(6), N3-O3 = 1.337(6), Ag1-O3 = 2.351(4), Ag1-O1 = 2.354(4), Ag1-O4 = 2.401(4), Ag1-O2 = 2.408(4).

The average N-O<sub>ligand</sub> and Ag-O<sub>ligand</sub> bond distances in complex **3.23** are 1.339 Å and 2.378 Å, which are longer than the values observed in complex **3.22**. Throughout complex **3.23**, ligands **3.1** preferred one type of coordination mode [Bipy – 3], as shown in figure 3.10b, with torsion angles 67.46° higher than Bipy – 1 and Bipy – 2 in complex **3.22**. The distance between the metal bound ligand oxygens, O1 and O2, is 2.910 Å, which is shorter than the values observed for **3.1** ligand molecules in complex **3.22**. Complex **3.23** is a 1D polymer extended along the *b*-direction, as shown in figure 3.10a. The average Ag-O<sub>ligand</sub> bond distances are 2.378 Å around the distorted square planar Ag1 ion [ $\tau_4 = 0.05$ ], which is slightly longer than the values shown in table 3.2 for complexes **3.22**, **3.26** and **3.27** with ligand **3.1**. However, this value is still within the range of reported O-donor silver(I) square planar complexes.<sup>[153]</sup> The angles between the *trans* oxygens around Ag1 are O4-Ag1-O2 = 175.82(2)° and O3-Ag1-O1 = 176.66(2)° and the sum of the internal angles around each Ag(I) center is 359.81°, which is equal to complex **3.22** [360°].

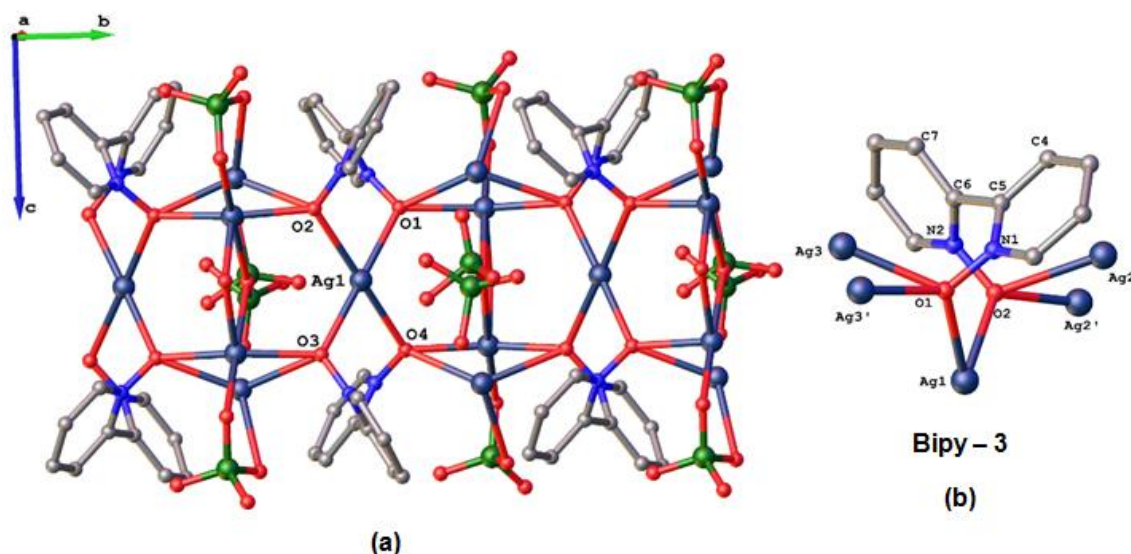


Figure 3.10 – (a) View of the 1D polymeric structure of complex **3.23**, and (b) coordination mode adopted by ligand **3.1** in complex **3.23**. Hydrogen atoms are omitted for clarity. Selected bond lengths (Å) and bond angles (°): O1-Ag1-O4 = 102.67(2), O3-Ag1-O4 = 75.58(2), O3-Ag1-O2 = 106.30(1), O1-Ag1-O2 = 75.26(1), O4-Ag1-O2 = 175.82(2), O3-Ag1-O1 = 176.66(2).

#### With silver(I) trifluoroacetate (1:2) **3.24**

Colourless thin plate crystals of complex **3.24** are obtained by mixing ligand **3.1** with AgOCOCF<sub>3</sub> in a 1:2 ratio, which solved in the monoclinic *P2/c* space group with 0.5:1 ligand to silver(I) ratio, as shown in figure 3.11. The asymmetric unit of complex **3.24** contains half a **3.1** ligand molecule, which has monodentate coordination with Ag1, as shown in figure 3.11. The N1-O1 and Ag1-O1 bond distances are 1.314(5) Å and 2.424(3) Å, respectively, with a coordination angle of

111.30(2)° [N1-O1-Ag1]. These distances show that the **3.1** ligand molecules are weakly coordinated to silver(I) ions with O1  $\pi$ -electrons back donated to the aromatic ring. The Ag $\cdots$ Ag distances of 2.893(2) Å, with trifluoroacetate anions bridged on either side, are shorter than the distances observed in AgOCOCF<sub>3</sub> complexes of pyridine N-oxides.

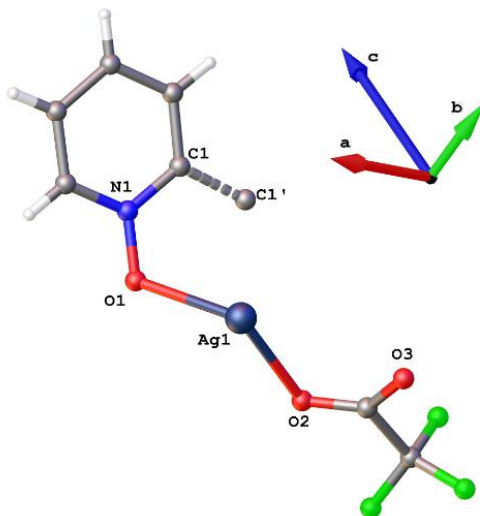


Figure 3.11 – Asymmetric unit of complex **3.24**. Selected bond lengths (Å) and bond angles (°): N1-O1 = 1.314(5), Ag1-O1 = 2.424(3), N1-O1-Ag1 = 111.30(2).

Complex **3.24** is a 1D linear polymer that propagates along the *c*-axis, as shown in figure 3.12a. Each of these strong Ag $\cdots$ Ag bridged trifluoroacetate anions is isolated by *anti*- $\mu_2$ -O, O' **3.1** ligand molecules [Bipy – 4], which are twisted at torsion angles of 67.44°, as shown in figure 3.12c. This value is similar to that in a reported copper<sup>[155]</sup> complex of ligand **3.1**. A chelating coordination mode has been commonly reported in ligand **3.1** complexes. However, the bridging coordination mode, shown in complex **3.24**, has only been previously reported twice.<sup>[155a, 155b]</sup> The distance between the Ag(I) ion bound oxygens is 2.944 Å, which is less than previous reports for ligand **3.1** [3.046(2) Å].<sup>[155a]</sup> Each Ag1 ion and O2 further interacts with O2 and Ag1 of adjacent 1D polymers, to form a 2D layered structure, as shown in figure 3.12b. These Ag1-O2 interactions between 1D polymers form an Ag<sub>2</sub>O<sub>2</sub> four-membered ring with Ag1-O2/Ag1'-O2' distances of 2.575(3) Å.

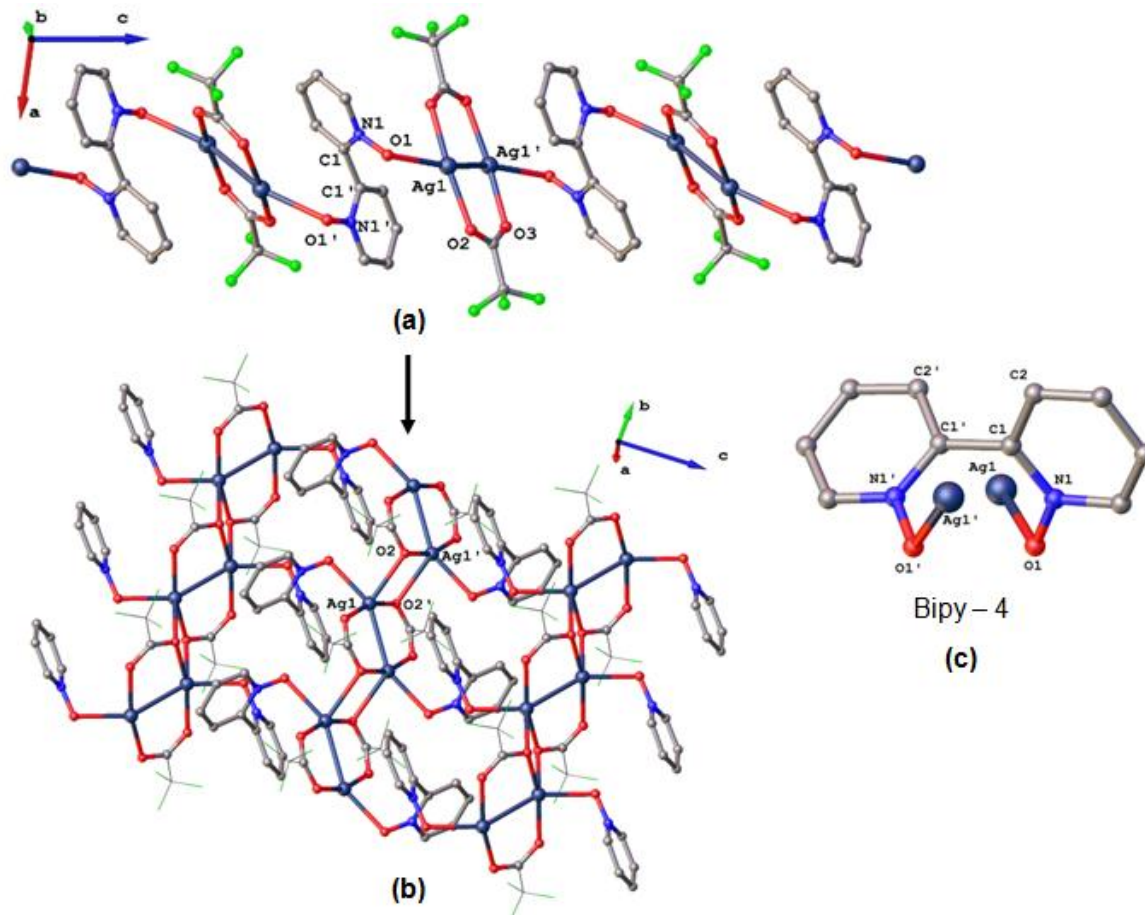


Figure 3.12 – (a) 1D Polymeric view of complex **3.24**, (b) extended 2D layer using  $\text{Ag}\cdots\text{O}$  interactions [– $\text{CF}_3$  groups are shown in wireframe for clarity], and (c) preferred coordination mode by ligand **3.1** in complex **3.24**. Hydrogen atoms are omitted for clarity. Selected bond lengths (Å) and bond angles ( $^\circ$ ):  $\text{Ag1-O2} = 2.575(3)$ ,  $\text{Ag1'-O3} = 2.232(3)$ ,  $\text{Ag1-Ag1''} = 2.892(6)$ ,  $\text{N1-C1-C1'-N1'} = 67.44(6)$ .

### With silver(I) triflate (1:2) **3.25**

The asymmetric unit of complex **3.25**, solved in the triclinic  $P-1$  space group, comprises ten silver(I) ions with two of them [Ag2 and Ag9] on inversion centers, nine triflate anions, four **3.1** ligands, and four water molecules, as shown in figure 3.13a. Interestingly, in complex **3.25**, the ligands **3.1**,  $\text{AgSO}_3\text{CF}_3$  and water molecules show a diverse range of coordination modes. The triflate anions show four types of coordination modes: S5 as non-coordinating; S1, S4, S6 and S9 as monodentate; S2 and S8 as bidentate and S3 and S9 as bidentate, which are all shown in detail in figure 3.31a. Interestingly, even the water oxygen molecules assemble in non-coordinating [O39], monodentate [O36] and also bridging [O38 and O37] coordination modes.

In complex **3.25**, the ligand molecules **3.1** have  $\mu_4\text{-O, O, O', O'}$  [Bipy – 5],  $\mu_5\text{-O, O, O', O', O'}$  [Bipy – 6] and  $\mu_6\text{-O, O, O, O', O', O'}$  [Bipy – 7] coordination modes, as shown in figure 3.13b. Interestingly,

complex **3.25** has Bipy – 7\* which is similar to Bipy – 7, but with different bond parameters, as shown in table 3.4.

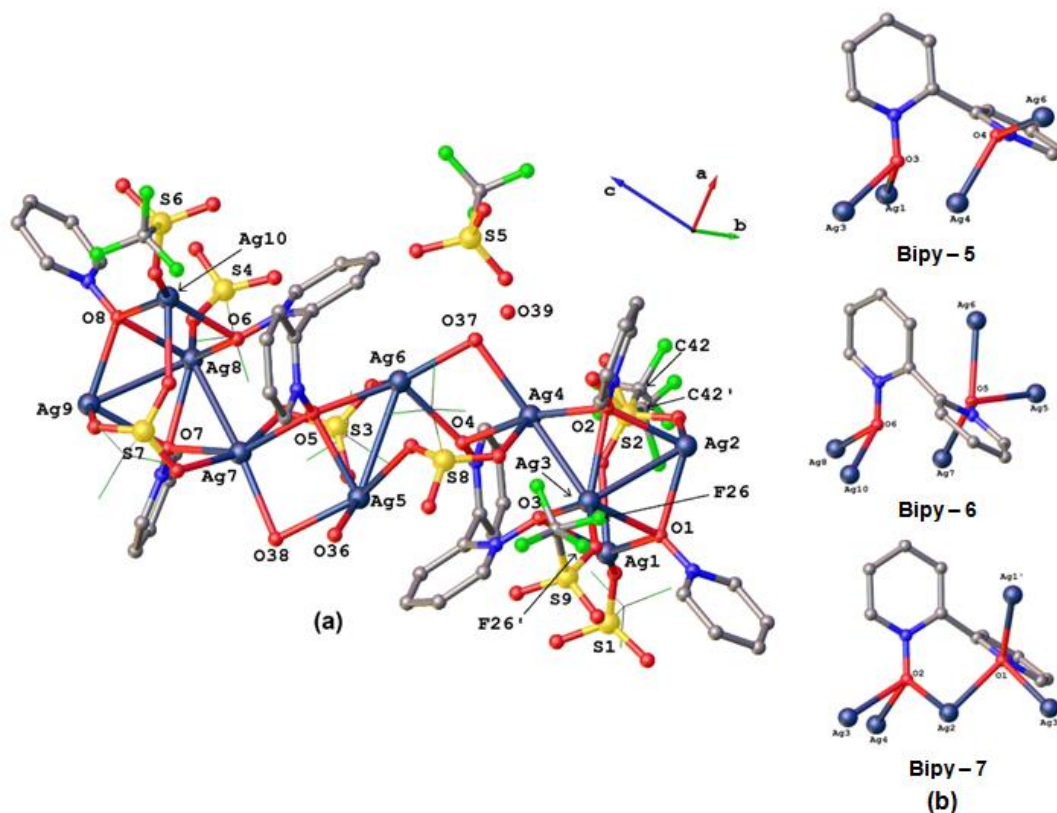


Figure 3.13 – (a) Asymmetric unit of complex **3.25** [selected  $-\text{CF}_3$  groups are shown in wireframe for clarity], and (b) preferred coordination modes of ligand **3.1** in complex **3.25**. Hydrogen atoms are omitted for clarity. Selected bond lengths (Å) and bond angles ( $^\circ$ ): N1-O1 = 1.332(4), N2-O2 = 1.347(4), N3-O3 = 1.331(4), N4-O4 = 1.325(4), N5-O5 = 1.331(4), N6-O6 = 1.330(4), N7-O7 = 1.340(4), N8-O8 = 1.337(4), Ag1-O1 = 2.395(3), Ag2-O1 = 2.448(3), Ag3-O1 = 2.502(3), Ag2-O2 = 2.448(3), Ag3-O2 = 2.491(3), Ag4-O2 = 2.344(3), Ag1-O3 = 2.459(3), Ag3-O3 = 2.337(3), Ag4-O4 = 2.320(3), Ag6-O4 = 2.383(3), Ag5-O5 = 2.509(3), Ag6-O5 = 2.477(3), Ag7-O5 = 2.496(3), Ag8-O6 = 2.297(3), Ag10-O6 = 2.467(3), Ag7-O7 = 2.477(3), Ag8-O7 = 2.392(3), Ag9-O7 = 2.468(3), Ag8-O8 = 2.525(3), Ag9-O8 = 2.400(3), Ag10-O8 = 2.419(3), N1-O1-Ag1 = 121.1(2), N1-O1-Ag2 = 115.7(2), N1-O1-Ag3 = 120.7(2), N2-O2-Ag4 = 125.9(2), N2-O2-Ag2 = 115.1(2), N2-O2-Ag3 = 116.8(2), N3-O3-Ag3 = 122.5(2), N3-O3-Ag1 = 116.2(2), N4-O4-Ag4 = 115.5(2), N4-O4-Ag6 = 132.9(2), N5-O5-Ag6 = 109.7(2), N5-O5-Ag7 = 112.5(2), N5-O5-Ag5 = 127.8(2), N6-O6-Ag8 = 119.1(2), N6-O6-Ag10 = 118.0(2), N7-O7-Ag8 = 118.9(2), N7-O7-Ag9 = 113.4(2), N7-O7-Ag7 = 128.4(2), N8-O8-Ag9 = 114.7(2), N8-O8-Ag10 = 119.9(2), N8-O8-Ag8 = 122.9(2), Ag2-Ag3 = 3.103(4), Ag2-Ag3' = 3.103(3), Ag3-Ag4 = 3.070(5), Ag5-Ag6 = 3.230(5), Ag4-Ag3-Ag2 = 83.89(2).

Taking into account the values shown in table 3.4, as the number of coordination modes of ligands **3.1** increase their coordination ability decreases in the following order:

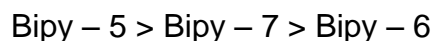




Table – 3.4 Bonding parameters observed for ligand **3.1** in its different coordination modes.

Bipy – X	Average			Torsional angles(°)
	N-O <sub>ligand</sub> (Å)	Ag-O <sub>ligand</sub> (Å)	N-O <sub>ligand</sub> -Ag (°)	
Bipy – 5	1.330	2.374	121.77	71.43
Bipy – 6	1.328	2.449	117.42	71.38
Bipy – 7	1.339	2.438	120.21	75.70
Bipy – 7*	1.338	2.446	119.70	72.17

Complex **3.25** is a 1D polymer that extends along the *c*-axis with inversion centers on the silver(I) ions [Ag2 and Ag9], which are eight-coordinate with distorted hexagonal bipyramidal geometry in an Ag<sub>2</sub>O<sub>6</sub> coordination environment. The base coordination plane of the Ag2 ion is surrounded with oxygens of Bipy – 7 and Bipy – 7\* **3.1** ligand molecules, while the apices are capped with triflate anion oxygens. Interestingly the *trans*- positions of the Ag2 centers are capped with oxygens of bidentate triflate anions, whereas the Ag9 centers have oxygens of tridentate anions as illustrated in figure 3.14b [these bonds are highlighted in red]. Two silver(I) ions Ag3 and Ag4, which are six- and five- [ $\tau_5 = 0.33$ ] coordinate, respectively, interact with Ag2 at near right angles Ag4-Ag3-Ag2 = 83.89(1)° at mean distances of 3.086 Å. Ag2 also interacts with Ag3 and Ag3' at a distance of 3.103(3) Å in a linear fashion [Ag3-Ag2-Ag3 = 180.0].

The eight-coordinate Ag9 center has interactions and bond parameters with the neighboring silver(I) ions similar to the Ag2 center, except that for Ag9 the coordination sphere is surrounded with oxygens of two tridentate triflate anions at *trans*- positions and two Bipy – 7\* **3.1** ligand molecules over the base. Between the two eight-coordinate centers, Ag2 and Ag9, a six-coordinate [Ag5] and a five-coordinate [Ag6] silver(I) are interacting at a distance of 3.229(5) Å. These Ag5-Ag6 bonds are connected to six- [Ag7] and five- [Ag4] coordinate silver(I) ions, as shown in figure 3.14b. Also, these Ag5-Ag6 bonds are bridged to six- [Ag7] and five- [Ag4] coordinate metals with tridentate and bidentate triflate anions. Interestingly, these Ag5-Ag6 interactions are connected to Ag7, Ag8 and Ag10 by Bipy – 6, and to Ag4, Ag3 and Ag1 by Bipy – 5 ligand molecules.

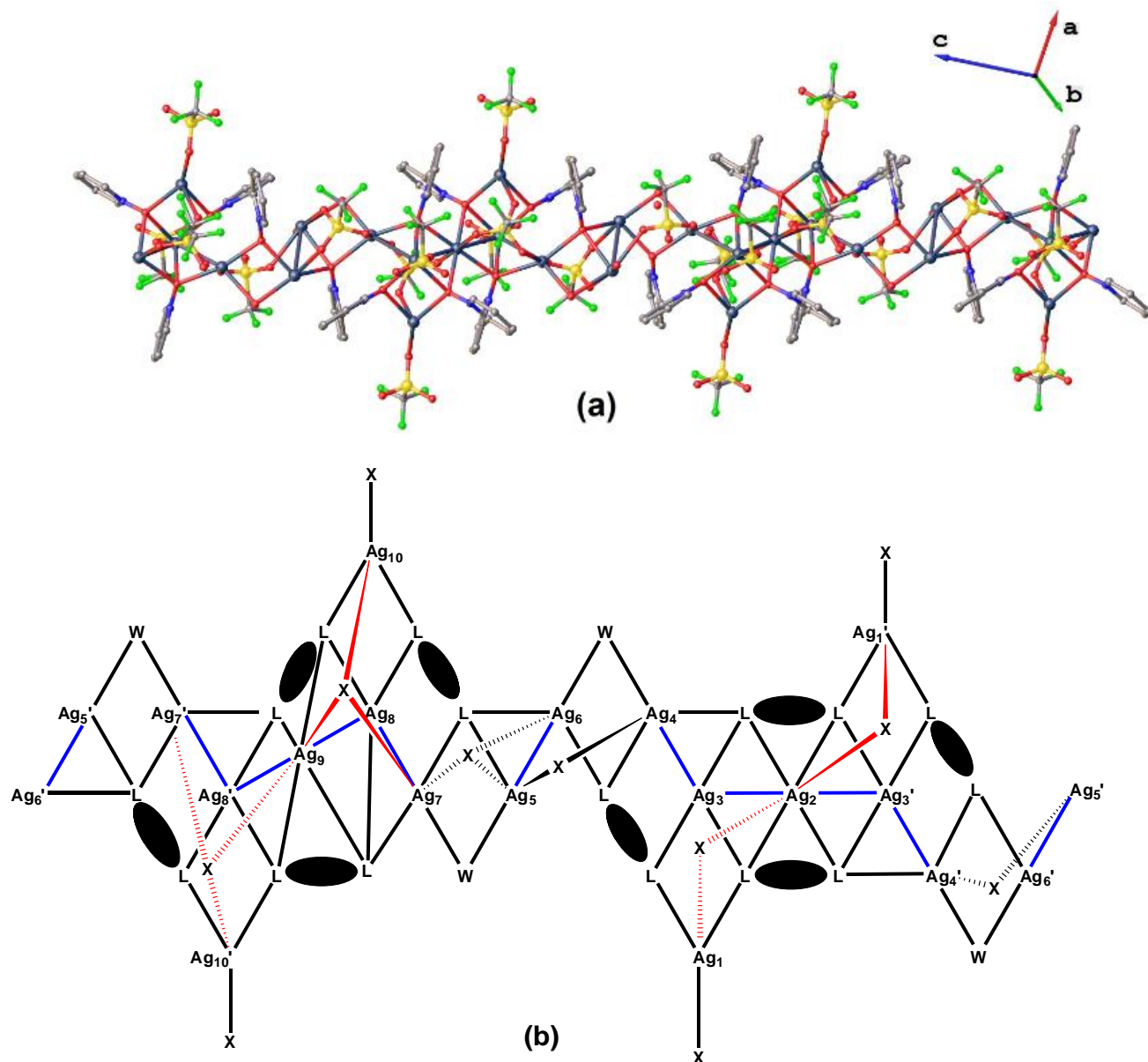


Figure 3.14 – (a) 1D Polymeric view of complex **3.25**. Hydrogen atoms are omitted for clarity, and (b) topological view of complex **3.25** [red colour bonds represent *trans*- bicapped triflate anions over eight-coordinate silver(I) ions and blue colour bonds represent Ag $\cdots$ Ag interactions].

#### With silver(I) nitrate (1:2) **3.28**

Complex **3.28** is a discrete structure as shown in figure 3.15b, with its asymmetric unit [figure 3.15a] solved in the triclinic *P*-1 space group. The asymmetric unit contains one whole ligand and one AgNO<sub>3</sub>, and the complex has a 1:1 ligand to silver(I) ratio. The ligands **3.1** adopt a  $\mu_3$ -O, O', O' coordination [Bipy – 2] mode, as shown in figure 3.6b. The ligands average N-O bond lengths [1.320 Å] are close to other values obtained in the distorted square planar complexes **3.22**, **3.26** and **3.37**. The Ag-O<sub>ligand</sub> bond lengths of the monodentate N-O groups [2.329(1) Å] are shorter than the bidentate bridging N2-O2 groups [2.461(1) Å], due to shared electron density over two

silver(I) ions. The twist between the pyridine N-oxide rings results in a torsion angle of  $61.77^\circ$  [N1-C5-C6-N2]

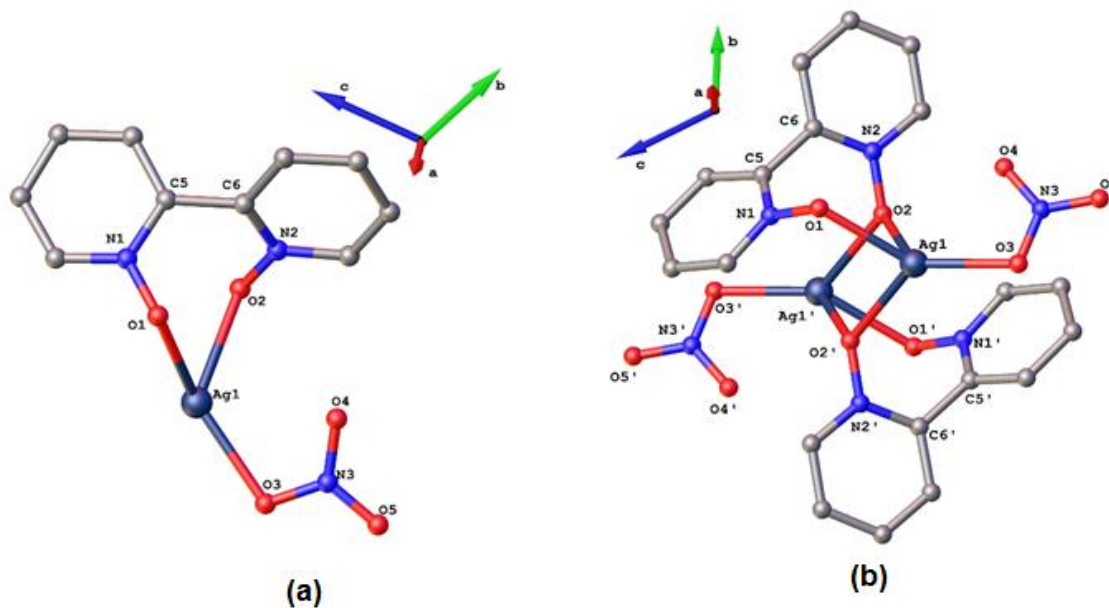


Figure 3.15 – (a) Asymmetric unit of complex **3.28**, and (b) discrete structure of complex **3.28**. Hydrogen atoms are omitted for clarity. Selected bond lengths (Å) and torsional angle ( $^\circ$ ): N1-O1 = 1.321(2), N2-O2 = 1.320(2), Ag1-O1 = 2.329(1), Ag1-O2' = 2.443(1) Ag1-O2 = 2.479(1), N1-C5-C6-N2 =  $61.77^\circ$ .

Within the discrete structure, two bidentate N2-O2 groups bridge two silver(I) ions, Ag1 and Ag1', to form an  $\text{Ag}_2\text{O}_2$  ring [Ag1-O2' = 2.443(1) Å and Ag1-O2 = 2.479(1) Å]. As a consequence of symmetry, the  $\text{Ag}_2\text{O}_2$  ring is planar in the form of a parallelogram with two unequal Ag-O distances, with a non-bonded  $\text{Ag}\cdots\text{Ag}$  distance of 4.003 Å. Each silver(I) ion adopts a four-coordinate distorted tetrahedral [ $\tau_4 = 0.73$ ] geometry with monodentate nitrate anions oriented up and down on either side of the four-membered rings at angles of  $138.57^\circ$  [O3-Ag1-Ag1'], as shown in figure 3.16a. Although the structure is discrete, the monodentate oxygens [N1-O1] weakly interact with Ag1 ions of adjacent units at a distance of 2.821 Å, as shown in figure 3.16b. The crystal packing also has  $\pi$ - $\pi$  interactions between the aromatic rings with centroid-centroid distances of 3.522 Å and 3.596 Å, as shown in figure 3.16b.

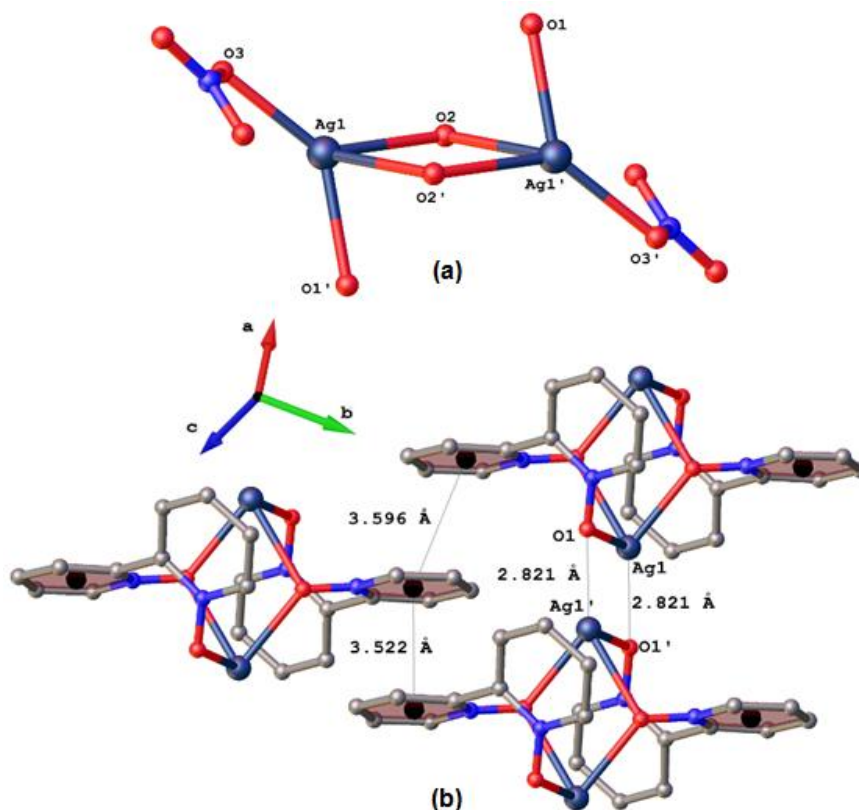
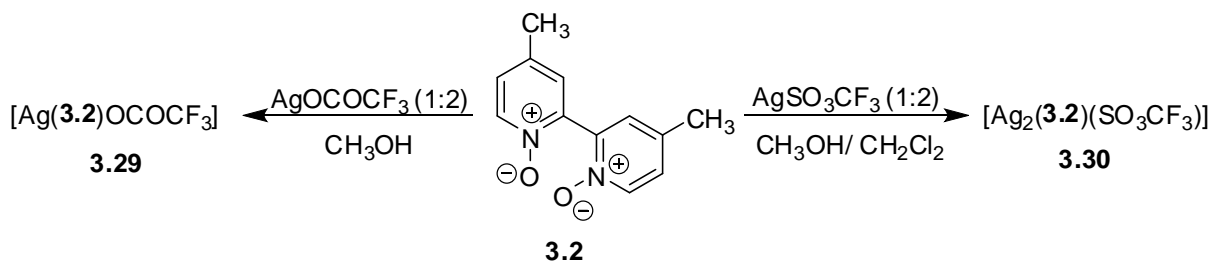


Figure 3.16 – (a) Ag<sub>2</sub>O<sub>2</sub> ring in complex **3.28** and (b) crystal packing showing  $\pi$ - $\pi$  and weak Ag $\cdots$ O interactions [nitrate anions and hydrogen atoms are omitted for clarity].

### 3.3.2 Complexes with 4,4'-dimethyl-2,2'-bipyridine N,N'-dioxide **3.2**

The  $\mu_5$ -O,O,O',O',O' ligand **3.1** in complex **3.25** increased our interest in synthesizing derivatives of ligand **3.1** with electron donating substituents, such as ligand **3.2**. Although several attempts to synthesise complexes with AgClO<sub>4</sub>, AgPF<sub>6</sub> and AgBF<sub>4</sub> were unsuccessful, the results shown in scheme **3.11** were still pleasing. Ligand **3.2** adopted a  $\mu_3$ -O,O',O' coordination mode, when reacted with AgOCOCF<sub>3</sub> in a 1:2 ratio.



Scheme 3.11 – Syntheses of complexes **3.29** – **3.30**.

#### With silver(I) trifluoroacetate (1:2) **3.29**

Complex **3.29** was solved in the monoclinic space group *C2/c* with a 1:2 ligand to silver(I) ratio, as shown in figure 3.17a. The asymmetric unit contains a  $\mu_3$ -O,O',O' ligand **3.2** and two silver(I)

ions and two trifluoroacetates coordinated to Ag1 and Ag2 which are interacting at a distance of 3.048(2) Å. One CF<sub>3</sub> group is disordered over two fluorine atoms [F1 and F2] with 90:10 occupancy ratios, as shown in figure 3.17a. The N1-O1 and N2-O2 bond distances are 1.316(3) Å and 1.333(3) Å, respectively, with their average N-O<sub>ligand</sub> distance [1.324(3) Å] greater than the N-O distances of ligand **3.1** observed in complex **3.24**. The N1-O1 is coordinated to Ag1 in a monodentate fashion, while the  $\mu_2$ -O,O N2-O2 bridges Ag1 and Ag2 at an angle of 76.19(6)°. The torsion angle between the two pyridine rings is 76.8(3)° [N1-C1-C11-N2], which shows a greater twist than ligand **3.1** in complex **3.24** [67.44(6)°]. Consistent with this, the distance between the O1 and O2 oxygens is 3.101 Å, which is slightly longer than the value observed in complex **3.24** [3.046 Å] for ligand **3.1**. The average Ag-O<sub>ligand</sub> bond distance [2.429(2) Å] is similar to the values of ligand **3.1** [2.424(3) Å] in its silver(I) trifluoroacetate complex.

Complex **3.29** is a discrete structure, as shown in figure 3.18, with ligand **3.2** in 'Bipy – 8' coordination mode, as shown in figure 3.17b. Ag1 and Ag2 have adopted distorted octahedral geometries with Ag $\cdots$ Ag interactions. Ag1-Ag2' and Ag2-Ag1' are interacting at distances of 2.878(3) Å with trifluoroacetate anions bridging on either side.

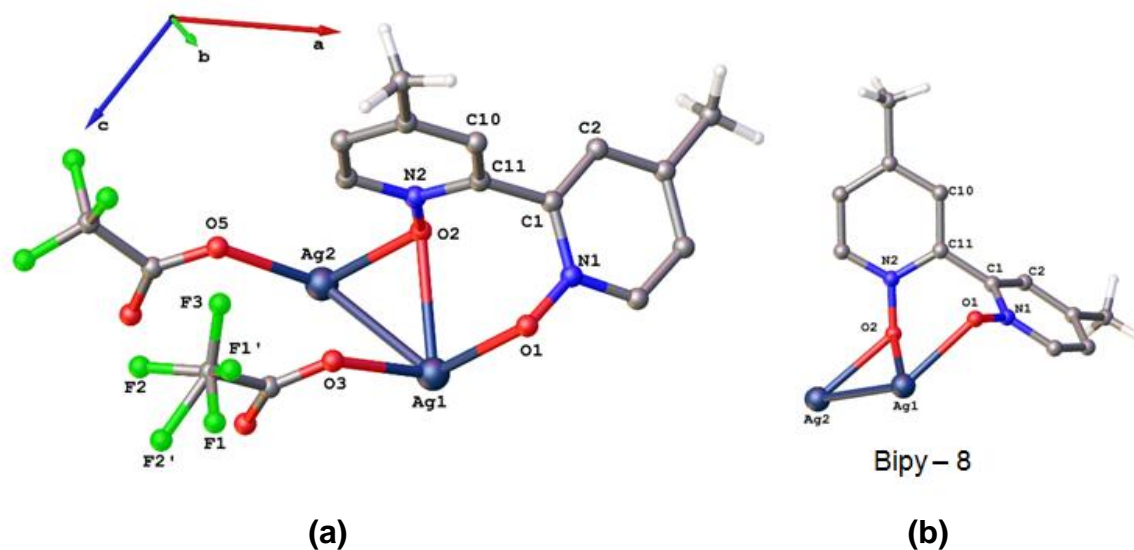


Figure 3.17 – (a) Asymmetric unit of complex **3.29**, and (b) coordination mode displayed by ligand **3.2** in complex **3.29**. Selected hydrogen atoms are omitted for clarity. Selected bond lengths(Å) and bond angles(°): N1-O1 = 1.316(3), N2-O2 = 1.333(3), Ag1-O1 = 2.352(2), Ag1-O2 = 2.555(2), Ag2-O2 = 2.381(1), N1-O1-Ag1 = 113.02(5), N2-O2-Ag2 = 127.94(5), N2-O2-Ag1 = 108.51(5), Ag2-O2-Ag1 = 76.19(6), Ag1-Ag2 = 3.047(6), Ag1-Ag2' = 2.877(6), Ag2-Ag2' = 3.077(1), Ag2-Ag1-Ag2' = 62.51(1), Ag1-Ag2-Ag1' = 117.52(7), Ag1-Ag2'-Ag2 = 61.47(6), Ag1-Ag2-Ag2' = 56.06(3), N1-C1-C11-N2 = 76.8(3).

Ag1, Ag2, Ag1' and Ag2' forms a parallelogram with two unequal sides, interacting at distances of 2.877(6) Å [Ag1-Ag2'/Ag2-Ag1'] and 3.047(6) Å [Ag1-Ag2/Ag1'-Ag2'], with angles 62.51(1)° [Ag2-Ag1-Ag2'] and 117.52(7)° [Ag1-Ag2-Ag1']. Ag2...Ag2' is interacting diagonally at a distance of 3.077(1) Å, dividing the parallelogram into two triangles with angles of 62.51(1)° [Ag2-Ag1-Ag2'], 61.47(6)° [Ag1-Ag2'-Ag2] and 56.06(3)° [Ag1-Ag2-Ag2'], as seen in figure 3.18.

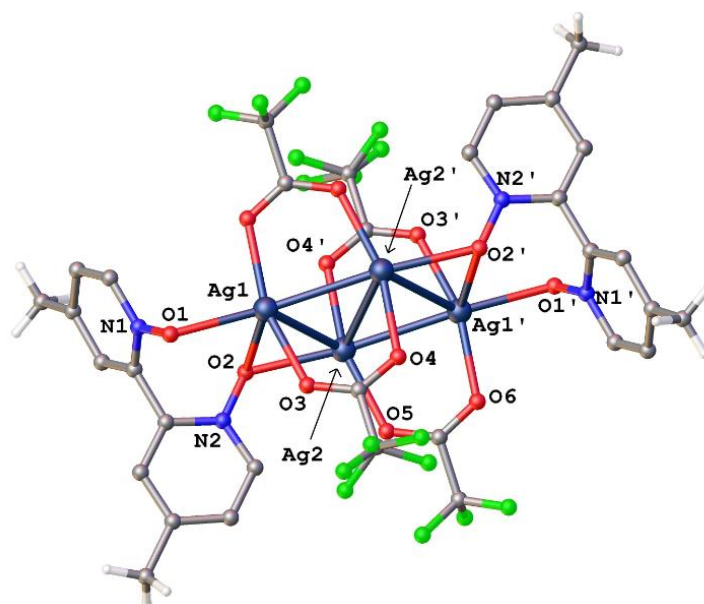


Figure 3.18 – Discrete structure of complex **3.29**, selected hydrogen atoms are excluded for clarity.

#### With silver(I) triflate (1:2) **3.30**

The asymmetric unit of complex **3.30** was solved in the monoclinic  $P2_1/n$  space group, and contains one ligand and two  $\text{AgSO}_3\text{CF}_3$  in a 1:2 ligand to silver(I) ratio, as shown in figure 3.19a. The N1-O1 and N2-O2 bond distances are 1.338(3) Å and 1.320(3) Å, respectively, which suggests that the ligand oxygen orbitals [O1 and O2] are  $sp^3$  and  $sp^2$  hybridized with single and double bond character. Hence, N1-O1 with single bond character is  $\mu_3$ -O,O,O tridentate with Ag1, Ag2 and Ag2', while the  $\mu_2$ -O,O oxygen [O2] bridges Ag1 and Ag1' at an angle of 109.04(7)°, as seen in figure 3.19a. The coordination abilities of bidentate N2-O2 [average Ag-O2 = 2.399(5) Å] is stronger than N1-O1 [average Ag-O1 = 2.503(3) Å] and, their average, 2.457(3) Å, is close to that seen for ligand **3.2** in complex **3.29** [2.429(3) Å].

The distances between metal bound oxygens O1 and O2 [3.007(1) Å], are close to the non-bonded distance [2.980 Å] previously reported<sup>[156]</sup> for ligand **3.2**. The torsional angle between the pyridine rings [70.91(3)°] is smaller than the value obtained for ligand **3.2** in complex **3.29** [76.8(3)°].

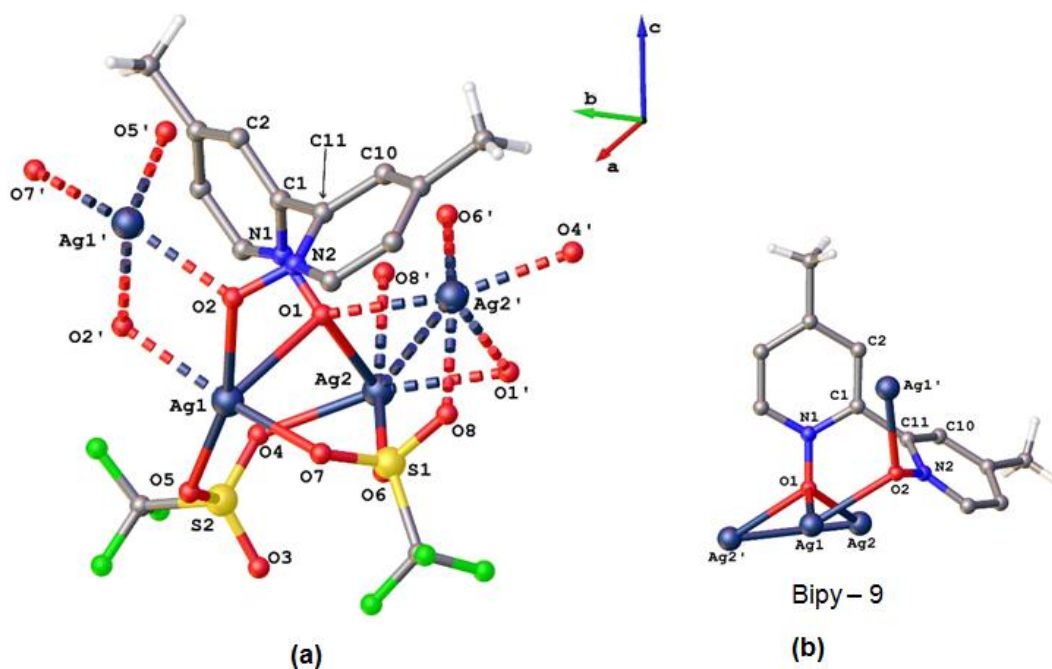


Figure 3.19 – (a) Asymmetric unit of complex **3.30**, and (b) preferred coordination mode of ligand **3.2** in complex **3.30**. Selected hydrogen atoms are omitted for clarity. Selected bond lengths(Å) and bond angles(°): N1-O1 = 1.338(3), N2-O2 = 1.320(3), Ag1-O1 = 2.528(1), Ag2-O1 = 2.474(2), Ag2'-O1 = 2.511(2), Ag1-O2 = 2.424(7), Ag1'-O2 = 2.375(3), Ag2-Ag2' = 3.337(4), N1-O1-Ag1 = 102.02(2), N1-O1-Ag2 = 123.54(4), N1-O1-Ag2' = 117.33(4), N2-O2-Ag1 = 121.55(4), N2-O2-Ag1' = 117.67(4), Ag2-O1-Ag1 = 102.48(6), Ag2-O1-Ag2' = 84.07(5), Ag2'-O1-Ag1 = 127.91(8), Ag1-O2-Ag1' = 109.04(7), N1-C1-C11-N2 = 70.91(3).

Complex **3.30** is a 1D polymer, as shown in figure 3.20, with ligands **3.2** in Bipy – 9 coordination mode, as shown in figure 3.19b. Ag1 is five-coordinated [ $\tau_5 = 0.20$ ], with distorted square pyramidal geometry in an O<sub>5</sub> environment. The oxygens for the base vertices are supplied by two ligand **3.2** oxygens, O2 and O2'; O5 from a bidentate triflate [S2] and O7 from a tridentate triflate [S1]. The apex position is occupied by a tridentate ligand **3.2** oxygen, O1. Ag2 is six-coordinate with an Ag<sub>1</sub>O<sub>5</sub> environment, interacting with symmetry related Ag2' at a distance of 3.337(4) Å. Oxygens for the six-coordinate Ag2 center are supplied from two bridging ligands **3.2** [O1 and O1'], two tridentate triflates [O6 and O8] and a bidentate triflate [O4], as shown in figure 3.20.

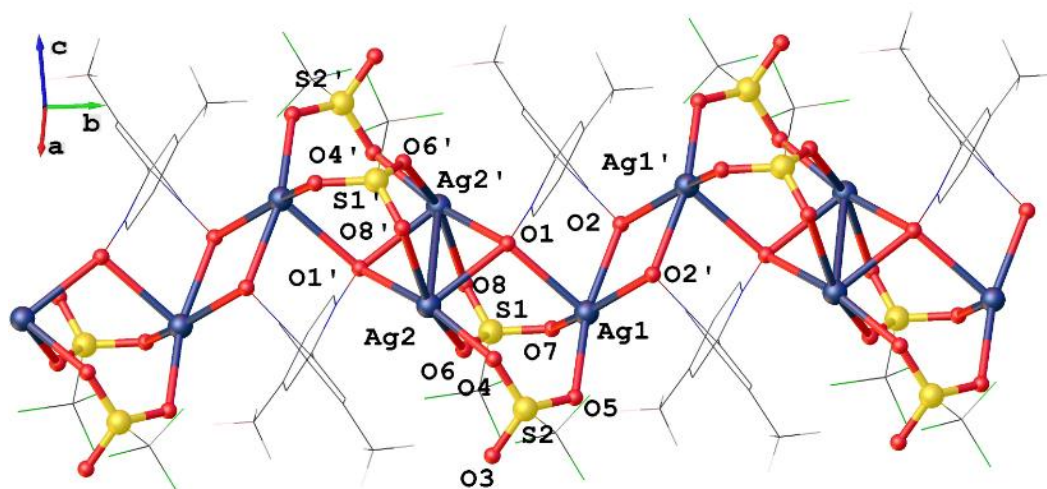


Figure 3.20 – 1D Polymeric view of complex **3.30** [ligands **3.2** are shown in wireframe for clarity], and hydrogen atoms are excluded for clarity.

### 3.3.3 Crystal structure of 4,4'-diphenyl-2,2'-bipyridine N,N'-dioxide **3.3**

Attempts to grow crystals with silver(I) salts using ligand **3.3** were unsuccessful. In most cases, the ligand preferentially crystallised, as shown in figure 3.21. The crystal structure of ligand **3.3** was solved in the monoclinic  $C2/c$  space group, which is similar to the other 4,4'-disubstituted ligand **3.2**,<sup>[156]</sup> with half a ligand molecule of **3.3** in the asymmetric unit. The crystal structure of ligand **3.3** has not been reported to date, based on *Cambridge Crystallographic Database* and *Sci-Finder* searches. The torsional angle between the pyridine rings [N1-C1-C1'-N1'] is  $71.11(3)^\circ$ , which is larger than other reported 4,4'-disubstituted ligand systems, such as **3.2**.<sup>[156]</sup> The phenyl substituents are twisted at torsional angles of  $16.95(2)^\circ$  with respect to the pyridine N-oxide rings with the distance between the non-bonded oxygen atoms being  $3.017(2) \text{ \AA}$ , as shown in figure 3.21. The N-O bond distance of  $1.304(1) \text{ \AA}$  is equivalent to that in ligand **2.10**.

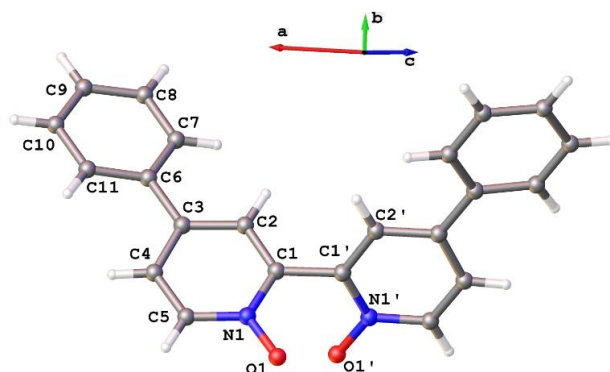


Figure 3.21 – Structure of ligand **3.3**. Selected bond lengths ( $\text{\AA}$ ) and bond angles ( $^\circ$ ): N1-O1 =  $1.304(1)$ , N1-C1-C1'-N1' =  $71.11(3)$ , C4-C3-C6-C11 =  $16.95(2)$ .

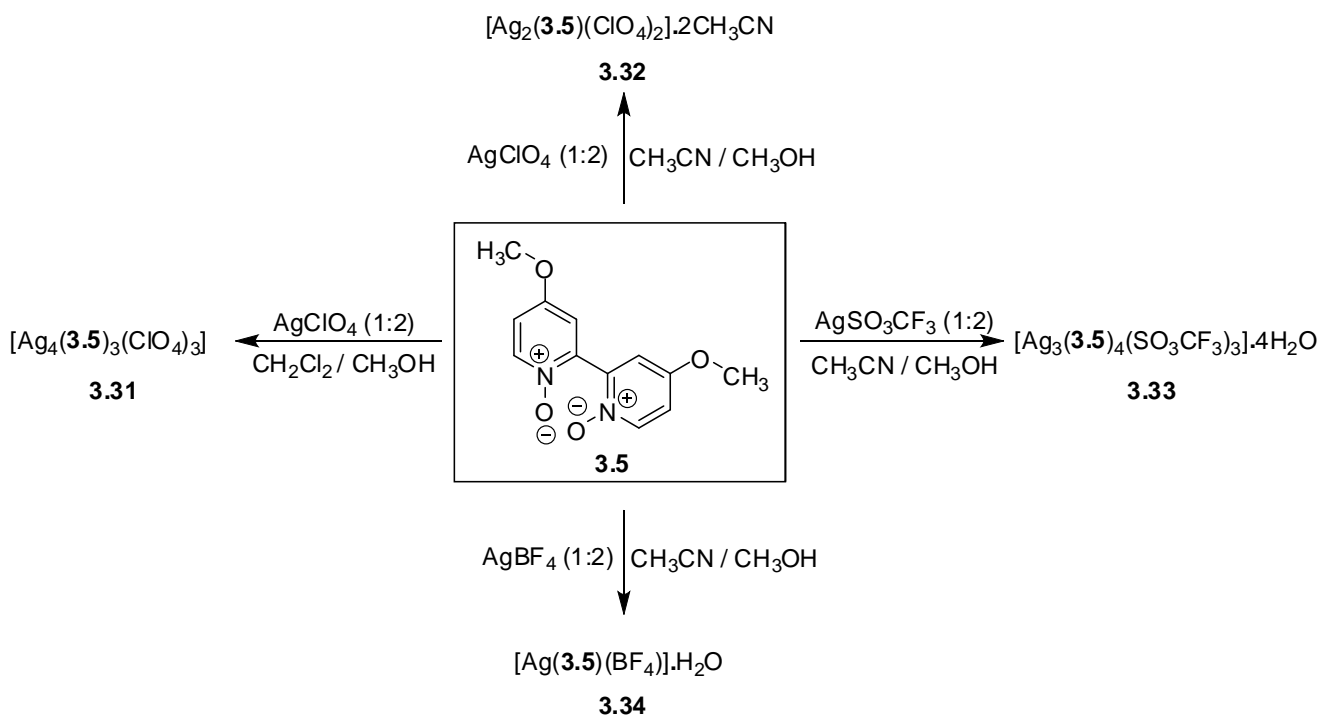


### 3.3.4 Complexes with 4,4'-di-tert-butyl-2,2'-bipyridine N,N'-dioxide 3.4

Syntheses of complexes of ligand **3.4** with different silver(I) salts, such as  $\text{AgClO}_4$ ,  $\text{AgOCOCF}_3$ ,  $\text{AgSO}_3\text{CF}_3$ ,  $\text{AgBF}_4$ ,  $\text{AgPF}_6$  and  $\text{AgNO}_3$ , were attempted. Unfortunately, none of these attempts was successful and, instead, resulted in gummy globules. Multiple crystallisation attempts with different ligand to silver(I) ratios using a range of solvent systems were also unsuccessful.

### 3.3.5 Complexes with 4,4'-dimethoxy-2,2'-bipyridine N,N'-dioxide 3.5

Complexes of ligand **3.5** with different silver(I) salts were obtained by slow evaporation of solvents, as shown in scheme 3.12. The first two complexes **3.31** and **3.32** solved in the monoclinic space groups  $C2/c$  and  $P2_1/n$  respectively, whereas **3.33** and **3.34** solved in the triclinic  $P-1$  space group. The solvent combinations,  $\text{CH}_2\text{Cl}_2/\text{CH}_3\text{OH}$  and  $\text{CH}_3\text{CN}/\text{CH}_3\text{OH}$ , used to prepare  $\text{AgClO}_4$  complexes resulted in two different structures **3.31** and **3.32**, due to the coordination of  $\text{CH}_3\text{CN}$  solvent molecules in complex **3.32**. Although the  $-\text{OCH}_3$  groups improve the electron donation of the coordinating N-O compared to  $-\text{CH}_3$  in ligand **3.2**, the maximum denticity shown by ligand **3.5** was  $\mu_4\text{-O, O, O', O'}$  in complexes **3.30**, **3.31** and **3.32**.



Scheme 3.12 – Syntheses of complexes **3.31** – **3.34**.

#### With silver(I) perchlorate (1:2) 3.31

Complex **3.31** crystallised and solved in the monoclinic  $C2/c$  space group and contains two **3.5** ligands, one and a half silver(I) ions and one and a half perchlorate anions, as shown in figure 3.22.  $\text{Ag}1$  and  $\text{Cl}2$  occupy special positions, and complex **3.31** has a 4:3 ligand to silver(I) ratio.

Ligands **3.5** adopted  $\mu_2$ -O,O' [Bipy – 10] and  $\mu_4$ -O,O',O',O' [Bipy – 11] coordination modes, as shown in figure 3.22b. The average N-O<sub>ligand</sub> and Ag-O<sub>ligand</sub> bond lengths are 1.340(3) Å and 2.395(2) Å, respectively, which are longer than the values obtained for ligand **3.2** in complexes **3.28** and **3.29**. These two values show that the –OCH<sub>3</sub> groups in ligand **3.5** are more electron donating giving a greater N-O single bond character. The N-O<sub>ligand</sub>-Ag angles in complex **3.31** range from 109.32(2)° to 130.56(2)°. The torsion angle between the pyridine rings for the chelating Bipy – 10 is 66.54(4)° [N3-C17-C19-N4], which has a bite angle of 76.91(8)° [O5-Ag2-O7]. The torsional angle between the pyridine rings for Bipy – 11 is 72.62(4)° [N1-C5-C7-N2] with silver(I) bound oxygen distances [O1-O3 = 3.147 Å] higher than Bipy – 10 [O5-O7 = 2.966 Å]. The longer O1-O3 distance reflects the larger twist required for Bipy – 11 to bridge Ag2, Ag1 and Ag2'', as shown in figure 3.22b.

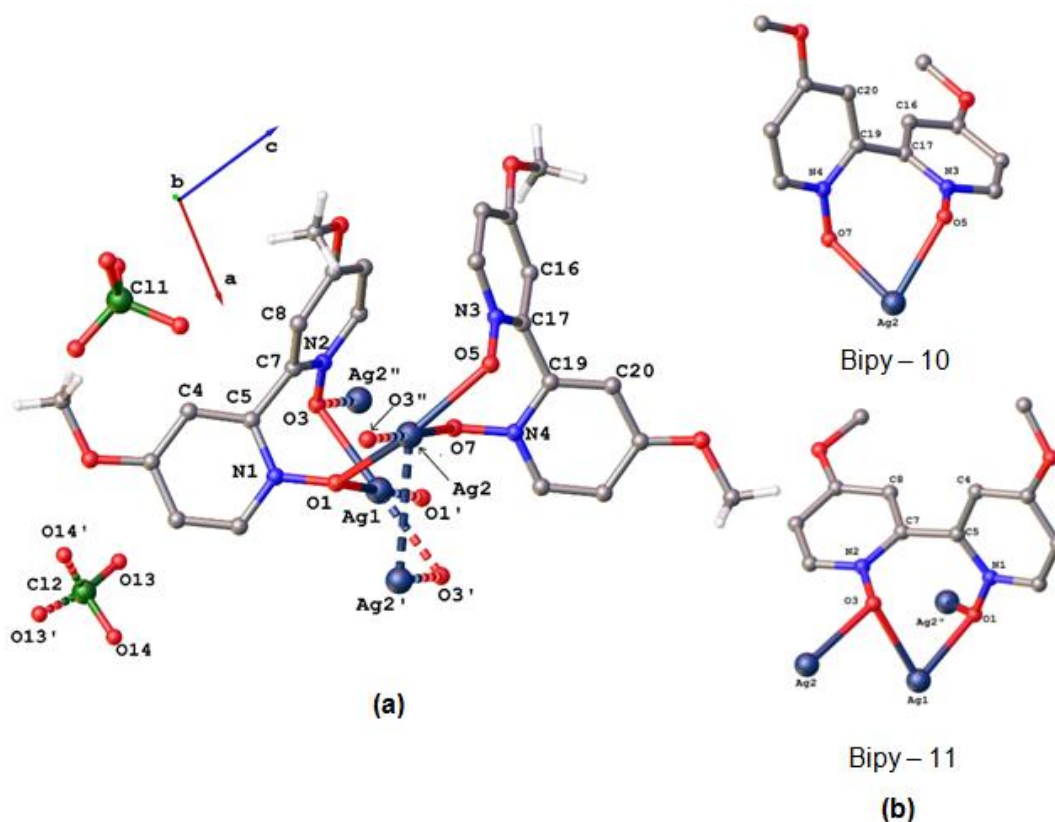


Figure 3.22 – (a) Asymmetric unit of complex **3.31**, and (b) coordination modes for ligand **3.5** in complex **3.31**. Hydrogen atoms have been omitted for clarity. Selected bond lengths (Å) and bond angles (°): N1-O1 = 1.345(3), N2-O2 = 1.338(3), N3-O5 = 1.333(3), N4-O7 = 1.344(3), Ag1-O1 = 2.341(2), Ag1-O3 = 2.373(2), Ag2-O7 = 2.378(2), Ag2-O5 = 2.392(2), Ag2-O1 = 2.493(2), Ag2-O3 = 2.456(2), N1-O1-Ag1 = 109.32(2), N1-O1-Ag2 = 130.56(2), N2-O3-Ag1 = 110.51(2), N2-O3-Ag2' = 126.49(2), N3-O5-Ag2 = 119.32(2), N4-O7-Ag2 = 116.34(2), Ag1-O1-Ag2 = 110.38(8), Ag1-O3-Ag2'' = 89.88(7), O7-Ag2-O5 = 76.91(8), Ag2-Ag2' = 3.357(5), N1-C5-C7-N2 = 72.6(4), N3-C17-C19-N4 = 66.5(4).

Ag1 [ $\tau_4 = 0$ ] and Ag2 [ $\tau_5 = 0.49$ ] are four- and five-coordinate with square planar and distorted square pyramidal geometries respectively. The Ag-O<sub>ligand</sub> bond distances around Ag1 are 2.341(2)

Å [Ag1-O1/O1'] and 2.373(2) Å [Ag1-O3/O3'] and, at an average of 2.357(2) Å, falls within the range of O-donor silver(I) square planar complexes previously reported by Hanton and coworkers.<sup>[153]</sup> Complex **3.31** is a 1D polymer [figure 3.23a] with alternate four- and five-coordinate silvers bridged by two Bipy – 11 ligands [shown in black bonds], as shown in figure 3.23b. The five-coordinate silvers weakly interact at a distance of 3.356(5) Å, and in turn are chelated with Bipy – 10 ligands [shown in red bonds] on either side, as shown in figure 3.25b.

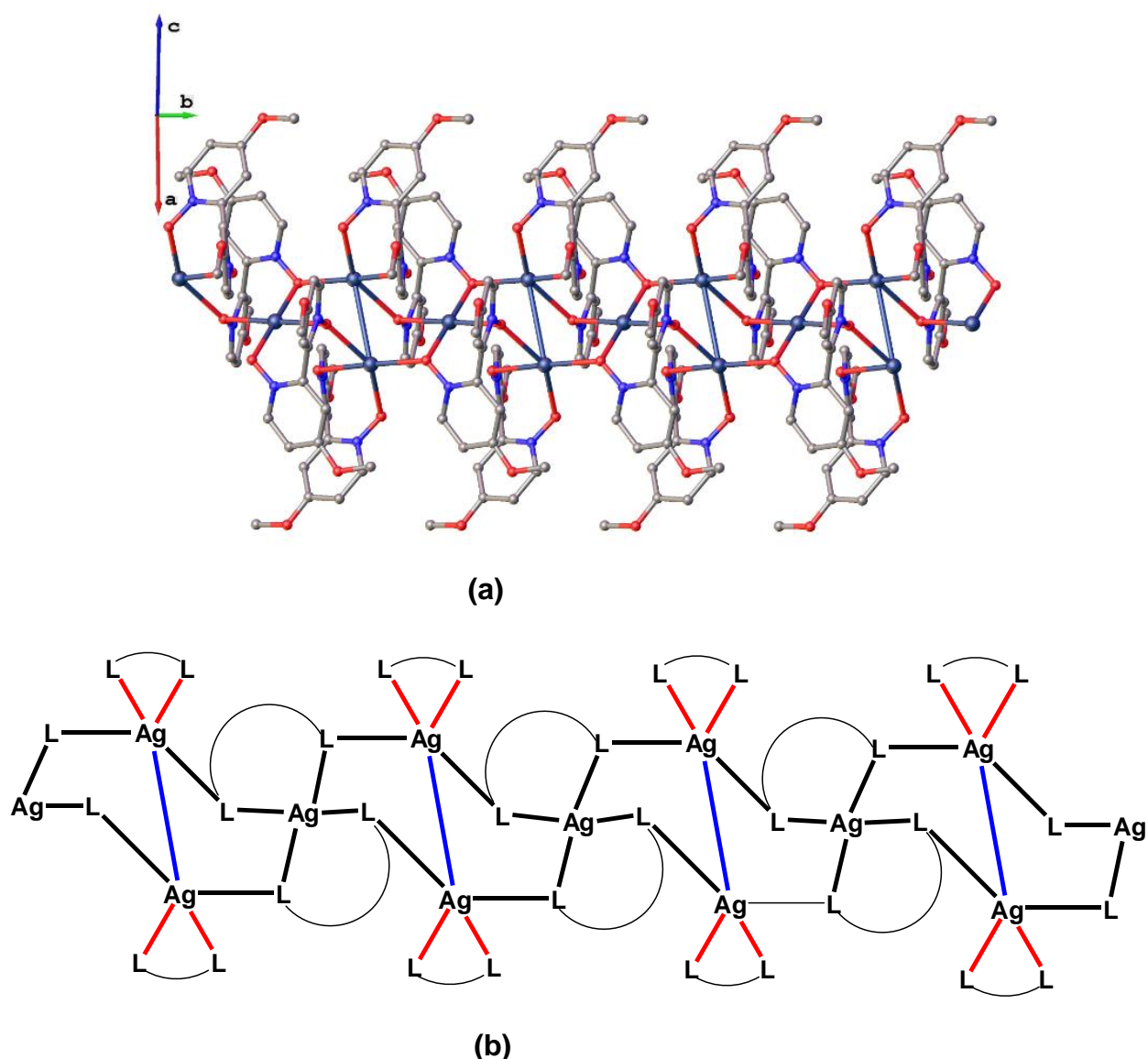


Figure 3.23 – (a) 1D Polymeric structure of complex **3.31**. Hydrogen atoms have been omitted for clarity, and (b) topological view of complex **3.30** related to figure 3.23a.

### With silver(I) perchlorate (1:2) **3.32**

The complex **3.32** solved in the monoclinic  $P2_1/n$  space group, and contains one ligand **3.5**, two silver(I) ions [Ag1 and Ag2], two perchlorate anions and two acetonitrile molecules in the asymmetric unit, as shown in figure 3.24a. The ligand **3.5** adopts a  $\mu_4$ -O,O,O',O' coordination

mode [Bipy – 12] with N-O groups bridging Ag1, Ag2 and Ag1'. The average N-O<sub>ligand</sub> and Ag-O<sub>ligand</sub> bond distances are 1.341(3) Å and 2.359(2) Å, respectively, which are similar to the values observed in complex **3.31**. However, the N-O<sub>ligand</sub>-Ag [113.15(2)°] angles are less than for ligand **3.5** in complex **3.31** [118.75(2)°].

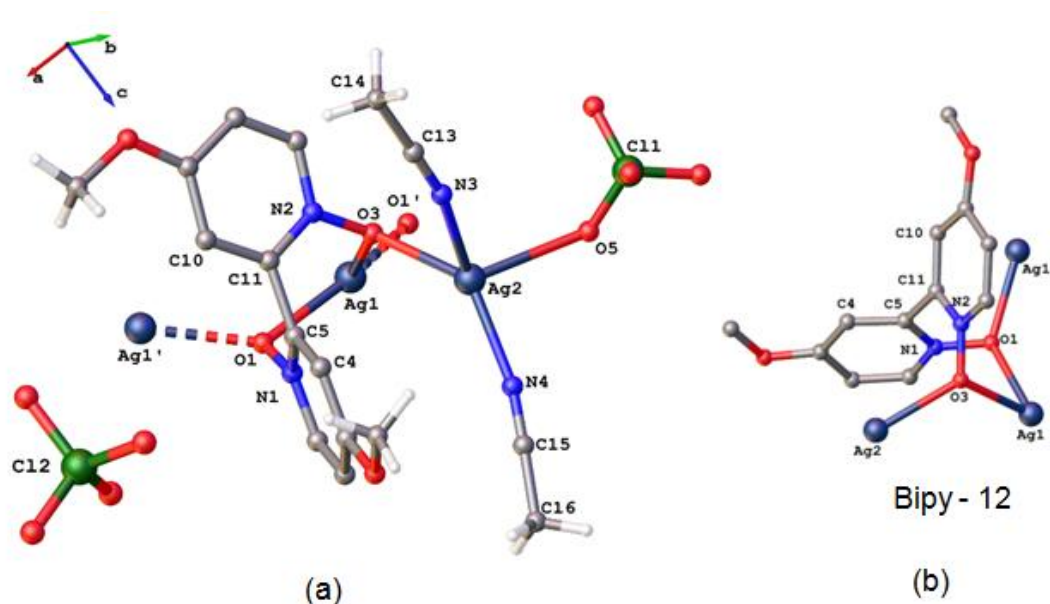


Figure 3.24 – (a) The asymmetric unit of complex **3.32**, and (b) coordination mode of ligand **3.5** in complex **3.32**. Selected hydrogen atoms have been omitted for clarity. Selected bond lengths (Å) and bond angles (°): N1-O1 = 1.342(3), N2-O3 = 1.341(3), Ag1-O1 = 2.361(2), Ag1-O3 = 2.389(2), Ag2-O3 = 2.364(2), Ag1'-O1 = 2.322(2), N1-O1-Ag1' = 109.95(2), N1-O1-Ag1 = 110.12(2), N2-O3-Ag2 = 119.79(2), N2-O3-Ag1 = 112.75(2), Ag1-O1-Ag1' = 133.37(9), Ag2-O3-Ag1 = 119.97(9), O1-Ag1-O1' = 158.95(2), O1-Ag1-O3 = 80.30(7), O3-Ag1-O1' = 119.24(7), N1-C5-C11-N2 = 73.4(4).

Ag1 and Ag2 [ $\tau_4 = 0.69$ ] are three- and four-coordinate with O<sub>3</sub> and N<sub>2</sub>O<sub>2</sub> coordination environments. Complex **3.32** is a 1D polymer extending along the *b*-axis with three-coordinate Ag1 centers bridged by O1 oxygens at angles of 133.37(9)° [Ag1-O1-Ag1'] and, Ag1 and Ag2 by O3 oxygens at angles of 119.97(9)°, as shown in figure 3.25a. Also, two acetonitrile molecules and one monodentate perchlorate anion are coordinated to each Ag2 as shown in figure 3.25a. The torsional angle between the pyridine rings is 73.4(4)° [N1-C5-C11-N2], with the O1-O3 distance being 3.063(3) Å. The O1-Ag1-O1', O1-Ag1-O3 and O3-Ag1-O1' angles around the three-coordinate Ag1 are 158.95(2)°, 80.30(7)° and 119.24(7)°, respectively.

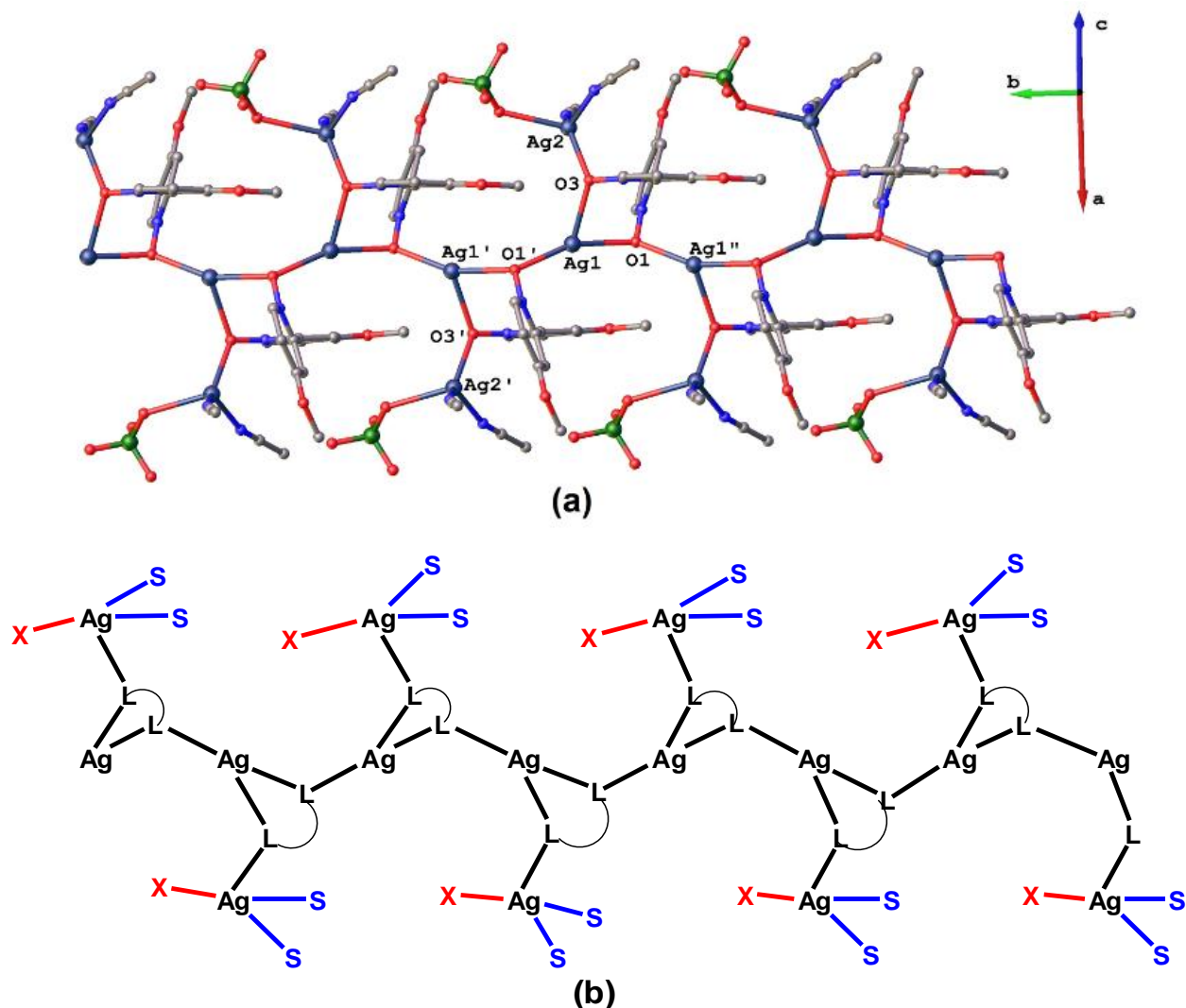


Figure 3.25 – (a) One-dimensional structure of complex **3.31**. Hydrogen atoms are omitted for clarity and (b) topology view of complex **3.31** [representation: blue – Ag-CH<sub>3</sub>CN molecules (S), red – Ag-anions (X) and black – Ag-bridging ligands (L)]. The non-coordinated perchlorate anions are not shown.

### With silver(I) triflate (1:2) **3.33**

The asymmetric unit of complex **3.33** solved in the triclinic *P*-1 space group with four **3.5** ligands, three silver(I) ions and two coordinated and two non-coordinated water molecules, as shown in figure 3.26. The three triflate anions are non-coordinating with one disordered over two sites at S1 with a 70:30 occupancy ratio. The ligands **3.5** have adopted  $\mu_2$ -O, O' [Bipy – 13],  $\mu_3$ -O, O', O' [Bipy – 14] and  $\mu_4$ -O, O, O', O' in two ways as Bipy – 15 & 16 coordination modes, as shown in figure 3.27. The N-O bond lengths range from 1.323(3) Å to 1.351(3) Å with an average Ag-O<sub>ligand</sub> bond length of 2.455(2) Å, similar to the values of ligands **3.1** and **3.2** in their silver(I) triflate complexes.

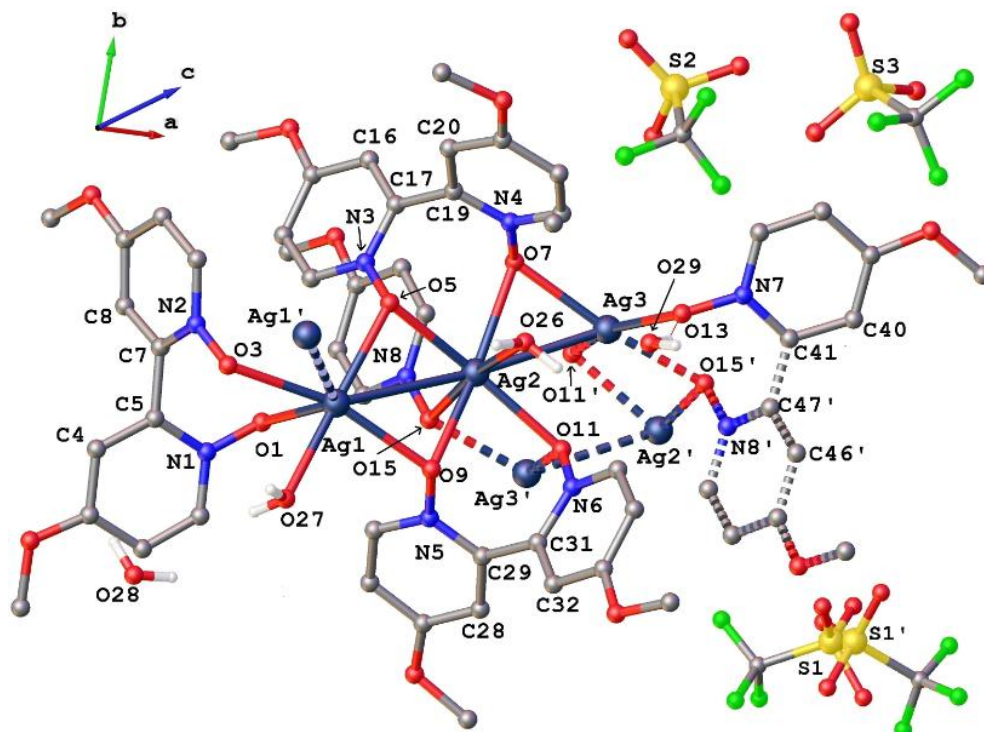


Figure 3.26 – Asymmetric unit of complex **3.33**. Hydrogen atoms have been excluded for clarity. Selected bond lengths (Å) and bond angles (°): N1-O1 = 1.323(3), N2-O3 = 1.343(3), N3-O5 = 1.348(3), N4-O7 = 1.348(3), N5-O9 = 1.329(3), N6-O11 = 1.351(3), N7-O13 = 1.338(3), N8-O15 = 1.341(3), Ag1-O1 = 2.522(2), Ag1-O3 = 2.493(2), Ag1-O5 = 2.448(2), Ag2-O5 = 2.455(2), Ag2-O7 = 2.526(2), Ag3-O7 = 2.396(2), Ag1-O9 = 2.468(2), Ag2-O9 = 2.418(2), Ag2-O11 = 2.422(2), Ag2-O15 = 2.513(2), Ag3'-O11 = 2.498(2), Ag3-O13 = 2.440(2), N1-O1-Ag1 = 115.64(2), N2-O3-Ag1 = 116.33(2), N3-O5-Ag1 = 123.27(2), N3-O5-Ag2 = 111.90(2), N4-O7-Ag3 = 122.54(2), N4-O7-Ag2 = 107.92(2), N5-O9-Ag2 = 111.02(2), N5-O9-Ag1 = 123.05(2), N6-O11-Ag2 = 111.44(2), N6-O11-Ag3' = 133.14(2), N7-O13-Ag3 = 121.81(2), N8-O15-Ag3' = 115.75(2), Ag1-Ag1' = 3.218(5), Ag1-Ag2 = 3.353(3), Ag2-Ag3 = 3.070(3).

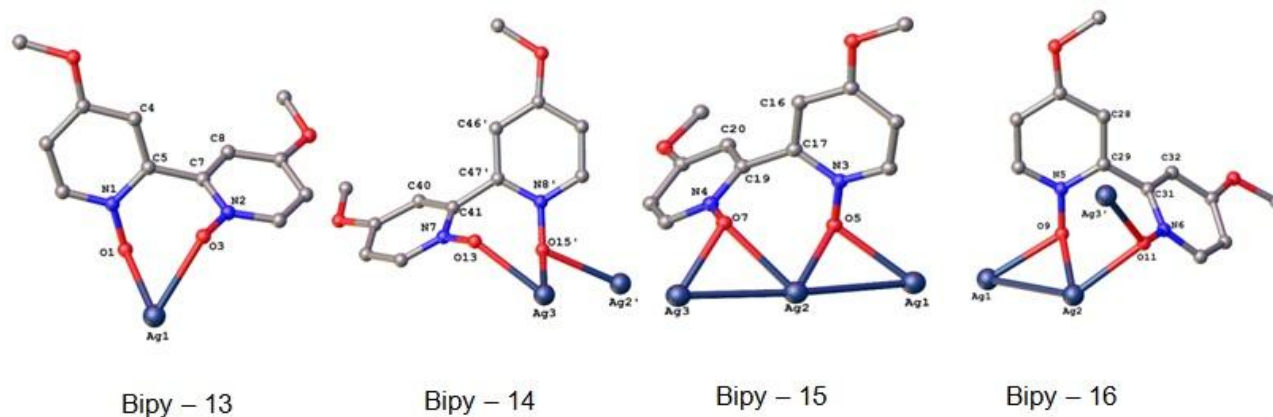


Figure 3.27 – Coordination modes of ligand **3.5** displayed in complex **3.33**. Hydrogen atoms are omitted for clarity.

The torsional angles and distances between the silver(I) bound **3.5** ligand oxygens in complex **3.33** are shown in table 3.7. The N-O<sub>ligand</sub>-Ag angles for Bipys are shown in figure 3.26 and range between 107.92(2)° and 133.14(2)°. Bipy – 13 chelates Ag1 forming a skew-type seven-membered ring with a bite angle of 76.10(7)° [O3-Ag1-O1]. Ag1 is seven-coordinate, with two oxygens supplied from Bipy – 13 [O1 and O3], two from bridging ligand **3.5** [O5 and O9] and one from a monodentate water molecule [O27], as shown in figure 3.26. Also, Ag1 interacts with Ag2 and Ag1' at distances of 3.353(3) Å and 3.218(5) Å and angles of 119.82(1)° [Ag1'-Ag1-Ag2], as shown in figure 3.26.

Table – 3.7 Comparison between ligands **3.5** in complex **3.33**.

Bond parameters → Ligand ↓	Torsional angles (°)	Distance between silver(I) coordinated ligand <b>3.5</b> oxygens (Å)	Average Ag...O <sub>ligand</sub> (Å)
Bipy – 13	73.9(4) [N1-C5-C7-N2]	O1-O3 = 3.091	2.507(2)
Bipy – 14	66.1(4) [N7-C41-C47'-N8']	O13-O15' = 2.910	2.445(2)
Bipy – 15	74.0(4) [N3-C17-C19-N4]	O5-O7 = 3.162	2.456(2)
Bipy – 16	70.0(4) [N5-C29-C31-N6]	O9-O11 = 3.070	2.451(2)

Ag2 is eight-coordinate similar to that in complex **3.25**, with distorted hexagonal bipyramidal geometry and is *trans*-bicapped by a ligand **3.5** oxygen [O15] and a water molecule [O26]. The five-coordinate Ag3 exhibits distorted square pyramidal geometry with a  $\tau_5$  index of 0.22. Four vertices are occupied by O7, O11', O15' and O13 of the ligand **3.5**, while the apical position has Ag2 at a distance of 3.070(3) Å. Each eight-coordinate Ag2 interacts at near linear angle with Ag1 and Ag3 [170.90(2)°] at distances of 3.353(3) Å and 3.070(3) Å, respectively.

The complex **3.33** is a 1D polymer [figure 3.28a] connected at seven-coordinate Ag1 to form five successive Ag...Ag interactions [red bonds] in a zigzag shape, as shown in figure 3.28b.

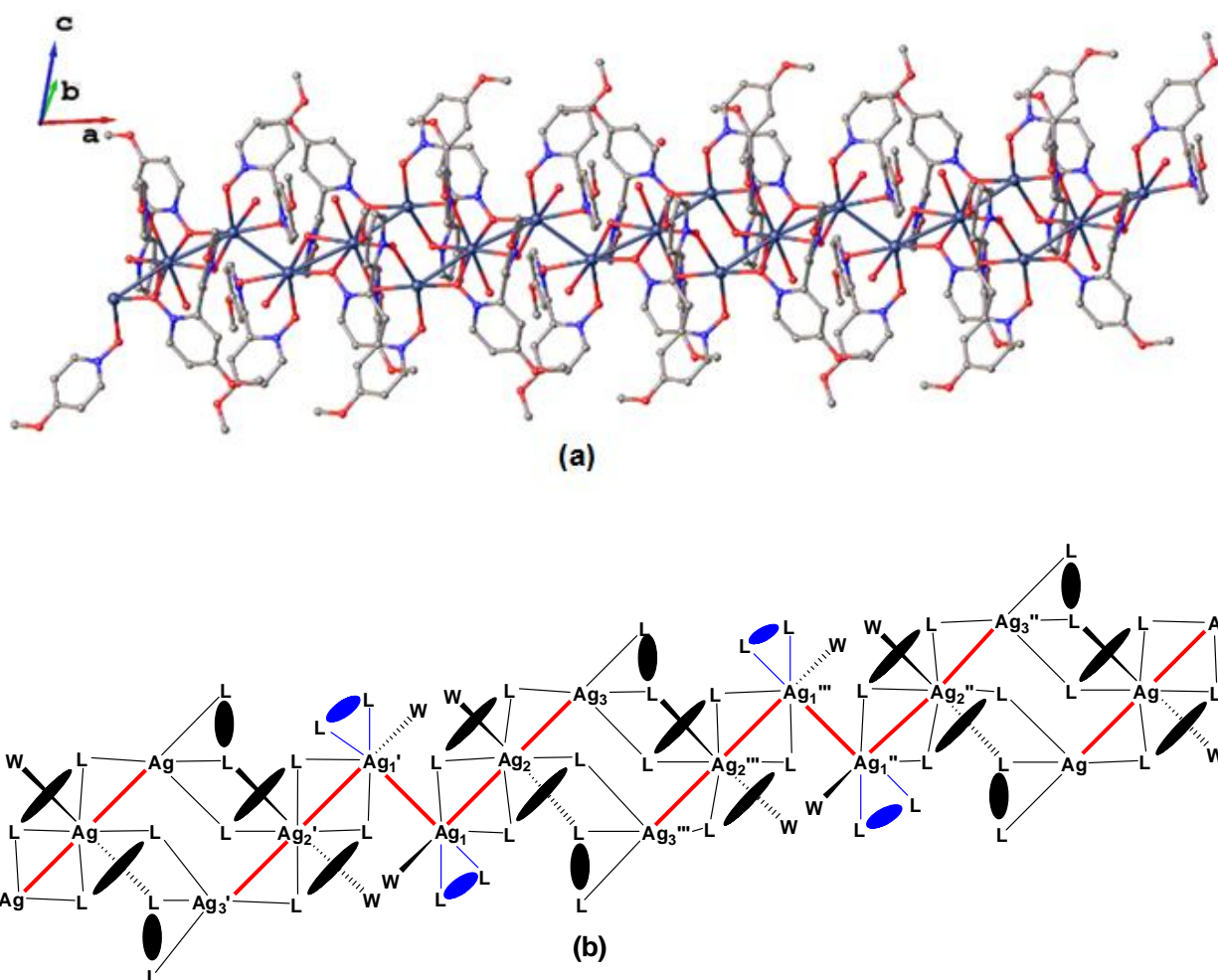


Figure 3.28 – (a) 1D Polymeric structure of complex **3.33**. Hydrogen atoms and triflate anions have been excluded for clarity and (b) topological view of complex **3.33** [Ag<sup>III</sup>–Ag zigzag interactions are shown in red and the skew ligands **3.5** are indicated in blue].

#### With silver(I) tetrafluoroborate (1:2) **3.34**

The asymmetric unit of complex **3.34** solved in the triclinic  $P-1$  space group with ligand **3.5** chelating to Ag1 to form a skewed seven-membered ring. A non-coordinated BF<sub>4</sub> anion interacts with a monodentate water molecule through a hydrogen bond at 2.730(2) Å [O5⋯F4], as shown in figure 3.29a. The ligands **3.5** are in a  $\mu_3$ -O,O',O' coordination mode with an average N–O<sub>ligand</sub>–Ag angle of 116.73(9)° similar to complex **3.28**. Complex **3.34** is a discrete structure with similar N1–O1 [1.339(3) Å] and N2–O3 [1.341(3) Å] bond distances.

The Ag–O<sub>ligand</sub> bond distances [2.350(2) Å] are close to those observed in complexes **3.31** [2.395(2) Å], **3.32** [2.371(2) Å] and **3.33** [2.455(2) Å]. Two four-coordinate silvers [ $\tau_4 = 0.59$ ], Ag1 and Ag1', and two oxygens, O3 and O3', form a four-membered ring with two unequal Ag–O<sub>ligand</sub> distances of 2.295(1) Å and 2.510(1) Å. Due to symmetry, the Ag<sub>2</sub>O<sub>2</sub> ring is planar and a



parallelogram, with a non-bonding  $\text{Ag}\cdots\text{Ag}$  distance of 3.781(3) Å. The two monodentate water molecules [O5 and O5'] are coordinated in a *trans*- fashion about the  $\text{Ag}_2\text{O}_2$  ring at an angle of 145.95(3)° [Ag1-Ag1'-O5'].

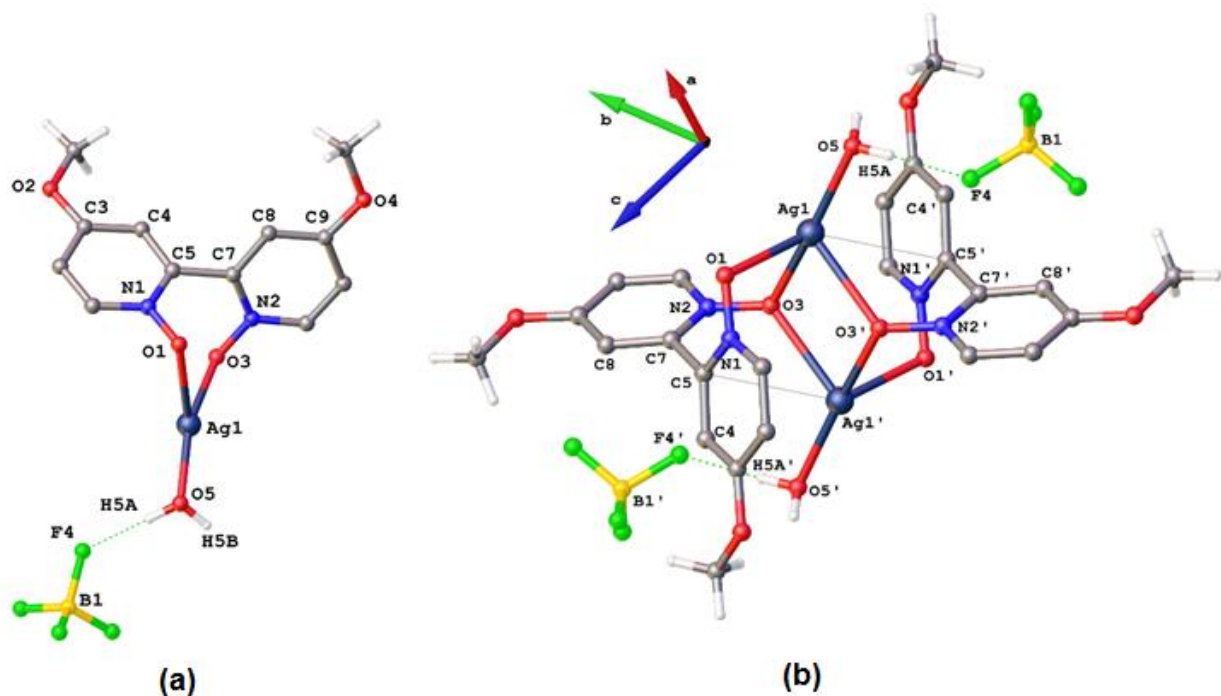


Figure 3.29 – (a) Asymmetric unit of complex **3.34**, and (b) discrete structure of complex **3.34**. Selected hydrogen atoms have been omitted for clarity. Selected bond lengths (Å) and bond angles (°): N1-O1 = 1.339(3), N2-O3 = 1.341(3), Ag1-O3 = 2.297(2), Ag1-O1 = 2.404(2), Ag1'-O3 = 2.512(2), N1-O1-Ag1 = 108.47(8), N2-O3-Ag1 = 117.35(9), N2-O3-Ag1' = 124.37(9), Ag1-O3-Ag1' = 103.67(4), Ag1-Ag1'-O5' = 145.95(3), N1-C5-C7-N2 = 70.52(2).

Although the complex **3.34** is a discrete structure, the crystal packing revealed weak interactions between the Ag1 centers and  $-\text{OCH}_3$  groups, as shown in figure 3.30a. The oxygens [O4/O4'] of the  $-\text{OCH}_3$  groups on the bidentate pyridine N-oxide ring system interact with Ag1/Ag1' at a distance of 3.017(1) Å. In complex **3.34**, ligand **3.5** has opted for a Bipy – 17 coordination mode, as shown in figure 3.30b. The torsional angle between the pyridine rings is 70.52(2)° [N1-C5-C7-N2] with the distance between the two Ag(I) bound oxygens [O1 and O3] being 3.020(2) Å.

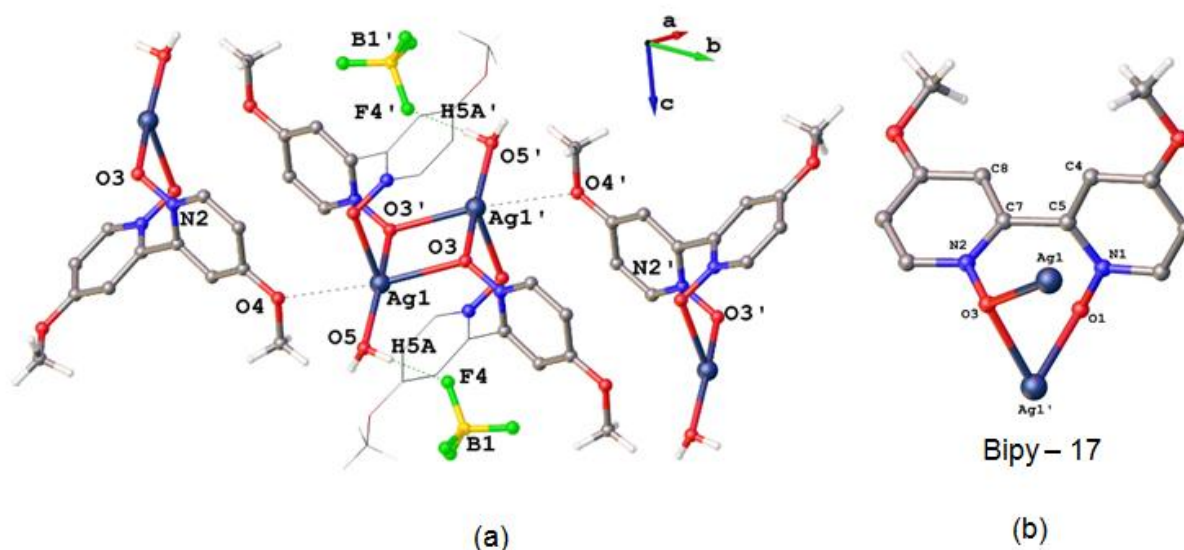


Figure 3.30 – (a) Section of the crystal packing structure in complex **3.34** displaying Ag $\cdots$ O interactions, and (b) coordination mode of ligand **3.5** in complex **3.34**. Selected hydrogen atoms have been omitted for clarity.

### 3.3.6 Complexes with 4,4'-dinitro-2,2'-bipyridine N,N'-dioxide **3.6**

Complexes of ligand **3.6** were attempted with a range of silver(I) salts, such as AgClO<sub>4</sub>, AgOCOCF<sub>3</sub>, AgSO<sub>3</sub>CF<sub>3</sub>, AgBF<sub>4</sub>, AgPF<sub>6</sub> and AgNO<sub>3</sub>. However, none of the attempts were successful, returning crystals of ligand **3.6** as yellow blocks.

### 3.3.7 Complexes with 2,2'-biquinoline N,N'-dioxide **3.7**

Attempts to grow crystals of silver(I) complexes with ligand **3.7** were unsuccessful resulting in thin needle-shape crystals, which were not suitable for X-ray analysis. Using a wide range of crystallisation methods, solvent combinations and different stoichiometric ratios of ligands to silver(I) were unsuccessful in producing good quality crystals for X-ray analysis.

### 3.3.8 Complexes with di-2-pyridylketone N,N'-dioxide **3.8**

Attempts to synthesise silver(I) complexes with ligand **3.8** were also unsuccessful and resulted in a green oily substance. However, ligand **3.8** crystallised and its crystal structure is shown in figure 3.31. Ligand **3.8** crystallised from a CDCl<sub>3</sub> solution as brown blocks, which were solved in the triclinic *P*-1 space group. The asymmetric unit contains one ligand **3.8** and a water molecule, as shown in figure 3.31. The N-O bond distances are 1.340(1) Å and the distance between the oxygens of N-oxide groups is 3.059(1) Å. The two pyridine N-oxide rings are twisted around the planar ketone functional group [C5-C6(O3)-C7] at torsional angles of 130.0(1)° [N1-C5-C6-O3] and 154.0(9)° [N2-C7-C6-O3]. The hydrogen bond parameters are shown in table 3.8.

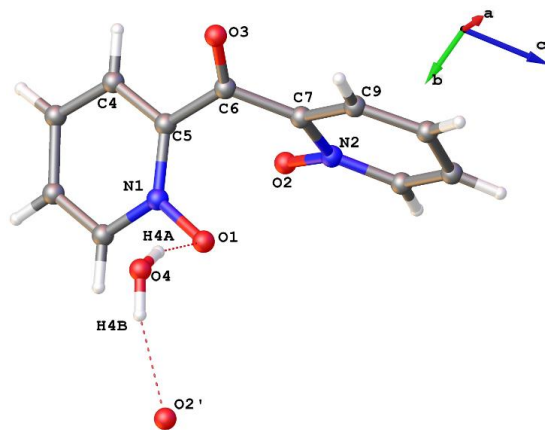


Figure 3.31 – Crystal structure of ligand **3.8**. Selected bond lengths (Å) and bond angles (°): N1-O1 = 1.340(1), N2-O2 1.340(1), C6-O3 = 1.1800(9), N1-C5-C6-O3 = 130.0(1), N2-C7-C6-O3 = 154.0(9).

Table – 3.8 Hydrogen bond parameters in ligand **3.8**.

D-H $\cdots$ A	<i>d</i> D-H(Å)	<i>d</i> H $\cdots$ A(Å)	<i>d</i> D $\cdots$ A(Å)	$\angle$ D-H $\cdots$ A(°)
O4-H4A $\cdots$ O1	0.773	2.001	2.745	161.28
O4-H4B $\cdots$ O2'	0.814	1.981	2.773	164.39

### 3.3.9 Complexes with 2,2'-bipyridylamine N,N'-dioxide **3.9**

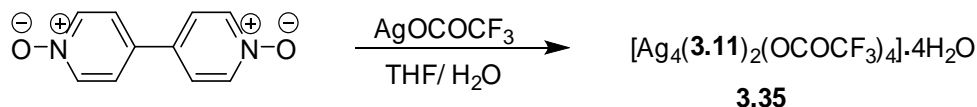
Ligand **3.9** was reacted with a range of silver(I) salts such as AgClO<sub>4</sub>, AgOCOCF<sub>3</sub>, AgSO<sub>3</sub>CF<sub>3</sub>, AgBF<sub>4</sub>, AgPF<sub>6</sub> and AgNO<sub>3</sub> using different solvent combinations and crystal growth techniques. However none of these attempts gave silver(I) complexes suitable for crystallography.

### 3.3.10 Complexes with 1,10-phenanthroline N,N'-dioxide **3.10**

Due to difficulty in synthesising large quantities of ligand **3.10** and associated solubility issues, the synthesis of silver(I) complexes was a difficult task with ligand **3.10**. Attempts to dissolve the ligand **3.10** with silver(I) salts at high temperatures resulted in reduction of the silver(I) ion.

### 3.3.11 Complex with 4,4'-bipyridine-N,N'-dioxide **3.11**

Complex **3.35** was obtained when ligand **3.11** was reacted with silver(I) trifluoroacetate, as shown in scheme 3.13. Attempts to obtain crystals suitable for X-ray analysis with other silver(I) salts were unsuccessful. In complex **3.35**, the anions are bridging Ag $\cdots$ Ag dimers with water molecules coordinating, as was seen in other AgOCOCF<sub>3</sub> complexes in chapter 2.

Scheme 3.13 – Synthesis of complex **3.35**.With silver(I) trifluoroacetate (1:2) **3.35**

The discrete structure of complex **3.35** was solved in the triclinic *P*-1 space group and contains  $[\text{Ag}_2(\text{H}_2\text{O})_2(\text{OCOCF}_3)_2]_2$  (**3.11**)<sub>2</sub> in a 1:2 ligand to silver(I) ratio, as shown in figure 3.32. The asymmetric unit of complex **3.35** contains two non-coordinated ligands **3.11**, four silver(I) trifluoroacetates and four monodentate water molecules. The trifluoroacetate anions bridge Ag–Ag dimers, with one on either side. The Ag<sup>+</sup>–Ag interactions have mean distances of 2.877(8) Å. The average N–O<sub>ligand</sub> bond distances are 1.338(6) Å, which are similar to the values observed in complexes **3.24** [1.314(5) Å] and **3.29** [1.324(3) Å]. The coordinated water molecules, O15 and O16, are coordinated in the Ag<sub>3</sub>–Ag<sub>4</sub> dimer in a *trans*-fashion, while O13 and O14 are in a *cis*-fashion in the Ag<sub>1</sub>–Ag<sub>2</sub> dimer, with mean Ag–O distances of 2.380(5) Å. The two pyridine rings of the ligand **3.11** close to co-planar with torsional angles of 7.7(6)° [C2–C3–C8–C9] and 0.9(6)° [C12–C13–C18–C17], which are close to the values reported in the literature.<sup>[62, 157]</sup>

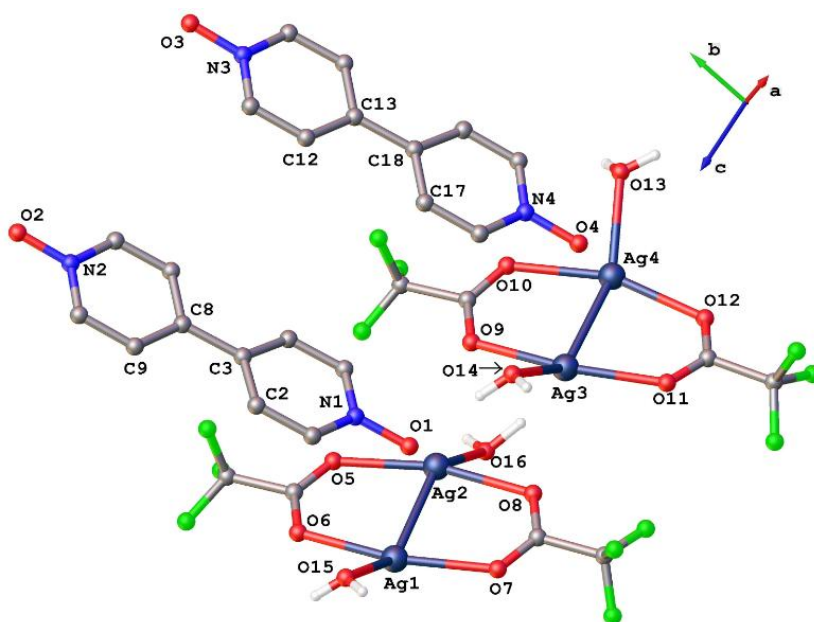
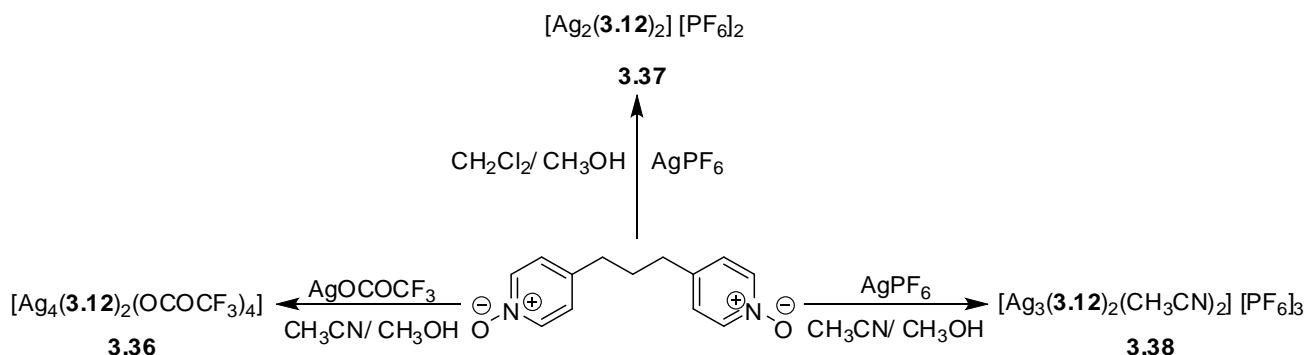


Figure 3.32 – Asymmetric unit and discrete structure of complex **3.35**. Selected hydrogen atoms are omitted for clarity. Selected bond lengths (Å) and bond angles (°): N1–O1 = 1.340(5), N2–O2 = 1.331(6), N3–O3 = 1.338(6), N4–O4 = 1.344(5), Ag4–O13 = 2.341(4), Ag3–O14 = 2.376(5), Ag1–O15 = 2.387(5), Ag2–O16 = 2.417(4), Ag1–Ag2 = 2.900(8), Ag3–Ag4 = 2.855(8), C2–C3–C8–C9 = 7.7(6), C12–C13–C18–C17 = 0.9(6).

### 3.3.12 Complexes with 1,3-bis(4-pyridyl)propane N,N'-dioxide 3.12

Due to the flexible  $-\text{CH}_2\text{CH}_2\text{CH}_2-$  spacer group, ligand **3.12** can adopt many conformations, as was discussed in Chapter 1. The reactions of ligand **3.12** with silver(I) salts, shown in scheme 3.14, resulted in TT and TG conformations. The maximum denticity obtained for ligand **3.12** was  $\mu_5\text{-O, O, O', O', O'}$ , which is similar to previously reported complexes containing ligand **3.12**.<sup>[14]</sup> For the syntheses of complexes **3.36** and **3.38**, the solvent used was a mixture of acetonitrile and methanol (1:1). A  $\text{CH}_3\text{CN}$  molecule is found to coordinate in complex **3.38** but not in **3.36**. The use of a non-coordinating anion  $[\text{PF}_6]$  as opposed to the coordinating  $\text{CF}_3\text{COO}$  anion has allowed coordination of  $\text{CH}_3\text{CN}$ .



Scheme 3.14 – Syntheses of complexes **3.36** – **3.38**.

#### With silver(I) trifluoroacetate (1:2) 3.36

Single crystal X-ray diffraction analysis reveals that complex **3.36** crystallised in the monoclinic space group *Cc*. The asymmetric unit consists of two ligands **3.12** and four silver(I) ions in a 1:2 ligand to silver(I) ratio, as shown in figure 3.33. The ligands **3.12** are functioning in  $\mu_4\text{-O, O, O', O'}$  coordination modes with average N-O [1.336(3) Å] and Ag-O<sub>ligand</sub> [2.438(2) Å] bond distances close to those reported with ligand **3.12** by Mak *et al.*<sup>[14]</sup> The trifluoroacetate anions bridge Ag1, Ag2 and Ag3, Ag4 which are interacting at distances of 2.979(7) Å and 3.037(6) Å, respectively. Oxygens, O1 and O2, bridge Ag1 and Ag4' at average angles of 85.54(7)° [Ag1-O-Ag4'], smaller than O3 and O4 bridging Ag2 and Ag3 at angles of 94.47(7)° [Ag2-O-Ag3].

The N-O<sub>ligand</sub>-Ag angles range from 111.44(2)° to 136.12(2)° with their average, 121.08(2)°, being close to the value [124.73(4)°] previously reported in the literature.<sup>[14]</sup> Complex **3.36** contains two five- [Ag2 and Ag3] and two six- [Ag1 and Ag4] coordinate silver centers, as shown in figure 3.33. The five-coordinate Ag2 and Ag3 atoms have distorted square pyramidal geometries with  $\tau_5$  indexes of 0.44 and 0.42, respectively. The asymmetric unit grows into a three-dimensional

network, to give an H-shape arrangement when viewed down the *a*-axis, as shown in figure 3.34a.

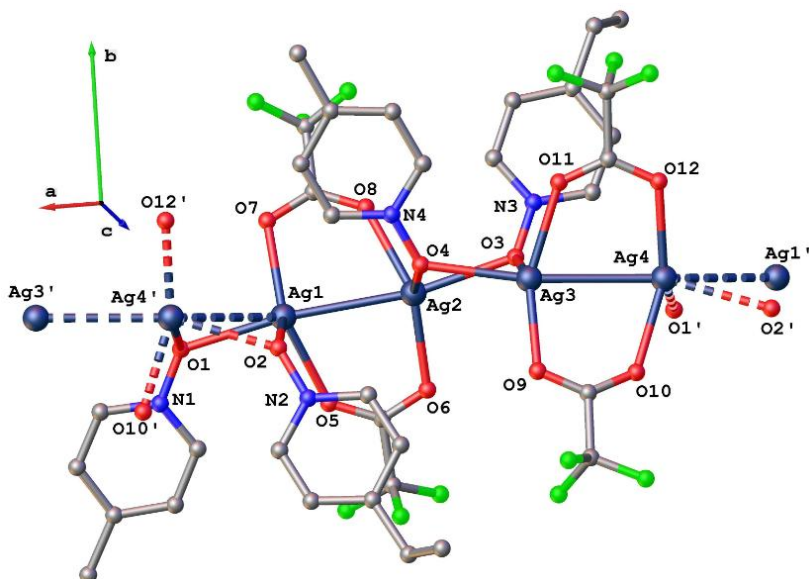


Figure 3.33 – Asymmetric unit of complex **3.36**. Hydrogen atoms are excluded for clarity. Selected bond lengths (Å) and bond angles (°): N1-O1 = 1.337(3), N2-O2 = 1.341(3), N3-O3 = 1.332(3), N4-O4 = 1.337(3), Ag1-O1 = 2.420(2), Ag4'-O1 = 2.432(2), Ag1-O2 = 2.419(2), Ag4'-O2 = 2.517(2), Ag2-O3 = 2.432(2), Ag3-O3 = 2.444(2), Ag2-O4 = 2.457(2), Ag3-O4 = 2.458(2), N1-O1-Ag1 = 128.47(2), N1-O1-Ag4' = 114.38(15), N2-O2-Ag1 = 113.57(1), N2-O2-Ag4' = 136.12(2), N3-O3-Ag2 = 125.87(2), N3-O3-Ag3 = 111.44(2), N4-O4-Ag2 = 112.98(2), N4-O4-Ag3 = 125.82(2), Ag1-O1-Ag4' = 86.46(7), Ag1-O2-Ag4' = 84.62(6), Ag2-O3-Ag3 = 94.98(7), Ag2-O4-Ag3 = 93.97(7), Ag1-Ag2 = 2.979(7), Ag3-Ag4 = 3.037(6), Ag1-Ag4' = 3.323(7).

The ligands **3.12** have adopted a TT conformation [figure 3.34b] to link H-shape 1D polymer units, which are grown along the *a*-axis. These TT conformational spacer ligands **3.12** are oriented up and down [marked with arrows], when viewed along the *a*-axis, as shown in figure 3.34a. The  $\mu_4$ -O,O,O',O' ligand **3.12**, shown in figure 3.34b has a distance of 11.941 Å between the oxygen atoms O3 and O4. The two pyridine rings are twisted at torsional angles of 68.9(3)° [C15-C16-C19-C20] and 75.4(3)° [C24-C23-C26-C20] relative to the -CH<sub>2</sub>- groups [C19-C20-C26].

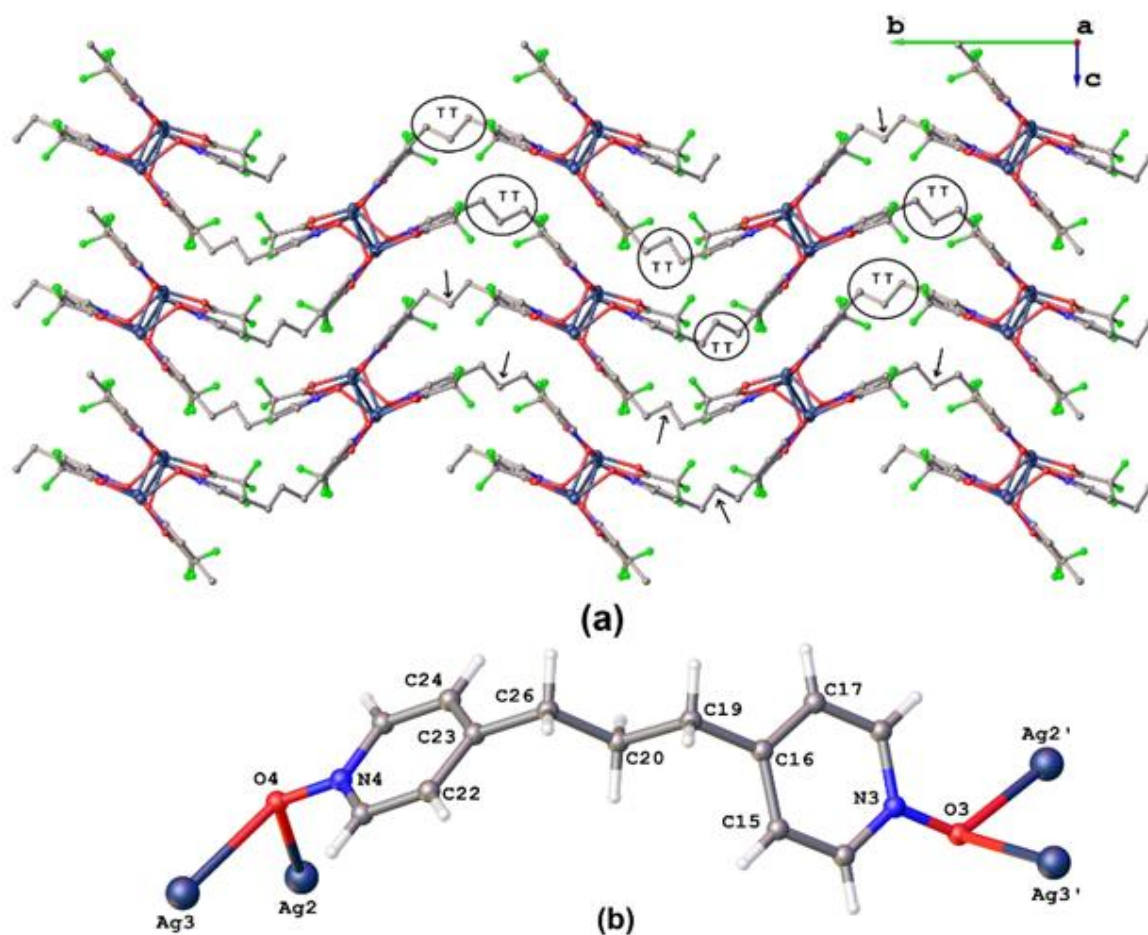


Figure 3.34 – (a) 3D Polymeric structure of complex **3.36**. Hydrogen atoms are omitted for clarity, and (b) TT conformation mode adopted by ligand **3.12** in complex **3.36**. Selected torsional angles (°): C15-C16-C19-C20 = 68.9(3), C24-C23-C26-C20 = 75.4(3).

#### With silver(I) hexafluorophosphate (1:2) **3.37**

The crystal structure of complex **3.37** solved in the monoclinic  $P2_1/m$  space group with the asymmetric unit comprising one and a half silver(I) ions coordinated with four half ligands in a 4:3 ligand **3.12** to silver(I) ratio. It contains three half  $PF_6$  anions, one of which [P3] lies on a center of inversion and the other two [P1 and P2] on mirror planes, as shown in figure 3.35. The ligands **3.12** have adopted a  $\mu_2$ -O,O' coordination mode in complex **3.37** with their average N-O bond lengths [1.335(4) Å] similar to ligand **3.12** with  $\mu_4$ -O,O,O',O' coordination mode [1.336(3) Å] in complex **3.36**. The average Ag-O<sub>ligand</sub> bond distances [2.264(3) Å] are shorter than the distances seen in complex **3.36** [2.438(2) Å]. The average N-O<sub>ligand</sub>-Ag angles [119.12(2)°] are close to the values obtained for ligand **3.12** in complex **3.36** [121.08(2)°].

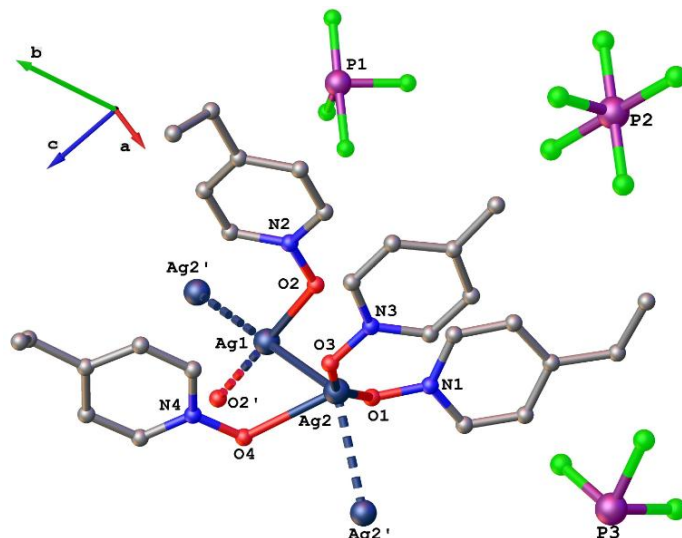


Figure 3.35 – Asymmetric unit of complex **3.37**. Hydrogen atoms are excluded for clarity. Selected bond lengths (Å) and bond angles (°): N1-O1 = 1.334(4), N2-O2 = 1.347(4), N3-O3 = 1.332(5), N4-O4 = 1.330(5), Ag2-O1 = 2.250(3), Ag1-O2 = 2.240(3), Ag2-O3 = 2.180(3), Ag2-O4 = 2.439(3), N1-O1-Ag2 = 115.1(2), N2-O2-Ag1 = 124.3(2), N3-O3-Ag2 = 119.7(2), N4-O4-Ag2 = 117.4(2), Ag1-Ag2 = 3.151(4), Ag2-Ag2' = 2.819(7).

Ag1 and Ag2, are four- [ $\tau_4 = 0$ ] and five- [ $\tau_4 = 0.50$ ] coordinate with square planar and distorted square pyramidal geometries. The interaction between adjacent five-coordinate silver centers, Ag2 $\cdots$ Ag2' [2.819(7) Å], is stronger than the interaction between four- and five-coordinate silver centers, Ag1 $\cdots$ Ag2 [3.151(4) Å]. The asymmetric unit shown in figure 3.35 grows one-dimensionally along the *a*-axis *via* Ag $\cdots$ Ag interactions, which in turn are linked by the ligands **3.12** in TT and TG conformations along the *b*- and *c*-axis respectively, to give a 3D polymeric structure, as shown in figure 3.36.

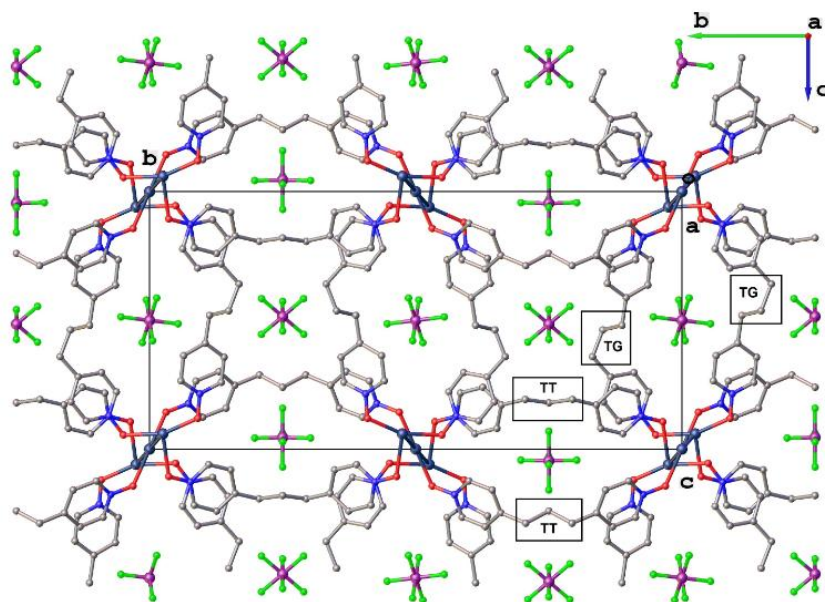


Figure 3.36 – 3D Polymeric structure of complex **3.37**.



TT and TG ligands produce a  $M_2L_2$  metallocycle, when they grow along the  $a$ -axis, with non-coordinated  $PF_6$  anions in the crystal packing, as shown in figure 3.36. A topological view of the crystal packing of complex **3.37** is shown in figure 3.37. The distances between the silver atoms bridged by TT and TG ligands **3.12** are 12.79 Å and 12.74 Å, respectively. The distances between the oxygens atoms in  $\mu_2$ -O, O' TT and TG ligands **3.12** are 12.46 Å and 11.99 Å.

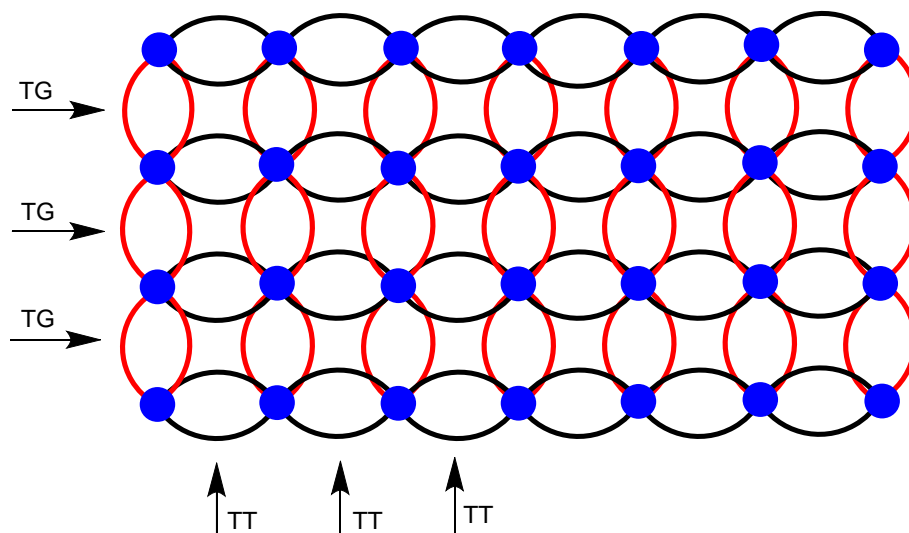


Figure 3.37 – Topological view of complex **3.37** [bonds in red and the black colour represents the TG and TT conformational ligands, respectively; dark blue circles are the  $Ag \cdots Ag$  interactions along the  $a$ -axis].

#### With silver(I) hexafluorophosphate (1:2) **3.38**

The crystal structure of the complex **3.38** solved in the orthorhombic space group  $P2_212_1$  and contains three silver(I) ions, two coordinated acetonitrile molecules and three ligands **3.12** in the asymmetric unit. It also has two full  $PF_6$  and two half  $PF_6$  anions, which lie on two-fold rotation axes, as shown in figure 3.38. The ligands **3.12** have adopted  $\mu_4$ -O, O, O', O' and  $\mu_5$ -O, O, O', O', O' coordination modes, with average N-O bond distances of 1.336(6) Å, similar to the values obtained in complexes **3.36** [1.336(3) Å] and **3.37** [1.335(4) Å]. The average Ag-O<sub>ligand</sub> bond distances [2.463(4) Å] are close to the values obtained in complex **3.36** [2.438(2) Å] and longer than complex **3.37** [2.264(3) Å]. The average N-O<sub>ligand</sub>-Ag angles [121.9(3)°] are close to the values observed in complex **3.37** [119.12(2)°]. The N2-O2 group displays a tridentate coordination mode, while the others displays a bidentate bridging coordination mode, with Ag-O<sub>ligand</sub>-Ag angles ranging from 77.63(1)° to 120.84(2)°.

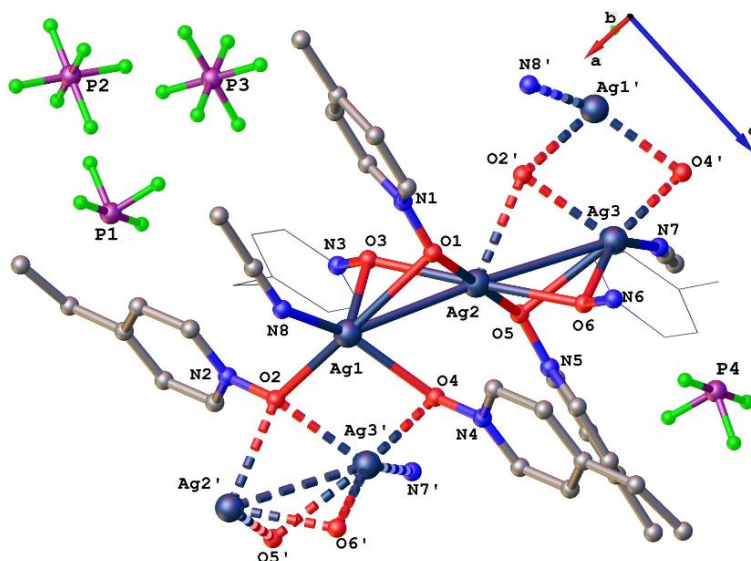


Figure 3.38 – Asymmetric unit of complex **3.38**. Hydrogen atoms are excluded for clarity. Selected ligands **3.12** are shown in wireframe for clarity. Selected bond lengths (Å) and bond angles (°): N1-O1 = 1.319(6), N2-O2 = 1.332(6), N3-O3 = 1.344(6), N4-O4 = 1.344(6), N5-O5 = 1.339(6), N6-O6 = 1.343(6), Ag1-O1 = 2.575(5), Ag1-O2 = 2.483(4), Ag1-O3 = 2.454(4), Ag1-O4 = 2.337(4), Ag2-O5 = 2.521(4), Ag3-O5 = 2.593(5), Ag2-O6 = 2.315(4), Ag3-O6 = 2.427(4), N1-O1-Ag2 = 133.8(3), N1-O1-Ag1 = 108.8(3), N2-O2-Ag3' = 130.0(4), N2-O2-Ag1 = 125.2(3), N2-O2-Ag2' = 102.1(3), N3-O3-Ag2 = 126.0(3), N3-O3-Ag1 = 122.0(3), N4-O4-Ag1 = 125.7(3), N4-O4-Ag3' = 126.1(3), N5-O5-Ag2 = 130.7(3), N5-O5-Ag3 = 103.4(3), N6-O6-Ag2 = 127.1(3), N6-O6-Ag3 = 123.8(3), Ag1-Ag2 = 3.220(9), Ag2-Ag3 = 3.335(9), Ag1-Ag2-Ag3 = 176.45(2), Ag2-O1-Ag1 = 77.63(1), Ag3-O2-Ag1' = 89.79(1), Ag1-O2-Ag2' = 120.84(2), Ag2-O3-Ag1 = 84.51(1), Ag1-O4-Ag3' = 91.83(1), Ag2-O5-Ag3 = 81.37(1), Ag2-O6-Ag3 = 89.33(1).

The complex **3.38** contains two six- [Ag1 and Ag3] and one seven- [Ag2] coordinate silver center which interact in a near linear fashion with an angle of 176.45(2)° and at a mean distance of 3.277(9) Å, as shown in figure 3.38. O2 [tridentate] and O4 [bidentate] bridge Ag1 and Ag3 to give a one-dimensional polymer along the *a*-axis, as shown in figure 3.39b. Each one-dimensional polymer is extended three-dimensionally by ligands **3.12** in a TT conformation, as seen in the crystal packing structure depicted in figure 3.39a.

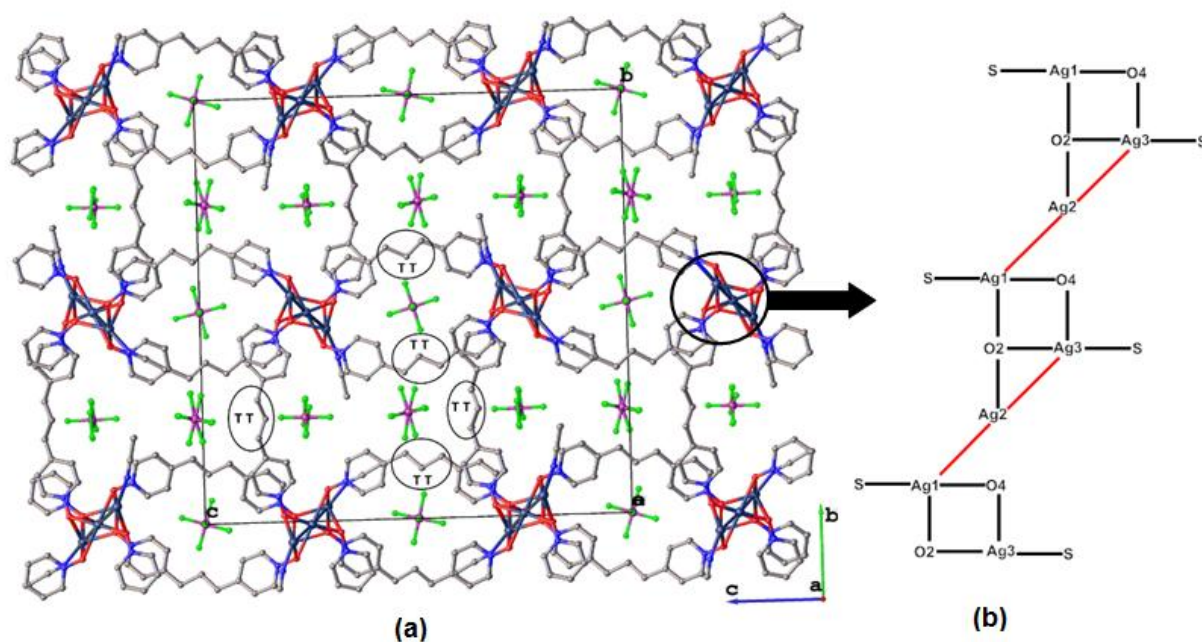


Figure 3.39 – 3D polymeric structure of complex **3.37**. Hydrogen atoms are omitted for clarity. [Representation of bonds: black colour – coordination modes of ligand **3.12**, red colour – Ag<sup>+</sup>...Ag<sup>+</sup> linear interactions coordinated with CH<sub>3</sub>CN molecules].

The distances between silver bound oxygens in the  $\mu_4$ -O,O,O',O' and  $\mu_5$ -O,O,O',O',O' ligands **3.12** along the *c*-axis are 12.262 Å [O4-O5] and 12.234 Å [O2-O1], while along the *b*-axis, the distances are 12.669 Å [O3-O6], as shown in figure 3.40a. The topology of complex **3.37** is shown in figure 3.40b.

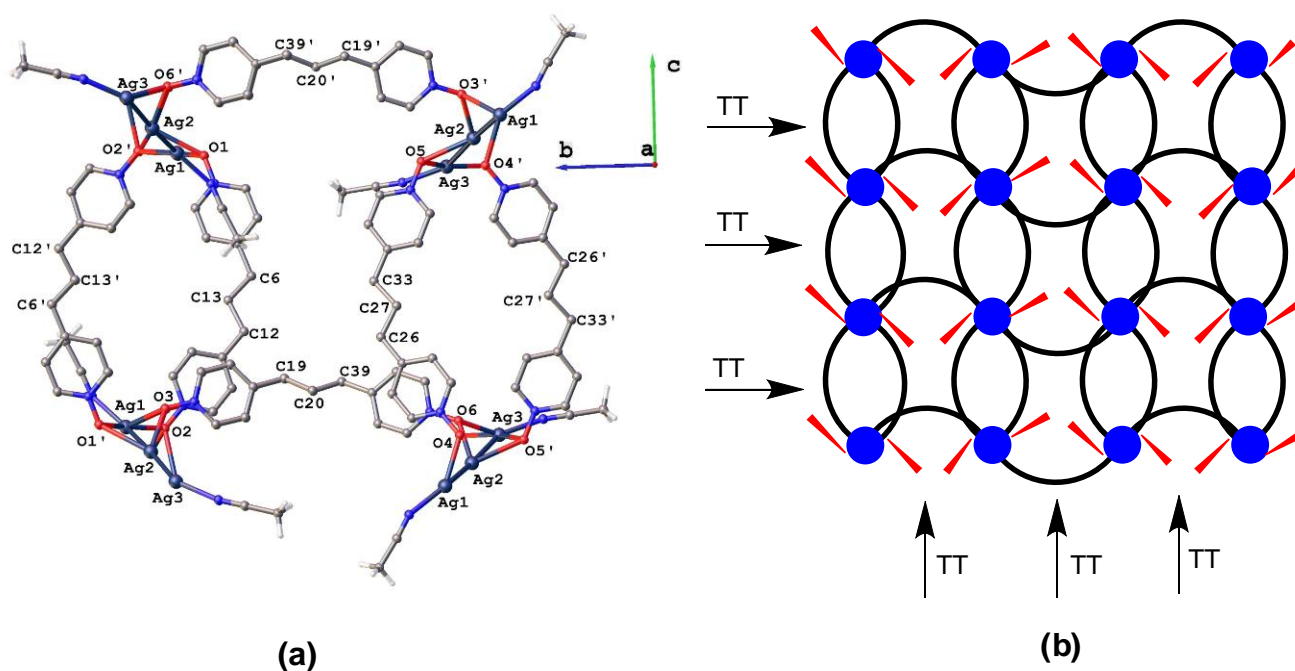
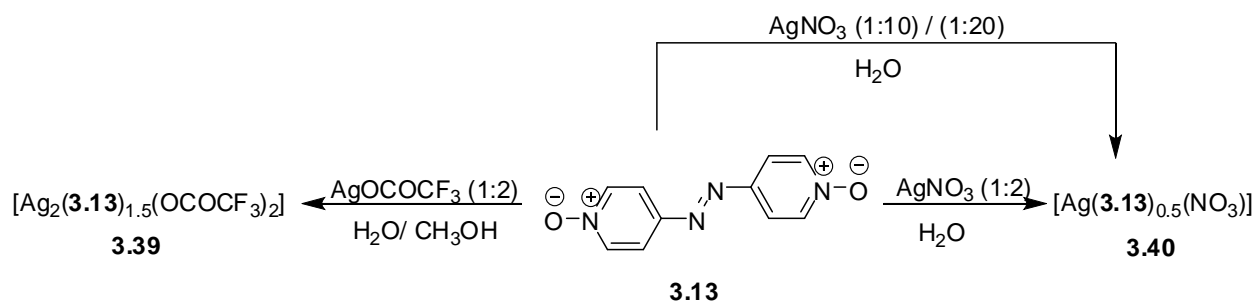


Figure 3.40 – (a) Section of complex **3.39**, and (b) topological view of complex **3.39** [representation: black colour – TT conformations of **3.12**, blue colour – silver(I) interactions, red colour – CH<sub>3</sub>CN molecules].

### 3.3.13 Complexes with 4,4'-azobis(pyridine N-oxide) **3.13**

Red needle shaped crystals of complexes **3.39** and **3.40** were obtained when ligand **3.13** reacted with AgX [X = CF<sub>3</sub>COO and NO<sub>3</sub>] in a 1:2 ratio, as shown in scheme 3.15.



Scheme 3.15 – Syntheses of complexes **3.39** and **3.40**.

#### With silver(I) trifluoroacetate **3.39**

The crystal structure of complex **3.39** was solved in the triclinic space group *P*-1 and the asymmetric unit comprises one and a half ligands **3.13**, two silvers [Ag1 and Ag2], with trifluoroacetate anions bridging on either side, as shown in figure 3.41. Complex **3.38** has a 3:4 ligand to silver(I) ratio. The average N-O<sub>ligand</sub> and –N=N– bond distances are 1.318(2) Å and 1.256(3) Å respectively, which are higher than the values reported for non-coordinated ligand **3.13** [1.283(1) Å and 1.228(2) Å].<sup>[158]</sup> The C–N<sub>azo</sub> bond lengths [1.422(3) Å] are similar to reported distances for non-coordinated ligand **3.13** [1.419(1) Å].<sup>[158]</sup> It is likely that upon complex formation, the π-electrons in the azo functional group are distributed over the aromatic rings to stabilize the charged nitrogen atoms, as evidenced by an increase in the N-O and –N=N– bond distances. The average N-O<sub>ligand</sub>-Ag angles and Ag-O<sub>ligand</sub> bond distances are 120.53(1)° and 2.497(2) Å, respectively. Ag1 and Ag2 are interacting at a distance of 3.045(3) Å, similar to the values observed in the AgOCOCF<sub>3</sub> complex **3.29** [3.077(1) Å].

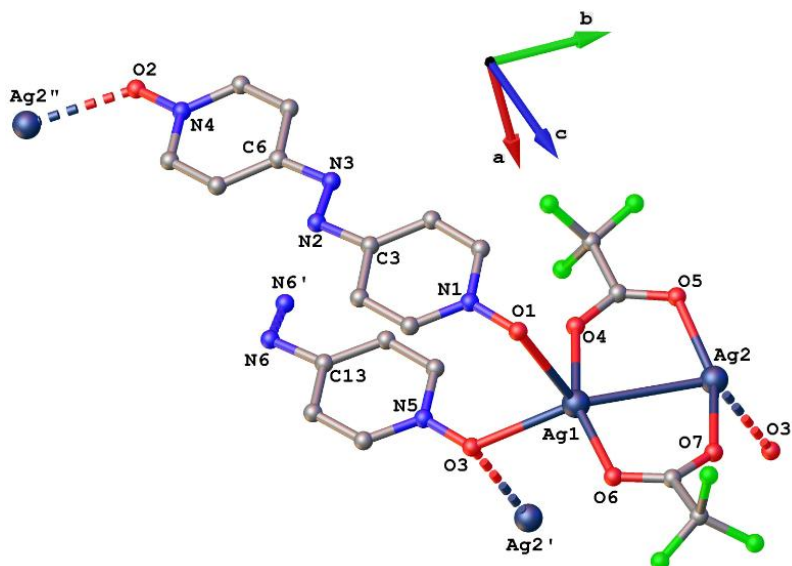
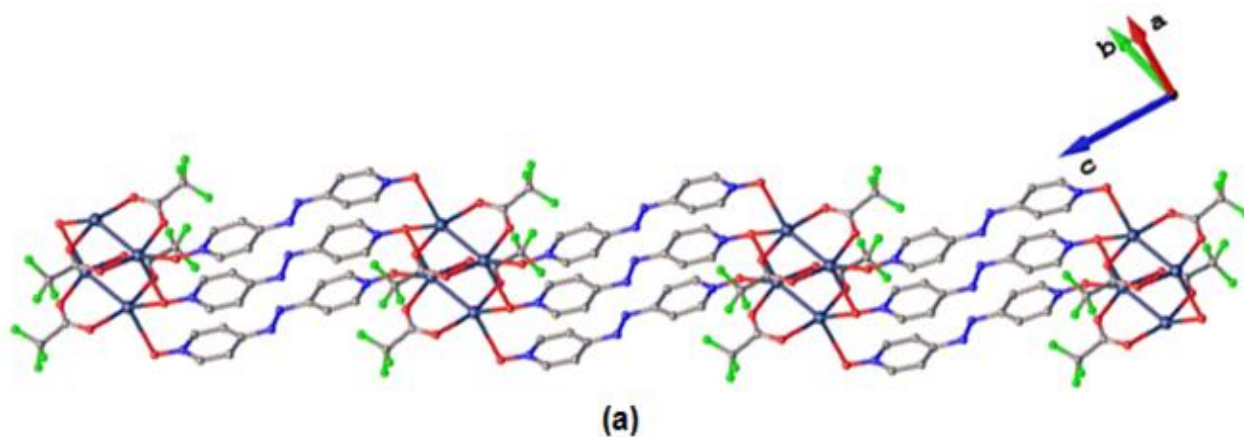


Figure 3.41 – Asymmetric unit of complex **3.39**. Hydrogen atoms are omitted for clarity. Selected bond lengths (Å) and bond angles (°): N1-O1 = 1.317(2), N4-O2 = 1.311(2), N5-O3 = 1.326(2), N2-N3 = 1.258(3), N6-N6' = 1.255(4), Ag1-O3 = 2.483(2), Ag1-O1 = 2.549(2), Ag2-O2 = 2.459(2), N1-O1-Ag1 = 110.68(1), N5-O3-Ag1 = 130.38(1), Ag1-O3-Ag2' = 90.03(5), Ag1-Ag2 = 3.045(3), N2-C3 = 1.424(3), N3-C6 = 1.420(3), N6-C13 = 1.426(3).

Complex **3.39** is a 1D linear polymer, as shown in figure 3.42a. Four silvers and two  $\mu_4$ -O,O,O',O' ligand **3.13** oxygens form a six-membered  $\text{Ag}_4\text{O}_2$  [Ag1-O3-Ag2-Ag1''-O3''-Ag2'] ring with two trifluoroacetate anions bridging on both side of each  $\text{Ag}^{\cdots}\text{Ag}$  bond, as depicted in figure 3.42b. O3 bridges Ag1 and Ag2 at an angle of 90.03(5)° [Ag1-O3-Ag2]. Also, each  $\mu_4$ -O,O,O',O' ligand **3.13** is sandwiched by  $\mu_2$ -O,O' ligands **3.13**, as shown in figure 3.42b. There also exists weak  $\pi$ - $\pi$  interactions between these sandwiched ligands **3.13** at centroid-centroid distances of 3.580(1) Å and 3.607(1) Å.



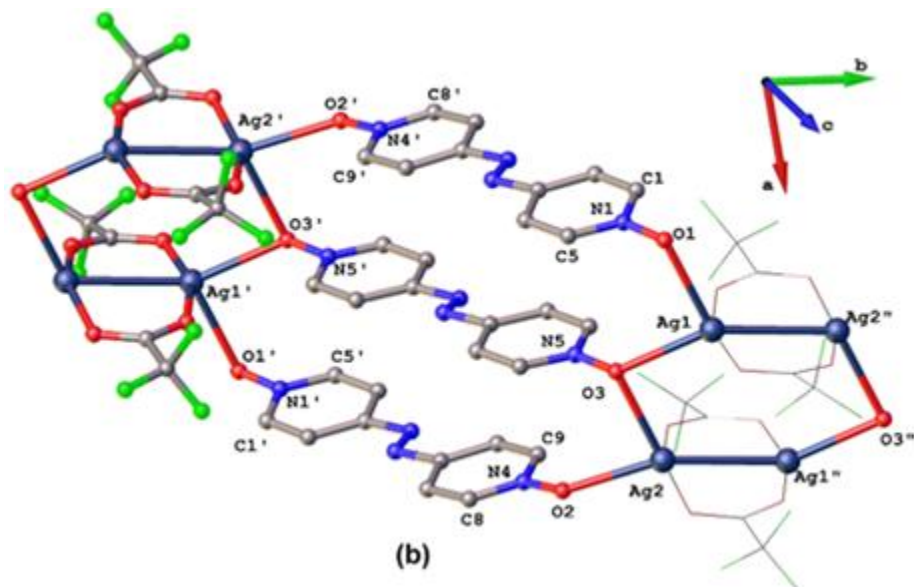


Figure 3.42 – (a) 1D Polymeric structure of complex **3.39**, and (b) section of the 1D polymeric structure. Hydrogen atoms are excluded for clarity [selected trifluoroacetate anions are in wireframes to show the six-membered ring clearly].

#### With silver(I) nitrate **3.40**

X-Ray analysis confirms the asymmetric unit of complex **3.40** contains half a ligand **3.13**, one silver(I) and a nitrate anion, as shown in figure 3.43. The crystal structure was solved in the monoclinic  $P2_1/n$  space group with a 1:2 ligand to silver(I) ratio. The N1-O1 [1.320(6) Å] and –N2'=N2- [1.260(9) Å] bond distances are similar to the values obtained for ligand **3.13** in complex **3.39** [1.318(2) Å and 1.256(3) Å]. The ligand **3.13** is monodentate with an Ag-O bond distance of 2.297(4) Å and coordination angle of 126.2(3)° [N1-O1-Ag1].

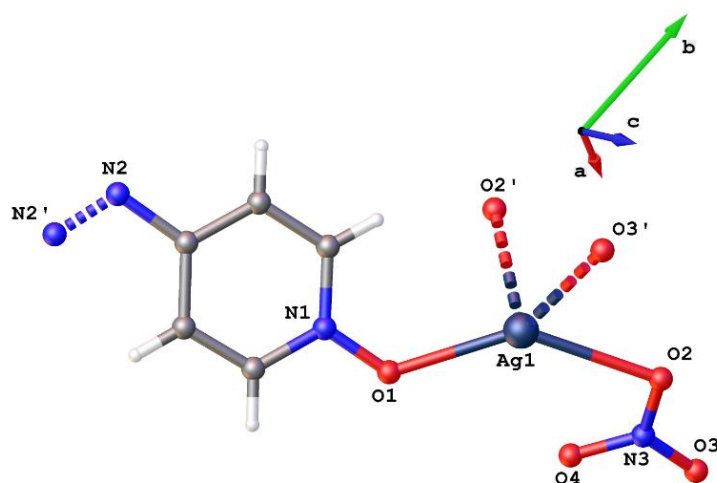


Figure 3.43 – Asymmetric unit of complex **3.40**. Selected bond lengths (Å) and bond angles (°): N1-O1 = 1.320(6), N2'-N2 = 1.260(9), Ag1-O1 = 2.297(4), N1-O1-Ag1 = 126.2(3).

Complex **3.40** forms a herringbone structure with zigzag units of figure 3.44b linked by ligands **3.13** coordinating in a *trans*- fashion, as shown in figure 3.44. The nitrate anion bridging modes can be explained from figure 3.44b and 3.45. Each of the marked letters 'R' is a 10-membered ring, which has a Z-shape arrangement, when viewed down the *a*-axis, as shown in figure 3.44b. The actual nitrate anion bridging mode seen in figure 3.44b looks like a stair-case of 2D nets, as illustrated in figure 3.45a.

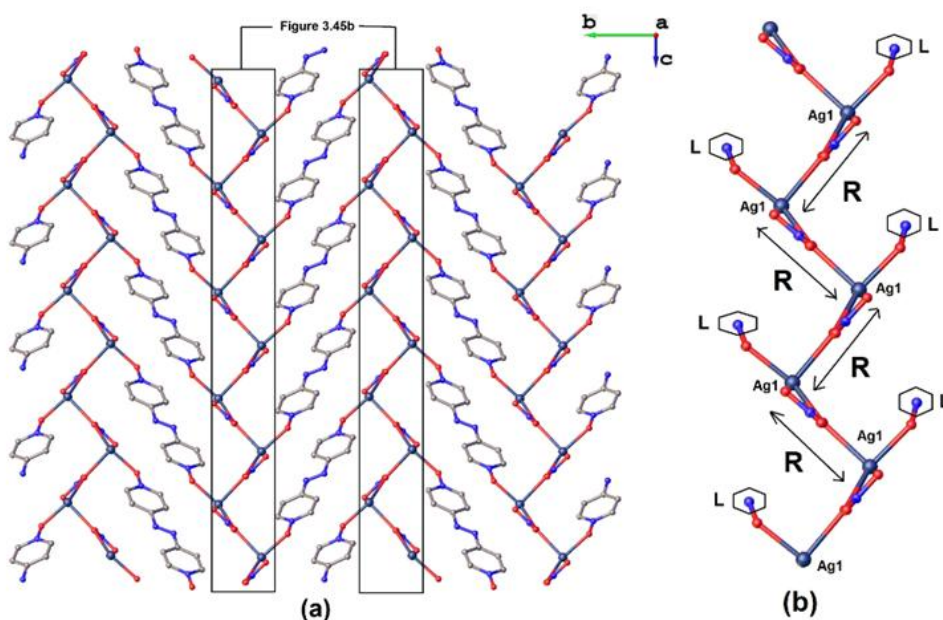


Figure 3.44 – (a) Herringbone pattern of complex **3.40**. Hydrogen atoms are omitted for clarity, and (b) section of polymeric unit of silver(I) nitrate bridges [L represents *trans*- coordination ligand **3.13**].

A section of the 2D net, shown in figure 3.45a, was looked at more closely in order to explain the bridging modes of the nitrate anions shown in figure 3.45b. One  $\mu_2$ - and two  $\mu_3$ - nitrate anions bridge three silvers to form a 10-membered  $\text{Ag}_3\text{N}_2\text{O}_5$  ring, with a monodentate ligand **3.13** coordinated to Ag1, as shown in figure 3.45b. The four  $\mu_3$ -nitrate anions, O2, O3 and O2'', O3'' bridge Ag1, Ag1' and Ag1, Ag1'', with Ag-O bond distances of 2.556(5) Å [Ag1-O2] and 2.515(5) Å [Ag1'-O3], respectively. The  $\mu_2$ -nitrate oxygen O2' bridges Ag1' and Ag1'' at distances 2.503(5) Å and 2.556(5) Å with angles 150.49(2)° [Ag1'-O2'-Ag1'']. Each 10-membered ring grows two-dimensionally to give a stair-case like structure [figure 3.45b] when viewed down the *b*-axis, and a 'Z-shape' arrangement when viewed along the *a*-axis [figure 3.44b]. The Ag1-Ag1', Ag1'-Ag1'' and Ag1''-Ag1 non-bond distances in the 10-membered rings are 5.565 Å, 4.893 Å and 5.360 Å, respectively. The difference in Ag-Ag non-bond distances is due to the different coordination modes adopted by the nitrate anions.

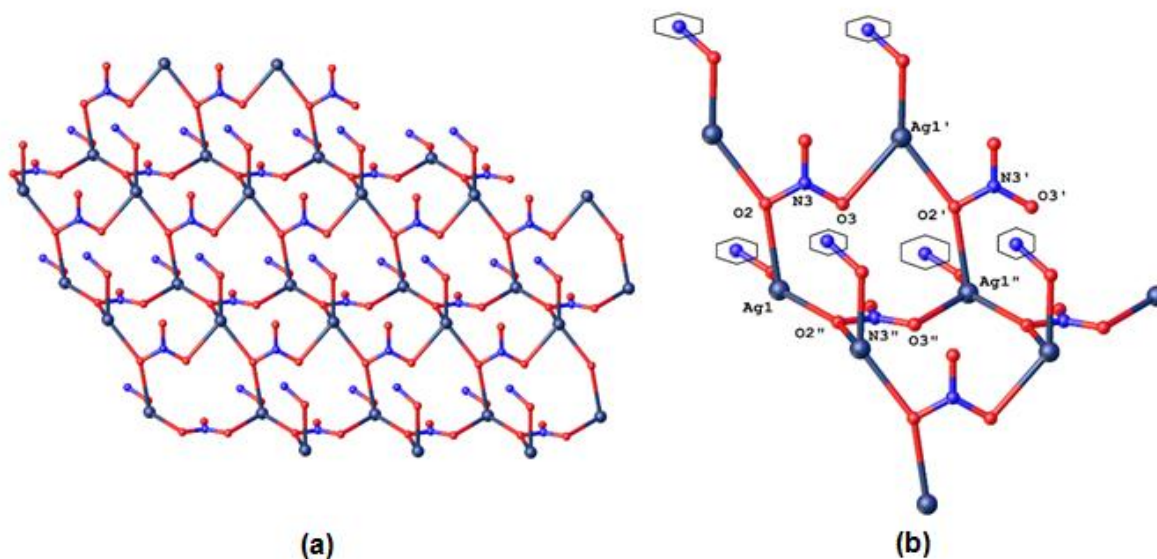


Figure 3.45 – (a) Two-dimensional view of figure 3.44b, (b) a section of the 2D polymer from figure 3.45a. Selected bond lengths (Å) and bond angles (°): Ag1'-O2' = 2.503(5), Ag1'-O3 = 2.515(5), Ag1-O2 = 2.556(5), Ag1-O2-Ag1 = 150.49(2).

Ligand **3.13** was reacted with AgNO<sub>3</sub> in 1:10 and 1:20 ratios in order to encourage a silver(I) interaction with the azo functional group. However, in both cases, silver(I) ion preferred to coordinate to the N-O groups rather than the azo groups of ligand **3.13** to give complex **3.40**. The observation is supported using X-ray powder diffraction, as shown in figure 3.46.

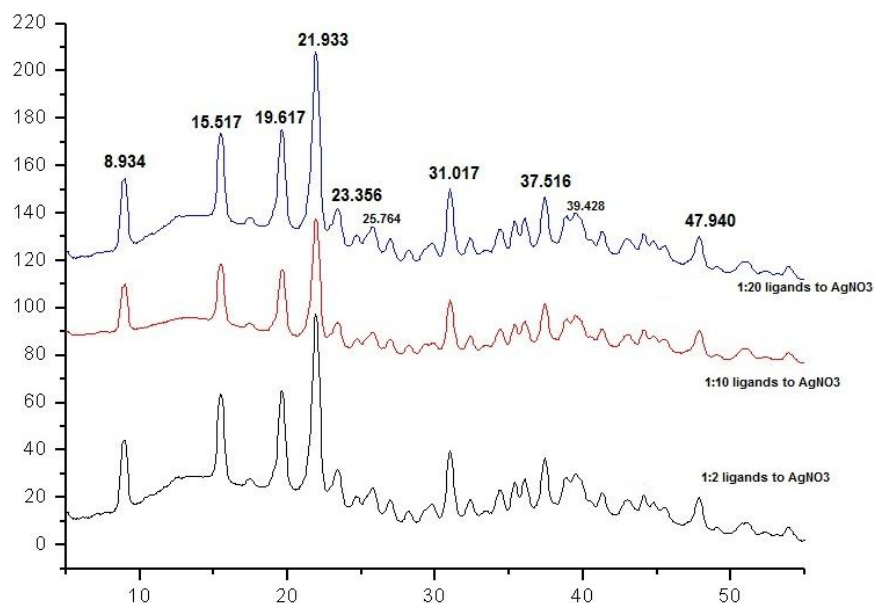


Figure 3.46 – Comparison of XRPD of complex **3.40** with 1:2 [black trace], 1:10 [red trace] and 1:20 [blue trace] ligand **3.13** to AgNO<sub>3</sub> ratios.



### 3.3.14 Crystal structure of (methylenedi-p-phenylene)bis(pyridine-4-carboxamide N,N'-dioxide) **3.14**

Attempts to grow crystals with silver(I) salts using ligand **3.14** were unsuccessful. In most cases a hydrated form of the ligand preferentially crystallised, as shown in figure 3.47. However, the crystal structure of ligand **3.14** has not been reported in the literature. Ligand **3.14** crystallised in the chiral orthorhombic  $P2_12_12_1$  space group, and the asymmetric unit contains one ligand **3.14** and two water molecules, as shown in figure 3.47. The water molecules [O5 and O6] are interacting with O3 and O2 at distances of 2.844 Å [O5⋯O3] and 2.875 Å [O6⋯O2], respectively. The N-O bond lengths [1.317 Å] show double bond character with a distance between oxygens, O1 and O2, of 20.923 Å. Selected torsional angles related to ligand **3.14** are shown in table 3.9.

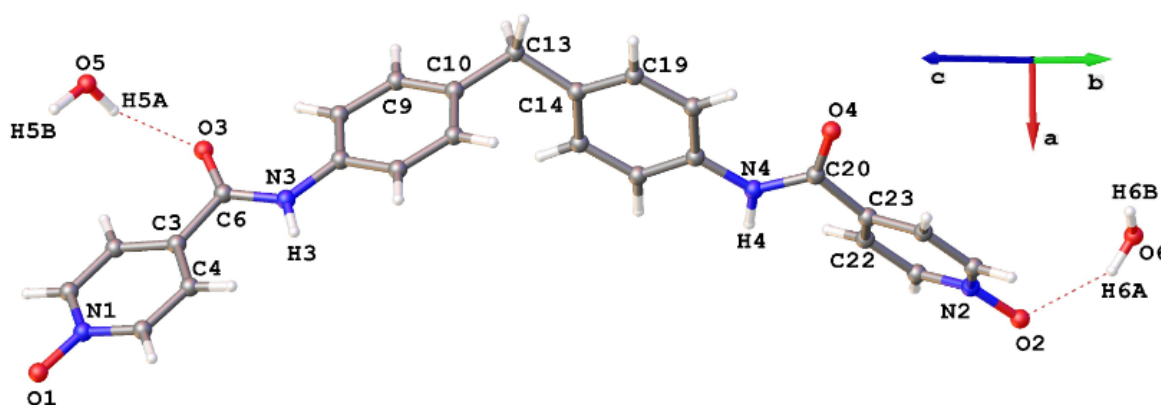


Figure 3.47 – Asymmetric unit of ligand **3.14**. Selected bond lengths (Å) and bond angles (°): N1-O1 = 1.318(2), N2-O2 = 1.316(2), C6-O3 = 1.227(2), C20-O4 = 1.229(2).

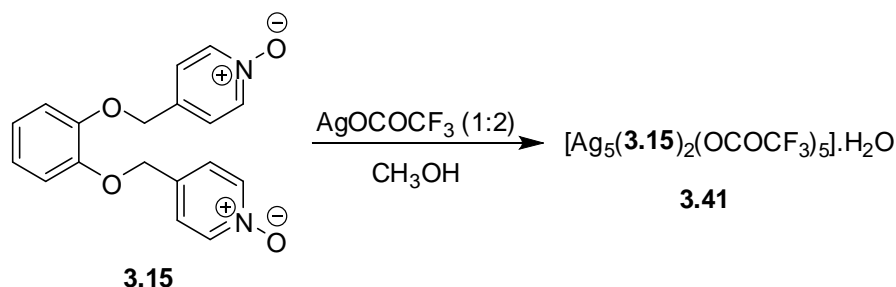
Table – 3.9 List of torsional angles in ligand **3.14**.

	Torsional angles (°)
N3-C6-C3-C4	14.1(2)
N4-C20-C23-C22	37.6(2)
C9-C10-C13-C14	129.98(2)
C19-C14-C13-C10	128.81(2)

### 3.3.15 Complexes with 1,2-bis(4-pyridylmethoxy)benzene N,N'-dioxide **3.15**

Ligand **3.15a** with the flexible  $-\text{CH}_2\text{O}-$  spacer groups has been prepared previously by preceding members of the Steel group in order to study silver(I) metallosupramolecular chemistry. The silver(I) nitrate complex synthesised by Fitchett showed zigzag structures, with the nitrogen

atoms of ligand **3.15a** being monodentate and the silver(I) ions in linear geometries. In complex **3.41** the ligand is present in  $\mu_4$ -O,O,O',O' and  $\mu_5$ -O,O,O',O',O' bridging modes to give a zigzag 1D polymeric structure, with these 1D polymers linked *via*  $\pi$ - $\pi$  interactions to give a 3D polymeric network.



Scheme 3.16 – Synthesis of complex **3.41**.

### With silver(I) trifluoroacetate **3.41**

Complex **3.41** was crystallised and solved in the triclinic *P*-1 space group. The asymmetric unit of complex **3.41** contains two ligands **3.15**, five silver(I) ions, five trifluoroacetates and a monodentate water molecule [O19], as shown in figure 3.48. The complex **3.41** has a 2:5 ligand to silver(I) ratio. Two of the trifluoroacetate groups are disordered; oxygens O18 and O18' with a 87:13 occupancy ratio, while the  $-\text{CF}_3$  group is disordered over F4 and F4' with a 50:50 ratio. Ligand **3.15** adopted  $\mu_4$ -O,O,O',O' and  $\mu_5$ -O,O,O',O',O' coordination modes with N-O<sub>ligand</sub> and Ag-O<sub>ligand</sub> bond distances ranging from 1.328(4) Å to 1.342(4) Å and 2.249(3) Å to 2.525(3) Å, respectively.

N1-O1 has a  $\mu_3$ -O,O,O coordination mode while N2-O4, N3-O5 and N4-O8 are in the  $\mu_2$ -O,O coordination mode. The average N-O<sub>ligand</sub>-Ag and Ag-O<sub>ligand</sub>-Ag angles range from 108.2(2)° to 129.6(2)° and 81.92(9)° to 105.69(1)°. Unlike previous complexes the trifluoroacetate anions adopt monodentate,  $\mu_2$ - and  $\mu_3$ - modes in complex **3.41**. Complex **3.41** contains one four- [Ag4 ( $\tau_4 = 0.45$ )], two five- [Ag1 ( $\tau_5 = 0.57$ ) and Ag5 ( $\tau_5 = 0.05$ )], one six- [Ag2] and one seven- [Ag3] coordinate silver center, as shown in figure 3.48. A chain of Ag $\cdots$ Ag interactions exists from Ag1 to Ag4. The weak Ag $\cdots$ Ag interactions start with 3.351(5) Å [Ag1-Ag3], 3.233(5) Å [Ag3-Ag5], 3.285(6) Å [Ag2-Ag5] and ends with 3.221(5) Å [Ag2-Ag4]. After this there is one bond break and again the silver bonding starts with 3.351(5) Å [Ag1-Ag3] and continues.

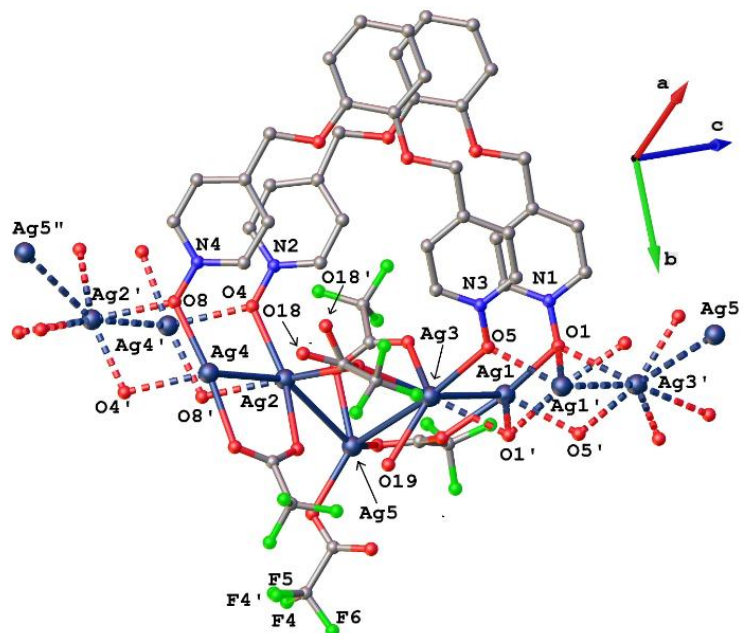


Figure 3.48 – Asymmetric unit of complex **3.41**. Hydrogen atoms are omitted for clarity. Selected bond lengths (Å) and bond angles (°): N1-O1 = 1.342(4), N2-O4 = 1.329(5), N3-O5 = 1.328(4), N4-O8 = 1.338(4), Ag1-O1 = 2.249(3), Ag3'-O1 = 2.525(3), Ag1'-O1 = 2.586(3), Ag1-O5 = 2.428(3), Ag2-O4 = 2.328(3), Ag2'-O8 = 2.478(3), Ag3-O5 = 2.391(3), Ag4'-O4 = 2.511(3), Ag4-O8 = 2.286(3), N1-O1-Ag1 = 121.8(2), N1-O1-Ag3' = 128.1(2), N1-O1-Ag1' = 108.2(2), N2-O4-Ag2 = 127.8(2), N2-O4-Ag4' = 129.6(2), N3-O5-Ag3 = 125.0(2), N3-O5-Ag1' = 129.0(2), N4-O8-Ag4 = 122.3(2), N4-O8-Ag2' = 132.9(2), Ag1-O1-Ag3' = 107.0(1), Ag1-O1-Ag1' = 95.23(1), Ag3'-O1-Ag1' = 81.92(9), Ag2-O4-Ag4' = 102.33(1), Ag3-O5-Ag1' = 105.69(1), Ag4-O8-Ag2' = 104.61(1), Ag1-Ag3 = 3.351(5), Ag2-Ag4 = 3.221(5), Ag2-Ag5 = 3.285(6), Ag3-Ag5 = 3.233(5).

From figure 3.49, the average N-O and Ag-O<sub>ligand</sub> bond lengths in complex **3.41** of ligand **3.15** with -OCH<sub>2</sub>- donating groups are close to the average values obtained for ligands **3.2** and **3.5** with -CH<sub>3</sub> and -OCH<sub>3</sub> groups.

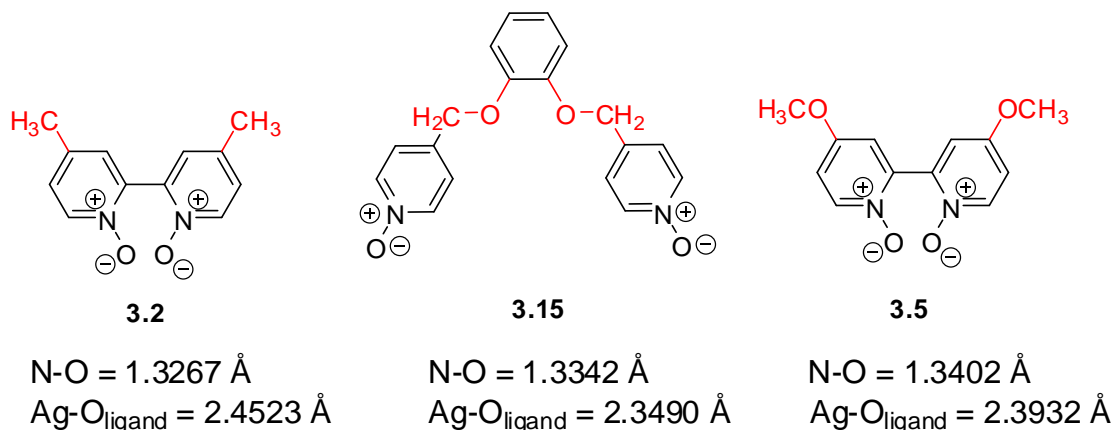


Figure 3.49 – Comparison of the average N-O<sub>ligand</sub> and Ag-O<sub>ligand</sub> bond parameters in complexes of ligands **3.2**, **3.5** and **3.15**.

As seen in the asymmetric unit, the ligands **3.15** are slightly offset and grow one-dimensionally with distances between the silver(I) bound N-oxide oxygens of 8.973 Å [O1-O4] and 9.179 Å [O5-O9]. The 1D polymeric structure looks like a sinusoidal chain (period 20.302 Å), as shown in figure 3.50.

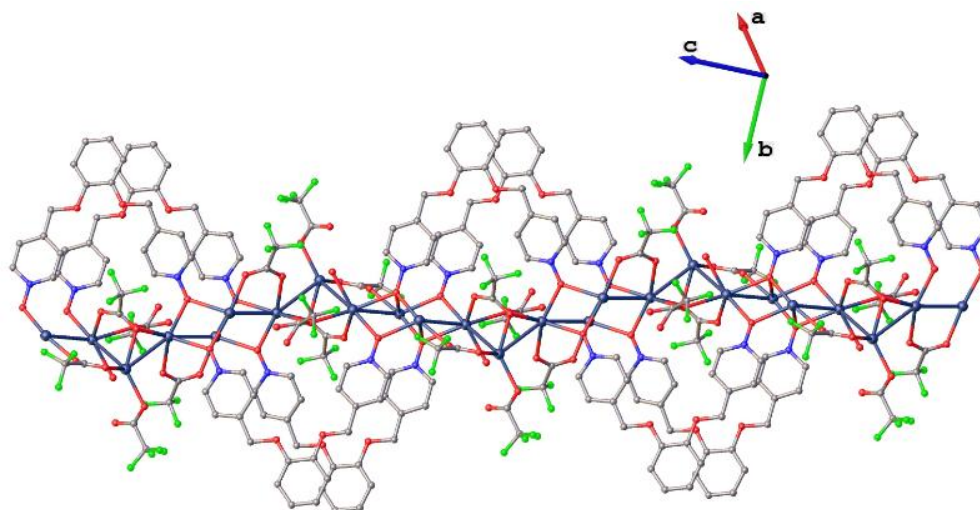


Figure 3.50 – 1D Polymeric zigzag structure of complex **3.41**.

Adjacent chains interact to give a 3D structure using  $\pi$ - $\pi$  interactions, as shown in figure 3.51. The  $\pi$ - $\pi$  interactions between pyridine N-oxide rings have centroid-centroid distances of 3.739(2) Å and 3.773(2) Å, while the distance between the benzene ring and a pyridine N-oxide in the adjacent 1D polymer is 3.627(1) Å, as shown in figure 3.51.

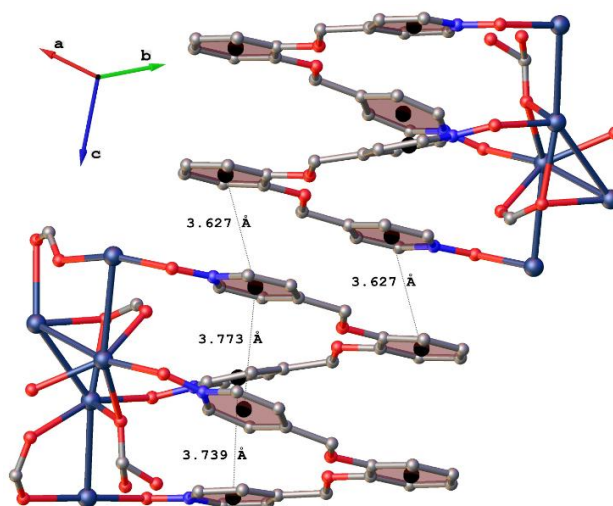


Figure 3.51 – Aromatic  $\pi$ - $\pi$  interactions in the crystal pack structure. Hydrogen atoms and anions are excluded for clarity.

### 3.3.16 Complexes with pyrazine N,N'-dioxide 3.18

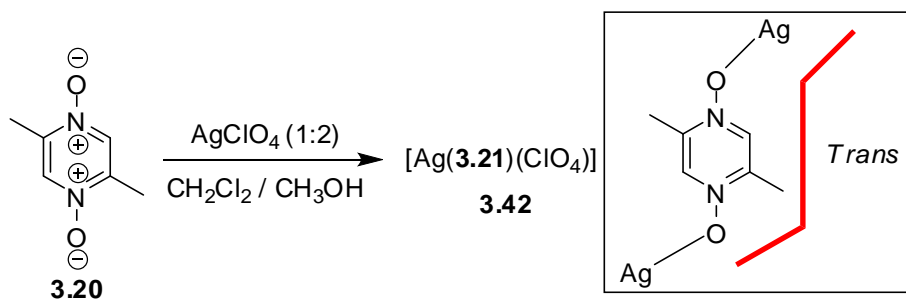
Due to solubility issues with ligand **3.18**, the synthesis of silver(I) complexes was a difficult task. Attempts to dissolve the ligand **3.18** with silver(I) salts at room and high temperatures resulted in yellow powders. Attempts to grow crystals with varied silver(I) ratios using different solvent combinations and crystal growth techniques were also unsuccessful.

### 3.3.17 Complexes with 2,3-dimethylpyrazine N,N'-dioxide 3.19

Ligand **3.19** was reacted with a range of silver(I) salts such as  $\text{AgClO}_4$ ,  $\text{AgOCOCF}_3$ ,  $\text{AgSO}_3\text{CF}_3$ ,  $\text{AgBF}_4$ ,  $\text{AgPF}_6$  and  $\text{AgNO}_3$  using different solvent combinations and crystal growth techniques. However none of these attempts gave silver(I) complexes suitable for crystallography.

### 3.3.18 Complexes with 2,5-dimethylpyrazine N,N'-dioxide 3.20

The bridging mode of pyrazine is linear,<sup>[159]</sup> whereas at least two kinds of bridging modes are expected for the pyrazine N,N'-dioxides when substituents are introduced in the pyrazine ring. Pyrazine N,N'-dioxides, similar to 4,4-bipyridine N,N'-dioxide, have a variety of potential bridging modes. For example, a  $\mu_2\text{-O,O'}$  coordination can have *cis*-, *gauche*- and *trans*- connection modes based on the “torsional angles” of  $\text{M1-O1-O1a-M1a}$  [ $0^\circ$ ,  $90^\circ$  and  $180^\circ$ ; M = metal ion and O = N-oxide oxygen].<sup>[160]</sup> Also, based on the number and position of substituents on these pyrazine N,N'-dioxides, different types of coordination modes could be obtained in supramolecular networks. Ligand **3.20** adopted a  $\mu_2\text{-O,O'}$  *trans*- coordination mode when reacted with  $\text{AgClO}_4$  in a 1:2 ratio, as shown in scheme 3.17.



Scheme 3.17 – Synthesis of complex **3.42**.

#### With silver(I) perchlorate 3.42

The asymmetric unit of complex **3.42**, solved in the monoclinic  $P2_1/c$  space group, consists of a silver(I) ion [Ag1] coordinated by two half ligand molecules **3.20** and a non-coordinated perchlorate anion, as shown in figure 3.52a. The asymmetric unit propagates into a 1D linear stair-case polymer as shown in figure 3.52b. In the 1D polymer, the Ag(I) ions are bridged by

ligands **3.20** in a *trans*- mode at average Ag-O distances of 2.287(2) Å, with torsional angles 180° [Ag1-O1-O1'-Ag1], which is similar to the previously reported values of *trans*- ligand **3.20** in manganese complexes.<sup>[135c]</sup> The N-O groups are monodentate with distances of 1.320(3) Å, which is also similar to those of reported ligand **3.20** in manganese complexes.<sup>[135d]</sup> The two half ligands coordinate Ag1 in near linear coordination geometry at angles of 175.95(7)° [O2-Ag1-O1]. The Ag<sup>+</sup>⋯Ag separations [8.779 Å] through the μ<sub>2</sub>-O,O' ligand **3.20** are similar to the distances found in ligand **3.20** manganese<sup>[135d]</sup> and cobalt<sup>[136]</sup> complexes.

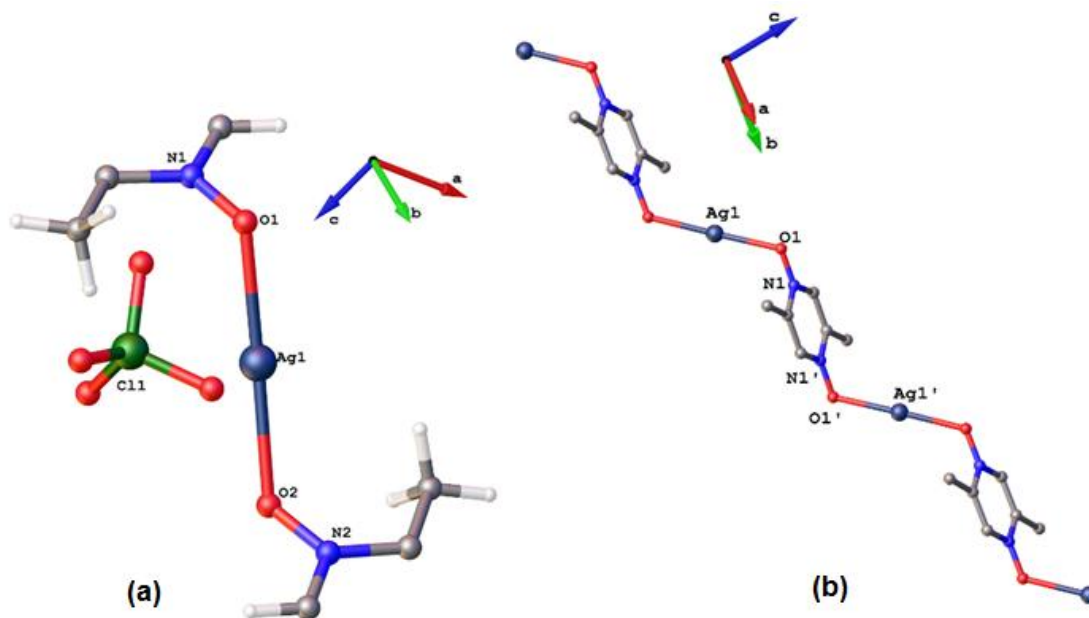


Figure 3.52 – (a) Asymmetric unit of complex **3.42** and (b) 1D stair case like polymer of complex **3.42**, anions are omitted for clarity. Hydrogen atoms are omitted for clarity. Selected bond lengths (Å) and bond angles (°): N1-O1 = 1.320(3), N2-O2 = 1.316(3), Ag1-O2 = 2.286(2), Ag1-O1 = 2.289(2), O2-Ag1-O1 = 175.95(7).

The complex **3.42** extends into a 3D network through weak Ag<sup>+</sup>⋯Ag interactions at distances of 3.657 Å, as shown in figure 3.53d. The N-oxide oxygen Ag1 distances are 2.758 Å [Ag1'-O2] and 2.746 Å [Ag1''-O1], as shown in figure 3.53d.

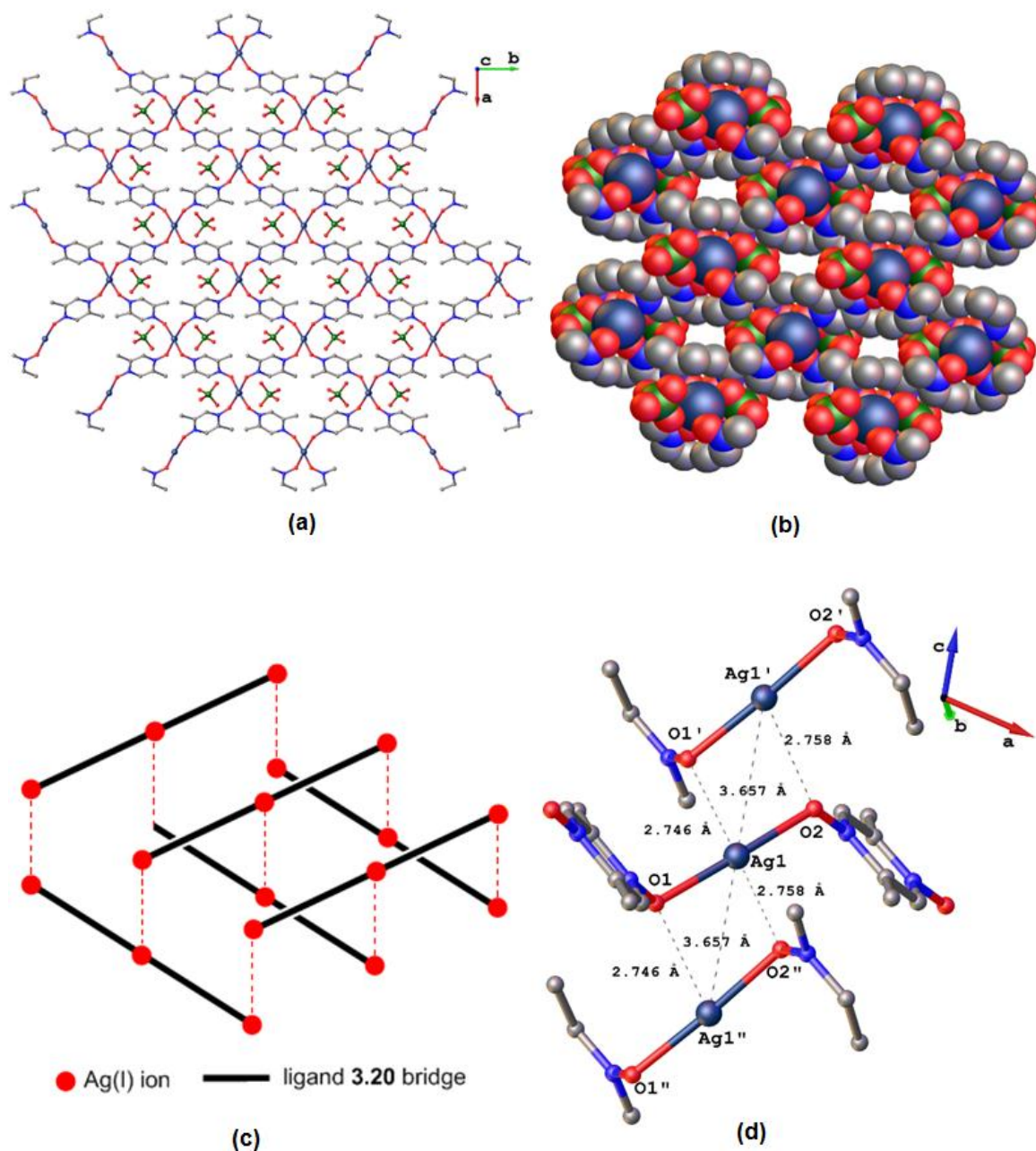
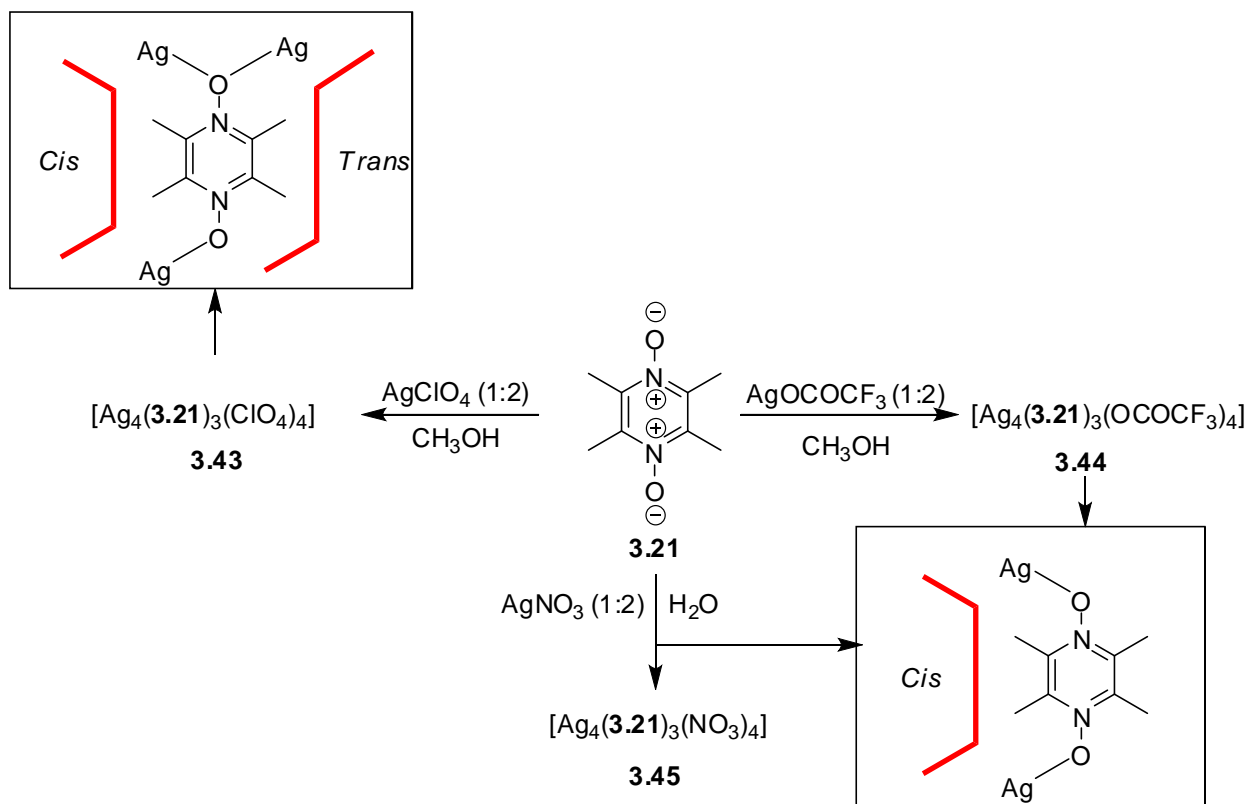


Figure 3.53 – (a) 3D crystal packing of complex **3.42**, (b) space filling structure of complex **3.42**, (c) topology view of Ag<sup>+</sup>–Ag interactions in the crystal packing, and (d) perspective view of Ag<sup>+</sup>–Ag interactions in the crystal packing.

### 3.3.19 Complexes with 2,3,5,6-tetramethylpyrazine N,N'-dioxide **3.21**

The asymmetric unit compositions shown in scheme **3.17** were obtained when ligand **3.21** was reacted with AgX (X = ClO<sub>4</sub>, CF<sub>3</sub>COO and NO<sub>3</sub>) in a 1:2 ratio. In complex **3.43**, the ligands **3.21** display μ<sub>4</sub>-O,O,O',O' and μ<sub>3</sub>-O,O,O' coordination modes, whereas in **3.44** and **3.45** they display μ<sub>4</sub>-O,O,O',O' and μ<sub>2</sub>-O,O' coordination modes to give 2D layered polymeric structures. Although the anions employed in complexes **3.44** and **3.45** are different, the μ<sub>2</sub>-O,O' ligands **3.21** adopted

*cis*-coordination modes, while in complex **3.43** a  $\mu_3$ -O,O,O' ligand exhibits both *cis*- and *trans*-coordination modes, as shown in scheme 3.18.



Scheme 3.18 – Syntheses of complexes **3.43** – **3.45**.

#### With silver(I) perchlorate (1:2) **3.43**

The asymmetric unit of complex **3.43** solved in the triclinic *P*-1 space group and contains three ligands **3.21** and four silver(I) ions in a 3:4 ligand to silver(I) ratio. The asymmetric unit also contains one non-coordinated [Cl2], two monodentate [Cl1 and Cl4] and one bidentate bridging perchlorate anion, as shown in figure 3.54. The ligand **3.21** exhibits  $\mu_4$ -O,O,O',O' [Pyz – 1] and  $\mu_3$ -O,O,O' [Pyz – 2] coordination modes, as shown in figure 3.54b. The *cis*- and *trans*- torsional angles for Pyz – 1 are  $10.31^\circ$  [Ag2'-O6-O5-Ag4],  $21.20^\circ$  [Ag1-O6-O5-Ag3] and  $165.22^\circ$  [Ag4-O5-O6-Ag1]  $163.26^\circ$  [Ag3-O5-O6-Ag2'], respectively. As seen in figure 3.54, ligand **3.21** adopted Pyz – 2 bridging modes between Ag1 and Ag2, Ag2 and Ag3 with *cis*- and *trans*- torsional angles of  $4.93^\circ$  [Ag1-O1-O2-Ag4'],  $18.25^\circ$  [Ag2-O3-O4-Ag3] and  $161.32^\circ$  [Ag1-O1-O2-Ag2] and  $165.94^\circ$  [Ag2-O3-O4-Ag1'], respectively.



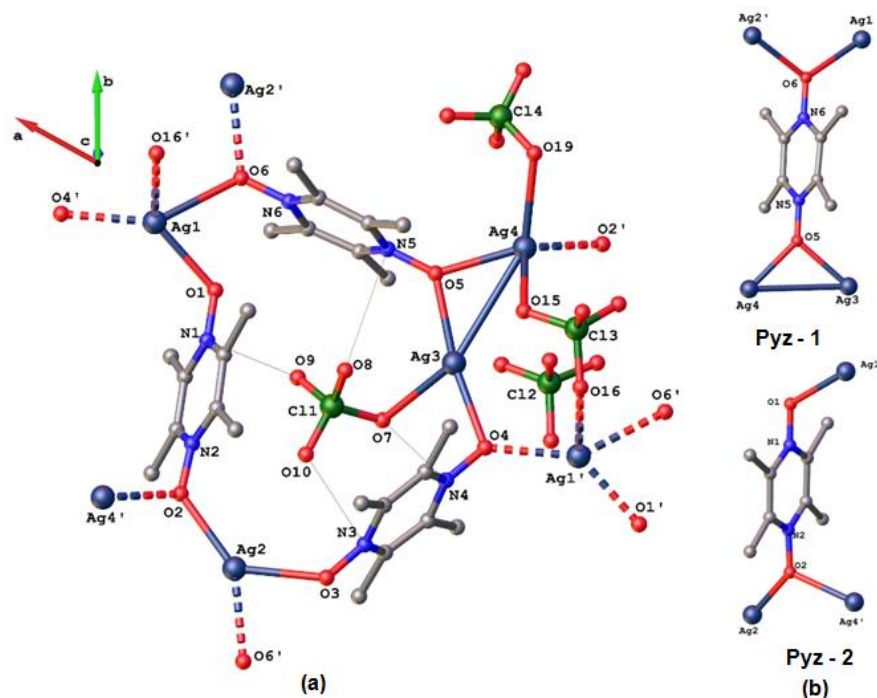


Figure 3.54 – (a) Asymmetric unit of complex **3.43**, and (b) coordination mode of ligands **3.21** in complex **3.43**. Hydrogen atoms are omitted for clarity. Selected bond lengths (Å) and bond angles (°): N1-O1 = 1.308(6), N2-O2 = 1.335(6), N3-O3 = 1.317(5), N4-O4 = 1.324(5), N5-O5 = 1.325(6), N6-O6 = 1.314(5), Ag1-O1 = 2.271(4), Ag1-O4' = 2.322(4), Ag1-O6 = 2.496(4), Ag1'-O16 = 2.525(4), Ag2-O2 = 2.287(4), Ag2-O3 = 2.292(4), Ag2-O6' = 2.400(4), Ag3-O5 = 2.251(4), Ag4-O5 = 2.286(4), Ag3-O4 = 2.278(4), Ag3-O7 = 2.558(4), Ag4-O19 = 2.464(5), Ag4-O15 = 2.525(4), Ag3-O7 = 2.558(4), N1-O1-Ag1 = 123.5(3), N2-O2-Ag4' = 112.4(3), N2-O2-Ag2 = 131.9(3), N3-O3-Ag2 = 127.3(3), N4-O4-Ag3 = 112.7(3), N4-O4-Ag1' = 134.1(3), N5-O5-Ag3 = 128.6(3), N5-O5-Ag4 = 136.5(3), N6-O6-Ag2' = 120.8(3), N6-O6-Ag1 = 124.2(3), Ag3-Ag4 = 3.338(7), Ag3-O5-Ag4 = 94.71(1), O7-Ag3-Ag4 = 142.51(1), O19-Ag4-Ag3 = 146.19(1).

The N-O bond distances range from 1.308(6) Å to 1.335(6) Å. The N-O<sub>ligand</sub>-Ag angles range between 112.4(3)° and 136.5(3)°, with their average, 125.2(3)°, higher than the values reported for ligand **3.21** in cadmium complexes.<sup>[135a]</sup> The complex **3.43** consists of one three- [Ag2], two four- [Ag1 ( $\tau_4 = 0.54$ ) and Ag3 ( $\tau_4 = 0.36$ )] and one five- [Ag4 ( $\tau_5 = 0.03$ )] coordinate silvers, as shown in figure 3.54a. The three-coordinate Ag2 is surrounded by oxygens [O2, O3 and O6'] of ligands **3.21** in a distorted trigonal planar geometry with Ag2-O distances ranging between 2.287(4) Å and 2.400(4) Å. The four-coordinate Ag1 has seesaw geometry with an O<sub>4</sub> environment, and is bound by oxygen atoms from three ligands **3.21** [O1, O4', and O6] and a perchlorate [O16'] anion. The Ag1-O distances range from 2.271(4) Å to 2.525(4) Å. Ag3 and Ag4 are bridged by O5 at an angle of 94.71(1)°, and are interacting at a distance of 3.338(7) Å. Two monodentate perchlorate [Cl1 and Cl4] anions coordinate Ag3 and Ag4 at distances of 2.558(4) Å [Ag3-O7] and 2.464(5) Å [Ag4-O19], as shown in figure 3.54. Also, a bidentate perchlorate [Cl3] bridges Ag1' and Ag4 at a mean distance of 2.525(4) Å.

The non-bonded N-O distances between the pyrazine nitrogens and perchlorate oxygens are 3.063 Å [N4-O7], 3.240 Å [N5-O8], 3.046 Å [N1-O9] and 3.255 Å [N3-O10]. The asymmetric unit grows into 2D sheet-like polymer, as shown in figure 3.55.

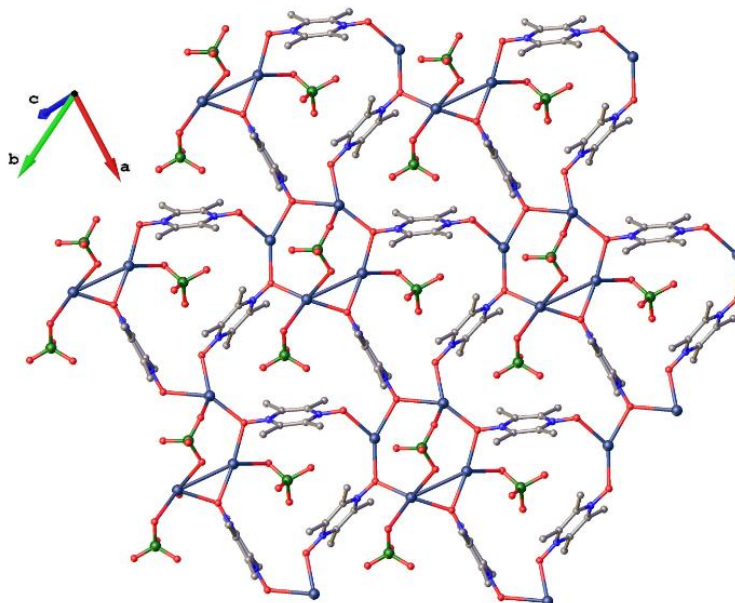


Figure 3.55 – 2D polymeric structure of complex **3.43**. Hydrogen atoms and non-coordinating perchlorate anions are omitted for clarity.

#### With silver(I) trifluoroacetate **3.44**

The asymmetric unit of complex **3.44**, shown in figure 3.56, was solved in the monoclinic  $C2/c$  space group, and comprises two trifluoroacetate anions bridging Ag1 and Ag2 with one and a half ligand **3.21** molecules in a 3:4 ligand to silver(I) ratio. Ag1...Ag2 are interacting at a distance of 2.874(3) Å. Ligand **3.21** adopted  $\mu_2-O, O'$  and  $\mu_4-O, O, O', O'$  connection modes to give 2D sheets. The  $\mu_4-O, O, O', O'$  ligands **3.21** bridge Ag2 centers to form a four-membered  $Ag_2O_2$  ring with two unequal Ag-O distances of 2.417(2) Å [Ag2-O3] and 2.484(2) Å [Ag2'-O3]. The N3-O3 bond distance shows double bond character with a distances of 1.316(3) Å, bridging Ag2 centers at an angle of 104.71(7)° [Ag2-O3-Ag2']. Due to the difference in Ag2-O<sub>ligand</sub> bond lengths, the ligand **3.21** displays two coordination angles of 117.49(2)° [N3-O3-Ag2] and 137.77(2)° [N3-O3-Ag2']. The average N-O bond distances of 1.313(3) Å is close to the values obtained for ligand **3.21** in complex **3.43** [1.320(6) Å]. The N-O<sub>ligand</sub>-Ag angles range from 106.15(2)° to 137.77(2)°.

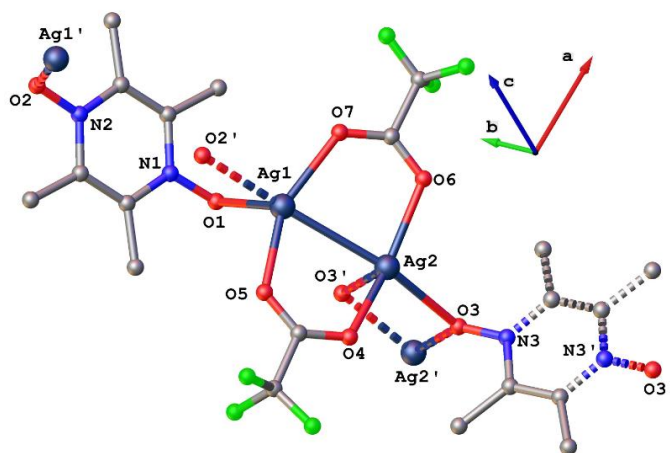


Figure 3.56 – Asymmetric unit of complex **3.44**. Hydrogen atoms are omitted for clarity. Selected bond lengths (Å) and bond angles (°): N1-O1 = 1.316(3), N2-O2 = 1.311(3), N3-O3 = 1.316(3), Ag1-O1 = 2.448(2), Ag2-O3 = 2.417(2), Ag2'-O3 = 2.484(2), Ag2-O4 = 2.231(2), Ag1-O5 = 2.230(2), Ag2-O6 = 2.222(2), Ag1-O7 = 2.236(2), Ag1-Ag2 = 2.877(3), N1-O1-Ag1 = 106.15(2), N2-O2-Ag1' = 113.71(2), N3-O3-Ag2 = 117.49(15), N3-O3-Ag2' = 137.77(2), Ag2-O3-Ag2 = 104.71(7).

The five-coordinate Ag1 and Ag2 atoms have distorted square pyramidal geometries with  $\tau_5$  parameters of 0.18 and 0.19, respectively. The complex **3.44** is a 2D sheet-like polymer, as shown in figure 3.57. The *cis*- $\mu_2$ -O,O' and  $\mu_4$ -O,O,O',O' ligands **3.21** in the 2D layered structure are orthogonal to the four-membered Ag<sub>2</sub>O<sub>2</sub> rings, as shown in figure 3.57. The *cis*-torsional angles for  $\mu_2$ -O,O' and  $\mu_4$ -O,O,O',O' ligands **3.21** are 0.97° and 2.36° respectively, while the *trans*-angles for tetradentate ligand **3.21** are 180°.

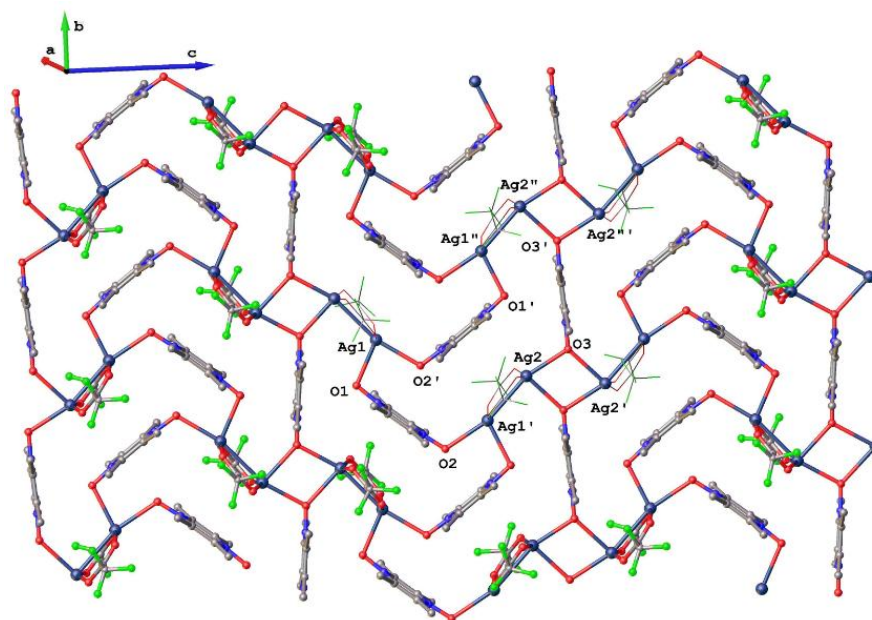


Figure 3.57 – 2D Polymeric structure of complex **3.44**. Hydrogen atoms are omitted for clarity and selected trifluoroacetate anions are shown in wireframe for clarity.

### With silver(I) nitrate **3.45**

The asymmetric unit of complex **3.45**, solved in the triclinic  $P-1$  space group, contains one and a half ligands **3.21**, two silver(I) ions, two nitrate anions and a water molecule, as shown in figure 3.58. Complex **3.45** has a 3:4 ligand to silver(I) ratio. The ligands **3.21** display  $\mu_4-O,O,O',O'$  and  $\mu_2-O,O'$  coordination modes, as shown in figure 3.59. The average  $N-O_{\text{ligand}}$  bond distance of 1.317(3) Å is similar to that obtained for ligand **3.21** in complex **3.44** [1.313(3) Å]. The average  $Ag-O_{\text{ligand}}$  bond distance for the  $\mu_2-O,O$  ligand [2.272(2) Å] is shorter than the  $\mu_4-O,O,O',O'$  [2.430(2) Å] ligands **3.21**, with overall  $N-O_{\text{ligand}}-Ag$  angles ranging from 115.54(2)° to 119.80(1)°. Ag1 and Ag2 are in five- and six-coordinate geometries, respectively, with the coordination sphere of Ag1 [ $\tau_5 = 0.06$ ] filled by two oxygens from two ligands **3.21** [O3 and O1], two from nitrate anions [O4 and O4'], and a water oxygen O10'. Ag2 adopts an  $O_6$  coordination sphere, with oxygens supplied by O3 and O2'' of bridging and monodentate ligands **3.21**, two from a bidentate nitrate anion [O7 and O8], one from a bridging nitrate anion [O5], and a water molecule [O10], as seen in figure 3.58.

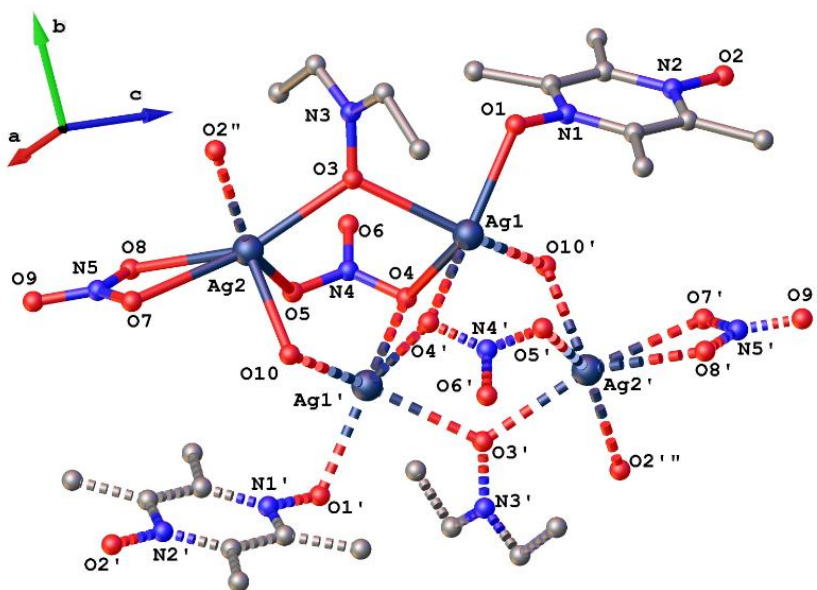


Figure 3.58 – Asymmetric unit of complex **3.45**. Hydrogen atoms are omitted for clarity. Selected bond lengths (Å) and bond angles (°): N1-O1 = 1.316(3), N2-O2 = 1.303(3), N3-O3 = 1.325(3), Ag1-O1 = 2.272(2), Ag1-O3 = 2.456(2), Ag2-O3 = 2.406(2), Ag1-O4 = 2.562(2), Ag1'-O4 = 2.397(2), N1-O1-Ag1 = 115.54(2), N3-O3-Ag2 = 119.80(1), N3-O3-Ag1 = 118.33(1), Ag2-O3-Ag1 = 120.03(7), Ag1-O4-Ag1' = 88.55(7), Ag2-O10-Ag1' = 88.56(7).

Two oxygens, O3 and O3', from ligands **3.21** and two oxygens [O10 and O10'] of water molecules bridge Ag1, Ag2, Ag1' and Ag2' to form an eight-membered ring with two bridging tridentate nitrate anions, as shown in figure 3.58. The  $Ag_2O_2$  ring is a parallelogram with two

unequal sides of 2.562(2) Å [Ag1-O4] and 2.397(2) Å [Ag1'-O4]. The oxygens O3, O4 and O10 bridges Ag1 and Ag2 at angles of 120.03(7)°, 88.55(7)° and 88.56(7)°, respectively. These eight-membered rings lie at four corners of the unit cell bridged by centrosymmetric  $\mu_4$ -O,O,O',O' ligands **3.21**, as shown in figure 3.59. The structure propagates in the *ab*-plane to form a 2D polymeric sheet, as shown in figure 3.60.

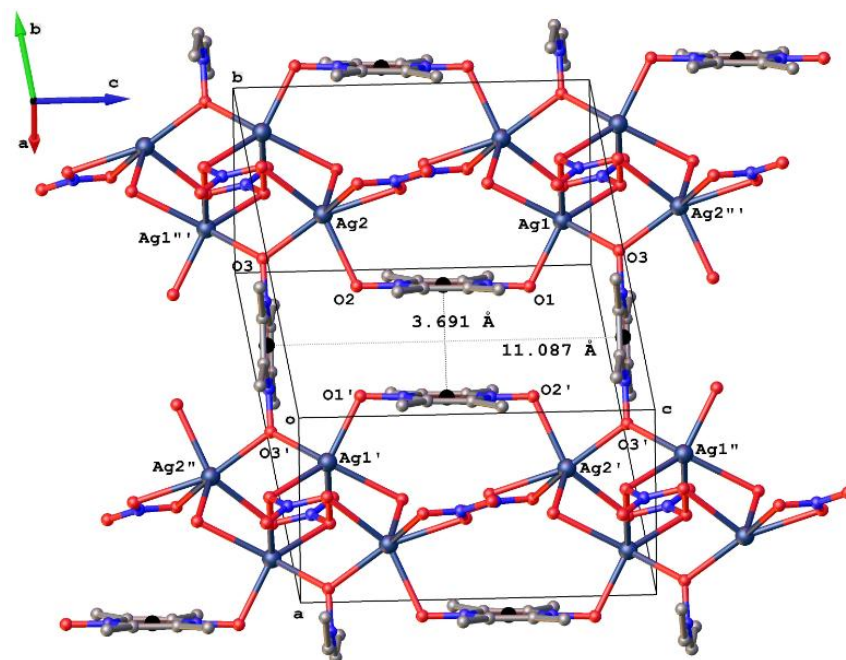


Figure 3.59 – A section of the 2D polymeric structure to explain the coordination modes of ligand **3.21**. Hydrogen atoms are omitted for clarity.

A *Cambridge Crystallographic Database* and *Sci-Finder* search revealed only one reported complex containing ligand **3.21** in a  $\mu_4$ - coordination mode.<sup>[135a]</sup> The ligand **3.21** adopts a *cis*-coordination mode with Ag1 and Ag2, and has torsional angles of 0.42° [Ag1-O1-O2-Ag2], which are close to the reported values in the literature.<sup>[135a-c, 160]</sup> The *cis*- and *trans*- torsional angles for  $\mu_4$ -O,O,O',O' ligand **3.21** are 14.91° [Ag1-O3-O3'-Ag2' and Ag1''-O3'-O3-Ag2'''] and 180° [Ag1-O3-O3'-Ag1'' and Ag2'-O3'-O3-Ag2'''], respectively. The centroid-centroid distances between  $\mu_4$ -O,O,O',O' and  $\mu_2$ -O,O' ligands **3.21** are 11.087(2) Å and 3.691(2) Å, as shown in figure 3.59.

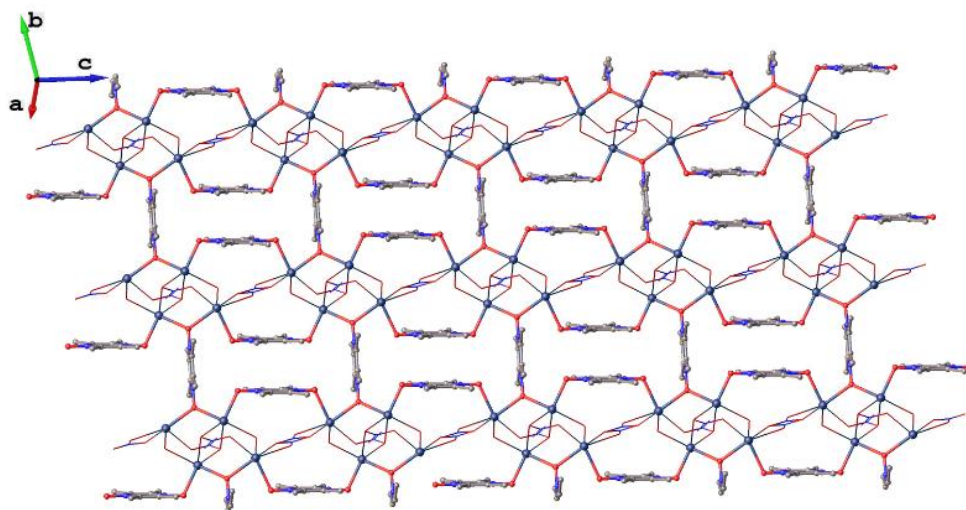


Figure 3.60 – 2D polymeric structure of complex **3.45**. Hydrogen atoms are omitted for clarity.

### 3.4 Conclusions

Polymeric coordination network synthesis is a procedure in which the final architecture depends on the building blocks [organic ligands, metal ions, counter ions, solvent molecules etc.] and on the interactions of self-assembled building blocks [metal ion coordination, hydrogen bonding interactions,  $\pi$ - $\pi$ -interactions and metal–metal interactions etc.]. To investigate these different factors that influence the formation of a particular crystal structure, 22 N,N'-dioxide ligands [16 known and 5 new] with different substituents and different sized spacers were studied in this chapter, as listed in figure 3.1. This chapter describes a total of 27 new crystal structures with 23 being silver(I) complexes, 1 molecular co-crystal and 3 unreported ligand structures.

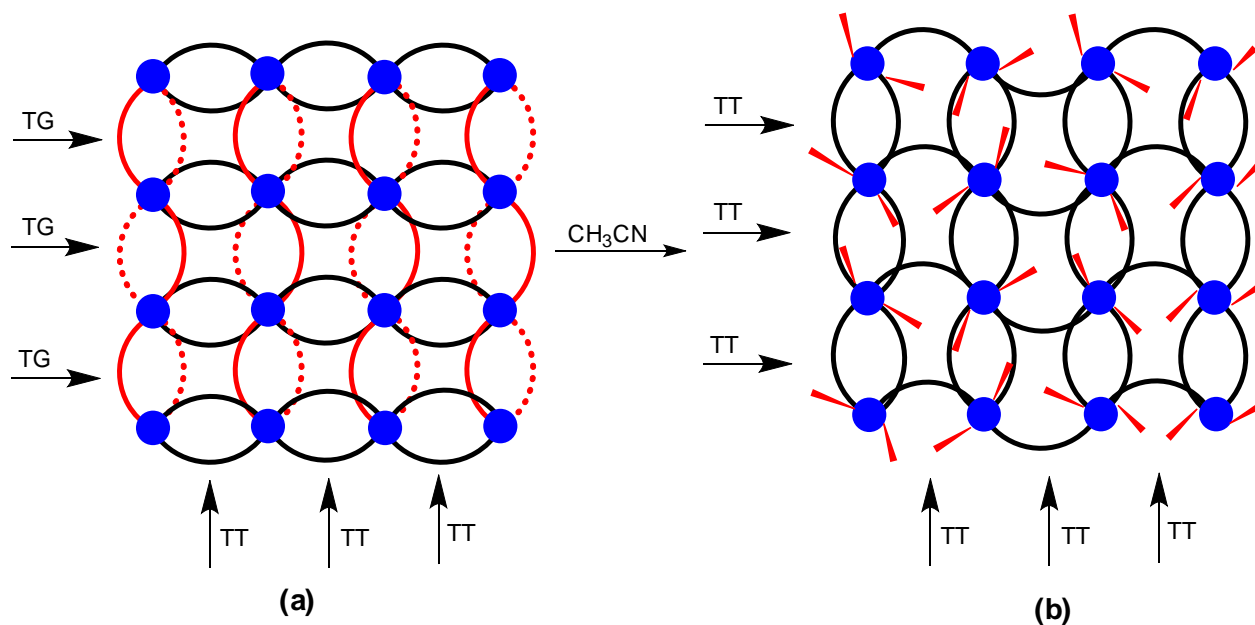
Non-coordinating counterions provide an advantage in which the silver(I) can fill its coordination sphere with either N,N'-dioxide ligands or N,N'-dioxide ligands and aqua-ligands. Examples of the coordination sphere of silver(I) filled with N,N'-dioxide ligands only are observed in complexes **3.22**, **3.26**, **3.27**, **3.31**, **3.37** and **3.40**, while the coordination sphere with N,N'-dioxide ligands and aqua-ligands are seen in **3.33** and **3.34** complexes. Since the coordination sphere of silver(I) is flexible, a wide range of coordination numbers, from 2 to 8, are adopted in these silver(I) non-coordinating anion complexes. In some cases, solvent molecule coordination can alter the silver(I) coordination number. For example, in complex **3.31** the silver(I) atoms display 4 and 5 coordination numbers, while in **3.32**, with CH<sub>3</sub>CN coordinating molecules, it is 3 and 4.

Reaction of ligand **3.1** with AgClO<sub>4</sub> [**3.22**], AgPF<sub>6</sub> [**3.26**] and AgBF<sub>4</sub> [**3.37**] in 1:2 ratios resulted in isomorphous crystal structures with their anions being non-coordinated. The ClO<sub>4</sub> anion is non-

coordinated in complex **3.22** and coordinated in **3.23** when reacted in 1:1 ligand to silver(I) ratio. When ligand **3.1** was reacted in a 1:2 ligand to  $\text{AgSO}_3\text{CF}_3$  [**3.25**] ratio, silver(I) adopted a maximum coordination number of 8 and ligand **3.1** a maximum denticity as  $\mu_6\text{-O,O,O,O',O',O'}$ . The dimensionalities obtained with ligand **3.1** are 0, 1 and 2. The ligand **3.1** gives a 2D polymer with a rare bridging type of coordination when reacted with  $\text{AgOCOCF}_3$  [**3.24**] in a 1:2 ratio and a discrete structure with  $\text{AgNO}_3$  [**3.28**].

Ligand **3.2** resulted in a discrete and a 1D polymeric structure when reacted with  $\text{AgOCOCF}_3$  [**3.29**] and  $\text{AgSO}_3\text{CF}_3$  [**3.30**] in a 1:2 ligand to silver(I) ratio. In these complexes, a maximum denticity of  $\mu_5\text{-O,O,O',O',O'}$  was adopted by ligand **3.2** with a silver(I) coordination number of 6. Ligand **3.5** produced three one-dimensional polymers and a discrete structure when reacted with  $\text{AgClO}_4$  [two complexes, **3.31** and **3.32**],  $\text{AgSO}_3\text{CF}_3$  [**3.33**] and  $\text{AgBF}_4$  [**3.34**] in 1:2 ligand to silver(I) ratios. A common maximum denticity of  $\mu_4\text{-O,O,O',O'}$  was obtained in all three complexes **3.31**, **3.32** and **3.33**. Ag(I) adopted a coordination number of 8 in complex **3.33**, similar to complex **3.25**.

Ligand **3.11** resulted in a molecular complex when reacted with silver(I) trifluoroacetate similar to complexes discussed in chapter 2. The change in network morphology by a conformationally free ligand [**3.12**] with solvent molecule coordination is shown in scheme 3.19. Ligands **3.12** adopted TG and TT conformations along the *b*- and *c*-axis when crystals were grown in a 1:1 mixture of  $\text{CH}_2\text{Cl}_2$  and  $\text{CH}_3\text{OH}$ . In complex **3.37**, no coordination with solvent molecules was observed. However, when  $\text{CH}_3\text{CN}$  was used instead of  $\text{CH}_2\text{Cl}_2$ , the ligands **3.12** display TT conformations throughout the polymeric network along with coordination of  $\text{CH}_3\text{CN}$  molecules, as shown in scheme 3.19b. Although the average N-O bond length of ligands **3.12** are similar in scheme 3.19a [1.335(4) Å] and scheme 3.19b [1.336(6) Å], the Ag-O<sub>ligand</sub> bond distances are shortened by 0.186 Å in the latter.



Scheme 3.19 – Conformational changes observed in ligand **3.12** due to  $\text{CH}_3\text{CN}$  coordination in complexes **3.36** (a) and **3.37** (b).

We also report the first X-ray crystal structures [**3.39** and **3.40**] of complexes with ligand **3.13** having both *cis*- and *trans*- coordination modes with silver(I) ions. A review by Young and Hanton presents an elaborate summary on the coordination number of silver(I) complexes based on a CSD search.<sup>[153]</sup> In this review, the search revealed a total of 3319 crystallographically characterised silver(I) structures. Of these, 24.2% are two-, 22.7% are three-, 43.9% are four-, 4.7% are five-, 3.9% are six-, 0.3% are seven- and 0.3% are eight-coordinate. Despite the huge family of silver(I) compounds, there are relatively few examples in which silver(I) ions exhibit two or three different coordination numbers in the same structure. Based on the CSD search, four different coordination spheres in the same compound has been reported only once in the literature.<sup>[161]</sup> In this chapter, we report the second complex [**3.41**] with a continuous silver(I)-polyhedral-framework containing four kinds [4, 5, 6 and 7] of coordination spheres. These types of metal-polyhedra networks are an active area of research due to their potential applications in various fields of research.<sup>[162]</sup>

It is possible to identify some trends in the coordination behaviour of ligands **3.20** and **3.21** [figure 3.64]. The  $\text{N-O}_{\text{ligand}}\text{-Ag}$  angles ranges from  $106.15(2)^\circ$  to  $137.77(2)^\circ$  with an average of  $120.13^\circ$ , suggesting  $\text{sp}^2$  hybridization of the N-oxide oxygens. Also, as seen from the crystal structures, with just one exception in complex **3.43**, the *trans*- bridging ligands lie on inversion centers with  $\text{Ag-O-O-Ag}$  torsional angles of  $180^\circ$ ; the exceptions deviate little from the ideal *trans*- bridging mode and the values range from  $161.32^\circ$  to  $165.94^\circ$ . A *Cambridge Crystallographic Database* and *Sci-Finder* search revealed that this type of *trans*- bridging modes are extensively studied



and reported with 4,4'-bipyridine N,N'-dioxide as ligand<sup>[45a, 60, 62, 123, 127, 157, 163]</sup> but is very rare with 1,4-pyrazine N,N'-dioxide and its derivatives.<sup>[135, 160]</sup>

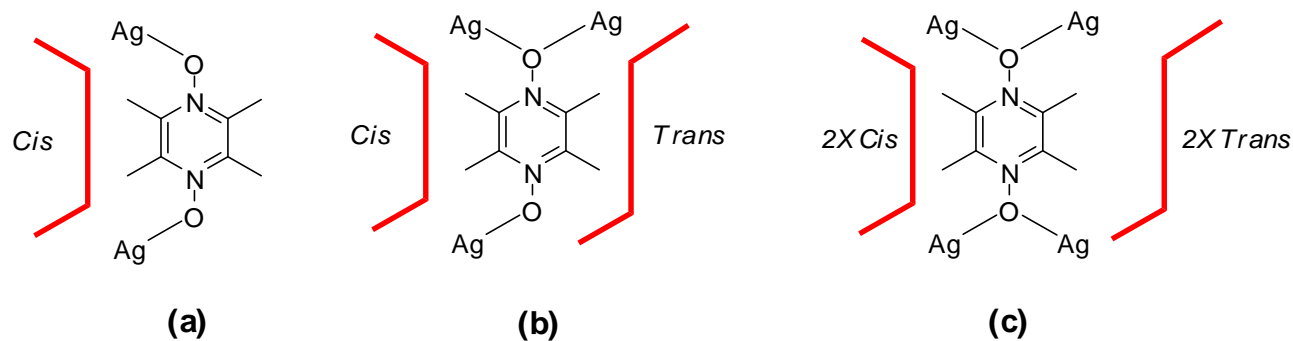
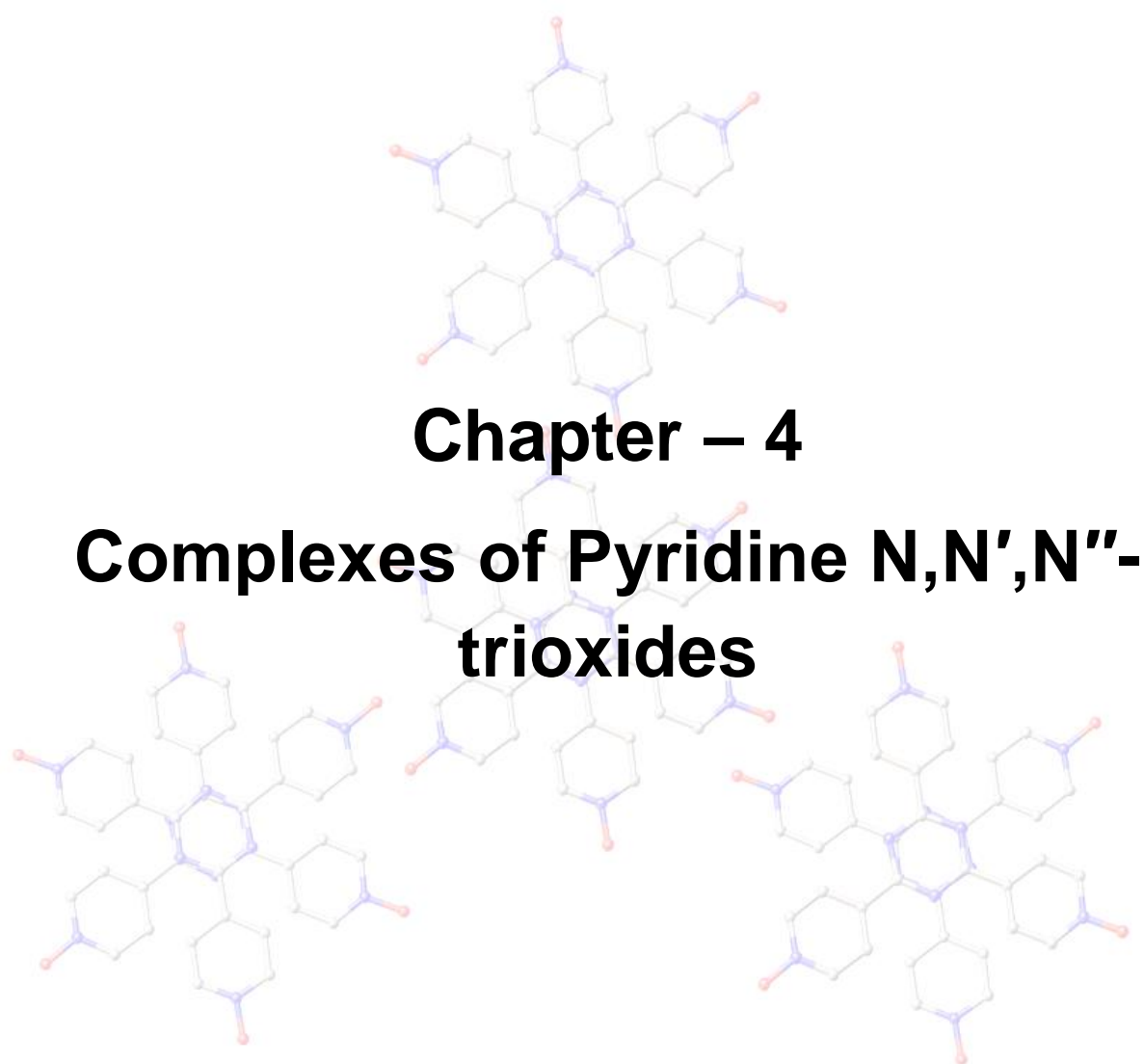


Figure 3.64 – Types of coordination modes obtained for ligands **3.20** and **3.21**.



## 4.1 Introduction

Terpyridine units have been used with great success in areas such as molecular electronics,<sup>[164]</sup> lanthanide luminescence<sup>[165]</sup> and as a part of longer chain ligands.<sup>[166]</sup> We are interested in the oxidised form of such ligands, as their poly-N-oxides. These ligands should have a greater affinity for metals than their parent pyridyl ligands, due to the harder oxygen donor atoms. These polydentate ligands are of interest due to their interesting coordination properties. Such multidentate pyridine N-oxide ligands have produced numerous coordination complexes<sup>[167]</sup> with useful magnetic properties. Some of these ligands are highly reactive and give good selectivity in asymmetric catalysis.<sup>[168]</sup> Due to the range of coordination modes formed by N-O groups, numerous research works have developed many neutral polydentate pyridine N-oxide ligands especially in the field of asymmetric catalysis.<sup>[169]</sup> Recently Amoroso *et al.*<sup>[65-66, 68]</sup> reported on the coordination properties of the flexible ligand **4.1**. The complexes were discrete with ligands coordinated to the metal center via stable, seven membered chelate rings. We synthesised **4.1** to study its coordination modes with the silver(I) ion, as it could potentially coordinate up to nine silver(I) ions per ligand and also, to avoid the steric repulsion between the lone pairs on the oxygens, could cause C-C bond rotation between the aromatic rings.

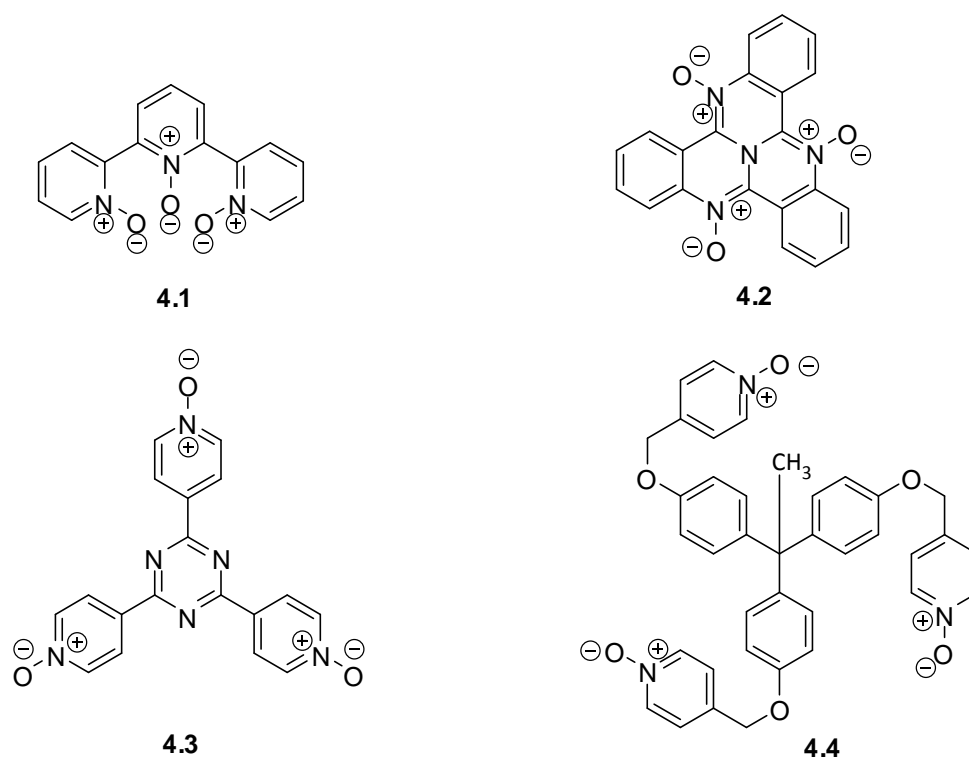
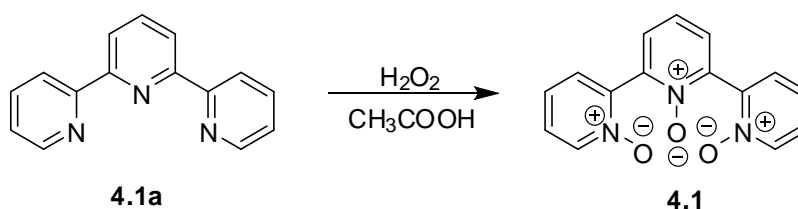


Figure 4.1 – List of poly N-oxides.

Despite numerous reports on the N-oxides of pyridine and diazines, relatively little is known about N,N',N''-trioxides. The syntheses of poly N-oxides were avoided by chemists due to several factors such as steric, solubility, isolation and characterisation issues. Here, we report some new poly-N-oxides [4.2, 4.3 and 4.4] shown in figure 4.1 to compare their coordination chemistry with mono- and di-N-oxides discussed in chapters 2 and 3.

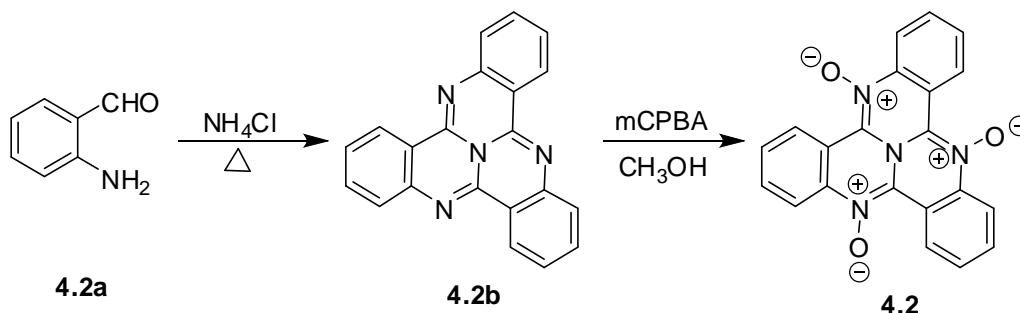
## 4.2 Syntheses of ligands

The general synthesis involves oxidising the respective nitrogen heterocycles using either mCPBA or hydrogen peroxide as oxidant. Ligand 4.1 was prepared in a satisfactory yield of 74% by the action of hydrogen peroxide in acetic acid on 4.1a according to the literature method.<sup>[170]</sup>



Scheme 4.1 – Synthesis of ligand 4.1.

Ligand 4.2 was prepared from 4.2b, which has been shown to have carcinogenic properties.<sup>[171]</sup> Ligand 4.2b was prepared by the Steel group using o-aminobenzaldehyde and ammonium chloride as reported by Patridge *et al.*<sup>[172]</sup> and this was then oxidized to 4.2 by reaction with mCPBA in methanol in 89% yield.

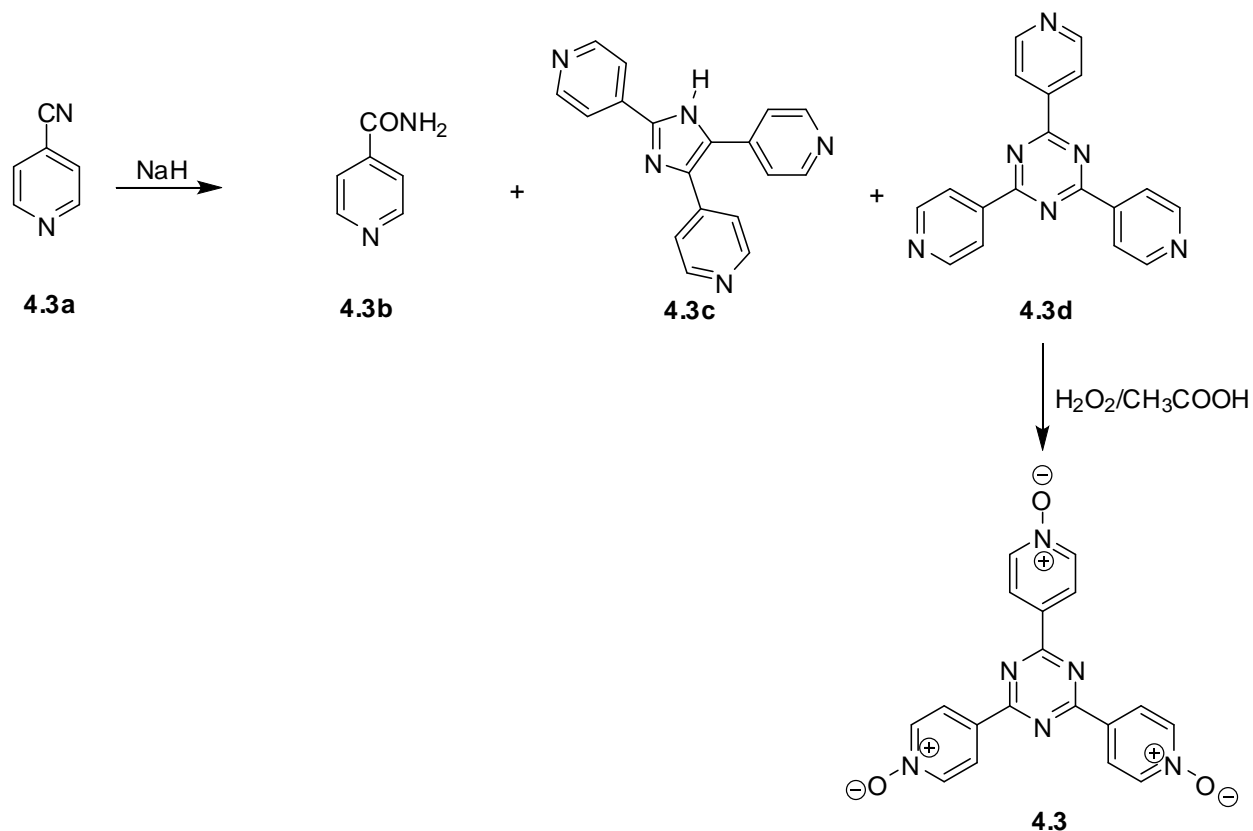


Scheme 4.2 – Synthesis of ligand 4.2.

The exo-tridentate ligand 4.3d and its analogues are widely used as herbicides, drugs and polymers that have excellent thermal and electrical properties. Due to the rigidity and triangular geometry in ligand 4.3d, these type of ligand systems can lead to the formation of porous frameworks. Furthermore, a large number of supramolecular assemblies have been reported with ligand 4.3d by Fujita<sup>[173]</sup> and others.<sup>[174]</sup>

Ligand **4.3d** can be prepared in many ways. A mixture of 4-cyanopyridine and NaH were heated to 180 °C which, after purification, gave **4.3d**<sup>[175]</sup> in 77% yield. The reaction formed several other products which were methanol soluble. From these **4.3b** and **4.3c** [scheme 4.3] were isolated and **4.3c** was characterised by X-ray analysis. The transformation of the CN group of 4-cyanopyridine in the presence of NaH changes the hybridization of the orbitals on both the C and N atoms from  $sp$  to  $sp^2$ . This leads to polymerization of 4-cyanopyridine to give multiple products. The distribution of products mainly depends on the reaction temperature.

Since the triazine **4.3d** was insoluble in deuterated solvents, NMR could not be used to characterize the product. However the insoluble compound **4.3d** was soluble in acetic acid and 50% hydrogen peroxide. When heated at 80 °C for 40 minutes this gave **4.3**, which was characterised by X-ray analysis.



Scheme 4.3 – Synthesis of ligand **4.3**.

### Crystal structure of **4.3c**

The crystal structure of **4.3c** [2,4,5-tris(4-pyridyl)-imidazole] as a hydrate has been reported<sup>[176]</sup> and it has been a ligand of interest in coordination chemistry for the construction of metal-organic coordination polymers in recent years.<sup>[177]</sup> The crystal structure was solved in the triclinic *P*-1 space group with one water molecule [O1] hydrogen bonded to the imidazole proton [H2] as shown in the figure 4.2. The hydrogen bond parameters are listed in table 4.1. The torsional

angles between the five membered cyclic spacer and the pyridyl rings are  $106.44(1)^\circ$  [N2-C2-C11-C12],  $168.68(1)^\circ$  [N1-C3-C6-C7] and  $172.88(1)^\circ$  [N1-C1-C16-C15].

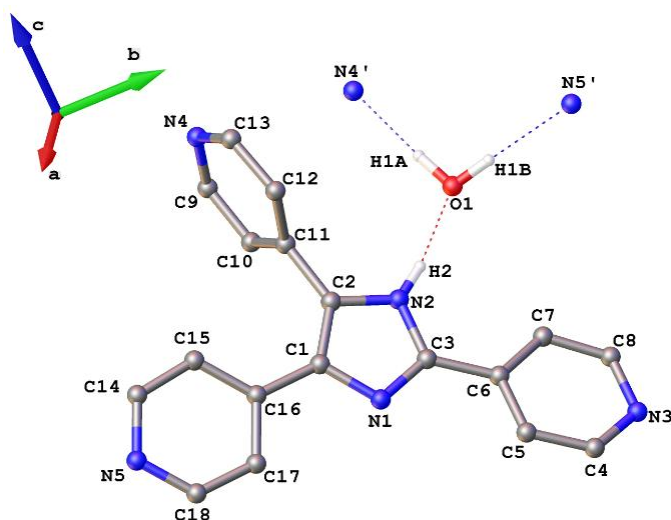


Figure 4.2 – Crystal structure of **4.3c** as its hydrate. Selected hydrogen atoms are omitted for clarity. Selected bond lengths (Å) and bond angles: C1-C2 = 1.385(2), C1-N1 = 1.382(1), C3-N1 = 1.322(2), C3-N2 = 1.362(1), C2-N2 = 1.364(1), N2-C2-C11-C12 =  $106.44(1)^\circ$ , N1-C3-C6-C7 =  $168.68(1)^\circ$ , N1-C1-C15-C16 =  $172.88(1)^\circ$ .

Table – 4.1 Hydrogen bond parameter in **4.3c**.

D-H $\cdots$ A	$d_{D-H}$ (Å)	$d_{H\cdots A}$ (Å)	$d_{D\cdots A}$ (Å)	$\angle D-H\cdots A$ ( $^\circ$ )
N2-H2 $\cdots$ O1	0.860	1.894	2.746	170.31
O1-H1A $\cdots$ N4'	0.922	1.883	2.804	177.03
O1-H1B $\cdots$ N5'	0.893	1.974	2.863	172.63

### Crystal structure of 4.3

Due to solubility issues, crystals of ligand **4.3** suitable for X-ray analysis were obtained from acidic deuterated [D<sub>2</sub>O/DCI] solvents. The crystal structure of the protonated ligand **4.3** solved in the triclinic *P*-1 space group with two water molecules and three chloride anions, as shown in figure 4.3. The N-O bond distances of 1.360(3) Å – 1.367(3) Å in ligand **4.3**, implies that the N-O bonds have significant single bond character. In the solid state, all four- six-membered rings are essentially coplanar with a maximum torsional angle of  $1.9(4)^\circ$  [N2-C1-C6-C5]. The C-N distances of 1.340(4) Å – 1.351(4) Å of the pyridine rings are slightly longer than in the protonated ligand **4.3d** [1.327(3) Å – 1.340(3) Å].<sup>[178]</sup> The triazine C-N bond distances of 1.336(4) Å – 1.341(4) Å are similar to protonated **4.3d**,<sup>[178]</sup> indicating the triazines are not protonated. All the hydrogens attached to oxygen atoms shown in figure 4.3 are involved in hydrogen bonding to acceptor atoms in the adjacent unit cell.

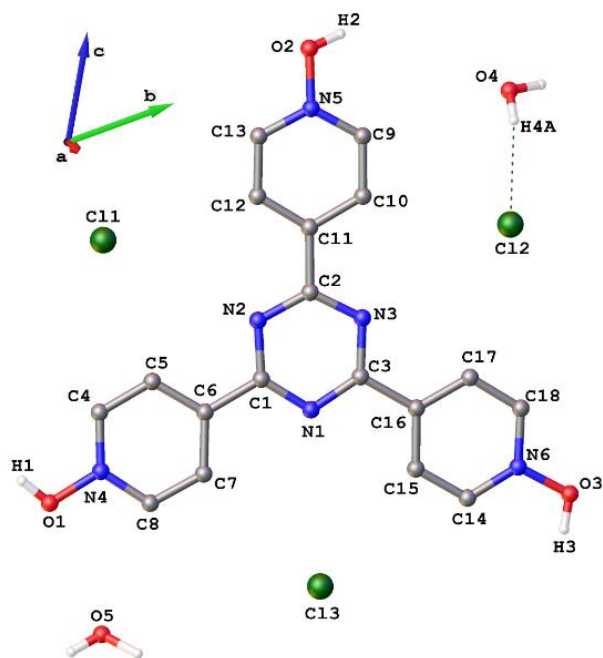
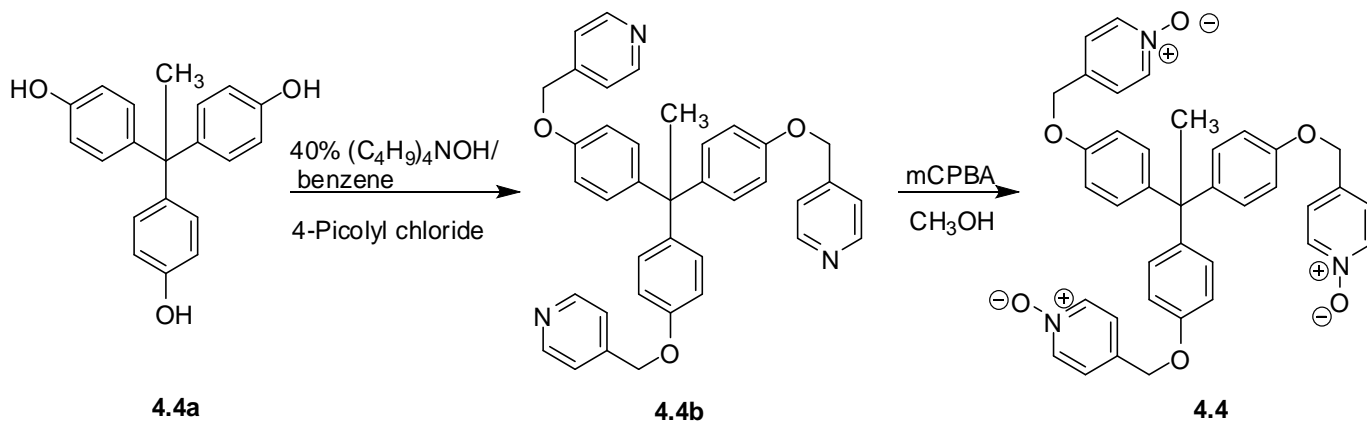


Figure 4.3 – Crystal structure of **4.3**. Selected hydrogen atoms were omitted for clarity. Selected bond lengths (Å) and bond angles: N4-O1 = 1.363(3), N5-O2 = 1.367(3), N6-O3 = 1.360(3), C1-N1 = 1.337(4), C1-N2 = 1.341(4), C2-N3 = 1.336(4), C2-N2 = 1.340(4), C3-N3 = 1.337(4), C4-N4 = 1.342(4), C8-N4 = 1.341(4), C9-N5 = 1.340(4), C13-N5 = 1.345(4), C14-N6 = 1.351(4), C18-N6 = 1.342(4).

Tripodal ligands with flexible chains show particularly interesting coordinating capacity due to their flexible binding modes. Tripodal ligands such as **4.4b** are of interest due to their formation of cavity sizes with potential applications. Ligand **4.4b** was prepared by Cottam,<sup>[179]</sup> in a metallosupramolecular chemistry study to investigate the flexible coordinate modes offered by the pyridine donors. The ligand **4.4b** was oxidized to **4.4** with mCPBA in methanol in 55% yield, giving a ligand which can potentially bind up to nine silver(I) ions. Ligand **4.4** is a new compound and was characterised by <sup>1</sup>H NMR, <sup>13</sup>C NMR, elemental analysis, mass and IR spectra. The <sup>1</sup>H NMR and <sup>13</sup>C NMR spectra were recorded in CDCl<sub>3</sub> and the assignments are shown in figure 4.4



Scheme 4.4 – Synthesis of ligand **4.4**.

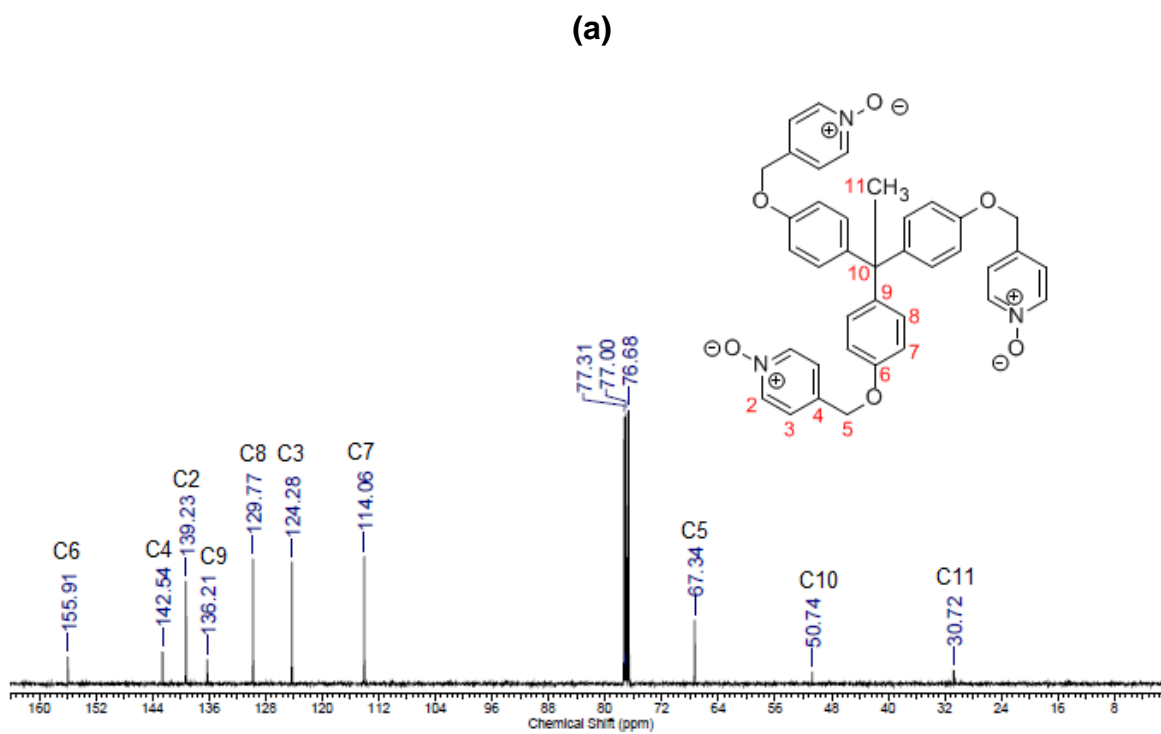
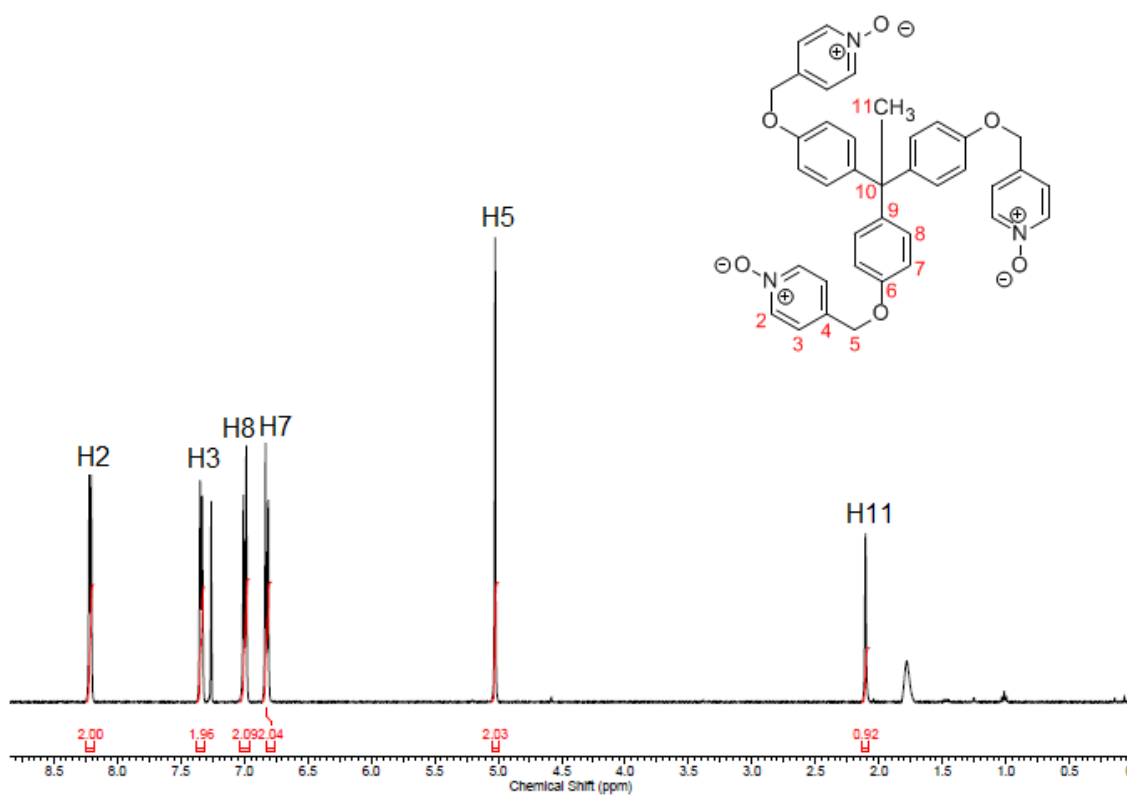


Figure 4.4 –  $^1\text{H}$  NMR (a) and  $^{13}\text{C}$  NMR (b) spectra and the assignments of ligand **4.4**.

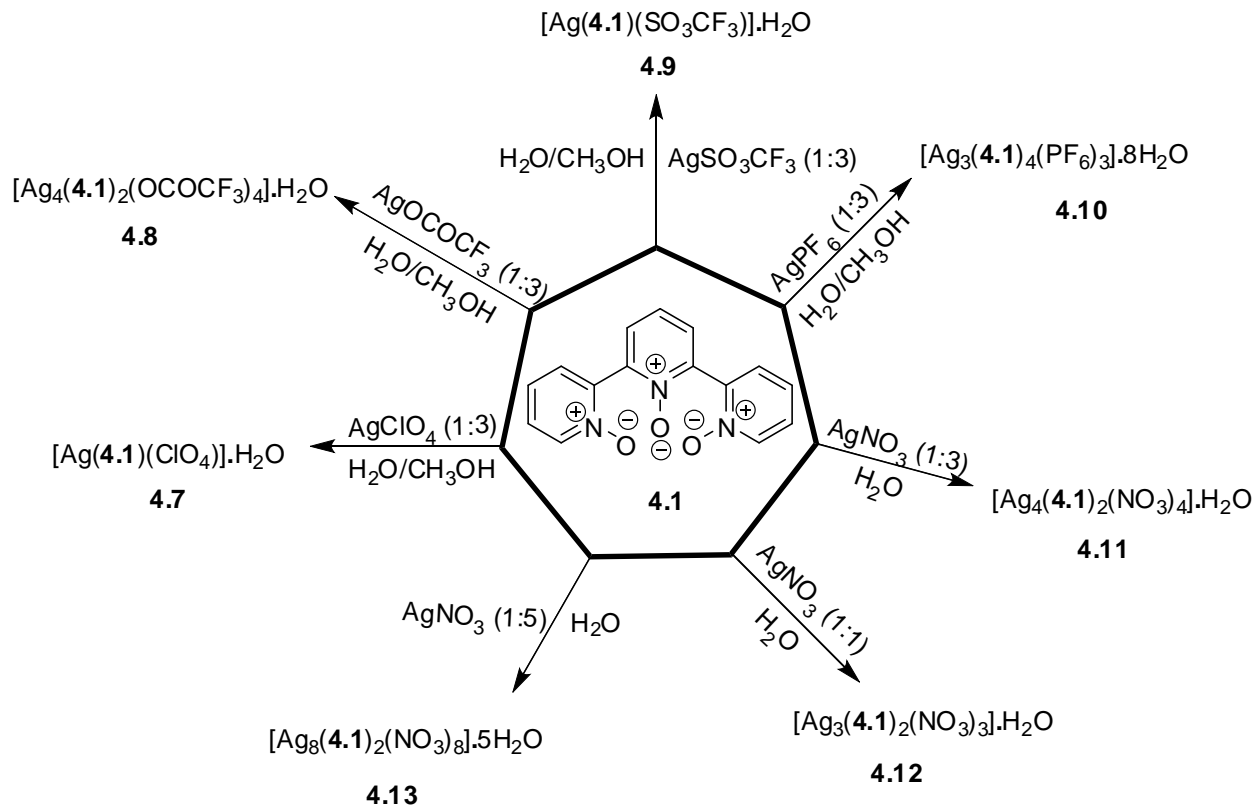


### 4.3 Syntheses of silver(I) complexes

Attempts to grow crystals of silver(I) complexes with ligand **4.2**, **4.3** and **4.4** were unsuccessful and resulted in yellow powders. Using a wide range of crystallisation methods, solvent combinations and different stoichiometric ratios of ligands to silver(I), all attempts were unsuccessful in producing good quality crystals for X-ray crystallography.

Due to the limited publications on the donor properties of terpyO<sub>3</sub> (**4.1**) and the characterisation of its complexes, we undertook a study of the silver(I) complexes to examine the effects of its C-C flexibility and its ability to coordinate metal centers. In this section, we describe the novel products from the reactions of the salts AgClO<sub>4</sub>, AgOCOCF<sub>3</sub>, AgSO<sub>3</sub>CF<sub>3</sub>, AgPF<sub>6</sub> and AgNO<sub>3</sub> with ligand **4.1** in the molar ratios shown in scheme 4.5. All the complexes were prepared by dissolving the silver(I) salts either in water or methanol and adding this to the ligand **4.1** dissolved in water. Water molecules were included in the asymmetric unit, as shown in scheme 4.5. The complexes obtained from AgClO<sub>4</sub> and AgPF<sub>6</sub> are discrete, whilst from other silver(I) salts complexes **4.8**, **4.9**, **4.10**, **4.11** and **4.12** were infinite one-dimensional polymers and **4.13** was three dimensional.

The counter-anion plays a significant role in influencing the network structures. The silver(I) nitrate complexes **4.11** – **4.13** display a variety of coordination modes, and ligand **4.1** adopted a  $\mu_6$ -O,O,O',O',O'',O'' coordination mode in complex **4.13**, which has a 1:4 ligand:AgNO<sub>3</sub> ratio. The nitrate anion has shown seven different coordination modes depending on the ratios of the reactants.

Scheme 4.5 – Syntheses of complexes **4.7** – **4.13**.

#### With silver(I) perchlorate (1:3) **4.7**

The asymmetric unit of complex **4.7** contains one ligand **4.1**, one silver(I) ion, a monodentate perchlorate anion [Cl1] and a water molecule. The complex is a discrete structure and solved in the monoclinic  $P2_1/n$  space group with a 1:1 ligand to silver(I) ratio, as shown in figure 4.5. The **4.1** molecules show  $\mu_4-O, O', O'', O'''$  coordination modes with N-O<sub>ligand</sub>-Ag angles ranging from 113.37(1)° to 121.60(1)°. The Ag-O<sub>ligand</sub> bond lengths to **4.1** vary from 2.355(2) Å to 2.539(2) Å. The average Ag-O bond lengths are longer than typical bond lengths observed in Cu<sup>2+</sup> and Ni<sup>2+</sup> complexes with ligand **4.1**.<sup>[66, 180]</sup> The N2-O2 and N3-O3 groups are monodentate and are skewed with a bite angle of 78.94(6)° [O2-Ag1-O3], while the N1-O1 groups bridge Ag1 ions at an angle of 98.62(6)° [Ag1-O1-Ag1], forming a four-membered Ag<sub>2</sub>O<sub>2</sub> rhombus core around the inversion center. Each of these Ag1 ions adopt a five coordinate geometry with five oxygens. The five-coordinate Ag1 has a  $\tau_5$  parameter<sup>[181]</sup> of 0.032, implying square pyramidal geometry with only 3.2% trigonal bipyramidal character. The observed torsion angles between the aromatic rings [N1-C5-C6-N2 = 68.6(3)°, N2-C10-C11-N3 = 70.7(3)°] of the terpyridine moieties are higher than the reported angles in Cu<sup>2+</sup> and Ni<sup>2+</sup> complexes.<sup>[66, 180]</sup>

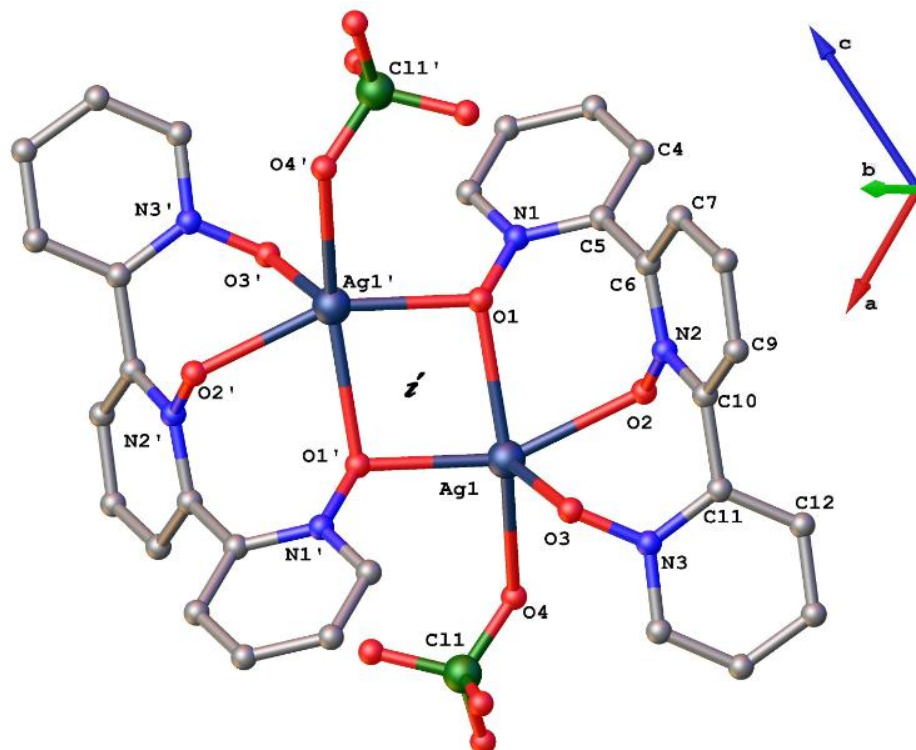


Figure 4.5 – Discrete structure of complex **4.7**. Hydrogen atoms and water molecules are excluded for clarity. Selected bond lengths (Å) and bond angles (°): N1-O1 = 1.323(3), N2-O2 = 1.310(3), N3-O3 = 1.313(3), Ag1-O1 = 2.539(2), Ag1'-O1 = 2.299(2), Ag1-O2 = 2.355(2), Ag1-O3 = 2.417(2), Ag1-O4 = 2.573(2), N1-O1-Ag1 = 121.60(1), N1-O1-Ag1' = 120.36(1), N2-O2-Ag1 = 113.37(1), N3-O3-Ag1 = 113.63(2), Ag1-O1-Ag1' = 98.62(6), O1'-Ag1-O2 = 155.46(6), O1-Ag1-O4 = 157.43(7), O1-Ag1-O3 = 105.79(7), O2-Ag1-O3 = 78.95(6), O1-Ag1-O1' = 81.38(6), O2-Ag1-O1 = 74.08(6), O2-Ag1-O3 = 78.94(6), O2-Ag1-O4 = 107.44(7), O3-Ag1-O1 = 100.71(6), O3-Ag1-O4 = 101.67(7), N1-C5-C6-N2 = 68.6(3), N2-C10-C11-N3 = 70.7(3).

As a consequence of the symmetry, the four-membered ring forms a parallelogram with two unequal distances 2.539(2) Å [Ag1-O1] and 2.299(2) Å [Ag1'-O1]. The non-bonding Ag-Ag distance is 3.672(1) Å. Two monodentate perchlorate anions are coordinated to the silver(I) ions at distances of 2.573(2) Å, *syn* to the O3 oxygen at an angle 101.67(7)° [O3-Ag1-O4] relative to the four-membered Ag<sub>2</sub>O<sub>2</sub> ring, as shown in figure 4.5. In the extended structure, the terminal and middle monodentate pyridine N-oxides exhibit  $\pi$ - $\pi$  interactions with a centroid-centroid distance of 3.788 Å, as shown in figure 4.6.

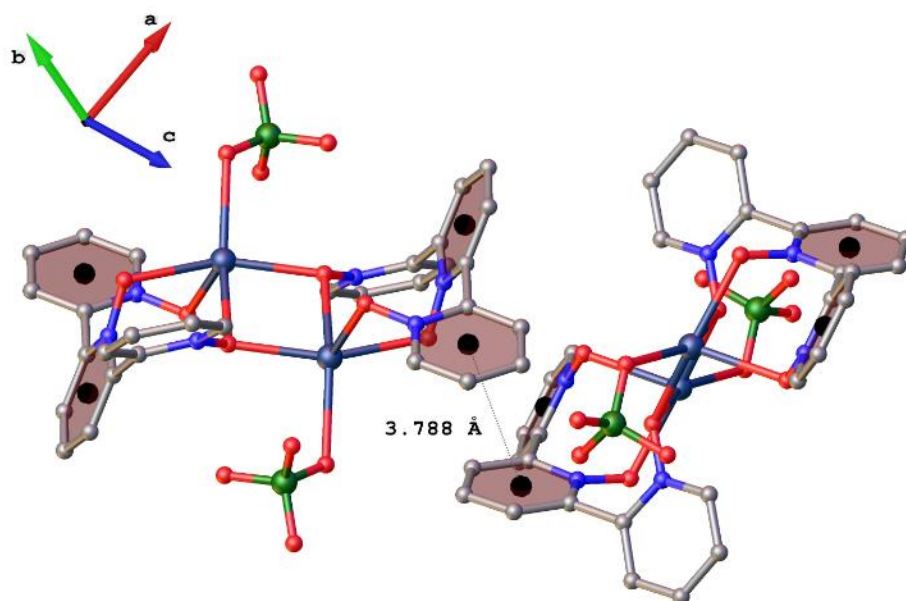


Figure 4.6 – A section of the crystal packing of complex **4.7**, showing  $\pi$ - $\pi$  interactions. Hydrogen atoms are excluded for clarity.

#### With silver(I) trifluoroacetate (1:3) **4.8**

Complex **4.8** crystallised in the triclinic  $P-1$  space group with two **4.1** ligand molecules, four silver(I) trifluoroacetates and a coordinated monodentate water molecule [O15], as shown in figure 4.7. The complex has a 1:2 ligand to silver(I) ratio. The ligand molecules adopted two coordination modes with  $\mu_5$ -O,O,O',O',O'' and  $\mu_3$ -O,O,O'' coordination. The average N-O bond distances 1.316 Å are smaller than reported for  $\text{Cu}^{2+}$ [180] [1.347 Å],  $\text{Ni}^{2+}$ [66] [1.334 Å] and  $\text{Eu}^{3+}$ [68] [1.329 Å] complexes, but greater than the reported ligand **4.1** [1.297 Å] N-O distances.<sup>[182]</sup> Of the two ligand molecules shown in the asymmetric unit, the shortest N-O bond distance is the non-coordinated N5-O5 group, whilst the longest are N3-O3 and N4-O4 [1.325 Å] groups coordinating to the Ag3 and Ag3' silver(I) ions. The non-bonding distance between O5 and Ag3' is 2.659 Å. As seen in figure 4.7, two hydrogens [H15A and H15B] of the water [O15] and the terminal proton [H1] of ligand **4.1** are interacting with oxygens [O6, O10' and O11] at D $\cdots$ A distances of 2.719 Å, 2.736 Å and 3.069 Å respectively. Other parameters related to the hydrogen bonds are shown in table 4.2.

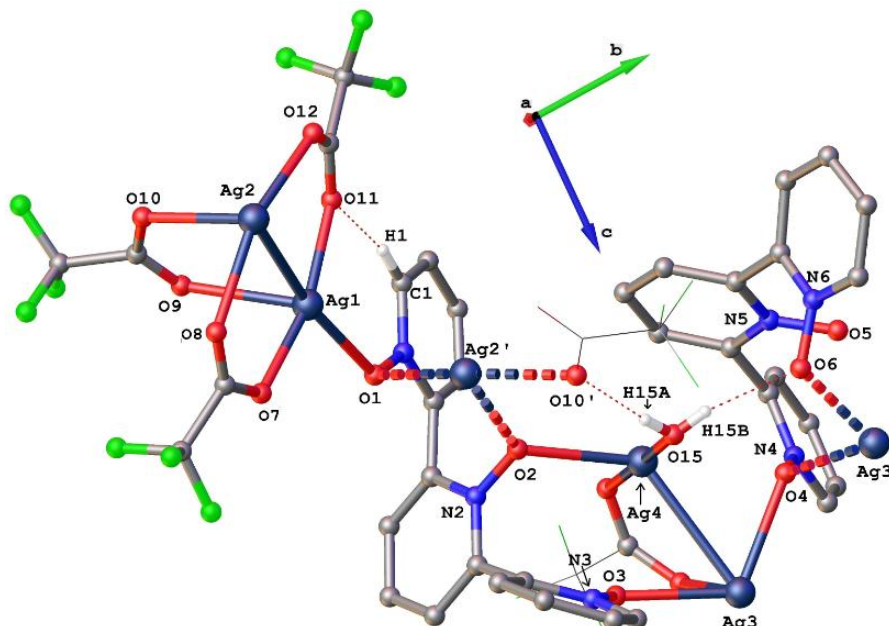


Figure 4.7 – Asymmetric unit of complex **4.8**. Selected  $-\text{CF}_3$  groups are shown in wireframe for clarity. Selected hydrogen atoms are omitted for clarity. Selected bond lengths ( $\text{\AA}$ ) and bond angles ( $^\circ$ ): N1-O1 = 1.313(3), N2-O2 = 1.316(3), N3-O3 = 1.326(3), N4-O4 = 1.324(3), N5-O5 = 1.300(3), N6-O6 = 1.317(3), Ag1-O1 = 2.548(2), Ag2'-O1 = 2.507(2), Ag4-O2 = 2.500(2), Ag2'-O2 = 2.495(2), Ag3-O3 = 2.370(2), Ag3-O4 = 2.455(2), Ag3'-O4 = 2.489(2).

Table – 4.2 Hydrogen bond parameters for complex **4.8**.

D-H $\cdots$ A	$d_{\text{D-H}}(\text{\AA})$	$d_{\text{H}\cdots\text{A}}(\text{\AA})$	$d_{\text{D}\cdots\text{A}}(\text{\AA})$	$\angle \text{D-H}\cdots\text{A}(^\circ)$
O15-H15A $\cdots$ O10'	0.757	1.980	2.745	175.75
O15-H15B $\cdots$ O6	0.744	1.987	2.719	168.13
C1-H1 $\cdots$ O11	0.930	2.164	3.069	164.17

Complex **4.8** is a 1D polymer with an AB connection mode as shown in figure 4.8. Unit – A comprises four silver(I) ions bridged by six trifluoroacetate groups in a paddle wheel arrangement, as shown in figure 4.9. Unit – B contains four **4.1** ligand molecules bridged over four silver(I) ions with two coordinated water molecules, as shown in figure 4.10.

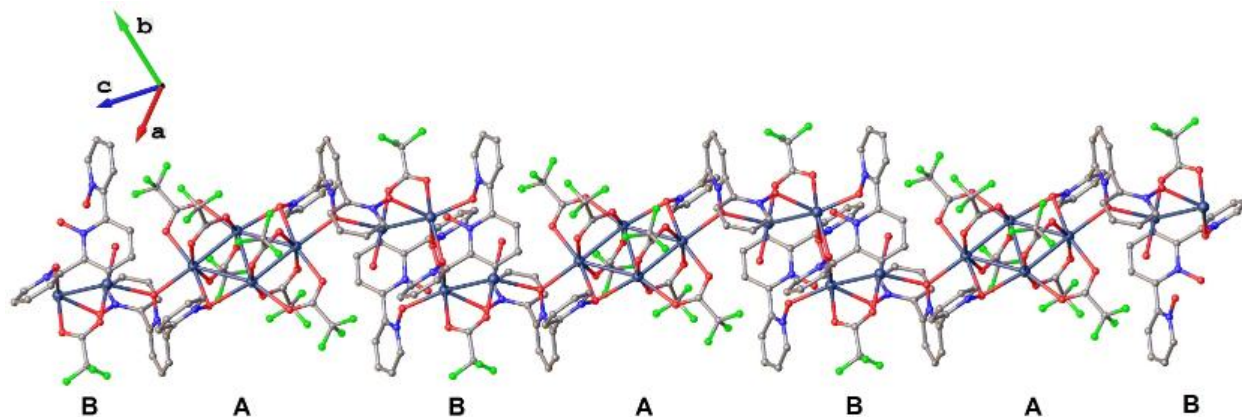


Figure 4.8 – The 1D polymeric structure of complex **4.8**. Hydrogen atoms are omitted for clarity.

### Unit – A

Four silver(I) ions, Ag1 and Ag2 and the inversion center related Ag1' and Ag2', form a four-membered rhombus Ag<sub>4</sub> core with two unequal Ag-Ag bond distances of 2.894(3) Å [Ag1-Ag2] and 3.243(3) Å [Ag1-Ag2'], as shown in figure 4.9. Four trifluoroacetate anions bridge the Ag1...Ag2 and Ag1'...Ag2' interactions. Ag1 and Ag1' interact diagonally at a distance of 2.990(4) Å, dividing the parallelogram into two triangles. The angles at the seven-coordinate Ag1 and Ag2 ions are Ag2-Ag1-Ag2' = 122.02(8)° and Ag1-Ag2-Ag1' = 57.98(8)° whilst the angles at the diagonal are Ag1-Ag1'-Ag2' = 55.19(7)° and Ag2-Ag1-Ag1' = 66.87(8)°. The Ag-O<sub>anion</sub> bond lengths in unit – A vary from 2.220(2) Å to 2.507(2) Å, with seven [Ag1] and six [Ag2] coordinate geometry silver(I) ions.

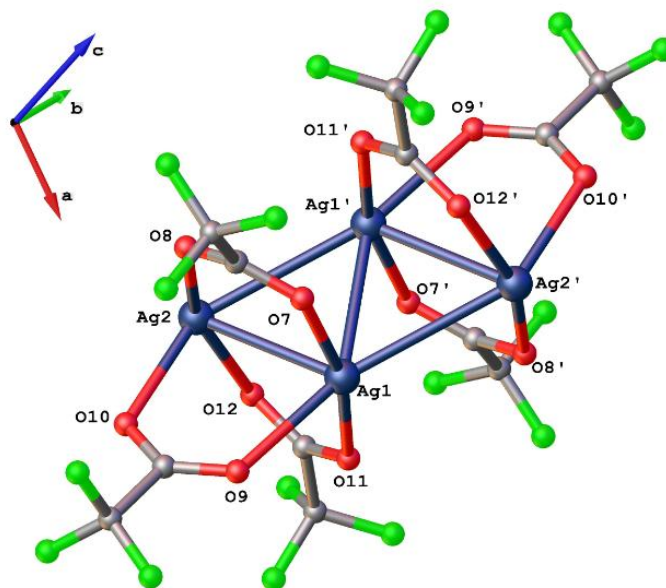


Figure 4.9 – Section of the 1D polymeric structure of complex **4.8**, unit – A. Hydrogen atoms are excluded for clarity. Selected bond lengths (Å) and bond angles (°): Ag2-O2 = 2.495(2), Ag1-O7 = 2.220(2), Ag2-O8 = 2.370(2), Ag1-O9 = 2.507(2), Ag2-O10 = 2.402(2), Ag1-O11 = 2.234(2), Ag2-O12 = 2.342(2), Ag1-

Ag2 = 2.894(3), Ag1-Ag2' = 3.243(3), Ag3-Ag4 = 3.076(3), Ag1-Ag1' = 2.990(4), Ag1-O1 = 2.548(2), O1-Ag2' = 2.507(2), Ag2-Ag1-Ag2' = 122.02(8), Ag1-Ag1'-Ag2' = 55.19(7), Ag2-Ag1-Ag1' = 66.87(8), Ag1-Ag2-Ag1' = 57.98(8), O1-Ag1-Ag2 = 170.83(4), O2-Ag2-Ag1 = 176.91(4).

### Unit – B

Unit – B consists of four molecules of **4.1** and four silver(I) ions around an inversion center in a four-membered Ag<sub>2</sub>O<sub>2</sub> [Ag3-O4-Ag3'-O4'] ring formed from two terminal pyridine N-oxides bridging the Ag3 and Ag3' ions. Only half the structure of unit – B is shown in figure 4.10. Ligand molecules in unit – B have  $\mu_5$ -O,O,O',O',O'' and  $\mu_3$ -O,O,O'' coordination modes with silver(I) ions Ag3 and Ag4 in six- and four-coordinate geometry, respectively. The four-coordinate Ag4 atom has a seesaw geometry with a  $\tau_4$  index<sup>[183]</sup> of 0.36. The  $\mu_3$ -O,O,O'' ligand has a non-coordinating N5-O5 group with the external oxygens [O4 and O6] attached to the Ag3 ion, forming a ten-membered ring with a bite angle [O6-Ag3-O4] 97.0(6)°. O4 also bridges Ag3 and Ag3' with an angle of 107.13(7)°. The  $\mu_5$ -O,O,O',O',O'' ligand is coordinated to all four silver(I) ions [Ag1 to Ag4], as shown in figure 4.10. To the best of our knowledge, the bridging angle made by O2 with Ag2 and Ag4 [131.27(7)°], is the largest to date in a pyridine N-oxide metal complex. Ag3 and Ag4 interact at a distance of 3.076(3) Å with a bridging trifluoroacetate anion [shown in wire frame for clarity]. The average bond lengths [Ag-O<sub>ligand</sub> = 2.480 Å] of the ligand molecules in complex **4.8** are longer than those in the previously reported metal complexes of ligand **4.1**. Finally, the observed torsional angles for the ligands **4.1** vary from 64.5(3)° to 88.4(3)°.

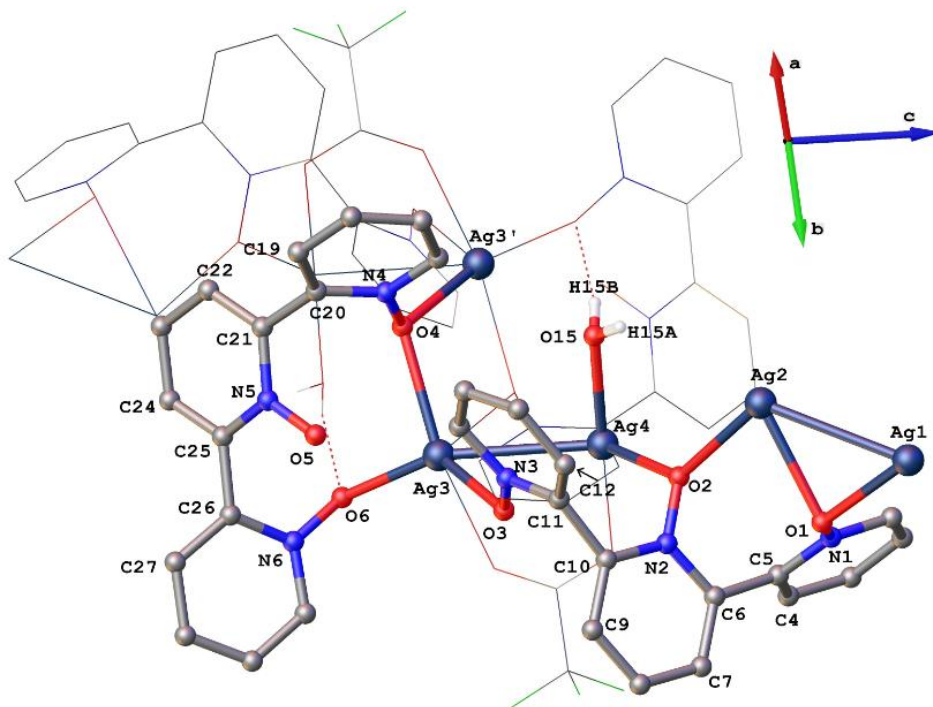


Figure 4.10 – Section of the 1D polymeric structure of complex **4.8**. Selected atoms and bonds are shown in wireframe for clarity. Selected hydrogen atoms are excluded for clarity. Selected bond lengths (Å) and

bond angles ( $^{\circ}$ ): Ag3-Ag4 = 3.076(3), Ag3-O4-Ag3 = 107.13(7), Ag2-O2-Ag4 = 131.27(7), O6-Ag3-O4 = 97.0(6), N1-C5-C6-N2 = 72.9(3), N2-C10-C11-N3 = 88.4(3), N4-C20-C21-N5 = 65.7(3), N5-C25-C26-N6 = 64.5(3).

#### With silver(I) triflate (1:3) 4.9

The complex **4.9** crystallised as colourless rectangular blocks and was solved in the triclinic  $P-1$  space group. The asymmetric unit of complex **4.9** comprises one ligand, two silver(I) triflates and a bidentate bridging water [O10], as shown in figure 4.11. The complex has a 1:2 ligand to silver(I) ratio. The oxygens O1 and O2 are monodentate while O3 bridges Ag2 and Ag1' at an angle of 126.11(6) $^{\circ}$ . Oxygens O2 and O3 are skewed at Ag2 to form a stable seven-membered ring, as observed in other reported metal complexes of **4.1**.<sup>[65, 68]</sup> Two oxygens, O1 and O2, coordinate Ag1 and Ag2 in a monodentate fashion, while O10 bridges Ag1 and Ag2 at an angle, Ag2-O10-Ag1 = 102.23(6) $^{\circ}$  to form a nine-membered ring, as shown in figure 4.11. The ligand **4.1** has a  $\mu_4$ -O,O',O'',O''' coordination mode with an average N-O bond length of 1.320(2) Å. These are slightly longer than in complex **4.8** but exhibit stronger coordination as measured by the Ag-O<sub>ligand</sub> bond length [2.435(2) Å]. The torsion angles for ligand **4.1** 67.9(3) $^{\circ}$  [N1-C5-C6-N2] and 72.2(2) $^{\circ}$  [N2-C10-C11-N3] fall in the range of angles obtained in complex **4.8**.

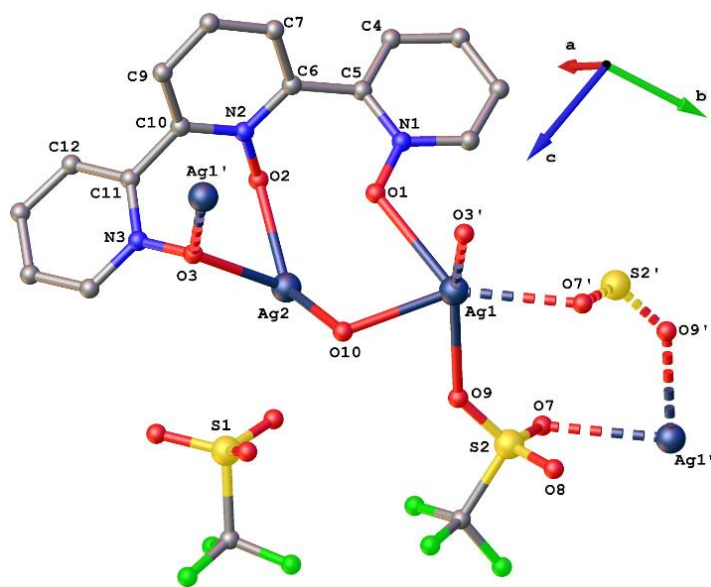


Figure 4.11 – Asymmetric unit of complex **4.9**. Hydrogen atoms are excluded for clarity. Selected bond lengths (Å) and bond angles ( $^{\circ}$ ): N1-O1 = 1.328(2), N2-O2 = 1.310(2), N3-O3 = 1.324(2), Ag1-O1 = 2.568(2), Ag2-O2 = 2.363(2), Ag2-O3 = 2.445(2), Ag1'-O3 = 2.366(2), Ag2-O3-Ag1 = 126.11(6), Ag2-O10-Ag1 = 102.23(6), N1-C5-C6-N2 = -67.9(3), N2-C10-C11-N3 = 72.2(2).

Ag1 and Ag2 silver(I) ions have five- and three-coordinate geometry respectively, with a bridging bidentate triflate [S2] and a non-coordinating [S1] triflate anion, as shown in figure 4.11. The five-coordinate Ag1 has a  $\tau_5$  parameter<sup>[183]</sup> of 0.030, implying square pyramidal geometry with only



3% trigonal bipyramidal character. Two ligand **4.1** [O3] oxygens and two water [O10] oxygens bridge four silver(I) ions in a zigzag arrangement to form an eight membered  $\text{Ag}_4\text{O}_4$  ring arrangement [viewed in the *ab*-plane] as shown in figure 4.12b. Each  $\text{Ag}_4\text{O}_4$  eight-membered ring is linked to another eight-membered ring of two Ag1 ions bridged by bidentate triflate anions to give a 1D polymeric structure, as shown in figure 4.12a.

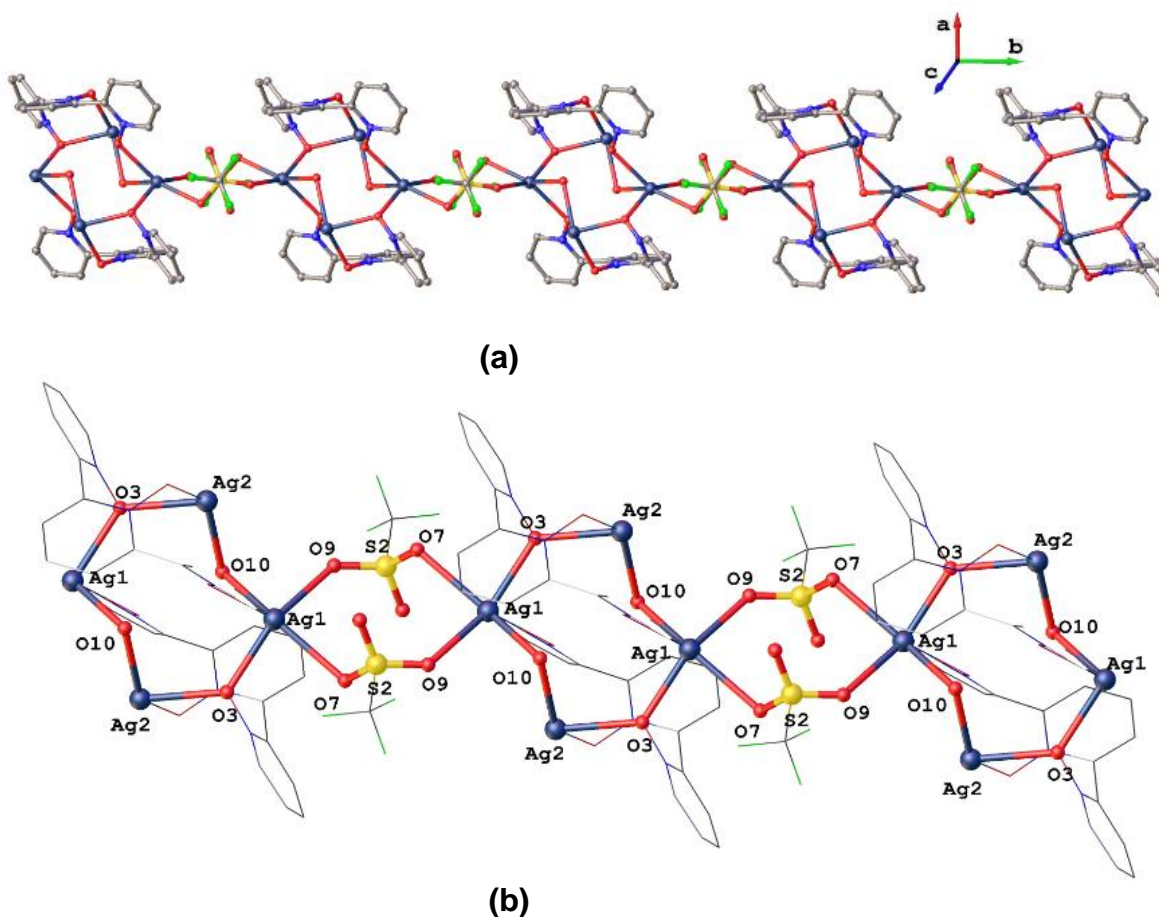


Figure 4.12 – (a, b) Perspective view of the 1D polymeric structure in complex **4.9**. Ligand molecules in 4.12b are shown in wireframe for clarity.

Elemental analysis for complex **4.9** was consistently low in carbon and nitrogen and a satisfactory agreement could not be obtained due to the presence of two complexes with 1:2 and 1:3 ligand to silver(I) ratio in the bulk sample. Crystals of the second complex were separated by hand. Due to serious disorder in the crystal structure of this complex, it is not discussed in this thesis. In order to confirm the homogeneity of the sample, XRPD was recorded. The data shown in figure 4.13, indicates that the bulk sample [red trace] best fits with the 1:2 complex [black trace] and not with the 1:3 complex [blue trace], inspite of being a mixture.

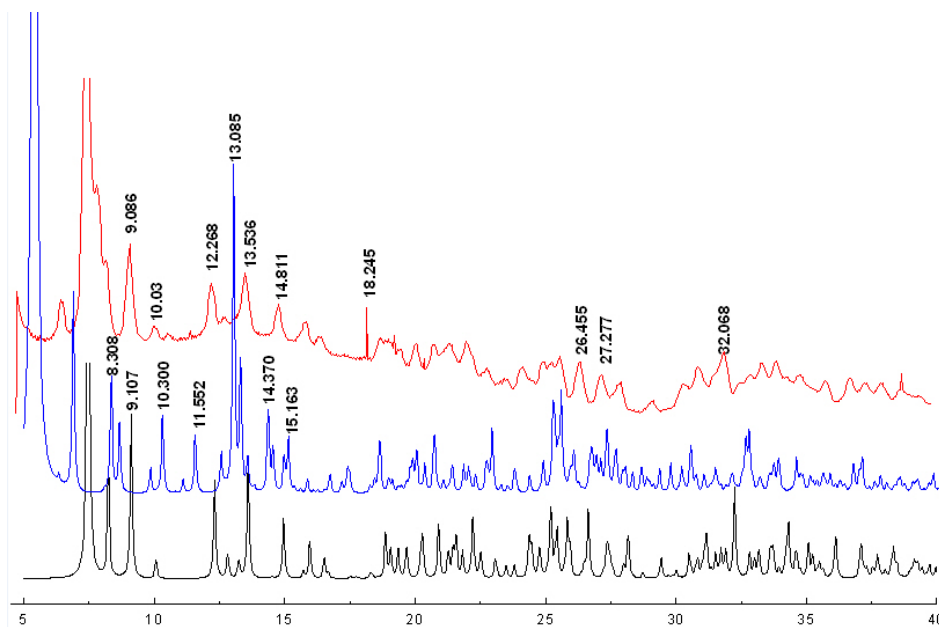


Figure 4.13 – PXRD pattern of complexes: Red trace – bulk sample PXRD from complex **4.9**. Black trace – computer generated PXRD of complex **4.9** [1:2 ligand to silver(I) ratio]. Blue trace – computer generated PXRD spectrum of disorder complex solved with 1:3 ligand to silver(I) ratio.

#### With silver(I) hexafluorophosphate (1:3) **4.10**

The structure of complex **4.10** solved in the monoclinic  $C2/c$  space group and has a six-coordinate Ag(I) center in a slightly distorted octahedral geometry with two ligand **4.1** molecules coordinated facially, as shown in figure 4.14. The asymmetric unit has a 4:3 ligand to silver(I) ratio with four water molecules, one of which has monodentate coordination to Ag<sub>2</sub> at a distance of 2.387(2) Å [Ag<sub>2</sub>-O7], as shown in figure 4.14. The ligands **4.1** have  $\mu_4-O,O',O'',O''$  and  $\mu_3-O,O',O''$  coordination modes with Ag(I) ions with N-O<sub>ligand</sub>-Ag angles ranging from 113.06(1)° to 117.49(1)°. This facial arrangement is similar to that previously reported for Cu<sup>2+</sup> and Ni<sup>2+</sup> complexes of **4.1**.<sup>[66, 180]</sup> The N-O bond distances range from 1.302(3) Å to 1.330(3) Å, and these bond lengths are comparable to those observed in Eu<sup>3+</sup> complexes of **4.1**.<sup>[68]</sup> The O-Ag-O bond angles around Ag1 ion are 167.57(6)° [O2-Ag1-O6], 163.63(6)° [O3-Ag1-O5] and 155.15(6)° [O4-Ag1-O1]. These O-Ag-O bond angles around the octahedral metal vary greatly in terpyO<sub>3</sub> based ligand complexes due to C-C bond rotations. The Ag-O bond distances range from 2.408(2) Å to 2.454(2) Å, and their average is higher than values observed for an octahedral Cu<sup>2+</sup> surrounded by two **4.1** molecules.<sup>[180]</sup>

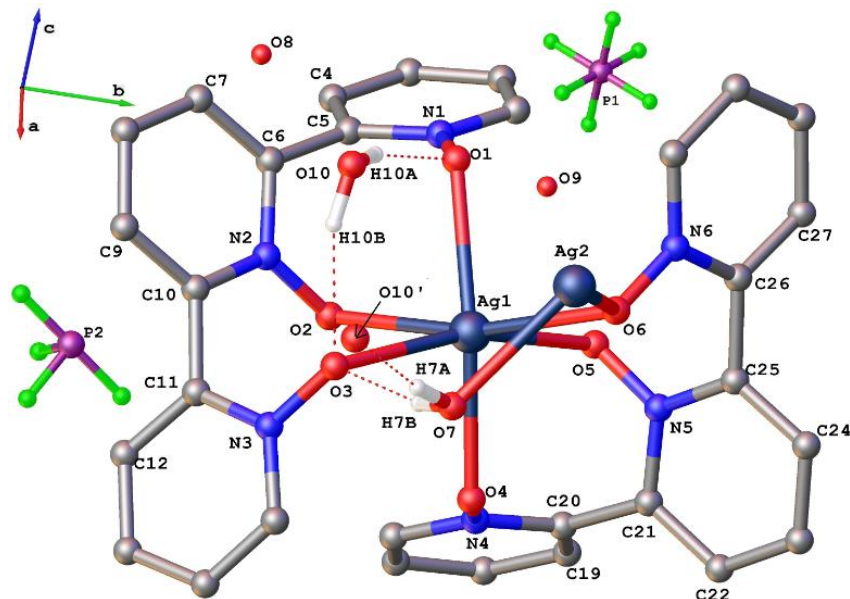


Figure 4.14 – Asymmetric unit of complex **4.10**. Selected hydrogen atoms are omitted for clarity. Selected bond lengths (Å) and bond angles (°): N1-O1 = 1.324(3), N2-O2 = 1.306(2), N3-O3 = 1.328(3), N4-O4 = 1.307(3), N5-O5 = 1.302(3), N6-O6 = 1.330(3), Ag1-O1 = 2.440(2), Ag1-O2 = 2.416(2), Ag1-O3 = 2.449(2), Ag1-O4 = 2.408(2), Ag1-O5 = 2.430(2), Ag1-O6 = 2.454(2), Ag2-O7 = 2.387(2), O4-Ag1-O1 = 155.15(6), O5-Ag1-O3 = 163.63(6), O2-Ag1-O6 = 167.57(6), N1-O1-Ag1 = 115.94(1), N2-O2-Ag1 = 113.06(1), N3-O3-Ag1 = 115.38(13), N4-O4-Ag1 = 117.16(13), N5-O5-Ag1 = 109.90(1), N6-O6-Ag1 = 111.26(1), N6-O6-Ag2 = 117.49(1), Ag2-O6-Ag1 = 109.65(7), O2-Ag1-O1 = 75.36(5), O2-Ag1-O3 = 75.41(6), O4-Ag1-O5 = 75.51(6), O5-Ag1-O6 = 78.36(6).

Complex **4.10** has a discrete structure with two octahedral Ag1 ions surrounded by ligands **4.1** in a facial manner, and connected by a four-coordinate, tetrahedral Ag2 ion, as shown in figure 4.15. In figure 4.15, both ligands coordinate to Ag1 ion forming stable seven-membered rings but only one ligand uses its terminal pyridine N-oxide oxygen [O6/O6'] to bridge Ag1 and Ag2 at an angle of 109.65(7)°. The average bite angle for the seven-membered rings formed by the oxygen donors is 75.41(6)°, O5-Ag1-O6 = 78.36(6)° is unique due to the oxygen O5 bridging the Ag1 and Ag2 ions. Ag2 has a distorted tetrahedral geometry [ $\tau_4 = 0.810$ ]<sup>[183]</sup> with an AgO<sub>4</sub> coordination sphere. The angles around Ag2 are 137.05(9)° [O6-Ag2-O6'], 106.04(1)° [O7-Ag2-O7'] and 108.62(6)° [O6-Ag2-O7].

The hydrogens of the O7 and O10 water molecules interact with the O3 and O1 oxygens of the terminal pyridine N-oxide rings at distances of 1.922 Å [O7-H7B...O3], 1.871 Å [O10-H10A...O1] and 1.896 Å [O10-H10B...O3] to form six-membered rings as shown in figure 4.14. The hydrogen bond parameters are shown in table 4.3. The  $\mu_3$ -O, O', O'' ligand around Ag1 show  $\pi$ - $\pi$  interactions in the crystal packing with a centroid-centroid distance of 3.616 Å. The PF<sub>6</sub> anions are non-coordinating as shown in figure 4.14.

Table – 4.3 Hydrogen bond parameters in complex **4.10**

D-H...A	$d_{D-H}(\text{Å})$	$d_{H...A}(\text{Å})$	$d_{D...A}(\text{Å})$	$\angle D-H...A(^{\circ})$
O10-H10A...O1	0.888	1.871	2.740	165.81
O10-H10B...O3	0.971	1.896	2.836	162.09
O7-H7A...O10'	0.847	1.916	2.576	171.50
O7-H7B...O3	0.889	1.922	2.790	164.73

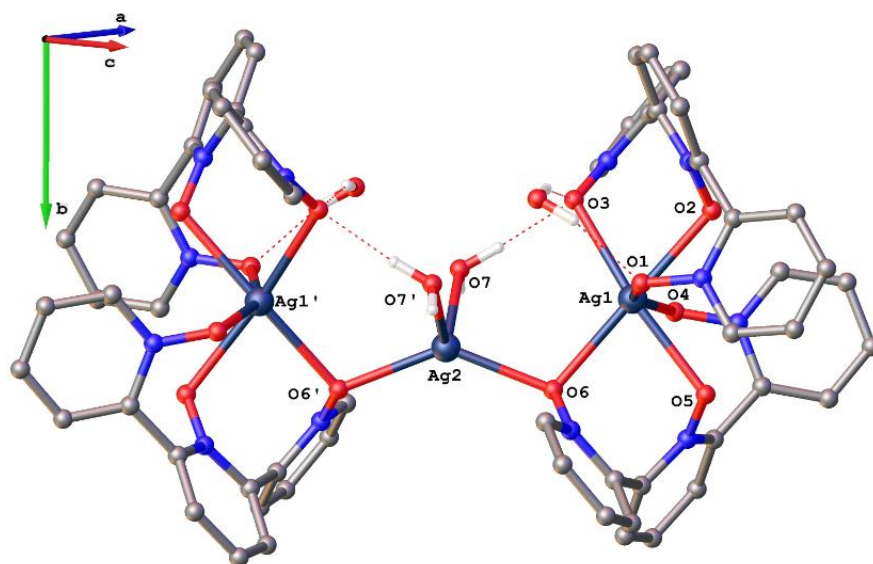


Figure 4.15 – Discrete unit of complex **4.10**. Selected hydrogen atoms are omitted for clarity. Selected bond lengths (Å) and bond angles ( $^{\circ}$ ): O6-Ag2-O6' = 137.05(9), O7-Ag2-O7' = 106.04(1), O6-Ag2-O7 = 108.62(6).

#### With silver(I) nitrate (1:3) **4.11**

The complex **4.11** of silver(I) nitrate with ligand **4.1** was solved in the monoclinic  $P2_1/n$  space group. Complex **4.11** was prepared by reacting a 1:3 equivalent ratio of ligand to  $\text{AgNO}_3$ . The asymmetric unit contains two **4.1** ligand molecules and four  $\text{AgNO}_3$  in a 1:2 ligand to silver(I) ratio with a coordinating [O19] monodentate water molecule interacting with a non-coordinated [O20] water molecule as shown in figure 4.16. The hydrogen bond parameters, are shown in table 4.4. The H19A and H19B hydrogens shown in figure 4.16 are involved in hydrogen bonding to acceptor atoms in the adjacent unit cell. Ligand **4.1** molecules have a  $\mu_5\text{-O,O,O',O'',O''}$  coordination mode with the external N-O and middle N-O groups in bidentate and monodentate coordination modes, respectively. The N-O distances range from 1.304(2) Å to 1.329(3) Å. The average of 1.317 Å shows that the N-O bond distances are double bond in character. The **4.1**

molecules exhibits weak interactions with the silver(I) ions at an average distance of 2.432 Å, similar to the Ag-O<sub>ligand</sub> distances observed in complex **4.9**. The  $\mu_2$ -O,O N3-O3 [135.22(8)°] and N6-O6 [137.82(7)°] groups bridge the silver(I) ions at angles larger than N1-O1 [105.54(7)°] and N4-O4 [93.09(6)°]. The N-O<sub>ligand</sub>-Ag angles range from 101.99(1)° to 126.63(1)°. The torsion angles [N<sub>ligand</sub>-C-C-N<sub>ligand</sub>] vary from 68.7(3)° to 69.2(3)°, as shown in figure 4.16, which fall in the range of those observed in complex **4.8**.

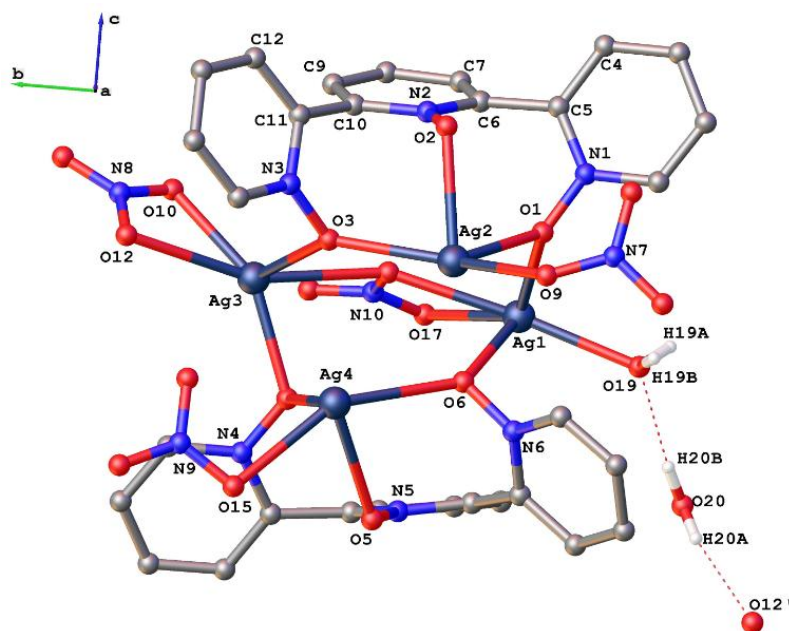


Figure 4.16 – Asymmetric unit of complex **4.11**. Selected hydrogen atoms are omitted for clarity. Selected bond lengths (Å) and bond angles (°): N1-O1 = 1.315(3), N-O2 = 1.311(2), N3-O3 = 1.329(3), N4-O4 = 1.322(3), N5-O5 = 1.304(2), N6-O6 = 1.322(2), Ag1-O1 = 2.412(2), Ag2-O1 = 2.369(2), Ag2-O2 = 2.452(2), Ag2-O3 = 2.395(2), Ag3-O3 = 2.433(2), Ag3-O4 = 2.275(2), Ag4-O4 = 2.432(2), Ag4-O5 = 2.499(2), Ag1-O6 = 2.517(2), Ag4-O6 = 2.568(2), N1-O1-Ag1 = 126.63(1), N1-O1-Ag2 = 126.62(1), N2-O2-Ag2 = 107.87(1), N3-O3-Ag2 = 121.09(1), N3-O3-Ag3 = 101.99(1), N4-O4-Ag3 = 123.96(1), N4-O4-Ag4 = 115.93(1), N5-O5-Ag4 = 115.51(1), N6-O6-Ag1 = 104.65(1), N6-O6-Ag4 = 114.72(1), Ag2-O1-Ag1 = 105.54(7), Ag2-O3-Ag3 = 135.22(8), Ag3-O4-Ag4 = 93.09(6), Ag1-O6-Ag4 = 137.82(7), N1-C5-C6-N2 = 69.2(3), N2-C10-C11-N3 = 69.6(3), N4-C20-C21-N5 = 66.2(3), N5-C25-C26-N6 = 68.7(3).

Table – 4.4 Hydrogen bond parameters in complex **4.11**.

D-H $\cdots$ A	<i>d</i> D-H(Å)	<i>d</i> H $\cdots$ A(Å)	<i>d</i> D $\cdots$ A(Å)	$\angle$ D-H $\cdots$ A(°)
O20-H20B $\cdots$ O19	0.850	1.957	2.786	164.49
O20-H20B $\cdots$ O19	0.850	2.018	2.833	160.48

The complex **4.11** is a 1D polymer running parallel to the *a*-axis [figure – 4.17a] with silver(I) ions in four- [Ag2 (seesaw:  $\tau_4 = 0.68$ )], five- [Ag3 (distorted square pyramidal:  $\tau_5 = 0.36$ ) and Ag4 (distorted square pyramidal:  $\tau_5 = 0.11$ )]<sup>[181, 183]</sup> and six- [Ag1] coordinate geometry, as shown in

figure 4.17b. The central pyridine N-oxide rings of the **4.1** ligand in the 1D polymer point in one direction along the *a*-axis [indicated by the solid black arrows]. The presence of four nitrates with different bonding modes in a silver(I) complex is very rare. The monodentate nitrate [N9] anion is coordinated to Ag4 at a distance of 2.522(2) Å, which in turn connects to Ag1' and Ag3' by a tetradentate nitrate anion [N10]. The two oxygens [O17 and O18] of N10 bridge three silver(I) ions in a tetradentate fashion at a mean Ag-N distance of 2.558 Å, as shown in figure 4.17b. Oxygen O9 of the N7 nitrate bridges Ag1 and Ag2' at an angle of 112.13(7)°, which is greater than those of the N1-O1 and N4-O4 groups of ligand **4.1**. The unsymmetrically chelating bidentate nitrate anion [N8] binds to Ag3 using two oxygens O10 and O12 at distances of 2.342(2) Å and 2.591(2) Å, with an internal bite angle of 50.41(7)° [O10-Ag3-O12].

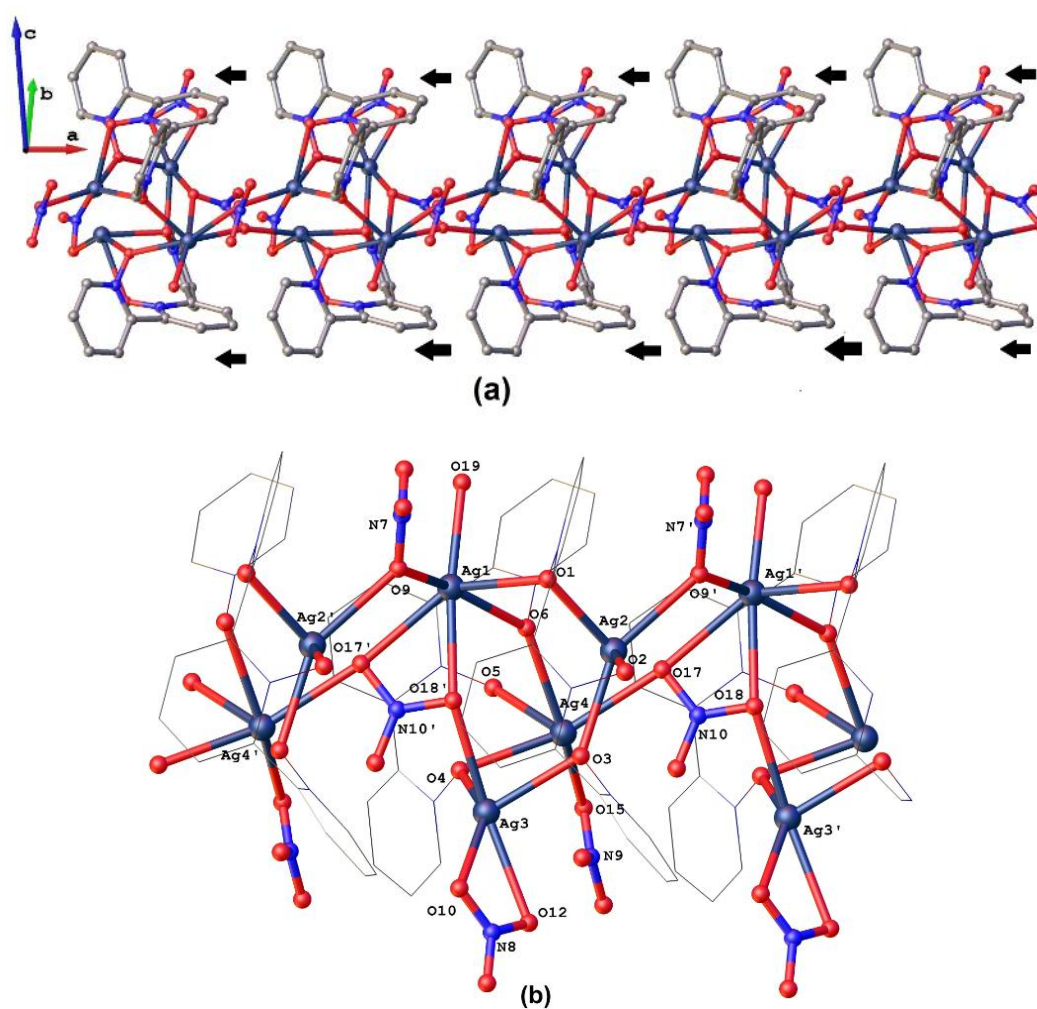


Figure 4.17 – (a) 1D Polymeric structure of complex **4.11**. Hydrogen atoms are omitted for clarity, and (b) a section of the polymer showing the nitrate anion bonding modes. **4.1** molecules are shown in wireframe for clarity. Selected bond lengths (Å) and bond angles (°): Ag4-O15 = 2.522(2), Ag1-O17 = 2.570(2), Ag4-O17 = 2.575(2), Ag3-O18 = 2.594(2), Ag1-O18 = 2.496(2), Ag3-O10 = 2.342(2), Ag3-O12 = 2.591(2), Ag1-O9-Ag2' = 112.13(7), O10-Ag3-O12 = 50.41(7).

### With silver(I) nitrate **4.12**

Complex **4.12** crystallized in the monoclinic  $P2_1/n$  space group and contains two **4.1** molecules, three  $\text{AgNO}_3$ , a coordinated water molecule [O16] and two non-coordinating water molecules [O17 and O18], as shown in figure 4.18. The bonding parameters are also shown in figure 4.18. The ligands **4.1** have a  $\mu_4\text{-O, O', O'', O''}$  and  $\mu_5\text{-O, O, O', O'', O''}$  coordination modes with N-O bond distances ranging from 1.297(6) Å to 1.342(7) Å and an average N-O bond distance of 1.323 Å, which is greater than in complex **4.11**. The average coordination abilities [ $\text{Ag-O} = 2.452$  Å] are weaker than in complex **4.11**, due to decreased denticity of the **4.1** molecules. The non-bonded distance between Ag1 and O6 is ca 2.661 Å, which is within the sum of the Van der Waals radii<sup>[184]</sup> for silver and oxygen (3.24 Å). The N3-O3 group in ligand **4.1** bridges Ag1 and Ag2 at an angle [ $\text{Ag1-O3-Ag2} = 94.44(2)^\circ$ ] which is smaller than the N6-O6 group [ $\text{Ag2-O6-Ag3} = 133.37(2)^\circ$ ].

The N-O<sub>ligand</sub>-Ag bond angles of ligand **4.1** range from  $109.3(3)^\circ$  to  $126.3(3)^\circ$ . Decreasing the reaction stoichiometry from 1:3 to 1:1 has caused some significant changes in the resulting structure. The coordination mode of the nitrate anions to silver(I) ions varies from  $\mu_4$ ,  $\mu_2$ ,  $\mu_1$ - in complex **4.11** to  $\mu_1$ - in complex **4.12**, which has a mean Ag-O distance of 2.374 Å, which is close to the distance of the monodentate water molecule [ $\text{Ag3-O16} = 2.349(5)$  Å] in complex **4.12**. The torsion angles [ $\text{N}_{\text{ligand}}\text{-C-C-N}_{\text{ligand}}$ ] of the ligands **4.1** varies from  $57.8(8)^\circ$  to  $66.6(8)^\circ$ .

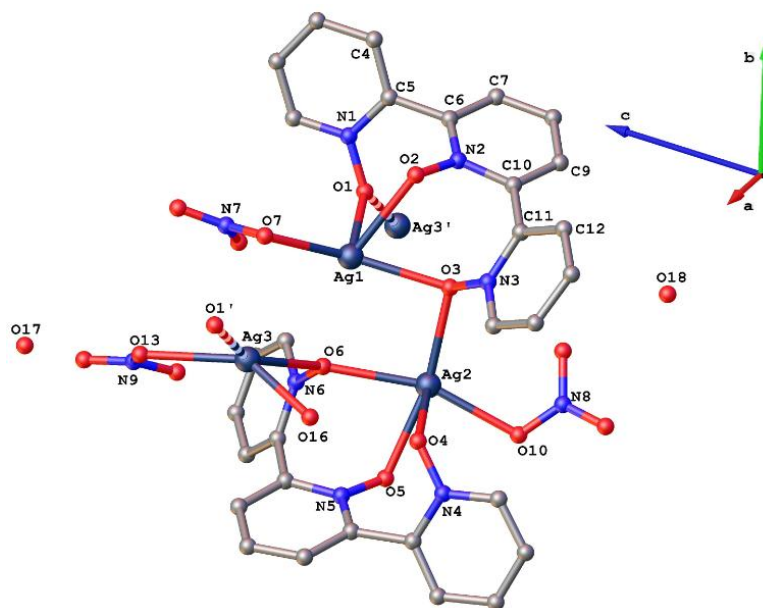


Figure 4.18– Asymmetric unit of complex **4.12**. Hydrogen atoms are excluded for clarity. Selected bond lengths (Å) and bond angles ( $^\circ$ ): N1-O1 = 1.335(8), N2-O2 = 1.297(6), N3-O3 = 1.342(7), N4-O4 = 1.322(7), N5-O5 = 1.312(6), N6-O6 = 1.331(7), Ag1-O1 = 2.421(5), Ag3'-O1 = 2.459(5), Ag1-O2 = 2.499(4), Ag1-O3 = 2.367(4), Ag2-O3 = 2.392(4), Ag2-O4 = 2.547(5), Ag2-O5 = 2.386(4), Ag2-O6 =

2.432(4), Ag3-O6 = 2.568(4), Ag1-O7 = 2.311(8), Ag2-O10 = 2.353(5), Ag3-O13 = 2.460(6), Ag3-O16 = 2.349(5), N1-O1-Ag1 = 114.4(4), N1-O1-Ag3' = 122.2(4), N2-O2-Ag1 = 116.3(3), N3-O3-Ag1 = 126.3(3), N3-O3-Ag2 = 116.7(3), N4-O4-Ag2 = 114.3(3), N5-O5-Ag2 = 117.5(3), N6-O6-Ag2 = 113.0(3), N6-O6-Ag3 = 109.3(3), Ag1-O1-Ag3' = 123.2(2), Ag1-O3-Ag2 = 94.44(16), Ag2-O6-Ag3 = 133.37(2), N1-C5-C6-N2 = -66.6(8), N2-C10-C11-N3 = 57.8(8), N4-C20-C21-N5 = 64.1(7), N5-C25-C26-N6 = -66.5(8).

Complex **4.12** is a one-dimensional polymer as shown in figure 4.19, with the four-coordinate Ag1 and Ag3 silver(I) ions in seesaw and tetrahedral geometries with  $\tau_4$  indexes of 0.69 and 1.0. The five coordinate Ag2 ion has distorted square pyramidal geometry with a  $\tau_5$  parameter<sup>[181]</sup> of 0.09. Though both complexes **4.11** and **4.12** crystallized in the monoclinic  $P2_1/n$  space group and grow along the *a*-direction, the central pyridine N-oxide rings point in opposite directions in complex **4.12**, which is different to complex **4.11**, as shown in figure 4.17a.

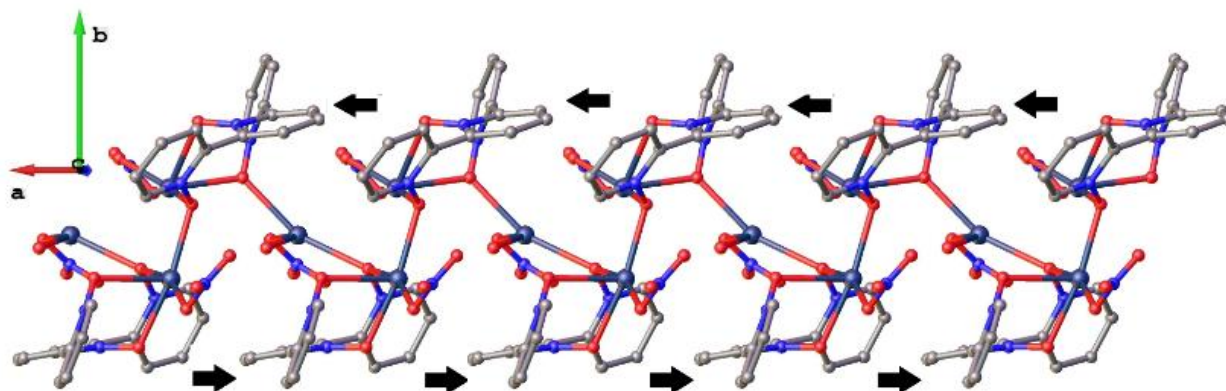


Figure 4.19 – (a) 1D Polymeric structure of complex **4.12**. Hydrogen atoms are omitted for clarity.

#### With silver(I) nitrate **4.13**

Complex **4.13** was formed from a reaction mixture containing a 1:5 ligand to AgNO<sub>3</sub> ratio. The asymmetric unit of complex **4.13**, solved in the triclinic  $P-1$  space group, contains two **4.1** molecules, eight silver(I) nitrates and five water molecules. Four waters are coordinated to Ag3, Ag4 and Ag7 ions in a monodentate fashion at distances of 2.324(3) Å [Ag7-O31], 2.432(3) Å [Ag7-O32], 2.375(3) Å [Ag3-O33] and 2.444(3) Å [Ag4-O34], as shown in figure 4.20. The complex **4.13** has a 1:4 ligand to silver(I) ratio. The **4.1** molecules have  $\mu_6$ -O, O, O', O', O'', O'' and  $\mu_5$ -O, O, O', O', O'' coordination modes with N-O bond distances ranging from 1.319(3) Å to 1.333(4) Å, the average N-O bond distance [1.327 Å] of  $\mu_5$ -O, O, O', O', O'' ligand **4.1** is similar to those observed in complex **4.11**. The coordination angles range from 116.68(2)° to 124.77(2)°, whilst the N-O bidentate groups Ag-O<sub>ligand</sub>-Ag bridging angles vary from 92.13(8)° to 116.50(9)°.



Complex **4.13** is a 3D polymer as shown in figure 4.23. The silver(I) ions have three- [Ag1], four- [Ag3 (seesaw:  $\tau_4 = 0.64$ ), Ag4 (seesaw:  $\tau_4 = 0.34$ ), Ag5 (seesaw:  $\tau_4 = 0.37$ ), Ag7 (seesaw:  $\tau_4 = 0.37$ ) and Ag8 (distorted trigonal pyramidal:  $\tau_4 = 0.77$ )]<sup>[183]</sup> and six- [Ag2 and Ag6] coordinate geometries with Ag(I) ion coordination spheres surrounded by the oxygen donors of ligands **4.1** and nitrate anions. The Ag-O distances around the Ag(I) ions range from 2.346(2) Å to 2.529(2) Å for ligands **4.1**, and vary from 2.307(3) Å to 2.580(3) Å for the nitrate anions. The silvers Ag5 and Ag6 are weakly interacting with a separation of 3.340(4) Å.

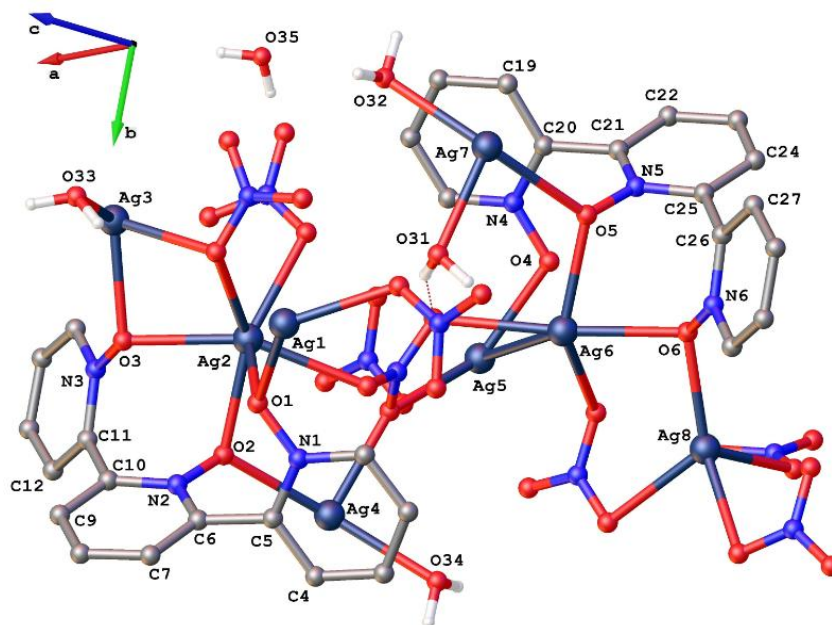


Figure 4.20 – Asymmetric unit of complex **4.13**. Selected hydrogen atoms are omitted for clarity. Selected bond lengths (Å) and bond angles: N1-O1 = 1.333(4), N2-O2 = 1.319(3), N3-O3 = 1.324(4), N4-O4 = 1.330(4), N5-O5 = 1.325(4), N6-O6 = 1.328(4), Ag7-O31 = 2.324(3), Ag7-O32 = 2.432(3), Ag3-O33 = 2.375(3), Ag4-O34 = 2.444(3), Ag5-Ag6 = 3.340(4), N1-O1-Ag1 = 116.68(2), N1-O1-Ag2 = 111.71(2), N2-O2-Ag2 = 111.94(2), N2-O2-Ag4 = 124.77(2), N3-O3-Ag3 = 124.52(2), N3-O3-Ag2 = 119.64(2), N4-O4-Ag5 = 113.29(2), N5-O5-Ag6 = 112.77(2), N5-O5-Ag7 = 124.30(2), N6-O6-Ag8 = 124.34(2), N6-O6-Ag6 = 116.55(2), Ag1-O1-Ag2 = 108.96(1), Ag2-O2-Ag4 = 112.11(9), Ag3-O3-Ag2 = 92.13(8), Ag6-O5-Ag7 = 116.50(9), Ag8-O6-Ag6 = 97.37(9).

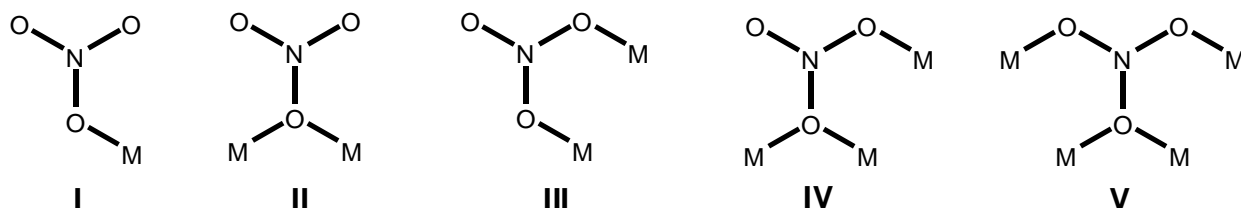


Figure 4.21 – Coordination modes of nitrate anions in complex **4.13**.

In some cases, nitrate anions exist simply as counter-ions in supramolecular assemblies but others are coordinated ligands. In complex **4.13**, the nitrate anions have five different coordination modes with Ag(I) ions [figure – 4.22], which is higher than in complex **4.11**. Modes I

to **IV** are the most commonly observed coordination modes in which the nitrate anions act as bridging ligands that make appropriate coordination sites for other ligand systems. Here we report the new mode **V** bridging four silver(I) ions, as shown in figure 4.21.

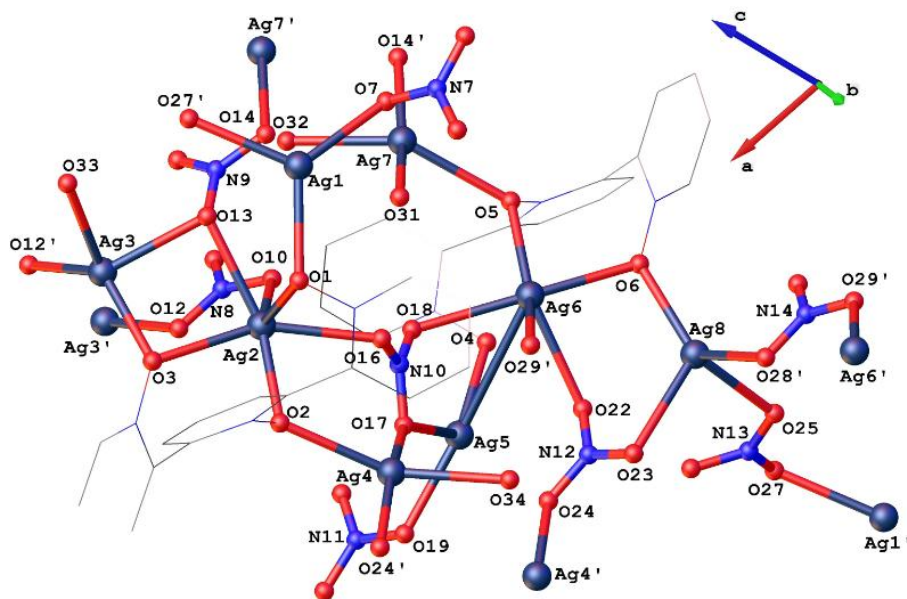


Figure 4.22 – Section of the 3D polymeric structure of complex **4.13**. Hydrogen atoms are omitted, and ligands **4.1** are shown in wireframe for clarity. Selected bond lengths (Å) and bond angles: Ag1-O1 = 2.346(2), Ag1-O7 = 2.384(3), Ag1-O27 = 2.429(3), Ag2-O2 = 2.376(2), Ag2-O3 = 2.423(2), Ag2-O10 = 2.436(3), Ag2-O16 = 2.483(3), Ag2-O13 = 2.493(3), Ag2-O1 = 2.500(2), Ag3-O3 = 2.386(2), Ag3-O12' = 2.466(3), Ag3-O13 = 2.522(3), Ag4-O24 = 2.388(3), Ag4-O17 = 2.415(3), Ag4-O2 = 2.529(2), Ag5-O19 = 2.307(3), Ag5-O4 = 2.370(3), Ag5-O17 = 2.550(4), Ag6-O5 = 2.350(2), Ag6-O29 = 2.392(3), Ag6-O6 = 2.410(2), Ag6-O18 = 2.531(3), Ag6-O22 = 2.580(3), Ag7-O14 = 2.421(3), Ag7-O5 = 2.569(2), Ag8-O6 = 2.375(2), Ag8-O25 = 2.479(4), Ag8-O28 = 2.519(3), Ag8-O23 = 2.559(3).

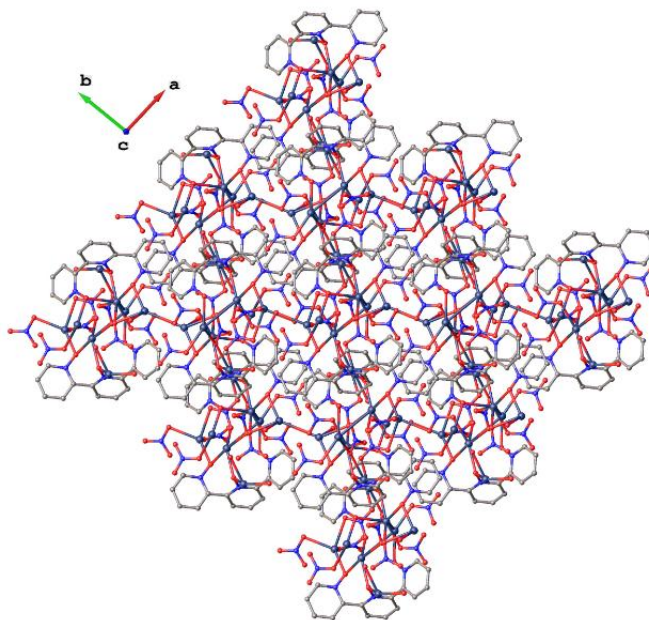


Figure 4.23 – 3D Polymer structure of complex **4.13** viewed down the *c*-axis. Hydrogen atoms are excluded for clarity.

## 4.4 Conclusions

We have synthesised seven new silver(I) coordination polymers of ligand **4.1** under similar conditions. This study demonstrates that the nature of the silver(I) salts employed plays a key role in tuning the structures from discrete to 3D coordination polymers. Also, the synthesis and characterisation of complexes **4.7– 4.13** has enabled the investigation of the structural diversity inherent to the polyvalent coordination ability of ligand **4.1**. Self-assembly between the chelating ligand **4.1** and  $\text{AgClO}_4$  resulted in a structure similar to Watson's dimeric bridges discussed in chapters 2 and 3. The competition between ligands **4.1** and silver(I) ions for coordination disfavour strong  $\text{Ag}\cdots\text{Ag}$  interactions in most of the complexes, except for **4.8**. The presence of strong  $\text{Ag}\cdots\text{Ag}$  interactions in complex **4.8** is probably related to the bridging nature of the trifluoroacetates.

With nitrate alone, three complexes **4.11 – 4.13** were synthesised and characterised by crystallographic methods. Significant differences were observed due to the variable coordinating behaviour of the nitrate anion towards silver(I) ions. This behaviour has influenced the other weak supramolecular forces present within the crystal packing structure, thus controlling the final motif in the solid state.

# **Chapter – 5**

## **Conclusions and future prospects**

This thesis reports the syntheses of three classes of pyridine N-oxides and their coordination chemistry with various silver(I) salts. Coordination polymers are constructed from pyridine N-oxides with silver(I) salts and show a preference to self-assemble into one dimensional motifs, as shown in figure 5.1. The pyridine N-oxide ligands coordinate to silver(I) through the oxygens of the N-O groups. The construction of more elaborate motifs was later driven by other weak interactions involving pyridine N-oxide ligands, substituents in the pyridine rings, counterions, and solvents. The effect of anions, ligand to silver(I) ratio and solvents on the network polymers was also studied.

Nitrate anions are very flexible and exhibit a variety of coordination modes as discussed in Chapter 4 [figure 4.21]. Non-coordinating anions such as  $\text{PF}_6^-$ ,  $\text{BF}_4^-$  and sometimes  $\text{ClO}_4^-$  can change the nature of the polymeric networks allowing other weak interactions in the crystal packing. Thus, the counterions can have a strong influence over the coordination sphere of silver(I) and other long range weak interactions. However, in silver(I) trifluoroacetate complexes, it is the nature of the pyridine N-oxide ligand which changes the dimensionality of the networks. In silver(I) triflate complexes, the final outcome of the silver(I) network depends on both the triflate anion and the pyridine N-oxide ligand. Silver(I) adopted a coordination number of eight in a silver(I) triflate complex with  $\text{Ag} \cdots \text{Ag}$  interactions, as shown in figure 5.1.

As shown in figure 5.1, the  $\mu_3\text{-O, O, O}$  denticity was obtained for pyridine N-oxide ligands **2.1**, **2.2** and **2.14**, and  $\mu_5\text{-O, O, O', O', O'}$  and  $\mu_6\text{-O, O, O, O', O', O'}$  with spacer **3.12**, **3.15** and **3.1** N,N'-dioxide ligands, respectively. Despite great progress with N,N',N''-trioxides, the probability of the formation of product mixtures through self-assembly process is high, due to the spherical coordination sphere of silver(I) and the range of possible coordination modes offered by ligand **4.1**. This conclusion from N,N',N''-trioxides is also supported by elemental analysis shown in Chapter 6. The  $\mu_6\text{-O, O, O', O', O'', O''}$  denticity with ligand **4.1** was obtained once in its silver(I) nitrate complex.

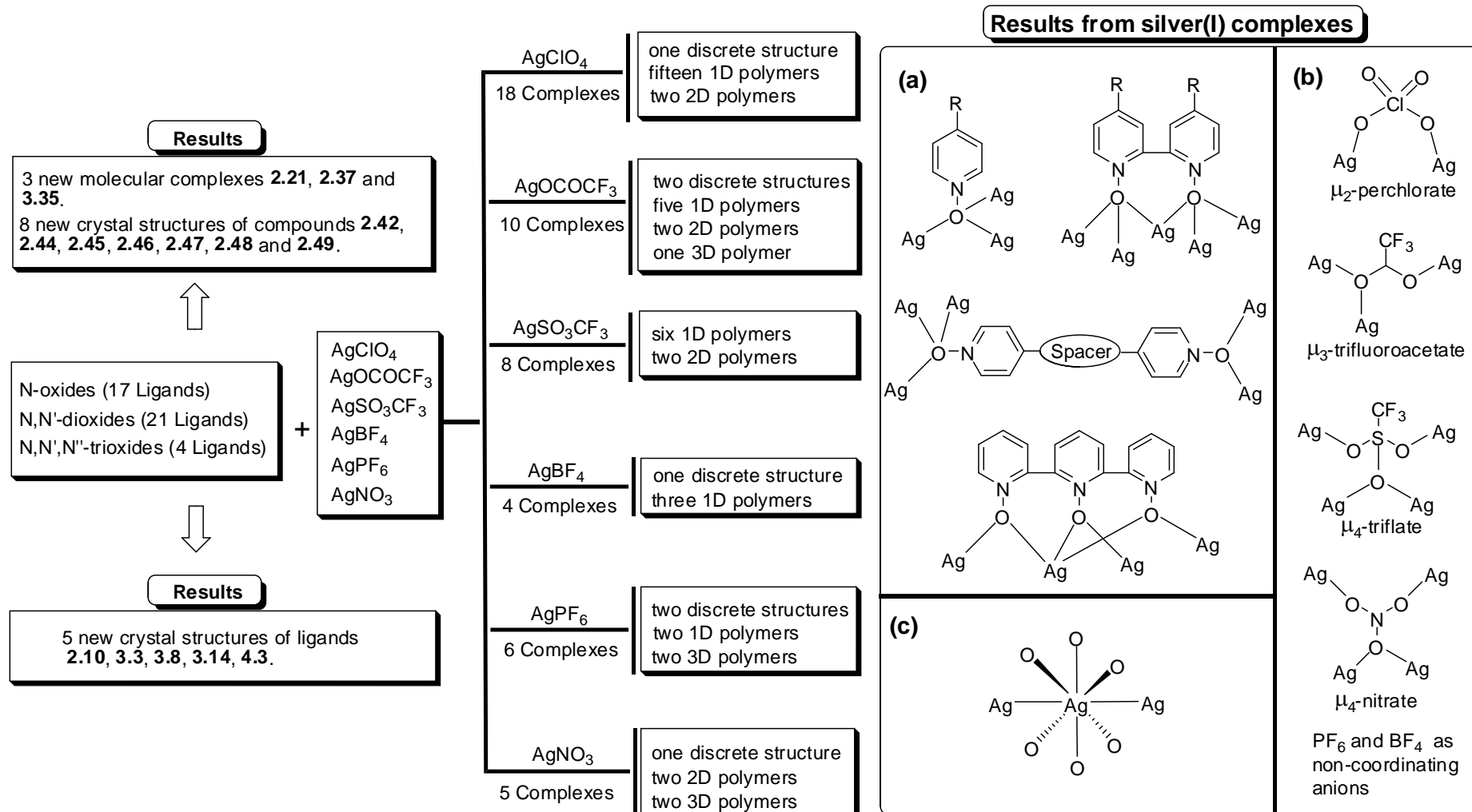


Figure 5.1 – Summary of results (a) maximum denticities adopted by various pyridine N-oxide ligands in silver(I) complexes, (b) coordination modes adopted by anions, and (c) coordination number eight adopted by silver(I).

The reactivity of these pyridine N-oxides with silver(I) and the range of their bridging modes should hopefully generate more interest for researchers in using such bridging ligands with other metals, leading to potential applications in metallosupramolecular chemistry. With this success, future projects could involve the use of various isoelectronic phenoxides as ligands for silver(I) to compare to the N-O ligands, as shown in figure 5.2.

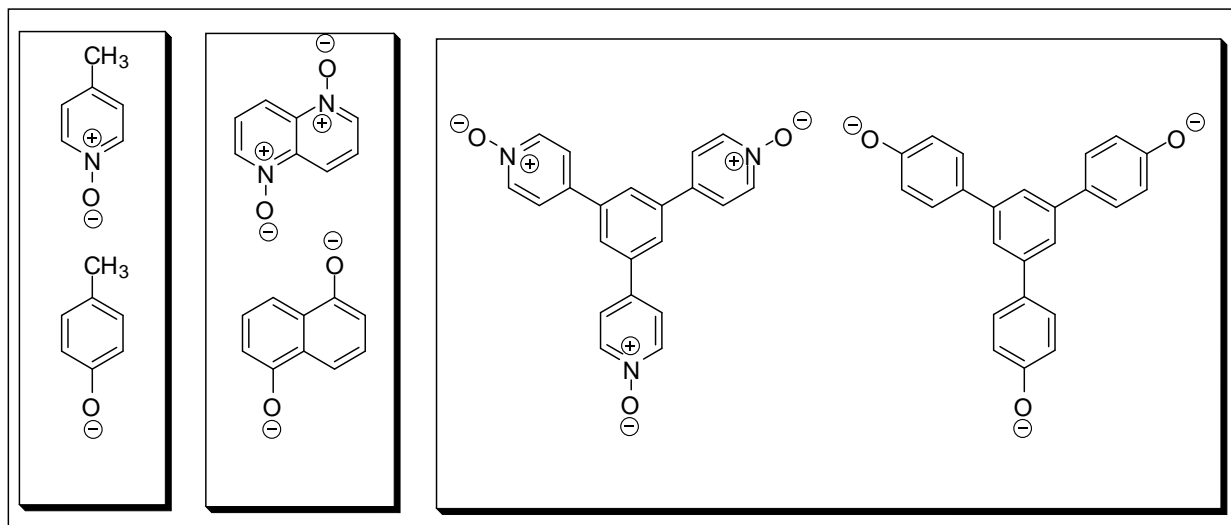


Figure 5.2 – Future work: comparison of the coordination modes N-O and C-O containing ligands with silver(I).

The present research focuses on the syntheses of pyridine N-oxides and their metallosupramolecular chemistry. A wide range of structures, from discrete structures to 3D polymers through N-O groups coordination with silver(I) metals, was obtained, as shown in figure 5.1. The most common dimensionality observed was one, and the highest dimensionality of these solid state structures was mostly anion directed. However, design and construction of higher dimensional polymers with secondary donor groups, such as  $-\text{COOH}$ ,  $-\text{CN}$  etc. using the bridging pyridine N-oxides is a new class of ligands [figure 5.3a] in metallosupramolecular chemistry. On the other hand, the prospect of having these secondary functional groups opens up a whole new area of research in metal-coordination networks. Another interest is to develop new synthetic routes for a new class of chelating ligands similar to 2,2'-bipyridine N,N'-dioxide and oxine N-oxide containing N-O and C-O groups, as shown in figure 5.3b.

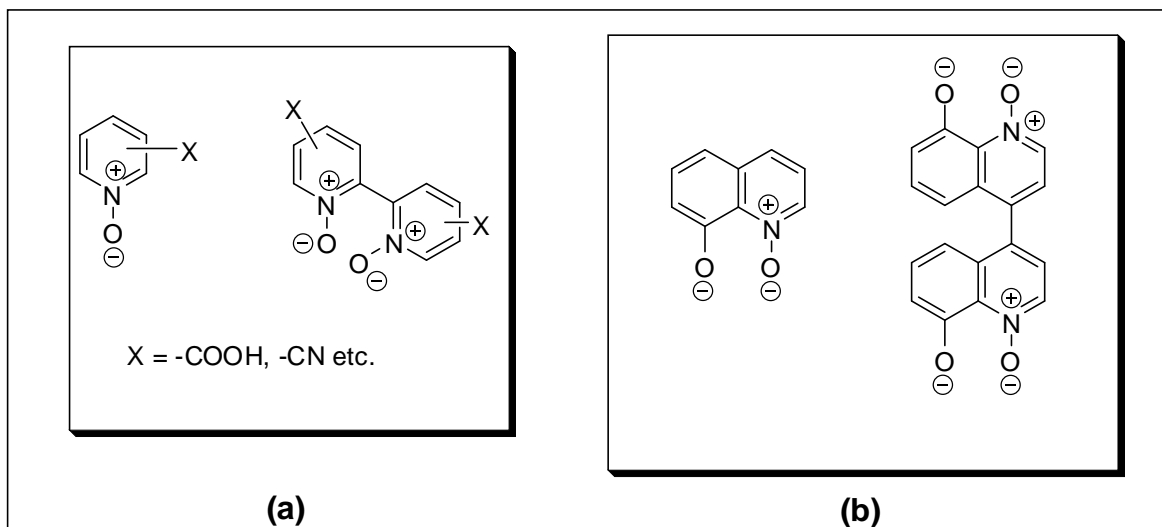


Figure 5.3 – Future work: (a) ligands with functional groups for the construction of higher dimensional polymers, and (b) new class of N-O and C-O containing groups as chelating ligands for silver(I).



# **Chapter – 6**

## **Experimental**

## 6.1 General Information

All the starting materials and reagents were reagent grade and used as received. Solvents used were reagent grade and used as received both for synthetic reactions and crystal growth. Melting points were recorded on an Electrothermal melting point apparatus and are uncorrected. Elemental analysis was carried out by the Campbell Microanalytical Laboratory, University of Otago. Except where otherwise specified, all reactions were carried out in air.

### 6.1.1 Nuclear Magnetic Resonance

Spectra were recorded on a Varian INOVA 300 or Varian Unity 400 instrument, operating at 300 and 400 MHz, respectively, for  $^1\text{H}$ , and 75 and 100 MHz, respectively, for  $^{13}\text{C}$  NMR. All the samples were dissolved in commercially available deuterated solvents  $\text{d}_6\text{-DSMO}$ ,  $\text{CDCl}_3$ ,  $\text{CD}_3\text{OD}$ ,  $\text{D}_2\text{O}$  or  $\text{DCI/D}_2\text{O}$ . Spectra were referenced to the residual solvent peaks and/or TMS. TOCSY, COSY, HSQC and HMBC experiments are employed where required. Data are reported as follows: chemical shift ( $\delta/\text{ppm}$ ), multiplicity (s = singlet, bs = broad singlet, d = doublet, t = triplet, q = quartet, quin = quintet, dd = doublet of doublets, dt = doublet of triplets, sp = septet, m = multiplet), coupling constant Hz and integration.

### 6.1.2 Mass Spectrometry

Mass spectra were recorded on a maXis 3G UHR-Qq-TOF mass spectrometer coupled to a Dionex Ultimate 3000 LC system, which were operated in high resolution positive ion electrospray mode. Samples were dissolved and diluted to the required concentration in water or methanol, and or water/formic acid.

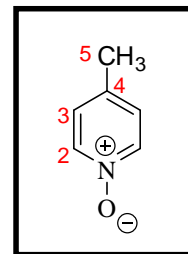
### 6.1.3 Infrared Spectroscopy

All infrared spectra were recorded on a Perkin-Elmer Spectrum One FTIR instrument operating in diffuse reflectance mode with samples prepared as KBr pellets, or in transmittance mode with liquid samples pressed between KBr discs (neat).

## 6.2 Preparation of pyridine N-oxides

### 6.2.1 Synthesis of 4-methylpyridine N-oxide 2.2

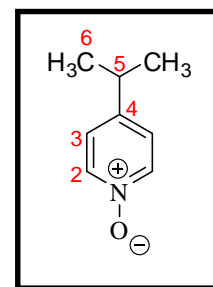
MCPBA (3.05 g, 17.7 mmol) was added to a solution of 4-methylpyridine (1.50 g, 16.1 mmol) in methanol (10 ml) at room temperature and heated to reflux for 15 minutes. The reaction was cooled to room temperature, and concentrated to dryness under vacuum. The crude product was purified by silica gel flash chromatography using 4% methanol:dichloromethane as elutant to give **2.2**, as an off-white solid. Yield 0.525 g (27%), m.p. 180°C [Lit<sup>[185]</sup>: m.p. 181 – 185°C].



<sup>1</sup>H NMR<sup>[186]</sup> (400MHz, CDCl<sub>3</sub>) δ/ppm: 8.11 (d, *J* = 6.6 Hz, 2H, H<sub>2</sub>), 7.08 (d, *J* = 6.7 Hz, 2H, H<sub>3</sub>), 2.34 (s, 3H, H<sub>5</sub>). <sup>13</sup>C NMR<sup>[187]</sup> (100MHz, CDCl<sub>3</sub>) δ/ppm: 138.73 (C<sub>2</sub>), 138.16 (C<sub>4</sub>), 126.79 (C<sub>3</sub>), 20.31 (C<sub>5</sub>). IR (KBr) ν<sub>max</sub>/cm<sup>-1</sup>: 3111, 1957, 1670, 1488, 1460, 1226, 1181, 1042, 854, 763. ESI-MS *m/z*: Found [L+H]<sup>+</sup> 110.0603, C<sub>6</sub>H<sub>8</sub>NO requires [L+H]<sup>+</sup> 110.0600.

### 6.2.2 Synthesis of 4-isopropylpyridine N-oxide 2.3

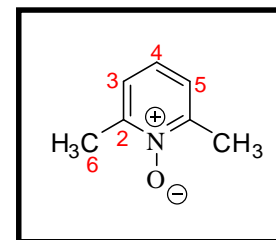
4-Isopropylpyridine (1.00 g, 8.25 mmol) and mCPBA (1.56 g, 9.07 mmol) were dissolved in methanol (20 ml) at room temperature and heated to reflux for 10 minutes. The reaction was then cooled to room temperature and concentrated to dryness under vacuum. The crude product was purified by silica gel flash chromatography using 5% hexane:dichloromethane as elutant to give **2.3**, as a pale yellow semi-solid. Yield 0.618 g (54%), m.p. 74°C [Lit<sup>[188]</sup>: m.p. 78 – 79°C].



<sup>1</sup>H NMR<sup>[86]</sup> (400MHz, CDCl<sub>3</sub>) δ/ppm: 8.14 (d, *J* = 7.0 Hz, 2H, H<sub>2</sub>), 7.13 (d, *J* = 7.0 Hz, 2H, H<sub>3</sub>), 2.90 (sp, *J* = 6.9 Hz, 1H, H<sub>5</sub>), 1.23 (d, *J* = 7.0 Hz, 6H, H<sub>6</sub>). <sup>13</sup>C NMR (100MHz, CDCl<sub>3</sub>) δ/ppm: 148.73 (C<sub>2</sub>), 138.84 (C<sub>4</sub>), 124.15 (C<sub>3</sub>), 32.88 (C<sub>5</sub>), 22.96 (C<sub>6</sub>). IR (KBr) ν<sub>max</sub>/cm<sup>-1</sup>: 2963, 1941, 1654, 1490, 1449, 1227, 1182, 1058, 846, 720. ESI-MS *m/z*: Found [L+H]<sup>+</sup> 138.0915, C<sub>8</sub>H<sub>12</sub>NO requires [L+H]<sup>+</sup> 138.0913.

### 6.2.3 Synthesis of 2,6-dimethylpyridine N-oxide 2.4

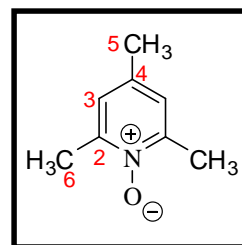
To a mixture of 25 ml of acetic acid and 1.00 g (9.33 mmol) of 2,6-dimethylpyridine was added 5 ml of 50% H<sub>2</sub>O<sub>2</sub> at room temperature. The reaction mixture was stirred at 80°C for 5 hours, then cooled to room temperature and concentrated to dryness under vacuum. The crude product was recrystallized from diethyl ether and dichloromethane to give **2.4**, as an off-white solid. Yield 1.04 g (90%), m.p. 49°C [Lit<sup>[185a]</sup>: m.p. 52°C].



<sup>1</sup>H NMR<sup>[189]</sup> (400MHz, CDCl<sub>3</sub>) δ/ppm: 7.16 (s, 3H, H<sub>3</sub> H<sub>4</sub> H<sub>5</sub>), 2.55 (s, 6H, H<sub>6</sub>). <sup>13</sup>C NMR<sup>[189]</sup> (100MHz, CDCl<sub>3</sub>) δ/ppm: 149.71 (C<sub>2</sub>), 126.42 (C<sub>3</sub>), 124.10 (C<sub>4</sub>), 18.32 (C<sub>6</sub>). IR (KBr) ν<sub>max</sub>/cm<sup>-1</sup>: 3414, 1950, 1711, 1574, 1499, 1460, 1376, 1271, 1101, 828, 783. ESI-MS *m/z*: Found [L+H]<sup>+</sup> 124.0760, C<sub>7</sub>H<sub>10</sub>NO requires [L+H]<sup>+</sup> 124.0757.

### 6.2.4 Synthesis of 2,4,6-trimethylpyridine N-oxide 2.5

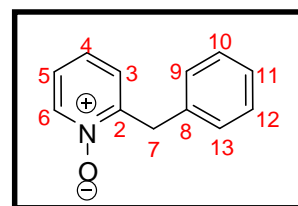
To a solution of 2,4,6-trimethylpyridine (1.49 g, 8.25 mmol) in methanol (10 ml), mCPBA (1.70 g, 9.90 mmol) was added at room temperature. The resulting mixture was heated to reflux for 1 hour, then cooled to room temperature, and concentrated to dryness under vacuum. The crude product was purified by silica gel flash chromatography with 4% methanol:dichloromethane as eluant to give **2.5**, as a pale yellow oil. Yield 0.353 g (31%). [Lit<sup>[190]</sup>: m.p. 45°C].



<sup>1</sup>H NMR<sup>[189]</sup> (400MHz, CDCl<sub>3</sub>) δ/ppm: 6.98 (s, 2H, H<sub>3</sub>), 2.49 (s, 6H, H<sub>6</sub>), 2.28 (s, 3H, H<sub>5</sub>). <sup>13</sup>C NMR<sup>[189]</sup> (100MHz, CDCl<sub>3</sub>) δ/ppm: 148.54 (C<sub>2</sub>), 137.24 (C<sub>4</sub>), 124.87 (C<sub>3</sub>), 19.40 (C<sub>5</sub>), 18.21 (C<sub>6</sub>). IR (KBr) ν<sub>max</sub>/cm<sup>-1</sup>: 2961, 1671, 1504, 1470, 1426, 1318, 1234, 1094, 1037, 791. ESI-MS m/z: Found [L+H]<sup>+</sup> 138.0917, C<sub>8</sub>H<sub>12</sub>NO requires [L+H]<sup>+</sup> 138.0913.

### 6.2.5 Synthesis of 2-benzylpyridine N-oxide 2.7

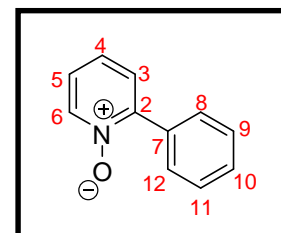
50% H<sub>2</sub>O<sub>2</sub> (5 ml) was added to 2-benzylpyridine (1.50 g, 8.86 mmol) in 20 ml of acetic acid at room temperature. This mixture was then stirred at 80°C for 30 minutes. The reaction mixture was cooled to room temperature and concentrated to dryness under vacuum. The crude residue was dissolved in chloroform (20 ml) and washed with water (4x50 ml). The organic layer was dried over anhydrous MgSO<sub>4</sub> and concentrated under reduced pressure to give **2.6**. Yield 0.966 g (59%), m.p. 98 – 100°C [Lit<sup>[191]</sup>: 98 – 99°C].



<sup>1</sup>H NMR<sup>[191]</sup> (400MHz, CDCl<sub>3</sub>) δ/ppm: 8.32 (t, *J* = 3.7 Hz, 1H, H<sub>6</sub>), 7.35 (t, *J* = 7.2 Hz, 2H, H<sub>9</sub>, H<sub>13</sub>), 7.28 (t, *J* = 7.4 Hz, 3H, H<sub>10</sub>, H<sub>11</sub>, H<sub>12</sub>), 7.16 (t, *J* = 4.3 Hz, 2H, H<sub>4</sub>, H<sub>5</sub>), 6.95 (t, *J* = 4.9 Hz, 1H, H<sub>3</sub>). <sup>13</sup>C NMR<sup>[192]</sup> (100MHz, CDCl<sub>3</sub>) δ/ppm: 150.30 (C<sub>2</sub>), 139.44 (C<sub>6</sub>), 136.14 (C<sub>8</sub>), 129.71 (C<sub>10</sub>), 128.87 (C<sub>9</sub>), 127.09 (C<sub>11</sub>), 126.01 (C<sub>4</sub>), 125.86 (C<sub>3</sub>), 125.58 (C<sub>5</sub>), 36.51 (C<sub>7</sub>). IR (KBr) ν<sub>max</sub>/cm<sup>-1</sup>: 2913, 1952, 1855, 1490, 1406, 1250, 1223, 1101, 1075, 931, 861. ESI-MS m/z: Found [L+H]<sup>+</sup> 186.0916, C<sub>12</sub>H<sub>12</sub>NO requires [L+H]<sup>+</sup> 186.0913.

### 6.2.6 Synthesis of 2-phenylpyridine N-oxide 2.8

2-Phenylpyridine (1.50 g, 9.67 mmol) and 50% H<sub>2</sub>O<sub>2</sub> (5 ml) were dissolved in acetic acid (20 ml) at room temperature and the reaction mixture was heated to 80°C for 4 hours. The reaction mixture was cooled to room temperature, and then concentrated to dryness under vacuum to give a pale yellow-oil. The residue was recrystallized from hexane/dichloromethane to give **2.7**, as an off-white solid. Yield 0.550 g (33%), m.p. 156 – 158°C [Lit<sup>[193]</sup>: m.p. 155°C].



<sup>1</sup>H NMR<sup>[194]</sup> (400MHz, CDCl<sub>3</sub>) δ/ppm: 8.33 (d, *J* = 6.3 Hz, 1H, H<sub>6</sub>), 7.81 (dd, *J* = 1.2 Hz, 8.2 Hz, 2H, H<sub>8</sub>, H<sub>12</sub>), 7.44 – 7.50 (m, 3H, H<sub>9</sub>, H<sub>10</sub>, H<sub>11</sub>), 7.42 (dd, *J* = 2.5 Hz, 6.2 Hz, 1H, H<sub>3</sub>), 7.29 (td, *J* = 1.2 Hz, 7.4 Hz, 1H, H<sub>4</sub>), 7.22 (td, *J* = 1.9 Hz, 6.6 Hz, 1H, H<sub>5</sub>). <sup>13</sup>C NMR<sup>[194]</sup> (100MHz, CDCl<sub>3</sub>) δ/ppm: 149.32 (C<sub>2</sub>), 140.52

(C<sub>6</sub>), 132.63 (C<sub>7</sub>), 129.59 (C<sub>10</sub>), 129.25 (C<sub>9</sub>), 128.94 (C<sub>8</sub>), 127.38 (C<sub>3</sub>), 125.57 (C<sub>4</sub>), 124.48 (C<sub>5</sub>). **IR (KBr)**  $\nu_{\max}/\text{cm}^{-1}$ : 3045, 2467, 1919, 1638, 1477, 1420, 1241, 1101, 841, 759. **ESI-MS**  $m/z$ : Found [L+H]<sup>+</sup> 172.0759, C<sub>11</sub>H<sub>10</sub>NO requires [L+H]<sup>+</sup> 172.0757.

### 6.2.7 Synthesis of 4-(diphenylmethyl)pyridine 2.9b

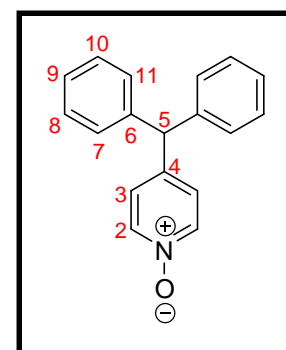
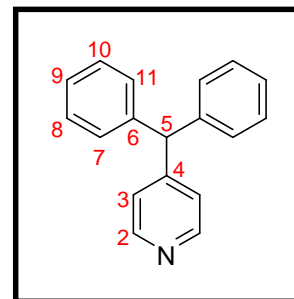
To a solution of 4-pyridinecarboxaldehyde (0.200 g, 1.86 mmol) in benzene (1.75 g, 22.4 mmol), triflic acid (5.08 g, 33.9 mmol) was added at room temperature. The reaction mixture was stirred till the consumption of 4-pyridinecarboxaldehyde (monitored by TLC). The reaction mixture was then poured over crushed ice, neutralized with NaOH and extracted with chloroform (3x20 ml). The organic layers were combined, washed with brine (15 ml), dried over anhydrous MgSO<sub>4</sub> and concentrated to dryness under vacuum. The crude residues were purified by silica gel flash chromatography with 5% ethyl acetate:hexane as elutant to give **2.9b**, as an off-white solid. Yield 0.489 g (quantitative), m.p. 76 – 78°C [Lit<sup>[195]</sup>: m.p. 74 – 75°C].

**<sup>1</sup>H NMR** (300MHz, CDCl<sub>3</sub>)  $\delta/\text{ppm}$ : 8.51 (d,  $J = 6.0$  Hz, 2H, H<sub>2</sub>), 7.26 – 7.34 (m, 6H, H<sub>8</sub>, H<sub>9</sub>, H<sub>10</sub>), 7.04 – 7.11 (m, 6H, H<sub>7</sub>, H<sub>11</sub>, H<sub>3</sub>), 5.50 (s, 1H, H<sub>5</sub>).

### 6.2.8 Synthesis of 4-(diphenylmethyl)pyridine N-oxide 2.9

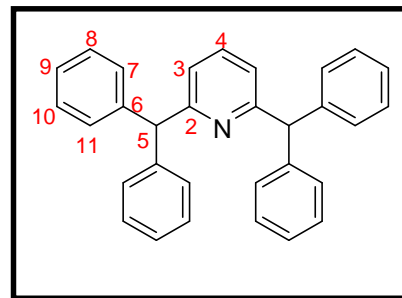
Compound **2.9b** (0.400 g, 1.63 mmol) and mCPBA (0.340 g, 1.95 mmol) were dissolved in methanol (10 ml) at room temperature and heated to reflux for 30 minutes. After TLC analysis, the reaction mixture was cooled to room temperature, then concentrated to dryness under vacuum. The crude product were purified by silica gel flash chromatography with 15% ethyl acetate:hexane as elutant to give **2.9b** as an off-white solid. Yield 0.302 g (71%), m.p. 153°C [Lit<sup>[86]</sup>: m.p. 156.3°C].

**<sup>1</sup>H NMR**<sup>[86]</sup> (400MHz, CDCl<sub>3</sub>)  $\delta/\text{ppm}$ : 8.27 (d,  $J = 6.7$  Hz, 2H, H<sub>2</sub>), 7.27 – 7.36 (m, 6H, H<sub>8</sub>, H<sub>9</sub>, H<sub>10</sub>), 7.07 – 7.12 (m, 6H, H<sub>7</sub>, H<sub>11</sub>, H<sub>3</sub>), 5.52 (s, 1H, H<sub>5</sub>). **<sup>13</sup>C NMR** (100MHz, CDCl<sub>3</sub>)  $\delta/\text{ppm}$ : 140.93 (C<sub>4</sub>), 138.87 (C<sub>2</sub>), 129.12 (C<sub>7</sub>), 128.98 (C<sub>8</sub>), 127.45 (C<sub>9</sub>), 127.03 (C<sub>3</sub>), 55.53 (C<sub>5</sub>), C<sub>6</sub> carbon was not observed even with prolonged scans. **IR (KBr)**  $\nu_{\max}/\text{cm}^{-1}$ : 3404, 2034, 1640, 1617, 1475, 1251, 1170, 1034, 841, 695. **ESI-MS**  $m/z$ : Found [L+Na]<sup>+</sup> 284.1042, C<sub>18</sub>H<sub>15</sub>NNaO requires [L+Na]<sup>+</sup> 284.1046.



### 6.2.9 Synthesis of 2,6-bis(diphenylmethyl)pyridine 2.10b

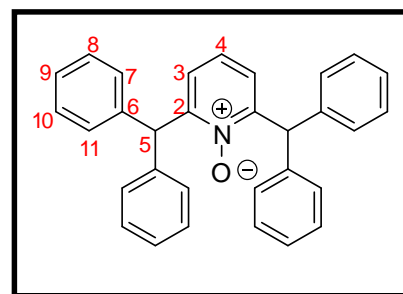
To 2,6-pyridine-dicarboxaldehyde (0.200 g, 1.48 mmol) in 1.5 ml of benzene (1.75 g, 16.8 mmol), was added 3 ml of triflic acid (5.08 g, 22.4 mmol) at room temperature. The reaction mixture was stirred to completion at room temperature, then poured over crushed ice, neutralized with NaOH and extracted with chloroform (2x10 ml). The organic layers were combined and washed with brine solution, dried over anhydrous MgSO<sub>4</sub> and concentrated to dryness under vacuum. The crude residues were purified by silica gel flash chromatography with 5% ethyl acetate:hexane as elutant to give **2.10b**. Yield 0.372 g (61%), m.p. 99°C [Lit<sup>[78]</sup>: m.p. 94 – 101°C].



<sup>1</sup>H NMR (300MHz, CDCl<sub>3</sub>) δ/ppm: 7.49 (t, *J* = 7.6 Hz, 1H, H<sub>4</sub>), 7.15 – 7.33 (m, 20H, Ar), 6.98 (d, *J* = 7.6 Hz, 2H, H<sub>3</sub>), 5.56 (s, 2H, H<sub>5</sub>).

### 6.2.10 Synthesis of 2,6-bis(diphenylmethyl)pyridine N-oxide 2.10

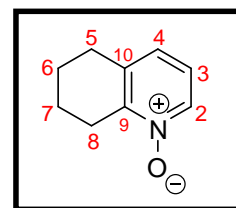
Compound **2.10b** (0.370 g, 0.899 mmol) and mCPBA (0.186 g, 1.07 mmol) were dissolved in chloroform (20 ml) at room temperature and heated to reflux for 60 minutes. After TLC analysis, the reaction was cooled to room temperature, then concentrated to dryness under vacuum. The crude product was purified by silica gel flash chromatography with 15% ethyl acetate:hexane as elutant to give **2.10**, as a white solid. Yield 0.133 g (34%), m.p. 64 – 66°C.



<sup>1</sup>H NMR (400MHz, CD<sub>3</sub>OD) δ/ppm: 7.24 – 7.36 (m, 13H, H<sub>8-10</sub>, H<sub>4</sub>), 7.05 – 7.07 (d, *J* = 8.6 Hz, 8H, H<sub>7</sub>, H<sub>11</sub>), 6.98 (d, *J* = 7.6 Hz, 2H, H<sub>3</sub>), 5.56 (s, 2H, H<sub>5</sub>). <sup>13</sup>C NMR (100MHz, CD<sub>3</sub>OD) δ/ppm: 140.27(C<sub>4</sub>), 128.75, 128.37, 126.78, 125.45, 51.03 (C<sub>5</sub>), two carbons were not observed even with prolonged scans. IR (KBr) ν<sub>max</sub>/cm<sup>-1</sup>: 3424, 1696, 1634, 1574, 1494, 1305, 1251, 1075, 852, 699. ESI-MS *m/z*: Found [L+H]<sup>+</sup> 428.2005, C<sub>31</sub>H<sub>26</sub>NO requires [L+H]<sup>+</sup> 428.2009; Found [L+Na]<sup>+</sup> 450.1828, C<sub>31</sub>H<sub>25</sub>NNaO requires [L+Na]<sup>+</sup> 450.1828.

### 6.2.11 Synthesis of 5,6,7,8-tetrahydroquinoline N-oxide 2.14

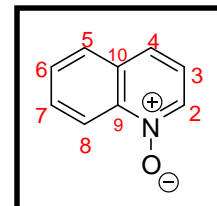
Compound **2.14a** (1.50 g, 11.2 mmol) and 50% H<sub>2</sub>O<sub>2</sub> (3 ml) were dissolved in acetic acid (10 ml) at room temperature and heated at 80°C for 12 hours. The reaction mixture was cooled to room temperature, then concentrated to dryness under vacuum to give a black liquid. The crude product was purified by silica gel flash chromatography using 5% methanol:dichloromethane as elutant to give **2.14**, as a brown oil. Yield 0.628 g (37%).



**$^1\text{H NMR}^{[196]}$**  (400MHz,  $\text{CDCl}_3$ )  $\delta/\text{ppm}$ : 8.31 (d,  $J = 6.3$  Hz, 1H,  $\text{H}_2$ ), 7.15 (d,  $J = 7.8$  Hz, 1H,  $\text{H}_4$ ), 7.09 (t,  $J = 7.0$  Hz, 1H,  $\text{H}_3$ ), 2.97 (t,  $J = 6.4$  Hz, 2H,  $\text{H}_8$ ), 2.78 (t,  $J = 6.1$  Hz, 2H,  $\text{H}_5$ ), 1.75 – 1.91 (m, 4H,  $\text{H}_6$ ,  $\text{H}_7$ ).  **$^{13}\text{C NMR}^{[196]}$**  (100MHz,  $\text{CDCl}_3$ )  $\delta/\text{ppm}$ : 149.26 ( $\text{C}_9$ ), 137.34 ( $\text{C}_2$ ), 136.99 ( $\text{C}_{10}$ ), 129.23 ( $\text{C}_4$ ), 122.24 ( $\text{C}_3$ ), 28.55 ( $\text{C}_5$ ), 24.88 ( $\text{C}_8$ ), 21.58 ( $\text{C}_7$ ), 21.39 ( $\text{C}_6$ ). **IR (KBr)**  $\nu_{\text{max}}/\text{cm}^{-1}$ : 2857, 1699, 1595, 1485, 1434, 1335, 1256, 1191, 1072, 970, 902. **ESI-MS  $m/z$** : Found  $[\text{L}+\text{H}]^+$  150.0916,  $\text{C}_9\text{H}_{12}\text{NO}$  requires  $[\text{L}+\text{H}]^+$  150.0913.

### 6.2.12 Synthesis of quinoline N-oxide 2.15

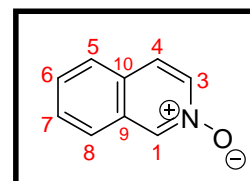
3 ml of 50%  $\text{H}_2\text{O}_2$  was added to a solution of quinoline (1.00 g, 7.74 mmol) in acetic acid (20 ml) at room temperature and the mixture heated at  $80^\circ\text{C}$  for 5 hours. This was then cooled to room temperature and the solvents were removed under reduced pressure to give a brown liquid, which solidified. The hygroscopic solid was recrystallized from methanol to give **2.15**, as a brown solid, and stored in an air tight container. Yield 0.600 g (53%), m.p.  $58^\circ\text{C}$  [Lit<sup>[41p]</sup>: m.p.  $52 - 54^\circ\text{C}$ ].



**$^1\text{H NMR}^{[197]}$**  (400MHz,  $\text{CDCl}_3$ )  $\delta/\text{ppm}$ : 8.74 (d,  $J = 8.6$  Hz, 1H,  $\text{H}_8$ ), 8.54 (d,  $J = 5.8$  Hz, 1H,  $\text{H}_2$ ), 7.86 (d,  $J = 8.2$  Hz, 1H,  $\text{H}_5$ ), 7.73 – 7.78 (m, 1H,  $\text{H}_4$ ,  $\text{H}_7$ ), 7.64 (t,  $J = 7.2$  Hz, 1H,  $\text{H}_6$ ), 7.29 (dd,  $J = 6.3$  Hz, 8.2 Hz, 1H,  $\text{H}_3$ ).  **$^{13}\text{C NMR}^{[197]}$**  (100MHz,  $\text{CDCl}_3$ )  $\delta/\text{ppm}$ : 141.55 ( $\text{C}_9$ ), 135.67 ( $\text{C}_2$ ), 130.53 ( $\text{C}_{10}$ ), 130.48 ( $\text{C}_7$ ), 128.79 ( $\text{C}_6$ ), 128.12 ( $\text{C}_5$ ), 126.11 ( $\text{C}_4$ ), 120.95 ( $\text{C}_3$ ), 119.80 ( $\text{C}_8$ ). **IR (KBr)**  $\nu_{\text{max}}/\text{cm}^{-1}$ : 1658, 1573, 1451, 1393, 1309, 1206, 1139, 882, 796, 766. **ESI-MS  $m/z$** : Found  $[\text{L}+\text{H}]^+$  146.0601,  $\text{C}_9\text{H}_8\text{NO}$  requires  $[\text{L}+\text{H}]^+$  146.0600.

### 6.2.13 Synthesis of isoquinoline N-oxide 2.16

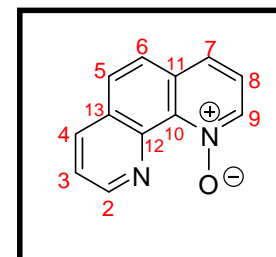
Isoquinoline (1.00 g, 7.74 mmol) and 5ml of 50%  $\text{H}_2\text{O}_2$  were dissolved in acetic acid (20 ml) at room temperature and heated at  $80^\circ\text{C}$  for 13 hours. The reaction mixture was then cooled to room temperature and the solvents were concentrated to dryness under vacuum. The crude residue was recrystallized from methanol to give **2.16**, as an off-white solid. Yield 0.682 g (60%), m.p.  $105^\circ\text{C}$  [Lit<sup>[41p]</sup>: m.p.  $103 - 105^\circ\text{C}$ ].



**$^1\text{H NMR}^{[198]}$**  (400MHz,  $\text{CDCl}_3$ )  $\delta/\text{ppm}$ : 8.74 (bs, 1H,  $\text{H}_1$ ), 8.11 (dd,  $J = 1.6$  Hz, 7.1 Hz, 1H,  $\text{H}_3$ ), 7.76 (d,  $J = 7.3$  Hz, 1H,  $\text{H}_8$ ), 7.70 (d,  $J = 7.4$  Hz, 1H,  $\text{H}_5$ ), 7.64 (d,  $J = 7.4$  Hz, 1H,  $\text{H}_4$ ), 7.55 – 7.62 (m, 2H,  $\text{H}_6$ ,  $\text{H}_7$ ).  **$^{13}\text{C NMR}^{[199]}$**  (100MHz,  $\text{CDCl}_3$ )  $\delta/\text{ppm}$ : 136.75 ( $\text{C}_3$ ), 136.18 ( $\text{C}_1$ ), 129.54 ( $\text{C}_7$ ), 129.51 ( $\text{C}_9$ ), 129.10 ( $\text{C}_6$ ), 128.86 ( $\text{C}_{10}$ ), 126.67 ( $\text{C}_8$ ), 125.01 ( $\text{C}_5$ ), 124.27 ( $\text{C}_4$ ). **IR (KBr)**  $\nu_{\text{max}}/\text{cm}^{-1}$ : 2510, 1690, 1491, 1337, 1290, 1206, 1124, 909, 874, 771. **ESI-MS  $m/z$** : Found  $[\text{L}+\text{H}]^+$  146.0603,  $\text{C}_9\text{H}_8\text{NO}$  requires  $[\text{L}+\text{H}]^+$  146.0600.

### 6.2.14 Synthesis of 1,10-phenanthroline N-oxide 2.17

To a solution of 1,10-phenanthroline monohydrate (1.00 g, 5.04 mmol) in acetic acid (15 ml), 50%  $\text{H}_2\text{O}_2$  (6 ml) was added. The temperature was maintained at  $80^\circ\text{C}$  for 5 hours, after which an additional portion of 50%  $\text{H}_2\text{O}_2$  (3 ml) was added and the heating was continued for an further 2



hours. After cooling to room temperature, solid  $K_2CO_3$  was added, followed by water (20 ml); the reaction mixture was concentrated to a volume of approximately 3 ml. Acetone (10 ml) was added to the resulting mixture and stored overnight in a fridge to give brown solids which are collected by filtration. The filtrate was concentrated and purified by silica gel column chromatography using 10% methanol:dichloromethane as elutant to give **2.17**, as a light-brown solid. Yield 0.741 g (74%), m.p. 175°C [Lit<sup>[200]</sup>: m.p. 176°C].

<sup>1</sup>H NMR<sup>[201]</sup> (400MHz, CD<sub>3</sub>OD) δ/ppm: 9.33 (bs, 1H, H<sub>2</sub>), 9.26 (d, *J* = 8.2 Hz, 1H, H<sub>4</sub>), 9.07 (d, *J* = 6.3 Hz, 1H, H<sub>9</sub>), 8.53 (d, *J* = 8.2 Hz, 1H, H<sub>7</sub>), 8.42 (dd, *J* = 2.7 Hz, 5.5 Hz, 1H, H<sub>3</sub>), 8.38 (bs, 2H, H<sub>5</sub>, H<sub>6</sub>), 8.07 (t, *J* = 7.5 Hz, 1H, H<sub>8</sub>). <sup>13</sup>C NMR<sup>[201]</sup> (100MHz, CD<sub>3</sub>OD) δ/ppm: 144.17 (C<sub>4</sub>), 142.37 (C<sub>2</sub>), 140.74 (C<sub>12</sub>), 139.60 (C<sub>9</sub>), 134.84 (C<sub>13</sub>), 133.46 (C<sub>11</sub>), 130.55 (C<sub>7</sub>), 129.73 (C<sub>10</sub>), 129.15 (C<sub>6</sub>), 128.14 (C<sub>5</sub>), 125.98 (C<sub>8</sub>), 125.79 (C<sub>3</sub>). IR (KBr)  $\nu_{max}/cm^{-1}$ : 3552, 3482, 3415, 1725, 1217, 1619, 1460, 1281, 1237, 962, 766. ESI-MS *m/z*: Found [L+H]<sup>+</sup> 197.0711, C<sub>12</sub>H<sub>9</sub>N<sub>2</sub>O requires [L+H]<sup>+</sup> 197.0709.

### 6.3 Preparation of silver(I) complexes with pyridine N-oxides

#### 6.3.1 Complexes of pyridine N-oxide 2.1

##### With silver(I) perchlorate (1:1) 2.18

Silver(I) perchlorate (32 mg, 0.15 mmol) dissolved in methanol (2 ml) was added to an acetone (2 ml) solution of ligand **2.1** (15 mg, 0.15 mmol). The solution was left in darkness at room temperature and allowed to evaporate slowly to give colourless crystals suitable for X-ray crystallography. Yield 24 mg (53%), m.p. 78°C.

**Elemental Analysis:** calculated for C<sub>5</sub>H<sub>5</sub>NO.AgClO<sub>4</sub>: C, 19.86; H, 1.67; N, 4.63. Found: C, 19.43; H, 2.00; N, 4.32. IR (KBr)  $\nu_{max}/cm^{-1}$ : 3103, 2012, 1649, 1469, 1505, 1232, 1140, 1090, 837, 770, 675. ESI-MS *m/z*: Found [L+Ag]<sup>+</sup> 201.9414, C<sub>5</sub>H<sub>5</sub>AgNO requires [L+Ag]<sup>+</sup> 201.9417; Found [L+Ag+CH<sub>3</sub>CN]<sup>+</sup> 242.9677, C<sub>7</sub>H<sub>8</sub>AgN<sub>2</sub>O requires [L+Ag+CH<sub>3</sub>CN]<sup>+</sup> 242.9682.

##### With silver(I) perchlorate (2:1) 2.19

A solution of silver(I) perchlorate (10 mg, 0.048 mmol) in methanol (1 ml) was added to a solution of ligand **2.1** (9.1 mg, 0.096 mmol) in methanol (2 ml). The mixture was then left in darkness and allowed to evaporate slowly at room temperature. This produced colourless crystals suitable for X-ray crystallography. Yield 16 mg (84%), m.p. 88°C.

**Elemental Analysis:** calculated for 2(C<sub>5</sub>H<sub>5</sub>NO).AgClO<sub>4</sub>: C 32.99; H 2.71; N 7.60. Found: (inconsistent with the proposed structure) C 30.21; H 2.54; N 7.05. IR (KBr)  $\nu_{max}/cm^{-1}$ : 3110, 1653, 1466, 1226, 1176, 1144, 1086, 1019, 835, 770, 674. ESI-MS *m/z*: Found [L+Ag]<sup>+</sup> 201.9415, C<sub>5</sub>H<sub>5</sub>AgNO requires [L+Ag]<sup>+</sup> 201.9417; Found [2L+Ag]<sup>+</sup> 296.9785, C<sub>10</sub>H<sub>10</sub>AgN<sub>2</sub>O<sub>2</sub> requires [2L+Ag]<sup>+</sup> 296.9788.

##### With silver(I) perchlorate (3:1) 2.20

Silver(I) perchlorate (10 mg, 0.048 mmol) dissolved in methanol (1 ml) was added to a methanol (2 ml) solution of ligand **2.1** (13.7 mg, 0.144 mmol). The solution was left in darkness at room



temperature and allowed to evaporate slowly to give crystals suitable for X-ray analysis. Yield 9 mg (38%), m.p. 67°C.

**Elemental Analysis:** calculated for  $3(\text{C}_5\text{H}_5\text{NO})\cdot\text{AgClO}_4$ : C, 36.57; H, 3.06; N 8.53. Found: C, 37.06; H, 3.14; N, 8.60. **IR (KBr)**  $\nu_{\text{max}}/\text{cm}^{-1}$ : 3110, 1659, 1469, 1226, 1177, 1120, 1140, 1019, 835, 771, 675. **ESI-MS**  $m/z$ : No sign of  $[\text{L}+\text{Ag}]^+$  peaks.

#### **With silver(I) trifluoroacetate (1:1) 2.21**

Complex **2.21** was obtained by the reaction of silver(I) trifluoroacetate (33 mg, 0.15 mmol) solution in methanol (1 ml) added to a solution of ligand **2.1** (15 mg, 0.15 mmol) in acetone (2 ml). Single crystals were obtained by a slow evaporation of the colourless solution. Yield 21 mg (44%), m.p. 92°C.

**Elemental Analysis:** calculated for  $\text{C}_5\text{H}_5\text{NO}\cdot\text{AgOCOCF}_3\cdot 0.5(\text{CH}_3\text{OH})$ : C, 27.13; H, 2.13; N, 4.22. Found: C, 27.54; H, 1.59; N, 4.52. **IR (KBr)**  $\nu_{\text{max}}/\text{cm}^{-1}$ : 3112, 1683, 1470, 1430, 1238, 1206, 1129, 1018, 836, 802, 769. **ESI-MS**  $m/z$ : No sign of  $[\text{L}+\text{Ag}]^+$  peaks.

#### **With silver(I) triflate (1:1) 2.22**

A methanol (1ml) solution of silver(I) triflate (37.8 mg, 0.147 mmol) was added into a methanol (3ml) solution of ligand **2.1** (14 mg, 0.14 mmol). The solution was left in darkness at room temperature and allowed to evaporate slowly to give crystals suitable for X-ray analysis. Yield 14 mg (27%), m.p. 122°C.

**Elemental Analysis:** calculated for  $\text{C}_5\text{H}_5\text{NO}\cdot\text{AgSO}_3\text{CF}_3$ : C, 20.47; H, 1.43; N, 3.98. Found: C, 20.73; H, 1.51; N, 3.97. **IR (KBr)**  $\nu_{\text{max}}/\text{cm}^{-1}$ : 3121, 2465, 1686, 1473, 1266, 1166, 1037, 838, 766, 673, 646. **ESI-MS**  $m/z$ : Found  $[\text{L}+\text{Ag}]^+$  201.9416,  $\text{C}_5\text{H}_5\text{AgNO}$  requires  $[\text{L}+\text{Ag}]^+$  201.9417.

#### **With silver(I) hexafluorophosphate (1:1) 2.23**

Silver(I) hexafluorophosphate (25 mg, 0.10 mmol) dissolved in methanol (1 ml) was added to a methanol (2 ml) solution of ligand **2.1** (10 mg, 0.10 mmol). The solution was left in darkness at room temperature and allowed to evaporate slowly to give crystals suitable for X-ray crystallography. Yield 18 mg (14%), m.p. 119°C.

**Elemental Analysis:** calculated for  $5(\text{C}_5\text{H}_5\text{NO})\cdot 3(\text{AgPF}_6)\cdot\text{CH}_3\text{COCH}_3$ : C, 26.03; H, 2.42; N, 5.42. Found: C, 26.52; H, 2.25; N, 6.12. **IR (KBr)**  $\nu_{\text{max}}/\text{cm}^{-1}$ : 2994, 1712, 1470, 1082, 987, 742, 548. **ESI-MS**  $m/z$ : No sign of  $[\text{L}+\text{Ag}]^+$  peaks.

### **6.3.2 Complexes of 2,6-dimethylpyridine N-oxide 2.4**

#### **With silver(I) trifluoroacetate (1:1) 2.24**

To a solution of ligand **2.4** (13 mg, 0.10 mmol) in methanol was added silver(I) trifluoroacetate (24 mg, 0.10 mmol) in methanol (1 ml). The resulting solution was allowed to evaporate slowly at

room temperature in darkness. Colourless crystals suitable for X-ray crystallography were thus obtained. Yield 25 mg (72%), m.p. 148°C.

**Elemental Analysis:** calculated for  $C_7H_9NO \cdot AgOCOCF_3$ : C, 31.42; H, 2.64; N, 4.07. Found: C, 31.40; H, 2.53; N, 3.96. **IR (KBr)**  $\nu_{max}/cm^{-1}$ : 1722, 1679, 1574, 1410, 1245, 1207, 1131, 1109, 836, 802, 772. **ESI-MS**  $m/z$ : No sign of  $[L+Ag]^+$  peaks.

#### **With silver(I) triflate (1:1) 2.25**

Silver(I) triflate (28 mg, 0.10 mmol) dissolved in methanol (1 ml) was added to a methanol (2 ml) solution of ligand **2.4** (13 mg, 0.10 mmol). The solution was left in darkness at room temperature and allowed to evaporate slowly to give crystals suitable for X-ray crystallography. Yield 22 mg (34%), m.p. 129°C.

**Elemental Analysis:** calculated for  $C_7H_9NO \cdot 2(AgSO_3CF_3) \cdot CH_3OH$ : C, 17.95; H, 1.96; N, 2.09. Found: C, 17.81; H, 1.48; N, 2.35. **IR (KBr)**  $\nu_{max}/cm^{-1}$ : 3414, 2023, 1638, 1615, 1430, 1380, 1177, 1131, 838, 582. **ESI-MS**  $m/z$ : Found  $[L+Ag]^+$  229.9727,  $C_7H_9AgNO$  requires  $[L+Ag]^+$  229.9730; Found  $[2L+Ag]^+$  353.0412,  $C_{14}H_{18}AgN_2O_2$  requires  $[2L+Ag]^+$  353.0414.

#### **With silver(I) nitrate (1:1) 2.26**

A solution of silver(I) nitrate (24 mg, 0.13 mmol) in water (1 ml) was dropped slowly into a water (3 ml) solution of ligand **2.4** (17 mg, 0.13 mmol). The mixture was then evaporated slowly over a period of a few days left in darkness at room temperature. Colourless crystals suitable for X-ray crystallography were obtained. Yield 28 mg (73%), m.p. 162°C.

**Elemental Analysis:** calculated for  $C_7H_9NO \cdot AgNO_3 \cdot H_2O$ : C, 27.84; H, 3.34; N, 9.27. Found: C, 27.44; H, 2.86; N, 9.36. **IR (KBr)**  $\nu_{max}/cm^{-1}$ : 2400, 1761, 1574, 1496, 1460, 1380, 1232, 1099, 826, 789. **ESI-MS**  $m/z$ : Found  $[L+Ag]^+$  229.9729,  $C_7H_9AgNO$  requires  $[L+Ag]^+$  229.9730.

### **6.3.3 Complexes of 2-benzylpyridine N-oxide 2.6**

#### **With silver(I) perchlorate (1:1) 2.27**

The reaction used 1 equivalent of silver(I) perchlorate (20 mg, 0.10 mmol) in methanol (1 ml) added to a 1 equivalent solution of ligand **2.6** (15 mg, 0.10 mmol) in methanol (2 ml). Crystallization formed colourless blocks, obtained by slow evaporation of the mother solution at room temperature in darkness. Yield 11 mg (28%), m.p. 114°C.

**Elemental Analysis:** calculated for  $C_{12}H_{11}NO \cdot AgClO_4$ : C, 36.72; H, 2.82; N, 3.57. Found: C, 37.16; H, 2.79; N, 3.59. **IR (KBr)**  $\nu_{max}/cm^{-1}$ : 3060, 1489, 1438, 1249, 1226, 1148, 1088, 932, 860, 777, 697. **ESI-MS**  $m/z$ : Found  $[L+Ag]^+$  291.9888,  $C_{12}H_{11}AgNO$  requires  $[L+Ag]^+$  291.9886.

### **With silver(I) perchlorate (1:2) 2.28**

To the solution of silver(I) perchlorate (22.3 mg, 0.10 mmol) in methanol (1 ml) was added slowly a solution of ligand **2.6** (10 mg, 0.053 mmol) in methanol (2 ml). The clear solution was left in darkness at room temperature for days to evaporate slowly, to give crystals suitable for X-ray analysis. Yield 9 mg (43%), m.p. 66°C.

**Elemental Analysis:** calculated for  $C_{12}H_{11}NO \cdot AgClO_4$ : C 36.72; H 2.82; N 3.57. Found: C 37.16; H 2.79; N 3.59. **IR (KBr)**  $\nu_{max}/cm^{-1}$ : 3060, 2012, 1490, 1438, 1250, 1146, 1086, 932, 861, 778, 730, 627. **ESI-MS**  $m/z$ : Found  $[L+Ag]^+$  291.9883,  $C_{12}H_{11}AgNO$  requires  $[L+Ag]^+$  291.9886; Found  $[2L+Ag]^+$  477.0729,  $C_{24}H_{22}AgN_2O_2$  requires  $[2L+Ag]^+$  477.0727.

### **With silver(I) hexafluorophosphate (1:1) 2.29**

A solution of silver(I) hexafluorophosphate (25 mg, 0.10 mmol) in methanol (1 ml) was dropped slowly into a solution of ligand **2.6** (10 mg, 0.10 mmol) in methanol (2 ml). The mixture was then slowly evaporated over a period of two weeks, and colourless block crystals suitable for X-ray analysis were obtained. Yield 13 mg (20%), m.p. 152°C.

**Elemental Analysis:** calculated for  $2(C_{12}H_{11}NO) \cdot AgPF_6$ : C 46.25; H 3.56; N 4.49. Found: (inconsistent with the proposed structure) C 36.22; H 2.79; N 3.51. **IR (KBr)**  $\nu_{max}/cm^{-1}$ : 2431, 1663, 1603, 1491, 1439, 1286, 1226, 1103, 847, 770, 740. **ESI-MS**  $m/z$ : Found  $[L+Ag]^+$  291.9883,  $C_{12}H_{11}AgNO$  requires  $[L+Ag]^+$  291.9886; Found  $[2L+Ag]^+$  477.0728,  $C_{24}H_{22}AgN_2O_2$  requires  $[2L+Ag]^+$  477.0727.

## **6.3.4 Complexes of 2-phenylpyridine N-oxide 2.7**

### **With silver(I) trifluoroacetate (1:1) 2.30**

A solution of silver(I) trifluoroacetate (14 mg, 0.058 mmol) in methanol (1 ml) was added to a methanol (2 ml) solution of ligand **2.7** (10 mg, 0.058 mmol). The reaction solution was then left in darkness at room temperature to evaporate slowly to yield crystals suitable for X-ray crystallography. Yield 18 mg (79%), m.p. 122 – 124°C.

**Elemental Analysis:** calculated for  $C_{11}H_9NO \cdot AgOCOCF_3$ : C, 40.01; H, 2.15; N, 3.56. Found: C, 39.82; H, 2.31; N, 3.57. **IR (KBr)**  $\nu_{max}/cm^{-1}$ : 1679, 1478, 1423, 1243, 1208, 1131, 841, 802, 761, 724, 695. **ESI-MS**  $m/z$ : Found  $[L+Ag]^+$  277.9727,  $C_{11}H_9AgNO$  requires  $[L+Ag]^+$  277.9730; Found  $[2L+Ag]^+$  449.0417,  $C_{20}H_{18}AgN_2O_2$  requires  $[2L+Ag]^+$  449.0414.

## **6.3.5 Complexes of 4-phenylpyridine N-oxide 2.8**

### **With silver(I) perchlorate (1:1) 2.31**

Silver(I) perchlorate (25 mg, 0.11 mmol) dissolved in methanol (1 ml) was added to a solution of ligand **2.8** (20 mg, 0.11 mmol) in methanol (3 ml). The solution was left in darkness at room

temperature and allowed to evaporate slowly to give colourless crystals suitable for X-ray analysis. Yield 11 mg (10%), m.p. 82°C.

**Elemental Analysis:** calculated for  $4(\text{C}_{11}\text{H}_9\text{NO}) \cdot 1.5(\text{AgClO}_4) \cdot \text{H}_2\text{O}$ : C, 52.13; H, 3.78; N, 5.53. Found: C, 52.17; H, 3.60; N, 5.46. **IR (KBr)**  $\nu_{\text{max}}/\text{cm}^{-1}$ : 3105, 1509, 1475, 1429, 1236, 1178, 1116, 1095, 850, 764, 696. **ESI-MS**  $m/z$ : Found  $[\text{L}+\text{Ag}]^+$  277.9727,  $\text{C}_{11}\text{H}_9\text{AgNO}$  requires  $[\text{L}+\text{Ag}]^+$  277.9730.

#### **With silver(I) trifluoroacetate (1:1) 2.32**

Silver(I) trifluoroacetate (21 mg, 0.093 mmol) dissolved in methanol (1 ml) was added to a solution of ligand **2.8** (16 mg, 0.093 mmol) in methanol (3 ml). The solution was left in darkness at room temperature and allowed to evaporate slowly to give colourless crystals suitable for X-ray crystallography. Yield 14 mg (38%), m.p. 114 – 116°C.

**Elemental Analysis:** calculated for  $\text{C}_{11}\text{H}_9\text{NO} \cdot \text{AgOCOCF}_3$ : C, 39.82; H, 2.27; N, 3.48. Found: C, 39.92; H, 2.31; N, 3.57. **IR (KBr)**  $\nu_{\text{max}}/\text{cm}^{-1}$ : 3104, 2402, 1703, 1679, 1478, 1246, 1178, 1039, 851, 765, 722. **ESI-MS**  $m/z$ : Found  $[\text{L}+\text{Ag}]^+$  277.9728,  $\text{C}_{11}\text{H}_9\text{AgNO}$  requires  $[\text{L}+\text{Ag}]^+$  277.9730.

#### **With silver(I) triflate (1:1) 2.33**

Silver(I) triflate (34 mg, 0.13 mmol) dissolved in methanol (1 ml) was added to a solution of ligand **2.8** (23 mg, 0.13 mmol) in methanol (4 ml). The solution was left in darkness at room temperature and allowed to evaporate slowly to give colourless crystals, suitable for X-ray crystallography. Yield 17 mg (30%), m.p. 114°C.

**Elemental Analysis:** calculated for  $\text{C}_{11}\text{H}_9\text{NO} \cdot \text{AgSO}_3\text{CF}_3$ : C, 35.15; H, 2.95; N, 3.15. Found: (inconsistent with the proposed structure) C, 37.36; H, 2.30; N, 3.63. **IR (KBr)**  $\nu_{\text{max}}/\text{cm}^{-1}$ : 3110, 1509, 1479, 1432, 1277, 1256, 1163, 1048, 1028, 849, 764. **ESI-MS**  $m/z$ : Found  $[\text{L}+\text{Ag}]^+$  277.9725,  $\text{C}_{11}\text{H}_9\text{AgNO}$  requires  $[\text{L}+\text{Ag}]^+$  277.9730.

#### **With silver(I) tetrafluoroborate (1:1) 2.34**

Silver(I) tetrafluoroborate (22 mg, 0.11 mmol) dissolved in methanol (1 ml) was added to a solution of ligand **2.8** (20 mg, 0.11 mmol) in methanol (3 ml). The solution was left in darkness at room temperature and allowed to evaporate slowly to give colourless crystals, suitable for X-ray crystallography. Yield 15 mg (37%), m.p. 62°C.

**Elemental Analysis:** calculated for  $\text{C}_{11}\text{H}_9\text{NO} \cdot \text{AgBF}_4 \cdot \text{H}_2\text{O}$ : C, 35.42; H, 2.89; N, 3.65. Found: C, 35.11; H, 2.76; N, 3.73. **IR (KBr)**  $\nu_{\text{max}}/\text{cm}^{-1}$ : 3106, 1896, 1509, 1475, 1428, 1235, 1180, 850, 764, 696, 578. **ESI-MS**  $m/z$ : No sign of  $[\text{L}+\text{Ag}]^+$  peaks.

### 6.3.6 Complexes of 4-(diphenylmethyl)pyridine N-oxide 2.9

#### With silver(I) perchlorate (1:1) 2.35

Silver(I) perchlorate (12 mg, 0.05 mmol) dissolved in methanol (1 ml) was added to a solution of ligand **2.9** (11 mg, 0.04 mmol) in methanol (3 ml). The solution was left in darkness at room temperature and allowed to evaporate slowly to give light yellow block crystals suitable for X-ray crystallography. Yield 14 mg (75%), m.p. 158°C.

**Elemental Analysis:** calculated for  $C_{18}H_{15}NO \cdot AgClO_4$ : C 46.13; H 3.23; N 2.99. Found: (inconsistent with the proposed structure) C 34.89; H 2.72; N 2.38. **IR (KBr)**  $\nu_{max}/cm^{-1}$ : 3421, 3051, 2019, 1628, 1493, 1450, 1312, 1092, 832, 628, 493. **ESI-MS**  $m/z$ : Found  $[L+Ag]^+$  368.0200,  $C_{18}H_{15}AgNO$  requires  $[L+Ag]^+$  368.0199.

### 6.3.7 Complexes of 4-methoxypyridine N-oxide 2.11

#### With silver(I) perchlorate (1:1) 2.36

Silver(I) perchlorate (32 mg, 0.15 mmol) dissolved in methanol (1 ml) was added to a solution of ligand **2.11** (19 mg, 0.15 mmol) in methanol (3 ml). The solution was left in darkness at room temperature and allowed to evaporate slowly to give colourless crystals suitable for X-ray crystallography. Yield 18 mg (26%), m.p. 168°C.

**Elemental Analysis:** calculated for  $2(C_6H_7NO_2) \cdot AgClO_4$ : C, 31.50; H, 3.08; N, 6.12. Found: C, 31.31; H, 2.96; N, 5.96. **IR (KBr)**  $\nu_{max}/cm^{-1}$ : 3112, 2043, 1628, 1499, 1464, 1298, 1213, 1150, 846, 759, 626. **ESI-MS**  $m/z$ : Found  $[L+Ag]^+$  231.9522,  $C_6H_7AgNO_2$  requires  $[L+Ag]^+$  231.9522.

#### With silver(I) trifluoroacetate (1:1) 2.37

A solution of silver(I) trifluoroacetate (32 mg, 0.14 mmol) in methanol (1 ml) was dropped slowly into a solution of ligand **2.11** (18 mg, 0.14 mmol) in methanol (2 ml). The resulting clear solution was left to stand in darkness at room temperature and allowed to evaporate slowly for a few days to give colourless crystals suitable for X-ray analysis. Yield 19 mg (24%), mp. 56°C.

**Elemental Analysis:** calculated for  $C_6H_7NO_2 \cdot 2(AgOCOCF_3)$ : C, 21.19; H, 1.24; N, 2.47. Found: (inconsistent with the proposed structure) C, 28.36; H, 2.01; N, 4.07. **IR (KBr)**  $\nu_{max}/cm^{-1}$ : 3038, 1685, 1634, 1504, 1441, 1296, 1213, 1136, 1020, 846, 762. **ESI-MS**  $m/z$ : Found  $[L+Ag]^+$  231.9518,  $C_6H_7AgNO_2$  requires  $[L+Ag]^+$  231.9522.

#### With silver(I) tetrafluoroborate (1:1) 2.38

Silver(I) tetrafluoroborate (54 mg, 0.27 mmol) dissolved in methanol (1 ml) was added to a solution of ligand **2.11** (35 mg, 0.27 mmol) in methanol (3 ml). The reaction solution was left in

darkness at room temperature and allowed to evaporate slowly to give colourless crystals suitable for X-ray crystallography. Yield 26 mg (22%), m.p. 184°C.

**Elemental Analysis:** calculated for  $2(\text{C}_6\text{H}_7\text{NO}_2)\cdot\text{AgBF}_4\cdot 2(\text{H}_2\text{O})$ : C, 29.97; H, 3.77; N, 5.82. Found: C, 30.25; H, 2.89; N, 5.76. **IR (KBr)**  $\nu_{\text{max}}/\text{cm}^{-1}$ : 3137, 1926, 1630, 1505, 1445, 1312, 1097, 1039, 852, 750, 529. **ESI-MS**  $m/z$ : Found  $[\text{L}+\text{Ag}]^+$  231.9521,  $\text{C}_6\text{H}_7\text{AgNO}_2$  requires  $[\text{L}+\text{Ag}]^+$  231.9522.

### 6.3.8 Complex of di-(2-pyridyl)ketone N-oxide 2.13

#### With silver(I) perchlorate (1:2) 2.39

A solution of silver(I) perchlorate (23 mg, 0.12 mmol) in methanol (1 ml) was added to a solution of ligand **2.13** (13 mg, 0.064 mmol) in toluene:chloroform (1:1, 4 ml). The solution was left in darkness at room temperature and allowed to evaporate slowly to give large block shaped green coloured crystals suitable for X-ray crystallography. Yield 21 mg (81%), m.p. 206°C.

**Elemental Analysis:** calculated for  $\text{C}_{11}\text{H}_8\text{N}_2\text{O}_2\cdot\text{AgClO}_4$ : C, 32.42; H, 1.98; N, 6.87. Found: C, 32.04; H, 1.85; N, 6.72. **IR (KBr)**  $\nu_{\text{max}}/\text{cm}^{-1}$ : 3090, 2000, 1683, 1597, 1438, 1323, 1247, 1213, 1094, 842, 775. **ESI-MS**  $m/z$ : Found  $[\text{L}+\text{Ag}]^+$  306.9631,  $\text{C}_{11}\text{H}_8\text{AgN}_2\text{O}_2$  requires  $[\text{L}+\text{Ag}]^+$  306.9631.

### 6.3.9 Complexes of 5,6,7,8-tetrahydroquinoline N-oxide 2.14

#### With silver(I) perchlorate (1:1) 2.40

A silver(I) perchlorate (14 mg, 0.067 mmol) solution in methanol (1 ml) was added to a solution of ligand **2.14** (10 mg, 0.067 mmol) in dichloromethane (4 ml). The solution was left to stand in darkness at room temperature, and allowed to evaporate slowly to give colourless needle shape crystals. Yield 22 mg (65%), m.p. 138°C.

**Elemental Analysis:** calculated for  $2(\text{C}_9\text{H}_{11}\text{NO})\cdot\text{AgClO}_4\cdot\text{H}_2\text{O}$ : C, 41.28; H, 4.62; N, 5.35. Found: C, 40.64; H, 4.18; N, 5.24. **IR (KBr)**  $\nu_{\text{max}}/\text{cm}^{-1}$ : 2940, 1486, 1438, 1335, 1254, 1146, 1038, 844, 787, 698, 626, 557. **ESI-MS**  $m/z$ : No sign of  $[\text{L}+\text{Ag}]^+$  peaks.

#### With silver(I) perchlorate (1:2) 2.41

Silver(I) perchlorate (58 mg, 0.28 mmol) dissolved in methanol (2 ml) was added to a solution of ligand **2.14** (21 mg, 0.14 mmol) in dichloromethane (4 ml). The solution was left in darkness at room temperature and allowed to evaporate slowly to give colourless crystals. Yield 17 mg (34%), m.p. 162°C.

**Elemental Analysis:** calculated for  $\text{C}_9\text{H}_{11}\text{NO}\cdot\text{AgClO}_4$ : C 30.32; H 3.11; N 3.93. Found: (inconsistent with the proposed structure) C 32.04; H 1.85; N 6.72. **IR (KBr)**  $\nu_{\text{max}}/\text{cm}^{-1}$ : 3419, 2942, 1701, 1485, 1437, 1148, 1088, 1213, 791, 626. **ESI-MS**  $m/z$ : Found  $[\text{L}+\text{Ag}]^+$  255.9881,  $\text{C}_9\text{H}_{11}\text{AgNO}$  requires  $[\text{L}+\text{Ag}]^+$  255.9886; Found  $[\text{2L}+\text{Ag}]^+$  405.0727,  $\text{C}_{18}\text{H}_{22}\text{AgN}_2\text{O}_2$  requires  $[\text{2L}+\text{Ag}]^+$  405.0727.

**With silver(I) perchlorate (1:3) 2.42**

Silver(I) perchlorate (42 mg, 0.20 mmol) dissolved in methanol (2 ml) was added to a solution of ligand **2.14** (10 mg, 0.067 mmol) in dichloromethane (5 ml). The solution was left in darkness at room temperature and allowed to evaporate slowly to give colourless needles. Yield 3 mg (7%), m.p. 231°C.

**Elemental Analysis:** Insufficient and impure sample for analysis. **IR (KBr)**  $\nu_{\max}/\text{cm}^{-1}$ : 3413, 2940, 1707, 1486, 1438, 1256, 1148, 1092, 791, 626. **ESI-MS**  $m/z$ : No sign of  $[\text{L}+\text{Ag}]^+$  peaks.

**With silver(I) triflate (1:1) 2.43**

To a solution of silver(I) perchlorate (18 mg, 0.067 mmol) in methanol (1 ml) was added a dichloromethane (4 ml) solution of ligand **2.14** (10 mg, 0.067 mmol). The resulting solution was left to stand in darkness at room temperature. Slow evaporation furnished needle shaped brown crystals. Yield 9 mg (25%), m.p. 182°C.

**Elemental Analysis:** calculated for  $\text{C}_9\text{H}_{11}\text{NO} \cdot \text{AgSO}_3\text{CF}_3 \cdot 2(\text{H}_2\text{O})$ : C, 27.16; H, 3.42; N, 3.17. Found: C, 27.73; H, 2.53; N, 2.93. **IR (KBr)**  $\nu_{\max}/\text{cm}^{-1}$ : 2944, 1683, 1487, 1439, 1258, 1210, 1129, 972, 837, 803, 723. **ESI-MS**  $m/z$ : No sign of  $[\text{L}+\text{Ag}]^+$  peaks.

**6.3.10 Compounds from isoquinoline N-oxide 2.16****With silver(I) perchlorate (1:1) 2.44**

Silver(I) perchlorate (15 mg, 0.068 mmol) dissolved in methanol (2 ml) was added to a solution of ligand **2.16** (10 mg, 0.068 mmol) in acetonitrile (2 ml). The solution was left in darkness at room temperature and allowed to evaporate slowly to give colourless needle shaped crystals suitable for X-ray crystallography. Yield 8 mg (48%).

**With silver(I) trifluoroacetate (1:1) 2.45**

Silver(I) trifluoroacetate (16 mg, 0.068 mmol) dissolved in methanol (2 ml) was added to a solution of ligand **2.16** (10 mg, 0.068 mmol) in acetonitrile (2 ml). The resulting solution was left in darkness at room temperature and allowed to evaporate slowly to give colourless needle shaped crystals suitable for X-ray analysis. Yield 12 mg (56%).

**With silver(I) tetrafluoroborate (1:1) 2.46**

Silver(I) tetrafluoroborate (14 mg, 0.068 mmol) dissolved in methanol (2 ml) was added to a solution of ligand **2.16** (10 mg, 0.068 mmol) in acetonitrile (2 ml). The solution was left in

darkness at room temperature and allowed to evaporate slowly to give colourless crystals, suitable for X-ray crystallography. Yield 6 mg (41%).

#### **With sodium tetraphenylborate (1:1) 2.47**

A 1:1 equivalent ratio of sodium tetraphenylborate (24 mg, 0.068 mmol) dissolved in methanol (2 ml) was added to a solution of ligand **2.16** (10 mg, 0.068 mmol) in acetonitrile (2 ml). This yellow colour solution was then left at room temperature to slowly evaporate. After a few days orange block shaped crystals were obtained suitable for X-ray crystallography, which are highly hygroscopic.

#### **With silver(I) hexafluorophosphate (1:1) 2.48**

Solutions of silver(I) hexafluorophosphate (47 mg, 0.18 mmol) in methanol (2 ml) and ligand **2.16** (27.3 mg, 0.188 mmol) in acetonitrile (2 ml) were mixed together. Upon slow evaporation of the solution in darkness at room temperature, colourless crystals of **2.48** were obtained. Yield 11 mg (20%).

### **6.3.11 Compound from 1,10-phenanthroline N-oxide 2.17**

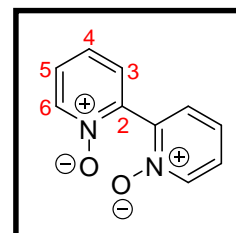
#### **With silver(I) perchlorate (1:2) 2.49**

Silver(I) perchlorate (21 mg, 0.10 mmol) dissolved in acetone (2 ml) was added to a solution of ligand **2.17** (10 mg, 0.050 mmol) in acetone (5 ml). The solution was left in darkness at room temperature, which resulted in one single pale orange crystal suitable for X-ray crystallography, m.p. 138°C. Insufficient sample for further analysis.

## **6.4 Preparation of pyridine N,N'-dioxides**

### **6.4.1 Synthesis of 2,2'-bipyridine N,N'-dioxide 3.1<sup>[202]</sup>**

To a solution of 2,2'-bipyridine (10.0 g, 64.0 mmol) in acetic acid, 50% H<sub>2</sub>O<sub>2</sub> (10 ml) was added at room temperature and the reaction mixture was heated at 70 – 80°C for 11 hours. The reaction mixture was then cooled to room temperature and concentrated to dryness under vacuum to give a yellow oily liquid. The crude residue gave a precipitate with acetone (80 ml), which was filtered and dried to give **3.1**, as a white solid. Yield 9.27 g (76%), m.p. 308 – 310°C [Lit<sup>[138b]</sup>: 307 – 309°C].

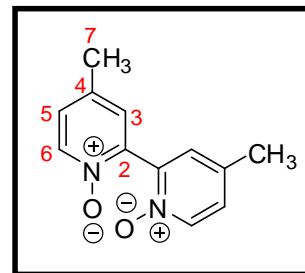




$^1\text{H NMR}$  (400MHz,  $\text{D}_2\text{O}$ )  $\delta/\text{ppm}$ : 8.37 (d,  $J = 6.6$  Hz, 2H,  $\text{H}_6$ ), 7.75 (t, 7.8 Hz, 2H,  $\text{H}_4$ ), 7.64 – 7.67 (m, 4H,  $\text{H}_3$ ,  $\text{H}_5$ ).  $^{13}\text{C NMR}$  (100MHz,  $\text{D}_2\text{O}$ )  $\delta/\text{ppm}$ : 141.75 ( $\text{C}_2$ ), 139.69 ( $\text{C}_6$ ), 131.43 ( $\text{C}_3$ ), 128.84 ( $\text{C}_5$ ), 128.42 ( $\text{C}_4$ ). **IR (KBr)**  $\nu_{\text{max}}/\text{cm}^{-1}$ : 3043, 1929, 1617, 1477, 1428, 1256, 1021, 836, 768, 582. **ESI-MS**  $m/z$ : Found  $[\text{L}+\text{H}]^+$  189.0659,  $\text{C}_{10}\text{H}_9\text{N}_2\text{O}_2$  requires  $[\text{L}+\text{H}]^+$  189.0659.

#### 6.4.2 Synthesis of 4,4'-dimethyl-2,2'-bipyridine N,N'-dioxide **3.2**<sup>[156]</sup>

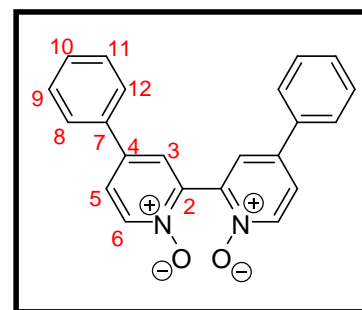
4,4'-Dimethyl-2,2'-bipyridine (0.900 g, 4.88 mmol) and mCPBA (1.70 g, 10.2 mmol) were dissolved in methanol (20 ml) at room temperature and heated to reflux for 1 hour. The reaction mixture was then cooled to room temperature, and concentrated to dryness under vacuum to give a yellow-white solid. The crude residue was purified by silica gel flash column chromatography with 2% methanol:dichloromethane as elutant to give **3.2**, as an off-white solid. Yield 0.367 g (35%), m.p. 238°C [Lit: m.p. not reported].



$^1\text{H NMR}$ <sup>[202]</sup> (400MHz,  $\text{CDCl}_3$ )  $\delta/\text{ppm}$ : 8.22 (d,  $J = 6.6$  Hz, 2H,  $\text{H}_6$ ), 7.48 (bs, 2H,  $\text{H}_3$ ), 7.12 (dd,  $J = 2.0$  Hz, 6.7 Hz 2H,  $\text{H}_5$ ), 2.36 (s, 6H,  $-\text{CH}_3$ ).  $^{13}\text{C NMR}$ <sup>[202]</sup> (100MHz,  $\text{CDCl}_3$ )  $\delta/\text{ppm}$ : 141.30 ( $\text{C}_2$ ), 139.44 ( $\text{C}_4$ ), 136.65 ( $\text{C}_6$ ), 128.94 ( $\text{C}_3$ ), 127.26 ( $\text{C}_5$ ), 20.29 ( $\text{C}_7$ ). **IR (KBr)**  $\nu_{\text{max}}/\text{cm}^{-1}$ : 3060, 2043, 1636, 1617, 1453, 1469, 1224, 1217, 1051, 843, 793. **ESI-MS**  $m/z$ : Found  $[\text{L}+\text{H}]^+$  217.0969,  $\text{C}_{12}\text{H}_{13}\text{N}_2\text{O}_2$  requires  $[\text{L}+\text{H}]^+$  217.0972; Found  $[\text{L}+\text{Na}]^+$  239.0789,  $\text{C}_{12}\text{H}_{12}\text{N}_2\text{NaO}_2$  requires  $[\text{L}+\text{Na}]^+$  239.0791.

#### 6.4.3 Synthesis of 4,4'-diphenyl-2,2'-bipyridine N,N'-dioxide **3.3**

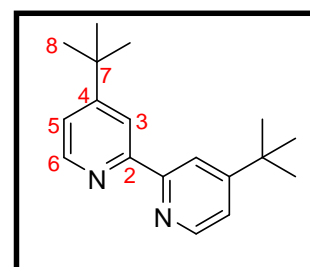
4,4'-Diphenyl-2,2'-bipyridine (1.00 g, 3.24 mmol) and mCPBA (1.20 g, 6.81 mmol) were dissolved in chloroform (20 ml) at room temperature and heated to reflux for 30 minutes. The reaction mixture was then cooled to room temperature, and concentrated to dryness under vacuum to give brown solid. The crude residue was purified by silica gel flash column chromatography with 5% methanol:dichloromethane as elutant to give **3.3**, as a pale brown solid. Yield 0.410 g (37%), m.p. 281°C.



$^1\text{H NMR}$  (400MHz,  $\text{CDCl}_3$ )  $\delta/\text{ppm}$ : 8.39 (d,  $J = 7.1$  Hz, 2H,  $\text{H}_6$ ), 7.97 (d,  $J = 2.7$  Hz, 2H,  $\text{H}_3$ ), 7.62 (d,  $J = 7.0$  Hz 4H,  $\text{H}_8$ ,  $\text{H}_{12}$ ), 7.58 (dd,  $J = 2.4$  Hz, 6.7 Hz, 2H,  $\text{H}_5$ ) 7.40 – 7.49 (m, 6H,  $\text{H}_9$ ,  $\text{H}_{10}$ ,  $\text{H}_{11}$ ).  $^{13}\text{C NMR}$  (100MHz,  $\text{CDCl}_3$ )  $\delta/\text{ppm}$ : 142.07 ( $\text{C}_2$ ), 140.14 ( $\text{C}_6$ ), 137.87 ( $\text{C}_4$ ), 136.09 ( $\text{C}_7$ ), 129.29 ( $\text{C}_9$ ), 129.12 ( $\text{C}_{10}$ ), 126.52 ( $\text{C}_5$ ), 126.18 ( $\text{C}_3$ ), 124.14 ( $\text{C}_8$ ). **IR (KBr)**  $\nu_{\text{max}}/\text{cm}^{-1}$ : 3043, 2034, 1617, 1636, 1453, 1236, 1262, 888, 763, 624. **ESI-MS**  $m/z$ : Found  $[\text{L}+\text{Na}]^+$  363.1103,  $\text{C}_{22}\text{H}_{16}\text{N}_2\text{NaO}_2$  requires  $[\text{L}+\text{Na}]^+$  363.1104.

#### 6.4.4 Synthesis of 4,4'-di-tert-butyl-2,2'-bipyridine **3.4b**<sup>[203]</sup>

4-*tert*-Butylpyridine (14.90 g, 110.1 mmol) was refluxed with 10% Pd/C (600 mg, 5.63 mmol) for 4 days. The reaction mixture was diluted with chloroform (50 ml) and filtered through Celite. The filtrate was concentrated to dryness under vacuum to give a pale yellow liquid, which

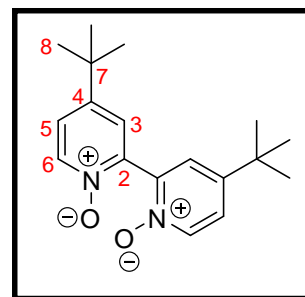


solidified on cooling. The unreacted 4-tert-butylpyridine was recovered by distillation and the remaining crude residue was recrystallized from pentane to give **3.4b**, as a white powder. Yield 1.69 g (6%), m.p. 158°C. [Lit<sup>[204]</sup>: m.p. 159 – 160°C].

<sup>1</sup>H NMR<sup>[204]</sup> (400MHz, CDCl<sub>3</sub>) δ/ppm: 8.59 (d, *J* = 5.4 Hz, 2H, H<sub>6</sub>), 8.42 (bs, 2H, H<sub>3</sub>), 7.30 (dd, *J* = 2.0 Hz, 5.1 Hz, 2H, H<sub>5</sub>), 1.39 (s, 18H, H<sub>8</sub>). <sup>13</sup>C NMR<sup>[204]</sup> (100MHz, CDCl<sub>3</sub>) δ/ppm: 160.94 (C<sub>4</sub>), 156.52 (C<sub>2</sub>), 149.01 (C<sub>6</sub>), 120.69 (C<sub>3</sub>), 118.26 (C<sub>5</sub>), 34.96 (C<sub>7</sub>), 30.61 (C<sub>8</sub>). IR (KBr)  $\nu_{\max}/\text{cm}^{-1}$ : 3409, 2957, 1932, 1585, 1545, 1375, 1267, 1204, 838, 669. ESI-MS *m/z*: Found [L+H]<sup>+</sup> 269.2019, C<sub>18</sub>H<sub>25</sub>N<sub>2</sub> requires [L+H]<sup>+</sup> 269.2012.

#### 6.4.5 Synthesis of 4,4'-di-tert-butyl-2,2'-bipyridine N,N'-dioxide **3.4**<sup>[140]</sup>

To a solution of 4,4'-di-tert-butyl-2,2'-bipyridine (1.00 g, 3.72 mmol) in acetic acid (10 ml), was added 50% H<sub>2</sub>O<sub>2</sub> (6 ml) at room temperature. The solution was heated at 80°C for 14 hours. After cooling, the reaction mixture was concentrated to dryness under vacuum to give a white foam. The crude product was purified by silica gel column chromatography with 5% hexane:dichloromethane as elutant to give **3.4** as a gummy liquid. To

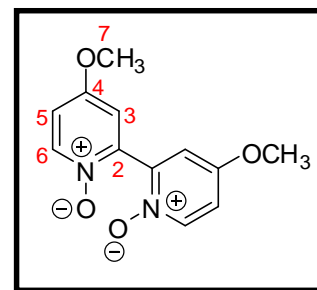


the liquid reaction mixture, hexane (50 ml) was added and stored overnight in a freezer. The hexanes layers were discarded and the liquid was dried under vacuum to give **3.4**, as a beige solid. Yield 0.550 g (49%), m.p. 52°C.

<sup>1</sup>H NMR<sup>[205]</sup> (400MHz, CDCl<sub>3</sub>) δ/ppm: 8.25 – 8.32 (m, 2H, H<sub>6</sub>), 7.67 – 7.71 (m, 2H, H<sub>3</sub>), 7.32 – 7.39 (m, 2H, H<sub>5</sub>), 1.37 (s, 18H, H<sub>8</sub>). <sup>13</sup>C NMR (100MHz, CDCl<sub>3</sub>) δ/ppm: 150.27 (C<sub>2</sub>), 141.39 (C<sub>4</sub>), 139.31 (C<sub>6</sub>), 125.55 (C<sub>3</sub>), 123.85 (C<sub>5</sub>), 34.74 (C<sub>7</sub>), 30.48 (C<sub>8</sub>). IR (KBr)  $\nu_{\max}/\text{cm}^{-1}$ : 3000, 2998, 1480, 1366, 1254, 1144, 832, 574, 547, 453. ESI-MS *m/z*: Found [L+H]<sup>+</sup> 301.1918, C<sub>18</sub>H<sub>25</sub>N<sub>2</sub>O<sub>2</sub> requires [L+H]<sup>+</sup> 301.1911.

#### 6.4.6 Synthesis of 4,4'-dimethoxy-2,2'-bipyridine N,N'-dioxide **3.5**

Compound **3.6** (1.00 g, 3.59 mmol) was added to a freshly prepared solution of sodium methoxide (0.300 g of Na in 50 ml of methanol) at room temperature. The yellow-red solution was stirred at 35°C on a water bath for 2 hours. This was then cooled to 0°C, and 3-4 drops of concentrated sulphuric acid were added. The resulting suspension was filtered through Celite, and the filtrate was concentrated to dryness

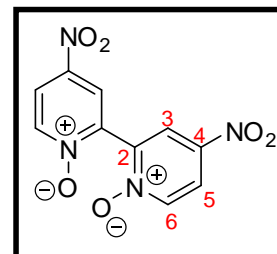


under vacuum to give a yellow solid. The crude residue was diluted with water (15 ml) and extracted with hot chloroform (5x50 ml). The combined organic layers were separated, dried over anhydrous MgSO<sub>4</sub> and concentrated to dryness. The crude residue was recrystallized from dichloromethane/hexanes to give **3.5**, as a white powder. Yield 0.312 g (35%), m.p. 226 – 228°C [Lit<sup>[138b]</sup>: 223 – 226°C].

$^1\text{H NMR}^{[202]}$  (400MHz,  $\text{CD}_3\text{OD}$ )  $\delta/\text{ppm}$ : 8.30 (d,  $J = 7.5$  Hz, 2H,  $\text{H}_6$ ), 7.33 (d,  $J = 3.2$  Hz, 2H,  $\text{H}_3$ ), 7.24 (dd,  $J = 3.5$  Hz, 7.4 Hz, 2H,  $\text{H}_5$ ), 3.29 (s, 6H,  $\text{H}_7$ ).  $^{13}\text{C NMR}^{[202]}$  (100MHz,  $\text{CD}_3\text{OD}$ )  $\delta/\text{ppm}$ : 161.47 ( $\text{C}_4$ ), 144.48 ( $\text{C}_2$ ), 141.98 ( $\text{C}_6$ ), 115.22 ( $\text{C}_3$ ), 114.85 ( $\text{C}_5$ ), 57.43 ( $\text{C}_7$ ) **IR (KBr)**  $\nu_{\text{max}}/\text{cm}^{-1}$ : 3052, 1550, 1567, 1477, 1300, 1212, 1017, 837, 779, 722. **ESI-MS**  $m/z$ : Found  $[\text{L}+\text{H}]^+$  249.0871,  $\text{C}_{11}\text{H}_{11}\text{N}_4\text{O}_4$  requires  $[\text{L}+\text{H}]^+$  249.0870.

#### 6.4.7 Synthesis of 4,4'-dinitro-2,2'-bipyridine N,N'-dioxide **3.6**<sup>[202]</sup>

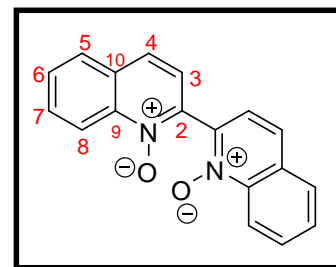
To a mixture of 2,2'-bipyridine N,N'-dioxide (4.40 g, 23.3 mmol) and concentrated sulphuric acid (15.8 ml) cooled over an ice bath, fuming nitric acid (7.4 ml) was added dropwise. The mixture was stirred at room temperature for one hour, and then at 80°C for 12 hours. The reaction mixture was then cooled to room temperature and was added slowly onto crushed ice. The solution turned green with the evolution of a reddish-brown gas, and was stirred at room temperature for 1 hour. The yellow precipitates were washed thoroughly with plenty of water (3x100 ml), filtered and dried under vacuum to give **3.6**, as a yellow powder. Yield 1.10 g (17%), m.p. 270 – 272°C [ $\text{Lit}^{[138b]}$ : 271 – 272°C].



$^1\text{H NMR}^{[202]}$  (400MHz, DMSO)  $\delta/\text{ppm}$ : 8.67 (d,  $J = 3.5$  Hz, 2H,  $\text{H}_3$ ), 8.57 (d,  $J = 7.5$  Hz, 2H,  $\text{H}_6$ ), 8.35 (dd,  $J = 3.1$  Hz, 7.0 Hz, 2H,  $\text{H}_5$ ).  $^{13}\text{C NMR}^{[202]}$  (100MHz,  $\text{CDCl}_3$ )  $\delta/\text{ppm}$ : 142.56 ( $\text{C}_2$ ), 141.62 ( $\text{C}_4$ ), 140.93 ( $\text{C}_6$ ), 124.24 ( $\text{C}_3$ ), 122.37 ( $\text{C}_5$ ). **IR (KBr)**  $\nu_{\text{max}}/\text{cm}^{-1}$ : 3094, 1886, 1516, 1344, 1292, 1129, 931, 910, 836, 748. **ESI-MS**  $m/z$ : Found  $[\text{L}+\text{H}]^+$  279.0359,  $\text{C}_{10}\text{H}_7\text{N}_4\text{O}_6$  requires  $[\text{L}+\text{H}]^+$  279.0360.

#### 6.4.8 Synthesis of 2,2'-biquinoline N,N'-dioxide **3.7**

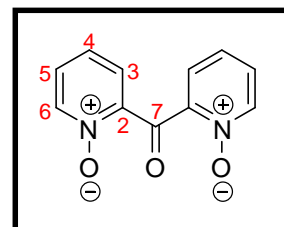
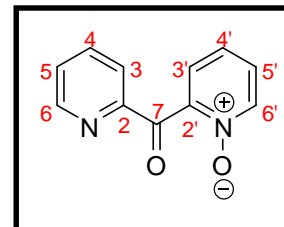
To a solution of 2,2'-biquinoline (1.50 g, 5.85 mmol) in acetic acid (25 ml), 50%  $\text{H}_2\text{O}_2$  (7 ml) was added and the reaction mixture was heated at 90°C for 24 hours, then was cooled to room temperature, and concentrated to dryness under vacuum to give a yellow solid. The crude residue was dissolved in methanol (20 ml) and left overnight in a fridge to give **3.7**, as yellow needles. Yield 0.140 g (8%), m.p. 258°C [ $\text{Lit}^{[206]}$ : m.p. 257°C].



$^1\text{H NMR}^{[207]}$  (400MHz,  $\text{CD}_3\text{OD}$ )  $\delta/\text{ppm}$ : 8.76 (d,  $J = 9.0$  Hz, 2H,  $\text{H}_8$ ), 8.34 (d,  $J = 8.6$  Hz, 2H,  $\text{H}_3$ ), 8.30 (d,  $J = 9.0$  Hz, 2H,  $\text{H}_4$ ), 8.17 (d,  $J = 8.3$  Hz, 2H,  $\text{H}_5$ ), 8.03 (t,  $J = 8.0$  Hz, 2H,  $\text{H}_7$ ), 7.91 (t,  $J = 7.8$  Hz, 2H,  $\text{H}_6$ ).  $^{13}\text{C NMR}^{[207]}$  (100MHz,  $\text{CD}_3\text{OD}$ )  $\delta/\text{ppm}$ : 132.56 ( $\text{C}_7$ ), 131.44 ( $\text{C}_9$ ), 130.96 ( $\text{C}_3$ ), 130.72 ( $\text{C}_6$ ), 128.61 ( $\text{C}_5$ ), 121.53 ( $\text{C}_4$ ), 118.79 ( $\text{C}_8$ ),  $\text{C}_2$  and  $\text{C}_{10}$  carbons were not observed even with prolonged scans. **IR (KBr)**  $\nu_{\text{max}}/\text{cm}^{-1}$ : 3421, 2034, 1619, 1634, 1578, 1372, 1299, 1178, 1088, 897, 761. **ESI-MS**  $m/z$ : Found  $[\text{L}+\text{H}]^+$  289.0970,  $\text{C}_{18}\text{H}_{13}\text{N}_2\text{O}_2$  requires  $[\text{L}+\text{H}]^+$  289.0972.

### 6.4.9 Synthesis of di-2-pyridylketone N,N'-dioxide 3.8

Di-2-pyridyl ketone (0.600 g, 3.25 mmol) and mCPBA (1.18 g, 6.84 mmol) were dissolved in methanol (15 ml) at room temperature and heated to reflux for 1 hour. After TLC analysis, the reaction mixture was allowed to cool to room temperature, and concentrated to dryness under vacuum to give brown solid. The crude residue was purified by silica gel column chromatography with 4% methanol:dichloromethane as elutant to give **2.13**, as a brown solid and **3.8**, as a light green solid.



**Di-(2-pyridyl)ketone N-dioxide 2.13** Yield 0.430 g (66%), m.p.132°C

[Lit<sup>[90a]</sup>: m.p. not reported].

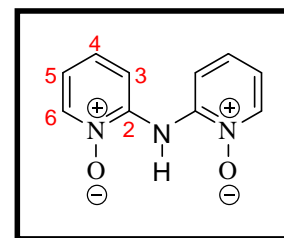
<sup>1</sup>H NMR (400MHz, CDCl<sub>3</sub>) δ/ppm: 8.60 (d, *J* = 4.7 Hz, 1H, H<sub>6</sub>), 8.18 (dd, *J* = 2.7 Hz, 5.0 Hz, 1H, H<sub>6'</sub>), 8.10 (d, *J* = 7.8 Hz, 1H, H<sub>3</sub>), 7.89 (td, *J* = 1.6 Hz, 7.6 Hz, 1H, H<sub>4</sub>), 7.45 – 7.49 (m, 2H, H<sub>5</sub>, H<sub>4'</sub>), 7.38 – 7.41 (m, 2H, H<sub>5'</sub>, H<sub>3'</sub>). <sup>13</sup>C NMR (100MHz, CDCl<sub>3</sub>) 190.26 (C<sub>7</sub>), 152.97 (C<sub>2</sub>), 149.46 (C<sub>6</sub>), 147.76 (C<sub>2'</sub>), 139.60 (C<sub>6'</sub>), 137.13 (C<sub>4</sub>), 127.36 (C<sub>5</sub>), 126.97 (C<sub>5'</sub>), 125.52, 122.55 (C<sub>3</sub>), one carbon was not observed even with prolonged scans. IR (KBr) ν<sub>max</sub>/cm<sup>-1</sup>: 3056, 1696, 1617, 1436, 1318, 1241, 1180, 993, 948, 847, 787. ESI-MS *m/z*: Found [L+H]<sup>+</sup> 201.0661, C<sub>11</sub>H<sub>9</sub>N<sub>2</sub>O<sub>2</sub> requires [L+H]<sup>+</sup> 201.0480; Found [L+Na]<sup>+</sup> 223.0480, C<sub>11</sub>H<sub>8</sub>N<sub>2</sub>NaO<sub>2</sub> requires [L+Na]<sup>+</sup> 223.0478.

**Di-(2-pyridyl)ketone N,N'-dioxide 3.8** Yield 0.150 g (21%), m.p. 186°C.

<sup>1</sup>H NMR (400MHz, CDCl<sub>3</sub>) δ/ppm: 8.08 (dd, *J* = 2.0 Hz, 5.1 Hz, 2H, H<sub>6</sub>), 7.68 – 7.70 (m, 2H, H<sub>3</sub>), 7.36 – 7.40 (m, 4H, H<sub>4</sub>, H<sub>5</sub>). <sup>13</sup>C NMR (100MHz, CDCl<sub>3</sub>) δ/ppm: 183.80 (C<sub>7</sub>), 147.22 (C<sub>2</sub>), 138.88 (C<sub>6</sub>), 127.71 (C<sub>4</sub>), 126.25 (C<sub>3</sub>), 126.09 (C<sub>5</sub>). IR (KBr) ν<sub>max</sub>/cm<sup>-1</sup>: 3073, 2189, 1673, 1602, 1436, 1318, 1219, 1172, 946, 841, 641. ESI-MS *m/z*: Found [L+H]<sup>+</sup> 217.0605, C<sub>11</sub>H<sub>9</sub>N<sub>2</sub>O<sub>3</sub> requires [L+H]<sup>+</sup> 217.0608; Found [L+Na]<sup>+</sup> 239.0424, C<sub>11</sub>H<sub>8</sub>N<sub>2</sub>NaO<sub>3</sub> requires [L+Na]<sup>+</sup> 239.0427.

### 6.4.10 Synthesis of 2,2'-dipyridylamine N,N'-dioxide 3.9

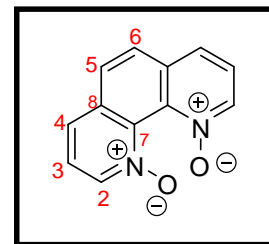
2,2'-Dipyridylamine (0.800 g, 4.67 mmol) and mCPBA (1.70 g, 10.2 mmol) were dissolved in methanol (15 ml) at room temperature and heated to reflux for one hour. The reaction mixture was cooled to room temperature, and concentrated to dryness under vacuum to give a brown solid. The crude residue was purified by silica gel column with 10% methanol:dichloromethane as elutant to give **3.9**, as a pale red powder. Yield 0.121 g (13%), m.p. 230°C [Lit<sup>[208]</sup>: m.p. 233°C].



<sup>1</sup>H NMR (400MHz, CDCl<sub>3</sub>) δ/ppm: 8.36 (d, *J* = 6.3 Hz, 2H, H<sub>6</sub>), 7.39 (d, *J* = 8.2 Hz, 2H, H<sub>3</sub>), 7.31 (t, *J* = 7.8 Hz, 2H, H<sub>4</sub>), 6.95 (t, *J* = 7.0 Hz, 2H, H<sub>5</sub>). <sup>13</sup>C NMR (100MHz, CDCl<sub>3</sub>) δ/ppm: 144.73 (C<sub>2</sub>), 138.63 (C<sub>6</sub>), 126.99 (C<sub>4</sub>), 117.35 (C<sub>3</sub>), 110.39 (C<sub>5</sub>). IR (KBr) ν<sub>max</sub>/cm<sup>-1</sup>: 3069, 1703, 1610, 1567, 1539, 1453, 1327, 1257, 1204, 1118, 838. ESI-MS *m/z*: Found [L+H]<sup>+</sup> 204.0770, C<sub>10</sub>H<sub>10</sub>N<sub>3</sub>O<sub>2</sub> requires [L+H]<sup>+</sup> 204.0768.

### 6.4.11 Synthesis of 1,10-phenanthroline N,N'-dioxide 3.10

To a solution of 1,10-phenanthroline (2.00 g, 11.0 mmol) in trifluoroacetic acid (20 ml), 50% H<sub>2</sub>O<sub>2</sub> (10 ml) was added and the reaction mixture was heated at 80°C for 9 days. The consumption of starting material was monitored using mass spectroscopy. The reaction was cooled to room temperature and neutralized with 10% KOH solution, and concentrated to dryness under vacuum to give a brown liquid. To the brown liquid, acetone and water (1:1) was added and the mixture kept in a freezer for 4 days. The brown solids formed were filtered and characterized. The filtrate was concentrated to dryness under vacuum and the addition of acetone and water (1:1) was continued till no precipitates were seen. Yield 72 mg (3%), m.p. 202°C [Lit<sup>[150]</sup>: m.p. 200°C].

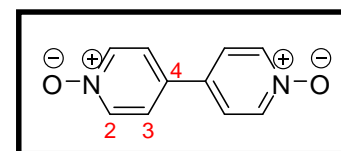


To the brown liquid, acetone and water (1:1) was added and the mixture kept in a freezer for 4 days. The brown solids formed were filtered and characterized. The filtrate was concentrated to dryness under vacuum and the addition of acetone and water (1:1) was continued till no precipitates were seen. Yield 72 mg (3%), m.p. 202°C [Lit<sup>[150]</sup>: m.p. 200°C].

<sup>1</sup>H NMR (400MHz, D<sub>2</sub>O) δ/ppm: 8.70 (bs, 2H, H<sub>5</sub>, H<sub>6</sub>), 8.38 (d, *J* = 6.7 Hz, 2H, H<sub>2</sub>), 8.14 (d, *J* = 8.2 Hz, 2H, H<sub>4</sub>), 7.60 (t, *J* = 7.2 Hz, 2H, H<sub>3</sub>). <sup>13</sup>C NMR (100MHz, CDCl<sub>3</sub>) δ/ppm: 166.03 (C<sub>7</sub>), 141.93 (C<sub>2</sub>), 139.89 (C<sub>5</sub>), 132.67 (C<sub>4</sub>), 131.71 (C<sub>8</sub>), 127.14 (C<sub>3</sub>). IR (KBr) ν<sub>max</sub>/cm<sup>-1</sup>: 3077, 1638, 1434, 1322, 1217, 1198, 1114, 1019, 933, 763. ESI-MS *m/z*: Found [L+H]<sup>+</sup> 197.0711, C<sub>12</sub>H<sub>9</sub>N<sub>2</sub>O requires [L+H]<sup>+</sup> 197.0709.

### 6.12 Synthesis of 4,4'-bipyridine N,N'-dioxide 3.11

4,4'-Bipyridine (1.00 g, 6.40 mmol) and mCPBA (3.57 g, 20.6 mmol) were dissolved in dichloromethane (20 ml) at room temperature and heated to reflux for 12 hours. After the consumption of 4,4'-bipyridine

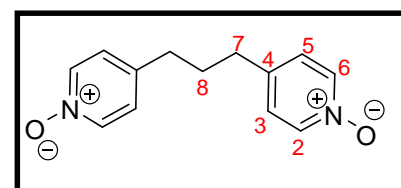


(monitored by TLC), the reaction mixture was cooled to room temperature, and concentrated to dryness under vacuum to give pale yellow-white solids. The crude residue was purified by silica gel column chromatography with 5% methanol:dichloromethane to give 4,4'-bipyridine N,N'-dioxide as brown solid and **3.11**, as yellow solid. Yield 0.560 g (46%), m.p. 302°C [Lit<sup>[209]</sup>: m.p. 299°C].

<sup>1</sup>H NMR<sup>[210]</sup> (400MHz, D<sub>2</sub>O) δ/ppm: 8.33 (d, *J* = 7.0 Hz, 4H, H<sub>2</sub>), 7.88 (d, *J* = 7.1 Hz, 4H, H<sub>3</sub>). <sup>13</sup>C NMR<sup>[210]</sup> (100MHz, D<sub>2</sub>O) δ/ppm: 139.50 (C<sub>2</sub>), 138.41 (C<sub>4</sub>), 124.94 (C<sub>3</sub>). IR (KBr) ν<sub>max</sub>/cm<sup>-1</sup>: 3073, 1638, 1475, 1432, 1241, 1185, 1023, 836, 546, 471. ESI-MS *m/z*: Found [L+H]<sup>+</sup> 189.0653, C<sub>10</sub>H<sub>9</sub>N<sub>2</sub>O<sub>2</sub> requires [L+H]<sup>+</sup> 189.0659; Found [L+Na]<sup>+</sup> 211.0471, C<sub>10</sub>H<sub>8</sub>N<sub>2</sub>NaO<sub>2</sub> requires [L+Na]<sup>+</sup> 211.0471.

### 6.4.13 Synthesis of 1,3-bis(4-pyridyl)propane N,N'-dioxide 3.12<sup>[141]</sup>

MCPBA (2.61 g, 15.1 mmol) was added to a solution of 1,3-bis(4-pyridyl)propane (1.00 g, 5.04 mmol) in dichloromethane (20 ml) at room temperature and the reaction mixture was stirred at room temperature for 13 hours. After TLC analysis, the reaction mixture

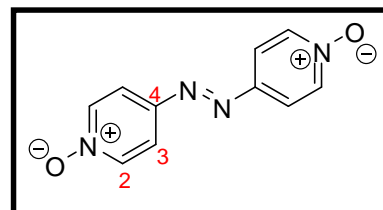


was cooled to room temperature, concentrated to dryness under vacuum to give brownish white solids. The crude residue was purified by silica gel flash column chromatography with 5% methanol: dichloromethane as elutant to give **3.12**, as a brown solid. Yield 0.564 g (48%), m.p. 196°C [Lit: m.p. not reported].

$^1\text{H NMR}^{[141]}$  (400MHz,  $\text{D}_2\text{O}$ )  $\delta/\text{ppm}$ : 8.09 (d,  $J = 7.1$  Hz, 4H,  $\text{H}_2$ ), 7.34 (d,  $J = 7.0$  Hz, 4H,  $\text{H}_3$ ), 2.66 (t, 4H,  $J = 7.4$  Hz,  $\text{H}_7$ ), 1.93 (quin,  $J = 7.6$  Hz, 2H,  $\text{H}_8$ ).  $^{13}\text{C NMR}$  (100MHz,  $\text{D}_2\text{O}$ )  $\delta/\text{ppm}$ : 148.64 ( $\text{C}_4$ ), 138.32 ( $\text{C}_2$ ), 127.19 ( $\text{C}_3$ ), 33.06 ( $\text{C}_7$ ), 29.31 ( $\text{C}_8$ ). **IR (KBr)**  $\nu_{\text{max}}/\text{cm}^{-1}$ : 3120, 1688, 1491, 1486, 1447, 1230, 1115, 1047, 865, 766. **ESI-MS**  $m/z$ : Found  $[\text{L}+\text{H}]^+$  231.1120 and  $\text{C}_{13}\text{H}_{15}\text{N}_2\text{O}_2$  requires 231.1128; Found  $[\text{L}+\text{Na}]^+$  253.0949 and  $\text{C}_{13}\text{H}_{14}\text{N}_2\text{NaO}_2$  requires 253.0947.

#### 6.4.14 Synthesis of 4,4'-azobis(pyridine-N-oxide) **3.13**<sup>[211]</sup>

To tetrahydrofuran (50 ml) was added dropwise with stirring  $\text{TiCl}_4$  (2.00 ml, 18.0 mmol), followed by addition of  $\text{SnCl}_2$  (3.50 g, 18.0 mmol) to the solution. The reaction mixture was stirred at room temperature for 30 minutes. 4-Nitropyridine N-oxide (1.26 g, 9.00 mmol) was added to the reaction mixture at room temperature and

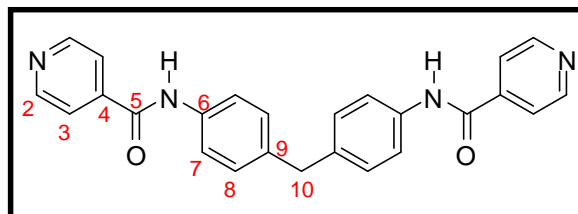


stirred for an additional 30 minutes. The reaction mixture was quenched with water (50 ml), 25% ammonia (25 ml) and 20% KOH solution (45 ml). The aqueous layer was extracted with chloroform (2x25 ml). The combined organic layers were dried over anhydrous  $\text{MgSO}_4$ , and concentrated to dryness under vacuum. The crude residue was recrystallized from ethanol: acetone (1:1, 20 ml) to give **3.13**. Yield 0.661 g (34%), m.p. 261°C [Lit<sup>[211]</sup>: m.p. 262.1°C].

$^1\text{H NMR}$  (400MHz,  $\text{D}_2\text{O}$ )  $\delta/\text{ppm}$ : 8.38 (d,  $J = 7.4$  Hz, 4H,  $\text{H}_2$ ), 7.98 (d,  $J = 7.1$  Hz, 4H,  $\text{H}_3$ ).  $^{13}\text{C NMR}$  (100MHz,  $\text{D}_2\text{O}$ )  $\delta/\text{ppm}$ : 150.67 ( $\text{C}_2$ ), 140.64 ( $\text{C}_3$ ), 120.57 ( $\text{C}_4$ ). **IR (KBr)**  $\nu_{\text{max}}/\text{cm}^{-1}$ : 3094, 3034, 1916, 1604, 1477, 1264, 1156, 1019, 860, 553. **ESI-MS**  $m/z$ : Found  $[\text{L}+\text{H}]^+$  217.0720,  $\text{C}_{10}\text{H}_9\text{N}_4\text{O}_2$  requires 217.0720.

#### 6.4.15 Synthesis of (methylene-di-*p*-phenylene)bis(pyridine-4-carboxamide) **3.14b**

4,4'-Diaminodiphenylmethane (1.98 g, 10.0 mmol), isonicotinic acid (2.46 g, 20.0 mmol) and triphenylphosphite (6.83 g, 22.0 mmol) were dissolved in anhydrous pyridine (45 ml) and heated to reflux for 4 hours. The reaction mixture was cooled to



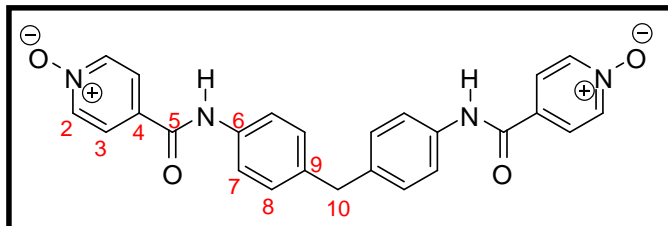
room temperature, poured onto ice cold water and stirred for 30 minutes. The precipitates formed were filtered, washed with an excess of distilled water (6x80 ml) and dried under vacuum to give **3.14b**, as a pale yellow powder. Yield 4.46 g (quantitative), m.p. 192°C. [Lit<sup>[147]</sup>: m.p. not reported]

$^1\text{H NMR}^{[147]}$  (400MHz, DMSO)  $\delta/\text{ppm}$ : 10.41 (s, 2H, NH), 8.74 (d,  $J = 5.5$  Hz, 4H,  $\text{H}_2$ ), 7.81 (d,  $J = 5.9$  Hz, 4H,  $\text{H}_3$ ), 7.66 (d,  $J = 8.3$  Hz, 4H,  $\text{H}_7$ ), 7.20 (d,  $J = 8.2$  Hz, 4H,  $\text{H}_8$ ), 3.88 (s, 2H,  $\text{H}_{10}$ ).  $^{13}\text{C NMR}$  (100MHz,  $\text{CDCl}_3$ )  $\delta/\text{ppm}$ : 164.24 ( $\text{C}_5$ ), 150.68 ( $\text{C}_2$ ), 142.39 ( $\text{C}_6$ ), 137.70 ( $\text{C}_4$ ), 130.02 ( $\text{C}_9$ ), 129.33 ( $\text{C}_8$ ), 121.98 ( $\text{C}_7$ ), 121.09 ( $\text{C}_3$ ), 40.07 ( $\text{C}_{10}$ ). **IR (KBr)**  $\nu_{\text{max}}/\text{cm}^{-1}$ : 3038, 1655, 1594, 1529, 1414, 1323, 1262, 834, 751. **ESI-MS**  $m/z$ : Found  $[\text{L}+\text{H}]^+$  409.1665,  $\text{C}_{25}\text{H}_{21}\text{N}_4\text{O}_2$  requires 409.1659.

#### 6.4.16 Synthesis of (methylenedi-p-phenylene)bis(pyridine-4-carboxamide N,N'-dioxide)

##### 3.14

Compound **3.14b** (1.00 g, 2.45 mmol) and mCPBA (1.26 g, 7.35 mmol) were dissolved in dichloromethane (20 ml) at room temperature and heated to reflux for 3 hours. The reaction mixture was cooled to room temperature,

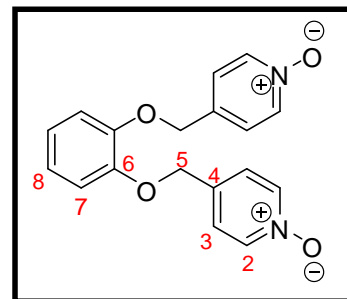


concentrated to dryness under vacuum to give yellow solids. The crude residue was purified by silica gel column chromatography with 5% methanol:dichloromethane as elutant to give **3.14**, as a yellow powder. Yield 0.214 g (20%), m.p. 141°C.

$^1\text{H NMR}$  (400MHz, DMSO)  $\delta/\text{ppm}$ : 10.35 (s, 2H, NH), 8.36 (d,  $J = 7.1$  Hz, 4H,  $\text{H}_2$ ), 7.96 (d,  $J = 6.7$  Hz, 4H,  $\text{H}_3$ ), 7.67 (d,  $J = 8.2$  Hz, 4H,  $\text{H}_7$ ), 7.23 (d,  $J = 8.4$  Hz, 4H,  $\text{H}_8$ ), 3.91 (s, 2H,  $\text{H}_{10}$ ).  $^{13}\text{C NMR}$  (100MHz,  $\text{CDCl}_3$ )  $\delta/\text{ppm}$ : 162.30 ( $\text{C}_5$ ), 139.29 ( $\text{C}_2$ ), 137.61 ( $\text{C}_6$ ), 137.06 ( $\text{C}_4$ ), 130.50 ( $\text{C}_9$ ), 129.30 ( $\text{C}_8$ ), 125.68 ( $\text{C}_7$ ), 121.10 ( $\text{C}_3$ ), 40.47 ( $\text{C}_{10}$ ). **IR (KBr)**  $\nu_{\text{max}}/\text{cm}^{-1}$ : 3036, 2077, 1649, 1539, 1509, 1486, 1413, 1245, 1178, 856. **ESI-MS**  $m/z$ : Found  $[\text{L}+\text{Na}]^+$  463.1367,  $\text{C}_{25}\text{H}_{20}\text{N}_4\text{NaO}_4$  requires 463.1377.

#### 6.4.17 Synthesis of 1,2-bis(4-pyridylmethoxy)benzene N,N'-dioxide 3.15

Compound **3.15a** (0.500 g, 1.71 mmol) and mCPBA (0.590 g, 3.42 mmol) were dissolved in methanol (10 ml) and heated to reflux for 40 minutes. The reaction mixture was cooled to room temperature, and concentrated to dryness under vacuum. The crude residue was purified by silica gel column chromatography with 5% methanol:dichloromethane as elutant to give **3.15**, as an off-white solid.

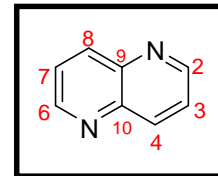


Yield 36 mg (7%), m.p. 128°C.

$^1\text{H NMR}$  (400MHz,  $\text{CDCl}_3$ )  $\delta/\text{ppm}$ : 8.20 (d,  $J = 7.0$  Hz, 2H,  $\text{H}_2$ ), 7.33 (d,  $J = 6.6$  Hz, 2H,  $\text{H}_3$ ), 6.93 – 6.97 (m, 2H,  $\text{H}_8$ ), 6.88 – 6.91 (m, 2H,  $\text{H}_7$ ), 5.10 (s, 4H,  $\text{H}_5$ ).  $^{13}\text{C NMR}$  (100MHz,  $\text{CDCl}_3$ )  $\delta/\text{ppm}$ : 147.98 ( $\text{C}_4$ ), 139.27 ( $\text{C}_2$ ), 135.93 ( $\text{C}_6$ ), 124.23 ( $\text{C}_3$ ), 122.61 ( $\text{C}_8$ ), 115.10 ( $\text{C}_7$ ), 68.75 ( $\text{C}_5$ ). **IR (KBr)**  $\nu_{\text{max}}/\text{cm}^{-1}$ : 3417, 2043, 1769, 1636, 1509, 1236, 1129, 1045, 832, 770. **Elemental Analysis**: calculated for  $\text{C}_{18}\text{H}_{16}\text{N}_2\text{O}_4 \cdot 3\text{H}_2\text{O}$ : C, 57.14; H, 5.86; N, 7.40. Found: C, 57.08; H, 5.73; N, 7.24. **ESI-MS**  $m/z$ : Found  $[\text{L}+\text{H}]^+$  325.1170,  $\text{C}_{18}\text{H}_{17}\text{N}_2\text{O}_4$  requires  $[\text{L}+\text{H}]^+$  325.1183; found  $[\text{L}+\text{Na}]^+$  345.0991,  $\text{C}_{18}\text{H}_{16}\text{N}_2\text{NaO}_4$  requires  $[\text{L}+\text{Na}]^+$  345.1002.

### 6.4.18 Synthesis of 1,5-Naphthyridine 3.16a

(i) Sulfo-mix was prepared by adding nitrobenzene into 20% oleum at room temperature. The reaction mixture was then heated at 70°C for 12 hours, until a sample was completely soluble in water.

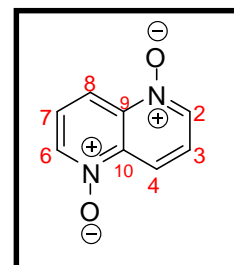


(ii) Glycerol (20.72 g, 223.9 mmol) was added dropwise to an ice-cold mixture of sulfo-mix (98.0 g). To this was added 3-aminopyridine (6.20 g, 65.0 mmol), followed by rapid addition of water (32 ml). The reaction mixture was heated at 140°C for 48 hours. After TLC analysis, the reaction mixture was cooled to room temperature and poured onto crushed ice. The black reaction mixture was basified with NaOH pellets to pH 14. The reaction mixture was filtered through Celite and the filtrate was extracted with hot chloroform (8x200 ml). The combined organic layers was washed with water, dried over anhydrous MgSO<sub>4</sub> and concentrated to dryness under vacuum. The crude residue was purified by flash silica gel chromatography using 5% methanol:dichloromethane as elutant to give **3.16a**, as a brown solid. Yield 5.12 g (60%), m.p. 74°C [Lit<sup>[148]</sup>: m.p. 72°C].

<sup>1</sup>H NMR<sup>[212]</sup> (300MHz, CD<sub>3</sub>CN) δ/ppm: 8.51 (d, *J* = 5.8 Hz 2H, H<sub>2</sub>), 8.34 (d, *J* = 8.9 Hz, 2H, H<sub>4</sub>), 7.58 (dd, *J* = 6.0 Hz, 8.6 Hz, 2H, H<sub>3</sub>). <sup>13</sup>C NMR<sup>[212]</sup> (100MHz, CDCl<sub>3</sub>) δ/ppm: 151.10 (C<sub>2</sub>), 143.84 (C<sub>9</sub>, C<sub>10</sub>), 137.39 (C<sub>4</sub>), 124.34 (C<sub>3</sub>). IR (KBr) ν<sub>max</sub>/cm<sup>-1</sup>: 3409, 2024, 1637, 1494, 1402, 1301, 1113, 1216, 837, 821. ESI-MS *m/z*: Found [L+H]<sup>+</sup> 131.0605, C<sub>8</sub>H<sub>7</sub>N<sub>2</sub> requires [L+H]<sup>+</sup> 131.0604.

### 6.4.19 Synthesis of 1,5-Naphthyridine N,N'-dioxide 3.16

1,5-Naphthyridine (5.00 g, 38.4 mmol) was dissolved in acetic acid (25 ml) and 50% H<sub>2</sub>O<sub>2</sub> (7 ml) was added at room temperature, and the mixture heated to reflux for 5 hours. The reaction mixture was monitored using mass spectrometry. The reaction was cooled to room temperature and concentrated to the minimum volume (~5 ml). The reaction mixture was basified with 10% KOH to pH 12 and the aqueous layer was extracted with chloroform (3x100 ml). The organic layers were combined, dried over anhydrous MgSO<sub>4</sub> and concentrated to give **3.16**. Yield 0.420 g (7%), m.p. 298°C [Lit<sup>[148]</sup>: m.p. 299 – 300°C].

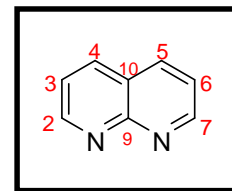


<sup>1</sup>H NMR (400MHz, D<sub>2</sub>O) δ/ppm: 8.77 (d, *J* = 6.3 Hz, 2H, H<sub>2</sub>), 8.62 (d, *J* = 9.4 Hz, 2H, H<sub>4</sub>), 7.83 (dd, *J* = 6.3 Hz, 9.0 Hz, 2H, H<sub>3</sub>). <sup>13</sup>C NMR (100MHz, D<sub>2</sub>O) δ/ppm: 139.80 (C<sub>4</sub>), 125.96 (C<sub>2</sub>), 121.67 (C<sub>3</sub>), C<sub>9</sub> and C<sub>10</sub> carbons were not observed even with prolonged scans. IR (KBr) ν<sub>max</sub>/cm<sup>-1</sup>: 3047, 1636, 1548, 1413, 1284, 1183, 1148, 1071, 961, 793. ESI-MS *m/z*: Found [L+H]<sup>+</sup> 163.0502, C<sub>8</sub>H<sub>8</sub>N<sub>2</sub>O<sub>2</sub> requires [L+H]<sup>+</sup> 163.0502.



### 6.4.20 Synthesis of 1,8-Naphthyridine 3.17a

Glycerol (10.36 g, 111.9 mmol) was added dropwise to an ice-cold mixture of sulfo-mix (49.0 g). To this was added 2-aminopyridine (3.10 g, 32.9 mmol), followed by the rapid addition of water (16 ml). The reaction mixture was heated to 140°C for 48 hours. The reaction was cooled to room temperature

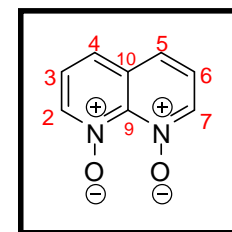


and then poured onto crushed ice. The reaction mixture was then basified with NaOH pellets to pH 14. The aqueous layer was extracted with chloroform (6x200 ml); the combined organic layers were dried over anhydrous MgSO<sub>4</sub> and concentrated to dryness under vacuum. The crude residue was purified by flash silica gel column chromatography with 5% methanol:dichloromethane as elutant to give **3.17a**, as a brown solid. Yield 1.69 g (39%), m.p. 94°C [Lit<sup>[213]</sup>: m.p. 96 – 97°C].

<sup>1</sup>H NMR<sup>[212]</sup> (400MHz, CDCl<sub>3</sub>) δ/ppm: 9.13 (d, *J* = 4.0 Hz, 2H, H<sub>2</sub>), 8.19 (d, *J* = 8.2 Hz, 2H, H<sub>4</sub>), 7.49 (dd, *J* = 4.3 Hz, 8.2 Hz, 2H, H<sub>3</sub>). <sup>13</sup>C NMR<sup>[212]</sup> (100MHz, CDCl<sub>3</sub>) δ/ppm: 153.62 (C<sub>2</sub>), 137.09 (C<sub>4</sub>), 122.15 (C<sub>3</sub>), C<sub>9</sub> and C<sub>10</sub> carbons were not observed even with prolonged scan. IR (KBr) ν<sub>max</sub>/cm<sup>-1</sup>: 3409, 1601, 1571, 1494, 1395, 1294, 1228, 1130, 834, 807. ESI-MS *m/z*: Found [L+H]<sup>+</sup> 131.0603, C<sub>8</sub>H<sub>7</sub>N<sub>2</sub> requires [L+H]<sup>+</sup> 131.0604. Found [L+Na]<sup>+</sup> 153.0424, C<sub>8</sub>H<sub>6</sub>N<sub>2</sub>Na requires [L+Na]<sup>+</sup> 153.0423.

### 6.4.21 Synthesis of 1,8-Naphthyridine N,N'-dioxide 3.17

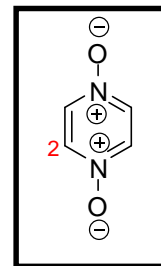
A mixture of 1,8-naphthyridine (1.60 g, 12.2 mmol), trifluoroacetic acid (15 ml) and 50% H<sub>2</sub>O<sub>2</sub> (5 ml) was heated at 140°C for 8 days. Additional portions of 50% H<sub>2</sub>O<sub>2</sub> (2 ml) were added every alternate day to the reaction mixture. The reaction mixture was then cooled to room temperature and concentrated to minimum volume (~5 ml). The reaction mixture was basified with 10% KOH to pH 12. The aqueous layers were concentrated to dryness under vacuum, and purified by silica gel column chromatography with water as elutant. The combined elutants were concentrated under vacuum and recrystallised from acetone (5 ml) to give **3.17**, as a brown solid. Yield 0.105 g (5%), m.p. >300°C [Lit: m.p. not reported].



<sup>1</sup>H NMR (400MHz, D<sub>2</sub>O) δ/ppm: 8.22 (d, *J* = 6.3 Hz, 2H, H<sub>2</sub>), 7.75 (d, *J* = 7.8 Hz, 2H, H<sub>4</sub>), 7.24 (t, *J* = 7.0 Hz, 2H, H<sub>3</sub>). <sup>13</sup>C NMR (100MHz, D<sub>2</sub>O) δ/ppm: 141.74 (C<sub>9</sub>), 135.33 (C<sub>2</sub>), 129.18 (C<sub>10</sub>), 119.11 (C<sub>4</sub>), 112.22 (C<sub>3</sub>). IR (KBr) ν<sub>max</sub>/cm<sup>-1</sup>: 3405, 1660, 1619, 1507, 1288, 1215, 1155, 1058, 873, 821. ESI-MS *m/z*: Found [L+H]<sup>+</sup> 163.0505, C<sub>8</sub>H<sub>7</sub>N<sub>2</sub>O<sub>2</sub> requires [L+H]<sup>+</sup> 163.0503.

#### 6.4.22 Synthesis of pyrazine N,N'-dioxide 3.18

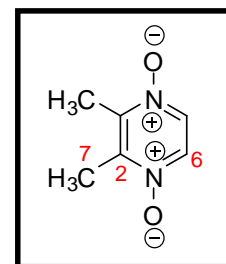
Pyrazine (0.700 g, 8.68 mmol) and mCPBA (3.00 g, 17.3 mmol) were dissolved in methanol (10 ml) at room temperature and heated to reflux for 4 days. After TLC analysis, an additional portion of mCPBA (3.00 g, 17.3 mmol) was added and the heating was continued for another 4 days. The reaction mixture was then cooled to room temperature, and concentrated to dryness under vacuum. The crude residue was purified by silica gel flash chromatography column with 2% methanol:dichloromethane as elutant to give **3.18**, as a white powder. Yield 0.123 g (12%), m.p. 292°C [Lit<sup>[214]</sup>: m.p. 295°C].



<sup>1</sup>H NMR<sup>[215]</sup> (400MHz, DMSO) δ/ppm: 8.24 (d, 4H, H<sub>2</sub>) <sup>13</sup>C NMR<sup>[216]</sup> (100MHz, DMSO) δ/ppm: 136.99 (C<sub>2</sub>). IR (KBr)<sup>[217]</sup> ν<sub>max</sub>/cm<sup>-1</sup>: 3416, 2552, 1638, 1619, 1483, 1462, 1261, 1054, 848, 816, 477. ESI-MS m/z: Found [L+H]<sup>+</sup> 113.0344, C<sub>4</sub>H<sub>5</sub>N<sub>2</sub>O<sub>2</sub> requires [L+H]<sup>+</sup> 113.0346.

#### 6.4.23 Synthesis of 2,3-dimethylpyrazine N,N'-dioxide 3.19

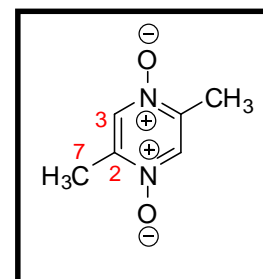
2,3-Dimethylpyrazine (1.00 g, 9.24 mmol) was dissolved in 10ml of acetic acid, to which was added 50% H<sub>2</sub>O<sub>2</sub> (3.2 ml) at room temperature. The reaction mixture was heated at 80°C for 40 minutes, then cooled to room temperature, and concentrated to dryness under vacuum. The crude residue was purified by silica gel flash chromatography column with 5% methanol:dichloromethane as elutant to give **3.19**, as a white powder. Yield 0.320 g (24%), m.p. 212°C [Lit<sup>[218]</sup>: m.p. 214°C].



<sup>1</sup>H NMR (400MHz, CDCl<sub>3</sub>) δ/ppm: 7.99 (s, 2H, H<sub>6</sub>), 2.54 (s, 6H, H<sub>7</sub>). <sup>13</sup>C NMR<sup>[216]</sup> (100MHz, CDCl<sub>3</sub>) δ/ppm: 145.89 (C<sub>2</sub>), 133.38 (C<sub>6</sub>), 14.17 (C<sub>7</sub>). IR (KBr) ν<sub>max</sub>/cm<sup>-1</sup>: 3058, 1889, 1509, 1405, 1389, 1289, 1225, 1109, 848, 788. ESI-MS m/z: Found [L+H]<sup>+</sup> 141.0661, C<sub>6</sub>H<sub>9</sub>N<sub>2</sub>O<sub>2</sub> requires [L+H]<sup>+</sup> 141.0659.

#### 6.4.24 Synthesis of 2,5-dimethylpyrazine N,N'-dioxide 3.20

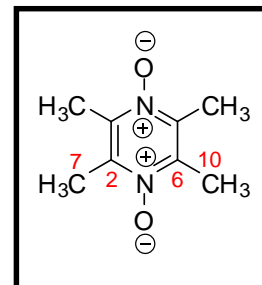
2,5-Dimethylpyrazine (0.800 g, 7.39 mmol) was dissolved in 3 ml of acetic acid, to which was added 50% H<sub>2</sub>O<sub>2</sub> (3 ml) at room temperature. The colourless solution was heated for one hour at 80°C, then cooled to room temperature, and concentrated to dryness under vacuum to give a white solid. The solid was purified by silica gel flash chromatography with 5% methanol:dichloromethane as elutant to give **3.20**, as a white powder. Yield 0.811 g (78%), m.p. >330°C [Lit<sup>[41a]</sup>: m.p. 360°C].



<sup>1</sup>H NMR (400MHz, CDCl<sub>3</sub>) δ/ppm: 8.38 (s, 2H, H<sub>3</sub>), 2.32 (s, 6H, H<sub>7</sub>). <sup>13</sup>C NMR (100MHz, CDCl<sub>3</sub>) δ/ppm: 146.07 (C<sub>2</sub>), 136.26 (C<sub>3</sub>), 13.87 (C<sub>7</sub>). IR (KBr) ν<sub>max</sub>/cm<sup>-1</sup>: 2038, 1787, 1542, 1638, 1400, 1357, 1275, 1198, 871, 710. ESI-MS m/z: Found [L+H]<sup>+</sup> 141.0665, C<sub>6</sub>H<sub>9</sub>N<sub>2</sub>O<sub>2</sub> requires [L+H]<sup>+</sup> 141.0659.

### 6.4.25 Synthesis of 2,3,5,6-tetramethylpyrazine N,N'-dioxide 3.21

2,3,5,6-Tetramethylpyrazine (0.700 g, 5.13 mmol) and mCPBA (1.77 g, 10.2 mmol) were dissolved in methanol (10 ml) at room temperature and heated to reflux for 30 minutes. After TLC analysis, an additional portion of mCPBA (0.880 g, 5.09 mmol) was added and the heating was continued for another 1 hour. The reaction mixture was then cooled to room temperature, and concentrated to dryness under vacuum. The crude residues were purified by silica gel flash chromatography with 5% methanol:dichloromethane as elutant to give **3.21**, as a white powder. Yield 0.532 g (61%), m.p. 226°C [Lit<sup>[41a]</sup>: m.p. 224°C].



<sup>1</sup>H NMR (400MHz, CDCl<sub>3</sub>) δ/ppm: 2.56 (s, 12H, H<sub>7</sub>). <sup>13</sup>C NMR (100MHz, CDCl<sub>3</sub>) δ/ppm: 142.57 (C<sub>2</sub>), 14.39 (C<sub>7</sub>). IR (KBr) ν<sub>max</sub>/cm<sup>-1</sup>: 2957, 1719, 1525, 1449, 1335, 1309, 1119, 1035, 1254, 867. ESI-MS m/z: Found [L+H]<sup>+</sup> 169.0972, C<sub>8</sub>H<sub>13</sub>N<sub>2</sub>O<sub>2</sub> requires [L+H]<sup>+</sup> 169.0972.

### 6.5 Preparation of silver(I) complexes with pyridine N,N'-dioxides

#### 6.5.1 Complexes of 2,2'-bipyridine N,N'-dioxide 3.1

##### With silver(I) perchlorate (1:2) 3.22

Silver(I) perchlorate (22 mg, 0.10 mmol) dissolved in acetone (2 ml) was added to a solution of ligand **3.1** (10 mg, 0.053 mmol) in water (2 ml). The solution was left in darkness at room temperature and allowed to evaporate slowly to give colourless block crystals, suitable for X-ray crystallography. Yield 28 mg (54%), m.p. 236 – 238°C.

**Elemental Analysis:** calculated for 3(C<sub>10</sub>H<sub>8</sub>N<sub>2</sub>O<sub>2</sub>).2(AgClO<sub>4</sub>): C, 36.80; H, 2.47; N, 8.58. Found: (inconsistent with the proposed structure) C, 32.04; H, 1.90; N, 6.72. IR (KBr) ν<sub>max</sub>/cm<sup>-1</sup>: 3421, 3094, 1618, 1479, 1431, 1258, 1207, 1086, 845, 833, 771. ESI-MS m/z: Found [L+Ag]<sup>+</sup> 294. 9630, C<sub>10</sub>H<sub>8</sub>AgN<sub>2</sub>O<sub>2</sub> requires [L+Ag]<sup>+</sup> 294.9631.

##### With silver(I) perchlorate (1:1) 3.23

Silver(I) perchlorate (11 mg, 0.053 mmol) dissolved in acetone (2 ml) was added to a solution of ligand **3.1** (10 mg, 0.053 mmol) in water (2 ml). The solution was left in darkness at room temperature and allowed to evaporate slowly to give colourless block crystals, suitable for X-ray crystallography. Yield 14 mg (26%), m.p. 236 – 238°C.

IR (KBr) ν<sub>max</sub>/cm<sup>-1</sup>: 3086, 2012, 1477, 1428, 1255, 1112, 1144, 841, 851, 769, 626. ESI-MS m/z: Found [L+Ag]<sup>+</sup> 294.9626, C<sub>10</sub>H<sub>8</sub>AgN<sub>2</sub>O<sub>2</sub> requires [L+Ag]<sup>+</sup> 294.9631; Found [2L+Ag]<sup>+</sup> 483.0216, C<sub>20</sub>H<sub>16</sub>AgN<sub>4</sub>O<sub>4</sub> requires [2L+Ag]<sup>+</sup> 483.0217.

**With silver(I) trifluoroacetate (1:2) 3.24**

Silver(I) trifluoroacetate (40 mg, 0.18 mmol) dissolved in acetone (2 ml) was added to a solution of ligand **3.1** (17 mg, 0.090 mmol) in water (2 ml). The solution was left in darkness at room temperature and allowed to evaporate slowly to give colourless block crystals, suitable for X-ray crystallography. Yield 16 mg (28%), m.p. 184°C.

**Elemental Analysis:** calculated for  $C_{10}H_8N_2O_2 \cdot 2(AgOCOCF_3)$ : C, 26.61; H, 1.59; N, 4.23. Found: C, 26.25; H, 1.22; N, 4.23. **IR (KBr)**  $\nu_{max}/cm^{-1}$ : 3425, 3043, 1681, 1479, 1428, 1254, 1210, 1137, 841, 803, 769. **ESI-MS**  $m/z$ : Found  $[L+Ag]^+$  294.9620,  $C_{10}H_8AgN_2O_2$  requires  $[L+Ag]^+$  294.9631.

**With silver(I) triflate (1:2) 3.25**

Silver(I) triflate (38 mg, 0.14 mmol) dissolved in acetone (2 ml) was added to a solution of ligand **3.1** (14 mg, 0.074 mmol) in water (2 ml). The solution was left in darkness at room temperature and allowed to evaporate slowly to give colourless block crystals suitable for X-ray crystallography. Yield 21 mg (9%), m.p. 114°C.

**Elemental Analysis:** calculated for  $C_{10}H_8N_2O_2 \cdot 2(AgSO_3CF_3) \cdot H_2O$ : C 18.76; H 1.29; N 3.57. Found: C 15.44; H 1.22; N 2.69. **IR (KBr)**  $\nu_{max}/cm^{-1}$ : 3039, 1658, 1479, 1427, 1254, 1036, 852, 839, 768, 654, 581. **ESI-MS**  $m/z$ : Found  $[L+Ag]^+$  294.9627,  $C_{10}H_8AgN_2O_2$  requires  $[L+Ag]^+$  294.9631; found  $[2L+Ag]^+$  483.0216,  $C_{20}H_{16}AgN_4O_4$  requires  $[2L+Ag]^+$  483.0217.

**With silver(I) hexafluorophosphate (1:2) 3.26**

Silver(I) hexafluorophosphate (40 mg, 0.15 mmol) dissolved in acetone (2 ml) was added to a solution of ligand **3.1** (15 mg, 0.079 mmol) in water (2 ml). The solution was left in darkness at room temperature and allowed to evaporate slowly to give colourless block crystals, suitable for X-ray crystallography. Yield 29 mg (34%), m.p. 236 – 238°C.

**Elemental Analysis:** calculated for  $3(C_{10}H_8N_2O_2) \cdot 2(AgPF_6)$ : C, 33.67; H, 2.26; N, 7.85. Found: C, 33.10; H, 2.15; N, 7.64. **IR (KBr)**  $\nu_{max}/cm^{-1}$ : 3051, 1477, 1434, 1423, 1237, 1208, 1030, 875, 834, 768, 582. **ESI-MS**  $m/z$ : Found  $[L+Ag]^+$  294.9627,  $C_{10}H_8AgN_2O_2$  requires  $[L+Ag]^+$  294.9631; found  $[2L+Ag]^+$  483.0217,  $C_{20}H_{16}AgN_4O_4$  requires  $[2L+Ag]^+$  483.0217.

**With silver(I) tetrafluoroborate (1:2) 3.27**

Silver(I) tetrafluoroborate (30 mg, 0.15 mmol) dissolved in acetone (2 ml) was added to a solution of ligand **3.1** (15 mg, 0.079 mmol) in water (2 ml). The solution was left in darkness at room temperature and allowed to evaporate slowly to give colourless block crystals, suitable for X-ray crystallography. Yield 13 mg (17%), m.p. 242°C.

**Elemental Analysis:** calculated for  $3(C_{10}H_8N_2O_2) \cdot 2(AgBF_4)$ : C 37.77; H 2.54; N 8.81. Found: (inconsistent with the proposed structure) C 22.94; H 2.33; N 5.30, **IR (KBr)**  $\nu_{max}/cm^{-1}$ : 3054, 1475, 1427,

1297, 1255, 1082, 961, 839, 768, 738, 581. **ESI-MS**  $m/z$ : Found  $[L+Ag]^+$  294.9628,  $C_{10}H_8AgN_2O_2$  requires  $[L+Ag]^+$  294.9631; Found  $[2L+Ag]^+$  483.0218,  $C_{20}H_{16}AgN_4O_4$  requires  $[2L+Ag]^+$  483.0218.

### **With silver(I) nitrate (1:2) 3.28**

To ligand **3.1** (25 mg, 0.13 mmol) in water (2 ml) (heated to dissolve at 50°C) was added silver(I) nitrate (45 mg, 0.27 mmol) dissolved in water (2 ml). The solution was allowed to cool and left in darkness at room temperature resulting in yellow crystals suitable for X-ray crystallography. Yield 39 mg (84%), m.p. 146°C.

**Elemental Analysis**: calculated for  $C_{10}H_8N_2O_2 \cdot AgNO_3$ : C, 33.54; H, 2.25; N, 11.74. Found: C 33.60; H 2.12; N 11.75. **IR (KBr)**  $\nu_{max}/cm^{-1}$ : 3040, 1932, 1477, 1426, 1387, 1298, 1255, 837, 852, 768, 624. **ESI-MS**  $m/z$ : Found  $[L+Ag]^+$  294.9628,  $C_{10}H_8AgN_2O_2$  requires  $[L+Ag]^+$  294.9631; Found  $[2L+Ag]^+$  483.0218,  $C_{20}H_{16}AgN_4O_4$  requires  $[2L+Ag]^+$  483.0217.

## **6.5.2 Complexes of 4,4'-dimethyl-2,2'-bipyridine N,N'-dioxide 3.2**

### **With silver(I) trifluoroacetate (1:2) 3.29**

Silver(I) trifluoroacetate (35 mg, 0.15 mmol) dissolved in methanol (2 ml) was added to a solution of ligand **3.2** (17 mg, 0.078 mmol) in methanol (2 ml). The solution was left in darkness at room temperature to give crystals suitable for X-ray crystallography. Yield 27 mg (53%), m.p. 152°C.

**Elemental Analysis**: calculated for  $C_{12}H_{12}N_2O_2 \cdot 2(AgOCOCF_3)$ : C, 29.21; H, 1.84; N, 4.26. Found: C, 29.65; H, 1.60; N, 4.16. **IR (KBr)**  $\nu_{max}/cm^{-1}$ : 2477, 1680, 1477, 1427, 1207, 1177, 1131, 842, 805, 720, 529. **ESI-MS**  $m/z$ : Found  $[L+Ag]^+$  322.9944,  $C_{12}H_{12}AgN_2O_2$  requires  $[L+Ag]^+$  322.9944.

### **With silver(I) triflate (1:2) 3.30**

Silver(I) triflate (39 mg, 0.15 mmol) dissolved in methanol (2 ml) was added to a solution of ligand **3.2** (17 mg, 0.078 mmol) in dichloromethane (2 ml). The solution was left in darkness at room temperature and allowed to evaporate slowly to give crystals suitable for X-ray crystallography. Yield 19 mg (33%), m.p. 298 – 300°C.

**Elemental Analysis**: calculated for  $C_{12}H_{12}N_2O_2 \cdot 2(AgSO_3CF_3) \cdot H_2O$ : C 22.48; H 1.89; N 3.74. Found: C 22.26; H 1.78; N 3.78. **IR (KBr)**  $\nu_{max}/cm^{-1}$ : 2021, 1632, 1476, 1458, 1262, 1226, 1165, 1034, 827, 775, 634. **ESI-MS**  $m/z$ : Found  $[L+Ag]^+$  322.9945,  $C_{12}H_{12}AgN_2O_2$  requires  $[L+Ag]^+$  322.9944.

## **6.5.3 Complexes of 4,4'-dimethoxy-2,2'-bipyridine N,N'-dioxide 3.5**

### **With silver(I) perchlorate (1:2) 3.31**

Silver(I) perchlorate (25 mg, 0.12 mmol) dissolved in methanol (2 ml) was added to a solution of ligand **3.5** (15 mg, 0.060 mmol) in dichloromethane (2 ml). The solution was left in darkness at

room temperature and gave pale yellow block crystals, suitable for X-ray crystallography. Yield 17 mg (17%), m.p. 216°C.

**Elemental Analysis:** calculated for  $4(\text{C}_{12}\text{H}_{12}\text{N}_2\text{O}_4) \cdot 3(\text{AgClO}_4)$ : C, 35.70; H, 3.00; N, 6.94. Found: (inconsistent with the proposed structure) C, 31.57; H, 2.87; N, 6.02. **IR (KBr)**  $\nu_{\text{max}}/\text{cm}^{-1}$ : 3077, 1567, 1479, 1426, 1300, 1208, 1089, 1020, 834, 797, 723. **ESI-MS**  $m/z$ : No sign of  $[\text{L}+\text{Ag}]^+$  peaks.

### **With silver(I) perchlorate (1:2) 3.32**

Silver(I) perchlorate (25 mg, 0.12 mmol) dissolved in methanol (2 ml) was added to a solution of ligand **3.5** (15 mg, 0.060 mmol) in acetonitrile (2 ml). The solution was left in darkness at room temperature and left to slowly evaporate to give colourless needle shaped crystals, suitable for X-ray crystallography. Yield 22 mg (55%), m.p. 168°C.

**Elemental Analysis:** calculated for  $\text{C}_{12}\text{H}_{12}\text{N}_2\text{O}_4 \cdot 2(\text{AgClO}_4) \cdot 2(\text{CH}_3\text{CN})$ : C 26.83; H 2.91; N 7.36. Found: (inconsistent with the proposed structure) C 15.36; H 1.22; N 2.69. **IR (KBr)**  $\nu_{\text{max}}/\text{cm}^{-1}$ : 3091, 1625, 1482, 1421, 1303, 1206, 1107, 1090, 834, 797, 626. **ESI-MS**  $m/z$ : No sign of  $[\text{L}+\text{Ag}]^+$  peaks.

### **With silver(I) triflate (1:2) 3.33**

Silver(I) trifluoroacetate (31 mg, 0.12 mmol) dissolved in methanol (2 ml) was added to a solution of ligand **3.5** (15 mg, 0.060 mmol) in acetonitrile (2 ml). The solution was left in darkness at room temperature and allowed to evaporate slowly to give crystals suitable for X-ray crystallography. Yield 11 mg (10%), m.p. 144°C.

**Elemental Analysis:** calculated for  $4(\text{C}_{12}\text{H}_{12}\text{N}_2\text{O}_4) \cdot 3(\text{AgSO}_3\text{CF}_3)$ : C, 34.73; H, 2.74; N, 6.35. Found: (inconsistent with the proposed structure) C, 15.36; H, 1.22; N, 2.69. **IR (KBr)**  $\nu_{\text{max}}/\text{cm}^{-1}$ : 1629, 1572, 1557, 1487, 1425, 1279, 1258, 1204, 1034, 800, 640. **ESI-MS**  $m/z$ : Found  $[\text{L}+\text{Ag}-2\text{O}]^+$  322.9944,  $\text{C}_{12}\text{H}_{12}\text{AgN}_2\text{O}_2$  requires  $[\text{L}+\text{Ag}-2\text{O}]^+$  322.9944.

### **With silver(I) tetrafluoroborate (1:2) 3.34**

Silver(I) trifluoroacetate (24 mg, 0.12 mmol) dissolved in methanol (2 ml) was added to a solution of ligand **3.5** (15 mg, 0.060 mmol) in acetonitrile (2 ml). The solution was left in darkness at room temperature and allowed to evaporate slowly to give crystals suitable for X-ray crystallography. Yield 16 mg (60%), m.p. 216°C.

**Elemental Analysis:** calculated for  $\text{C}_{12}\text{H}_{12}\text{N}_2\text{O}_4 \cdot \text{AgBF}_4 \cdot 2(\text{H}_2\text{O})$ : C, 30.09; H, 3.37; N, 5.85. Found: C, 30.55; H, 2.91; N, 5.87. **IR (KBr)**  $\nu_{\text{max}}/\text{cm}^{-1}$ : 3074, 1627, 1484, 1422, 1301, 1206, 1084, 1054, 800, 523. **ESI-MS**  $m/z$ : Found  $[\text{L}+\text{Ag}]^+$  354.9841,  $\text{C}_{12}\text{H}_{12}\text{AgN}_2\text{O}_4$  requires  $[\text{L}+\text{Ag}]^+$  354.9843.

### 6.5.4 Complexes of 4,4'-bipyridine N,N'-dioxide 3.11

#### With silver(I) trifluoroacetate (1:2) 3.35

Silver(I) trifluoroacetate (23 mg, 0.10 mmol) dissolved in tetrahydrofuran (THF) (2 ml) was added to a solution of ligand **3.11** (10 mg, 0.053 mmol) in water (2 ml). The solution was left in darkness at room temperature and allowed to evaporate slowly to give colourless thin rectangular shaped crystals, suitable for X-ray crystallography. Yield 14 mg (42%), m.p. 196°C.

**Elemental Analysis:** calculated for  $C_{10}H_8N_2O_2 \cdot 2(AgOCOCF_3) \cdot 3(H_2O)$ : C, 24.58; H, 2.06; N, 4.10. Found: C, 24.84; H, 1.44; N, 3.37. **IR (KBr)**  $\nu_{max}/cm^{-1}$ : 2496, 1679, 1478, 1430, 1266, 1209, 1022, 838, 803, 767, 723(s). **ESI-MS**  $m/z$ : Found  $[L+Ag]^+$  294.9629,  $C_{10}H_8AgN_2O_2$  requires  $[L+Ag]^+$  294.9631.

### 6.5.5 Complexes of 1,3-bis(4-pyridyl)propane N,N'-dioxide 3.12

#### With silver(I) trifluoroacetate (1:2) 3.36

Silver(I) trifluoroacetate (30 mg, 0.13 mmol) dissolved in methanol (2 ml) was added to a solution of ligand **3.12** (16 mg, 0.069 mmol) in acetonitrile (2 ml). The solution was left in darkness at room temperature and allowed to evaporate slowly to give colourless crystals, suitable for X-ray crystallography. Yield 15 mg (32%), m.p. 168°C.

**Elemental Analysis:** calculated for  $C_{13}H_{14}N_2O_2 \cdot 2(AgOCOCF_3)$ : C, 30.38; H, 2.10; N, 4.17. Found: C, 30.30; H, 1.93; N, 4.06. **IR (KBr)**  $\nu_{max}/cm^{-1}$ : 1688, 1491, 1447, 1428, 1207, 1183, 836, 801, 723, 486. **ESI-MS**  $m/z$ : Found  $[L+Ag]^+$  337.0101,  $C_{13}H_{14}AgN_2O_2$  requires  $[L+Ag]^+$  337.0101; Found  $[2L+Ag]^+$  567.1162,  $C_{26}H_{28}AgN_4O_4$  requires  $[2L+Ag]^+$  567.1156.

#### With silver(I) hexafluorophosphate (1:2) 3.37

Silver(I) hexafluorophosphate (22 mg, 0.086 mmol) dissolved in methanol (2 ml) was added to a solution of ligand **3.12** (10 mg, 0.043 mmol) in dichloromethane (2 ml). The solution was left in darkness at room temperature and allowed to evaporate slowly to give crystals suitable for X-ray crystallography. Yield 6 mg (8%), m.p. 168°C.

**Elemental Analysis:** Insufficient and impure sample for analysis. **IR (KBr)**  $\nu_{max}/cm^{-1}$ : 1699, 1490, 1453, 1212, 1178, 1094, 864, 843, 766, 727, 626, 559. **ESI-MS**  $m/z$ : Found  $[L+Ag]^+$  337.0098,  $C_{13}H_{14}AgN_2O_2$  requires  $[L+Ag]^+$  337.0101.

#### With silver(I) hexafluorophosphate (1:2) 3.38

Silver(I) hexafluorophosphate (21 mg, 0.086 mmol) dissolved in methanol (2 ml) was added to a solution of ligand **3.12** (10 mg, 0.043 mmol) in acetonitrile (2 ml). The solution was left in darkness at room temperature to give crystals suitable for X-ray crystallography. Yield 11 mg (53%), m.p. 168°C.

**Elemental Analysis:** calculated for  $3(\text{C}_{13}\text{H}_{14}\text{N}_2\text{O}_2) \cdot 3(\text{AgPF}_6) \cdot \text{CH}_3\text{CN}$ : C, 33.03; H, 3.04; N, 6.58. Found: C, 32.51; H, 3.08; N, 6.88. **IR (KBr)**  $\nu_{\text{max}}/\text{cm}^{-1}$ : 3410, 1905, 1636, 1618, 1490, 1450, 1226, 1180, 834, 559. **ESI-MS**  $m/z$ : Found  $[\text{L}+\text{Ag}]^+$  337.0097,  $\text{C}_{13}\text{H}_{14}\text{AgN}_2\text{O}_2$  requires  $[\text{L}+\text{Ag}]^+$  337.0101.

### 6.5.6 Complexes of 4,4'-azobis(pyridine-N-oxide) 3.13

#### With silver(I) trifluoroacetate (1:2) 3.39

Silver(I) trifluoroacetate (16 mg, 0.092 mmol) dissolved in methanol (2 ml) was added to a solution of ligand **3.13** (10 mg, 0.046 mmol) in water (2 ml). The solution was left in darkness at room temperature and allowed to evaporate slowly to give thin red needles, suitable for X-ray crystallography. Yield 23 mg (32%), m.p. 216°C.

**Elemental Analysis:** calculated for  $3(\text{C}_{10}\text{H}_8\text{N}_4\text{O}_2) \cdot 4(\text{AgOCOCF}_3)$ : C, 29.79; H, 1.58; N, 10.97. Found: C, 29.68; H, 1.58; N, 10.64. **IR (KBr)**  $\nu_{\text{max}}/\text{cm}^{-1}$ : 1928, 1686, 1606, 1550, 1475, 1451, 1212, 1146, 864, 840, 801. **ESI-MS**  $m/z$ : No sign of  $[\text{L}+\text{Ag}]^+$  peaks.

#### With silver(I) nitrate (1:2) 3.40

Silver(I) nitrate (16 mg, 0.092 mmol) dissolved in water (2 ml) was added to a solution of ligand **3.13** (10 mg, 0.046 mmol) in water (2 ml). The solution was left in darkness at room temperature and allowed to evaporate slowly to give thin red crystals, suitable for X-ray crystallography. Yield 17 mg (66%), m.p. 78 – 80°C.

**Elemental Analysis:** calculated for  $\text{C}_{10}\text{H}_8\text{N}_4\text{O}_2 \cdot 2(\text{AgNO}_3) \cdot \text{H}_2\text{O}$ : C, 20.93; H, 1.76; N, 14.64. Found: C, 21.14; H, 1.42; N, 14.34. **IR (KBr)**  $\nu_{\text{max}}/\text{cm}^{-1}$ : 3471, 2023, 1644, 1621, 1477, 1384, 1220, 1148, 851, 792. **ESI-MS**  $m/z$ : No sign of  $[\text{L}+\text{Ag}]^+$  peaks.

### 6.5.7 Complexes of 1,2-bis(4-pyridylmethoxy)benzene N,N'-dioxide 3.15

#### With silver(I) trifluoroacetate (1:2) 3.41

Silver(I) trifluoroacetate (9 mg, 0.03 mmol) dissolved in methanol (2 ml) was added to a solution of ligand **3.15** (6 mg, 0.01 mmol) in methanol (2 ml). The solution was left in darkness at room temperature and allowed to evaporate slowly to give pale orange crystals, suitable for X-ray crystallography. Yield 6 mg (34%), m.p. 62 – 64°C.

**Elemental Analysis:** calculated for  $2(\text{C}_{18}\text{H}_{16}\text{N}_2\text{O}_4) \cdot 5(\text{AgOCOCF}_3)$ : C 31.52; H 1.84; N 3.20. Found: C 31.29; H 1.80; N 3.16. **IR (KBr)**  $\nu_{\text{max}}/\text{cm}^{-1}$ : 1686, 1595, 1508, 1496, 1450, 1210, 1131, 836, 802, 772, 723. **ESI-MS**  $m/z$ : Found  $[\text{L}+\text{Ag}]^+$  431.0156,  $\text{C}_{18}\text{H}_{16}\text{AgN}_2\text{O}_4$  requires 431.0156.



### 6.5.8 Complexes of 2,5-dimethylpyrazine N,N'-dioxide 3.20

#### With silver(I) perchlorate (1:2) 3.42

Silver(I) perchlorate (36 mg, 0.17 mmol) dissolved in methanol (2 ml) was added to a solution of ligand **3.20** (12 mg, 0.085 mmol) in dichloromethane (2 ml). The solution was left in darkness at room temperature and allowed to evaporate slowly to give colourless block crystals, suitable for X-ray crystallography. Yield 18 mg (61%), m.p. 206°C.

**Elemental Analysis:** calculated for  $C_6H_8N_2O_2 \cdot AgClO_4 \cdot H_2O$ : C, 19.72; H, 2.76; N, 7.66. Found: C, 19.82; H, 2.26; N, 7.67. **IR (KBr)**  $\nu_{max}/cm^{-1}$ : 1675, 1458, 1524, 1450, 1356, 1274, 1140, 1090, 906, 712, 627. **ESI-MS**  $m/z$ : Found  $[L+Ag]^+$  246.9626,  $C_6H_8AgN_2O_2$  requires  $[L+Ag]^+$  246.9631.

### 6.5.9 Complexes of 2,3,5,6-tetramethylpyrazine N,N'-dioxide 3.21

#### With silver(I) perchlorate (1:2) 3.43

Silver(I) perchlorate (25 mg, 0.11 mmol) dissolved in methanol (2 ml) was added to a solution of ligand **3.21** (10 mg, 0.059 mmol) in methanol (2 ml). The solution was left in darkness at room temperature and allowed to evaporate slowly to give colourless block crystals, suitable for X-ray crystallography. Yield 12 mg (15%).

**Elemental Analysis:** calculated for  $3(C_8H_{12}N_2O_2) \cdot 4(AgClO_4)$ : C, 21.61; H 2.72; N, 6.30. Found: C, 21.18; H, 2.68; N, 6.29. **IR (KBr)**  $\nu_{max}/cm^{-1}$ : 2924, 1941, 1518, 1432, 1335, 1308, 1120, 1099, 866, 625. **ESI-MS**  $m/z$ : Found  $[L+Ag]^+$  274.9940,  $C_8H_{12}AgN_2O_2$  requires  $[L+Ag]^+$  274.9944.

#### With silver(I) trifluoroacetate (1:2) 3.44

Silver(I) trifluoroacetate (26 mg, 0.11 mmol) dissolved in methanol (2 ml) was added to a solution of ligand **3.21** (10 mg, 0.059 mmol) in methanol (2 ml). The solution was left in darkness at room temperature and allowed to evaporate slowly to give colourless block crystals, suitable for X-ray crystallography. Yield 22 mg (27%), m.p. 248°C.

**Elemental Analysis:** calculated for  $3(C_8H_{12}N_2O_2) \cdot 4(AgOCOCF_3)$ : C, 27.69; H 2.61; N, 6.05. Found: C, 27.31; H, 2.70; N, 5.76. **IR (KBr)**  $\nu_{max}/cm^{-1}$ : 1692, 1527, 1437, 1338, 1318, 1208, 1185, 1131, 841, 800, 722. **ESI-MS**  $m/z$ : Found  $[L+Ag]^+$  274.9941,  $C_8H_{12}AgN_2O_2$  requires  $[L+Ag]^+$  274.9944.

#### With silver(I) nitrate (1:2) 3.45

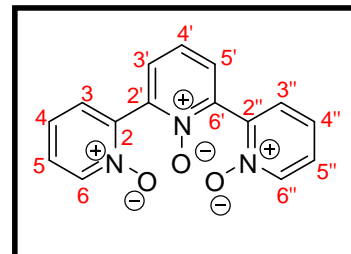
Silver(I) nitrate (20 mg, 0.11 mmol) dissolved in water (2 ml) was added to a solution of ligand **3.21** (10 mg, 0.059 mmol) in water (2 ml). The solution was left in darkness at room temperature and allowed to evaporate slowly to give colourless block crystals, suitable for X-ray crystallography. Yield 13 mg (19%), m.p. 132°C.

**Elemental Analysis:** calculated for  $3(\text{C}_8\text{H}_{12}\text{N}_2\text{O}_2) \cdot 4(\text{AgNO}_3)$ : C 24.34; H 3.06; N 11.83. Found: (inconsistent with the proposed structure) C 18.38; H 2.31; N 10.34. **IR (KBr)**  $\nu_{\text{max}}/\text{cm}^{-1}$ : 3038, 2425, 1525, 1447, 1385, 1335, 1309, 1120, 1026, 865, 622. **ESI-MS**  $m/z$ : Found  $[\text{L}+\text{Ag}]^+$  274.9940,  $\text{C}_8\text{H}_{12}\text{AgN}_2\text{O}_2$  requires  $[\text{L}+\text{Ag}]^+$  274.9944.

## 6.6 Preparation of pyridine N,N',N''-trioxides

### 6.6.1 Synthesis of 2,6':2',6''-terpyridine N,N',N''-trioxide 4.1

2,6':2',6''-Terpyridine (0.800 g, 3.42 mmol) and 50%  $\text{H}_2\text{O}_2$  (4 ml) were dissolved in glacial acetic acid (15 ml) at room temperature and heated at  $90^\circ\text{C}$  for 6 hours. The reaction mixture was cooled to room temperature and concentrated to dryness under vacuum to give a yellow liquid. To the crude residue 30 ml of acetone was added to give

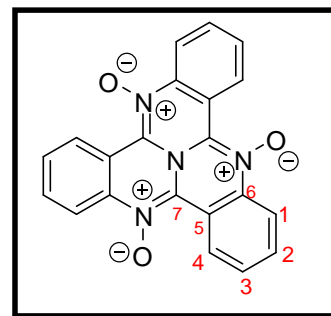


**4.1**, as a yellow solid, which was filtered and dried. Yield 0.718 g (74%), m.p.  $318^\circ\text{C}$  [Lit<sup>[170]</sup>: m.p.  $322^\circ\text{C}$ ].

**$^1\text{H NMR}$**  <sup>[219]</sup> (400MHz,  $\text{D}_2\text{O}$ )  $\delta/\text{ppm}$ : 8.38 (d,  $J = 6.2$  Hz, 2H,  $\text{H}_6, \text{H}_{6''}$ ), 7.81 (bs, 3H,  $\text{H}_{3'}, \text{H}_{4'}, \text{H}_{5'}$ ), 7.71 – 7.79 (m, 4H,  $\text{H}_3, \text{H}_{3''}, \text{H}_4, \text{H}_{4''}$ ), 7.66 (td,  $J = 2.4$  Hz, 6.7 Hz, 2H,  $\text{H}_5, \text{H}_{5''}$ ).  **$^{13}\text{C NMR}$**  (100MHz,  $\text{CDCl}_3$ )  $\delta/\text{ppm}$ : 142.47, 141.48, 139.65, 131.49, 129.93, 129.87, 129.00, 128.42. **IR (KBr)**  $\nu_{\text{max}}/\text{cm}^{-1}$ : 3068, 2478, 1640, 1466, 1423, 1275, 1241, 1255, 1034, 860, 793. **ESI-MS**  $m/z$ : Found  $[\text{L}+\text{H}]^+$  282.0874,  $\text{C}_{15}\text{H}_{12}\text{N}_3\text{O}_3$  requires  $[\text{L}+\text{H}]^+$  282.0873; Found  $[\text{L}+\text{Na}]^+$  304.0694,  $\text{C}_{15}\text{H}_{11}\text{N}_3\text{NaO}_3$  requires 304.0693.

### 6.6.2 Synthesis of tricycloquinazoline N,N',N''-trioxide 4.4

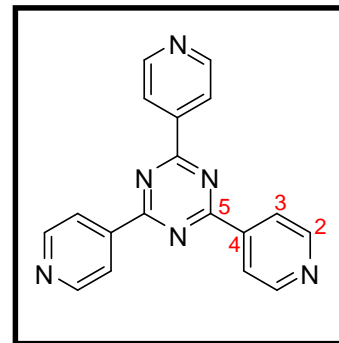
To a solution of **4.2b** (1.50 g, 4.68 mmol) in 25 ml of chloroform, was added mCPBA (2.90 g, 16.3 mmol) and the reaction mixture was heated at reflux for 7 hours. The reaction was cooled to room temperature and concentrated to dryness under vacuum to give a yellow solid, which was recrystallized from hexane /dichloromethane to give **4.4**. Yield 1.53 g (89%), m.p.  $156^\circ\text{C}$ .



**$^1\text{H NMR}$**  (400MHz,  $\text{CDCl}_3$ )  $\delta/\text{ppm}$ : 8.10 (bs, 3H,  $\text{H}_4$ ), 8.00 (d,  $J = 7.8$  Hz, 3H,  $\text{H}_1$ ), 7.59 (d,  $J = 8.3$  Hz, 3H,  $\text{H}_3$ ), 7.43 (t,  $J = 8.0$  Hz, 3H,  $\text{H}_2$ ).  **$^{13}\text{C NMR}$**  (100MHz,  $\text{CDCl}_3$ )  $\delta/\text{ppm}$ : 170.44 ( $\text{C}_7$ ), 135.72 ( $\text{C}_6$ ), 133.88 ( $\text{C}_3$ ), 130.90 ( $\text{C}_5$ ), 130.26 ( $\text{C}_4$ ), 129.84 ( $\text{C}_2$ ), 128.31 ( $\text{C}_1$ ). **IR (KBr)**  $\nu_{\text{max}}/\text{cm}^{-1}$ : 2551, 2012, 1692, 1572, 1426, 1262, 1146, 1075, 914, 852, 748. **ESI-MS**  $m/z$ : Found  $[\text{L}+\text{H}]^+$  369.0968,  $\text{C}_{21}\text{H}_{13}\text{N}_4\text{O}_3$  requires  $[\text{L}+\text{H}]^+$  369.0982; Found  $[\text{L}+\text{Na}]^+$  391.0788,  $\text{C}_{21}\text{H}_{12}\text{N}_4\text{NaO}_3$  requires 391.0802.

### 6.6.3 Synthesis of 2,4,6-tris(4-pyridyl)-1,3,5-triazine 4.3d.

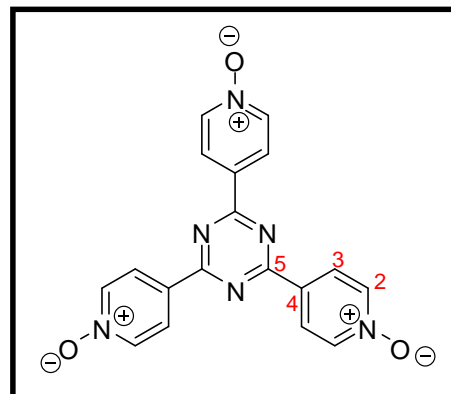
4-Cyanopyridine (5.00 g, 48.0 mmol) and 50% sodium hydride (0.500 g, 9.60 mmol) were heated to 180°C for one hour. Upon cooling, methanol (50 ml) was added to the reaction mixture and stirred at room temperature for 30 minutes. The solid thus obtained was filtered to give **4.3d**, as an off-white solid. This was used as such in further reactions. Yield 11.60 g (77%), m.p. >330°C [Lit<sup>[220]</sup>: m.p. 372 – 374°C].



<sup>1</sup>H NMR<sup>[221]</sup> (400MHz, D<sub>2</sub>O-DCI) δ/ppm: 7.05 (d, *J* = 5.8 Hz, 6H, H<sub>2</sub>), 6.81 (d, *J* = 5.9 Hz, 3H, H<sub>3</sub>). <sup>13</sup>C NMR (100MHz, D<sub>2</sub>O-DCI) δ/ppm: 169.48, 150.65, 128.54, 126.52. IR (KBr) ν<sub>max</sub>/cm<sup>-1</sup>: 3052, 1636, 1582, 1373, 1318, 1264, 1160, 1054, 852, 798. ESI-MS *m/z*: Found [L+H]<sup>+</sup> 313.1201, C<sub>18</sub>H<sub>13</sub>N<sub>6</sub> requires [L+H]<sup>+</sup> 313.1169.

### 6.6.4 Synthesis of 1,3,5-triazine-2,4,6-tris(4-pyridyl) N,N',N''-trioxide 4.3

To a solution of **4.3d** (3.00 g, 9.61 mmol) in acetic acid (25 ml) 50% H<sub>2</sub>O<sub>2</sub> (8 ml) was added, and the reaction mixture was heated to 80°C for 40 minutes. The reaction mixture changed colour from grey to orange then deep red and finally colourless. After 40 minutes, a white precipitate started to form. At this point, the reaction mixture was cooled to room temperature, filtered and dried to give **4.3**, as a white solid. Yield 1.56 g (45%), m.p. >360°C.

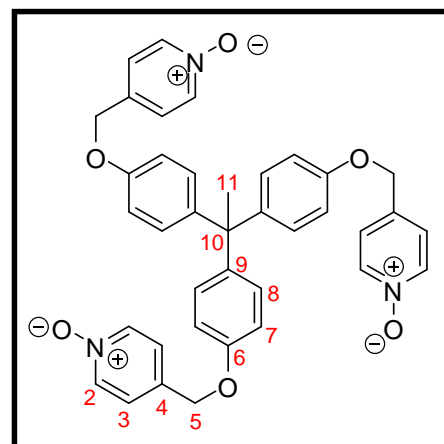


<sup>1</sup>H NMR (400MHz, D<sub>2</sub>O-DCI) δ/ppm: 7.0 (d, *J* = 7.1 Hz, 6H, H<sub>2</sub>), 6.84 (d, *J* = 7.0 Hz, 6H, H<sub>3</sub>). <sup>13</sup>C NMR (100MHz, D<sub>2</sub>O-DCI) δ/ppm: 166.92 (C<sub>5</sub>), 144.03 (C<sub>4</sub>), 138.58 (C<sub>2</sub>), 126.06 (C<sub>3</sub>). IR (KBr) ν<sub>max</sub>/cm<sup>-1</sup>: 3073, 2517, 1608, 1561, 1511, 1363, 1264, 1178, 1092, 869, 813. ESI-MS *m/z*: No sign of [L+H]<sup>+</sup> peaks.

### 6.6.5 Synthesis of 1,1',1''-tris[4-(4-pyridylmethoxy)phenyl]ethane N,N',N''-trioxide 4.4

MCPBA (0.416 g, 2.41 mmol) was added to a methanolic solution (20 ml) of compound **4.4b** (0.400 g, 0.690 mmol), and the mixture was heated to reflux for 4 hours. The reaction was cooled to room temperature, then concentrated to dryness under vacuum and purified by silica gel flash chromatography with 5% methanol:dichloromethane to give **4.4**, as an off-white solid. Yield 0.239 g (55%), m.p. 76°C.

<sup>1</sup>H NMR (400MHz, CDCl<sub>3</sub>) δ/ppm: 8.21 (d, *J* = 7.1 Hz, 6H, H<sub>2</sub>), 7.33 (d, *J* = 7.0 Hz, 6H, H<sub>3</sub>), 6.99 (d, *J* = 8.7 Hz, 6H, H<sub>8</sub>), 6.82 (d, *J* = 9.0



Hz, 6H, H<sub>7</sub>), 5.02 (s, 6H, H<sub>5</sub>), 2.10 (s, 3H, H<sub>11</sub>). <sup>13</sup>C NMR (100MHz, CDCl<sub>3</sub>) δ/ppm: 155.92 (C<sub>6</sub>), 142.54 (C<sub>4</sub>), 139.23 (C<sub>2</sub>), 136.21 (C<sub>9</sub>), 129.77 (C<sub>8</sub>), 124.28 (C<sub>3</sub>), 114.06 (C<sub>7</sub>), 67.34 (C<sub>5</sub>), 50.74 (C<sub>10</sub>), 30.72 (C<sub>11</sub>). **IR (KBr)**  $\nu_{\max}/\text{cm}^{-1}$ : 3033, 2474, 1893, 1507, 1488, 1445, 1378, 1230, 1180, 1038, 829. **Elemental Analysis:** calculated for C<sub>38</sub>H<sub>33</sub>N<sub>3</sub>O<sub>6</sub>·3H<sub>2</sub>O: C, 66.95; H, 5.77; N, 6.16. Found: C, 67.06; H, 5.75; N, 6.10. **ESI-MS**  $m/z$ : Found [L+H]<sup>+</sup> 628.2461, C<sub>38</sub>H<sub>34</sub>N<sub>3</sub>O<sub>6</sub> requires [L+H]<sup>+</sup> 628.2442.

## 6.7 Preparation of silver(I) complexes with pyridine N,N',N''-trioxides

### 6.7.1 Complexes of 2,6':2',6''-terpyridine N,N',N''-trioxide 4.1

#### With silver(I) perchlorate (1:3) 4.7

To a solution of ligand **4.1** (10 mg, 0.035 mmol) in water (1 ml) was added a methanol (2 ml) solution of AgClO<sub>4</sub> (20 mg, 0.10 mmol) at room temperature. The solution was left in darkness at room temperature and subjected to slow evaporation to give colourless crystals. Yield 14 mg (80%), m.p. 259°C.

**Elemental Analysis:** calculated for C<sub>15</sub>H<sub>11</sub>N<sub>3</sub>O<sub>3</sub>·AgClO<sub>4</sub>: C 36.87; H 2.27; N 8.60. Found: (inconsistent with the proposed structure) C 21.55; H 1.39; N 5.02. **IR (KBr)**  $\nu_{\max}/\text{cm}^{-1}$ : 3080, 1503, 1468, 1437, 1384, 1275, 1247, 1142, 1086, 852, 774. **ESI-MS**  $m/z$ : Found [L+Ag]<sup>+</sup> 387.9843, C<sub>15</sub>H<sub>11</sub>AgN<sub>3</sub>O<sub>3</sub> requires [L+Ag]<sup>+</sup> 387.9846.

#### With silver(I) trifluoroacetate (1:3) 4.8

To a solution of ligand **4.1** (15 mg, 0.053 mmol) of water (1 ml) was added a methanol (2 ml) solution of AgOCOCF<sub>3</sub> (35 mg, 0.16 mmol) at room temperature. Slow evaporation of the solution at room temperature in darkness afforded colourless crystals suitable for X-ray crystallography. Yield 7 mg (18%), m.p. 146°C.

**Elemental Analysis:** Insufficient sample for analysis **IR (KBr)**  $\nu_{\max}/\text{cm}^{-1}$ : 3096, 1681, 1470, 1433, 1390, 1271, 1209, 838, 803, 723. **ESI-MS**  $m/z$ : Found [L+Ag]<sup>+</sup> 387.9846, C<sub>15</sub>H<sub>11</sub>AgN<sub>3</sub>O<sub>3</sub> requires [L+Ag]<sup>+</sup> 387.9846.

#### With silver(I) triflate (1:3) 4.9

To a water solution of ligand **4.1** (15 mg, 0.053 mmol) was added AgSO<sub>3</sub>CF<sub>3</sub> (41 mg, 0.16 mmol) dissolved in methanol (2 ml) Slow evaporation gave a colourless crystalline solid suitable for X-ray crystallography. Yield 22 mg (52%), m.p. 182°C.

**Elemental Analysis:** calculated for C<sub>15</sub>H<sub>11</sub>N<sub>3</sub>O<sub>3</sub>·2(AgSO<sub>3</sub>CF<sub>3</sub>)·H<sub>2</sub>O: C 25.11; H 1.61; N 5.15. Found: (inconsistent with the proposed structure) C 21.14; H 1.43; N 4.19. **IR (KBr)**  $\nu_{\max}/\text{cm}^{-1}$ : 2422, 1660, 1503, 1468, 1433, 1391, 1256, 1175, 1034, 851, 776. **ESI-MS**  $m/z$ : Found [L+Ag]<sup>+</sup> 387.9846, C<sub>15</sub>H<sub>11</sub>AgN<sub>3</sub>O<sub>3</sub> requires [L+Ag]<sup>+</sup> 387.9846. Found [L+2Ag]<sup>+</sup> 496.9603, C<sub>15</sub>H<sub>11</sub>Ag<sub>2</sub>N<sub>3</sub>O<sub>3</sub> requires [L+2Ag]<sup>+</sup> 496.8894.

### **With silver(I) hexafluorophosphate (1:3) 4.10**

To a water solution of ligand **4.1** (10 mg, 0.035 mmol) was added AgPF<sub>6</sub> (25 mg, 0.10 mmol) dissolved in methanol (2 ml). Slow evaporation gave a colourless crystalline solid suitable for X-ray crystallography. Yield 11 mg (16%), m.p. 204°C.

**Elemental Analysis:** calculated for 2(C<sub>15</sub>H<sub>11</sub>N<sub>3</sub>O<sub>3</sub>).1.5(AgPF<sub>6</sub>): C 38.26; H 2.35; N 8.92. Found: (inconsistent with the proposed structure) C 31.40; H 2.21; N 7.27. **IR (KBr)**  $\nu_{\max}/\text{cm}^{-1}$ : 3095, 2435, 1499, 1467, 1433, 1391, 1243, 1216, 845, 773, 559. **ESI-MS**  $m/z$ : Found [L+Ag]<sup>+</sup> 387.9849, C<sub>15</sub>H<sub>11</sub>AgN<sub>3</sub>O<sub>3</sub> requires [L+Ag]<sup>+</sup> 387.9846; Found [2L+Ag]<sup>+</sup> 669.0654, C<sub>30</sub>H<sub>22</sub>AgN<sub>6</sub>O<sub>6</sub> requires [2L+Ag]<sup>+</sup> 669.0646.

### **With silver(I) nitrate (1:3) 4.11**

Silver(I) nitrate (30 mg, 0.18 mmol) dissolved in water (1 ml) was combined with a water (2 ml) solution of ligand **4.1** (17 mg, 0.060 mmol). Colourless needle shaped crystals were formed when the solution was left to evaporate slowly in darkness. Yield 24 mg (64%), m.p. 162°C.

**Elemental Analysis:** calculated for 2(C<sub>15</sub>H<sub>11</sub>N<sub>2</sub>O<sub>2</sub>).4(AgNO<sub>3</sub>).2(H<sub>2</sub>O): C 28.19; H 2.05; N 10.96. Found: (inconsistent with the proposed structure) C 25.76; H 1.64; N 10.40. **IR (KBr)**  $\nu_{\max}/\text{cm}^{-1}$ : 3081, 2424, 1385, 1243, 1032, 852, 822, 796, 781, 568. **ESI-MS**  $m/z$ : [L+Ag]<sup>+</sup> 387.9847, C<sub>15</sub>H<sub>11</sub>AgN<sub>3</sub>O<sub>3</sub> requires [L+Ag]<sup>+</sup> 387.9846; Found [2L+Ag]<sup>+</sup> 669.0654, C<sub>30</sub>H<sub>22</sub>AgN<sub>6</sub>O<sub>6</sub> requires [2L+Ag]<sup>+</sup> 669.0646.

### **With silver(I) nitrate (1:1) 4.12**

Ligand **4.1** (17 mg, 0.060 mmol) and silver(I) nitrate (10 mg, 0.060 mmol) were both dissolved in water, the solutions mixed and on standing for several days in darkness gave colourless crystals suitable for X-ray analysis. Yield 6 mg (10%), m.p. 102°C.

**Elemental Analysis:** insufficient sample for analysis. **IR (KBr)**  $\nu_{\max}/\text{cm}^{-1}$ : 3076, 2426, 1496, 1460, 1426, 1301, 1251, 1218, 853, 834, 772. **ESI-MS**  $m/z$ : Found [L+Ag]<sup>+</sup> 387.9841, C<sub>15</sub>H<sub>11</sub>AgN<sub>3</sub>O<sub>3</sub> requires [L+Ag]<sup>+</sup> 387.9846; Found [2L+Ag]<sup>+</sup> 669.0646, C<sub>30</sub>H<sub>22</sub>AgN<sub>6</sub>O<sub>6</sub> requires [2L+Ag]<sup>+</sup> 669.0633.

### **With silver(I) nitrate (1:5) 4.13**

A solution of silver(I) nitrate (44.5 mg, 0.265 mmol) in water (1 ml) was added to a solution of ligand **4.1** (15 mg, 0.053 mmol) in water (2 ml). The resultant solution was kept at room temperature in darkness to give colourless needle shaped crystals. Yield 18 mg (35%), m.p. 121°C.

**Elemental Analysis:** calculated for 2(C<sub>15</sub>H<sub>11</sub>N<sub>2</sub>O<sub>2</sub>).8AgNO<sub>3</sub>.5H<sub>2</sub>O: C 17.14; H 2.01; N 9.33. Found: (inconsistent with the proposed structure) C 16.23; H 1.15; N 9.61. **IR (KBr)**  $\nu_{\max}/\text{cm}^{-1}$ : 3069, 2421, 1501, 1466, 1383, 1245, 1213, 1030, 851, 835, 781. **ESI-MS**  $m/z$ : Found [L+Ag]<sup>+</sup> 387.9846, C<sub>15</sub>H<sub>11</sub>AgN<sub>3</sub>O<sub>3</sub> requires [L+Ag]<sup>+</sup> 387.9846; Found [2L+Ag]<sup>+</sup> 669.0649, C<sub>30</sub>H<sub>22</sub>AgN<sub>6</sub>O<sub>6</sub> requires [2L+Ag]<sup>+</sup> 669.0646.

## **Appendix: Crystallography**

## X-Ray Crystallography

Tables A1 – A14 list the crystal data and X-ray experimental details for the 68 fully refined crystal structures discussed in this thesis. Throughout the text, selected bond lengths and angles are discussed and listed under the appropriate figures, while the remaining distances and angles, as well as the coordinates, anisotropic displacement parameters and hydrogen atom coordinates are available on request from the Department of Chemistry, University of Canterbury, New Zealand.

X-Ray data were collected either on a Bruker APEX-II instrument with graphite-monochromatised Mo K $\alpha$  radiation [ $\lambda = 0.71073 \text{ \AA}$ ] radiation, or on an Oxford-Agilent Supernova instrument with focused microsource Mo K $\alpha$  [ $\lambda = 0.71073 \text{ \AA}$ ] radiation and ATLAS CCD area detector. CrysAlisPro was used for the data collection and data processing. All structures were solved using direct methods with SHELXS<sup>[222]</sup> and refined on  $F^2$  using all data by full matrix least square procedures with SHELXL-97<sup>[223]</sup> using either XP or OLEX-2<sup>[224]</sup> for visualisation. Multi-scan absorption corrections were done using SADABS or SCALE3 ABSPACK. Hydrogen atoms were included in calculated positions for carbons and manually located from residual electron density for heteroatoms, with isotropic displacement parameters 1.2 or 1.5 times the isotropic equivalent of their carrier atoms. Graphical presentation of crystallographic data was prepared using OLEX-2.<sup>[224]</sup>

## X-Ray Powder Diffraction

X-Ray Powder Diffraction data were collected using an Oxford-Agilent Supernova instrument using Cu K $\alpha$  [ $\lambda = 1.5418 \text{ \AA}$ ] radiation and an ATLAS CCD area detector. Samples were prepared by grinding ca. 5mg of analyte with a minimum quantity of perfluorinated-PEG and applying a sample of approximately 0.5 mm diameter to a thin glass fibre mounted on a goniometer head, which was mounted directly in the beam path. Diffraction data were recorded using 360°  $\Phi$  scans with 300 second exposure time per rotation frame. The diffraction data were integrated radially and background correction manually applied, using a 6<sup>th</sup> order polynomial to approximate the absorbance due to the fibre and oil. The graphical presentation of X-ray Powder Diffraction data was prepared using Origin version-8.<sup>[225]</sup>

Table – A1 Crystal data and X-ray experimental data for complexes **2.18**, **2.19**, **2.20**, **2.21** and **2.22**.

Complex Code	<b>2.18</b> [3RPUA]	<b>2.19</b> [3RPU146]	<b>2.20</b> [3RPU156]	<b>2.21</b> [3RPUB]	<b>2.22</b> [3RPU142]
Empirical formula	C <sub>10</sub> H <sub>14</sub> N <sub>2</sub> O <sub>12</sub> Cl <sub>2</sub> Ag <sub>2</sub>	C <sub>20</sub> H <sub>20</sub> N <sub>4</sub> O <sub>12</sub> Cl <sub>2</sub> Ag <sub>2</sub>	C <sub>15</sub> H <sub>15</sub> N <sub>3</sub> O <sub>8</sub> ClAg	C <sub>7</sub> H <sub>7</sub> NO <sub>4</sub> F <sub>3</sub> Ag	C <sub>12</sub> H <sub>10</sub> N <sub>2</sub> O <sub>8</sub> S <sub>2</sub> F <sub>6</sub> Ag <sub>2</sub>
Formula weight	640.87	795.04	508.62	334.01	704.08
Temperature (K)	113.0	120.0	120.0	113.0	120.0
Crystal system	Triclinic	Trigonal	Hexagonal	Monoclinic	Triclinic
Space group	<i>P</i> -1	<i>R</i> 3	<i>P</i> 6 <sub>3</sub> / <i>m</i>	<i>P</i> 2 <sub>1</sub> / <i>c</i>	<i>P</i> -1
Unit cell dimensions: a (Å)	7.3920(2)	21.9957(2)	13.3014(3)	5.8783(2)	8.26718(8)
b (Å)	10.7920(3)	21.9957(2)	13.3014(3)	22.9077(7)	10.26639(13)
c (Å)	11.6410(4)	14.07390(14)	5.9918(2)	7.4993(2)	11.74637(13)
α (°)	80.286(1)	90.00	90.00	90.00	86.5046(9)
β (°)	88.272(1)	90.00	90.00	106.0930(10)	81.1991(9)
γ (°)	77.080(1)	120.00	120.00	90.00	88.2690(9)
Volume / Å <sup>3</sup>	892.14(5)	5896.88(10)	918.09(5)	970.27(5)	983.172(19)
Z	2	9	2	4	2
Density (calculated) mg/m <sup>3</sup>	2.386	2.015	1.840	2.286	2.378
Absorption Coefficient mm <sup>-1</sup>	2.562	1.768	1.294	2.123	2.306
F(000)	624	3528	492	648	680
Crystal size (mm <sup>3</sup> )	0.48 x 0.37 x 0.13	0.31 x 0.27 x 0.13	0.22 x 0.14 x 0.10	0.52 x 0.40 x 0.06	0.20 x 0.16 x 0.09
2θ range for data collection (°)	4.84 to 60.00	6.18 to 54.94	6.12 to 54.86	5.92 to 55.00	5.46 to 55.00
Reflections collected [R(int)]	24007 [0.0322]	95119 [0.0573]	22378 [0.0376]	21712 [0.0274]	148021 [0.0528]
Independent reflections	5214	6016	767	2233	4516
Data completeness (%)	99.0	100	100	100	99.9
Data/ restraints/ parameters	5164/0/272	6016/0/361	767/0/56	2233/0/153	4516/0/289
Goodness-of-fit on F <sup>2</sup>	1.107	1.159	1.168	1.110	1.095
Final R <sub>1</sub> indices [I>2σ(I)]	R <sub>1</sub> = 0.0211 wR <sub>2</sub> = 0.0547	R <sub>1</sub> = 0.0203 wR <sub>2</sub> = 0.0504	R <sub>1</sub> = 0.0412 wR <sub>2</sub> = 0.1014	R <sub>1</sub> = 0.0175 wR <sub>2</sub> = 0.0446	R <sub>1</sub> = 0.0206 wR <sub>2</sub> = 0.0475
Final R indices [all data]	R <sub>1</sub> = 0.0220 wR <sub>2</sub> = 0.0553	R <sub>1</sub> = 0.0215 wR <sub>2</sub> = 0.0512	R <sub>1</sub> = 0.0454 wR <sub>2</sub> = 0.1047	R <sub>1</sub> = 0.0185 wR <sub>2</sub> = 0.0452	R <sub>1</sub> = 0.0239 wR <sub>2</sub> = 0.0500
Largest diff. peak/hole (e.Å <sup>-3</sup> )	0.53/-0.90	0.76/-0.42	0.87/-1.00	0.41/-0.70	0.72/-0.54



Table – A2 Crystal data and X-ray experimental data for complexes 2.23, 2.24, 2.25, 2.26 and 2.27.

Complex Code	2.23 [3RPU139]	2.24 [3RPUZ]	2.25 [3RPU9]	2.26 [3RPU19]	2.27 [3RPU100]
Empirical formula	C <sub>25</sub> H <sub>27</sub> N <sub>5</sub> O <sub>6</sub> P <sub>3</sub> F <sub>18</sub> Ag <sub>3</sub>	C <sub>9</sub> H <sub>9</sub> NO <sub>3</sub> F <sub>3</sub> Ag	C <sub>9</sub> H <sub>9</sub> NO <sub>7</sub> S <sub>2</sub> F <sub>6</sub> Ag <sub>2</sub>	C <sub>14</sub> H <sub>18</sub> N <sub>4</sub> O <sub>8</sub> Ag <sub>2</sub>	C <sub>12</sub> H <sub>11</sub> NO <sub>5</sub> ClAg
Formula weight	1252.04	344.04	637.03	586.06	392.54
Temperature (K)	120.0	114.0	120.0	113.0	120.0
Crystal system	Monoclinic	Monoclinic	Triclinic	Monoclinic	Monoclinic
Space group	<i>P</i> 2 <sub>1</sub> / <i>a</i>	<i>P</i> 2 <sub>1</sub> / <i>c</i>	<i>P</i> -1	<i>P</i> 2 <sub>1</sub> / <i>n</i>	<i>P</i> 2 <sub>1</sub> / <i>c</i>
Unit cell dimensions: a (Å)	26.5946(7)	10.0386(3)	8.3124(4)	13.8718(4)	8.52135(8)
b (Å)	11.0166(2)	16.5102(6)	9.7965(5)	8.4073(2)	11.71872(10)
c (Å)	28.6114(8)	6.7291(2)	11.6154(7)	18.1038(5)	12.91370(14)
α (°)	90.00	90.00	79.201(5)	90.00	90.00
β (°)	117.329(4)	91.916(2)	78.572(4)	111.5620(10)	103.7560(10)
γ (°)	90.00	90.00	68.501(4)	90.00	90.00
Volume / Å <sup>3</sup>	7447.0(3)	1114.65(6)	855.76(8)	1963.59(9)	1252.57(2)
Z	8	4	2	4	4
Density (calculated) mg/m <sup>3</sup>	2.233	2.050	2.472	1.982	2.082
Absorption Coefficient mm <sup>-1</sup>	1.830	1.845	2.629	2.043	1.841
F(000)	4864	672	612	1152	776
Crystal size (mm <sup>3</sup> )	0.24 x 0.21 x 0.17	0.50 x 0.40 x 0.20	0.24 x 0.17 x 0.06	0.52 x 0.48 x 0.36	0.27 x 0.20 x 0.07
2θ range for data collection (°)	5.66 to 55.00	6.40 to 54.98	5.32 to 55.00	5.42 to 55.00	6.02 to 54.98
Reflections collected [R(int)]	121515 [0.0446]	24215 [0.0293]	16493 [0.0443]	42508 [0.0489]	102473 [0.0466]
Independent reflections	17077	2554	3894	4492	2872
Data completeness (%)	99.8	99.7	100	99.9	100
Data/ restraints/ parameters	17077/0/1097	2554/0/184	3894/0/246	4492/0/257	2872/0/189
Goodness-of-fit on F <sup>2</sup>	1.221	1.109	1.116	1.013	1.116
Final R <sub>1</sub> indices [I>2σ(I)]	R <sub>1</sub> = 0.0652 wR <sub>2</sub> = 0.1386	R <sub>1</sub> = 0.0217 wR <sub>2</sub> = 0.0572	R <sub>1</sub> = 0.0303 wR <sub>2</sub> = 0.0655	R <sub>1</sub> = 0.0260 wR <sub>2</sub> = 0.0651	R <sub>1</sub> = 0.0166 wR <sub>2</sub> = 0.0390
Final R indices [all data]	R <sub>1</sub> = 0.0706 wR <sub>2</sub> = 0.1407	R <sub>1</sub> = 0.0229 wR <sub>2</sub> = 0.0580	R <sub>1</sub> = 0.0446 wR <sub>2</sub> = 0.0758	R <sub>1</sub> = 0.0313 wR <sub>2</sub> = 0.0676	R <sub>1</sub> = 0.0195 wR <sub>2</sub> = 0.0410
Largest diff. peak/hole (e.Å <sup>-3</sup> )	1.72/-2.02	1.44/-0.72	1.51/-1.08	0.68/-0.71	0.38/-0.47

Table – A3 Crystal data and X-ray experimental data for complexes **2.28**, **2.29**, **2.30**, **2.31** and **2.32**.

Complex Code	<b>2.28</b> [3RPU163]	<b>2.29</b> [3RPU164]	<b>2.30</b> [3RPU21]	<b>2.31</b> [3RPU86]	<b>2.32</b> [3RPUS]
Empirical formula	C <sub>48</sub> H <sub>44</sub> N <sub>4</sub> O <sub>20</sub> Cl <sub>4</sub> Ag <sub>4</sub>	C <sub>48</sub> H <sub>44</sub> N <sub>4</sub> O <sub>4</sub> P <sub>2</sub> F <sub>12</sub> Ag <sub>2</sub>	C <sub>26</sub> H <sub>18</sub> N <sub>2</sub> O <sub>6</sub> F <sub>6</sub> Ag <sub>2</sub>	C <sub>88</sub> H <sub>72</sub> N <sub>8</sub> O <sub>21</sub> Cl <sub>3</sub> Ag <sub>3</sub>	C <sub>26</sub> H <sub>18</sub> N <sub>2</sub> O <sub>6</sub> F <sub>6</sub> Ag <sub>2</sub>
Formula weight	1570.15	1246.55	784.16	2007.50	784.16
Temperature (K)	120.0	120.0	113.0	120.0	113.0
Crystal system	Monoclinic	Triclinic	Triclinic	Triclinic	Tetragonal
Space group	<i>P</i> 2 <sub>1</sub> / <i>c</i>	<i>P</i> -1	<i>P</i> -1	<i>P</i> -1	<i>P</i> 4 <sub>1</sub> 2 <sub>1</sub> 2
Unit cell dimensions: a (Å)	15.0704(5)	9.6514(3)	5.9134(2)	7.5210(4)	10.9416(4)
b (Å)	10.3103(4)	10.7688(4)	10.7520(3)	15.7390(4)	10.9416(4)
c (Å)	33.2645(13)	12.4502(5)	11.5231(4)	19.0404(8)	44.554(2)
α (°)	90.00	79.907(3)	64.2720(10)	111.559(3)	90.00
β (°)	100.678(4)	70.633(3)	80.3630(10)	100.393(4)	90.00
γ (°)	90.00	75.729(3)	74.1410(10)	94.618(3)	90.00
Volume / Å <sup>3</sup>	5079.2(3)	1176.91(8)	633.89(4)	2035.06(14)	5334.0(4)
Z	4	1	1	1	8
Density (calculated) mg/m <sup>3</sup>	2.053	1.759	2.054	1.638	1.953
Absorption Coefficient mm <sup>-1</sup>	1.816	0.998	1.636	0.895	1.556
F(000)	3104	624	384	1016	3072
Crystal size (mm <sup>3</sup> )	0.33 x 0.26 x 0.22	0.13 x 0.13 x 0.10	0.52 x 0.52 x 0.48	0.22 x 0.17 x 0.06	0.40 x 0.30 x 0.20
2θ range for data collection (°)	5.44 to 55.00	5.36 to 54.98	6.92 to 55.00	5.20 to 55.00	4.14 to 55.00
Reflections collected [R(int)]	51163 [0.0683]	31585 [0.0338]	14266 [0.0258]	92255 [0.0509]	121434 [0.0437]
Independent reflections	11669	5396	2904	9338	3630
Data completeness (%)	100	99.9	100	99.8	100
Data/ restraints/ parameters	11669/0/721	5396/0/325	2904/0/190	9338/0/575	3630/0/379
Goodness-of-fit on F <sup>2</sup>	1.079	1.070	1.090	1.191	1.305
Final R <sub>1</sub> indices [I>2σ(I)]	R <sub>1</sub> = 0.0475 wR <sub>2</sub> = 0.0843	R <sub>1</sub> = 0.0214 wR <sub>2</sub> = 0.0483	R <sub>1</sub> = 0.0182 wR <sub>2</sub> = 0.0536	R <sub>1</sub> = 0.0464 wR <sub>2</sub> = 0.1187	R <sub>1</sub> = 0.0324 wR <sub>2</sub> = 0.0718
Final R indices [all data]	R <sub>1</sub> = 0.0689 wR <sub>2</sub> = 0.0908	R <sub>1</sub> = 0.0239 wR <sub>2</sub> = 0.0495	R <sub>1</sub> = 0.0187 wR <sub>2</sub> = 0.0540	R <sub>1</sub> = 0.0555 wR <sub>2</sub> = 0.1240	R <sub>1</sub> = 0.0338 wR <sub>2</sub> = 0.0724
Largest diff. peak/hole (e.Å <sup>-3</sup> )	2.03/-1.48	0.49/-0.37	0.42/-0.51	1.59/-1.03	0.53/-1.01

Table – A4 Crystal data and X-ray experimental data for complexes 2.33, 2.34, 2.35, 2.36 and 2.37.

Complex Code	2.33 [3RPU90]	2.34 [3RPU8]	2.35 [3RPU26]	2.36 [3RPU17]	2.37 [3RPU3]
Empirical formula	C <sub>12</sub> H <sub>9</sub> NO <sub>4</sub> SF <sub>3</sub> Ag	C <sub>11</sub> H <sub>11</sub> NO <sub>2</sub> BF <sub>4</sub> Ag	C <sub>18</sub> H <sub>15</sub> NO <sub>5</sub> ClAg	C <sub>36</sub> H <sub>42</sub> N <sub>6</sub> O <sub>24</sub> Cl <sub>3</sub> Ag <sub>3</sub>	C <sub>30</sub> H <sub>27</sub> N <sub>3</sub> O <sub>21</sub> F <sub>18</sub> Ag <sub>6</sub>
Formula weight	428.13	383.89	468.63	1372.72	1754.77
Temperature (K)	120.0	120.0	120.0	113.0	120.0
Crystal system	Orthorhombic	Monoclinic	Monoclinic	Monoclinic	Monoclinic
Space group	<i>Pbca</i>	<i>P2<sub>1</sub>/n</i>	<i>P2<sub>1</sub>/n</i>	<i>P2<sub>1</sub>/n</i>	<i>P2<sub>1</sub>/n</i>
Unit cell dimensions: a (Å)	8.2101(2)	7.15767(13)	9.10616(11)	18.6132(10)	19.14913(13)
b (Å)	10.8412(3)	10.73700(17)	18.83466(19)	10.2467(5)	9.59167(6)
c (Å)	30.7539(9)	16.3544(3)	10.83429(14)	24.9577(13)	25.4038(2)
α (°)	90.00	90.00	90.00	90.00	90.00
β (°)	90.00	91.8065(17)	109.3642(13)	101.410(3)	95.7068(7)
γ (°)	90.00	90.00	90.00	90.00	90.00
Volume / Å <sup>3</sup>	2737.33(13)	1256.24(4)	1753.09(4)	4666.0(4)	4642.85(6)
Z	8	4	4	4	4
Density (calculated) mg/m <sup>3</sup>	2.078	2.030	1.767	1.954	2.510
Absorption Coefficient mm <sup>-1</sup>	1.677	1.653	1.325	1.513	2.635
F(000)	1680	752	936	2736	3360
Crystal size (mm <sup>3</sup> )	0.25 x 0.16 x 0.08	0.22 x 0.17 x 0.08	0.35 x 0.28 x 0.08	0.52 x 0.52 x 0.48	0.22 x 0.20 x 0.04
2θ range for data collection (°)	5.62 to 55.00	6.14 to 54.98	5.22 to 55.00	4.30 to 55.00	5.34 to 55.00
Reflections collected [R(int)]	32691 [0.0450]	19242 [0.0349]	44455 [0.0248]	103071 [0.0563]	248578 [0.0377]
Independent reflections	3141	2866	4020	10712	10651
Data completeness (%)	99.9	100	99.9	99.9	99.8
Data/ restraints/ parameters	3141/0/199	2866/0/186	4020/0/235	10712/0/649	10651/0/796
Goodness-of-fit on F <sup>2</sup>	1.372	1.002	1.048	1.061	1.048
Final R <sub>1</sub> indices [I>2σ(I)]	R <sub>1</sub> = 0.0417 wR <sub>2</sub> = 0.0691	R <sub>1</sub> = 0.0212 wR <sub>2</sub> = 0.0457	R <sub>1</sub> = 0.0221 wR <sub>2</sub> = 0.0548	R <sub>1</sub> = 0.0399 wR <sub>2</sub> = 0.1075	R <sub>1</sub> = 0.0334 wR <sub>2</sub> = 0.0776
Final R indices [all data]	R <sub>1</sub> = 0.0479 wR <sub>2</sub> = 0.0714	R <sub>1</sub> = 0.0277 wR <sub>2</sub> = 0.0495	R <sub>1</sub> = 0.0231 wR <sub>2</sub> = 0.0555	R <sub>1</sub> = 0.0511 wR <sub>2</sub> = 0.1134	R <sub>1</sub> = 0.0393 wR <sub>2</sub> = 0.0832
Largest diff. peak/hole (e.Å <sup>-3</sup> )	1.12/-0.55	0.39/-0.38	1.02/-0.60	1.75/-1.33	4.55/-2.88

Table – A5 Crystal data and X-ray experimental data for complexes **2.38**, **2.39**, **2.40**, **2.41** and **2.42**.

Complex Code	<b>2.38</b> [3RPU62]	<b>2.39</b> [3RPU52]	<b>2.40</b> [3RPU114]	<b>2.41</b> [3RPU114.1]	<b>2.42</b> [3RPU158]
Empirical formula	C <sub>36</sub> H <sub>42</sub> N <sub>6</sub> O <sub>12</sub> B <sub>3</sub> F <sub>12</sub> Ag <sub>3</sub>	C <sub>22</sub> H <sub>16</sub> N <sub>4</sub> O <sub>12</sub> Cl <sub>2</sub> Ag <sub>2</sub>	C <sub>18</sub> H <sub>22</sub> N <sub>2</sub> O <sub>6</sub> ClAg	C <sub>18</sub> H <sub>22</sub> N <sub>2</sub> O <sub>10</sub> Cl <sub>2</sub> Ag <sub>2</sub>	C <sub>18</sub> H <sub>23</sub> N <sub>2</sub> O <sub>6</sub> Cl
Formula weight	1334.80	815.03	505.70	713.02	398.83
Temperature (K)	113.0	120.0	120.0	120.0	120.0
Crystal system	Triclinic	Triclinic	Monoclinic	Triclinic	Monoclinic
Space group	<i>P</i> -1	<i>P</i> -1	<i>P</i> 2 <sub>1</sub> / <i>n</i>	<i>P</i> -1	<i>P</i> 2 <sub>1</sub> / <i>c</i>
Unit cell dimensions: a (Å)	10.2012(3)	7.5933(3)	6.96356(10)	8.09382(14)	16.932(3)
b (Å)	14.1759(5)	7.8776(3)	19.2620(3)	11.6657(2)	14.526(3)
c (Å)	17.2837(5)	11.4805(4)	14.6859(2)	13.2207(2)	14.956(3)
α (°)	71.712(3)	85.447(2)	90.00	109.6979(17)	90.00
β (°)	76.452(3)	80.991(2)	98.9710(14)	95.9735(15)	99.73(3)
γ (°)	77.743(3)	67.726(2)	90.00	97.5384(14)	90.00
Volume / Å <sup>3</sup>	2280.91(12)	627.50(4)	1945.75(5)	1150.30(4)	3625.6(13)
Z	2	1	4	2	8
Density (calculated) mg/m <sup>3</sup>	1.944	2.157	1.726	2.059	1.461
Absorption Coefficient mm <sup>-1</sup>	1.391	1.850	1.211	1.993	0.250
F(000)	1320	400	1024	704	1680
Crystal size (mm <sup>3</sup> )	0.30 x 0.24 x 0.18	0.45 x 0.42 x 0.40	0.34 x 0.24 x 0.22	0.21 x 0.18 x 0.06	0.30 x 0.14 x 0.05
2θ range for data collection (°)	5.52 to 52.00	5.58 to 54.98	5.62 to 55.00	5.66 to 55.00	5.52 to 55.00
Reflections collected [R(int)]	16643 [0.0198]	14144 [0.0319]	108347 [0.0530]	54170 [0.0523]	54145 [0.0407]
Independent reflections	8960	2879	4459	5295	8304
Data completeness (%)	99.8	100	99.9	100	99.9
Data/ restraints/ parameters	8960/0/693	2879/0/219	4459/0/253	5295/0/316	8304/0/495
Goodness-of-fit on F <sup>2</sup>	1.038	1.044	1.120	1.070	1.036
Final R <sub>1</sub> indices [I>2σ(I)]	R <sub>1</sub> = 0.0306 wR <sub>2</sub> = 0.0649	R <sub>1</sub> = 0.0216 wR <sub>2</sub> = 0.0607	R <sub>1</sub> = 0.0240 wR <sub>2</sub> = 0.0591	R <sub>1</sub> = 0.0265 wR <sub>2</sub> = 0.0599	R <sub>1</sub> = 0.0701 wR <sub>2</sub> = 0.1888
Final R indices [all data]	R <sub>1</sub> = 0.0388 wR <sub>2</sub> = 0.0704	R <sub>1</sub> = 0.0232 wR <sub>2</sub> = 0.0616	R <sub>1</sub> = 0.0273 wR <sub>2</sub> = 0.0615	R <sub>1</sub> = 0.0350 wR <sub>2</sub> = 0.0657	R <sub>1</sub> = 0.0813 wR <sub>2</sub> = 0.1988
Largest diff. peak/hole (e.Å <sup>-3</sup> )	1.32/-1.23	0.39/-0.72	0.55/-0.69	0.91/-0.50	2.77/-0.69

Table – **A6** Crystal data and X-ray experimental data for complexes **2.43**, **2.44**, **2.45**, **2.46**, **2.47\*** and **2.48**.

Complex Code	<b>2.43</b> [3RPU128]	<b>2.44</b> [3RPU73]	<b>2.45</b> [3RPU84]	<b>2.46</b> [3RPU76]	<b>2.48</b> [3RPU123]
Empirical formula	C <sub>20</sub> H <sub>22</sub> N <sub>2</sub> O <sub>8</sub> S <sub>2</sub> F <sub>6</sub> Ag <sub>2</sub>	C <sub>9</sub> H <sub>10</sub> NO <sub>6</sub> Cl	C <sub>17</sub> H <sub>13</sub> NO <sub>5</sub>	C <sub>9</sub> H <sub>7</sub> NOBF <sub>3</sub>	C <sub>18</sub> H <sub>15</sub> N <sub>2</sub> O <sub>2</sub> PF <sub>6</sub>
Formula weight	812.28	263.63	311.28	212.97	435.29
Temperature (K)	120.0	120.0	120.0	120.0	120.0
Crystal system	Triclinic	Triclinic	Triclinic	Orthorhombic	Monoclinic
Space group	<i>P</i> -1	<i>P</i> -1	<i>P</i> -1	<i>Pbca</i>	<i>C2/c</i>
Unit cell dimensions: a (Å)	8.30232(9)	7.2057(5)	7.0894(5)	10.5168(4)	14.7979(9)
b (Å)	12.31343(15)	8.1460(5)	7.3285(5)	8.5571(3)	13.3496(7)
c (Å)	12.96229(14)	10.4964(7)	14.1838(9)	19.5676(8)	10.2391(7)
α (°)	99.2705(10)	68.479(6)	101.570(6)	90.00	90.00
β (°)	97.9089(9)	74.416(6)	103.371(5)	90.00	117.061(9)
γ (°)	95.2925(9)	84.832(5)	91.634(6)	90.00	90.00
Volume / Å <sup>3</sup>	1286.49(2)	552.07(6)	700.20(8)	1760.96(12)	1801.26(19)
Z	2	2	2	8	4
Density (calculated) mg/m <sup>3</sup>	2.097	1.586	1.476	1.607	1.609
Absorption Coefficient mm <sup>-1</sup>	1.778	0.363	0.110	0.146	0.231
F(000)	800	272	324	864	888
Crystal size (mm <sup>3</sup> )	0.26 x 0.24 x 0.14	0.14 x 0.12 x 0.06	0.22 x 0.17 x 0.08	0.48 x 0.37 x 0.22	0.36 x 0.27 x 0.19
2θ range for data collection (°)	5.5 to 55.00	5.38 to 54.98	5.70 to 54.98	5.68 to 54.98	6.10 to 52.48
Reflections collected [R(int)]	67952 [0.0509]	4030 [0.0218]	23377 [0.0279]	33101 [0.0407]	5370 [0.0238]
Independent reflections	5907	2439	3208	2017	1743
Data completeness (%)	100	95.9	97.6	100	95.3
Data/ restraints/ parameters	5907/0/361	2439/0/162	3208/0/216	2017/0/136	1743/0/134
Goodness-of-fit on F <sup>2</sup>	1.089	1.116	1.022	1.074	1.033
Final R <sub>1</sub> indices [I>2σ(I)]	R <sub>1</sub> = 0.0272 wR <sub>2</sub> = 0.0610	R <sub>1</sub> = 0.0484 wR <sub>2</sub> = 0.1192	R <sub>1</sub> = 0.0343 wR <sub>2</sub> = 0.0868	R <sub>1</sub> = 0.0390 wR <sub>2</sub> = 0.1012	R <sub>1</sub> = 0.0330 wR <sub>2</sub> = 0.0883
Final R indices [all data]	R <sub>1</sub> = 0.0370 wR <sub>2</sub> = 0.0681	R <sub>1</sub> = 0.0611 wR <sub>2</sub> = 0.1275	R <sub>1</sub> = 0.0386 wR <sub>2</sub> = 0.0895	R <sub>1</sub> = 0.0448 wR <sub>2</sub> = 0.1052	R <sub>1</sub> = 0.0402 wR <sub>2</sub> = 0.0940
Largest diff. peak/hole (e.Å <sup>-3</sup> )	1.65/-0.49	0.42/-0.47	0.35/-0.22	0.33/-0.20	0.28/-0.30

\*Crystal data for complex **2.47** are not listed due to severe disorder problems.

Table – **A7** Crystal data and X-ray experimental data for complexes **2.49**, **3.22**, **3.23**, **3.24**, and **3.25**.

Complex Code	<b>2.49</b> [3RPU16]	<b>3.22</b> [3RPU47]	<b>3.23</b> [3RPU103]	<b>3.24</b> [3RPU55]	<b>3.25</b> [3RPU53]
Empirical formula	C <sub>12</sub> H <sub>9</sub> N <sub>2</sub> O <sub>5</sub> Cl	C <sub>15</sub> H <sub>12</sub> N <sub>3</sub> O <sub>7</sub> ClAg	C <sub>22</sub> H <sub>19</sub> N <sub>5</sub> O <sub>17</sub> Cl <sub>3</sub> Ag <sub>3</sub>	C <sub>7</sub> H <sub>4</sub> NO <sub>3</sub> F <sub>3</sub> Ag	C <sub>49</sub> H <sub>40</sub> N <sub>8</sub> O <sub>39</sub> F <sub>27</sub> S <sub>9</sub> Ag <sub>9</sub>
Formula weight	296.66	489.60	1055.38	314.98	3133.10
Temperature (K)	120.0	110.0	120.0	120.0	120.0
Crystal system	Triclinic	Monoclinic	Monoclinic	Monoclinic	Triclinic
Space group	<i>P</i> -1	<i>C</i> 2/ <i>c</i>	<i>P</i> 2 <sub>1</sub> / <i>n</i>	<i>P</i> 2/ <i>c</i>	<i>P</i> -1
Unit cell dimensions: a (Å)	5.8217(4)	22.5763(9)	9.54572(12)	10.102(2)	13.1634(5)
b (Å)	9.4836(4)	13.0278(5)	12.51108(13)	5.4090(11)	14.9367(6)
c (Å)	10.6047(6)	13.5406(5)	26.0066(3)	15.326(3)	23.0757(9)
α (°)	92.195(4)	90.00	90.00	90.00	98.804(2)
β (°)	101.203(5)	123.260(2)	90.4262(10)	96.17(3)	95.188(2)
γ (°)	97.901(4)	90.00	90.00	90.00	104.708(2)
Volume / Å <sup>3</sup>	567.60(6)	3330.2(2)	3105.81(6)	832.6(3)	4296.9(3)
Z	2	8	4	4	2
Density (calculated) mg/m <sup>3</sup>	1.736	1.953	2.257	2.513	2.422
Absorption Coefficient mm <sup>-1</sup>	0.361	1.418	2.219	2.457	2.375
F(000)	304	1944	2056	604	3016
Crystal size (mm <sup>3</sup> )	0.20 x 0.17 x 0.09	0.50 x 0.42 x 0.26	0.18 x 0.16 x 0.16	0.36 x 0.32 x 0.32	0.42 x 0.38 x 0.36
2θ range for data collection (°)	5.66 to 55.00	6.00 to 55.00	5.36 to 52.00	4.06 to 52.54	3.48 to 55.00
Reflections collected [R(int)]	21397 [0.0341]	37475 [0.0499]	89920 [0.0538]	4682 [0.0534]	97622 [0.0488]
Independent reflections	2611	3822	6105	1659	19730
Data completeness (%)	99.7	100	99.9	100	99.9
Data/ restraints/ parameters	2611/0/217	3822/0/274	6105/0/512	1659/0/136	19730/0/1327
Goodness-of-fit on F <sup>2</sup>	1.077	1.068	1.092	1.095	1.124
Final R <sub>1</sub> indices [I>2σ(I)]	R <sub>1</sub> = 0.0308 wR <sub>2</sub> = 0.0811	R <sub>1</sub> = 0.0240 wR <sub>2</sub> = 0.0560	R <sub>1</sub> = 0.0542 wR <sub>2</sub> = 0.1339	R <sub>1</sub> = 0.0399 wR <sub>2</sub> = 0.1163	R <sub>1</sub> = 0.0337 wR <sub>2</sub> = 0.0658
Final R indices [all data]	R <sub>1</sub> = 0.0368 wR <sub>2</sub> = 0.0856	R <sub>1</sub> = 0.0295 wR <sub>2</sub> = 0.0576	R <sub>1</sub> = 0.0579 wR <sub>2</sub> = 0.1362	R <sub>1</sub> = 0.0414 wR <sub>2</sub> = 0.1192	R <sub>1</sub> = 0.0388 wR <sub>2</sub> = 0.0679
Largest diff. peak/hole (e.Å <sup>-3</sup> )	0.39/-0.47	0.39/-0.59	1.94/-2.07	1.67/-0.91	1.64/-1.21

Table – A8 Crystal data and X-ray experimental data for complexes **3.26**, **3.27**, **3.28**, **3.29**, and **3.30**.

Complex Code	<b>3.26</b> [3RPU125]	<b>3.27</b> [3RPU148]	<b>3.28</b> [3RPU160]	<b>3.29</b> [3RPU91]	<b>3.30</b> [3RPU1]
Empirical formula	C <sub>15</sub> H <sub>12</sub> N <sub>3</sub> O <sub>3</sub> PF <sub>6</sub> Ag	C <sub>15</sub> H <sub>12</sub> N <sub>3</sub> O <sub>3</sub> BF <sub>4</sub> Ag	C <sub>10</sub> H <sub>8</sub> N <sub>3</sub> O <sub>5</sub> Ag	C <sub>32</sub> H <sub>24</sub> N <sub>4</sub> O <sub>12</sub> F <sub>12</sub> Ag <sub>4</sub>	C <sub>14</sub> H <sub>12</sub> N <sub>2</sub> O <sub>8</sub> S <sub>2</sub> F <sub>6</sub> Ag <sub>2</sub>
Formula weight	535.12	476.96	358.06	1316.03	730.12
Temperature (K)	120.0	120.0	120.0	120.0	110.0
Crystal system	Monoclinic	Monoclinic	Triclinic	Monoclinic	Monoclinic
Space group	<i>C2/c</i>	<i>C2/c</i>	<i>P-1</i>	<i>C2/c</i>	<i>P2<sub>1</sub>/n</i>
Unit cell dimensions: a (Å)	23.4319(6)	22.655(5)	6.97784(10)	26.272(5)	14.5925(6)
b (Å)	13.14761(16)	12.852(3)	8.66814(15)	8.9020(18)	9.7010(4)
c (Å)	13.5859(4)	13.556(3)	10.2043(2)	19.610(4)	15.0640(6)
α (°)	90.00	90.00	113.0722(17)	90.00	90.00
β (°)	123.536(4)	124.17(3)	97.9192(14)	118.48(3)	96.668(2)
γ (°)	90.00	90.00	102.6672(13)	90.00	90.00
Volume / Å <sup>3</sup>	3488.71(14)	3265.5(11)	536.533(16)	4031.1(18)	2118.06(15)
Z	8	8	1	4	4
Density (calculated) mg/m <sup>3</sup>	2.038	1.940	2.216	2.168	2.290
Absorption Coefficient mm <sup>-1</sup>	1.334	1.301	1.902	2.035	2.145
F(000)	2104	1880	352	2544	1416
Crystal size (mm <sup>3</sup> )	0.36 x 0.24 x 0.15	0.18 x 0.09 x 0.04	0.32 x 0.30 x 0.24	0.22 x 0.12 x 0.04	0.48 x 0.26 x 0.22
2θ range for data collection (°)	5.94 to 55.00	6.02 to 55.00	5.28 to 54.98	5.80 to 55.00	5.00 to 55.00
Reflections collected [R(int)]	55789 [0.0376]	40775 [0.0508]	52305 [0.0507]	60881 [0.0366]	48080 [0.0419]
Independent reflections	4004	3753	2451	4630	4866
Data completeness (%)	99.8	99.0	100	100	100
Data/ restraints/ parameters	4004/0/263	3753/0/246	2451/0/172	4630/0/299	4866/0/309
Goodness-of-fit on F <sup>2</sup>	1.080	1.046	1.072	1.059	1.041
Final R <sub>1</sub> indices [I>2σ(I)]	R <sub>1</sub> = 0.0262 wR <sub>2</sub> = 0.0576	R <sub>1</sub> = 0.0298 wR <sub>2</sub> = 0.0722	R <sub>1</sub> = 0.0180 wR <sub>2</sub> = 0.0460	R <sub>1</sub> = 0.0256 wR <sub>2</sub> = 0.0622	R <sub>1</sub> = 0.0186 wR <sub>2</sub> = 0.0481
Final R indices [all data]	R <sub>1</sub> = 0.0338 wR <sub>2</sub> = 0.0621	R <sub>1</sub> = 0.0371 wR <sub>2</sub> = 0.0776	R <sub>1</sub> = 0.0190 wR <sub>2</sub> = 0.0468	R <sub>1</sub> = 0.0320 wR <sub>2</sub> = 0.0666	R <sub>1</sub> = 0.0225 wR <sub>2</sub> = 0.0491
Largest diff. peak/hole (e.Å <sup>-3</sup> )	0.74/-0.79	1.11/-1.04	0.60/-0.76	0.87/-0.57	0.47/-0.38

Table – A9 Crystal data and X-ray experimental data for complexes 3.31, 3.32, 3.33, 3.34, and 3.35.

Complex Code	3.31 [3RPU99]	3.32 [3RPU94]	3.33 [3RPU78]	3.34 [3RPU7]	3.35 [3RPUX]
Empirical formula	C <sub>48</sub> H <sub>48</sub> N <sub>8</sub> O <sub>28</sub> Cl <sub>3</sub> Ag <sub>3</sub>	C <sub>16</sub> H <sub>18</sub> N <sub>4</sub> O <sub>12</sub> Cl <sub>2</sub> Ag <sub>2</sub>	C <sub>51</sub> H <sub>56</sub> N <sub>8</sub> O <sub>29</sub> S <sub>3</sub> F <sub>9</sub> Ag <sub>3</sub>	C <sub>24</sub> H <sub>28</sub> N <sub>4</sub> O <sub>10</sub> B <sub>2</sub> F <sub>8</sub> Ag <sub>2</sub>	C <sub>28</sub> H <sub>24</sub> N <sub>4</sub> O <sub>16</sub> F <sub>12</sub> Ag <sub>4</sub>
Formula weight	1614.90	744.98	1835.83	921.86	1331.99
Temperature (K)	120.0	120.0	120.0	120.0	110.0
Crystal system	Monoclinic	Monoclinic	Triclinic	Triclinic	Triclinic
Space group	<i>C2/c</i>	<i>P2<sub>1</sub>/n</i>	<i>P-1</i>	<i>P-1</i>	<i>P-1</i>
Unit cell dimensions: a (Å)	28.1985(3)	17.5545(4)	14.2197(3)	8.1324(2)	8.0428(12)
b (Å)	6.59792(5)	8.43633(12)	15.2870(5)	9.83519(19)	12.3476(17)
c (Å)	30.2752(3)	18.3296(4)	16.5707(5)	11.0489(3)	20.651(3)
α (°)	90.00	90.00	71.784(3)	74.7217(19)	80.860(7)
β (°)	103.4272(10)	117.565(3)	78.792(2)	84.024(2)	80.272(8)
γ (°)	90.00	90.00	74.218(2)	65.719(2)	73.609(8)
Volume / Å <sup>3</sup>	5478.77(9)	2406.38(8)	3268.93(16)	777.08(3)	1925.8(5)
Z	4	4	2	1	2
Density (calculated) mg/m <sup>3</sup>	1.958	2.056	1.865	1.970	2.297
Absorption Coefficient mm <sup>-1</sup>	1.311	1.918	1.105	1.369	2.139
F(000)	3232	1464	1840	456	1288
Crystal size (mm <sup>3</sup> )	0.27 x 0.07 x 0.07	0.26 x 0.24 x 0.22	0.36 x 0.22 x 0.14	0.48 x 0.44 x 0.36	0.30 x 0.20 x 0.08
2θ range for data collection (°)	5.54 to 55.00	5.44 to 55.00	5.34 to 55.00	5.28 to 55.00	3.8 to 55.00
Reflections collected [R(int)]	135733 [0.0367]	62416 [0.0347]	91220 [0.0574]	38863 [0.0371]	42353 [0.0339]
Independent reflections	6308	5517	14975	3576	8819
Data completeness (%)	100	99.9	99.7	99.7	99.6
Data/ restraints/ parameters	6308/0/412	5517/0/339	14975/0/1021	3576/0/237	8819/0/601
Goodness-of-fit on F <sup>2</sup>	1.043	1.049	1.057	1.056	1.065
Final R <sub>1</sub> indices [I>2σ(I)]	R <sub>1</sub> = 0.0409 wR <sub>2</sub> = 0.1020	R <sub>1</sub> = 0.0332 wR <sub>2</sub> = 0.0835	R <sub>1</sub> = 0.0386 wR <sub>2</sub> = 0.0917	R <sub>1</sub> = 0.0171 wR <sub>2</sub> = 0.0410	R <sub>1</sub> = 0.0454 wR <sub>2</sub> = 0.1073
Final R indices [all data]	R <sub>1</sub> = 0.0448 wR <sub>2</sub> = 0.1057	R <sub>1</sub> = 0.0381 wR <sub>2</sub> = 0.0875	R <sub>1</sub> = 0.0520 wR <sub>2</sub> = 0.1032	R <sub>1</sub> = 0.0182 wR <sub>2</sub> = 0.0416	R <sub>1</sub> = 0.0583 wR <sub>2</sub> = 0.1122
Largest diff. peak/hole (e.Å <sup>-3</sup> )	5.78/-0.85	2.77/-1.54	2.35/-1.01	0.64/-0.42	1.52/-1.08



Table – **A10** Crystal data and X-ray experimental data for complexes **3.36**, **3.37**, **3.38**, **3.39**, and **3.40**.

Complex Code	<b>3.36</b> [3RPU18]	<b>3.37</b> [3RPUD]	<b>3.38</b> [3RPU136]	<b>3.39</b> [3RPU147]	<b>3.40</b> [3RPU71]
Empirical formula	C <sub>34</sub> H <sub>27</sub> N <sub>4</sub> O <sub>12</sub> F <sub>12</sub> Ag <sub>4</sub>	C <sub>52</sub> H <sub>56</sub> N <sub>8</sub> O <sub>8</sub> P <sub>3</sub> F <sub>18</sub> Ag <sub>3</sub>	C <sub>43</sub> H <sub>48</sub> N <sub>8</sub> O <sub>6</sub> P <sub>3</sub> F <sub>18</sub> Ag <sub>3</sub>	C <sub>19</sub> H <sub>12</sub> N <sub>6</sub> O <sub>7</sub> F <sub>6</sub> Ag <sub>2</sub>	C <sub>5</sub> H <sub>4</sub> N <sub>3</sub> O <sub>4</sub> Ag
Formula weight	1343.07	1679.57	1531.42	766.09	277.98
Temperature (K)	120.0	114.0	120.0	120.0	120.0
Crystal system	Monoclinic	Monoclinic	Orthorhombic	Triclinic	Monoclinic
Space group	<i>Cc</i>	<i>P2<sub>1</sub>/m</i>	<i>P2<sub>2</sub>1<sub>2</sub>1</i>	<i>P-1</i>	<i>P2<sub>1</sub>/n</i>
Unit cell dimensions: a (Å)	11.129(2)	7.7069(3)	6.9800(14)	9.7740(3)	5.36001(12)
b (Å)	44.518(9)	28.4373(11)	27.754(6)	9.90307(15)	19.6602(4)
c (Å)	9.5060(19)	13.8911(6)	27.941(6)	12.2524(3)	7.03284(17)
α (°)	90.00	90.00	90.00	87.8589(17)	90.00
β (°)	116.97(3)	97.665(2)	90.00	75.255(2)	100.739(2)
γ (°)	90.00	90.00	90.00	78.5617(18)	90.00
Volume / Å <sup>3</sup>	4197.5(18)	3017.2(2)	5412.8(19)	1124.00(5)	728.14(3)
Z	4	2	4	2	4
Density (calculated) mg/m <sup>3</sup>	2.125	1.849	1.879	2.264	2.536
Absorption Coefficient mm <sup>-1</sup>	1.957	1.159	1.279	1.851	2.752
F(000)	2604	1672	3032	744	536
Crystal size (mm <sup>3</sup> )	0.32 x 0.16 x 0.08	0.45 x 0.40 x 0.28	0.30 x 0.16 x 0.11	0.15 x 0.11 x 0.04	0.48 x 0.34 x 0.18
2θ range for data collection (°)	5.14 to 55.00	5.22 to 55.00	5.26 to 55.00	5.38 to 55.00	6.24 to 55.00
Reflections collected [R(int)]	86763 [0.0504]	66903 [0.0625]	184779 [0.0528]	52933 [0.0404]	13272 [0.0373]
Independent reflections	4826	7055	6958	5152	1668
Data completeness (%)	100	99.9	100	99.9	99.8
Data/ restraints/ parameters	4826/0/595	7055/0/443	6958/0/773	5152 /0/361	1668/0/118
Goodness-of-fit on F <sup>2</sup>	1.133	1.029	1.168	1.068	1.145
Final R <sub>1</sub> indices [I>2σ(I)]	R <sub>1</sub> = 0.0162, wR <sub>2</sub> = 0.0398	R <sub>1</sub> = 0.0392 wR <sub>2</sub> = 0.0973	R <sub>1</sub> = 0.0473 wR <sub>2</sub> = 0.1069	R <sub>1</sub> = 0.0242 wR <sub>2</sub> = 0.0576	R <sub>1</sub> = 0.0427 wR <sub>2</sub> = 0.0991
Final R indices [all data]	R <sub>1</sub> = 0.0172, wR <sub>2</sub> = 0.0404	R <sub>1</sub> = 0.0540 wR <sub>2</sub> = 0.1033	R <sub>1</sub> = 0.0479 wR <sub>2</sub> = 0.1072	R <sub>1</sub> = 0.0303 wR <sub>2</sub> = 0.0615	R <sub>1</sub> = 0.0467 wR <sub>2</sub> = 0.1013
Largest diff. peak/hole (e.Å <sup>-3</sup> )	0.70/-0.48	1.22/-0.93	1.39/-1.54	1.04/-0.61	2.24/-0.95

Table – A11 Crystal data and X-ray experimental data for complexes **3.41**, **3.42**, **3.43**, **3.44**, and **3.45**.

Complex Code	<b>3.41</b> [3RPU51]	<b>3.42</b> [3RPU22]	<b>3.43</b> [3RPU79]	<b>3.44</b> [3RPU11]	<b>3.45</b> [3RPU134]
Empirical formula	C <sub>46</sub> H <sub>34</sub> N <sub>4</sub> O <sub>19</sub> F <sub>15</sub> Ag <sub>5</sub>	C <sub>6</sub> H <sub>8</sub> N <sub>2</sub> O <sub>6</sub> ClAg	C <sub>24</sub> H <sub>36</sub> N <sub>6</sub> O <sub>22</sub> Cl <sub>4</sub> Ag <sub>4</sub>	C <sub>16</sub> H <sub>18</sub> N <sub>3</sub> O <sub>7</sub> F <sub>6</sub> Ag <sub>2</sub>	C <sub>12</sub> H <sub>20</sub> N <sub>5</sub> O <sub>10</sub> Ag <sub>2</sub>
Formula weight	1769.11	347.46	1333.87	694.07	610.07
Temperature (K)	112.0	113.0	120.0	120.0	120.0
Crystal system	Triclinic	Monoclinic	Triclinic	Monoclinic	Triclinic
Space group	<i>P</i> -1	<i>P</i> 2 <sub>1</sub> / <i>c</i>	<i>P</i> -1	<i>C</i> 2/ <i>c</i>	<i>P</i> -1
Unit cell dimensions: a (Å)	12.4386(4)	11.4058(4)	11.91751(18)	21.0145(4)	8.87143(19)
b (Å)	13.3769(4)	12.6306(5)	12.2703(3)	8.29128(12)	10.7462(2)
c (Å)	17.8663(8)	7.3130(3)	16.6635(4)	26.0961(4)	11.0874(2)
α (°)	98.529(2)	90.00	70.352(2)	90.00	101.8118(16)
β (°)	93.232(2)	104.770(2)	87.9329(15)	99.7689(16)	97.0829(16)
γ (°)	115.780(2)	90.00	61.9362(19)	90.00	113.309(2)
Volume / Å <sup>3</sup>	2622.78(16)	1018.71(7)	2003.05(7)	4480.97(13)	925.32(3)
Z	2	4	2	8	2
Density (calculated) mg/m <sup>3</sup>	2.240	2.266	2.212	2.058	2.190
Absorption Coefficient mm <sup>-1</sup>	1.969	2.256	2.285	1.841	2.182
F(000)	1716	680	1308	2712	602
Crystal size (mm <sup>3</sup> )	0.48 x 0.46 x 0.38	0.58 x 0.52 x 0.28	0.24 x 0.20 x 0.06	0.24 x 0.20 x 0.02	0.26 x 0.24 x 0.09
2θ range for data collection (°)	2.32 to 53.20	6.46 to 55.00	5.26 to 55.00	5.30 to 55.00	5.68 to 55.00
Reflections collected [R(int)]	54394 [0.0454]	22446 [0.0301]	145871 [0.0473]	52494 [0.0402]	53222 [0.0495]
Independent reflections	10893	2338	9190	5143	4246
Data completeness (%)	99.0	99.9	99.9	99.9	99.8
Data/ restraints/ parameters	10893/0/822	2338/0/147	9190/0/553	5143/0/332	4246/0/276
Goodness-of-fit on F <sup>2</sup>	1.131	1.151	1.074	1.058	1.103
Final R <sub>1</sub> indices [I>2σ(I)]	R <sub>1</sub> = 0.0345 wR <sub>2</sub> = 0.0699	R <sub>1</sub> = 0.0268 wR <sub>2</sub> = 0.0662	R <sub>1</sub> = 0.0533 wR <sub>2</sub> = 0.1147	R <sub>1</sub> = 0.0261 wR <sub>2</sub> = 0.0610	R <sub>1</sub> = 0.0193 wR <sub>2</sub> = 0.0438
Final R indices [all data]	R <sub>1</sub> = 0.0385 wR <sub>2</sub> = 0.0720	R <sub>1</sub> = 0.0275 wR <sub>2</sub> = 0.0667	R <sub>1</sub> = 0.0625 wR <sub>2</sub> = 0.1207	R <sub>1</sub> = 0.0333 wR <sub>2</sub> = 0.0647	R <sub>1</sub> = 0.0227 wR <sub>2</sub> = 0.0455
Largest diff. peak/hole (e.Å <sup>-3</sup> )	0.87/-1.17	0.71/-0.53	8.09/-5.42	1.11/-0.52	0.41/-0.41

Table – A12 Crystal data and X-ray experimental data for complexes 4.7, 4.8, 4.9, 4.10, and 4.11.

Complex Code	4.7 [3RPU168]	4.8 [3RPU80]	4.9 [3RPU6-1]	4.10 [3RPU169]	4.11 [3RPU56]
Empirical formula	C <sub>60</sub> H <sub>47</sub> N <sub>12</sub> O <sub>30</sub> Cl <sub>4</sub> Ag <sub>4</sub>	C <sub>38</sub> H <sub>24</sub> N <sub>6</sub> O <sub>15</sub> F <sub>12</sub> Ag <sub>4</sub>	C <sub>17</sub> H <sub>13</sub> N <sub>3</sub> O <sub>10</sub> S <sub>2</sub> F <sub>6</sub> Ag <sub>2</sub>	C <sub>60</sub> H <sub>52</sub> N <sub>12</sub> O <sub>19</sub> P <sub>3</sub> F <sub>18</sub> Ag <sub>3</sub>	C <sub>30</sub> H <sub>26</sub> N <sub>10</sub> O <sub>20</sub> Ag <sub>4</sub>
Formula weight	1989.38	1464.11	813.18	2003.66	1278.09
Temperature (K)	120.0	120.0	120.0	120.0	120.0
Crystal system	Monoclinic	Triclinic	Triclinic	Monoclinic	Monoclinic
Space group	<i>P</i> 2 <sub>1</sub> / <i>n</i>	<i>P</i> -1	<i>P</i> -1	<i>C</i> 2/ <i>c</i>	<i>P</i> 2 <sub>1</sub> / <i>n</i>
Unit cell dimensions: a (Å)	11.6780(3)	11.39449(17)	8.7940(18)	15.3800(3)	7.01477(12)
b (Å)	8.6192(2)	12.8804(2)	11.366(2)	24.9844(6)	23.7507(4)
c (Å)	17.6473(5)	15.8288(3)	12.540(3)	19.4766(5)	22.3376(4)
α (°)	90.00	92.0504(15)	109.16(3)	90.00	90.00
β (°)	109.276(3)	101.2164(15)	91.52(3)	104.160(2)	92.5260(15)
γ (°)	90.00	103.4418(14)	91.41(3)	90.00	90.00
Volume / Å <sup>3</sup>	1676.70(7)	2208.32(7)	1182.8(4)	7256.7(3)	3717.96(11)
Z	4	2	2	4	4
Density (calculated) mg/m <sup>3</sup>	1.970	2.202	2.283	1.834	2.283
Absorption Coefficient mm <sup>-1</sup>	1.412	1.876	1.941	0.993	2.178
F(000)	987	1420	792	3984	2496
Crystal size (mm <sup>3</sup> )	0.28 x 0.17 x 0.05	0.28 x 0.16 x 0.08	0.36 x 0.32 x 0.24	0.21 x 0.18 x 0.05	0.27 x 0.24 x 0.20
2θ range for data collection (°)	5.32 to 54.98	5.32 to 55.00	5.68 to 55.00	5.4 to 55.00	5.46 to 55.00
Reflections collected [R(int)]	38288 [0.0357]	121325 [0.0509]	189336 [0.0515]	51675 [0.0375]	31279 [0.0222]
Independent reflections	3850	10135	5420	8330	8515
Data completeness (%)	99.9	99.8	99.8	99.9	99.9
Data/ restraints/ parameters	3850/0/257	10135/0/684	5420/0/369	8330/0/539	8515/0/581
Goodness-of-fit on F <sup>2</sup>	1.245	1.148	1.078	1.216	1.095
Final R <sub>1</sub> indices [I>2σ(I)]	R <sub>1</sub> = 0.0335 wR <sub>2</sub> = 0.0778	R <sub>1</sub> = 0.0241 wR <sub>2</sub> = 0.509	R <sub>1</sub> = 0.0201 wR <sub>2</sub> = 0.0484	R <sub>1</sub> = 0.0303 wR <sub>2</sub> = 0.0771	R <sub>1</sub> = 0.0242 wR <sub>2</sub> = 0.0537
Final R indices [all data]	R <sub>1</sub> = 0.0347 wR <sub>2</sub> = 0.0783	R <sub>1</sub> = 0.0329 wR <sub>2</sub> = 0.0572	R <sub>1</sub> = 0.0251 wR <sub>2</sub> = 0.0480	R <sub>1</sub> = 0.0355 wR <sub>2</sub> = 0.0802	R <sub>1</sub> = 0.0262 wR <sub>2</sub> = 0.0547
Largest diff. peak/hole (e.Å <sup>-3</sup> )	1.17/-0.66	0.75/-0.77	0.98/-0.58	2.99/-1.12	1.10/-1.28

Table – **A13** Crystal data and X-ray experimental data for complexes **4.12** and **4.13**, and for compounds **2.10**, **3.3**, and **3.8**.

Complex Code	<b>4.12</b> [3RPU87]	<b>4.13</b> [3RPU173]	<b>2.10</b> [3RPU39]	<b>3.3</b> [3RPUR]	<b>3.8</b> [3RPU129]
Empirical formula	C <sub>30</sub> H <sub>28</sub> N <sub>9</sub> O <sub>18</sub> Ag <sub>3</sub>	C <sub>30</sub> H <sub>32</sub> N <sub>14</sub> O <sub>35</sub> Ag <sub>8</sub>	C <sub>31</sub> H <sub>25</sub> NO	C <sub>22</sub> H <sub>16</sub> N <sub>2</sub> O <sub>2</sub>	C <sub>11</sub> H <sub>10</sub> N <sub>2</sub> O <sub>4</sub>
Formula weight	1126.21	2011.66	427.52	340.37	234.21
Temperature (K)	120.0	120.0	113.0	113.0	120.0
Crystal system	Monoclinic	Triclinic	Orthorhombic	Monoclinic	Triclinic
Space group	<i>P2<sub>1</sub>/c</i>	<i>P-1</i>	<i>Pbca</i>	<i>C2/c</i>	<i>P-1</i>
Unit cell dimensions: a (Å)	7.0279(5)	12.4304(2)	9.1942(4)	26.1127(12)	6.7060(13)
b (Å)	20.9594(13)	13.6176(5)	19.9611(9)	5.3620(2)	7.3820(15)
c (Å)	24.8833(14)	16.0283(5)	25.2120(11)	12.2356(6)	12.102(2)
α (°)	90.00	75.127(3)	90.00	90.00	101.01(3)
β (°)	106.406(2)	72.931(2)	90.00	102.632(3)	91.33(3)
γ (°)	90.00	89.469(2)	90.00	90.00	116.90(3)
Volume / Å <sup>3</sup>	3516.1(4)	2500.32(12)	4627.1(4)	1671.72(13)	520.30(18)
Z	4	2	8	4	2
Density (calculated) mg/m <sup>3</sup>	2.127	3.188	1.227	1.352	1.495
Absorption Coefficient mm <sup>-1</sup>	1.752	2.672	0.073	0.088	0.116
F(000)	2214.6	1932	1808	712	244
Crystal size (mm <sup>3</sup> )	0.26 x 0.04 x 0.02	0.13 x 0.07 x 0.04	0.50 x 0.28 x 0.24	0.50 x 0.38 x 0.13	0.28 x 0.24 x 0.14
2θ range for data collection (°)	5.48 to 55.00	5.36 to 55.00	6.34 to 53.78	6.40 to 54.98	3.46 to 52.62
Reflections collected [R(int)]	15030 [0.0368]	62545 [0.0331]	93390 [0.1157]	18204 [0.0412]	4850 [0.0338]
Independent reflections	7167	11468	4958	1907	2031
Data completeness (%)	88.8	99.9	99.3	100	96.3
Data/ restraints/ parameters	7167/0/547	11468/0/791	4991/0/373	1907/0/122	2031/0/157
Goodness-of-fit on F <sup>2</sup>	1.075	1.027	0.785	1.029	1.038
Final R <sub>1</sub> indices [I>2sigma(I)]	R <sub>1</sub> = 0.0496 wR <sub>2</sub> = 0.1111	R <sub>1</sub> = 0.0310 wR <sub>2</sub> = 0.0794	R <sub>1</sub> = 0.0365 wR <sub>2</sub> = 0.0636	R <sub>1</sub> = 0.0384 wR <sub>2</sub> = 0.1176	R <sub>1</sub> = 0.0441 wR <sub>2</sub> = 0.1143
Final R indices [all data]	R <sub>1</sub> = 0.0733 wR <sub>2</sub> = 0.1329	R <sub>1</sub> = 0.0357 wR <sub>2</sub> = 0.0827	R <sub>1</sub> = 0.0816 wR <sub>2</sub> = 0.0703	R <sub>1</sub> = 0.0472 wR <sub>2</sub> = 0.1268	R <sub>1</sub> = 0.0499 wR <sub>2</sub> = 0.1209
Largest diff. peak/hole (e.Å <sup>-3</sup> )	1.65/-2.45	6.07/-2.75	0.17/-0.24	0.31/-0.20	0.22/-0.33

Table – **A14** Crystal data and X-ray experimental data for compounds **3.14**, **4.3c**, and **4.3**.

Complex Code	<b>3.14</b> [3RPUE]	<b>4.3c</b> [RPU54]	<b>4.3</b> [3RPU140]
Empirical formula	C <sub>25</sub> H <sub>24</sub> N <sub>4</sub> O <sub>6</sub>	C <sub>18</sub> H <sub>15</sub> N <sub>5</sub> O	C <sub>18</sub> H <sub>19</sub> N <sub>6</sub> O <sub>5</sub> Cl <sub>3</sub>
Formula weight	476.48	317.35	505.74
Temperature (K)	113.0	113.0	120.0
Crystal system	Orthorhombic	Triclinic	Triclinic
Space group	<i>P</i> 2 <sub>1</sub> 2 <sub>1</sub> 2 <sub>1</sub>	<i>P</i> -1	<i>P</i> -1
Unit cell dimensions: a (Å)	8.6858(2)	8.7868(7)	6.60879(17)
b (Å)	8.6914(2)	9.3185(7)	13.5244(5)
c (Å)	29.2607(8)	10.5344(9)	13.5839(5)
α (°)	90.00	72.703(5)	60.238(4)
β (°)	90.00	71.814(5)	87.571(3)
γ (°)	90.00	78.617(5)	83.793(3)
Volume / Å <sup>3</sup>	2208.94(9)	777.19(11)	1047.71(6)
Z	4	2	2
Density (calculated) mg/m <sup>3</sup>	1.433	1.356	1.603
Absorption Coefficient mm <sup>-1</sup>	0.104	0.089	0.484
F(000)	1000	332	520
Crystal size (mm <sup>3</sup> )	0.50 x 0.23 x 0.09	0.36 x 0.32 x 0.18	0.19 x 0.09 x 0.04
2θ range for data collection (°)	4.90 to 54.96	4.60 to 55.00	6.20 to 55.00
Reflections collected [R(int)]	50174 [0.0443]	17578 [0.0792]	21496 [0.0491]
Independent reflections	2904	3571	4827
Data completeness (%)	100	99.9	99.9
Data/ restraints/ parameters	2904/0/322	3571/0/229	4827/0/312
Goodness-of-fit on F <sup>2</sup>	1.051	0.790	1.068
Final R <sub>1</sub> indices [I>2sigma(I)]	R <sub>1</sub> = 0.0302 wR <sub>2</sub> = 0.0783	R <sub>1</sub> = 0.0509 wR <sub>2</sub> = 0.1090	R <sub>1</sub> = 0.0604 wR <sub>2</sub> = 0.1654
Final R indices [all data]	R <sub>1</sub> = 0.0357 wR <sub>2</sub> = 0.0806	R <sub>1</sub> = 0.1032 wR <sub>2</sub> = 0.1329	R <sub>1</sub> = 0.0766 wR <sub>2</sub> = 0.1813
Largest diff. peak/hole (e.Å <sup>-3</sup> )	0.18/-0.18	0.27/-0.26	0.86/-0.97

# References

- [1] E. C. Constable, *Chemical industry* **1994**, 56.
- [2] a) L. F. Lindoy, I. M. Atkinson, *Self Assembly in Supramolecular Systems*, Cambridge University Press, UK, **2000**; b) P. J. Steel, *Accounts of Chemical Research* **2005**, 38, 243-250; c) T. R. Cook, Y.-R. Zheng, P. J. Stang, *Chemical Reviews* **2012**, 113, 734-777; d) M. W. Hosseini, *Accounts of Chemical Research* **2005**, 38, 313-323; e) J. W. Steed, J. L. Atwood, *Supramolecular Chemistry*, Wiley, **2009**.
- [3] C. M. Fitchett, P. J. Steel, *Polyhedron* **2007**, 26, 400-405.
- [4] a) C. O. Dietrich-Buchecker, J.-P. Sauvage, *Angewandte Chemie International Edition in English* **1989**, 28, 189-192; b) C. O. Dietrich-Buchecker, J. P. Sauvage, J. P. Kintzinger, *Tetrahedron Letters* **1983**, 24, 5095-5098.
- [5] C. H. M. Amijs, G. P. M. van Klink, G. van Koten, *Dalton Transactions* **2006**, 308-327.
- [6] a) M. Fujita, J. Yazaki, K. Ogura, *Journal of the American Chemical Society* **1990**, 112, 5645-5647; b) M. Fujita, S. Nagao, M. Iida, K. Ogata, K. Ogura, *Journal of the American Chemical Society* **1993**, 115, 1574-1576.
- [7] a) S. Banfi, L. Carlucci, E. Caruso, G. Ciani, D. M. Proserpio, *Journal of the Chemical Society, Dalton Transactions* **2002**, 2714-2721; b) A. J. Blake, N. R. Champness, P. Hubberstey, W.-S. Li, M. A. Withersby, M. Schröder, *Coordination Chemistry Reviews* **1999**, 183, 117-138.
- [8] S. H. Rahaman, H. Chowdhury, D. Bose, G. Mostafa, H.-K. Fun, B. K. Ghosh, *Inorganic Chemistry Communications* **2005**, 8, 1041-1044.
- [9] a) M. Loï, M. W. Hosseini, A. Jouaiti, A. De Cian, J. Fischer, *European Journal of Inorganic Chemistry* **1999**, 1999, 1981-1985; b) R. L. Paul, Z. R. Bell, J. C. Jeffery, J. A. McCleverty, M. D. Ward, *Proceedings of the National Academy of Sciences* **2002**, 99, 4883-4888; c) J. Lu, D. R. Turner, L. P. Harding, S. R. Batten, *Inorganic Chemistry* **2009**, 48, 7525-7527.
- [10] M.-L. Ma, X.-Y. Li, X.-L. Zhao, F. Guo, B. Jiang, K. Wen, *CrystEngComm* **2011**, 13, 1752-1754.
- [11] a) C. Richardson, P. J. Steel, *Dalton Transactions* **2003**, 992-1000; b) C. Richardson, C. M. Fitchett, F. R. Keene, P. J. Steel, *Dalton Transactions* **2008**, 2534-2537.
- [12] D. S. Cati, J. Ribas, J. Ribas-Ariño, H. Stoeckli-Evans, *Inorganic Chemistry* **2004**, 43, 1021-1030.
- [13] P. Jacopozzi, E. Dalcanale, *Angewandte Chemie International Edition in English* **1997**, 36, 613-615.
- [14] X.-L. Zhao, L.-P. Zhang, T. C. W. Mak, *Dalton Transactions* **2006**, 3141-3146.
- [15] R. Carballo, B. Covelo, E. García-Martínez, A. B. Lago, E. M. Vázquez-López, *Polyhedron* **2009**, 28, 923-932.
- [16] R. P. Feazell, C. E. Carson, K. K. Klausmeyer, *Inorganic Chemistry* **2005**, 45, 935-944.
- [17] R. P. Feazell, C. E. Carson, K. K. Klausmeyer, *Inorganic Chemistry* **2006**, 45, 2635-2643.
- [18] R. P. Feazell, C. E. Carson, K. K. Klausmeyer, *Inorganic Chemistry* **2006**, 45, 2627-2634.
- [19] a) D. L. Reger, R. F. Semeniuc, V. Rassolov, M. D. Smith, *Inorganic Chemistry* **2003**, 43, 537-554; b) D. L. Reger, R. P. Watson, J. R. Gardinier, M. D. Smith, *Inorganic Chemistry* **2004**, 43, 6609-6619.
- [20] A. N. Khlobystov, A. J. Blake, N. R. Champness, D. A. Lemenovskii, A. G. Majouga, N. V. Zyk, M. Schröder, *Coordination Chemistry Reviews* **2001**, 222, 155-192.
- [21] G. R. Desiraju, *Angewandte Chemie International Edition in English* **1995**, 34, 2311-2327.
- [22] N. Yanagihara, T. Gotoh, T. Ogura, *Polyhedron* **1996**, 15, 4349-4354.
- [23] M.-O. M. Piepenbrock, N. Clarke, J. W. Steed, *Langmuir* **2009**, 25, 8451-8456.

- [24] P. Pyykkö, *Chemical Reviews* **1997**, *97*, 597-636.
- [25] F. Robinson, M. J. Zaworotko, *Journal of the Chemical Society, Chemical Communications* **1995**, 2413-2414.
- [26] O. M. Yaghi, H. Li, *Journal of the American Chemical Society* **1996**, *118*, 295-296.
- [27] S.-i. Noro, H. Miyasaka, S. Kitagawa, T. Wada, T. Okubo, M. Yamashita, T. Mitani, *Inorganic Chemistry* **2004**, *44*, 133-146.
- [28] T. K. Maji, S. Konar, G. Mostafa, E. Zangrando, T.-H. Lu, N. Ray Chaudhuri, *Dalton Transactions* **2003**, 171-175.
- [29] a) B.-L. Fei, W.-Y. Sun, K.-B. Yu, W.-X. Tang, *Journal of the Chemical Society, Dalton Transactions* **2000**, 805-811; b) H.-P. Wu, C. Janiak, G. Rheinwald, H. Lang, *Journal of the Chemical Society, Dalton Transactions* **1999**, 183-190.
- [30] a) A. J. Blake, N. R. Champness, P. A. Cooke, J. E. B. Nicolson, C. Wilson, *Journal of the Chemical Society, Dalton Transactions* **2000**, 3811-3819; b) A. J. Blake, N. R. Champness, P. A. Cooke, J. E. B. Nicolson, *Chemical Communications* **2000**, 665-666; c) M. A. Withersby, A. J. Blake, N. R. Champness, P. Hubberstey, W.-S. Li, M. Schröder, *Angewandte Chemie International Edition in English* **1997**, *36*, 2327-2329.
- [31] a) I. Bassanetti, F. Mezzadri, A. Comotti, P. Sozzani, M. Gennari, G. Calestani, L. Marchiò, *Journal of the American Chemical Society* **2012**, *134*, 9142-9145; b) N. Gimeno, R. Vilar, *Coordination Chemistry Reviews* **2006**, *250*, 3161-3189.
- [32] J. Meisenheimer, *Berichte der deutschen chemischen Gesellschaft* **1926**, *59*, 1848-1853.
- [33] a) *Chemical & Engineering News Archive* **1954**, *32*, 3300-3302; b) F. E. Cislak, *Industrial & Engineering Chemistry* **1955**, *47*, 800-802.
- [34] A. R. Katritzky, J. M. Lagowski, "Chemistry of Heterocyclic N-Oxides," Academic, New York, **1971**.
- [35] E. N. Shaw, "Pyridine and Its Derivatives," Vol. 2, E. Klingsberg, Ed., Interscience, New York, **1961**, 97.
- [36] R. A. Abramovitch, J. G. Saha, "Advances in Heterocyclic Chemistry," Vol. 6, A. R. Katritzky, Ed., Academic, New York. **1966**. 229.
- [37] E. Ochiai, "Aromatic Amine Oxides," Elsevier, Amsterdam, **1967**.
- [38] E. P. Linton, *Journal of the American Chemical Society* **1940**, *62*, 1945-1948.
- [39] E. Ochiai, *Journal of Organic Chemistry* **1953**, *18*, 534-551.
- [40] C. M. Bax, A. R. Katritzky, L. E. Sutton, *Journal of the Chemical Society* **1958**, 1254-1257.
- [41] a) B. Klein, J. Berkowitz, *Journal of the American Chemical Society* **1959**, *81*, 5160-5166; b) G. B. Payne, P. H. Deming, P. H. Williams, *Journal of Organic Chemistry* **1961**, *26*, 659-663; c) R. A. Burrell, J. M. Cox, E. G. Savins, *Journal of the Chemical Society, Perkin Transactions* **1973**, 2707-2713; d) R. S. Varma, K. P. Naicker, *Organic Letters* **1999**, *1*, 189-192; e) R. Balicki, J. Golinski, *Synthetic Communications* **2000**, *30*, 1529-1534; f) S. M. Roberts, H. Suschitzky, *Journal of the Chemical Society C: Organic* **1968**, 1537-1541; g) S. Caron, N. M. Do, J. E. Sieser, *Tetrahedron Letters* **2000**, *41*, 2299-2302; h) L. Kaczmarek, R. Balicki, P. Nantka-Namirski, *Chemische Berichte* **1992**, *125*, 1965-1966; i) M. Carmeli, S. Rozen, *Journal of Organic Chemistry* **2005**, *70*, 2131-2134; j) B. Plesničar, G. A. Russell, *Angewandte Chemie International Edition in English* **1970**, *9*, 797-798; k) A. McKillop, D. Kemp, *Tetrahedron* **1989**, *45*, 3299-3306; l) X. Zhu, K. D. Kreutter, H. Hu, M. R. Player, M. D. Gaul, *Tetrahedron Letters* **2008**, *49*, 832-834; m) S. L. Jain, J.



- K. Joseph, B. Sain, *Synlett* **2006**, 2006, 2661-2663; n) G. Soldaini, F. Cardona, A. Goti, *Organic Letters* **2007**, 9, 473-476; o) R. W. Murray, K. Iyanar, J. Chen, J. T. Wearing, *Tetrahedron Letters* **1996**, 37, 805-808; p) C. Copéret, H. Adolfsson, T.-A. V. Khuong, A. K. Yudin, K. B. Sharpless, *Journal of Organic Chemistry* **1998**, 63, 1740-1741; q) K. Yamaguchi, T. Mizugaki, K. Ebitani, K. Kaneda, *New Journal of Chemistry* **1999**, 23, 799-801.
- [42] a) T. J. Kress, *Journal of Organic Chemistry* **1985**, 50, 3073-3076; b) A. R. Gallopo, J. O. Edwards, *Journal of Organic Chemistry* **1981**, 46, 1684-1688; c) A. E. C. Kettani, J. Bernadou, B. Meunier, *Journal of Organic Chemistry* **1989**, 54, 3213-3215; d) T.-C. Zheng, D. E. Richardson, *Tetrahedron Letters* **1995**, 36, 837-840; e) R. W. Murray, R. Jeyaraman, *Journal of Organic Chemistry* **1985**, 50, 2847-2853; f) V. A. Petrov, G. Resnati, *Chemical Reviews* **1996**, 96, 1809-1824.
- [43] V. P. Andreev, *Chemistry of Heterocyclic Compounds* **2010**, 46, 184-195.
- [44] V. P. Andreev, Y. P. Nizhnik, *Russian Journal of Coordination Chemistry* **2007**, 33, 692-697.
- [45] a) D.-L. Long, A. J. Blake, N. R. Champness, C. Wilson, M. Schröder, *Angewandte Chemie International Edition in English* **2001**, 40, 2443-2447; b) D.-L. Long, R. J. Hill, A. J. Blake, N. R. Champness, P. Hubberstey, D. M. Proserpio, C. Wilson, M. Schröder, *Angewandte Chemie International Edition in English* **2004**, 43, 1851-1854.
- [46] a) J. S. Wood, R. O. Day, C. P. Keijzers, E. De Boer, A. E. Yildirim, A. A. K. Klaassen, *Inorganic Chemistry* **1981**, 20, 1982-1987; b) A. Paduan-Filho, E. Sinn, R. D. Chirico, R. L. Carlin, *Inorganic Chemistry* **1981**, 20, 2688-2691; c) J. S. Wood, C. P. Keijzers, E. De Boer, A. Buttafava, *Inorganic Chemistry* **1980**, 19, 2213-2225.
- [47] A. R. Al-Karaghoul, J. S. Wood, *Inorganic Chemistry* **1979**, 18, 1177-1184.
- [48] a) J. Casellato, P. A. Vigato, S. Tamburini, R. Graziani, M. Vidali, *Inorganica Chimica Acta* **1983**, 72, 141-147; b) U. Casellato, S. Sitran, S. Tamburini, P. A. Vigato, R. Graziani, *Inorganica Chimica Acta* **1984**, 95, 37-42.
- [49] a) A. E. V. Gorden, J. Xu, G. Szigethy, A. Oliver, D. K. Shuh, K. N. Raymond, *Journal of the American Chemical Society* **2007**, 129, 6674-6675; b) U. Casellato, P. A. Vigato, S. Tamburini, M. Vidali, R. Graziani, *Inorganica Chimica Acta* **1983**, 69, 77-82.
- [50] K. Abu-Dari, K. N. Raymond, *Inorganic Chemistry* **1982**, 21, 1676-1679.
- [51] D. Z. Niu, Z. S. Lu, B. W. Sun, B. L. Song, *Chinese Journal of Structural Chemistry* **2001**, 20, 180-182.
- [52] a) H. Knuuttila, P. Knuuttila, *Acta Chemica Scandinavica Series* **1983**, 37A, 227-233; b) H. Knuuttila, *Acta Chemica Scandinavica Series* **1983**, 37A, 697-702; c) H. Knuuttila, *Acta Chemica Scandinavica Series* **1983**, 37A, 765-769; d) P. Knuuttila, H. Knuuttila, *Acta Chemica Scandinavica Series* **1985**, 39A, 307-316.
- [53] Y.-H. Zhao, H.-B. Xu, Y.-M. Fu, K.-Z. Shao, S.-Y. Yang, Z.-M. Su, X.-R. Hao, D.-X. Zhu, E.-B. Wang, *Crystal Growth & Design* **2008**, 8, 3566-3576.
- [54] J.-Q. Liu, W.-P. Wu, Y.-Y. Wang, W.-H. Huang, W.-H. Zhang, Q.-Z. Shi, J. S. Miller, *Inorganica Chimica Acta* **2009**, 362, 1295-1302.
- [55] H. Kanno, M. Yamada, K. Nakata, M. Nishimura, *Inorganica Chimica Acta* **2001**, 318, 181-185.
- [56] a) H. Kanno, T. Yano, K. Sato, S. Utsuno, J. Fujita, *Bulletin of the Chemical Society of Japan* **1997**, 70, 1085-1091; b) H. Kanno, J. Yamamoto, S. Utsuno, J. Fujita, *Bulletin of the Chemical Society of Japan* **1996**, 69, 665-671; c) H. Kanno, M. Tomita, S. Utsuno, J. Fujita, *Bulletin of the Chemical*

- Society of Japan* **1992**, *65*, 1233-1239; d) H. Kanno, T. Shimotori, S. Utsuno, J. Fujita, *Chemistry Letters* **1983**, *12*, 939-940.
- [57] P. Baran, M. Koman, D. Valigura, J. Mrozinski, *Journal of the Chemical Society, Dalton Transactions* **1991**, 1385-1390.
- [58] a) S. J. Loeb, *Chemical Communications* **2005**, 1511-1518; b) H. W. Roesky, M. Andruh, *Coordination Chemistry Reviews* **2003**, *236*, 91-119.
- [59] J. Jia, A. J. Blake, N. R. Champness, P. Hubberstey, C. Wilson, M. Schröder, *Inorganic Chemistry* **2008**, *47*, 8652-8664.
- [60] D.-L. Long, A. J. Blake, N. R. Champness, C. Wilson, M. Schröder, *Journal of the American Chemical Society* **2001**, *123*, 3401-3402.
- [61] R. J. Hill, D.-L. Long, M. S. Turvey, A. J. Blake, N. R. Champness, P. Hubberstey, C. Wilson, M. Schröder, *Chemical Communications* **2004**, 1792-1793.
- [62] D.-L. Long, A. J. Blake, N. R. Champness, C. Wilson, M. Schröder, *Chemistry – A European Journal* **2002**, *8*, 2026-2033.
- [63] D. González Mantero, A. Neels, H. Stoeckli-Evans, *Inorganic Chemistry* **2006**, *45*, 3287-3294.
- [64] a) W.-J. Lu, L.-P. Zhang, H.-B. Song, Q.-M. Wang, T. C. W. Mak, *New Journal of Chemistry* **2002**, *26*, 775-781; b) L.-P. Zhang, M. Du, W.-J. Lu, T. C. W. Mak, *Polyhedron* **2004**, *23*, 857-863.
- [65] A. J. Amoroso, M. W. Burrows, T. Gelbrich, R. Haigh, M. B. Hursthouse, *Journal of the Chemical Society, Dalton Transactions* **2002**, 2415-2416.
- [66] A. J. Amoroso, M. W. Burrows, A. A. Dickinson, C. Jones, D. J. Willock, W.-T. Wong, *Journal of the Chemical Society, Dalton Transactions* **2001**, 225-227.
- [67] G. Zheng, W. Fan, S. Song, H. Guo, H. Zhang, *Journal of Solid State Chemistry* **2010**, *183*, 1457-1463.
- [68] A. J. Amoroso, M. W. Burrows, R. Haigh, M. Hatcher, M. Jones, U. Kynast, K. M. A. Malik, D. Sendor, *Dalton Transactions* **2007**, 1630-1638.
- [69] L. C. Nathan, J. H. Nelson, G. L. Rich, R. O. Ragsdale, *Inorganic Chemistry* **1969**, *8*, 1494-1497.
- [70] S. K. Madan, W. E. Bull, *Journal of Inorganic and Nuclear Chemistry* **1964**, *26*, 2211-2217.
- [71] G. Schmauss, H. Specker, *Naturwissenschaften* **1967**, *54*, 442-442.
- [72] P. J. Huffman, J. E. House Jr, *Journal of Inorganic and Nuclear Chemistry* **1974**, *36*, 2618-2620.
- [73] T. S. Lobana, S. Paul, A. Castineiras, *Journal of the Chemical Society, Dalton Transactions* **1999**, 1819-1824.
- [74] M. Bagieu-Beucher, Y. Le Fur, J.-P. Levy, J.-P. Pecaut, *Acta Crystallographica Section C* **1994**, *50*, 1079-1084.
- [75] M. Du, C.-P. Li, J.-H. Guo, *CrystEngComm* **2009**, *11*, 1536-1540.
- [76] J. N. Gardner, A. R. Katritzky, *Journal of the Chemical Society* **1957**, 4375-4385.
- [77] a) D. W. Herlocker, R. S. Drago, V. I. Meek, *Inorganic Chemistry* **1966**, *5*, 2009-2015; b) L. Chmurzyński, *Analytica Chimica Acta* **1996**, *329*, 267-274.
- [78] D. A. Klumpp, Y. Zhang, P. J. Kindelin, S. Lau, *Tetrahedron* **2006**, *62*, 5915-5921.
- [79] a) G. Zohuri, S. Seyedi, R. Sandaroos, S. Damavandi, A. Mohammadi, *Catalysis Letters* **2010**, *140*, 160-166; b) C. Yoakim, P. R. Bonneau, R. Déziel, L. Doyon, J. Duan, I. Guse, S. Landry, E. Malenfant, J. Naud, W. W. Ogilvie, J. A. O'Meara, R. Plante, B. Simoneau, B. Thavonekham, M. Bös, M. G. Cordingley, *Bioorganic & Medicinal Chemistry Letters* **2004**, *14*, 739-742.

- [80] Z. Gross, S. Ini, *Inorganic Chemistry* **1999**, 38, 1446-1449.
- [81] T. Higuchi, H. Ohtake, M. Hirobe, *Tetrahedron Letters* **1989**, 30, 6545-6548.
- [82] a) A. R. Hands, A. R. Katritzky, *Journal of the Chemical Society* **1958**, 1754-1762; b) A. R. Katritzky, P. Simmons, *Journal of the Chemical Society* **1960**, 1511-1516.
- [83] a) H. Ban-Oganowska, *Chemical papers* **1999**, 53, 69-74; b) J. Xiang, Y. Luo, C.-H. Wang, *Journal of Applied and General Chemistry*. **2013**, 639, 563-568.
- [84] E. Barchiesi, S. Bradamante, C. Carfagna, R. Ferraccioli, G. A. Pagani, *Journal of the Chemical Society, Perkin Transactions 2* **1987**, 1009-1013.
- [85] H. P. Kokatla, P. F. Thomson, S. Bae, V. R. Doddi, M. K. Lakshman, *Journal of Organic Chemistry* **2011**, 76, 7842-7848.
- [86] V. J. Traynelis, K. Yamauchi, J. P. Kimball, *Journal of the American Chemical Society* **1974**, 96, 7289-7294.
- [87] T. L. Lemke, T. W. Shek, L. A. Cates, L. K. Smith, L. A. Cosby, A. C. Sartorelli, *Journal of Medicinal Chemistry* **1977**, 20, 1351-1354.
- [88] a) J. Wu, X. Cui, L. Chen, G. Jiang, Y. Wu, *Journal of the American Chemical Society* **2009**, 131, 13888-13889; b) R. Loska, M. Małkosza, *Chemistry – A European Journal* **2008**, 14, 2577-2589.
- [89] H.-R. Bjørsvik, C. Gambarotti, V. R. Jensen, R. R. González, *Journal of Organic Chemistry* **2005**, 70, 3218-3224.
- [90] a) C. Balsarini, B. Novo, G. Resnati, *Journal of Fluorine Chemistry* **1996**, 80, 31-34; b) B. N. P. Metrangolo, G. Resnati, Polytechnic of Milan, Milan, Italy, *Encyclopedia of Reagents for Organic Synthesis* **2005**.
- [91] J. F. J. Engbersen, A. Koudijs, M. H. A. Joosten, H. C. van der Plas, *Journal of Heterocyclic Chemistry* **1986**, 23, 989-990.
- [92] T. V. Rybalova, V. F. Sedova, Y. V. Gatilov, O. P. Shkurko, *Chemistry of Heterocyclic Compounds* **1998**, 34, 1161-1165.
- [93] W. H. Watson, *Inorganic Chemistry* **1969**, 8, 1879-1886.
- [94] J. J. R. F. da Silva, L. F. Volas Boas, R. Wootton, *Journal of Inorganic and Nuclear Chemistry* **1971**, 33, 2029-2036.
- [95] A. D. Mighell, C. W. Reimann, A. Santoro, *Journal of the Chemical Society D: Chemical Communications* **1970**, 204-204.
- [96] M. R. Bermejo, A. Castiñeiras, J. A. Garcia-Vazquez, W. Hiller, J. Strähle, *Journal of Crystallographic and Spectroscopic Research* **1991**, 21, 93-96.
- [97] a) M. Munakata, L. P. Wu, G. L. Ning, *Coordination Chemistry Reviews* **2000**, 198, 171-203; b) M. Munakata, L. P. Wu, T. Kuroda-Sowa, M. Maekawa, Y. Suenaga, T. Ohta, H. Konaka, *Inorganic Chemistry* **2003**, 42, 2553-2558.
- [98] a) M. A. Gutierrez, G. R. Newkome, J. Selbin, *Journal of Organometallic Chemistry* **1980**, 202, 341-350; b) E. C. Constable, A. M. W. Cargill Thompson, T. A. Leese, D. G. F. Reese, D. A. Tocher, *Inorganica Chimica Acta* **1991**, 182, 93-100.
- [99] a) C. P. Newman, K. Casey-Green, G. J. Clarkson, G. W. V. Cave, W. Errington, J. P. Rourke, *Dalton Transactions* **2007**, 3170-3182; b) G. L. Edwards, D. S. t. C. Black, G. B. Deacon, L. P. Wakelin, *Canadian Journal of Chemistry* **2005**, 83, 980-989.

- [100] Y. A. Hernández, J. López-Serrano, M. Paneque, M. L. Poveda, F. Vattier, V. Salazar, E. Álvarez, E. Carmona, *Chemistry – A European Journal* **2011**, *17*, 9302-9305.
- [101] a) B. Peña, N. A. Leed, K. R. Dunbar, C. Turro, *Journal of Physical Chemistry C* **2012**, *116*, 22186-22195; b) S. Fraysse, C. Coudret, J.-P. Launay, *European Journal of Inorganic Chemistry* **2000**, *2000*, 1581-1590.
- [102] H. Papadaki, A. Christofides, J. C. Jeffery, T. Bakas, *Journal of Coordination Chemistry* **1999**, *47*, 559-572.
- [103] a) M. Eddaoudi, D. B. Moler, H. Li, B. Chen, T. M. Reineke, M. O'Keeffe, O. M. Yaghi, *Accounts of Chemical Research* **2001**, *34*, 319-330; b) L. Brammer, M. D. Burgard, C. S. Rodger, J. K. Swearingen, N. P. Rath, *Chemical Communications* **2001**, 2468-2469; c) M. O. Awaleh, A. Badia, F. Brisse, X.-H. Bu, *Inorganic Chemistry* **2006**, *45*, 1560-1574.
- [104] S. O. Sommerer, B. L. Westcott, K. A. Abboud, *Acta Crystallographica Section C* **1994**, *50*, 48-52.
- [105] Z. Karczmarzyk, T. M. Lipinska, W. Wysocki, Z. Urbanczyk-Lipkowska, P. Kalicki, *Acta Crystallographica Section E* **2010**, *66*, o806-o807.
- [106] S. N. Ivashevskaja, L. A. Aleshina, V. P. Andreev, Y. P. Nizhnik, V. V. Chernyshev, *Acta Crystallographica Section E* **2002**, *58*, m721-m723.
- [107] a) V. P. Andreev, A. V. Ryzhǎlcov, *Chemistry of Heterocyclic Compounds* **1994**, *30*, 938-942; b) V. P. Andreev, E. G. Batotsyrenova, A. V. Ryzhakov, L. L. Rodina, *Chemistry of Heterocyclic Compounds* **1998**, *34*, 941-949.
- [108] Y. A. Gubarev, N. S. Lebedeva, V. P. Andreev, G. V. Girichev, *Russian Journal of General Chemistry* **2009**, *79*, 1183-1190.
- [109] Z. Dega-Szafran, Z. Kosturkiewicz, E. Tykarska, M. Szafran, D. Lemański, B. Nogaj, *Journal of Molecular Structure* **1997**, *404*, 25-32.
- [110] H. Nakai, T. Saito, M. Yamakawa, *Acta Crystallographica Section C* **1988**, *44*, 533-535.
- [111] A. Wawrzynów, K. Sokołowski, L. Chmurzyński, A. Liwo, *Journal of Molecular Structure* **1988**, *174*, 235-240.
- [112] A. Szemik-Hojniak, T. Głowiak, I. Deperasinska, A. Puszko, *Journal of Molecular Structure* **2001**, *597*, 279-291.
- [113] R. Moreno-Fuquen, A. M. Montano, R. Atencio, *Acta Crystallographica Section E* **2005**, *61*, o3061-o3062.
- [114] a) Y. P. Nizhnik, J. Lu, S. V. Rosokha, J. K. Kochi, *New Journal of Chemistry* **2009**, *33*, 2317-2325; b) D. S. Laitar, E. Y. Tsui, J. P. Sadighi, *Journal of the American Chemical Society* **2006**, *128*, 11036-11037.
- [115] a) M. Szafran, E. Tykarska, Z. Dega-Szafran, *Journal of Molecular Structure* **1997**, *416*, 81-90; b) J. Wąsicki, M. Jaskólski, Z. Pająk, M. Szafran, Z. Dega-Szafran, M. A. Adams, S. F. Parker, *Journal of Molecular Structure* **1999**, *476*, 81-95.
- [116] M. S. Hussain, S. A. A. Al-Hamoud, *Journal of the Chemical Society, Dalton Transactions* **1985**, 749-753.
- [117] a) E. Huskowska, I. Turowska-Tyrk, J. Legendziewicz, J. P. Riehl, *New Journal of Chemistry* **2002**, *26*, 1461-1467; b) G. A. van Albada, I. Mutikainen, U. Turpeinen, J. Reedijk, *Acta Crystallographica Section E* **2003**, *59*, m889-m891.

- [118] a) Y. P. Nizhnik, A. Szemik-Hojniak, I. Deperasińska, L. B. Jerzykiewicz, M. Korabik, M. Hojniak, V. P. Andreev, *Inorganic Chemistry* **2008**, *47*, 2103-2112; b) A. Puszko, A. Krojcer, M. Pelczynska, J. Wietrzyk, M. Cieślak-Golonka, J. Jezierska, A. Adach, M. Kubiak, *Journal of Inorganic Biochemistry* **2010**, *104*, 153-160.
- [119] a) J. Luo, F. Yang, L.-J. Qiu, X.-X. Wang, B.-S. Liu, *Acta Crystallographica Section E* **2009**, *65*, m547-m548; b) M. Yuan, S. Gao, F. Zhao, W. Zhang, Z. Wang, *Science in China Series B-Chemistry* **2009**, *52*, 266-275.
- [120] T. Linker, *Angewandte Chemie International Edition in English* **1997**, *36*, 2060-2062.
- [121] a) H.-J. Lu, F.-M. Wang, *Acta Crystallographica Section E* **2009**, *65*, m660; b) R. Puthiyottil, S. Varghese, U. Gopalakrishnapanicker, J. T. Guthrie, *Polymer Engineering & Science* **2013**, *53*, 119-124.
- [122] a) V. Chandrasekhar, P. Singh, *Dalton Transactions* **2011**, *40*, 114-123; b) L. Ducháčková, V. Steinmetz, J. I. Lemaire, J. Roithová, *Inorganic Chemistry* **2010**, *49*, 8897-8903.
- [123] S. Bruda, M. Andruh, H. W. Roesky, Y. Journaux, M. Noltemeyer, E. Rivière, *Inorganic Chemistry Communications* **2001**, *4*, 111-114.
- [124] a) D.-Q. Yuan, F.-Y. Lian, M.-C. Hong, *Acta Crystallographica Section E* **2007**, *63*, m1430; b) A. J. Dillner, C. P. Lilly, J. M. Knaust, *Acta Crystallographica Section E* **2010**, *66*, m1156-m1157.
- [125] a) R. Thaimattam, D. Shekhar Reddy, F. Xue, T. C. W. Mak, A. Nangia, G. R. Desiraju, *Journal of the Chemical Society, Perkin Transactions 2* **1998**, 1783-1790; b) C. Horn, M. Scudder, I. Dance, *CrystEngComm* **2001**, *3*, 1-8.
- [126] A. K. Ghosh, D. Ghoshal, E. Zangrando, J. Ribas, N. Ray Chaudhuri, *Inorganic Chemistry* **2005**, *44*, 1786-1793.
- [127] D.-L. Long, A. J. Blake, N. R. Champness, M. Schroder, *Chemical Communications* **2000**, 2273-2274.
- [128] H.-L. Sun, S. Gao, B.-Q. Ma, S. R. Batten, *CrystEngComm* **2004**, *6*, 579-583.
- [129] a) E. P. Boron, J. M. Knaust, *Acta Crystallographica Section E* **2009**, *65*, o2970; b) X.-J. Feng, W. Yao, M.-F. Luo, R.-Y. Ma, H.-W. Xie, Y. Yu, Y.-G. Li, E.-B. Wang, *Inorganica Chimica Acta* **2011**, *368*, 29-36.
- [130] a) Y.-F. Hsu, C.-H. Lin, J.-D. Chen, J.-C. Wang, *Crystal Growth & Design* **2008**, *8*, 1094-1096; b) Y.-F. Hsu, H.-L. Hu, C.-J. Wu, C.-W. Yeh, D. M. Proserpio, J.-D. Chen, *CrystEngComm* **2009**, *11*, 168-176.
- [131] M. Muniz-Miranda, B. Pergolese, G. Sbrana, A. Bigotto, *Journal of Molecular Structure* **2005**, *744-747*, 339-343.
- [132] D. J. W. Bullock, C. W. N. Cumper, A. I. Vogel, *Journal of the Chemical Society* **1965**, 5316-5323.
- [133] a) H.-H. Song, B.-Q. Ma, *CrystEngComm* **2007**, *9*, 625-627; b) H.-H. Song, B.-Q. Ma, *Acta Crystallographica Section E* **2007**, *63*, o1332-o1333.
- [134] B.-Q. Ma, H.-L. Sun, S. Gao, *Chemical Communications* **2004**, 2220-2221.
- [135] a) J. M. Shi, X. Zhang, H. Y. Xu, C. J. Wu, L. D. Liu, *Journal of Coordination Chemistry* **2007**, *60*, 647-654; b) H.-L. Sun, S. Gao, B.-Q. Ma, G. Su, *Inorganic Chemistry* **2003**, *42*, 5399-5404; c) B.-Q. Ma, H.-L. Sun, S. Gao, G. Su, *Chemistry of Materials* **2001**, *13*, 1946-1948; d) H.-L. Sun, S. Gao, B.-Q. Ma, G. Su, S. R. Batten, *Crystal Growth & Design* **2004**, *5*, 269-277.
- [136] H.-L. Sun, Z.-M. Wang, S. Gao, *Inorganic Chemistry* **2005**, *44*, 2169-2176.

- [137] C. J. Brown, III, J. M. Knaust, *Acta Crystallographica Section E* **2009**, *65*, o3052.
- [138] a) D. Zhang, J. P. Telo, C. Liao, S. E. Hightower, E. L. Clennan, *Journal of Physical Chemistry A* **2007**, *111*, 13567-13574; b) G.-J. ten Brink, I. W. C. E. Arends, M. Hoogenraad, G. Verspui, R. A. Sheldon, *Advanced Synthesis & Catalysis* **2003**, *345*, 497-505; c) D. Wenkert, R. B. Woodward, *Journal of Organic Chemistry* **1983**, *48*, 283-289.
- [139] H. Arzoumanian, R. Bakhtchadjian, G. Agrifoglio, R. Atencio, A. Briceño, *Transition Metal Chemistry* **2006**, *31*, 681-689.
- [140] F. W. Lewis, L. M. Harwood, M. J. Hudson, P. Distler, J. John, K. Stamberg, A. Núñez, H. Galán, A. G. Espartero, *European Journal of Organic Chemistry* **2012**, *2012*, 1509-1519.
- [141] L.-P. Zhang, W.-J. Lu, T. C. W. Mak, *Chemical Communications* **2003**, 2830-2831.
- [142] L. Della Ciana, I. Hamachi, T. J. Meyer, *Journal of Organic Chemistry* **1989**, *54*, 1731-1735.
- [143] O. Toma, N. Mercier, M. Bouilland, M. Allain, *CrystEngComm* **2012**, *14*, 7844-7847.
- [144] B. G. De Geest, A. G. Skirtach, T. R. M. De Beer, G. B. Sukhorukov, L. Bracke, W. R. G. Baeyens, J. Demeester, S. C. De Smedt, *Macromolecular Rapid Communications* **2007**, *28*, 88-95.
- [145] M. Malinowski, Ł. Kaczmarek, *Russian Journal of Applied Chemistry* **1988**, *330*, 154-158.
- [146] a) S. Youssif, *Arkivoc* **2001**, 242-268; b) M. Malinowski, Ł. Kaczmarek, F. Rozploch, *Journal of the Chemical Society, Perkin Transactions 2* **1991**, 879-883.
- [147] C.-W. Yeh, J.-D. Chen, J.-C. Wang, *Polyhedron* **2008**, *27*, 3611-3618.
- [148] E. P. Hart, *Journal of the Chemical Society* **1954**, 1879-1882.
- [149] A. N. Singh, R. P. Thummel, *Inorganic Chemistry* **2009**, *48*, 6459-6470.
- [150] S. Rozen, S. Dayan, *Angewandte Chemie International Edition in English* **1999**, *38*, 3471-3473.
- [151] W. W. Paudler, D. J. Pokorny, S. J. Cornrich, *Journal of Heterocyclic Chemistry* **1970**, *7*, 291-295.
- [152] a) J.-M. Shi, X.-Z. Meng, Y.-M. Sun, H.-Y. Xu, W. Shi, P. Cheng, L.-D. Liu, *Journal of Molecular Structure* **2009**, *917*, 164-169; b) J.-M. Shi, Y.-M. Sun, Z. Liu, L.-D. Liu, W. Shi, P. Cheng, *Dalton Transactions* **2006**, 376-380.
- [153] A. G. Young, L. R. Hanton, *Coordination Chemistry Reviews* **2008**, *252*, 1346-1386.
- [154] G. A. Bowmaker, Effendy, S. Marfua, B. W. Skelton, A. H. White, *Inorganica Chimica Acta* **2005**, *358*, 4371-4388.
- [155] a) R. Sarma, A. K. Boudalis, J. B. Baruah, *Inorganica Chimica Acta* **2010**, *363*, 2279-2286; b) Y.-Z. Tang, M. Zhou, H.-R. Wen, Z. Cao, X.-W. Wang, S. Huang, *CrystEngComm* **2011**, *13*, 3040-3045; c) J. R. Bowers, G. W. Hopkins, G. P. A. Yap, K. A. Wheeler, *Crystal Growth & Design* **2004**, *5*, 727-736.
- [156] H. Kanno, K. Iijima, *Acta Crystallographica Section C* **1997**, *53*, 498-499.
- [157] a) S. G. Ang, B. W. Sun, *Crystal Growth & Design* **2004**, *5*, 383-386; b) A. D. Jana, S. C. Manna, G. M. Rosair, M. G. B. Drew, G. Mostafa, N. Ray Chaudhuri, *Crystal Growth & Design* **2007**, *7*, 1365-1372; c) S. C. Manna, E. Zangrando, N. Ray Chaudhuri, *Journal of Molecular Structure* **2008**, *877*, 145-151; d) D.-L. Long, R. J. Hill, A. J. Blake, N. R. Champness, P. Hubberstey, C. Wilson, M. Schröder, *Chemistry – A European Journal* **2005**, *11*, 1384-1391.
- [158] E. Eichhorn, *Acta Crystallographica* **1959**, *12*, 746-754.
- [159] a) D. Venkataraman, S. Lee, J. S. Moore, P. Zhang, K. A. Hirsch, G. B. Gardner, A. C. Covey, C. L. Prentice, *Chemistry of Materials* **1996**, *8*, 2030-2040; b) C. M. Fitchett, P. J. Steel, *New Journal of Chemistry* **2000**, *24*, 945-947; c) F.-F. Li, J.-F. Ma, S.-Y. Song, J. Yang, Y.-Y. Liu, Z.-M. Su,

- Inorganic Chemistry* **2005**, *44*, 9374-9383; d) D. Sun, G.-G. Luo, N. Zhang, Q.-J. Xu, R.-B. Huang, L.-S. Zheng, *Polyhedron* **2010**, *29*, 1243-1250; e) P. J. Leszczynski, A. Budzianowski, L. Dobrzycki, M. K. Cyranski, M. Derzsi, W. Grochala, *Dalton Transactions* **2012**, *41*, 396-402; f) P. J. Steel, C. M. Fitchett, *Coordination Chemistry Reviews* **2008**, *252*, 990-1006.
- [160] H.-L. Sun, S. Gao, B.-Q. Ma, F. Chang, W.-F. Fu, *Microporous Mesoporous Materials* **2004**, *73*, 89-95.
- [161] Z.-P. Deng, Z.-B. Zhu, S. Gao, L.-H. Huo, H. Zhao, *Dalton Transactions* **2009**, 1290-1292.
- [162] P. J. Hagrman, D. Hagrman, J. Zubieta, *Angewandte Chemie International Edition in English* **1999**, *38*, 2638-2684.
- [163] a) B.-Q. Ma, H.-L. Sun, S. Gao, *Inorganic Chemistry* **2005**, *44*, 837-839; b) B.-Q. Ma, H.-L. Sun, S. Gao, G.-X. Xu, *Inorganic Chemistry* **2001**, *40*, 6247-6253; c) S. Tanase, M. Andruh, A. Muller, M. Schmidtman, C. Mathoniere, G. Rombaut, *Chemical Communications* **2001**, 1084-1085; d) A. Nedelcu, Z. Žak, A. M. Madalan, J. Pinkas, M. Andruh, *Polyhedron* **2003**, *22*, 789-794; e) D. Visinescu, G. I. Pascu, M. Andruh, J. Magull, H. W. Roesky, *Inorganica Chimica Acta* **2002**, *340*, 201-206.
- [164] a) P. Pechy, F. P. Rotzinger, M. K. Nazeeruddin, O. Kohle, S. M. Zakeeruddin, R. Humphry-Baker, M. Gratzel, *Journal of the Chemical Society, Chemical Communications* **1995**, 65-66; b) U. Ziener, J.-M. Lehn, A. Mourran, M. Möller, *Chemistry – A European Journal* **2002**, *8*, 951-957.
- [165] a) P. Zhang, Y. Wang, H. Liu, Y. Chen, *Journal of Materials Chemistry* **2011**, *21*, 18462-18466; b) B. Tong, S. Wang, Y. Meng, B. Wang, *Photochemical & Photobiological Sciences* **2007**, *6*, 519-520.
- [166] a) H. Hofmeier, U. S. Schubert, *Chemical Society Reviews* **2004**, *33*, 373-399; b) A. Khatyr, R. Ziessel, *Journal of Organic Chemistry* **2000**, *65*, 3126-3134; c) H. S. Chow, E. C. Constable, C. E. Housecroft, M. Neuburger, S. Schaffner, *Polyhedron* **2006**, *25*, 1831-1843.
- [167] K. Ito, T. Nagata, K. Tanaka, *Inorganic Chemistry* **2001**, *40*, 6331-6333.
- [168] a) W.-L. Wong, W.-S. Lee, H.-L. Kwong, *Tetrahedron: Asymmetry* **2002**, *13*, 1485-1492; b) G. Dyker, B. Hölzer, G. Henkel, *Tetrahedron: Asymmetry* **1999**, *10*, 3297-3307.
- [169] a) A. Winter, G. R. Newkome, U. S. Schubert, *ChemCatChem* **2011**, *3*, 1384-1406; b) W.-L. Wong, C.-S. Lee, H.-K. Leung, H.-L. Kwong, *Organic & Biomolecular Chemistry* **2004**, *2*, 1967-1969.
- [170] F. H. Case, *Journal of Organic Chemistry* **1962**, *27*, 640-641.
- [171] F. C. Cooper, M. W. Partridge, *Journal of the Chemical Society* **1954**, 3429-3435.
- [172] M. W. Partridge, H. J. Vipond, J. A. Waite, *Journal of the Chemical Society* **1962**, 2549-2556.
- [173] a) T. Kusukawa, M. Fujita, *Journal of the American Chemical Society* **1999**, *121*, 1397-1398; b) T. Kusukawa, M. Fujita, *Journal of the American Chemical Society* **2002**, *124*, 13576-13582.
- [174] a) A. Pitto-Barry, O. Zava, P. J. Dyson, R. Deschenaux, B. Therrien, *Inorganic Chemistry* **2012**, *51*, 7119-7124; b) F.-Y. Yi, J. Zhang, H.-X. Zhang, Z.-M. Sun, *Chemical Communications* **2012**, *48*, 10419-10421.
- [175] M. I. J. Polson, E. A. Medlycott, G. S. Hanan, L. Mikelsons, N. J. Taylor, M. Watanabe, Y. Tanaka, F. Loiseau, R. Passalacqua, S. Campagna, *Chemistry – A European Journal* **2004**, *10*, 3640-3648.
- [176] Q. Huang, *Acta Crystallographica Section E* **2009**, *65*, o2329.
- [177] X.-Q. Liang, X.-H. Zhou, C. Chen, H.-P. Xiao, Y.-Z. Li, J.-L. Zuo, X.-Z. You, *Crystal Growth & Design* **2009**, *9*, 1041-1053.

- [178] J. Janczak, M. Śledź, R. Kubiak, *Journal of Molecular Structure* **2003**, 659, 71-79.
- [179] J. R. A. Cottam, P. J. Steel, *Tetrahedron* **2009**, 65, 7948-7953.
- [180] A. J. Amoroso, M. W. Burrows, S. J. Coles, R. Haigh, R. D. Farley, M. B. Hursthouse, M. Jones, K. M. A. Malik, D. M. Murphy, *Dalton Transactions* **2008**, 506-513.
- [181] A. W. Addison, T. N. Rao, J. Reedijk, J. van Rijn, G. C. Verschoor, *Journal of the Chemical Society, Dalton Transactions* **1984**, 1349-1356.
- [182] S. E. McKay, K. A. Wheeler, S. C. Blackstock, *Acta Crystallographica Section E* **2004**, 60, 2258-2260.
- [183] L. Yang, D. R. Powell, R. P. Houser, *Dalton Transactions* **2007**, 955-964.
- [184] A. Bondi, *Journal of Physical Chemistry* **1964**, 68, 441-451.
- [185] a) P. Zhong, S.-r. Guo, C.-s. Song, *Synthetic Communications* **2004**, 34, 247-253; b) S. L. Jain, B. Sain, *Applied Catalysis A: General* **2006**, 301, 259-264.
- [186] D. Sanz, A. Perona, R. M. Claramunt, J. Elguero, *Tetrahedron* **2005**, 61, 145-154.
- [187] B. Brycki, B. Nowak-Wydra, M. Szafran, *Magnetic Resonance Chemistry* **1988**, 26, 303-306.
- [188] W. M. Schubert, J. Robins, J. M. Craven, *Journal of Organic Chemistry* **1959**, 24, 943-946.
- [189] M. Ferrer, F. Sánchez-Baeza, A. Messegue, *Tetrahedron* **1997**, 53, 15877-15888.
- [190] A. T. Balaban, C. D. Nenitzescu, *Journal of the Chemical Society* **1961**, 3566-3572.
- [191] A. Ohsawa, T. Kawaguchi, H. Igeta, *Journal of Organic Chemistry* **1982**, 47, 3497-3503.
- [192] W. Mai, J. Yuan, Z. Li, L. Yang, Y. Xiao, P. Mao, L. Qu, *Synlett* **2012**, 23, 938-942.
- [193] F. Zhang, S. Zhang, X.-F. Duan, *Organic Letters* **2012**, 14, 5618-5620.
- [194] S. H. Cho, S. J. Hwang, S. Chang, *Journal of the American Chemical Society* **2008**, 130, 9254-9256.
- [195] T. Niwa, H. Yorimitsu, K. Oshima, *Organic Letters* **2007**, 9, 2373-2375.
- [196] S. Kaiser, S. P. Smidt, A. Pfaltz, *Angewandte Chemie International Edition in English* **2006**, 45, 5194-5197.
- [197] G. Barbieri, R. Benassi, P. Lazzeretti, L. Schenetti, F. Taddei, *Organic Magnetic Resonance* **1975**, 7, 451-454.
- [198] J. Yin, B. Xiang, M. A. Huffman, C. E. Raab, I. W. Davies, *Journal of Organic Chemistry* **2007**, 72, 4554-4557.
- [199] J.-A. Su, E. Siew, E. V. Brown, S. L. Smith, *Organic Magnetic Resonance* **1978**, 11, 565-574.
- [200] E. J. Corey, A. L. Borrer, T. Foglia, *Journal of Organic Chemistry* **1965**, 30, 288-290.
- [201] Y. Engel, A. Dahan, E. Rozenshine-Kemelmakher, M. Gozin, *Journal of Organic Chemistry* **2007**, 72, 2318-2328.
- [202] A. Ouali, J.-F. Spindler, A. Jutand, M. Taillefer, *Advanced Synthesis & Catalysis* **2007**, 349, 1906-1916.
- [203] T. R. Amarante, S. Figueiredo, A. D. Lopes, I. S. Goncalves, F. A. Almeida Paz, *Acta Crystallographica Section E* **2009**, 65, o2047.
- [204] D. J. Awad, U. Schilde, P. Strauch, *Inorganica Chimica Acta* **2011**, 365, 127-132.
- [205] H. E. Katz, *Journal of Organic Chemistry* **1985**, 50, 2086-2091.
- [206] F. H. Case, J. M. Lesser, *Journal of Heterocyclic Chemistry* **1966**, 3, 170-173.
- [207] R. P. Thummel, F. Lefoulon, *Journal of Organic Chemistry* **1985**, 50, 666-670.
- [208] S. Kajihara, *Nippon Kagaku Zasshi* **1965**, 86, 839-849.



- [209] S. E. McKay, R. W. Lashlee, L. W. Maina, K. A. Wheeler, A. B. Brown, in *Heterocyclic Communications*, **2009**, *15*, 181.
- [210] D. Wang, W. E. Crowe, R. M. Strongin, M. Sibrian-Vazquez, *Chemical Communications* **2009**, 1876-1878.
- [211] Y. Y. Durmaz, Ö. Zaim, Y. Yagci, *Macromolecular Rapid Communications* **2008**, *29*, 892-896.
- [212] H. J. W. Van den Haak, H. C. Van der Plas, B. Van Veldhuizen, *Journal of Organic Chemistry* **1981**, *46*, 2134-2137.
- [213] W. W. Paudler, T. J. Kress, *Journal of Organic Chemistry* **1967**, *32*, 832-833.
- [214] C. F. Koelsch, W. H. Gumprecht, *Journal of Organic Chemistry* **1958**, *23*, 1603-1606.
- [215] N. J. Babu, A. Nangia, *CrystEngComm* **2007**, *9*, 980-983.
- [216] M. Matsuo, S. Matsumoto, T. Kurihara, Y. Akita, T. Watanabe, A. Ohta, *Organic Magnetic Resonance* **1980**, *13*, 172-179.
- [217] R. A. Yadav, V. Mukherjee, M. Kumar, R. Singh, *Spectrochimica Acta Part A: Molecular and Biomolecular Spectroscopy* **2007**, *66*, 964-971.
- [218] A. Ohta, S. Masano, S. Iwakura, A. Tamura, H. Watahiki, M. Tsutsui, Y. Akita, T. Watanabe, T. Kurihara, *Journal of Heterocyclic Chemistry* **1982**, *19*, 465-473.
- [219] R. P. Thummel, Y. Jahng, *Journal of Organic Chemistry* **1985**, *50*, 3635-3636.
- [220] J. Wang, F. Xu, T. Cai, Q. Shen, *Organic Letters* **2008**, *10*, 445-448.
- [221] J. S. Gardner, R. G. Harrison, J. D. Lamb, D. V. Dearden, *New Journal of Chemistry* **2006**, *30*, 1276-1282.
- [222] G. M. Sheldrick, *Acta Crystallographica Section A* **2008**, *64*, 112-122.
- [223] G. M. Sheldrick, SHELXL-97, Programs for X-ray Crystal Structure Refinement, **1997**, University of Göttingen.
- [224] O. V. Dolomanov, L. J. Bourhis, R. J. Gildea, J. A. K. Howard, H. Puschmann, *Journal of Applied Crystallography* **2009**, *42*, 339-341.
- [225] K. J. Stevenson, Origin (OriginLab, Northampton, MA), 2007, University of Texas at Austin.